ALD 2019

19th International Conference on Atomic Layer Deposition

ATOMIC LAYER ETCHING

Featuring the 6th International *Atomic Layer Etching* WORKSHOP

July 21-24, 2019 • Bellevue, Washington, USA

Technical Program & Abstracts

ALD/ALE 2019 PLATINUM SPONSORS

Air Liquide

APPLIED MATERIALS make possible

ARRADIANCE

ASM

EMD Performance Materials

EREZTECH BRIDGING CHEMICAL GAPS

EUGENUS

Kurt J. Lesker Company

Lam RESEARCH

Leadmicro 微导

OXFORD INSTRUMENTS The Business of Science®

picosun AGILE ALD

TEL™

VERSUM MATERIALS

Start using the ALD/ALE 2019 App

To login, enter your Registration Confirmation Number and Last Name to access messaging, enable the synchronization of notes, favorites, and scheduled items between devices and the online planner.

© Visit Bellevue Washington photo courtesy of Merrill Images

ALD 2019

19th International Conference on Atomic Layer Deposition

July 21-24, 2019 • Bellevue, Washington, USA

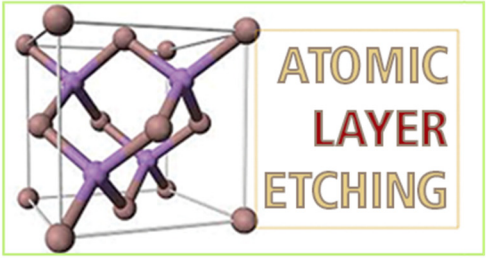

Table of Contents

Welcome 1
General Information 3
Conference Locations 5
Committees 6
Sponsors 7
Exhibitors 10
Sponsors Product Guide 11
Tutorial Schedule 12
Plenary Lecture Schedule 13
Technical Program Key 14
Technical Program Overview 15
Technical Program and Schedule (Oral & Poster) 16
Technical Program Author Index 42
Abstracts (Oral & Poster) 50
Abstracts Author Index 151
Sponsor Ads 159

AVS Meeting Code of Conduct

It is the policy of the AVS that all participants, including attendees, vendors, staff, volunteers, and all other stakeholders at AVS meetings will conduct themselves in a professional manner that is welcoming to all participants and free from any form of discrimination, harassment, or retaliation. Participants will treat each other with respect and consideration to create a collegial, inclusive, and professional environment at AVS Meetings. Creating a supportive environment to enable scientific disclosure at AVS meetings is the responsibility of all participants. Participants will avoid any inappropriate actions or statements based on individual characteristics such as age, race, ethnicity, sexual orientation, gender identity, gender expression, marital status, nationality, political affiliation, ability status, educational background, or any other characteristic protected by law. Disruptive or harassing behavior of any kind will not be tolerated. Harassment includes but is not limited to inappropriate or intimidating behavior and language, unwelcome jokes or comments, unwanted touching or attention, offensive images, photography without permission, and stalking. Violations of this code of conduct policy should be reported to the AVS Managing Director or Events Manager. Sanctions may range from verbal warning, to ejection from the meeting without refund, to notifying appropriate authorities. Retaliation for complaints of inappropriate conduct will not be tolerated. If a participant observes inappropriate comments/actions personal intervention seems appropriate and safe, they should be considerate of all parties before intervening.

Welcome

to the 19th International Conference on Atomic Layer Deposition (ALD 2019) featuring the 6th International Workshop on Atomic Layer Etching (ALE 2019). The Program Committees for both topics feel that members of the ALD and ALE communities benefit from close interaction to allow us to work collectively toward a future of atomic-scale processing. Therefore, conference registrants are invited to attend the joint tutorial session and the Welcome Reception on Sunday, the joint Plenary Session on Monday, and all parallel ALD and ALE oral sessions throughout the week. However, this year, the poster sessions will be held on separate days for better visibility: the ALE poster session will be on Sunday evening during the welcome reception, and the ALD poster sessions will be on Monday and Tuesday evenings. Given the large number of posters in ALD, we have made an effort to create subcategories of posters so attendees can quickly locate presentations related to their area of interest.

To accommodate the recent growth in the ALD and ALE community, in 2018 AVS fully assumed the conference leadership, taking on the financial management and all event management tasks of the ALD Conference and the ALE Workshop every year in both U.S. and international locations. This year the conference will take place from Sunday, July 21–24, 2019, at the Hyatt Regency in the beautiful city of Bellevue, Washington (East Seattle), which sits on the Puget Sound just across from Lake Washington. Close proximity to the Sea-Tac International Airport makes the location accessible to both the Asian and European attendees.

The Conference will begin with joint ALD/ALE Tutorials. For the ALD Tutorials, the Program Committee placed a focus on applications of ALD in various fields. The first tutorial by Stacey Bent (Stanford University, USA) will focus on “Area-Selective ALD for Semiconductor Manufacturing,” reflecting the importance of ALD in the semiconductor field and the need for new area-selective ALD processes. The next three Tutorials will be on energy-related applications of ALD with Andy Sun (Western University, Canada), Rong Chen (Huazhong University of Science and Technology, China), and Bart Macco (Eindhoven University of Technology, The Netherlands) presenting tutorials on applications of ALD in batteries, catalysis, and photovoltaics, respectively.

ALE Tutorials will cover two major areas of the technology. Thorsten Lill (Lam Research, USA) will discuss surface reaction control using a plasma-based approach through traditional dry etch processing parameters. The second tutorial, given by Steven George (University of Colorado at Boulder, USA) will cover the control and formation of volatile reaction products using thermal based ALE.

We are fortunate to have three distinguished plenary speakers. The Conference will open with the first Plenary Speaker, Erwin Kessels (Eindhoven University of Technology, The Netherlands) who is also the 2019 ALD Innovator Awardee “For Original Work and Leadership in ALD.” In his presentation, Prof. Kessels will address several recent and emerging trends in atomic scale processing and discuss how understanding of the underlying mechanisms has contributed to important innovations in the field, either in research or in industry. The ALD Innovator Award will be presented prior to Prof. Kessels’ lecture. In the next Plenary Lecture, Jeffrey Elam (Argonne National Laboratory, USA) will present an overview of how *in situ* measurements can reveal the fundamental mechanisms during ALD, and how these measurements can be combined with machine learning to accelerate ALD process development.
Last, Eric Joseph (IBM, USA) will discuss the coming paradigm shift from Moore’s Law towards accelerator technologies for AI applications. Examples of this paradigm shift will be discussed and a vision for future challenges of atomic scale processes will be reviewed.

A total of 402 abstracts were accepted for this year’s Conference, 59 of which were for the ALE sessions. This total is almost the same as in 2017 and 2018 conferences, which also had over 400 submitted abstracts. Of these 402 abstracts, there are 27 invited speakers, 200 contributed orals, and 175 posters. ALE has shown significant growth in 2019, and will be running a session until Wednesday morning. The diversity and reach of ALD/ALE can be seen in the abstracts submitted from 27 different countries this year. Given the consistency in the submitted abstracts over the past few years, and the growth in certain areas such as ALE, we feel the future of atomic layer processing remains bright.

To accommodate the large number of abstracts and to allow more attendees to give oral presentations, we have scheduled four parallel sessions. Following ALD 2016–2018, the ALE Workshop will be held as the fourth parallel session starting Monday afternoon, but this year will extend into Wednesday morning reflecting the increase in the number of abstracts. Although we have done our best to organize the program into logical groupings of talks, we understand that these many sessions may lead to difficult choices in deciding which talks to attend. However, since all talks are recorded and will be available after the Conference, we believe this approach to be most effective.

Lastly, we would like to sincerely thank the AVS staff for their dedication and hard work in the organization of this Conference. We would also like to express gratitude to all our committee members, sponsors, and exhibitors who have contributed to make this year's ALD/ALE Conference a success. We hope that the organization and structure of the Conference, as well as the special get-together opportunities provided by our industrial sponsors will allow you to meet new contacts and make new friends—enabling fruitful discussions and productive collaborations that will further brighten the future of ALD/ALE.

ALD 2019 Program Chairs:
Sumit Agarwal (Colorado School of Mines, USA)
Dennis Hausmann (Lam Research, USA)

ALE 2019 Program Chairs:
Craig Huffman (Micron Technology, USA)
Gottlieb Oehrlein (University of Maryland, USA)

General Information

Conference Location
Hyatt Regency Bellevue
900 Bellevue Way NE
Bellevue, WA 98004, USA

Tutorial Registration Hours

Sunday, July 21, 2019:	11:30 a.m.-1:00 p.m.	Grand Ballroom Foyer

Conference Registration Hours

Sunday, July 21, 2019:	4:00 p.m.-8:00 p.m.	Grand Ballroom Foyer
Monday, July 22, 2019:	7:00 a.m.-7:00 p.m.	Grand Ballroom Foyer
Tuesday, July 23, 2019:	7:00 a.m.-7:00 p.m.	Grand Ballroom Foyer
Wednesday, July 24, 2019:	7:00 a.m.-2:00 p.m.	Grand Ballroom Foyer

Exhibit Hours
The exhibit will take place in the Hyatt Regency Bellevue Evergreen Ballroom and Foyer during coffee and lunch breaks as well as poster sessions. This year it will also be open during the Welcome Reception.

Sunday, July 21, 2019:	6:00 p.m.-8:00 p.m.	Evergreen Ballroom and Foyer
Monday, July 22, 2019:	10:00 a.m.-7:30 p.m.	Evergreen Ballroom and Foyer
Tuesday, July 23, 2019:	10:00 a.m.-7:30 p.m.	Evergreen Ballroom and Foyer
Wednesday, July 24, 2019:	10:00 a.m.-1:30 p.m.	Evergreen Ballroom and Foyer

Poster Sessions
Poster Sessions will be held in the Hyatt Regency Bellevue Evergreen Ballroom and Foyer throughout the week. Poster presenters are requested to be present at (or near) their poster during the times scheduled for poster viewing.

Poster Hours:

Sunday, July 21, 2019 (ALE ONLY):	6:00 p.m.-8:00 p.m.	Evergreen Ballroom and Foyer
Monday, July 22, 2019:	5:45 p.m.-7:30 p.m.	Evergreen Ballroom and Foyer
Tuesday, July 23, 2019:	5:30 p.m.-7:30 p.m.	Evergreen Ballroom and Foyer

Poster Setup:

- Sunday Setup (ALE ONLY): After 5:45 p.m.
  Sunday posters will stay up until the end of lunch on Wednesday.
- Monday Setup: After 10:00 a.m.
  Monday posters will stay up until the end of lunch on Tuesday.
- Tuesday Setup: After 3:00 p.m.
  Tuesday posters will stay up until the end of lunch on Wednesday.

Poster Removal: Please note that we cannot take responsibility for any posters left on the boards after the session—any remaining posters will be discarded.

- Sunday (ALE ONLY) posters should be removed Wednesday by 1:20 p.m.
- Monday posters should be removed Tuesday by 1:20 p.m.
- Tuesday posters should be removed Wednesday by 1:20 p.m.

Welcome Reception
All registered attendees and exhibitors are invited to attend the Welcome Reception on Sunday, July 21, 2019, in the Evergreen Ballroom and Foyer from 6:00 p.m.-8:00 p.m.

Refreshment Breaks and Lunches

All refreshment breaks and strolling lunches will be held Monday-Wednesday in the Hyatt Regency Bellevue Evergreen Ballroom and Foyer *. Limited seating will be available**. *While supplies last.**

Internet Service

Free wireless is available in the Hyatt Regency Bellevue meeting rooms. The password is **ALD2019**.

Mobile App

Don't forget to download the ALD/ALE 2019 Mobile App from your devices App Store or at https://ald2019.avs.org/mobileapp/. Use the app and/or the online scheduler to view presentations, presenters, abstracts, sponsors, exhibitors, and to build your schedule. **Login using your confirmation/ID number and last name**.

Manuscript Submission

Journal of Vacuum Science & Technology A is soliciting research articles for publication in a 2020 Special Topic Collection on Atomic Layer Deposition and Atomic Layer Etching. Manuscripts are due November 1, 2019. Please see details at https://ald2019.avs.org/manuscripts/.

Conference Management

AVS
110 Yellowstone Dr., Suite 120
Chico CA 95973
Phone: 530-896-0477
Fax: 530-896-0487,
E-mail: events@avs.org
Website: www.ald-avs.org

Conference Locations

Exhibits and Posters

Lobby Level: Evergreen Ballroom and Foyer

Registration

Second Floor: Grand Ballroom Foyer

Technical Sessions

Second Floor: Grand Ballroom and Regency Ballroom

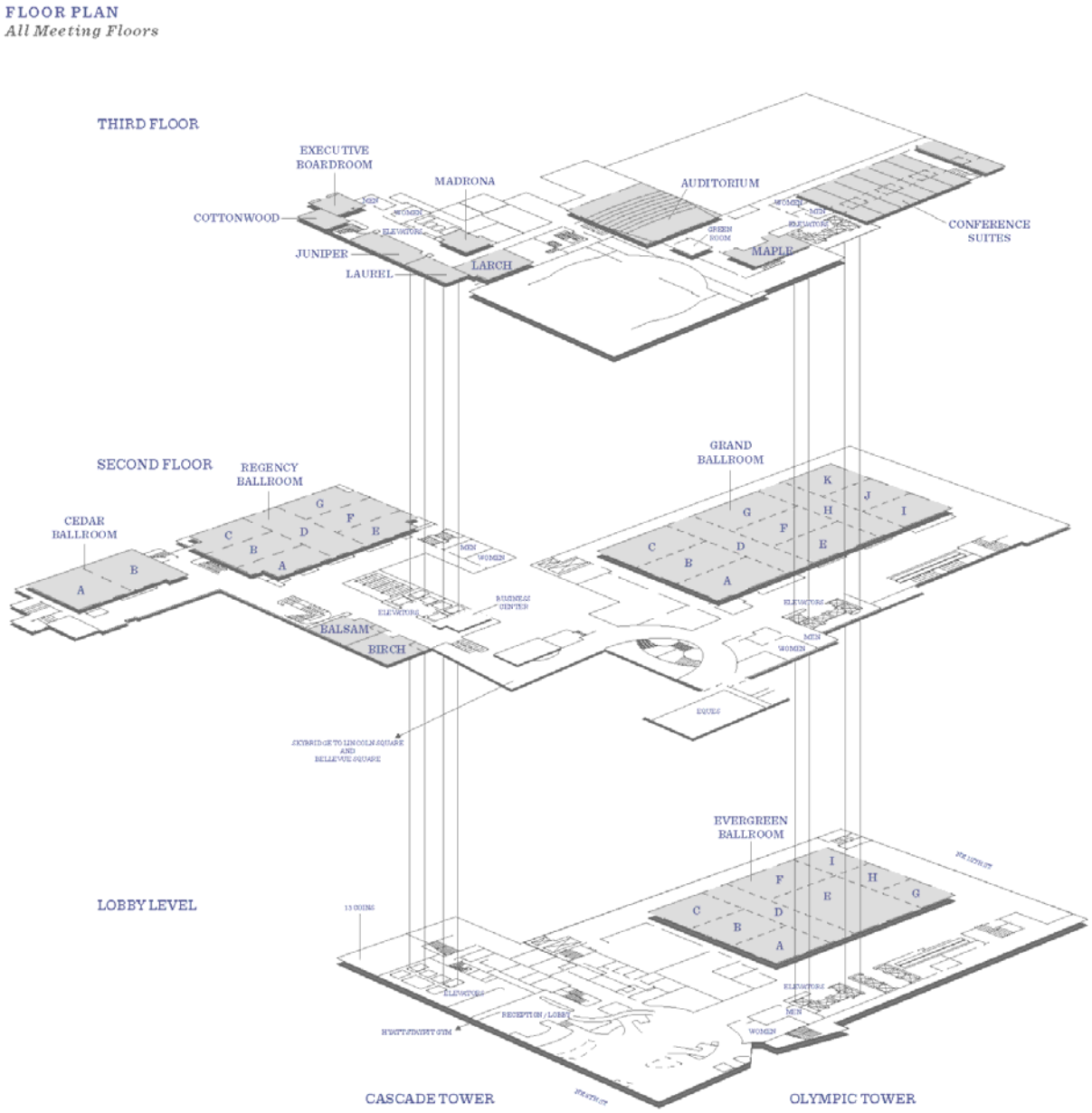

Committees

ALD 2019 Program Chairs

Program Chair: Sumit Agarwal (Colorado School of Mines, USA)
Program Co-Chair: Dennis Hausmann (Lam Research, USA)

ALD Program Committee

Parag Banerjee (Univ. of Central Florida, USA)
Sean Barry (Carlton Univ., Canada)
Stacey Bent (Stanford Univ., USA)
Iain Buchanan (Versum Materials, UK)
Robert Clark (TEL, USA)
Scott Clendenning (Intel, USA)
Rong Chen (Huazhong Univ. of Science and Technology, China)
John F. Conley, Jr. (Oregon State Univ., USA)
Arrelaine Dameron (Forge Nano, USA)
Neil Dasgupta (Univ. of Michigan, USA)
Charles Dezelah (ASM Microchemistry, USA)
Christophe Detavernier (Univ. of Ghent, Belgium)
Shi-Jin Ding (Fudan Univ., China)
Christian Dussarrat (Air Liquide, France)
Simon Elliott (Schrödinger, Ireland)
Ravi Kanjolia (EMD Performance Materials, USA)
Jiyoung Kim (Univ. of Texas at Dallas, USA)
Mato Knez (Nanogune, Spain)
Harm Knoops (Oxford Instruments, UK)
Se-Hun Kwon (Pusan National Univ., South Korea)
Adrien LaVoie (Lam Research, USA)
Han-Bo-Ram Lee (Incheon National Univ., South Korea)
Won-Jun Lee (Sejong Univ., South Korea)
Han-Jin Lim (Samsung Electronics, South Korea)
Mike McSwiney (Intel, USA)
Jin-Seong Park (Hanyang Univ., South Korea)
Paul Poodt (TNO/Holst Center, The Netherlands)
Matti Putkonen (VTT, Finland)
Somil Rathi (Eugenus, USA)
Mikko Ritala (Univ. of Helsinki, Finland)
Simon Rushworth (EpiValence, UK)
Seung Wook Ryu (SK Hynix, South Korea)
Uwe Schroeder (Namlab, Germany)
Nicholas Strandwitz (Lehigh Univ., USA)
Jonas Sundqvist (Fraunhofer IKTS, Germany)
Ganesh Sundaram (Veeco, USA)
Myung Mo Sung (Hanyang Univ., South Korea)
Christophe Vallee (LETI-LTM, France)
Charles Winter (Wayne State Univ., USA)
Angel Yanguas-Gil (Argonne National Lab, USA

ALD Poster Chairs

Adrie Mackus (Eindhoven Univ. of Technology, The Netherlands)
Virginia Wheeler (U.S. Naval Research Lab, USA)

ALD Social Media Chairs

Riikka Puurunen (Aalto Univ., Finland)

ALD International Advisory Committee

Annelies Delabie (imec, Belgium)
Anjana Devi (Ruhr-Univ. Bochum, Germany)
Jeffrey Elam (Argonne National Lab, USA)
Steven George (Univ. of Colorado at Boulder, USA)
Roy Gordon (Harvard Univ., USA)
Cheol Seong Hwang (Seoul National Univ., South Korea)
Hyeongtag Jeon (Hanyang Univ., South Korea)
Erwin Kessels (Eindhoven Univ. of Technology, The Netherlands)
Hyungjun Kim (Yonsei Univ., South Korea)
Sang In Lee (Synos Foundation, USA)
Markku Leskelä (Univ. of Helsinki, Finland)
Gregory N. Parsons (North Carolina State Univ., USA)
Viljami Pore (ASM, Finland)

ALD Steering Committee:

Steven George (Univ. of Colorado at Boulder, USA)
Erwin Kessels (Eindhoven Univ. of Technology, The Netherlands)
Hyungjun Kim (Yonsei Univ., South Korea)
Gregory N. Parsons (North Carolina State Univ., USA)

ALE 2019 Program Chairs

Program Chair: Craig Huffman (Micron Technology, USA)
Program Co-Chair: Gottlieb Oehrlein (Univ. of Maryland, USA)

ALE Program Committee

Ankur Agarwal (KLA, USA)
David Boris (Naval Research Lab, USA)
Jean-Francois de Marneffe (imec, Belgium)
Bert Ellingboe (Dublin City Univ., Ireland)
Steve George (Univ. of Colorado at Boulder, USA)
Satoshi Hamaguchi (Osaka Univ., Japan)
Keren Kanarik (Lam Research, USA)
Harm Knoops (Oxford Instruments, The Netherlands)
Venkat Pallem (Air Liquide, USA)
Alok Ranjan (Tokyo Electron, USA)
Fred Roozeboom (Eindhoven Univ. of Technology, The Netherlands)
Dmitry Suyatin (Lund Univ., Sweden)
Tetsuya Tatsumi (Sony Corp., Japan)
Wei Tian (Applied Materials, USA)
Geun Young Yeom (Sungkyunkwan Univ., South Korea)
Ishii Yohei (Hitachi High Technologies USA)

ALE Steering Committee:

Craig Huffman (Micron, USA)
Eric Joseph (IBM, USA)
Keren Kanarik (Lam Research, USA)
Steven George (Univ. of Colorado at Boulder, USA)

Platinum Sponsors

www.electronics-airliquide.com/our-brands

www.appliedmaterials.com

www.arradiance.com

www.asm.com

www.emdgroup.com/en/performance-materials.html

www.ereztech.com

www.eugenustech.com

www.lesker.com/newweb/ped/atomic-layer-deposition-systems.cfm

www.lamresearch.com

www.leadmicro.com

plasma.oxinst.com

www.picosun.com

www.tel.com

www.versummaterials.com

Gold Sponsors

www.adeka.co.jp/en/index.html

www.hansolchemical.com/main.do

www.pegasuschemicals.com

www.rasirc.com

www.tmeic.co.jp

www.upchem.co.kr

www.wimco.co.kr

Silver Sponsors

www.entegris.com

www.nsi-mfg.com

Bronze Sponsors

www.nanomaster.com/index.html

www.pall.com

www.schrodinger.com

www.sentech.com

Exhibitors

Exhibit Hours

The exhibit will take place in the Hyatt Regency Bellevue Evergreen Ballroom and Foyer during coffee and lunch breaks as well as poster sessions. This year it will also be open during the Welcome Reception.

Sunday, July 21, 2019:	6:00 p.m.-8:00 p.m.	Evergreen Ballroom and Foyer
Monday, July 22, 2019:	10:00 a.m.-7:30 p.m.	Evergreen Ballroom and Foyer
Tuesday, July 23, 2019:	10:00 a.m.-7:30 p.m.	Evergreen Ballroom and Foyer
Wednesday, July 24, 2019:	10:00 a.m.-1:30 p.m.	Evergreen Ballroom and Foyer

Please visit the Mobile App for the Exhibit Floor Plan.

Company Name	Booth #	Company Name	Booth #
Air Liquide	300/302	Kratos Analytical	612
Alicat Scientific	102	Kurt J. Lesker Company	100
Amuneal Manufacturing Corp.	208	Lotus Applied Technology	614
Annealsys	604	MKS Instruments	610
Anric Technologies	618	MSP Corporation	402
Beneq Oy	401/403	Nano-Master	400
Bruker Optics	404	NSI	201/203
ChemTrace	109	Oxford Instruments Plasma Technology	105
CN-1	410	Pall Corporation	206
Dockweiler Chemical GmbH	115	Park Systems	408
EMD Performance Materials	106	Pegasus Chemicals Ltd.	107
Ereztech	200/202	Picosun Group	511/513
Eurofins EAG Materials Science	212	PillarHall	500
Film Sense	204	RASIRC	101
Gelest, Inc.	315	Schrödinger	104
Gencoa, Ltd.	406	SEMILAB USA, INC.	210
Hansol Chemical	313	Sempa Systems GmbH	113
HORIBA	103	SENTECH Instruments GmbH	311
iCAM Engineering Ltd.	307	Strem Chemicals, Inc.	502
Integrated Surface Technologies-IST	214	SVCS Process Innovation	503
ION-TOF	602	Swagelok	414
ISAC Research, Inc.	505	TMEIC	620
J.A. Woollam	305	Tri Chemical Laboratories Inc.	412
KEMSTREAM	606	UC Components Inc.	309
KITZ-SCT Corporation	111	Veeco	301/303

Literature Display Tables

Evergreen Foyer

Hiden Analytical
Okyaytech

Sponsor Product Guide

ALD Precursors

Adeka Corporation
www.adeka.co.jp/en/

Air Liquide Advanced Materials
www.electronics-airliquide.com/our-brands

EMD Performance Materials
www.emdgroup.com

ErezTech
www.ereztech.com

Hansol Chemical
www.hansolchemical.com

Pegasus Chemicals Ltd.
www.pegasuschemicals.com/

RASIRC
www.rasirc.com

UP Chemical
www.upchem.co.kr

Versum Materials
www.versummaterials.com

Wonik Materials
www.wimco.co.kr

ALD Systems

Applied Materials
www.appliedmaterials.com

Arradiance
www.arradiance.com

ASM
www.asm.com

Eugenus, Inc.
www.eugenustech.com

Jiangsu Leadmicro Nano-Equipment Tech. Ltd.
www.leadmicro.com

Kurt J. Lesker Company
www.lesker.com

Lam Research Corp.
www.lamresearch.com

Oxford Instruments Plasma Technology
www.oxinst.com/plasma

Picosun
www.picosun.com

Tokyo Electron Ltd.
www.tel.com

ALD Components and Subsystems

TMEIC
www.tmeic.com/

ALE

Air Liquide Advanced Materials
www.electronics-airliquide.com/our-brands

Applied Materials
www.appliedmaterials.com

EMD Performance Materials
www.emdgroup.com

Lam Research Corp.
www.lamresearch.com

Oxford Instruments Plasma Technology
www.oxinst.com/plasma

Pegasus Chemicals Ltd.
www.pegasuschemicals.com/

Tokyo Electron Ltd.
www.tel.com

Other Products & Services

EMD Performance Materials
www.emdgroup.com

Pegasus Chemicals Ltd.
www.pegasuschemicals.com/

Picosun
www.picosun.com

Tutorial Schedule

Sunday, July 21, 2019, 1:00 p.m.-6:00 p.m.

1:00-1:05 p.m.	Tutorial Welcome
1:05-1:50 p.m.	**Area-selective ALD for Semiconductor Manufacturing** Stacey Bent (Stanford Univ., USA)
1:50-2:35 p.m.	**ALD for Battery Applications** Andy Sun (Western Univ., Canada)
2:35-3:20 p.m.	**ALD for Catalysis** Rong Chen (Huazhong Univ. of Science and Technology, China)
3:20-3:40 p.m.	Break
3:40-4:25 p.m.	**ALD for Photovoltaics** Bart Macco (Eindhoven Univ. of Technology, Netherlands)
4:25-5:10 p.m.	**Plasma Based ALE** Thorsten Lill, (Lam Research, USA)
5:10-5:55 p.m.	**Thermal Based ALE** Steve George (Univ. of Colorado at Boulder, USA)

Plenary Lecture Schedule

ALD 2019 Innovation Awardee Lecture

"Atomic Scale Processing: From Understanding to Innovation"
Erwin Kessels (Eindhoven University of Technology, The Netherlands)
Monday, July 22, 2019, 8:45 a.m., Grand Ballroom H-K

The ALD 2019 Innovator Award is being presented "for pioneering work on unraveling atomistic-level mechanisms during plasma-assisted ALD and leadership in ALD."

Biography: Erwin Kessels is a full professor at the Eindhoven University of Technology TU/e where he is also the scientific director of the NanoLab@TU/e clean room facilities. Erwin received his MSc and PhD degree (with highest honors) in Applied Physics from the TU/e in 1996 and 2000, respectively. His research interests cover the field of synthesis of ultrathin films and nanostructures using methods such as (plasma-enhanced) atomic layer deposition (ALD) and atomic layer etching (ALE). Within the field of ALD, he has contributed most prominently by his work on plasma-assisted ALD, his research related to ALD for photovoltaics, and ALD for nanopatterning (including area-selective ALD). Currently Erwin is focusing his research on atomic scale processing, a field which is believed to grow in importance quickly in the next decade for a wide variety of application domains. He was chair of the International Conference on Atomic Layer Deposition in 2008 (Bruges, Belgium) and he frequently (co-)organizes ALD-related workshops. He will serve as chair ALE workshop in 2020. Erwin is active within the American Vacuum Society and has been President of the Netherlands Vacuum Society. He is an associate editor of the Journal of Vacuum Science and Technology. He is also the founder of the blog AtomicLimits.com and of the ALD Academy.

ALD 2019 Plenary Lecture

"Elucidating the Mechanisms for Atomic Layer Growth through In Situ Studies"
Jeff Elam (Argonne National Lab, USA)
Monday, July 22, 2019, 9:30 a.m., Grand Ballroom H-K

ALE 2019 Plenary Lecture

"Mapping the Future Evolution of Atomic Scale Processing to Enable the World of Artificial Intelligence"
Eric Joseph (IBM, USA)
Monday, July 22, 2019, 11:00 a.m., Grand Ballroom H-K

Technical Program Key

Conference Topics

AA ALD Applications
AF ALD Fundamentals
ALE Atomic Layer Etching
AM ALD for Manufacturing
AS Area Selective ALD
EM Emerging Materials
NS Nanostructure Synthesis and Fabrication
PS Plenary Session

Key to Session/Paper Numbers

Sessions sponsored by multiple topics are labeled with all acronyms (e.g. **AC+EM+SS**),
then a number to indicate simultaneous sessions sponsored by the same topic(s) (e.g. SS**1**, SS**2**),
then a dash followed by the first two characters of the day of the week:
Monday, **Tu**esday, **We**dnesday, **Th**ursday, **Fr**iday,
then a single letter for **M**orning, **A**fternoon, **E**vening, **P**oster,
and finally a number indicating the starting time slot for the paper.
Example: SS1-MoM9 (Surface Science, Monday morning, 11:00 am).

Technical Program Overview

Room /Time	Evergreen Ballroom & Foyer	Grand Ballroom A-C	Grand Ballroom A-G	Grand Ballroom E-G	Grand Ballroom H-K	Regency Ballroom A-C
SuP	ALE Poster Session 6:00 pm-8:00 pm Welcome Reception & Exibits 6:00 pm-8:00 pm					
MoM	Exhibits 10:00 am-7:30 pm Morning Break 10:15 am-10:45 am		ALD 2019 Opening Remarks & ALD 2019 Innovation Award 8:30 am PS1-MoM: ALD Plenary Session ALE 2019 Opening Remarks 10:15 am PS2-MoM: ALE Plenary Session			
MoA	Lunch 12:00 pm-1:30 pm Afternoon Break 3:30 pm-4:00 pm	AA1-MoA: ALD for Biological & Space Applications AA2-MoA: ALD for Solar Cells, Fuel Cells, & H_2 Storage		AF2-MoA: ALD Precursors I AF3-MoA: Growth & Characterization I	AF1-MoA: ALD Growth Mechanisms I AF4-MoA: Growth Mechanisms II	ALE1-MoA: Energy-enhanced ALE ALE2-MoA: ALE of Compound Semiconductors
MoP	ALD/ALE Poster Session 5:45 pm-7:30 pm					
TuM	Exhibits 10:00 am-7:30 pm Morning Break 10:00 am-10:30 am	AF1-TuM: In-Situ Characterization of ALD Processes AF3-TuM: Growth & Characterization II		AA1-TuM: ALD for Catalysts, Electrocatalysts, & Photocatalysts AA2-TuM: ALD for Batteries I	AF2-TuM: ALD Precursors II AS1-TuM: Area-Selective ALD Techniques	ALE1-TuM: ALE: Gas-phase and/or Thermal ALE ALE2-TuM: Alternative Methods to ALE
TuA	Lunch 12:00 pm-1:30 pm Afternoon Break 3:30 pm-4:00 pm	AA3-TuA: ALD for Memory Applications I AF-TuA: Plasma ALD: Growth & Characterization		AA1-TuA: Emerging Applications I AA2-TuA: ALD for Batteries II	AS1-TuA: Area-Selective ALD by Area-Deactivation AS2-TuA1: Area-Selective ALD: Combinations with Etching AS2-TuA2: Late Breaking Abstracts	ALE1-TuA: Modeling & Instrumentation I ALE2-TuA: Modeling & Instrumentation II
TuP	ALD/ALE Poster Session 5:30 pm-7:30 pm					
WeM	Exhibits 10:00 am-1:30 pm Morning Break 10:00 am-10:30 am Lunch 12:00 pm-1:30 pm	EM1-WeM: Molecular Layer Deposition EM2-WeM: Organic-Inorganic Hybrid Materials		AM1-WeM: Spatial ALD, Fast ALD, and Large-Area ALD EM3-WeM: Epitaxial Growth and III-V Materials	AA1-WeM: ALD for Memory Applications II AA2-WeM: ALD for ULSI Applications I	ALE1-WeM: Integration & Application of ALE ALE2-WeM: Materials Selective ALE
WeA		AA1-WeA: Emerging Applications II		NS-WeA: 2D Nanomaterials by ALD (including Transition Metal Dichalcogenides)	AA2-WeA: ALD for ULSI Applications II ALD-ALE 2019 Closing Remarks & Student Awards 3:30 pm	EM1-WeA: Ternary & Quaternary Oxide Materials

Atomic Layer Etching
Evergreen Ballroom & Foyer - Session ALE-SuP
Atomic Layer Etching Poster Session
6:00pm

Note: ALE Posters Will Remain Posted All Week

ALE-SuP1 Mechanistic Thermal Desorption Studies of Thermal Dry Etching Reactions for Cobalt and Iron Thin Films, ***Mahsa Konh**, A. Teplyakov,* University of Delaware

ALE-SuP2 Mechanistic Study of the Thermal Atomic Layer Etch of Tungsten Metal Using O_2 and WCl_6, *S. Kondati Natarajan, M. Nolan,* Tyndall National Institute, Ireland; ***Patrick Theofanis**, C. Mokhtarzadeh, S.B. Clendenning,* Intel Corp.

~~**ALE-SuP3** Using Etching of the Atomic Layer to Remove Damaged Layers Obtained by Plasma-Chemical Etching with Subsequent Growth of GaAs Quantum Dots by the Method of Droplet Epitaxy, ***Victor Klimin**, A. Rezvan, O. Ageev,* Southern Federal University, Russia~~

ALE-SuP4 Atomic Layer Etching of Silicon Using a Conventional ICP Etch Chamber for Failure Analysis Applications, ***John Mudrick**, R. Shul, K.D. Greth, R. Goeke, D. Adams,* Sandia National Laboratories

~~**ALE-SuP5** Study of the Chemical Fabrication Process of NSOM Probes and the Modification of its Surface for Sensing Applications, ***Muhammad Nazmul Hussain**, J. Woehl,* University of Wisconsin-Milwaukee~~

ALE-SuP6 A Mechanistic Study of the HF Pulse in the Thermal Atomic Layer Etch of HfO_2 and ZrO_2, ***Rita Mullins**, S. Kondati Natarajan, M. Nolan,* Tyndall National Institute, Ireland

ALE-SuP7 Atomic Precision Processing of Aluminum Mirrors for Enhanced Ultra-violet Optical Properties, ***Scott Walton**, A. Kozen,* U.S. Naval Research Laboratory; *J. del Hoyo, M. Quijada,* NASA Goddard Space Flight Center; *D. Boris,* U.S. Naval Research Laboratory

~~**ALE-SuP8** Surface Reaction Analysis for Atomic-Layer Etching and Deposition by Means of Beam Experiments, ***Kazuhiro Karahashi**, T. Ito, S. Hamaguchi,* Osaka University, Japan~~

ALE-SuP9 Atomic Layer Etching of SiO_2 and Si_3N_4 with Fluorocarbon, Hydrofluorocarbon and Fluoroether Compounds, *H. Chae, **Yongjae Kim**, T. Cha, Y. Cho,* Sungkyunkwan University (SKKU), Republic of Korea

ALE-SuP10 Cyclic Etching of Copper Thin Films using Two Sequential Steps, ***Eun Tack Lim**, J.S. Choi, J.S. Ryu, M.H. Cha, C.W. Chung,* Inha University, Republic of Korea

ALE-SuP11 Analysis of Mechanisms Involved in Cryogenic ALE, ***Thomas Tillocher**, G. Antoun, P. Lefaucheux, R. Dussart,* GREMI Université d'Orléans/CNRS, France; *K. Yamazaki, K. Yatsuda,* Tokyo Electron Limited, Japan; *J. Faguet, K. Maekawa,* TEL Technology Center, America, LLC

ALE-SuP12 Study on Dry Etching Characteristics of Germanium Oxide by Atomic Layer Deposition, ***Donghyuk Shin**, J. Jeong, H. Song, H. Park, D.-H. Ko,* Yonsei University, Republic of Korea

ALE-SuP13 Laser Isotropic Atomistic Removal of Germanium, *D. Paeng, **He Zhang**, Y.S. Kim,* Lam Research Corp.

ALE-SuP14 Anisotropic Atomic Layer Etching of Tungsten using Reactive Ion Beam, ***Doo San Kim**, J.E. Kim, W.O. Lee, Y.J. Gill, B.H. Jeong, G.Y. Yeom,* Sungkyunkwan University, Republic of Korea

Monday Morning, July 22, 2019

	Grand Ballroom A-G	
8:30am	**ALD 2019 Opening Remarks and ALD 2019 Innovation Award Presentation**	**Plenary Session** **Session PS1-MoM** **ALD Plenary Session** **Moderators:** Sumit Agarwal, Colorado School of Mines Dennis Hausmann, Lam Research Corp.
8:45am	**INVITED: PS1-MoM2** Atomic Scale Processing: From Understanding to Innovation, ***Erwin Kessels,*** Eindhoven University of Technology, Netherlands	
9:00am	Invited talk continues.	
9:15am	Invited talk continues.	
9:30am	**INVITED: PS1-MoM5** Elucidating the Mechanisms for Atomic Layer Growth through In Situ Studies, ***Jeffrey W. Elam,*** Argonne National Laboratory	
9:45am	Invited talk continues.	
10:00am	Invited talk continues.	
10:15am	**Break & Exhibits**	
10:30am	**Break & Exhibits**	
10:45am	**ALE 2019 Opening Remarks**	
11:00am	**INVITED: PS2-MoM11** Mapping the Future Evolution of Atomic Scale Processing to enable the World of Artificial Intelligence, ***Eric A. Joseph,*** IBM T.J. Watson Research Center	**Plenary Session** **Session PS2-MoM** **ALE Plenary Session** **Moderators:** Craig Huffman, Micron Technology Gottlieb S. Oehrlein, University of Maryland
11:15am	Invited talk continues.	
11:30am	Invited talk continues.	
11:45am	**ALD/ALE 2019 Sponsor Preview**	
12:00pm	**Lunch & Exhibits**	

Monday Afternoon, July 22, 2019

	Grand Ballroom A-C	
1:30pm	**AA1-MoA1** Atomic Layer Deposition on Pharmaceutical Particles for Inhaled Drug Delivery, ***Damiano La Zara,*** Delft University of Technology, Netherlands*; D. Zhang, M.J. Quayle, G. Petersson, S. Folestad,* AstraZeneca, Sweden*; J.R. van Ommen,* Delft University of Technology, Netherlands	**ALD Applications** **Session AA1-MoA** **ALD for Biological and Space Applications** **Moderators:** Elton Graugnard, Boise State University Mato Knez, CIC nanoGUNE
1:45pm	**AA1-MoA2** The Use of Atomic Layer Deposition to Increase the Availability of Medical Radio-Isotopes, ***Ruud van Ommen****, J. Moret, B. Wolterbeek, E. Pidko, A. Denkova,* Delft University of Technology, Netherlands	
2:00pm	**AA1-MoA3** Atomic Layer Deposition for Biosensing Applications*, O. Graniel,* ***Matthieu Weber****, S. Balme, P. Miele, M. Bechelany,* Institut Européen des Membranes, France	
2:15pm	**AA1-MoA4** Multi-layer Stacked ALD Coating for Hermetic Encapsulation of Implantable Biomedical Microdevices*, J. Jeong,* Pusan National University, Republic of Korea*; S. Sigurdsson, F. Laiwalla,* Brown University*; R. Ritasalo, M. Pudas, T. McKee, T. Pilvi,* ***Juhana Kostama****,* Picosun Oy, Finland*; A. Nurmikko,* Brown University*; Tom Blomberg,* Picosun Oy/ASM, Finland	
2:30pm	**AA1-MoA5** Modification of Spaceflight Radiator Coating Pigments by Atomic Layer Deposition for Thermal Applications*,* ***Vivek Dwivedi****,* NASA Goddard Space Flight Center*; R. Adomaitis, H. Salami, A. Uy,* University of Maryland*; M. Hasegawa,* NASA Goddard Space Flight Center	
2:45pm	**AA1-MoA6** Novel Atomic Layer Deposition Process/Hardware for Superconducting Films for NASA Applications*,* ***Frank Greer****, D. Cunnane,* Jet Propulsion Laboratory	
3:00pm	**AA1-MoA7** Fluoride-based ALD Materials System for Optical Space Applications*,* ***John Hennessy****,* Jet Propulsion Laboratory, California Institute of Technology	
3:15pm	**AA1-MoA8** Atomic Layer Deposition of Aluminum Fluoride for use in Astronomical Optical Devices*,* ***Alan Uy****, H. Salami, A. Vadapalli, C. Grob, R. Adomaitis,* University of Maryland*; V. Dwivedi,* NASA Goddard Space Flight Center	
3:30pm	**Break & Exhibits**	
3:45pm	**Break & Exhibits**	
4:00pm	**AA2-MoA11** Nucleation Layer for Atomic Layer Deposition Enabling High Efficiency and Flexible Monolithic All-Perovskite Tandem Solar Cells*,* ***Axel F. Palmstrom****, G. Eperon, T. Leijtens,* National Renewable Energy Laboratory*; R. Prasanna,* Stanford University*; S. Nanayakkara, S. Christensen, K. Zhu,* National Renewable Energy Laboratory*; M. McGehee,* University of Colorado Boulder*; D. Moore, J.J. Berry,* National Renewable Energy Laboratory	**ALD Applications** **Session AA2-MoA** **ALD for Solar Cells, Fuel Cells, and H_2 Storage** **Moderators:** Christophe Detavernier, Ghent University Nicholas Strandwitz, Lehigh University
4:15pm	**AA2-MoA12** Perovskite Solar Cells Fabricated using Atomic Layer Deposited Doped ZnO as a Transparent Electrode*,* ***Louise Ryan****, M. McCarthy, S. Monaghan, M. Modreanu, S. O'Brien, M. Pemble, I. Povey,* Tyndall National Institute, Ireland	
4:30pm	**AA2-MoA13** Metal Oxide Barrier and Buffer Layers by Atomic Layer Deposition and Pulsed-Chemical Vapor Deposition for Semi-Transparent Perovskite Solar Cells*,* ***Helen Hejin Park****, T. Eom, R.E. Agbenyeke, S.M. Yeo, G.J. Kim, S.S. Shin, T.-Y. Yang, N.J. Jeon, Y.K. Lee, C.G. Kim, T.-M. Chung, J. Seo,* Korea Research Institute of Chemical Technology (KRICT), Republic of Korea	
4:45pm	**AA2-MoA14** Particle Atomic Layer Deposition of Tungsten Nitride Environmental Barrier Coatings from Bis(t-butylimido)bis(dimethylamino) tungsten(VI) and Ammonia*,* ***Sarah Bull****, A. Weimer,* University of Colorado - Boulder	
5:00pm	**AA2-MoA15** Atomic Layer Deposition on $Mg(BH_4)_2$: A Route to Improved Automotive H_2storage*,* ***Noemi Leick****,* National Renewable Energy Laboratory*; K. Gross,* H₂ Technology Consulting LLL*; T. Gennett, S. Christensen,* National Renewable Energy Laboratory	
5:15pm	**AA2-MoA16** Plasmonic Mediated Hydrogen Desorption from Metal Hydrides*,* ***Katherine Hurst****, A. Gaulding, M. Martinez, N. Leick, S. Christensen, T. Gennett,* National Renewable Energy Laboratory	
5:30pm	**AA2-MoA17** Surface Modification of Solid Oxide Fuel Cell Cathodes by Atomic Layer Deposition*,* ***Dong Hwan Kim****, H.J. Choi, J. Koo,* Korea University, Republic of Korea*; J.H. Park, J.-W. Son,* Korea Institute of Science and Technology (KIST), Republic of Korea*; J.H. Shim,* Korea University, Republic of Korea	
5:45pm	**Poster Session**	

Monday Afternoon, July 22, 2019

	Grand Ballroom E-G	
1:30pm	**INVITED: AF2-MoA1** The Materials Supplier Challenge: Flawless Execution from Precursor Design to High Volume Manufacturing, ***Madhukar B. Rao***, Versum Materials	**ALD Fundamentals** **Session AF2-MoA** **ALD Precursors I** **Moderators:** Daniel Alvarez, RASIRC Charles H. Winter, Wayne State University
1:45pm	Invited talk continues.	
2:00pm	**AF2-MoA3** Precursor and Co-Reactant Selection: A Figure of Merit, ***Seán Barry***, *M. Griffiths,* Carleton University, Canada	
2:15pm	**AF2-MoA4** Designing Thermal Atomic Layer Deposition Processes for Gold Metal using New Organogold Precursors and Co-reageants, ***Matthew Griffiths***, *G. Bačić, A. Varga, S. Barry,* Carleton University, Canada	
2:30pm	**AF2-MoA5** A New Carbene Based Silver Precursor Applied in APP-ALD Yielding Conductive and Transparent Ag Films: A Promising Precursor Class for Ag Metal ALD, ***Nils Boysen***, Ruhr University Bochum, Germany; *T. Hasselmann, D. Theirich, T. Riedl,* University of Wuppertal, Germany; *A. Devi,* Ruhr University Bochum, Germany	
2:45pm	**AF2-MoA6** Transition Metal β-ketoiminates: A Promising Precursor Class for Atomic Layer Deposition of Binary and Ternary Oxide Thin Films, ***Dennis Zywitzki***, *A. Devi,* Ruhr University Bochum, Germany	
3:00pm	**AF2-MoA7** A New and Promising ALD Process for Molybdenum Oxide Thin Films: From Process Development to Hydrogen Gas Sensing Applications, ***Jan-Lucas Wree***, Ruhr University Bochum, Germany; *M. Mattinen,* University of Helsinki, Finland; *E. Ciftyürek, K.D. Schierbaum,* Heinrich Heine University Düsseldorf, Germany; *M. Ritala, M. Leskelä,* University of Helsinki, Finland; *A. Devi,* Ruhr University Bochum, Germany	
3:15pm	**AF2-MoA8** Atomic Layer Deposition of Gallium Oxide Thin Films using Pentamethylcyclopentadienyl Gallium and Combinations of H_2O and O_2 Plasma, ***Fumikazu Mizutani***, *S. Higashi,* Kojundo Chemical Laboratory Co., Ltd., Japan; *M. Inoue, T. Nabatame,* National Institute for Materials Science, Japan	
3:30pm	**Break & Exhibits**	
3:45pm	**Break & Exhibits**	
4:00pm	**AF3-MoA11** Understanding Elemental Steps of ALD on Oxidation Catalysts, ***Kristian Knemeyer***, *M. Piernavieja Hermida, R. Naumann d'Alnoncourt,* Technische Universität Berlin, Germany; *A. Trunschke, R. Schlögl,* Fritz Haber Institute of the Max Planck Society, Germany; *M. Driess,* Technische Universität Berlin, Germany; *F. Rosowski,* BASF SE, Germany	**ALD Fundamentals** **Session AF3-MoA** **Growth and Characterization I** **Moderators:** Somilkumar Rathi, Eugenus, Inc. Sumit Agarwal, Colorado School of Mines
4:15pm	**AF3-MoA12** Advanced Lateral High Aspect Ratio Test Structures for Conformality Characterization by Optical Microscopy, *Oili Ylivaara, P. Hyttinen,* VTT Technical Research Centre of Finland Ltd, Finland; *K. Arts,* Eindhoven University of Technology, Netherlands; *F. Gao,* VTT Technical Research Centre of Finland Ltd, Finland; *W.M.M. Kessels,* Eindhoven University of Technology, Netherlands; *R. Puurunen,* Aalto University, Finland; ***M. Utriainen***, VTT Technical Research Centre of Finland Ltd, Finland	
4:30pm	**AF3-MoA13** Dopant Concentration Analysis of ALD Thin Films in 3D Structures by ToF-SIMS, *A.M. Kia,* ***Wenke Weinreich***, Fraunhofer-Institut fur Photonische Mikrosysteme (IPMS), Germany; *M. Utriainen,* VTT Technical Research Centre of Finland Ltd, Finland; *R. Puurunen,* Aalto University, Finland; *N. Haufe,* Fraunhofer-Institut fur Photonische Mikrosysteme (IPMS), Germany	
4:45pm	**AF3-MoA14** Metallic Ruthenium Coating on SiO_2 Powder by Atomic Layer Deposition using H_2O Reactant., ***Chi Thang Nguyen***, Incheon National University, Republic of Korea	
5:00pm	**AF3-MoA15** Low Energy Ion Scattering Study of Pt@Al_2O_3 Nanoparticle Coarsening, ***Philipp Brüner***, IONTOF GmbH, Germany; *E. Solano,* ALBA Synchrotron Light Source, Spain; *C. Detavernier, J. Dendooven,* Ghent University, Belgium	
5:15pm	**AF3-MoA16** Physical and Electrical Characterization of ALD Chalcogenide Materials for 3D Memory Applications, ***Vijay K. Narasimhan***, *V. Adinolfi, L. Cheng, M.E. McBriarty,* Intermolecular, Inc.; *M. Utriainen, F. Gao,* VTT Technical Research Centre of Finland Ltd, Finland; *R. Puurunen,* Aalto University, Finland; *K. Littau,* Intermolecular, Inc.	
5:30pm	**AF3-MoA17** The Tailoring of the Single Metal Atom-Oxide Interface, ***Bin Zhang***, *Y. Qin,* Institute of Coal Chemistry, Chinese Academy of Sciences, China	
5:45pm	**Poster Session**	

Monday Afternoon, July 22, 2019

	Grand Ballroom H-K	
1:30pm	**AF1-MoA1** Hybrid Computational Fluid Dynamics / Machine Learning Approaches to Reactor Scale Simulations and Optimization of ALD, ALEt, and LPCVD Processes, ***Angel Yanguas-Gil**, S. Letourneau, A. Lancaster, J.W. Elam,* Argonne National Laboratory	**ALD Fundamentals** **Session AF1-MoA** **ALD Growth Mechanisms I** **Moderators:** Simon Elliot, Schrödinger, Inc. Angel Yanguas-Gil, Argonne National Laboratory
1:45pm	**AF1-MoA2** Scalable Kinetic Monte-Carlo Model for Parasitic Reactions in Silicon Nitride Growth using 3DMAS Precursor, ***Gem Shoute**, T. Muneshwar,* Synthergy Inc., Canada*; D. Barlage, K. Cadien,* University of Alberta, Canada	
2:00pm	**INVITED: AF1-MoA3** Diffusion and Aggregation in Island-Growth and Area-Selective Deposition, ***Fabio Grillo**,* ETH Zurich, Switzerland	
2:15pm	Invited talk continues.	
2:30pm	**AF1-MoA5** Surface Kinetics in ALD and ALE: Computing the Cooperative Effect by Automated Enumeration of Reaction Pathways with Spectator Adsorbates, ***Thomas Mustard**,* Schrödinger, Inc.*; S. Elliot,* Schrödinger, Inc.*; T. Hughes, A. Bochevarov, L. Jacobson, S. Kwak,* Schrödinger, Inc.*; T. Morisato,* Schrödinger K.K., Japan*; J. Gavartin,* Schrödinger, Inc., UK*; S. Pandiyan,* Schrödinger, Inc., India*; M. Halls,* Schrödinger, Inc.	
2:45pm	**AF1-MoA6** An Immiscible Fluids Approach for Correctly Predicting Agglomerate Dynamics during Particle Atomic Layer Deposition (Particle ALD), ***Julia Hartig**, A. Weimer,* University of Colorado - Boulder	
3:00pm	**INVITED: AF1-MoA7** The Time-Resolved Interface between ALD and CVD, ***Henrik Pedersen**,* Linköping University, Sweden	
3:15pm	Invited talk continues.	
3:30pm	**Break & Exhibits**	
3:45pm	**Break & Exhibits**	
4:00pm		**ALD Fundamentals** **Session AF4-MoA** **Growth Mechanisms II** **Moderators:** Viljami Pore, ASM Mikko Ritala, University of Helsinki
4:15pm	**INVITED: AF4-MoA12** Monolithic Integration of Single Crystal Perovskites on Semiconductors with ALD, ***John Ekerdt**,* University of Texas at Austin	
4:30pm	Invited talk continues.	
4:45pm	**AF4-MoA14** Surface Enhanced Raman Spectroscopy Studies of Aluminum ALD Precursors for Al_2O_3 Growth, ***Michael Foody**,* Illinois Institute of Technology	
5:00pm	**AF4-MoA15** Atomic Layer Deposition of Aluminum, Hafnium and Zirconium Oxyfluoride Films with Tunable Stoichiometry, ***Neha Mahuli**, J. Wallas, S.M. George,* University of Colorado - Boulder	
5:15pm	**AF4-MoA16** Fundamental Study on the SiO_2 Growth Mechanism of Electronegativity Difference of Metal-O in the High-*k* Underlayers by PE-ALD Method, ***Erika Maeda**,* Shibaura Institute of Technology, Japan*; T. Nabatame,* National Institute for Materials Science, Japan*; M. Hirose,* Shibaura Institute of Technology, Japan*; M. Inoue, A. Ohi, N. Ikeda,* National Institute for Materials Science, Japan*; M. Takahashi, K. Ito,* Osaka University, Japan*; H. Kiyono,* Shibaura Institute of Technology, Japan	
5:30pm	**AF4-MoA17** Low Temperature Aluminium Nitride Deposition: Comparing Hydrazine and Ammonia, ***Aswin L.N. Kondusamy**, S.M. Hwang, A.T. Lucero, Z. Qin, X. Meng,* The University of Texas at Dallas*; D. Alvarez, J. Spiegelman,* RASIRC*; J. Kim,* The University of Texas at Dallas	
5:45 pm	**Poster Session**	

Monday Afternoon, July 22, 2019

	Regency Ballroom A-C	
1:30pm	**INVITED: ALE1-MoA1** Atomic Layer Etching – Advancing Its Application with a New Regime, ***Samantha Tan**, W. Yang, K.J. Kanarik, Y. Pan, R. Gottscho,* Lam Research Corp.	**Atomic Layer Etching** **Session ALE1-MoA** **Energy-enhanced ALE** **Moderators:** Keren J. Kanarik, Lam Research Corp. Harm Knoops, Oxford Instruments Plasma Technology
1:45pm	Invited talk continues.	
2:00pm	**ALE1-MoA3** Control of the Interface Layer in ALE Process by Alternating O_2 Plasma with Fluorocarbon Deposition for High Selectivity Etching, ***Takayoshi Tsutsumi**, A. Kobayashi,* Nagoya University, Japan*; N. Kobayashi,* ASM Japan K.K., Japan*; M. Hori,* Nagoya University, Japan	
2:15pm	**ALE1-MoA4** Self-limiting Atomic Layer Etching of SiO_2 using Low Temperature Cyclic Ar/CHF_3 Plasma, ***Stefano Dallorto**,* Lawrence Berkeley National Laboratory*; A. Goodyear, M. Cooke,* Oxford Instruments Plasma Technology, UK*; S. Dhuey,* Lawrence Berkeley National Laboratory*; J. Szornel,* Lawrence Livermore National Laboratory*; I. Rangelow,* Ilmenau University of Technology, Germany*; S. Cabrini,* Lawrence Berkeley National Laboratory	
2:30pm	**ALE1-MoA5** Evolution of Photoresist Layer Structure and Surface Morphology in a Fluorocarbon-Plasma-Based Atomic Layer Etching Process, ***Adam Pranda**, K-Y. Lin, S. Gutierrez Razo, J. Fourkas, G.S. Oehrlein,* University of Maryland	
2:45pm	**ALE1-MoA6** Optimized Radical Composition of C4F8/Ar Plasma to Improve Atomic Layer Etching of SiO_2, ***Young-Seok Lee**, J.-J. Lee, S.-W. Yoo, S.-H. Lee, I.-H. Seong, C.-H. Cho, S.-J. Kim, J.-P. Son, S-J. You,* Chungnam National University, Korea	
3:00pm	**ALE1-MoA7** Atomic Layer Etching of Silicon Nitride with Ultrahigh Etching Selectivity over Silicon and Oxide Materials by Utilizing Novel Etch Gas Molecule, ***Xiangyu Guo**,* American Air Liquide*; N. Stafford,* Air Liquide*; V. Pallem,* American Air Liquide	
3:15pm	**ALE1-MoA8** Atomic Layer Etching at Low Substrate Temperature, ***Gaëlle Antoun**, T. Tillocher, P. Lefaucheux, R. Dussart,* GREMI Université d'Orléans/CNRS, France*; K. Yamazaki, K. Yatsuda,* Tokyo Electron Limited, Japan*; J. Faguet, K. Maekawa,* TEL Technology Center, America, LLC	
3:30pm	**Break & Exhibits**	
3:45pm	**Break & Exhibits**	
4:00pm	**INVITED: ALE2-MoA11** Developments of Atomic Layer Etch Processes and their Applications in Fabricating III-V Compound Semiconductor Devices, ***Xu Li**, Y.-C. Fu, S.-J. Cho, D. Hemakumara, K. Floros, D. Moran, I. Thayne,* University of Glasgow, UK	**Atomic Layer Etching** **Session ALE2-MoA** **ALE of Compound Semiconductors** **Moderators:** David Boris, U.S. Naval Research Laboratory Ishii Yohei, Hitachi High Technologies
4:15pm	Invited talk continues.	
4:30pm	**ALE2-MoA13** GaN and Ga_2O_3 Thermal Atomic Layer Etching Using Sequential Surface Reactions, *N. Johnson, Y. Lee,* ***Steven M. George**,* University of Colorado - Boulder	
4:45pm	**ALE2-MoA14** Selective GaN Etching Process using Self-limiting Cyclic Approach for Power Device Applications, ***Frédéric Le Roux**, N. Posseme, P. Burtin, S. Barnola, A. Torres,* Univ. Grenoble Alpes, CEA, LETI, France	
5:00pm	**ALE2-MoA15** ALE of GaN (0001) by Sequential Oxidation and H_2/N_2 Plasma, ***Kevin Hatch**, D. Messina, H. Fu, K. Fu, X. Wang, M. Hao, Y. Zhao, R. Nemanich,* Arizona State University	
5:15pm	**ALE2-MoA16** Comparative Study of Two Atomic Layer Etching Processes for GaN, *Cédric Mannequin*, *C. You,* University of Tsukuba, Japan*; G. Jacopin, T. Chevolleau, C. Durand,* University Grenoble-Alpes, France*;* ***C. Vallée**,* LTM-UGA, France*; C. Dussarat, T. Teramoto,* Air Liquide Laboratories, Japan*; H. Mariette,* University Grenoble-Alpes, France*; K. Akimoto, M. Sasaki,* University of Tsukuba, Japan*; E. Gheeraert,* University Grenoble-Alpes, France	
5:30pm	**ALE2-MoA17** Chlorinated Surface Layer of GaN in Quasi Atomic Layer Etching of Cyclic Processes of Chlorine Adsorption and Ion Irradiation, ***Masaki Hasegawa**, T. Tsutsumi,* Nagoya University, Japan*; A. Tanide,* SCREEN Holdings Co., Ltd.*; H. Kondo, M. Sekine, K. Ishikawa, M. Hori,* Nagoya University, Japan	
5:45pm	**Poster Session**	

ALD Fundamentals
Evergreen Ballroom & Foyer - Session AF1-MoP
Precursor Synthesis and Process Development
Poster Session
5:45pm

AF1-MoP1 Atomic Layer Deposition of Molybdenum Films from Molybdenum Pentachloride Precursor, ***Changwon Lee**, S.-W. Lee, M.-S. Kim,* Versum Materials, Republic of Korea*; S. Ivanov,* Versum Materials, Inc.

AF1-MoP2 Atomic Layer Deposition of Silver Metal Films: Synthesis and Characterization of Thermally Stable Silver Metal Precursors, ***Harshani J. Arachchilage**, C.H. Winter,* Wayne State University

AF1-MoP3 Atomic Layer Deposition of Lanthanum Oxide Using Heteroleptic La Precursors, ***Daehyeon Kim**, J. Lee, W. Noh,* Air Liquide Laboratories Korea, South Korea

AF1-MoP4 Synthesis and Thermal Characterization of New Molybdenum Precursors for Atomic Layer Deposition of Molybdenum Metal, ***Michael Land**,* Carleton University, Canada*; K. Robertson,* Saint Mary's University, Canada*; S. Barry,* Carleton University, Canada

AF1-MoP6 A Novel Hf Precursor with Linked Cyclopentadienyl-Amido Ligand for Thermal Atomic Layer Deposition of HfO_2 Thin Film, ***Jeong do Oh**, M.-H. Nim, J.-S. An, J.-H. Seok, J.-W. Park,* Hansol Chemical, Republic of Korea

AF1-MoP7 Atomic Layer Deposition of WS_2 using a New Metal-Organic Precursor and H_2S Molecules, ***Deok Hyun Kim**, D.K. Nandi, S.-H. Kim,* Yeungnam University, Republic of Korea

AF1-MoP8 Recent Advances in the Development of Metal Organic Precursors for Atomic Layer Deposition, ***Anjana Devi**, L. Mai, D. Zywitzki, S.M.J. Beer, N. Boysen, D. Zanders, J.-L. Wree, M. Wilken, H. Parala,* Ruhr University Bochum, Germany

AF1-MoP9 Synthesis of Group VI Oxyhalide Adducts and Mo Metal Film Growth on TiN Surfaces, ***David Ermert**, R. Wright Jr., T. Baum,* Entegris, Inc.

AF1-MoP10 Gallium Precursor Development for ALD Film Applications, ***Atsushi Sakurai**, M. Hatase, N. Okada, A. Yamashita,* ADEKA Corporation, Japan

AF1-MoP11 Design and Optimization of Heteroleptic Zirconium Precursors by Density Function Theory Calculation, ***Romel Hidayat**,* Sejong University, Republic of Korea*; J.-H. Cho, H.-D. Lim, B.-I. Yang, J.J. Park, W.-M. Chae,* DNF Co. Ltd, Republic of Korea*; H.-L. Kim,* Sejong University, Republic of Korea*; S.I. Lee,* DNF Co. Ltd, Republic of Korea*; W.-J. Lee,* Sejong University, Republic of Korea

AF1-MoP12 Low Temperature Plasma-Enhanced Atomic Layer Deposition of ZnO from a New Non-Pyrophoric Zn Precursor, ***Lukas Mai**, F. Mitschker, P. Awakowicz, A. Devi,* Ruhr University Bochum, Germany

AF1-MoP13 Homoleptic and Heteroleptic Yttrium Precursor: Tuning of Volatility, Reactivity and Stability for ALD Applications, ***Sebastian Markus Josef Beer**, A. Devi,* Ruhr University Bochum, Germany

AF1-MoP14 Gallium ALD Precursor Development based on Mechanistic Study, *M. Foody, Y. Zhao,* ***Adam Hock**,* Illinois Institute of Technology

AF1-MoP15 Fluorine Doping of Aluminium Oxide Through In-situ Precursor Synthesis: Theory, Design and Application., ***Ben Peek**,* University of Liverpool, UK

ALD Fundamentals
Evergreen Ballroom & Foyer - Session AF2-MoP
Precursor Selection and Growth Optimization
Poster Session
5:45pm

AF2-MoP1 Atomic Layer Deposition of Cyclopentadienyl Based Hf Precursor With Various Oxidants, ***Jooho Lee**, D. Kim, W. Noh,* Air Liquide Laboratories Korea, South Korea

AF2-MoP2 Atomic Layer Deposition of Magnesium Oxide Thin Films by using Bis(ethylcyclopentadienyl)Magnesium Precursor and H_2O, O_2 Plasma and O_3 Reactants, ***Moo-Sung Kim**, S.-W. Lee,* Versum Materials Korea, Republic of Korea*; S. Ivanov,* Versum Materials, Inc.

AF2-MoP3 Comparative Study between $CpTi(OMe)_3$ and $CpTi(NMe_2)_3$ for Atomic Layer Deposition of Titanium Oxide, ***Jaemin Kim**, S. Kim, R. Hidayat, Y. Choi, H.-L. Kim, W.-J. Lee,* Sejong University, Republic of Korea

AF2-MoP4 Tin Nitride Atomic Layer Deposition using Hydrazine, ***Ann Greenaway**, A. Tamboli, S. Christensen,* National Renewable Energy Laboratory

~~**AF2-MoP5** Growing Polycrystalline Indium Oxide Film by Atomic Layer Deposition, ***Chien-Wei Chen**,* ITRC, NARL, Republic of China~~

~~**AF2-MoP6** Low Temperature Tin Oxide by Atomic Layer Deposition, ***Yu-Chiao Lin**, B. H. Liu, Y. S. Yu, C. C. Kei, C. L. Lin,* National Applied Research Laboratories, Republic of China~~

AF2-MoP7 Dielectric ALD with Hydrogen Peroxide: Comparitive Study of Growth and Film Characteristics for Anhydrous H_2O_2, H_2O_2/H_2O Mixtures and H_2O, ***Daniel Alvarez**,* RASIRC*; K. Andachi, G. Tsuchibuchi, K. Suzuki,* Taiyo Nippon Sanso Corporation*; J. Spiegelman,* RASIRC

AF2-MoP8 Atomic Layer Deposition of Carbon Doped Silicon Oxide and Effect of Thermal Treatment or Hydrogen Plasma Treatment on The Films, ***Meiliang Wang**, H. Chandra, X. Lei, A. Mallikarjunan, K. Cuthill, M. Xiao, M. Rao,* Versum Materials, Inc.

AF2-MoP9 DFT Study on Atomic Layer Deposition of Al_2O_3 with Various Oxidants, ***Seunggi Seo**, T. Nam,* Yonsei University, Republic of Korea*; H.B.R. Lee,* Incheon National University, Republic of Korea*; B. Shong,* Hongik University, Republic of Korea*; H. Kim,* Yonsei University, Republic of Korea

AF2-MoP10 Effect of Heteroleptic Structure on Atomic Layer Deposited HfO_2 Using $Hf(N(CH_3)_2)_4$ and $CpHf(N(CH_3)_2)_3$ Precursors, ***Sungmin Park**, B.-E. Park, S. Lee, H. Yoon,* Yonsei University, Republic of Korea*; M.Y. Lee, S.-H. Kim,* Yeungnam University, Republic of Korea*; H. Kim,* Yonsei University, Republic of Korea

AF2-MoP11 Effect of Co-Reactant on the Atomic Layer Deposition of Copper Oxide, ***Jason Avila**, N. Nepal, V. Wheeler,* U.S. Naval Research Laboratory

AF2-MoP12 A Systematic Study on Atomic Layer Deposition of ZrO_2 Thin Films, *X. Wang, J. Cai,* ***Xiangbo Meng**,* University of Arkansas

AF2-MoP13 Hydrophobic SiO_x Thin Film Deposition using Low-Temperature Atomic Layer Deposition, ***Taewook Nam**, H. Kim,* Yonsei University, Republic of Korea

AF2-MoP14 Characteristics of High-temperature ALD SiO_2 Thin Films Using a Si Precursor with Excellent Thermal Stability, ***Jae-Seok An**, J.-R. Park, M.-H. Nim,* Hansol Chemical, Republic of Korea*; Y. Kim, J. Gu, S. Kim,* Sejong University, Republic of Korea*; J.-H. Seok, J.-W. Park,* Hansol Chemical, Republic of Korea*; W.-J. Lee,* Sejong University, Republic of Korea

~~**AF2-MoP15** Developing Routes Toward Atomic Layer Deposition of Tungsten using Fluorine-Free W Precursor and Various Reactants with Density Functional Theory, ***Tae Hyun Kim**, D.K. Nandi, M.Y. Lee,* Yeungnam University, Republic of Korea*; R. Hidayat, S. Kim, W. J. Lee,* Sejong University, Republic of Korea*; S. H. Kim,* Yeungnam University, Republic of Korea~~

AF2-MoP16 ALD HfO_2 with Anhydrous H_2O_2 in a 300 mm Cross-flow Reactor – Comparison with H_2O and O_3 Oxidants, ***Steven Consiglio**, R. Clark, C. Wajda, G. Leusink,* TEL Technology Center, America, LLC

AF2-MoP17 Atomic Layer Deposition of Copper (I) Chloride using Liquid 1-Chlorobutane Precursor, ***Richard Krumpolec**, D. Cameron, D. Bača, J. Humlíček, O. Caha,* Masaryk University, Czech Republic

AF2-MoP18 Number Effect of Si Atoms Contained in Precursor for SiN Atomic Layer Deposition, ***Seungbae Park**, H. Ji, H. Yang, S. Yoon,* DUKSAN Techopia company, Republic of Korea*; I.-S. Park,* Hanyang University, Republic of Korea

ALD Fundamentals
Evergreen Ballroom & Foyer - Session AF3-MoP
Growth Mechanisms and In Situ Studies Poster Session
5:45pm

AF3-MoP1 Langasite Crystal Microbalance (LCM) for In-situ Process Monitoring of ALD up to 440 º C, ***Masafumi Kumano**,* Tohoku University, Japan*; K. Inoue,* Piezo Studio, Japan*; K. Hikichi,* Technofine co. Ltd, Japan*; M. Shimizu, S. Tanaka,* Tohoku University, Japan

AF3-MoP2 In-Situ Process Monitoring of Precursor Delivery Using Infra-Red Spectroscopic Method, ***Robert Wright**, T. Baum,* Entegris, Inc.

AF3-MoP3 Quantitative Analysis of High-k ALD Precursors for Trace Elemental Impurities by Inductively Coupled Plasma – Mass Spectrometry (ICP-MS), ***Jinjin Wang**, L. Mey-Ami, F. Li,* Air Liquide Electronics – Balazs NanoAnalysis

~~**AF3-MoP4** Numerical Studies of the Fluid Dynamics and Chemical Kinetics of Spatial Atomic Layer Deposition of Al_2O_3, ***Dongqing Pan,*** University of North Alabama~~

~~**AF3-MoP5** Mechanistic Understanding of Dicholosilane Thermal Decomposition during Atomic Layer Deposition of Silicon Nitride, ***Gyeong Hwang,*** *G. Hartmann,* University of Texas at Austin; ***P. Ventzek,*** Tokyo Electron America Inc.; *T. Iwao, K. Ishibashi,* Tokyo Electron Ltd~~.

AF3-MoP6 New Challenges of the Channeled Spectroscopic Ellipsometry for ALD Applications, ***Gai Chin,*** ULVAC Inc., Japan

AF3-MoP7 *In-situ Ellipsometric Analysis of the Plasma Influence on Atomic Layer Deposited AlN Thin Films,* ***Necmi Biyikli,*** *S. Ilhom, D. Shukla, A. Mohammad, B. Willis,* University of Connecticut

AF3-MoP8 Reaction Mechanisms of Thermal and Plasma-Modified ALD Growth Studied by *In-Situ* Mass Spectrometry, ***Thomas J. Larrabee,*** *L.B. Ruppalt,* U.S. Naval Research Laboratory

AF3-MoP10 In-situ Quartz Crystal Microbalance Study of Poly(3,4-ethylenedioxythiophene) (PEDOT) by Oxidative Molecular Layer Deposition (o-MLD), ***Jungsik Kim,*** *A. Volk,* North Carolina State University

ALD Fundamentals
Evergreen Ballroom & Foyer - Session AF4-MoP
Plasma Enhanced ALD Poster Session
5:45pm

AF4-MoP1 Low-temperature Atomic Layer Deposition of Yttrium Oxide using tris(butylcyclopentadienyl)yttrium and a Plasma-Excited Humidified Argon, ***Kentaro Saito,*** *K. Yosida, K. Kanomata, M. Miura, B. Ahmmad, K. Shigeru, F. Hirose,* Yamagata University, Japan

AF4-MoP2 Plasma Enhanced Atomic Layer Deposition of Silicon Nitride Thin Film by Organosilane Precursor and Process Engineering, ***Se-Won Lee,*** *C. Lee, M.-S. Kim,* Versum Materials Korea, Republic of Korea; *S. Yi, X. Lei,* Versum Materials, Inc.

AF4-MoP3 Understanding the Effect of Plasma Gas Chemistry and Reactor Pressure on the Crystallinity of AlN Films Grown via Plasma-Assisted Atomic Layer Deposition, ***Saidjafarzoda Ilhom,*** *D. Shukla, A. Mohammad, N. Biyikli, B. Willis,* University of Connecticut

AF4-MoP4 Plasma Enhanced Atomic Layer Deposition of Aluminum and Aluminum Fluoride, ***Daniel Messina,*** *Z. Haung, B. Eller, F. Koeck, P. Scowen, R. Nemanich,* Arizona State University

AF4-MoP5 High-temperature Hollow Cathode Plasma Enhanced Atomic Layer Deposition of Silicon Nitride (SiN_x) Thin Films using Hexachlorodisilane (HCDS), ***Su Min Hwang,*** *A.L.N. Kondusamy, Q. Zhiyang, H.S. Kim, J. Kim,* University of Texas at Dallas; *X. Zhou, B.K. Hwang,* Dow Chemicals

AF4-MoP6 Effects of Ion Bombardment in Plasma Enhanced Atomic Layer Deposition Processes, ***Hu Li,*** Tokyo Electron Technology Solutions Ltd., Japan; *T. Ito,* Osaka University, Japan; *M. Kagaya, T. Moriya,* Tokyo Electron Technology Solutions Ltd., Japan; *K. Karahashi, S. Hamaguchi,* Osaka University, Japan; *M. Matsukuma,* Tokyo Electron Technology Solutions Ltd., Japan

~~**AF4-MoP8** Microwave Generated Plasma Enhanced Atomic Layer Deposition of Oxides, ***Ji Hye Kim,*** *Y.D. Tak, Y.B. Lee,* ISAC Research Inc., Republic of Korea; *A. Poruba, J. Dolak,* SVCS Process Innovation s.r.o., Czech Republic; *H.S. Park,* ISAC Research Inc., Republic of Korea~~

~~**AF4-MoP9** Epitaxial Growth of GaN by Plasma-Enhanced Atomic Layer Deposition, ***Sanjie Liu,*** *X. Zheng,* University of Science and Technology Beijing, China~~

AF4-MoP10 Improving Plasma Enhanced Atomic Layer Deposition of Silicon Nitride with A Halodisilane, *B.K. Hwang, C. Lee,* ***Xiaobing Zhou,*** *A.E. Foss,* DuPont; *T.L. Sunderland, A.R. Millward,* Dow Chemicals; *S.M. Hwang, J.Y. Kim, A.T. Lucero, A.L.N. Kondusamy,* University of Texas at Dallas

AF4-MoP11 Characteristics of Silicon Nitride Film Deposited by Multi-electrode VHF (162 MHz)-PEALD, ***Ki Hyun Kim,*** *K.S. Kim, Y.J. Ji, J.Y. Byun,* Sungkyunkwan University, Republic of Korea; *A.R. Ellingboe,* Dublin City University; *G.Y. Yeom,* Sungkyunkwan University, Republic of Korea

AF4-MoP12 Characteristics of Low Damage Cobalt Films Deposited by Very High Frequency Plasma Enhanced Atomic Layer Deposition, ***Changhoon Song,*** *W.K. Yeom, Y. Shin, G.W. Kim, G.Y. Yeom,* Sungkyunkwan University, Republic of Korea

ALD Fundamentals
Evergreen Ballroom & Foyer - Session AF5-MoP
Characterization of ALD Films Poster Session
5:45pm

AF5-MoP1 Film Thickness and Trace Metal Analysis of Compound Semiconductor Stacks through Direct Film Stripping (DFS) followed by ICP-MS/OES, ***Vijay (Jaya) Chowdhury,*** *J. Huang,* ChemTrace; *P. Sun,* UCT - ChemTrace; *E. Appiah,* ChemTrace

AF5-MoP2 Overview of Doctoral Theses on Atomic Layer Deposition Worldwide - Outcome of the Virtual Project on the History of ALD, *J. Aarik,* University of Tartu, Estonia; *J. Aav, E. Ahvenniemi,* Aalto University, Finland; *A.R. Akbashev,* Stanford University; *S. Ali,* Aalto University, Finland; *M. Bechelany,* Institut Européen des Membranes, France; *M. Berdova,* Aalto University, Finland; *I. Bodalyov,* St. Petersburg State Institute of Technology, Russian Federation; *S. Boyadjiev,* Bulgarian Academy of Sciences, Bulgaria; *D. Cameron,* Masaryk University, Czech Republic; *N. Chekurov,* Oxford Instruments Analytical Oy, Finland; *R. Cheng,* Huazhong University of Science and Technology, China; *M. Chubarov,* The Pennsylvania State University; *V. Cremers,* Ghent University, Belgium; *A. Devi,* Ruhr University Bochum, Germany; *V.E. Drozd,* St. Petersburg State Institute of Technology, Russian Federation; *L. Elnikova,* Institute for Theoretical and Experimental Physics, Russian Federation; *G. Gottardi,* Fondazione Bruno Kessler, Center for Materials and Microsystems, Italy; ***J. Ruud van Ommen,*** Delft University of Technology, Netherlands; *R. Puurunen,* Aalto University, Finland

~~**AF5-MoP3** Nanoscale Chemical Characterization of Ultrathin Films via PiFM, ***Sung Park,*** *D. Nowak, W. Morrison,* Molecular Vista~~

AF5-MoP4 The Effect of Impurities on Film Properties in the $Y(MeCp)_3/O_3$ Process, *J. Kalliomäki, T. Lehto, M. Kääriä, T. Sarnet,* ***Jani Kivioja,*** Picosun Oy, Finland

AF5-MoP6 Internal Photoemission Spectroscopy Measurement of Barrier Heights between ALD Ru and Al_2O_3, ***Melanie Jenkins,*** *M.H. Hayes, K. Holden, J.F. Conley, Jr.,* Oregon State University

AF5-MoP7 Growth and Characterization: Low Temperature ALD, ***Birol Kuyel,*** *A. Alphonse, K.P. Hong, J. Marshall,* Nano-Master, Inc.

AF5-MoP8 Etch Rate Characterization of Oxide ALD Films, ***Martin M. Winterkorn,*** *H.J. Kim, J. Provine, F. Prinz, T.W. Kenny,* Stanford University

~~**AF5-MoP10** Structural Aspects of Nanometer Size Amorphous Materials, ***Yael Etinger Geller,*** *A. Katsman, B. Pokroy,* Technion - Israel Institute of Technology, Israel~~

ALD for Manufacturing
Evergreen Ballroom & Foyer - Session AM-MoP
ALD for Manufacturing Poster Session
5:45pm

AM-MoP1 Cobalt Precursor Supply Chain - Ethics and Risks, ***Andreas Wilk,*** *A. Frey, O. Briel,* Umicore AG & Co. KG, Germany; *D. Zeng,* Umicore AG & Co. KG

AM-MoP2 Homogeneous and Stress Controlled PEALD Films for Large Optics, ***Hassan Gargouri,*** *F. Naumann, S. Golka,* SENTECH Instruments GmbH, Germany; *K. Pfeiffer,* Fraunhofer Institute for Applied Optics and Precision Engineering IOF, Germany; *V. Beladiya,* Friedrich Schiller University, Germany; *A. Szeghalmi,* Fraunhofer Institute for Applied Optics and Precision Engineering IOF, Germany

~~**AM-MoP3** Sensing Response of ZnO Nanotube Gas Sensor Synthesized on Porous Substrate by Atomic Layer Deposition, ***Pengtao Lin,*** *K. Zhang, H. Baumgart,* Old Dominion University~~

AM-MoP4 Temperature-based Control of Liquid Precursor Delivery for ALD Processes, ***Egbert Woelk,*** CeeVeeTech; *K. Kimmerle, B. Kimmerle,* NSI; *J. Maslar,* National Institute of Standards and Technology

AM-MoP5 Design and Manufacturing of ICP-Type Remote Plasma ALD, ***Dohyun Go,*** *J.W. Shin, B.C. Yang, H.J. Kim,* Seoul National University of Science and Technology, Republic of Korea

AM-MoP6 ACS™ (Atomically Clean Surface™) Cleaning and Analytical Validation of Recycled ALD Chamber Parts for the Semiconductor Industry, ***Russell Parise,*** *I. Iordanov, B. Quinn,* UCT - QuantumClean; *P. Sun,* UCT - ChemTrace

AM-MoP8 Process Control and Mass Delivery Optimization from Low Vapor Pressure Precursors, ***Jeffrey Spiegelman,*** *C. Ramos, D. Alvarez, Z. Shamsi,* RASIRC

AM-MoP9 Scaling Low-temperature Thermal ALD of SiO_2 to Batch, *J. Kalliomäki, M. Mäntymäki, T. Lehto, S. Shukla, M. Kääriä, T. Sarnet,* ***Juhana Kostamo,*** Picosun Oy, Finland

Emerging Materials
Evergreen Ballroom & Foyer - Session EM-MoP
Emerging Materials Poster Session
5:45pm

Note: ALE Posters Will Remain Posted All Week

~~**EM-MoP1** Structure and Magnetism of Electrospun a- Fe_2O_3 Nanofibers SiO_2 Coated by ALD, *F. Pantò,* CNR-Istituto di Tecnologie Avanzate per l'Energia (ITAE), Italy*; H. Raza,* Humboldt-Universität zu Berlin, Germany*; A.M. Ferretti,* CNR-Istituto di Scienze e Tecnologie Molecolari (ISTM), Italy*; C. Triolo,* Università di Messina, Italy*; A. Ponti,* CNR-Istituto di Scienze e Tecnologie Molecolari, Italy*; S. Patanè,* Università di Messina, Italy*; N. Pinna,* Humboldt-Universität zu Berlin, Germany*; **Saveria Santangelo,*** Università Mediterranea, Italy~~

EM-MoP2 Fluidized Bed Molecular Layer Deposition of Ultrathin Poly(ethylene terephthalate) Films on TiO_2 P25 Nanoparticles, ***Damiano La Zara**, M. Bailey, D. Benz,* Delft University of Technology, Netherlands*; M.J. Quayle, G. Petersson, S. Folestad,* AstraZeneca, Sweden*; J.R. van Ommen,* Delft University of Technology, Netherlands

~~**EM-MoP3** Fabrication and Characterization of Organic-Inorganic Hybrid Thin Films, ***Chu Huong,*** Hanyang University, Republic of Korea~~

EM-MoP4 High Performance Encapsulation Polymer-Al_2O_3 Hybrid Thin Layer by Atomic Layer Infiltration, ***Hong Rho Yoon**, J. Park, N.V. Long, C. Huong,* Hanyang University, Republic of Korea

EM-MoP5 ALD of Metal Oxides Fabricated by using $La(NO_3)_3 \cdot 6H_2O$ Oxidant and their Applications, ***In-Sung Park**, S.Y. Kim, T. Lee, S. Seong, Y.C. Jung, J. Ahn,* Hanyang University, Republic of Korea

EM-MoP6 Bringing Higher Etch-resistance to Metal-infiltrated Polymer, ***Norikatsu Sasao**, K. Asakawa, S. Sugimura,* Toshiba Memory Corporation

~~**EM-MoP7** Magnetic and Electric Properties of Atomic Layer Deposited ZrO_2-based Thin Films, ***Kristjan Kalam,*** *H. Seemen, P. Ritslaid, T. Jõgiaas, M. Rähn, A. Kasikov, A. Tamm, K. Kukli, M. Mikkor,* University of Tartu, Estonia*; J. Link, R. Stern,* National Institute of Chemical Physics and Biophysics, Estonia*; S. Dueñas, H. Castán,* University of Valladolid~~

~~**EM-MoP8** Vapor Phase Infiltration as a New Approach in the Fabrication of Advanced Hybrid Thermoelectric Materials, ***Jaime DuMont,*** *M. Knez,* CIC nanoGUNE, Spain~~

EM-MoP9 Low-temperature Atomic Layer Deposition of Aluminum Oxide on Polymeric Powder Feedstocks for Improved Powder Rheology, ***John Miller**, C. Gillespie, J. Chesser,* Lawrence Livermore National Laboratory*; A. Scheppe,* United States Air Force Academy*; A. Nelson, N. Teslich, A. Lange, S. Elhadj, R. Reeves,* Lawrence Livermore National Laboratory

EM-MoP10 Atomic Layer Deposition of Molybdenum Oxide Carbide and Molybdenum Carbide Films, ***Michael D. Overbeek**, C.H. Winter,* Wayne State University

EM-MoP11 Solid Phase Epitaxy of ALD-Grown $PrAlO_3$ Films, ***Navoda Jayakodiarachchi**, W.L.I. Waduge,* Wayne State University*; Y. Chen, P. Zuo, T.F.T. Kuech, S.E. Babcock, P.G. Evans,* University of Wisconsin-Madison*; C.H. Winter,* Wayne State University

EM-MoP12 Homogenous Distribution of Dopants in ALD Films: Tin-Doped Zinc Oxide (ZTO) Case Study, ***Triratna Muneshwar**, D. Barlage, K. Cadien,* University of Alberta, Canada

EM-MoP13 Uniform, Thermal ALD of Al_2O_3 and ZnO on Zirconia Particles, ***Dhruv Shah**, D. Patel, J. O'Tani, M. Linford,* Brigham Young University

EM-MoP14 Composition Control of Ge-Sb-Te Film by Supercycles of ALD GeSb and ALD Sb Followed by Tellurization Annealing, ***Yewon Kim**, J. Lee,* Sejong University, Republic of Korea*; S.J. Baik,* Hankyong National University, Republic of Korea*; W. Koh,* UP Chemical Co., Ltd., Republic of Korea*; W.-J. Lee,* Sejong University, Republic of Korea

EM-MoP15 Study on The Crystallinity and The Dielectric Constant of $Zr_xGe_{1-x}O_2$ Films using Mixed Zr - Ge Precursor by Atomic Layer Deposition, ***Ju Young Jeong**, Y. Han, H. Sohn,* Yonsei University, Korea*; H. Noh, H. Park,* SK Hynix Inc

Tuesday Morning, July 23, 2019

	Grand Ballroom A-C	
8:00am	**AF1-TuM1** Surface Chemistry during ALD of Nickel Sulfide, ***Xinwei Wang***, Peking University, China	**ALD Fundamentals** **Session AF1-TuM** **In-Situ Characterization of ALD Processes** **Moderators:** Christophe Vallée, LTM-UGA Erwin Kessels, Eindhoven University of Technology
8:15am	**AF1-TuM2** In situ and In vacuo Studies on Plasma Enhanced Atomic Layer Deposited Cobalt Films, ***Johanna Reif***, *M. Knaut, S. Killge, N.A. Hampel, M. Albert, J.W. Bartha,* Technische Universität Dresden, Germany	
8:30am	**AF1-TuM3** Investigation of PEALD Grown HfO_2 Thin Films via Near Ambient Pressure XPS: Precursor Tuning, Process Design and a New In-situ Examination Approach for Studying Film Surfaces Exposed to Reactive Gases, ***David Zanders***, Ruhr University Bochum, Germany; *E. Ciftyurek,* Heinrich Heine University Düsseldorf, Germany; *C. Bock, A. Devi,* Ruhr University Bochum, Germany; *K.D. Schierbaum,* Heinrich Heine University Düsseldorf, Germany	
8:45am	**AF1-TuM4** Surface Science Studies of GaN Substrates Subjected to Plasma-Assisted Atomic Layer Processes, ***Samantha G. Rosenberg***, ASEE; *D.J. Pennachio,* University of California, Santa Barbara; *E.C. Young, Y.H. Chang, H.S. Inbar,* University of California Santa Barbara; *J.M. Woodward,* U.S. Naval Research Laboratory; *Z.R. Robinson,* SUNY College at Brockport; *J. Grzeskowiak,* University at Albany-SUNY; *C.A. Ventrice, Jr.,* SUNY Polytechnic Institute; *C.J. Palmstrøm,* University of California Santa Barbara; *C.R. Eddy, Jr.,* U.S. Naval Research Laboratory	
9:00am	**AF1-TuM5** Infrared and Optical Emission Spectroscopy on Atmospheric-Pressure Plasma-Enhanced Spatial ALD of Al_2O_3, ***Maria Antonietta Mione***, *R. Engeln, W.M.M. Kessels,* Eindhoven University of Technology, Netherlands; *F. Roozeboom,* Eindhoven University of Technology and TNO, Netherlands	
9:15am	**AF1-TuM6** Fingerprinting of ALD Reaction Products with Time-Resolved In situ Mass Spectrometry, ***Andreas Werbrouck***, *F. Mattelaer, J. Dendooven, C. Detavernier*, Ghent University, Belgium	
9:30am	**INVITED: AF1-TuM7** Studying Pt and Pd Nanoparticle ALD through X-ray based In situ Characterization, ***Jolien Dendooven***, *J.-Y. Feng,* Ghent University, Belgium; *E. Solano,* ALBA Synchrotron Light Source, Spain; *R. Ramachandran, M. Minjauw, M. Van Daele,* Ghent University, Belgium; *D. Hermida-Merino,* ESRF European Synchrotron, France; *A. Coati,* Synchrotron SOLEIL, France; *C. Detavernier,* Ghent University, Belgium	
9:45am	Invited talk continues.	
10:00am	**Break & Exhibits**	
10:15am	**Break & Exhibits**	
10:30am	**Break & Exhibits**	
10:45am	**AF3-TuM12** Enabling Nucleation Phenomena Studies of ALD Deposited Films by In-situ High-Resolution TEM, ***Stephanie Burgmann***, *A. Dadlani, A. Bin Afif,* Norwegian University of Science and Technology, Norway; *J. Provine,* Aligned Carbon; *A.T.J. van Helvoort, J. Torgesen,* Norwegian University of Science and Technology, Norway	**ALD Fundamentals** **Session AF3-TuM** **Growth and Characterization II** **Moderators:** Jolien Dendooven, Ghent University Henrik Pedersen, Linköping University
11:00am	**AF3-TuM13** *In-situ* ellipsometric analysis of plasma assisted ALD grown-stoichiometric and crystalline AlN films, ***Adnan Mohammad***, *D. Shukla, S. Ilhom, B. Willis,* University of Connecticut; *B. Johs,* Film Sense LLC; *A.K. Okyay,* Stanford University; *N. Biyikli,* University of Connecticut	
11:15am	**AF3-TuM14** Film Properties of ALD SiNx Deposited by Trisilylamine and N_2 Plasma, ***Markus Bosund***, *E. Salmi, K. Niiranen,* Beneq Oy, Finland	
11:30am	**AF3-TuM15** Comparison of Properties of Conductive Nitride Films Prepared by PEALD using Quartz and Sapphire Plasma Sources, *I. Krylov, X. Xu, K. Weinfeld,* ***Valentina Korchnoy***, *D. Ritter, M. Eizenberg,* Technion - Israel Institute of Technology, Israel	
11:45am	**AF3-TuM16** Role of Hydrogen Radicals in the Surface Reactions of Trimethyl-Indium (TMI) with Ar/N_2 Plasma in Hollow-Cathode Plasma-Assisted ALD, ***Saidjafarzoda Ilhom***, *A. Mohammad, D. Shukla, N. Biyikli, B. Willis,* University of Connecticut	
12:00pm	**Lunch & Exhibits**	

Tuesday Morning, July 23, 2019

	Grand Ballroom E-G	
8:00am 8:15am		**ALD Applications** **Session AA1-TuM** **ALD for Catalysts, Electrocatalysts, and Photocatalysts** **Moderators:** Jeffrey W. Elam, Argonne National Laboratory Parag Banerjee, University of Central Florida
8:30am	**AA1-TuM3** Plasma-Assisted ALD of Cobalt Phosphate: Process Development and Electro-Catalytic Activity Towards Oxygen Evolution Reaction*, V. Di Palma,* Eindhoven University of Technology, Netherlands*; G. Zafeiropoulos, R. van de Sanden,* Dutch Institute for Fundamental Energy Research*; W.M.M. Kessels,* Eindhoven University of Technology, Netherlands*; M. Tsampas,* Dutch Institute for Fundamental Energy Research*;* ***Mariadriana Creatore,*** Eindhoven University of Technology, Netherlands	
8:45am	**AA1-TuM4** Improved Electrochemical Activity of Pt Catalyst Fabricated by Vertical Forced-Flow Atomic Layer Deposition*,* ***Tzu-Kang Chin****, T.-P. Perng,* National Tsing Hua University, Republic of China	
9:00am	**AA1-TuM5** Improved Catalyst Selectivity and Longevity using Atomic Layer Deposition*, C. Marshall,* Argonne National Laboratory*; A. Dameron, R. Tracy,* Forge Nano*; C. Nicholas, L. Abrams, P. Barger,* Honeywell UOP*; T. Li,* ***Lu Zheng****,* Argonne National Laboratory	
9:15am	**AA1-TuM6** Enhancing Co_2C Activity for C_{2+} Oxygenate Production from Syngas using ALD Promoters*,* ***Sindhu Nathan****, J. Singh, A. Asundi, S.F. Bent,* Stanford University	
9:30am	**AA1-TuM7** Atomic Layer Deposition of Bismuth Vanadate Core-Shell Nanowire Photoanodes*,* ***Ashley Bielinski****, S. Lee, J. Brancho, S. Esarey, A. Gayle, E. Kazyak, K. Sun, B. Bartlett, N.P. Dasgupta,* University of Michigan	
9:45am	**AA1-TuM8** Improved Photocatalytic Efficiency by Depositing Pt and SiO_2 on TiO_2 (P25) using Atomic Layer Deposition in a Fluidized Bed*,* ***Dominik Benz****, H. Nugteren, H. Hintzen, M. Kreutzer, R. van Ommen,* Delft University of Technology, Netherlands	
10:00am	**Break & Exhibits**	
10:15am	**Break & Exhibits**	
10:30am	**Break & Exhibits**	
10:45am	**AA2-TuM12** Atomic Layer Deposition of Glassy Lithium Borate-Carbonate Electrolytes for Solid-State Lithium Metal Batteries*, E. Kazyak, A. Davis, S. Yu, K.-H. Chen, A. Sanchez, J. Lasso, T. Thompson, A. Bielinski, D. Siegel,* ***Neil P. Dasgupta****,* University of Michigan	**ALD Applications** **Session AA2-TuM** **ALD for Batteries I** **Moderators:** Neil P. Dasgupta, University of Michigan Noemi Leick, National Renewable Energy Laboratory
11:00am	**AA2-TuM13** ALD Interlayers for Stabilization of $Li_{10}GeP_2S_{12}$ Solid Electrolytes Against Li Metal Anodes*,* ***Andrew Davis****,* University of Michigan*; K. Wood,* National Renewable Energy Laboratory*; R. Garcia-Mendez, E. Kazyak, K.-H. Chen, J. Sakamoto,* University of Michigan*; G. Teeter,* National Renewable Energy Laboratory*; N.P. Dasgupta,* University of Michigan	
11:15am	**AA2-TuM14** ALD and MLD on Lithium Metal – A Practical Approach Toward Enabling Safe, Long Lasting, High Energy Density Batteries*,* ***Andrew Lushington****,* Arradiance*; Y. Zhao, L. Goncharova, Q. Sun, R. Li, X. Sun,* University of Western Ontario, Canada	
11:30am	**AA2-TuM15** Synergistic Effect of 3D Current Collectors and ALD Surface Modification for High Coulombic Efficiency Lithium Metal Anodes*,* ***Kuan-Hung Chen****, A. Sanchez, E. Kazyak, A. Davis, N.P. Dasgupta,* University of Michigan	
11:45am	~~**AA2-TuM16** Atomic Layer Deposition FeS@CNT from Elemental Sulfur as an Electrode for Lithium-Ion batteries*,* ***Hongzheng Zhu****, J. Liu,* University of British Columbia, Canada~~	
12:00pm	**Lunch & Exhibits**	

Tuesday Morning, July 23, 2019

	Grand Ballroom H-K	
8:00am	**AF2-TuM1** Characterizing Water Delivery for ALD Processes, ***James Maslar***, *B. Sperling, W. Kimes,* National Institute of Standards and Technology*; W. Kimmerle, K. Kimmerle,* NSI*; E. Woelk,* CeeVeeTech	**ALD Fundamentals** **Session AF2-TuM** **ALD Precursors II** **Moderators:** Jin-Seong Park, Hanyang University Seán Barry, Carleton University
8:15am	**AF2-TuM2** A Nickel Chloride Adduct Complex as a Precursor for Low-Resistivity Nickel Nitride Thin Films with Tert-butylhydrazine as a Coreactant*, K. Väyrynen, T. Hatanpää, M. Mattinen, M.J. Heikkilä, K. Mizohata, J. Räisänen,* University of Helsinki, Finland*; J. Link, R. Stern,* National Institute of Chemical Physics and Biophysics, Estonia*; M. Leskelä,* ***Mikko Ritala****,* University of Helsinki, Finland	
8:30am	**AF2-TuM3** Simple, Rationally Designed Aluminum Precursors for the Deposition of Low-impurity AlN Films*,* ***Sydney Buttera****, S. Barry,* Carleton University, Canada*; H. Pedersen,* Linköping University, Sweden	
8:45am	**AF2-TuM4** Atomic Layer Deposition of Lead(II) Sulfide at Temperatures Below 100 °C*,* ***Georgi Popov****,* University of Helsinki, Finland*; G. Bačić,* Carleton University, Canada*; M. Mattinen, M. Vehkamäki, K. Mizohata, M. Kemell,* University of Helsinki, Finland*; S. Barry,* Carleton University, Canada*; J. Räisänen, M. Leskelä, M. Ritala,* University of Helsinki, Finland	
9:00am	**AF2-TuM5** Development and Characterization of a Novel Atomic Layer Deposition Process for Transparent p-Type Semiconducting Nickel Oxide using $Ni(^{tBu2}DAD)_2$ and Ozone*,* ***Konner Holden****,* Oregon State University*; C.L. Dezelah,* EMD Performance Materials*; J.F. Conley, Jr.,* Oregon State University	
9:15am	**AF2-TuM6** Blocking Thermolysis in Diamido Plumbylenes*,* ***Goran Bacic****,* Carleton University, Canada*; D. Zanders,* Ruhr University Bochum, Germany*; I. Frankel,* Carleton University, Canada*; J. Masuda,* Saint Mary's University, Canada*; T. Zeng,* Carleton University, Canada*; B. Mallick, A. Devi,* Ruhr University Bochum, Germany*; S. Barry,* Carleton University, Canada	
9:30am	**AF2-TuM7** ALD of Sc_2O_3 with $Sc(cp)_3$ and a Novel Heteroleptic Precursors*, T. Ivanova,* ***Perttu Sippola****,* ASM, Finland*; G. Verni, Q. Xie,* ASM, Belgium*; M. Givens,* ASM, Finland	
9:45am	**AF2-TuM8** A Novel Self-limited Atomic Layer Deposition of WS_2 based on the Chemisorption and Reduction of bis(t-butylimido)bis(dimethylamino) Complexes*,* ***Nicola Pinna****,* Humboldt-Universtät zu Berlin, Germany	
10:00am	**Break & Exhibits**	
10:15am	**Break & Exhibits**	
10:30am	**Break & Exhibits**	
10:45am	**INVITED: AS1-TuM12** Overview of Wet And Dry Selective Processes Driven by Area Activation or Deactivation Down to Below 20nm Critical Dimensions*,* ***Silvia Armini****,* IMEC, Belgium	**Area Selective ALD** **Session AS1-TuM** **Area-Selective ALD Techniques** **Moderator:** Adrie Mackus, Eindhoven University of Technology
11:00am	Invited talk continues.	
11:15am	**AS1-TuM14** Electron-Enhanced Atomic Layer Deposition (EE-ALD) of Cobalt Metal Films at Room Temperature*,* ***Zach Sobell****, A. Cavanagh, S.M. George,* University of Colorado - Boulder	
11:30am	~~**AS1-TuM15** Area Selective Atomic Layer Deposition on Molecular Design, ***Akihiro Nishida****, T. Yoshino, N. Okada, A. Yamashita,* ADEKA Corporation, Japan~~	
11:45am	**AS1-TuM16** From Surface Dependence in Atomic Layer Deposition to Area-Selective Deposition of TiN in Nanoscale Patterns*,* ***Annelies Delabie****,* IMEC, Belgium*; D. Carbajal,* UNAM*; J. Soethoudt, B.T. Chan, E. Altamirano Sanchez, B. Meynaerts, J.-W. Clerix, S. Van Elshocht,* IMEC, Belgium	
12:00pm	**Lunch & Exhibits**	

Tuesday Morning, July 23, 2019

	Regency Ballroom A-C	
8:00am	**INVITED: ALE1-TuM1** Analyses of Hexafluoroacetylacetone (Hfac) Adsorbed on Transition Metal Surfaces, ***Tomoko Ito**, K. Karahashi, S. Hamaguchi,* Osaka University, Japan	**Atomic Layer Etching** **Session ALE1-TuM** **ALE: Gas-phase and/or Thermal ALE** **Moderators:** Steven M. George, University of Colorado – Boulder Venkateswara Pallem, American Air Liquide
8:15am	Invited talk continues.	
8:30am	**ALE1-TuM3** Thermal Atomic Layer Etching of Silicon Nitride using an Oxidation and "Conversion-Etch" Mechanism, ***Aziz Abdulagatov**, S.M. George,* University of Colorado - Boulder	
8:45am	**ALE1-TuM4** Thermal Dry Atomic Layer Etching of Cobalt with Sequential Exposure to Molecular Chlorine and Diketones, *M. Konh, C. He, X. Lin,* University of Delaware*; X. Guo, V. Pallem,* American Air Liquide*; R. Opila, **Andrew Teplyakov**, Z. Wang, B. Yuan,* University of Delaware	
9:00am	**ALE1-TuM5** Spontaneous Etching of B_2O_3 and TiO_2 by HF: Removal Reaction in WO_3 ALE and TiN ALE, ***Austin Cano**,* University of Colorado - Boulder*; S.K. Natarajan,* Tyndall National Institute, Ireland*; J. Clancey,* University of Colorado - Boulder*; S. Elliot,* Schrödinger Inc*; S.M. George,* University of Colorado - Boulder	
9:15am	**ALE1-TuM6** Thermal Based Atomic Layer Etching of Aluminum Oxide and Titanium Nitride, ***Varun Sharma**,* ASM, Finland*; T. Blomberg,* Picosun Oy/ASM, Finland*; M. Tuominen, S. Haukka,* ASM, Finland	
9:30am	**ALE1-TuM7** Thermal Atomic Layer Etching of Amorphous and Crystalline Hafnium Oxide, Zirconium Oxide and Hafnium Zirconium Oxide, ***Jessica A. Murdzek**, S.M. George,* University of Colorado - Boulder	
9:45am	**ALE1-TuM8** Isotropic Atomic Layer Etching of Cobalt with Smooth Etched Surfaces by using Cyclic Repetition of Plasma Oxidation and Organometallization, ***Sumiko Fujisaki**,* Hitachi R&D Group, Japan	
10:00am	**Break & Exhibits**	
10:15am	**Break & Exhibits**	
10:30am	**Break & Exhibits**	
10:45am	**ALE2-TuM12** Atomic Layer Etching for Germanium using Halogen Neutral Beam =Comparison between Br and Cl Chemistry=, *T. Fujii, **Daisuke Ohori**,* Tohoku University, Japan*; S. Noda,* National Institute of Advanced Industrial Science and Technology, Japan*; Y. Tanimoto, D. Sato, H. Kurihara,* Showa Denko K.k.*; W. Mizubayashi, K. Endo,* National Institute of Advanced Industrial Science and Technology, Japan*; Y. Li,* National Chiao Tung University*; Y.-J. Lee,* National Nano Device Laboratories*; T. Ozaki, S. Samukawa,* Tohoku University, Japan	**Atomic Layer Etching** **Session ALE2-TuM** **Alternative Methods to ALE** **Moderators:** Erwin Kessels, Eindhoven University of Technology Satoshi Hamaguchi, Osaka University
11:00am		
11:15am	**ALE2-TuM14** A New Etching / Passivation Process in Cyclic Mode for Spacer Etching in 3D CMOS Integrations, *O. Pollet,* CEA-LETI, France*; N. Posseme,* Univ. Grenoble Alpes, CEA, LETI, France*; V. Ah-Leung, **Valentin Bacquie**,* CEA-LETI, France	
11:30am	**ALE2-TuM15** Atomic Layer Etching of Transition Metals with Gas Cluster Ion Beam Irradiation and Acetylacetone, ***Noriaki Toyoda**, K. Uematsu,* University of Hyogo, Japan	
11:45am	**ALE2-TuM16** Atomic Layer Etching at Atmospheric Pressure, ***Eugen Shkura**, D. Theirich, K. Brinkmann, T. Haeger,* University of Wuppertal, Germany*; J. Schneidewind, M. Siebert,* SENTECH Instruments GmbH, Germany*; T. Riedl,* University of Wuppertal, Germany	
12:00pm	**Lunch & Exhibits**	

Tuesday Afternoon, July 23, 2019

	Grand Ballroom A-C	
1:30pm	**AF-TuA1** Low Temperature High Quality Silicon Dioxide by Neutral Beam Enhanced Atomic Layer Deposition, ***Hua-Hsuan Chen**, D. Ohori, T. Ozaki,* Tohoku University, Japan*; M. Utsuno, T. Kubota, T. Nozawa,* ASM Japan K.K., Japan*; S. Samukawa,* Tohoku University, Japan	**ALD Fundamentals** **Session AF-TuA** **Plasma ALD: Growth and Characterization** **Moderators:** Hyeongtag Jeon, Hanyang University Jiyoung Kim, The University of Texas at Dallas
1:45pm	**AF-TuA2** Radical Surface Recombination Probabilities during Plasma ALD of SiO_2, TiO_2 and Al_2O_3 Determined from Film Conformality, ***Karsten Arts**,* Eindhoven University of Technology, Netherlands*; M. Utriainen,* VTT Technical Research Centre of Finland, Finland*; R. Puurunen,* Aalto University, Finland*; W.M.M. Kessels,* Eindhoven University of Technology, Netherlands*; H. Knoops,* Oxford Instruments Plasma Technology, UK	
2:00pm	**AF-TuA3** A Robust Method for In-situ Gas Monitoring of ALD Processes using Optical Emission Spectroscopy of a Pulsed Remote Plasma, ***Joe Brindley**, B. Daniel, V. Bellido-Gonzalez,* Gencoa Limited, UK*; R. Potter, B. Peek,* University of Liverpool, UK	
2:15pm	**AF-TuA4** Near Room Temperature Plasma Enhanced Atomic Layer Deposition of Gold Metal, ***Michiel Van Daele**,* Ghent University, Belgium*; M. Griffiths,* Carleton University, Canada*; A. Raza,* Ghent University - IMEC, Belgium*; M. Minjauw,* Ghent University, Belgium*; S. Barry,* Carleton University, Canada*; R. Baets,* Ghent University - IMEC, Belgium*; C. Detavernier, J. Dendooven,* Ghent University, Belgium	
2:30pm	**AF-TuA5** Low-Temperature Deposition of Gallium Oxide and Aluminum Oxide with Arrays of Microcavity Plasma Enhanced Atomic Layer Deposition, ***Jinhong Kim**, A. Mironov, S.-J. Park, J.G. Eden,* University of Illinois at Urbana-Champaign	
2:45pm	**AF-TuA6** The Effects of Varying Plasma Conditions on Plasma Assisted Atomic Layer Epitaxy, ***David Boris**, V. Wheeler, N. Nepal, S.G. Rosenberg, J. Avila, J.M. Woodward, V. Anderson, S. Walton, C.R. Eddy, Jr.,* U.S. Naval Research Laboratory	
3:00pm	**INVITED: AF-TuA7** Plasma-Enhanced Atomic Layer Epitaxy of Ultra-wide Bandgap Ga_2O_3 and $(Al_xGa_{1-x})_2O_3$ Films, ***Virginia Wheeler**, N. Nepal, D. Boris, S. Walton, S. Qadri, J. Avila, D. Meyer, B. Downey, V. Gokhale,* U.S. Naval Research Laboratory*; L. Nyakiti,* Texas A&M University*; M. Tadjer,* U.S. Naval Research Laboratory*; M. Goorsky,* University of California Los Angeles*; C.R. Eddy Jr.,* U.S. Naval Research Laboratory	
3:15pm	Invited talk continues.	
3:30pm	**Break & Exhibits**	
3:45pm	**Break & Exhibits**	
4:00pm	**INVITED: AA3-TuA11** Doped Hi-K ALD Films of HfO_X and ZrO_X for Advanced Ferroelectric and Anti-Ferroelectric Memory Device Applications:, ***Niloy Mukherjee**, J. Mack, S. Rathi,* Eugenus, Inc.*; Z. Wang, A. Gaskell, N. Tasneem, A. Khan,* Georgia Institute of Technology*; M. Dopita, D. Kriegner,* Charles University	**ALD Applications** **Session AA3-TuA** **ALD for Memory Applications I** **Moderators:** Scott B. Clendenning, Intel Corp. Adrien LaVoie, Lam Research Corp.
4:15pm	Invited talk continues.	
4:30pm	**AA3-TuA13** ALD of La-Doped HfO_2 Films for Ferroelectric Applications, ***Tatiana Ivanova**, P. Sippola, M. Givens,* ASM, Finland*; H. Sprey,* ASM, Belgium*; T.M. Büttner, P. Polakowski, K. Seidel,* Fraunhofer IPMS-CNT, Germany	
4:45pm	**AA3-TuA14** Characterization of Multi-Domain Ferroelectric ZrO_2 Thin Films for Negative Capacitance and Inductive Responses, ***Yu-Tung Yin**, P.-H. Cheng, Y.-S. Jiang, J. Shieh, M.J. Chen,* National Taiwan University, Republic of China	
5:00pm	**AA3-TuA15** Scaling Ferroelectric $Hf_{0.5}Zr_{0.5}O_2$ on Metal-Ferroelectric-Metal (MFM) and Metal-Ferroelectric-Insulator-Semiconductor (MFIS) Structures, ***Jaidah Mohan**, H. Hernandez-Arriaga, H.S. Kim, A. Khosravi, A. Sahota,* The University of Texas at Dallas*; R. Wallace,* University of Texas at Dallas*; J. Kim,* The University of Texas at Dallas	
5:15pm	**AA3-TuA16** Interface Characteristics of MIM Capacitors using Vanadium Nitride Electrode and ALD-grown ZrO_2 High-k Dielectric Film, ***Jae Hyoung Choi**, Y. Kim, H.I. Lee, H.-J. Lim, K. Hwang, S.W. Nam, H.-K. Kang,* Samsung Electronics, Republic of Korea	
5:30pm	**Poster Session**	

Tuesday Afternoon, July 23, 2019

	Grand Ballroom E-G	
1:30pm	**INVITED: AA1-TuA1** Atomic Layer Deposition of Indium Gallium Zinc Oxide (IGZO) Semiconductor Thin Films: From Precursor to Thin Film Transistor Application, ***Jin-Seong Park***, Hanyang University, Republic of Korea	**ALD Applications** **Session AA1-TuA** **Emerging Applications I** **Moderators:** Anjana Devi, Ruhr University Bochum Han-Bo-Ram Lee, Incheon National University
1:45pm	Invited talk continues.	
2:00pm	**AA1-TuA3** ALD Growth of Ultra-thin Co Layers on the Topological Insulator Sb_2Te_3, ***Emanuele Longo***, *R. Mantovan, R. Cecchini,* CNR-IMM Unit of Agrate Brianza, Italy; *M.D. Overbeek,* Wayne State University; *M. Longo,* CNR-IMM Unit of Agrate Brianza, Italy; *L. Lazzarini,* CNR-IMEM, Italy; *M. Fanciulli,* Università degli Studi di Milano-Bicocca, Italy; *C.H. Winter,* Wayne State University; *C. Wiemer,* CNR-IMM Unit of Agrate Brianza, Italy	
2:15pm	**AA1-TuA4** Modifying Interfacial Chemistry of Cellulose-Reinforced Epoxy Resin Composites using Atomic Layer Deposition (ALD), ***Jamie Wooding***, *Y. Li, K. Kalaitzidou, M. Losego,* Georgia Institute of Technology	
2:30pm	**AA1-TuA5** Atomic Layer Deposition of Au Nanoparticles on Titania, *Fatemeh S.M. Hashemi,* Delft University of Technology, Netherlands; *F. Grillo,* ETH Zurich, Switzerland; *V. Ravikumar,* ***D. Benz***, *A. Shekhar,* Delft University of Technology, Netherlands; *M. Griffiths, S. Barry,* Carleton University, Canada; *J.R. van Ommen,* Delft University of Technology, Netherlands	
2:45pm	**AA1-TuA6** Multi-layer Protective Coatings on Silver for Protection of Historic Silver Artifacts, *E. Breitung,* Metropolitan Museum of Art; *S. Creange,* Rijks Museum, Netherlands; *G. Pribil,* J.A. Woollam; *A. Bertuch,* ***Ritwik Bhatia***, Veeco-CNT	
3:00pm	**AA1-TuA7** Nonlinear Optical Properties of TiO_2-Based ALD Thin Films, ***Theodosia Gougousi***, *R. Kuis, I. Basaldua, P. Burkins, J.A. Kropp, A. Johnson,* University of Maryland, Baltimore County	
3:15pm	**AA1-TuA8** Atomic Layer Deposition to Alter the Wetting and Thermal Properties of Lumber, ***Shawn Gregory***, *C. McGettigan, E. McGuinness, D. Rodin, S. Yee, M. Losego,* Georgia Institute of Technology	
3:30pm	**Break & Exhibits**	
3:45pm	**Break & Exhibits**	
4:00pm	**AA2-TuA11** Tunable Electrical Properties of Lithium Fluoride Thin Films using Different Fluorine Sources, ***Devika Choudhury***, *A. Mane, J.W. Elam,* Argonne National Laboratory	**ALD Applications** **Session AA2-TuA** **ALD for Batteries II** **Moderator:** Yong Qin, Institute of Coal Chemistry, Chinese Academy of Sciences
4:15pm	**AA2-TuA12** The Role of Al_2O_3 ALD Precursor Chemistry on the Electrochemical Performance of Lithium Ion Battery Cathode Mmaterials, ***Donghyeon Kang***, *A. Mane, J.W. Elam,* Argonne National Laboratory; *R.F. Warburton, J.P. Greeley,* Purdue University	
4:30pm	**AA2-TuA13** Spatial Atomic Layer Deposition of Hybrid Nanolaminates for High Capacity Li-ion Battery Electrodes, *E. Balder, L. Haverkate, M. Tulodziecki, F. van den Bruele, S. Unnikrishnan,* ***Paul Poodt***, TNO/Holst Center, Netherlands	
4:45pm	**AA2-TuA14** Lithium Organic Thin Films for Various Battery Components, ***Juho Heiska***, *M. Karppinen,* Aalto University, Finland	
5:00pm	**AA2-TuA15** ALD Infiltration of $LiCoO_2$ for High Rate Lithium Ion Batteries, ***Ian Povey***, *M. Modreanu, S. O'Brien,* Tyndall National Institute, Ireland; *T. Teranishi, Y. Yoshikawa, M. Yoneda, A. Kishimoto,* Okayama University, Japan	
5:15pm	**AA2-TuA16** ALD Al_2O_3 and MoS_2 Coated TiO_2 Nanotube Layers as Anodes for Lithium Ion Batteries, *H. Sopha,* University of Pardubice, Czech Republic; *A. Tesfaye,* Ecole Nationale Supérieure des Mines de Saint-Etienne, France; *R. Zazpe,* University of Pardubice, Czech Republic; *T. Djenizian,* Ecole Nationale Supérieure des Mines de Saint-Etienne, France; ***Jan Macak***, University of Pardubice, Czech Republic	
5:30pm	**Poster Session**	

Tuesday Afternoon, July 23, 2019

	Grand Ballroom H-K	
1:30pm	**AS1-TuA1** Elucidating Mechanisms of Selective ALD of Al_2O_3 by a Comparative Study of Precursors, ***Il-Kwon Oh***, *T.-L. Liu,* Stanford University; *T. Sandoval,* Technical University Federico Santa Maria; *R. Tonner,* Philipps-Universität Marburg, Germany; *S.F. Bent,* Stanford University	**Area Selective ALD** **Session AS1-TuA** **Area-Selective ALD by Area-Deactivation** **Moderators:** Rong Chen, Huazhong University of Science and Tech Jessica Kachian, Intel Corp.
1:45pm	**AS1-TuA2** Area-Selective Atomic Layer Deposition using Dodecanethiols: Comparison of Monolayer versus Multilayer, ***Tzu-Ling Liu***, Stanford University; *K. Nardi, N. Draeger, D. Hausmann,* Lam Research Corp.; *S.F. Bent,* Stanford University	
2:00pm	**AS1-TuA3** Mechanism for Breakdown in Selectivity During Area-Selective Atomic Layer Deposition of ZrO_2 on a SiO_2 Surface Functionalized with a Blocking Layer, ***Wanxing Xu***, Colorado School of Mines; *P.C. Lemaire, K. Sharma, D. Hausmann,* Lam Research Corp.; *S. Agarwal,* Colorado School of Mines	
2:15pm	**AS1-TuA4** Area Selective Chemical Vapor Deposition of Co from the Co (CO) Precursor: Use of Ammonia to Afford Dielectric-Dielectric Selectivity, ***Zhejun Zhang***, *S. Liu, G. Girolami, J. Abelson,* University of Illinois at Urbana-Champaign	
2:30pm	**AS1-TuA5** Area-Selective ALD of Silicon Oxide using Inhibitors in Four-step Cycles for Metal/Dielectric Selectivity, ***Marc Merkx***, *R. Jongen,* Eindhoven University of Technology, Netherlands; *A. Mameli,* TNO/Holst Center, Netherlands; *D. Hausmann,* Lam Research Corp.; *W.M.M. Kessels, A.J.M. Mackus,* Eindhoven University of Technology, Netherlands	
2:45pm	**AS1-TuA6** Selective Area Growth of Deactivating Polymers, ***Rudy Wojtecki***, IBM Research - Almaden; *T. Pattison,* University of Melbourne, Australia; *A. Hess, N. Arellano, A. Friz,* IBM Research - Almaden	
3:00pm	**AS1-TuA7** Area-Selective ALD of ZnO Films Patterned by Electrohydrodynamic Jet Printing of Polymers with Sub-Micron Resolution, ***Tae Cho***, *N. Farjam, C. Pannier, C. Huber, O. Trejo, C. Allemang, E. Kazyak, R. Peterson, K. Barton, N.P. Dasgupta,* University of Michigan	
3:15pm	**AS1-TuA8** Selective Deposition of Silicon Nitride, ***Han Wang***, *B. Hendrix, T. Baum,* Entegris Inc.	
3:30pm	**Break & Exhibits**	
3:45pm	**Break & Exhibits**	
4:00pm	**AS2-TuA111** Area-Selective Deposition and Smoothing of Ru by Combining Atomic Layer Deposition and Selective Etching, ***Martijn Vos***, Eindhoven University of Technology, Netherlands; *S. Chopra,* University of Texas at Austin; *M. Verheijen,* Eindhoven University of Technology, Netherlands; *J. Ekerdt,* University of Texas at Austin; *S. Agarwal,* Colorado School of Mines; *W.M.M. Kessels, A.J.M. Mackus,* Eindhoven University of Technology, Netherlands	**Area Selective ALD** **Session AS2-TuA1** **Area-Selective ALD: Combinations with Etching** **Moderators:** Silvia Armini, IMEC Dennis Hausmann, Lam Research Corp.
4:15pm	**AS2-TuA112** Single Batch Strategies for the Development of an Area Selective Deposition Process with the Deposition/Etch Approach, ***Christophe Vallée***, *M. Bonvalot,* LTM-UGA, France; *R. Gassilloud,* CEA-Leti, France; *V. Pesce, A. Chaker, S. Belahcen,* LTM-UGA, France; *N. Possémé,* CEA-Leti, France; *B. Pelissier, P. Gonon, A. Bsiesy,* LTM-UGA, France	
4:30pm	~~**AS2-TuA113** Surface Halogenation of Amorphous Carbon for Defect-free Area-Selective Deposition of Metal Oxides, ***Mikhail Krishtab***, KU Leuven, Belgium; *S. Armini,* IMEC, Belgium; *S. De Gendt,* KU Leuven/IMEC, Belgium; *R. Ameloot,* KU Leuven, Belgium~~	
4:45pm	**AS2-TuA214** Real-time Grazing Incidence Small-angle X-ray Scattering Studies of Indium Aluminum Nitride Growth, ***Jeffrey M. Woodward***, *S.G. Rosenberg,* ASEE (residing at U.S. Naval Research Laboratory); *S.D. Johnson, N. Nepal,* U.S. Naval Research Laboratory; *Z.R. Robinson,* SUNY College at Brockport; *K.F. Ludwig,* Boston University; *C.R. Eddy,* U.S. Naval Research Laboratory	**Area Selective ALD** **Session AS2-TuA2** **Late Breaking Abstracts** **Moderators:** Silvia Armini, IMEC, Dennis Hausmann, Lam Research Corp.
5:00pm	**AS2-TuA215** Expanding the Materials Library of Sequential Infiltration Synthesis: Conductive Indium and Gallium Oxides Grown in Polymers, ***Ruben Waldman***, University of Chicago; *N. Jeon, D. Mandia, O. Heinonen, S. Darling, A. Martinson,* Argonne National Laboratory	
5:15pm	~~**AS2-TuA216** Highly Efficient and Stable Organic – Inorganic Halide Perovskite Solar Cells with ALD-grown Charge Transport Layers, ***Hyunjung Shin***, Sungkyunkwan University, Republic of Korea~~	
5:30pm	**Poster Session**	

Tuesday Afternoon, July 23, 2019

	Regency Ballroom A-C	
1:30pm	**INVITED: ALE1-TuA1** Atomic Layer Etching of Nanostructures, ***Sabbir Khan,*** Niels Bohr Institute, University of Copenhagen, Denmark; *D. Suyatin,* Lund University, Sweden; *J. Sundqvist,* Fraunhofer Institute for Ceramic Technologies and Systems IKTS, Germany	**Atomic Layer Etching** **Session ALE1-TuA** **Modeling & Instrumentation I** **Moderators:** Ankur Agarwal, KLA-Tencor Angelique Raley, Tokyo Electron America Inc.
1:45pm	Invited talk continues.	
2:00pm	**ALE1-TuA3** Selectivity during Plasma ALE of Si-Compounds: Reaction Mechanism Studied by in-situ Surface Spectroscopy, ***René Vervuurt,*** ASM; *K. Nakane, T. Tsutsumi, M. Hori, N. Kobayashi,* Nagoya University, Japan	
2:15pm	**ALE1-TuA4** Chamber Vacuum Strategies to Enable High Productivity ALE, ***Declan Scanlan,*** *D. Stephenson, A. Stover,* Edwards Vacuum, Ireland	
2:30pm	**ALE1-TuA5** Mechanistic Study of the Thermal Atomic Layer Etch of Cobalt Metal Using Propene and CO, *S. Kondati Natarajan, M. Nolan,* Tyndall National Institute, Ireland; ***Patrick Theofanis,*** *C. Mokhtarzadeh, S.B. Clendenning,* Intel Corp.	
2:45pm	**ALE1-TuA6** Selective Quasi-ALE of SiO_2 over Si_3N_4 via Bottom-up Si_3N_4 Passivation: A Computational Study, ***Du Zhang,*** *Y. Tsai, Y. Shi, M. Wang,* TEL Technology Center, America, LLC	
3:00pm	**INVITED: ALE1-TuA7** Insights of Different Etching Properties between CW and ALE Processes using 3D Voxel-Slab Model, ***Nobuyuki Kuboi,*** *T. Tatsumi, J. Komachi, S. Yamakawa,* Sony Semiconductor Solutions Corp., Japan	
3:15pm	Invited talk continues.	
3:30pm	**Break & Exhibits**	
3:45pm	**Break & Exhibits**	
4:00pm	**ALE2-TuA11** First-principles Understanding of Atomic Layer Etching of Silicon Nitride using Hydrofluorocarbons, ***Gyeong Hwang,*** *E. Cheng,* University of Texas at Austin; *S. Sridhar,* TEL Technology Center, America; *P. Ventzek, A. Ranjan,* Tokyo Electron America Inc.	**Atomic Layer Etching** **Session ALE2-TuA** **Modeling & Instrumentation II** **Moderators:** Dmitry Suyatin, Lund University Tetsuya Tatsumi, Sony Semiconductor Solutions Corp.
4:15pm	**ALE2-TuA12** An Extended Knudsen Diffusion Model for Aspect Ratio Dependent Atomic Layer Etching, ***Luiz Felipe Aguinsky,*** *P. Manstetten,* TU Wien, Austria; *A. Hössinger,* Silvaco Europe Ltd., UK; *S. Selberherr, J. Weinbub,* TU Wien, Austria	
4:30pm	**ALE2-TuA13** Thermodynamics-Based Screening Approach for Atomic Layer Etching, ***Nagraj Kulkarni,*** Consultant	
4:45pm	**ALE2-TuA14** Always in Competition: Self-limiting Versus Continuous Reactions in ALD and ALEt, ***Simon D. Elliott,*** Schrödinger, Inc.; *S.K. Natarajan, R. Mullins, M. Nolan,* Tyndall National Institute, Ireland; *A. Cano, J. Clancey, S.M. George,* University of Colorado - Boulder	
5:00pm	~~**ALE2-TuA15** Variation of Etched Depth per Cycle and Removal of Reactive Species in Atomic-Layer Etching (ALE) : Molecular Dynamics Study, ***Satoshi Hamaguchi,*** *E.J. Tinacba, S. Shigeno, Y. Okada, M. Isobe, T. Ito, K. Karahashi,* Osaka University, Japan~~	
5:30 pm	**Poster Session**	

ALD Applications
Evergreen Ballroom & Foyer - Session AA1-TuP
Energy Harvesting and Storage Poster Session
5:30pm

~~**AA1-TuP1** Study on Atomic Layer Deposited Al_2O_3, TiO_2 and ZnO for the Application in Silicon Photovoltaics, ***Arun Haridas,*** *M.G. Sreenivasan,* Hind High Vacuum Company Pvt. Ltd., India; *A. Antony,* Indian Institute of Technology Bombay, India~~

AA1-TuP2 Nitrogen-Doped TiO_2 Film Deposited using Plasma-Enhanced Atomic Layer Deposition to Improve the Electrical Conductivity for Surface Passivation of Crystalline Silicon, *E.-J. Song,* Korea Institute of Materials Science, Republic of Korea; *J.-H. Ahn,* Korea Maritime and Ocean University, Republic of Korea; ***Jung-Dae Kwon,*** Korea Institute of Materials Science, Republic of Korea

AA1-TuP3 Multilayer Encapsulation for Highly Stable Perovskite Solar Cells with Atomic Layer Deposited Al_2O_3 and Chemical Vapor Deposited Flowable Oxide, ***Jungwoo Kim,*** *H. Hwangbo, S.J. Kim, J.H. Jang, H.C. Tran Vo, H. Chae,* Sungkyunkwan University (SKKU), Republic of Korea

AA1-TuP5 Oxide Buffer Layers for Perovskite Solar Cells Grown with a 200 mm Commercial ALD System Using Low-Temperature Process, *P. Rajbhandari,* ***Tara Dhakal,*** Binghamton University

AA1-TuP6 Ultra-thin Nickel Films for Energy Harvesting Applications, ***Ken Bosnick,*** *P. Motamedi,* National Research Council Canada, Canada; *K. Cadien,* University of Alberta, Canada; *K. Harris, J.-Y. Cho,* National Research Council Canada, Canada

AA1-TuP7 MoNx-Deposited on High-surface N-doped Carbon Coated-Carbon Cloth Substrates: The Best Possible Option for ALD in View of Energy Storage Application, *S.Y. Sawant, D.K. Nandi, R. Rahul, S.-H. Kim,* ***Moo Hwan Cho,*** Yeungnam University, Republic of Korea

AA1-TuP8 ALD Coatings for Nano Imprint Masks, ***Thomas Seidel,*** Seitek50

AA1-TuP9 The Investigation of Al_2O_3 Passivation Characteristics in the Condition of Growth Temperature and Ozone Concentration, ***Young Joon Cho,*** *H.S. Chang,* Chungnam National University, Republic of Korea

AA1-TuP10 Effect of Al2O3 Passivation on n-type Si Solar Cell with Passivated Emitter and Rear Cell (PERC), ***Kiryun Kim,*** *H.S. Chang,* Chungnam National University, Republic of Korea

AA1-TuP11 High Quality CaF_2 from a New ALD Process: Enabling New Approaches in Battery Technology and Optical Applications, ***Max Gebhard,*** *A. Mane, J.W. Elam,* Argonne National Laboratory

AA1-TuP12 Properties of Molybdenum Oxide Deposited by Plasma Enhanced Atomic Layer Deposition for High Efficiency Solar Cells, ***Taewan Lim,*** *H.S. Chang,* Chungnam National University, Republic of Korea

AA1-TuP13 Understanding and Mitigating F Migration in ALD Nanocomposite Coatings, ***Anil Mane,*** *M. Gebhard, J.W. Elam,* Argonne National Laboratory; *M. Popecki, T. Cremer,* Incom Inc.; *M. Minot,* incom

AA1-TuP14 Ultrathin Metal Oxide Passivation by Atomic Layer Deposition Enhances Stability and Performance of Visible Solar Water Splitting on Solution-Processed Organic Semiconductor Thin Films, *L. Wang, D. Yan,* Stony Brook University; *D. Shaffer,* Brookhaven National Laboratory; *X. Ye,* Stony Brook University; *B. Layne, J. Concepcion, M. Liu,* ***Chang-Yong Nam,*** Brookhaven National Laboratory

AA1-TuP15 Enhancement of Photovoltaic Efficiency using a Novel Nickel-4 Mercaptophenol Hybrid Interfacial Layer, ***Jinseon Park,*** *N.V. Long, H. Thu,* Hanyang University, Republic of Korea

AA1-TuP16 Enhancement of Photovoltaic Properties of Metal/III-V Schottky Solar Cells using Al2O3 Anti-Reflection and Passivation Layer, *A. Ghods, V. Saravade, C. Zhou,* ***Ian Ferguson,*** Missouri University of Science and Technology

AA1-TuP17 Investigation of ALD-grown i-ZnO Buffer Layer Properties for CIGS Solar Cell Application, ***Jeha Kim,*** *V. Arepalii,* Cheongju University, Republic of Korea; *W.-J. Lee, Y.-D. Chung,* Electronics and Telecommunications Research Institute, Republic of Korea

AA1-TuP18 Atomic Layer Deposited Zirconium-doped ZnO Transparent Conductive Oxides for Silicon Solar Cells, ***Geedhika Kallidil Poduval,*** *M.A. Hossain, B. Hoex,* University of New South Wales, Australia

AA1-TuP19 Atomic Layer Deposition of Few-Atom Cluster Arrays for Solar Fuel Catalysis, ***David Mandia,*** *N. Guisinger, A. Martinson,* Argonne National Laboratory

ALD Applications
Evergreen Ballroom & Foyer - Session AA2-TuP
Microelectronics Poster Session
5:30pm

AA2-TuP1 Chemically and Mechanically Activated Carbonaceous Materials for Supercapacitor, *D.V. Lam, J.-H. Kim,* ***Seung-Mo Lee,*** Korea Institute of Machinery and Materials, South Korea

~~**AA2-TuP2** Diamond Field Effect Transistors with Different Gate Lengths of HfO_2 Deposited by Atomic Layer Deposition, ***Changzhi Gu,*** Institute of Physics, Chinese Academy of Sciences, China~~

AA2-TuP3 Atomic Layer Deposition of IGZO Thin Films for BEOL Applications, ***Shóna Doyle,*** Tyndall National Institute, Ireland

AA2-TuP5 High Voltage MIM Capacitor based on ALD Deposited Crystalline $HfAlO_x$ Film, ***Valentina Korchnoy,*** Technion - Israel Institute of Technology, Israel; *M. Lisiansky,* Tower Semiconductor Ltd., Israel; *I. Popov, V. Uvarov,* The Hebrew University of Jerusalem, Israel; *B. Meyler,* Technion - Israel Institute of Technology, Israel

AA2-TuP6 Improved Performance of GaN Metal-Oxide-Semiconductor Capacitors byPplasma ALD of AlN Interlayer, ***Dilini Hemakumara,*** *X. Li, K. Floros, S. Cho,* University of Glasgow, UK; *I. Guinney, C. Humphreys,* University of Cambridge, UK; *I. Thayne,* University of Glasgow, UK; *A. O'Mahony,* Oxford Instruments Plasma Technology; *H. Knoops,* Oxford Instruments Plasma Technology, UK; *D. Moran,* University of Glasgow, UK

~~**AA2-TuP7** 2-Dimensional Perovskite Oxide Thin Films Deposited by ALD for High-k Application, ***Seung-Won Lee,*** Korea Maritime and Ocean University, Republic of Korea; *C. M. Kim, S. H. Kwon,* Pusan National University, Republic of Korea~~

AA2-TuP8 High Performance Atomic Layer Deposition (ALD) of Gate Dielectrics for 4H-SiC Power Device Application, *B. Lee, M. Kang,* North Carolina State University; ***Adam Bertuch,*** Veeco-CNT; *V. Misra,* North Carolina State University

~~**AA2-TuP9** Atomic Layer Deposted TiO_2-Based Memristors using In-situ Fabricated Al Doped ZnO Thin Film as Electrodes, ***Kai Zhang,*** *P. Lin,* Old Dominion University; *A. Pradhan,* Advance Material Solution LLC; *H. Baumgart,* Old Dominion University~~

AA2-TuP10 Homogeneously Doped Atomic Layer Deposition Zinc Tin Oxide Thin Films for Improving Contact Resistance in Semiconductor Device Applications, ***Alex Ma,*** University of Alberta, Canada; *T. Muneshwar,* Synthergy Inc., Canada; *D. Barlage, K. Cadien,* University of Alberta, Canada

~~**AA2-TuP11** AlGaN/GaN Layers Obtained by Atomic Layer Deposition Targeting Thin Film HEMT, ***Joaquin Alvarado,*** *M. Chávez,* Benemérita Universidad Autónoma de Puebla, Mexico; *S. Gallardo,* CINVESTAV-IPN, Mexico; *Y. Sheng, D. Muenstermann,* Lancaster University, UK~~

AA2-TuP12 High-Temperature Thermal Stability of ALD-TiN Metal Gate on *In-situ* Al_2O_3/Y_2O_3/(In)GaAs(001): Toward the Self-Aligned Gate-First Process, ***Lawrence Boyu Young,*** *H.-W. Wan, J.-H. Huang, K.-Y. Lin, J. Liu, Y.-H. Lin,* National Taiwan University, Republic of China; *J. Kwo,* National Tsing Hua University, Republic of China; *M. Hong,* National Taiwan University, Republic of China

AA2-TuP13 Identification of Interfacial Defect in ALD Grown Al_2O_3/GeO_x/Ge Gate Stack, ***Jinjuan Xiang,*** *L. Zhou, X. Wang, X. Ma, T. Li, W. Wang,* Institute of Microelectronics of Chinese Academy of Sciences, China

AA2-TuP15 Effect of Metal-insulator Interface on Dielectric Properties of Ultrathin Al_2O_3 and MgO Fabricated using *In-situ* Sputtering and Atomic Layer Deposition, ***Jagaran Acharya,*** *J. Wilt, R. Goul, B. Liu, J. Wu,* The University of Kansas

AA2-TuP16 Thermal and Plasma ALD Al_2O_3 Gate Insulator for GaN Electronic Devices Characterized by CV-Stress Measurements, ***Nicole Bickel,*** *E. Bahat Treidel, I. Ostermay, O. Hilt, O. Krüger,* Ferdinand-Braun-Institut, Germany; *F. Naumann, H. Gargouri,* SENTECH Instruments GmbH, Germany; *J. Würfl, G. Tränkle,* Ferdinand-Braun-Institut, Germany

AA2-TuP17 Variable Morphology Highly-Conformal Diffusion Barriers for Advanced Memory and Logic Applications, ***Hae Young Kim,*** *S. Rathi, B. Nie, N. Naghibolashrafi, Y. Okuyama, S. Chugh, J. Heo, S.H. Jung, J. Mack, N. Mukherjee,* Eugenus, Inc.

~~**AA2-TuP18** Room Temperature Deposition of Hafnium Oxide by Atomic Layer Deposition for Gating Applications, ***Pragya Shekhar,*** *S. Shamim, S. Hartinger, J. Kleinlein, R. Schlereth, H. Buhmann, L. Molenkamp,* University of Wuerzburg, Germany~~

AA2-TuP19 Influence of Surface Cleaning Process on Initial Growth of ALD-Al_2O_3 and Electrical Properties of Pt/Al_2O_3/*β*-Ga_2O_3 MOS Capacitors, ***Masafumi Hirose***, Shibaura Institute of Technology, Japan; *T. Nabatame*, National Institute for Materials Science, Japan; *E. Maeda*, Shibaura Institute of Technology, Japan; *A. Ohi, N. Ikeda, Y. Irokawa, Y. Koide*, National Institute for Materials Science, Japan; *H. Kiyono*, Shibaura Institute of Technology, Japan

~~**AA2-TuP20** Reliable Gate Stack Development Employing Plasma Assisted Atomic Layer Deposited HfO_xN_y on InGaAs Substrate, ***Sukeun Eom***, *M. Kong, K. Seo*, Seoul National University, Republic of Korea~~

ALD Applications
Evergreen Ballroom & Foyer - Session AA3-TuP
Catalysis and Sensor Applications Poster Session
5:30pm

AA3-TuP1 Highly Dispersed Uniform Pt Catalysts on Carbon Support by Atomic Layer Deposition with Fluidized Bed Reactor(FBR)., ***Jung-Yeon Park***, *W.P. Hong, S.-J. Oh*, Hyundai Motor Group, Republic of Korea; *W.-J. Lee, S.-H. Kwon*, Pusan National University, Republic of Korea

~~**AA3-TuP3** Stabilizing Ultrasmall Colloidal Platinum Diphosphide (PtP_2) Nanocrystals with Atomic Layer Deposition Oxide for Neutral H_2O_2 Electrosynthesis, ***Hui Li***, *S. Geyer*, Wake Forest University~~

AA3-TuP5 Synthesis of Core Shell Nanocatalysts using Atomic Layer Deposition with Fluidized Bed Reactor for PEMFC, ***Seung-Jeong Oh***, *W.P. Hong, J.Y. Park*, Hyundai Motor Group, Republic of Korea; *W.-J. Lee, S.-H. Kwon*, Pusan National University, Republic of Korea

~~**AA3-TuP6** Porous Nanomembranes Grown by Atomic Layer Deposition: Self-Rolling in Solvent and their Sensing Applications, ***F. Ma***, *Y.T. Zhao, G. Huang, Yong Feng Mei*, Fudan University, China~~

AA3-TuP7 Fabrication and Characterization of Atomic Layer Deposited ZnO-based Ultra-thin Films for Hydrogen Sensing, ***Yan-Qiang Cao***, *A.-D. Li*, Nanjing University, China

ALD Applications
Evergreen Ballroom & Foyer - Session AA4-TuP
Protective Coatings, Barrier Films, Membranes and Flexible Substrates Poster Session
5:30pm

AA4-TuP1 ALD for Membrane Applications, ***Matthieu Weber***, *M. Bechelany*, Institut Européen des Membranes, France

AA4-TuP2 Nano-Hardness of ALD Films, ***James Daubert***, *W. Sweet, J. Kelliher*, Northrop Grumman

AA4-TuP3 High Acid Corrosion Resistance of Nb_2O_5 Thin Film Deposited by Room Temperature ALD, ***Kazuki Yoshida***, *K. Saito, M. Miura, K. Kanomata, B. Ahmmad, S. Kubota, F. Hirose*, Yamagata University, Japan

AA4-TuP4 Effects of Composition Ratios on Mechanical and Electrical Properties of AZO – Zincone Composite Thin Film Deposited on Transparent Polyimide Film Using Atomic and Molecular Layer Depositions., ***Seung Hak Song***, *B.-H. Choi*, Korea University, Republic of Korea

AA4-TuP5 Room-temperature Atomic Layer Deposition of Aluminosilicate Thin Film on Flexible Films, ***Yoshiharu Mori***, *K. Yoshida, K. Kanomata, M. Miura, B. Ahmmad Arima, S. Kubota, F. Hirose*, Yamagata University, Japan

AA4-TuP6 ALD Layers for Reduced Wear on Micro Cutting Tools, *T. Junghans*, ***Hans-Dieter Schnabel***, Westsächsische Hochschule Zwickau, Germany

AA4-TuP7 Fabrication of Atomic Layer Deposited Alumina as Protective Coating of Silver, ***Gwon Deok Han***, *J.S. Park, J. Koo, J.H. Shim*, Korea University, Republic of Korea

AA4-TuP8 Characterization of Laminated Thin Films for Encapsulation using Single Si Precursor by PEALD, ***Joong Jin Park***, *S.D. Lee, H.-D. Lim, S.J. Jang, S.G. Kim, G.J. Park, S.I. Lee, M.W. Kim*, DNF Co. Ltd, Republic of Korea

AA4-TuP9 Low-cost Fabrication of Flexible Transparent Electrodes based on Sprayed Nanocomposites Silver Nanowires and Al Doped ZnO Deposited by Spatial ALD, *V.H. Nguyen, J. Resende, D. Papanastasiou, C. Jimenez, D. Bellet*, LMGP Grenoble INP/CNRS, France; *S. Aghazadehchors*, LMGP, France; *N.D. Nguyen*, Université de Liège; ***David Muñoz-Rojas***, LMGP Grenoble INP/CNRS, France

~~**AA4-TuP10** Nanomechanical Properties of Crystalline Anatase Titanium Oxide Films Synthesized using Atomic Layer Deposition, ***Yousuf Mohammed***, *P. Lin, K. Zhang, H. Baumgart, A. Elmustafa*, Old Dominion University~~

AA4-TuP11 Encapsulation of Magnetic Nanostructures by ALD for Improved Stability and Performance, ***Devika Choudhury***, *Y. Zhang, K. Gao, A. Mane, J.W. Elam*, Argonne National Laboratory

AA4-TuP12 Diffusion Barrier Properties of ALD TiSiN Films, ***Jerry Mack***, *J. Heo, S. Chugh, H.Y. Kim, S. Rathi, N. Mukherjee*, Eugenus, Inc.

ALD Applications
Evergreen Ballroom & Foyer - Session AA5-TuP
Emerging Applications Poster Session
5:30pm

AA5-TuP1 Bottom up Stabilization of Perovskite Quantum Dots LED via Atomic Layer Deposition, ***Rong Chen***, *K. Cao, Q. Xiang, B. Zhou*, Huazhong University of Science and Technology, China

AA5-TuP2 ALD Bilayers for X-ray Windows with Long Lifetime, ***Agnieszka Kurek***, *Y. Shu*, Oxford Instruments Plasma Technology; *H. Knoops*, Oxford Instruments Plasma Technology, UK; *A. O'Mahony, O. Thomas, R. Gunn*, Oxford Instruments Plasma Technology; *Y. Alivov, C. McKenzie, B. Grigsby, A. Degtyaryov*, Oxford Instruments X-ray Technology

AA5-TuP3 ALD for 3D Nano MEMS Applications, ***Dorothee Dietz***, Fraunhofer Institute for Microelectronic Circuits and Systems IMS, Germany

AA5-TuP4 Tribological Properties of Plasma Enhanced Atomic Layer Deposition TiMoN, ***Mark Sowa***, Veeco-CNT; *A. Kozen*, U.S. Naval Research Laboratory; *B. Krick, N. Strandwitz*, Lehigh University

AA5-TuP5 Thickness Optimization of Alumina Thin Film for Microchannel Plate Detector, ***Baojun Yan***, *S. Liu*, Institute of High Energy Physics, Chinese Academy of Sciences, China

~~**AA5-TuP6** Optical Coatings Deposited on Nonlinear Crystals by Atomic Layer Deposition, ***Ramutis Drazdys***, *R. Buzelis, M. Drazdys*, Center for Physical Sciences and Technology, Lithuania~~

AA5-TuP7 Atomic Layer Deposition of Nickel and Nickel Oxide Thin-Films for Astronomical X-ray Optics Applications, ***Hossein Salami***, *A. Uy, A. Vadapalli*, University of Maryland; *V. Dwivedi*, NASA Goddard Space Flight Center; *R. Adomaitis*, University of Maryland

AA5-TuP8 Atomic Layer Deposition and Chemical Vapor Deposition of Zirconium Boride for Various Applications: New Work Function, Barrier Metal, Hard Mask and Area Selective Deposition, ***Jun-Hee Cho***, *J.J. Park, W.-M. Chae, J.-H. Park, S.I. Lee, M.W. Kim*, DNF Co. Ltd, Republic of Korea

~~**AA5-TuP9** Comparative Study of $Mo_{1-x}W_xS_2$ Alloy Gas Sensor by Atomic Layer Deposition, ***Minjoo Lee***, *Y. Kim, J. Park, H. Kim*, Yonsei University, Republic of Korea~~

AA5-TuP10 Fabrication of High-Aspect-Ratio Nanometric Gold Gratings, *O. Makarova*, Creatv MicroTech Inc; ***Ralu Divan***, *L. Stan*, Argonne National Laboratory; *C.-M. Tang*, Creatv MicroTech Inc

Area Selective ALD
Evergreen Ballroom & Foyer - Session AS-TuP
Area Selective ALD Poster Session
5:30pm

AS-TuP1 Laterally-Structured Dielectrics by Area-Selective Atomic-Layer-Deposition on 3D Substrates, ***Philip Klement***, *D. Anders, F. Michel, J. Schörmann, S. Chatterjee*, Justus Liebig University Giessen, Germany

AS-TuP2 Light Assisted Area Selective Atomic Layer Deposition on Plasmonic Nanoantennas, ***Chengwu Zhang***, *T. Gao, B. Willis*, University of Connecticut

AS-TuP3 Area-Specific Atomic Layer Deposition (ALD) of Cobalt As Mediated by Thermally Induced Dehydrocoupled Self-Assembled Monolayers (SAMs), ***Barry Arkles***, *J. Goff, C. Brick*, Gelest, Inc.; *A. Kaloyeros*, SUNY Polytechnic Institute

AS-TuP4 Investigation of *In-situ* Surface Cleaning of Cu Films using O_3/O_2 and N_2H_4, ***Su Min Hwang***, *A.L.N. Kondusamy, Q. Zhiyang, H.S. Kim, L.F. Peña, K. Tan, J. Veyan*, University of Texas at Dallas; *D. Alvarez, J. Spiegelman*, RASIRC; *J. Kim*, University of Texas at Dallas

AS-TuP5 Area-Selective Deposition of SiO_2 based on Spatial ALD with Interleaved Etching Steps to Obtain High Selectivity, ***Alfredo Mameli***, TNO/Holst Center, Netherlands; *F. Roozeboom*, Eindhoven University of Technology and TNO, Netherlands; *P. Poodt*, TNO/Holst Center, Netherlands

AS-TuP6 Defect Mitigation Solution for Area-Selective Atomic Layer Deposition of Ru on TiN/SiO_2 Nanopatterns, *J. Soethoudt,* KU Leuven – University of Leuven/IMEC, Belgium*; F. Grillo,* ETH Zurich, Switzerland*; E. Marques, R. van Ommen,* Delft University of Technology, Netherlands*; B. Briggs, H. Hody, V. Spampinato, A. Franquet, B.T. Chan,* ***Annelies Delabie,*** IMEC, Belgium

Nanostructure Synthesis and Fabrication
Evergreen Ballroom & Foyer - Session NS-TuP
Nanostructures Synthesis and Fabrication Poster Session
5:30pm

NS-TuP1 Molybdenum Disulfides and Diselenides by Atomic Layer Deposition, ***Raul Zazpe****, J. Prikryl, M. Krbal, J. Charvot, F. Dvorak, F. Bures, J. Macak,* University of Pardubice, Czech Republic

NS-TuP2 Wafer-scale MoS_2 Thin Film Deposition via H_2S Plasma Sulfurization of ALD-grown MoO_3 at Low Temperature, ***Jeong-Hun Choi****,* Korea Maritime and Ocean University, Republic of Korea

NS-TuP3 ALD-based Synthesis of Few-layer Transition Metal Disulfides with Wafer-scale Uniformity for Device Integration, ***Tao Chen****, Y. Wang, H. Zhu, L. Chen, Q.Q. Sun, D.W. Zhang,* Fudan University, China

NS-TuP4 Overcoming Agglomeration and Adhesion in Particle ALD, ***Benjamin Greenberg****, J. Wollmershauser, B. Feigelson,* U.S. Naval Research Laboratory

NS-TuP5 Density Function Theory for Nucleation of MoF_6 with Oxide Surfaces in Atomic Layer Deposition of MoS_2, ***Matthew Lawson****,* Boise State University

Note: ALE Posters Will Remain Posted All Week

Wednesday Morning, July 24, 2019

	Grand Ballroom A-C	
8:00am	**EM1-WeM1** Molecular Layer Deposition of Titanicone Films using TiCl and Fumaric or Maleic Acid: Growth Mechanism and Ambient Stability, ***Yan-Qiang Cao**, A.-D. Li,* Nanjing University, China	**Emerging Materials** **Session EM1-WeM** **Molecular Layer Deposition** **Moderators:** Stacey F. Bent, Stanford University Charles L. Dezelah, ASM
8:15am	**EM1-WeM2** Temperature Dependent Surface Chemistry in Molecular Layer Deposition of Polyimide on Cu and Si, ***Chao Zhang**, M. Leskelä, M. Ritala,* University of Helsinki, Finland	
8:30am	**EM1-WeM3** Integrated MLD Supercycle for the Direct Deposition of Zeolitic Imidazolate Framework Films, ***Alexander John Cruz**, I. Stassen, R. Ameloot,* KU Leuven, Belgium	
8:45am	**EM1-WeM4** Understanding Molecular Layer Deposition Nucleation Mechanisms in Polyurea via Time Domain Thermoreflectance, ***Rachel Nye**, M. Fusco,* North Carolina State University*; E. Radue, A. Kelliher, P. Hopkins,* University of Virginia*; G.N. Parsons,* North Carolina State University	
9:00am	**EM1-WeM5** Molecular Layer Deposition of Indicone Thin film using Indium Precursor and Hydroquinone, ***Seung-Hwan Lee**, G.H. Baek, J.-H. Lee,* Hanyang University, Republic of Korea*; T.T. Ngoc Van, B. Shong,* Hongik University, Republic of Korea*; J.-S. Park,* Hanyang University, Republic of Korea	
9:15am	**EM1-WeM6** Air Stable Alucone Thin Film Deposited by Molecular Layer Deposition using Hetero Bifunctional Organic Reactant, ***GeonHo Baek**, S.-H. Lee, J.-H. Lee, J.-S. Park,* Hanyang University, Republic of Korea	
9:30am	**EM1-WeM7** Molecular Layer Deposition of "Magnesicone", a Magnesium-based Hybrid Material, as a Matrix Material for Solid Composite Electrolytes, *Jeroen Kint, F. Mattelaer, M. Minjauw,* Ghent University, Belgium*; P. Vereecken,* IMEC, Belgium*; J. Dendooven, **C. Detavernier**,* Ghent University, Belgium	
9:45am	**EM1-WeM8** Molecular Layer Deposition of Polyamide Films on Particles Using a Rotating Cylinder Reactor, ***Tyler Myers**, S.M. George,* University of Colorado - Boulder	
10:00am	**Break & Exhibits**	
10:15am	**Break & Exhibits**	
10:30am	**Break & Exhibits**	
10:45am	**EM2-WeM12** Vapor Phase Infiltration: A Route for Making Insulating Polymer Fibers Conductive, ***Mato Knez**,* CIC nanoGUNE, Spain*; I. Azpitarte,* CTECHnano, Spain	**Emerging Materials** **Session EM2-WeM** **Organic-Inorganic Hybrid Materials** **Moderators:** Gregory N. Parsons, North Carolina State University Jonas Sundqvist, Fraunhofer Institute for Ceramic Technologies and Systems IKTS
11:00am	**EM2-WeM13** Vapor Phase Infiltration of Metal Oxides into Microporous Polymers for Organic Solvent Separation Membranes, ***Emily McGuinness**, F. Zhang, Y. Ma, R. Lively, M. Losego,* Georgia Institute of Technology	
11:15am	**EM2-WeM14** ZnO-Infiltrated Hybrid Polymer Thin Films with Enhanced Gravimetric Water and Oxygen Vapor Sensing Properties, *E. Muckley, L. Collins, A. Ievlev,* Oak Ridge National Laboratory*; X. Ye, K. Kisslinger,* Brookhaven National Laboratory*; B. Sumpter, N. Lavrik,* Oak Ridge National Laboratory*; **Chang-Yong Nam**,* Brookhaven National Laboratory*; I. Ivanov,* Oak Ridge National Laboratory	
11:30am	**EM2-WeM15** Physically Interpenetrated Organic-Inorganic Sub-Surface Layers Created via Vapor Phase Infiltration for Improved Film Adhesion, ***Mark Losego**, S. Dwarakanath, R. Tummala,* Georgia Institute of Technology	
11:45am	**EM2-WeM16** Inorganic-Organic Thin Film Layer-Structures and Thermal Conductivity, ***Fabian Krahl**,* Aalto University, Finland*; A. Giri, P. Hopkins,* University of Virginia*; M. Karppinen,* Aalto University, Finland	
12:00pm	**Lunch & Exhibits**	

Wednesday Morning, July 24, 2019

	Grand Ballroom E-G	
8:00am	**AM1-WeM1** Impact of Operating Parameters on Precursor Separation in "Air Hockey" Spatial Atomic Layer Deposition Reactor, ***John Grasso**, B. Willis,* University of Connecticut	**ALD for Manufacturing** **Session AM1-WeM** **Spatial ALD, Fast ALD, and Large-Area ALD** **Moderators:** John F. Conley, Jr., Oregon State University Paul Poodt, TNO/Holst Center
8:15am	**AM1-WeM2** Plasma Enhanced Spatial ALD of Silver Thin Films at Atmospheric Pressure, ***Tim Hasselmann**,* University of Wuppertal, Germany*; N. Boysen,* Ruhr University Bochum, Germany*; D. Theirich,* University of Wuppertal, Germany*; A. Devi,* Ruhr University Bochum, Germany*; T. Riedl,* University of Wuppertal, Germany	
8:30am	**INVITED: AM1-WeM3** Low Temperature Spatial PEALD of Silicon Nitride Films from Aminosilane Precursors and DC Direct Plasma, ***Eric Dickey**,* Lotus Applied Technology	
8:45am	Invited talk continues.	
9:00am	**AM1-WeM5** Development and Characterization of an Atmospheric Pressure Plasma Reactor Compatible with Open-Air Spatial ALD, *H. Rabat, F. Zoubian, O. Aubry, N. Dumuis, S. Dozias,* GREMI Université d'Orléans/CNRS, France*; C. Masse de la Huerta, A. Sekkat, V.H. Nguyen,* LMGP Grenoble INP/CNRS, France*; M. Bonvalot, C. Vallée,* LTM-UGA, France*; D. Hong,* GREMI Université d'Orléans/CNRS, France*; **David Muñoz-Rojas**,* LMGP Grenoble INP/CNRS, France	
9:15am	**AM1-WeM6** Fast Plasma ALD Employing de Laval Nozzles for High Velocity Precursor Injection, ***Abhishekkumar Thakur**, J. Sundqvist,* Fraunhofer Institute for Ceramic Technologies and Systems IKTS, Germany*; S. Wege,* Plasway Technologies GmbH, Germany	
9:30am	**AM1-WeM7** Development of a Meter Scale ALD Optical Coating Tool for Astronomical Mirror (and other) Applications, *D. Fryauf,* University of California Santa Cruz*; A. Phillips,* University of California Observatories*; A. Feldman,* Structured Material Industries, Inc.*; N. Kobayashi,* University of California Santa Cruz*; **Gary Tompa**,* Structured Material Industries, Inc.	
9:45am	**AM1-WeM8** From Wet-lab to Cleanroom: An Integrated ALD-CVD Process for the Large-area Deposition of Ultrathin Zeolitic Imidazolate Framework Films, ***Ivo Stassen**, A.J. Cruz, R. Ameloot,* KU Leuven, Belgium	
10:00am	**Break & Exhibits**	
10:15am	**Break & Exhibits**	
10:30am	**Break & Exhibits**	
10:45am	**EM3-WeM12** Atomic Layer Epitaxy of Zinc Oxide on C-plane Sapphire from Diethylzinc and Water using Pulsed-Heating Atomic Layer Deposition, ***Brandon Piercy**, M. Losego,* Georgia Institute of Technology	**Emerging Materials** **Session EM3-WeM** **Epitaxial Growth and III-V Materials** **Moderator:** John Ekerdt, University of Texas at Austin
11:00am	**EM3-WeM13** Growth of AlN Barriers in Al/AlN/Al SIS Josephson Junctions by Low Temperature Atomic Layer Epitaxy, ***Charles Eddy, Jr.**,* U.S. Naval Research Laboratory*; D.J. Pennachio, J. Lee, A. McFadden,* University of California, Santa Barbara*; S.G. Rosenberg,* U.S. Naval Research Laboratory*; Y.H. Chang, C.J. Palmstrom,* University of California, Santa Barbara	
11:15am	**EM3-WeM14** Investigating Plasma Parameters and Influence of Argon to the Crystallinity of GaN Films Grown by Plasma-Assisted ALD, ***Deepa Shukla**, I. Saidjafarzoda, A. Mohammad, B. Brian Willis, N. Biyikli,* University of Connecticut	
11:30am	**EM3-WeM15** Ultrathin GaN Epilayer by Low-temperature Atomic Layer Annealing and Epitaxy, ***Wei-Chung Kao**, W.-H. Lee, Y.-T. Yin,* National Taiwan University, Republic of China*; J.-J. Shyue,* Academia Sinica*; H.-C. Lin, M.J. Chen,* National Taiwan University, Republic of China	
11:45am	~~**EM3-WeM16** High Quality ALD Formation of Group-III Nitrides and their Applications in FTO-based Thin Film Solar Cells, ***Xinhe Zheng**, H. Wei, P. Qiu, M. Peng, S. Liu, Y. He, Y. Song, Y. An,* University of Science and Technology Beijing, China~~	
12:00pm	**Lunch & Exhibits**	

Wednesday Morning, July 24, 2019

	Grand Ballroom H-K	
8:00am	**INVITED: AA1-WeM1** ALD/ALE Process in Commercially Available Leading-Edge Logic and Memory Devices, ***Rajesh Krishnamurthy***, TechInsights	**ALD Applications** **Session AA1-WeM** **ALD for Memory Applications II** **Moderators:** Seung Wook Ryu, SK Hynix
8:15am	Invited talk continues.	
8:30am	**AA1-WeM3** Atomic Layer Deposited Crystalline Zinc Oxide for Silver-based Ultra-Steep Threshold Switching Selector, ***Harrison Sejoon Kim***, *A. Sahota, J. Mohan, H. Hernandez-Arriaga, J. Kim,* The University of Texas at Dallas	
8:45am	**AA1-WeM4** ALD Ge-Se-Te OTS Selectors with Controlled Composition for PCM Applications, ***Valerio Adinolfi***, *L. Cheng, R. Clarke, S. Balatti, K. Littau,* Intermolecular, Inc.	
9:00am	**AA1-WeM5** Pulsed CVD of Amorphous GeSe for Application as OTS Selector, *A. Haider,* IMEC, Belgium; *Shaoren Deng,* ASM, Belgium; *E. Schapmans,* IMEC, Belgium; *J.W. Maes,* ASM, Belgium; *J.-M. Girard,* Air Liqude Advanced Materials, France; *G. Khalil,* imec; *G.S. Kar, L. Goux, R. Delhougne,* IMEC; ***M. Caymax***, IMEC, Belgium	
9:15am	**INVITED: AA1-WeM6** Thin Film Challenges in 3D NAND Scaling, ***Jessica Kachian***, *D. Pavlopoulos, D. Kioussis,* Intel Corporation	
9:30am	Invited talk continues.	
9:45am		
10:00am	**Break & Exhibits**	
10:15am	**Break & Exhibits**	
10:30am	**Break & Exhibits**	
10:45am	**INVITED: AA2-WeM12** The Journey of ALD High-k Metal Gate from Research to High Volume Manufacturing, ***Dina Triyoso***, *R. Clark, S. Consiglio, K. Tapily, C. Wajda, G. Leusink,* TEL Technology Center, America, LLC	**ALD Applications** **Session AA2-WeM** **ALD for ULSI Applications I** **Moderators:** Ravindra Kanjolia, EMD Performance Materials Jae Hyoung Choi, Samsung Electronics
11:00am	Invited talk continues.	
11:15am	**AA2-WeM14** Effects of Er Doping on Structural and Electrical Properties of HfO_2 Grown by Atomic Layer Deposition., ***Soo Hwan Min***, *B.-E. Park, C.W. Lee,* Yonsei University, Republic of Korea; *W. Noh,* Air Liquide Laboratories Korea, South Korea; *I.-K. Oh,* Yonsei University, Republic of Korea; *W.-H. Kim,* Hanyang University, Republic of Korea; *H. Kim,* Yonsei University, Republic of Korea	
11:30am	**AA2-WeM15** Improvement of Electrical Performances of Atomic Layer Deposited ZrO_2 MIM Capacitors with Ru Bottom Electrode, ***Jaehwan Lee***, *B.-E. Park,* Yonsei University, Republic of Korea; *W. Noh,* Air Liquide Laboratories Korea, South Korea; *I.-K. Oh,* Yonsei University, Republic of Korea; *W.-H. Kim,* Hanyang University, Republic of Korea; *H. Kim,* Yonsei University, Republic of Korea	
11:45am	**AA2-WeM16** Perfecting ALD-Y_2O_3/GaAs(001) Interface with Ultra-High Vacuum Annealing, *Keng-Yung Lin, Y.-H. Lin,* ***W.-S. Chen***, *H.-W. Wan, L.B. Young,* National Taiwan University, Republic of China; *C.-P. Cheng,* National Chia-Yi University, Republic of China; *T.-W. Pi,* National Synchrotron Radiation Research Center, Republic of China; *J. Kwo,* National Tsing Hua University, Republic of China; *M. Hong,* National Taiwan University, Republic of China	
12:00pm	**Lunch & Exhibits**	

Wednesday Morning, July 24, 2019

	Regency Ballroom A-C	
8:00am	**INVITED: ALE1-WeM1** ALD and Etch Synergy to Enable the Next Scaling Innovations, ***Angelique Raley***, *K.L. Lee, X. Sun, Q. Lou, Y.T. Lu, M. Edley, S. Oyola-Reynoso, P. Ventzek, R. Clark, P. Biolsi, H. Masanobu, A. Ranjan,* TEL Technology Center, America, LLC	**Atomic Layer Etching** **Session ALE1-WeM** **Integration & Application of ALE** **Moderators:** Wei Tian, Applied Materials
8:15am	Invited talk continues.	
8:30am	**INVITED: ALE1-WeM3** On the Role of Individual Etching Components in Selective Atomic Layer Processing: Etch and Deposit to Obtain High Selectivity, ***Alfredo Mameli***, TNO/Holst Center, Netherlands; *F. Roozeboom,* Eindhoven University of Technology and TNO, Netherlands; *P. Poodt,* TNO/Holst Center, Netherlands	
8:45am	Invited talk continues.	
9:00am	**ALE1-WeM5** Area-Selective Deposition of TiO_2 on Various Surfaces by Isothermal Integration of Thermal TiO_2 ALD and ALE, ***Seung Keun Song***, *G.N. Parsons,* North Carolina State University	
9:15am	**ALE1-WeM6** Limited Dose ALE and ALD Processes for Local Film Coatings on 3D Structures, ***Thomas Seidel***, Seitek50; *M. Current,* Current Scientific	
9:30am	**ALE1-WeM7** Formation of Ohmic Contacts to Si using In-situ Chemical Cleaning of the Substrate, ***Sara Iacopetti***, Technion - Israel Institute of Technology, Israel; *R. Tarafdar, S. Lai, M. Danek,* Lam Research Corp.; *M. Eizenberg,* Technion - Israel Institute of Technology, Israel	
9:45am	**ALE1-WeM8** SADP Spacer Profile Engineering by Quasi-Atomic Layer Etching, ***Tsai Wen (Maggie) Sung***, *C. Yan, H. Chung, J. Lo, D. Desai, P. Lembesis, R. Pakulski, M. Yang,* Mattson Technology, Inc.	
10:00am	**Break & Exhibits**	
10:15am	**Break & Exhibits**	
10:30am	**Break & Exhibits**	
10:45am	**ALE2-WeM12** Dynamic Temperature Control Enabled Atomic Layer Etching of Titanium Nitride, ***He Zhang***, *Y.S. Kim, D. Paeng,* Lam Research Corp.	**Atomic Layer Etching** **Session ALE2-WeM** **Materials Selective ALE** **Moderators:** Fred Roozeboom, Eindhoven University of Technology and TNO Geun Young Yeom, Sungkyunkwan University
11:00am	**INVITED: ALE2-WeM13** Rapid Thermal-Cyclic Atomic Layer Etching of Thin Films with Highly Selective, Self-Limiting, and Conformal Characteristics, ***Kazunori Shinoda***, Hitachi, Japan; *H. Kobayashi,* Hitachi; *N. Miyoshi, M. Izawa,* Hitachi High-Technologies; *K. Ishikawa, M. Hori,* Nagoya University, Japan	
11:15am	Invited talk continues.	
11:30am	**ALE2-WeM15** Atomic Layer Etching of HfO_2 with Selectivity to Si by Utilizing Material-Selective Deposition Phenomena, ***Kang-Yi Lin***, *C. Li,* University of Maryland; *S. Engelmann, R.L. Bruce, E.A. Joseph,* IBM T.J. Watson Research Center; *D. Metzler,* IBM Research - Albany; *G.S. Oehrlein,* University of Maryland	
11:45am	**ALE2-WeM16** Enhancing Etch Selectivity in Plasma-Assisted ALE of Silicon-Based Dielectrics using Surface Functionalization, ***Ryan Gasvoda***, Colorado School of Mines; *S. Wang, E. Hudson,* Lam Research Corp.; *S. Agarwal,* Colorado School of Mines	
12:00pm	**Lunch & Exhibits**	

Wednesday Afternoon, July 24, 2019

	ALD Applications **Grand Ballroom A-C - Session AA1-WeA** **Emerging Applications II** **Moderators:** Arrelaine Dameron, Forge Nano, Han-Bo-Ram Lee, Incheon National University	**ALD Applications** **Grand Ballroom H-K - Session AA2-WeA** **ALD for ULSI Applications II** **Moderators:** Haripin Chandra, Versum Materials, Inc., Robert Clark, TEL Technology Center, America, LLC
1:30pm	**AA1-WeA1** Atomic Layer Deposited Nano-Coatings to Protect $SrAl_2O_4$ Based Long-Life Phosphors from Environmental Degradation, ***Erkul Karacaoglu,*** Georgia Institute of Technology*; E. Ozturk,* Karamanoglu Mehmetbey University, Turkey*; M. Uyaner,* Necmettin Erbakan University, Turkey*; M. Losego,* Georgia Institute of Technology	**INVITED: AA2-WeA1** Silicon-Based Low k Dielectric Materials with Remote Plasma ALD, ***Hyeongtag Jeon,*** Hanyang University, Republic of Korea
1:45pm	**AA1-WeA2** Enhanced Interfacial Fracture Toughness of Polymer-Epoxy Interfaces using ALD Surface Treatments, ***Yuxin Chen****, N. Ginga, W. LePage, E. Kazyak, A. Gayle, J. Wang, M.D. Thouless, N.P. Dasgupta,* University of Michigan	Invited talk continues.
2:00pm	**AA1-WeA3** Atomic Layer Deposition of Pd on ZnO Nanorods for High Performance Photocatalysts, ***Jong Seon Park****, B.J. Kim, G.D. Han, K.-H. Park, E.H. Kang, H.-D. Park, J.H. Shim,* Korea University, Republic of Korea	**AA2-WeA3** SiOC Films by PEALD with Excellent Conformality and Wet Etch Resistance, ***Young Chol Byun****, E. Shero,* ASM
2:15pm	**AA1-WeA4** Accelerating Light Beam (ALB) Generation through Dielectric Optical Device Fabricated by Low Temperature Atomic Layer Deposition (ALD), *W. Zhu, C. Zhang, A. Agrawal, H. Lezec,* National Institute of Standards and Technology*; **Huazhi Li,*** Arradiance LLC	**AA2-WeA4** ALD TiN for Superconducting Through-Silicon Vias, ***Kestutis Grigoras****, S. Simbierowicz, L. Grönberg, J. Govenius, V. Vesterinen, M. Prunnila, J. Hassel,* VTT Technical Research Centre of Finland Ltd, Finland
2:30pm	**AA1-WeA5** Tunable Plasmonic Colours Preserved and Modified by Atomic Layer Deposition of Alumina, *J-M. Guay, A. Lesina, G. Killaire,* University of Ottawa, Canada*; **Peter Gordon,*** Carleton University, Canada*; C. Hahn,* University of Ottawa, Canada*; S. Barry,* Carleton University, Canada*; L. Ramunno, P. Berini, A. Weck,* University of Ottawa, Canada	**AA2-WeA5** Physical and Electronic Properties of Annealed ALD-deposited Ru from $Ru(DMBD)(CO)_3$ and Oxygen, ***Michael H. Hayes,*** Oregon State University*; C.L. Dezelah, J.H. Woodruff,* EMD Performance Materials*; J.F. Conley, Jr.,* Oregon State University
2:45pm	**AA1-WeA6** TFE of OLED Displays by Time-Space-Divided (TSD) PE-ALD and PE-CVD Hybrid System, ***Bongsik Kim,*** JUSUNG Engineering, Republic of Korea	**AA2-WeA6** Fluorine Free Boron-Containing Composite Layers for Shallow Dopant Source Applications, ***Anil Mane****, D. Choudhury, K. Pupek, R. Langeslay, M. Delferro, J.W. Elam,* Argonne National Laboratory
3:00pm	**AA1-WeA7** Tailoring the Ferroelectricity of ZrO_2 Thin Films using Ultrathin Interfacial Layers Prepared by Plasma-Enhanced Atomic Layer Deposition, ***Sheng-Han Yi****, B.-T. Lin, T.-Y. Hsu, J. Shieh, M.J. Chen,* National Taiwan University, Republic of China	**AA2-WeA7** Impact of Medium Energy Ions on the Microstructure and Physical Properties of TiN Thin Layers Grown by Plasma Enhanced Atomic Layer Deposition (PE-ALD)., *S. Belahcen, C. Vallée, A. Bsiesy,* ***Marceline Bonvalot,*** LTM-UGA, France
3:15pm	**AA1-WeA8** Spin-Hall-Active Platinum Thin Films Grown Via Atomic Layer Deposition, ***Michaela Lammel,*** IFW Dresden, Germany*; R. Schlitz,* Technische Universität Dresden, Germany*; A.A. Amusan,* IFW Dresden, Germany*; S. Schlicht,* FAU Erlangen, Germany*; T. Tynell,* IFW Dresden, Germany*; J. Bachmann,* FAU Erlangen, Germany*; G. Woltersdorf,* Martin-Luther-Universität Halle-Wittenberg, Germany*; K. Nielsch,* IFW Dresden, Germany*; S.T.B. Goennenwein,* Technische Universität Dresden, Germany*; A. Thomas,* IFW Dresden, Germany	**AA2-WeA8** ALD Process Monitoring for 3D Device Structures, ***Jiangtao Hu,*** Lam Research Corp.
3:30pm		**ALD/ALE 2019 Closing Remarks and Student Awards**

Wednesday Afternoon, July 24, 2019

	Emerging Materials **Regency Ballroom A-C - Session EM1-WeA** **Ternary and Quaternary Oxide Materials** **Moderator:** Bart Macco, Eindhoven University of Technology	**Nanostructure Synthesis and Fabrication** **Grand Ballroom E-G - Session NS-WeA** **2D Nanomaterials by ALD (including Transition Metal Dichalcogenides)** **Moderators:** Annelies Delabie, IMEC, Harm Knoops, Oxford Instruments Plasma Technology
1:30pm	**EM1-WeA1** Rhenium(III)-based Ternary Oxides: Novel Materials from Straightforward Synthesis *via* ALD Comprising Uncommon Reaction Pathways, ***Max Gebhard***, *S. Letourneau, D. Mandia, D. Choudhury, A. Yanguas-Gil, A. Mane, A. Sattelberger, J.W. Elam,* Argonne National Laboratory	**NS-WeA1** Modified ALD Process to Achieve Crystalline MoS_2Thin Films, ***Li Zeng***, *C. Maclsaac, J. Shi, N. Ricky, I.-K. Oh, S.F. Bent,* Stanford University
1:45pm	**EM1-WeA2** Growth Behavior and Electronic Characterization of $PbZrO_3$ and $PbZr_xTi_{1-x}O_3$ Grown by Atomic Layer Deposition with Several Zr Precursors, ***Nicholas Strnad***, University of Maryland; *D. Potrepka,* U.S. Army Research Laboratory; *A. Leff,* General Technical Services, LLC; *J. Pulskamp,* U.S. Army Research Laboratory; *R. Phaneuf,* University of Maryland; *R. Polcawich,* U.S. Army Research Laboratory	**NS-WeA2** Nucleation and Growth of ALD MoS_2 Films on Dielectric Surfaces, *S. Letourneau,* ***Anil Mane***, *J.W. Elam,* Argonne National Laboratory
2:00pm	**EM1-WeA3** Understanding Growth Characteristics of ALD $NiAl_yO_x$: The Role of Ozone, ***Jonathan Baker***, *J. Schneider, S.F. Bent,* Stanford University	**INVITED: NS-WeA3** Plasma-Enhanced Atomic Layer Deposition of Transition Metal Dichalcogenides: From 2D Monolayers to 3D Vertical Nanofins, ***Ageeth Bol***, Eindhoven University of Technology, Netherlands
2:15pm	~~**EM1-WeA4** Atomic Layer Deposition of $B_xMg_{1-x}O$ Films: Progress Towards Shallow Boron Doping, ***David Mandia***, *D. Choudhury, M. Gebhard,* Argonne National Laboratory; *J. Liu,* Northwestern University; *A. Yanguas-Gil, A.U. Mane, A. Nassiri, J.W. Elam,* Argonne National Laboratory~~	Invited talk continues.
2:30pm	**EM1-WeA5** Enhanced Doping Control of Metal Oxide Thin Films Using a Modified ALD Process, *E. Levrau,* IBM TJ Watson Research Center; ***Yohei Ogawa***, ULVAC, Japan; *M. Frank, M. Hopstaken, E. Cartier,* IBM T.J. Watson Research Center; *K. Schmidt,* IBM Research - Almaden; *M. Hatanaka,* ULVAC, Japan; *J. Rozen,* IBM T.J. Watson Research Center	**NS-WeA5** Atomic Layer Deposition of Emerging 2D Semiconductors HfS_2 and ZrS_2, ***Miika Mattinen***, *G. Popov, M. Vehkamäki, P. King, K. Mizohata, P. Jalkanen, J. Räisänen, M. Leskelä, M. Ritala,* University of Helsinki, Finland
2:45pm	**EM1-WeA6** As Deposited Epitaxial $LaNiO_3$ and $La(Ni,Cu)O_3$ with Controllable Electric Properties, ***Henrik Hovde Sønsteby***, University of Oslo / Argonne Natl. Labs, Norway; *O. Nilsen, H. Fjellvåg,* University of Oslo, Norway	**NS-WeA6** Low Temperature ALD for Phase-controlled Synthesis of 2D Transition Metal (M=Ti, Nb) *di-* (MX_2) and *Tri-* (MX_3) Sulfides, ***Saravana Balaji Basuvalingam***, *M. Verheijen, W.M.M. Kessels, A. Bol,* Eindhoven University of Technology, Netherlands
3:00pm	**EM1-WeA7** Time Dependence of Pyroelectric Response in Ferroelectric $Hf_{0.58}Zr_{0.42}O_2$ Films, ***Sean Smith***, *M.D. Henry, M. Rodriguez,* Sandia National Laboratories; *J. Ihlefeld,* University of Virginia	**NS-WeA7** ALD Boron Nitride Coated and Infiltrated Carbon Materials for Environmental Applications, *W. Hao, C. Journet, A. Brioude,* Université Lyon, France; *H. Okuno,* Université Grenoble-Alpes, France; ***Catherine Marichy***, Université Lyon, France
3:15pm	**EM1-WeA8** Tailoring Nickel Oxide Conductivity by Introducing Transition Metals: From First-principles to Experimental Demonstration, ***Md. Anower Hossain***, *T. Zhang, D. Lambert,* University of New South Wales, Australia; *Y. Zakaria,* Hamad Bin Khalifa University, Qatar; *P. Burr,* University of New South Wales, Australia; *S. Rashkeev, A. Abdallah,* Hamad Bin Khalifa University, Qatar; *B. Hoex,* University of New South Wales, Australia	

Author Index

Bold page numbers indicate presenter

— A —
Aarik, J.: AF5-MoP2, 23
Aav, J.: AF5-MoP2, 23
Abdallah, A.: EM1-WeA8, 41
Abdulagatov, A.: ALE1-TuM3, **28**
Abelson, J.: AS1-TuA4, 31
Abrams, L.: AA1-TuM5, 26
Acharya, J.: AA2-TuP15, **33**
Adams, D.: ALE-SuP4, 16
Adinolfi, V.: AA1-WeM4, **38**; AF3-MoA16, 19
Adomaitis, R.: AA1-MoA5, 18; AA1-MoA8, 18; AA5-TuP7, 34
Agarwal, S.: ALE2-WeM16, 39; AS1-TuA3, 31; AS2-TuA111, 31
Agbenyeke, R.E.: AA2-MoA13, 18
~~Ageev, O.~~: ~~ALE-SuP3~~, 16
Aghazadehchors, S.: AA4-TuP9, 34
Agrawal, A.: AA1-WeA4, 40
Aguinsky, L.F.: ALE2-TuA12, **32**
Ah-Leung, V.: ALE2-TuM14, 28
Ahmmad Arima, B.: AA4-TuP5, 34
Ahmmad, B.: AA4-TuP3, 34; AF4-MoP1, 23
Ahn, J.: EM-MoP5, 24
Ahn, J.-H.: AA1-TuP2, 33
Ahvenniemi, E.: AF5-MoP2, 23
Akbashev, A.R.: AF5-MoP2, 23
Akimoto, K.: **ALE2-MoA16**, 21
Albert, M.: AF1-TuM2, 25
Ali, S.: AF5-MoP2, 23
Alivov, Y.: AA5-TuP2, 34
Allemang, C.: AS1-TuA7, 31
Alphonse, A.: AF5-MoP7, 23
Altamirano Sanchez, E.: AS1-TuM16, 27
~~Alvarado, J.~~: ~~AA2-TuP11~~, **33**
Alvarez, D.: AF2-MoP7, **22**; AF4-MoA17, 20; AM-MoP8, 23; AS-TuP4, 34
~~Ameloot, R.~~: AM1-WeM8, 37; ~~AS2-TuA113~~, 31; EM1-WeM3, 36
Amusan, A.A.: AA1-WeA8, 40
An, J.-S.: AF1-MoP6, 22; AF2-MoP14, **22**
~~An, Y.~~: ~~EM3-WeM16~~, 37
Andachi, K.: AF2-MoP7, 22
Anders, D.: AS-TuP1, 34
Anderson, V.: AF-TuA6, 29
~~Antony, A.~~: ~~AA1-TuP1~~, 33
Antoun, G.: ALE1-MoA8, **21**; ALE-SuP11, 16
Appiah, E.: AF5-MoP1, 23
Arachchilage, H.J.: AF1-MoP2, **22**
Arellano, N.: AS1-TuA6, 31
Arepalii, V.: AA1-TuP17, 33
Arkles, B.: AS-TuP3, **34**
Armini, S.: AS1-TuM12, **27**; ~~AS2-TuA113~~, 31
Arts, K.: **AF3-MoA12**, 19; AF-TuA2, **29**
Asakawa, K.: EM-MoP6, 24
Asundi, A.: AA1-TuM6, 26
Aubry, O.: AM1-WeM5, 37
Avila, J.: AF2-MoP11, **22**; AF-TuA6, 29; AF-TuA7, 29
Awakowicz, P.: AF1-MoP12, 22
Azpitarte, I.: EM2-WeM12, 36
— B —
Babcock, S.E.: EM-MoP11, 24
Bača, D.: AF2-MoP17, 22
Bachmann, J.: AA1-WeA8, 40
Bacic, G.: AF2-TuM6, **27**
Bačić, G.: AF2-MoA4, 19; AF2-TuM4, 27
Bacquie, V.: ALE2-TuM14, **28**
Baek, G.H.: EM1-WeM5, 36; EM1-WeM6, **36**
Baets, R.: AF-TuA4, 29
Bahat Treidel, E.: AA2-TuP16, 33
Baik, S.J.: EM-MoP14, 24
Bailey, M.: EM-MoP2, 24
Baker, J.: EM1-WeA3, **41**
Balatti, S.: AA1-WeM4, 38
Balder, E.: AA2-TuA13, 30
Balme, S.: AA1-MoA3, 18
Barger, P.: AA1-TuM5, 26
Barlage, D.: AA2-TuP10, 33; AF1-MoA2, 20; EM-MoP12, 24
Barnola, S.: ALE2-MoA14, 21
Barry, S.: **AA1-TuA5**, 30; AA1-WeA5, 40; AF1-MoP4, 22; AF2-MoA3, **19**; AF2-MoA4, 19; AF2-TuM3, 27; AF2-TuM4, 27; AF2-TuM6, 27; AF-TuA4, 29
Bartha, J.W.: AF1-TuM2, 25
Bartlett, B.: AA1-TuM7, 26
Barton, K.: AS1-TuA7, 31
Basaldua, I.: AA1-TuA7, 30
Basuvalingam, S.B.: NS-WeA6, **41**
Baum, T.: AF1-MoP9, 22; AF3-MoP2, 22; AS1-TuA8, 31
~~Baumgart, H.~~: ~~AA2-TuP9~~, 33; ~~AA4-TuP10~~, 34; ~~AM-MoP3~~, 23
Bechelany, M.: AA1-MoA3, 18; AA4-TuP1, 34; AF5-MoP2, 23
Beer, S.M.J.: AF1-MoP13, **22**; AF1-MoP8, 22
Beladiya, V.: AM-MoP2, 23
Belahcen, S.: AA2-WeA7, 40; AS2-TuA112, 31
Bellet, D.: AA4-TuP9, 34
Bellido-Gonzalez, V.: AF-TuA3, 29
Bent, S.F.: AA1-TuM6, 26; AS1-TuA1, 31; AS1-TuA2, 31; EM1-WeA3, 41; NS-WeA1, 41
Benz, D.: **AA1-TuA5**, 30; AA1-TuM8, **26**; EM-MoP2, 24
Berdova, M.: AF5-MoP2, 23
Berini, P.: AA1-WeA5, 40
Berry, J.J.: AA2-MoA11, 18
Bertuch, A.: AA1-TuA6, 30; AA2-TuP8, **33**
Bhatia, R.: AA1-TuA6, **30**
Bickel, N.: AA2-TuP16, **33**
Bielinski, A.: AA1-TuM7, **26**; AA2-TuM12, 26
Bin Afif, A.: AF3-TuM12, 25
Biolsi, P.: ALE1-WeM1, 39
Biyikli, N.: AF3-MoP7, **23**; AF3-TuM13, 25; AF3-TuM16, 25; AF4-MoP3, 23; EM3-WeM14, 37
Blomberg, T.: AA1-MoA4, **18**; ALE1-TuM6, 28
Bochevarov, A.: AF1-MoA5, 20
Bock, C.: AF1-TuM3, 25
Bodalyov, I.: AF5-MoP2, 23
Bol, A.: NS-WeA3, **41**; NS-WeA6, 41
Bonvalot, M.: AA2-WeA7, **40**; AM1-WeM5, 37; AS2-TuA112, 31
Boris, D.: AF-TuA6, **29**; AF-TuA7, 29; ALE-SuP7, 16
Bosnick, K.: AA1-TuP6, **33**
Bosund, M.: AF3-TuM14, **25**
Boyadjiev, S.: AF5-MoP2, 23
Boysen, N.: AF1-MoP8, 22; AF2-MoA5, **19**; AM1-WeM2, 37
Brancho, J.: AA1-TuM7, 26
Breitung, E.: AA1-TuA6, 30
Brian Willis, B.: EM3-WeM14, 37
Brick, C.: AS-TuP3, 34
Briel, O.: AM-MoP1, 23
Briggs, B.: AS-TuP6, 35
Brindley, J.: AF-TuA3, **29**
Brinkmann, K.: ALE2-TuM16, 28
Brioude, A.: NS-WeA7, 41
Bruce, R.L.: ALE2-WeM15, 39
Brüner, P.: AF3-MoA15, **19**
Bsiesy, A.: AA2-WeA7, 40; AS2-TuA112, 31
~~Buhmann, H.~~: ~~AA2-TuP18~~, 33
Bull, S.: AA2-MoA14, **18**
Bures, F.: NS-TuP1, 35
Burgmann, S.: AF3-TuM12, **25**
Burkins, P.: AA1-TuA7, 30
Burr, P.: EM1-WeA8, 41
Burtin, P.: ALE2-MoA14, 21
Buttera, S.: AF2-TuM3, **27**
Büttner, T.M.: AA3-TuA13, 29
~~Buzelis, R.~~: ~~AA5-TuP6~~, 34
Byun, J.Y.: AF4-MoP11, 23
Byun, Y.C.: AA2-WeA3, **40**
— C —
Cabrini, S.: ALE1-MoA4, 21
Cadien, K.: AA1-TuP6, 33; AA2-TuP10, 33; AF1-MoA2, 20; EM-MoP12, 24
Caha, O.: AF2-MoP17, 22
Cai, J.: AF2-MoP12, 22
Cameron, D.: AF2-MoP17, 22; AF5-MoP2, 23
Cano, A.: ALE1-TuM5, **28**; ALE2-TuA14, 32
Cao, K.: AA5-TuP1, 34
Cao, Y.-Q.: AA3-TuP7, **34**; EM1-WeM1, **36**
Carbajal, D.: AS1-TuM16, 27
Cartier, E.: EM1-WeA5, 41
~~Castán, H.~~: ~~EM-MoP7~~, 24
Cavanagh, A.: AS1-TuM14, 27
Caymax, M.: AA1-WeM5, 38
Cecchini, R.: AA1-TuA3, 30
Cha, M.H.: ALE-SuP10, 16
Cha, T.: ALE-SuP9, 16
Chae, H.: AA1-TuP3, 33; ALE-SuP9, 16
Chae, W.-M.: AA5-TuP8, 34; AF1-MoP11, 22
Chaker, A.: AS2-TuA112, 31
Chan, B.T.: AS1-TuM16, 27; AS-TuP6, 35
Chandra, H.: AF2-MoP8, 22
Chang, H.S.: AA1-TuP10, 33; AA1-TuP12, 33; AA1-TuP9, 33
Chang, Y.H.: AF1-TuM4, 25; EM3-WeM13, 37
Charvot, J.: NS-TuP1, 35
Chatterjee, S.: AS-TuP1, 34
~~Chávez, M.~~: ~~AA2-TuP11~~, 33
Chekurov, N.: AF5-MoP2, 23
~~Chen, C. W.~~: ~~AF2-MoP5~~, **22**
Chen, H.-H.: AF-TuA1, **29**
Chen, K.-H.: AA2-TuM12, 26; AA2-TuM13, 26; AA2-TuM15, **26**
Chen, L.: NS-TuP3, 35
Chen, M.J.: AA1-WeA7, 40; AA3-TuA14, 29; EM3-WeM15, 37
Chen, R.: AA5-TuP1, **34**
Chen, T.: NS-TuP3, **35**
Chen, W.-S.: **AA2-WeM16**, 38
Chen, Y.: AA1-WeA2, **40**; EM-MoP11, 24
Cheng, C.-P.: **AA2-WeM16**, 38
Cheng, E.: ALE2-TuA11, 32
Cheng, L.: AA1-WeM4, 38; AF3-MoA16, 19
Cheng, P.-H.: AA3-TuA14, 29
Cheng, R.: AF5-MoP2, 23
Chesser, J.: EM-MoP9, 24
Chevolleau, T.: **ALE2-MoA16**, 21
Chin, G.: AF3-MoP6, **23**
Chin, T.-K.: AA1-TuM4, **26**
Cho, C.-H.: ALE1-MoA6, 21
Cho, J.-H.: AA5-TuP8, **34**; AF1-MoP11, 22
Cho, J.-Y.: AA1-TuP6, 33
Cho, M.H.: AA1-TuP7, **33**
Cho, S.: AA2-TuP6, 33
Cho, S.-J.: ALE2-MoA11, 21
Cho, T.: AS1-TuA7, **31**
Cho, Y.: ALE-SuP9, 16
Cho, Y.J.: AA1-TuP9, **33**
Choi, B.-H.: AA4-TuP4, 34
Choi, H.J.: AA2-MoA17, 18
Choi, J.H.: AA3-TuA16, **29**
Choi, J.-H.: NS-TuP2, **35**
Choi, J.S.: ALE-SuP10, 16
Choi, Y.: AF2-MoP3, 22
Chopra, S.: AS2-TuA111, 31

Author Index

Choudhury, D.: AA2-TuA11, **30**; AA2-WeA6, 40; AA4-TuP11, **34**; EM1-WeA1, 41; ~~EM1-WeA4~~, 41
Chowdhury, V,: AF5-MoP1, **23**
Christensen, S.: AA2-MoA11, 18; AA2-MoA15, 18; AA2-MoA16, 18; AF2-MoP4, 22
Chubarov, M.: AF5-MoP2, 23
Chugh, S.: AA2-TuP17, 33; AA4-TuP12, 34
Chung, C.W.: ALE-SuP10, 16
Chung, H.: ALE1-WeM8, 39
Chung, T.-M.: AA2-MoA13, 18
Chung, Y.-D.: AA1-TuP17, 33
Ciftyurek, E.: AF1-TuM3, 25
Ciftyürek, E.: AF2-MoA7, 19
Clancey, J.: ALE1-TuM5, 28; ALE2-TuA14, 32
Clark, R.: AA2-WeM12, 38; AF2-MoP16, 22; ALE1-WeM1, 39
Clarke, R.: AA1-WeM4, 38
Clendenning, S.B.: ALE1-TuA5, 32; ALE-SuP2, 16
Clerix, J.-W.: AS1-TuM16, 27
Coati, A.: AF1-TuM7, 25
Collins, L.: EM2-WeM14, 36
Concepcion, J.: AA1-TuP14, 33
Conley, Jr., J.F.: AA2-WeA5, 40; AF2-TuM5, 27; AF5-MoP6, 23
Consiglio, S.: AA2-WeM12, 38; AF2-MoP16, **22**
Cooke, M.: ALE1-MoA4, 21
Creange, S.: AA1-TuA6, 30
Creatore, M.: AA1-TuM3, **26**
Cremer, T.: AA1-TuP13, 33
Cremers, V.: AF5-MoP2, 23
Cruz, A.J.: AM1-WeM8, 37; EM1-WeM3, **36**
Cunnane, D.: AA1-MoA6, 18
Current, M.: ALE1-WeM6, 39
Cuthill, K.: AF2-MoP8, 22
— D —
Dadlani, A.: AF3-TuM12, 25
Dallorto, S.: ALE1-MoA4, **21**
Dameron, A.: AA1-TuM5, 26
Danek, M.: ALE1-WeM7, 39
Daniel, B.: AF-TuA3, 29
Darling, S.: AS2-TuA215, 31
Dasgupta, N.P.: AA1-TuM7, 26; AA1-WeA2, 40; AA2-TuM12, **26**; AA2-TuM13, 26; AA2-TuM15, 26; AS1-TuA7, 31
Daubert, J.: AA4-TuP2, **34**
Davis, A.: AA2-TuM12, 26; AA2-TuM13, **26**; AA2-TuM15, 26
~~De Gendt, S.~~: ~~AS2-TuA113~~, 31
Degtyaryov, A.: AA5-TuP2, 34
del Hoyo, J.: ALE-SuP7, 16
Delabie, A.: AS1-TuM16, **27**; AS-TuP6, **35**
Delferro, M.: AA2-WeA6, 40
Delhougne, R.: AA1-WeM5, 38
Dendooven, J.: AF1-TuM6, 25; AF1-TuM7, **25**; AF3-MoA15, 19; AF-TuA4, 29; **EM1-WeM7**, 36
Deng, S.: AA1-WeM5, **38**
Denkova, A.: AA1-MoA2, 18
Desai, D.: ALE1-WeM8, 39
Detavernier, C.: AF1-TuM6, 25; AF1-TuM7, 25; AF3-MoA15, 19; AF-TuA4, 29; **EM1-WeM7**, 36
Devi, A.: AF1-MoP12, 22; AF1-MoP13, 22; AF1-MoP8, **22**; AF1-TuM3, 25; AF2-MoA5, 19; AF2-MoA6, 19; AF2-MoA7, 19; AF2-TuM6, 27; AF5-MoP2, 23; AM1-WeM2, 37
Dezelah, C.L.: AA2-WeA5, 40; AF2-TuM5, 27
Dhakal, T.: AA1-TuP5, **33**
Dhuey, S.: ALE1-MoA4, 21
Di Palma, V.: AA1-TuM3, 26
Dickey, E.: AM1-WeM3, **37**
Dietz, D.: AA5-TuP3, **34**
Divan, R.: AA5-TuP10, **34**
Djenizian, T.: AA2-TuA16, 30
~~Dolak, J.~~: ~~AF4-MoP8~~, 23
Dopita, M.: AA3-TuA11, 29
Downey, B.: AF-TuA7, 29
Doyle, S.: AA2-TuP3, **33**
Dozias, S.: AM1-WeM5, 37
Draeger, N.: AS1-TuA2, 31
~~Drazdys, M.~~: ~~AA5-TuP6~~, 34
~~Drazdys, R.~~: ~~AA5-TuP6~~, **34**
Driess, M.: AF3-MoA11, 19
Drozd, V.E.: AF5-MoP2, 23
~~Dueñas, S.~~: ~~EM-MoP7~~, 24
~~DuMont, J.~~: ~~EM-MoP8~~, **24**
Dumuis, N.: AM1-WeM5, 37
Durand, C.: **ALE2-MoA16**, 21
Dussarat, C.: **ALE2-MoA16**, 21
Dussart, R.: ALE1-MoA8, 21; ALE-SuP11, 16
Dvorak, F.: NS-TuP1, 35
Dwarakanath, S.: EM2-WeM15, 36
Dwivedi, V.: AA1-MoA5, **18**; AA1-MoA8, 18; AA5-TuP7, 34
— E —
Eddy Jr., C.R.: AF-TuA7, 29
Eddy, C.R.: AS2-TuA214, 31
Eddy, Jr., C.R.: AF1-TuM4, 25; AF-TuA6, 29; EM3-WeM13, **37**
Eden, J.G.: AF-TuA5, 29
Edley, M.: ALE1-WeM1, 39
Eizenberg, M.: AF3-TuM15, 25; ALE1-WeM7, 39
Ekerdt, J.: AF4-MoA11, **20**; AS2-TuA111, 31
Elam, J.W.: AA1-TuP11, 33; AA1-TuP13, 33; AA2-TuA11, 30; AA2-TuA12, 30; AA2-WeA6, 40; AA4-TuP11, 34; AF1-MoA1, 20; EM1-WeA1, 41; ~~EM1-WeA4~~, 41; NS-WeA2, 41; PS1-MoM5, **17**
Elhadj, S.: EM-MoP9, 24
Eller, B.: AF4-MoP4, 23
Ellingboe, A.R.: AF4-MoP11, 23
Elliot, S.: AF1-MoA5, 20; ALE1-TuM5, 28
Elliott, S.D.: ALE2-TuA14, **32**
~~Elmustafa, A.~~: ~~AA4-TuP10~~, 34
Elnikova, L.: AF5-MoP2, 23
Endo, K.: ALE2-TuM12, 28
Engelmann, S.: ALE2-WeM15, 39
Engeln, R.: AF1-TuM5, 25
~~Eom, S.~~: ~~AA2-TuP20~~, **34**
Eom, T.: AA2-MoA13, 18
Eperon, G.: AA2-MoA11, 18
Ermert, D.: AF1-MoP9, **22**
Esarey, S.: AA1-TuM7, 26
~~Etinger-Geller, Y.~~: ~~AF5-MoP10~~, **23**
Evans, P.G.: EM-MoP11, 24
— F —
Faguet, J.: ALE1-MoA8, 21; ALE-SuP11, 16
Fanciulli, M.: AA1-TuA3, 30
Farjam, N.: AS1-TuA7, 31
Feigelson, B.: NS-TuP4, 35
Feldman, A.: AM1-WeM7, 37
Feng, J.-Y.: AF1-TuM7, 25
Ferguson, I.: AA1-TuP16, **33**
~~Ferretti, A.M.~~: ~~EM-MoP1~~, 24
Fjellvåg, H.: EM1-WeA6, 41
Floros, K.: AA2-TuP6, 33; ALE2-MoA11, 21
Folestad, S.: AA1-MoA1, 18; EM-MoP2, 24
Foody, M.: AF1-MoP14, 22; AF4-MoA14, **20**
Foss, A.E.: AF4-MoP10, 23
Fourkas, J.: ALE1-MoA5, 21
Frank, M.: EM1-WeA5, 41
Frankel, I.: AF2-TuM6, 27
Franquet, A.: AS-TuP6, 35
Frey, A.: AM-MoP1, 23
Friz, A.: AS1-TuA6, 31
Fryauf, D.: AM1-WeM7, 37
Fu, H.: ALE2-MoA15, 21
Fu, K.: ALE2-MoA15, 21
Fu, Y.-C.: ALE2-MoA11, 21
Fujii, T.: ALE2-TuM12, 28
Fujisaki, S.: ALE1-TuM8, **28**
Fusco, M.: EM1-WeM4, 36
— G —
~~Gallardo, S.~~: ~~AA2-TuP11~~, 33
Gao, F.: **AF3-MoA12**, 19; AF3-MoA16, 19
Gao, K.: AA4-TuP11, 34
Gao, T.: AS-TuP2, 34
Garcia-Mendez, R.: AA2-TuM13, 26
Gargouri, H.: AA2-TuP16, 33; AM-MoP2, **23**
Gaskell, A.: AA3-TuA11, 29
Gassilloud, R.: AS2-TuA112, 31
Gasvoda, R.: ALE2-WeM16, **39**
Gaulding, A.: AA2-MoA16, 18
Gavartin, J.: AF1-MoA5, 20
Gayle, A.: AA1-TuM7, 26; AA1-WeA2, 40
Gebhard, M.: AA1-TuP11, **33**; AA1-TuP13, 33; EM1-WeA1, **41**; ~~EM1-WeA4~~, 41
Gennett, T.: AA2-MoA15, 18; AA2-MoA16, 18
George, S.M.: AF4-MoA15, 20; ALE1-TuM3, 28; ALE1-TuM5, 28; ALE1-TuM7, 28; ALE2-MoA13, **21**; ALE2-TuA14, 32; AS1-TuM14, 27; EM1-WeM8, 36
~~Geyer, S.~~: ~~AA3-TuP3~~, 34
Gheeraert, E.: **ALE2-MoA16**, 21
Ghods, A.: AA1-TuP16, 33
Gill, Y.J.: ALE-SuP14, 16
Gillespie, C.: EM-MoP9, 24
Ginga, N.: AA1-WeA2, 40
Girard, J.-M.: AA1-WeM5, 38
Giri, A.: EM2-WeM16, 36
Girolami, G.: AS1-TuA4, 31
Givens, M.: AA3-TuA13, 29; AF2-TuM7, 27
Go, D.: AM-MoP5, **23**
Goeke, R.: ALE-SuP4, 16
Goennenwein, S.T.B.: AA1-WeA8, 40
Goff, J.: AS-TuP3, 34
Gokhale, V.: AF-TuA7, 29
Golka, S.: AM-MoP2, 23
Goncharova, L.: AA2-TuM14, 26
Gonon, P.: AS2-TuA112, 31
Goodyear, A.: ALE1-MoA4, 21
Goorsky, M.: AF-TuA7, 29
Gordon, P.: AA1-WeA5, **40**
Gottardi, G.: AF5-MoP2, 23
Gottscho, R.: ALE1-MoA1, 21
Gougousi, T.: AA1-TuA7, **30**
Goul, R.: AA2-TuP15, 33
Goux, L.: AA1-WeM5, 38
Govenius, J.: AA2-WeA4, 40
Graniel, O.: AA1-MoA3, 18
Grasso, J.: AM1-WeM1, **37**
Greeley, J.P.: AA2-TuA12, 30
Greenaway, A.: AF2-MoP4, **22**
Greenberg, B.: NS-TuP4, **35**
Greer, F.: AA1-MoA6, **18**
Gregory, S.: AA1-TuA8, **30**
Greth, K.D.: ALE-SuP4, 16
Griffiths, M.: **AA1-TuA5**, 30; AF2-MoA3, 19; AF2-MoA4, **19**; AF-TuA4, 29
Grigoras, K.: AA2-WeA4, **40**
Grigsby, B.: AA5-TuP2, 34
Grillo, F.: **AA1-TuA5**, 30; AF1-MoA3, **20**; AS-TuP6, 35
Grob, C.: AA1-MoA8, 18
Grönberg, L.: AA2-WeA4, 40
Gross, K.: AA2-MoA15, 18
Grzeskowiak, J.: AF1-TuM4, 25
~~Gu, C.~~: ~~AA2-TuP2~~, **33**
Gu, J.: AF2-MoP14, 22
Guay, J-M.: AA1-WeA5, 40
Guinney, I.: AA2-TuP6, 33

Author Index

Guisinger, N.: AA1-TuP19, 33
Gunn, R.: AA5-TuP2, 34
Guo, X.: ALE1-MoA7, **21**; ALE1-TuM4, 28
Gutierrez Razo, S.: ALE1-MoA5, 21
— H —
Haeger, T.: ALE2-TuM16, 28
Hahn, C.: AA1-WeA5, 40
Haider, A.: AA1-WeM5, 38
Halls, M.: AF1-MoA5, 20
~~Hamaguchi, S.~~: AF4-MoP6, 23; ALE1-TuM1, 28; ~~ALE2-TuA15~~, **32**; ~~ALE-SuP8~~, 16
Hampel, N.A.: AF1-TuM2, 25
Han, G.D.: AA1-WeA3, 40; AA4-TuP7, **34**
Han, Y.: EM-MoP15, 24
Hao, M.: ALE2-MoA15, 21
Hao, W.: NS-WeA7, 41
~~Haridas, A.~~: ~~AA1-TuP1~~, **33**
Harris, K.: AA1-TuP6, 33
Hartig, J.: AF1-MoA6, **20**
~~Hartinger, S.~~: ~~AA2-TuP18~~, 33
~~Hartmann, G.~~: ~~AF3-MoP5~~, 23
Hasegawa, M.: AA1-MoA5, 18; ALE2-MoA17, **21**
Hashemi, F.S.M.: **AA1-TuA5**, **30**
Hassel, J.: AA2-WeA4, 40
Hasselmann, T.: AF2-MoA5, 19; AM1-WeM2, **37**
Hatanaka, M.: EM1-WeA5, 41
Hatanpää, T.: AF2-TuM2, 27
Hatase, M.: AF1-MoP10, 22
Hatch, K.: ALE2-MoA15, **21**
Haufe, N.: AF3-MoA13, 19
Haukka, S.: ALE1-TuM6, 28
Haung, Z.: AF4-MoP4, 23
Hausmann, D.: AS1-TuA2, 31; AS1-TuA3, 31; AS1-TuA5, 31
Haverkate, L.: AA2-TuA13, 30
Hayes, M.H.: AA2-WeA5, **40**; AF5-MoP6, 23
He, C.: ALE1-TuM4, 28
~~He, Y.~~: ~~EM3-WeM16~~, 37
Heikkilä, M.J.: AF2-TuM2, 27
Heinonen, O.: AS2-TuA215, 31
Heiska, J.: AA2-TuA14, **30**
Hemakumara, D.: AA2-TuP6, **33**; ALE2-MoA11, 21
Hendrix, B.: AS1-TuA8, 31
Hennessy, J.: AA1-MoA7, **18**
Henry, M.D.: EM1-WeA7, 41
Heo, J.: AA2-TuP17, 33; AA4-TuP12, 34
Hermida-Merino, D.: AF1-TuM7, 25
Hernandez-Arriaga, H.: AA1-WeM3, 38; AA3-TuA15, 29
Hess, A.: AS1-TuA6, 31
Hidayat, R.: AF1-MoP11, **22**; ~~AF2-MoP15~~, 22; AF2-MoP3, 22
Higashi, S.: AF2-MoA8, 19
Hikichi, K.: AF3-MoP1, 22
Hilt, O.: AA2-TuP16, 33
Hintzen, H.: AA1-TuM8, 26
Hirose, F.: AA4-TuP3, 34; AA4-TuP5, 34; AF4-MoP1, 23
Hirose, M.: AA2-TuP19, **34**; AF4-MoA16, 20
Hock, A.: AF1-MoP14, **22**
Hody, H.: AS-TuP6, 35
Hoex, B.: AA1-TuP18, 33; EM1-WeA8, 41
Holden, K.: AF2-TuM5, **27**; AF5-MoP6, 23
Hong, D.: AM1-WeM5, 37
Hong, K.P.: AF5-MoP7, 23
Hong, M.: AA2-TuP12, 33; **AA2-WeM16**, 38
Hong, W.P.: AA3-TuP1, 34; AA3-TuP5, 34
Hopkins, P.: EM1-WeM4, 36; EM2-WeM16, 36
Hopstaken, M.: EM1-WeA5, 41
Hori, M.: ALE1-MoA3, 21; ALE1-TuA3, 32; ALE2-MoA17, 21; ALE2-WeM13, 39
Hossain, M.A.: AA1-TuP18, 33; EM1-WeA8, **41**
Hössinger, A.: ALE2-TuA12, 32
Hsu, T.-Y.: AA1-WeA7, 40
Hu, J.: AA2-WeA8, **40**
~~Huang, G.~~: ~~AA3-TuP6~~, 34
Huang, J.: AF5-MoP1, 23
Huang, J.-H.: AA2-TuP12, 33
Huber, C.: AS1-TuA7, 31
Hudson, E.: ALE2-WeM16, 39
Hughes, T.: AF1-MoA5, 20
Humlíček, J.: AF2-MoP17, 22
Humphreys, C.: AA2-TuP6, 33
~~Huong, C.~~: ~~EM-MoP3~~, **24**; EM-MoP4, 24
Hurst, K.: AA2-MoA16, **18**
~~Hussain, M.N.~~: ~~ALE-SuP5~~, **16**
Hwang, B.K.: AF4-MoP10, 23; AF4-MoP5, 23
~~Hwang, G.~~: ~~AF3-MoP5~~, **23**; ALE2-TuA11, **32**
Hwang, K.: AA3-TuA16, 29
Hwang, S.M.: AF4-MoA17, 20; AF4-MoP10, 23; AF4-MoP5, **23**; AS-TuP4, **34**
Hwangbo, H.: AA1-TuP3, 33
Hyttinen, P.: **AF3-MoA12**, 19
— I —
Iacopetti, S.: ALE1-WeM7, **39**
Ievlev, A.: EM2-WeM14, 36
Ihlefeld, J.: EM1-WeA7, 41
Ikeda, N.: AA2-TuP19, 34; AF4-MoA16, 20
Ilhom, S.: AF3-MoP7, 23; AF3-TuM13, 25; AF3-TuM16, **25**; AF4-MoP3, **23**
Inbar, H.S.: AF1-TuM4, 25
Inoue, K.: AF3-MoP1, 22
Inoue, M.: AF2-MoA8, 19; AF4-MoA16, 20
Iordanov, I.: AM-MoP6, 23
Irokawa, Y.: AA2-TuP19, 34
~~Ishibashi, K.~~: ~~AF3-MoP5~~, 23
Ishikawa, K.: ALE2-MoA17, 21; ALE2-WeM13, 39
~~Isobe, M.~~: ~~ALE2-TuA15~~, 32
Ito, K.: AF4-MoA16, 20
~~Ito, T.~~: AF4-MoP6, 23; ALE1-TuM1, **28**; ~~ALE2-TuA15~~, 32; ~~ALE-SuP8~~, 16
Ivanov, I.: EM2-WeM14, 36
Ivanov, S.: AF1-MoP1, 22; AF2-MoP2, 22
Ivanova, T.: AA3-TuA13, **29**; AF2-TuM7, 27
~~Iwao, T.~~: ~~AF3-MoP5~~, 23
Izawa, M.: ALE2-WeM13, 39
— J —
Jacobson, L.: AF1-MoA5, 20
Jacopin, G.: **ALE2-MoA16**, 21
Jalkanen, P.: NS-WeA5, 41
Jang, J.H.: AA1-TuP3, 33
Jang, S.J.: AA4-TuP8, 34
Jayakodiarachchi, N.: EM-MoP11, **24**
Jenkins, M.: AF5-MoP6, **23**
Jeon, H.: AA2-WeA1, **40**
Jeon, N.: AS2-TuA215, 31
Jeon, N.J.: AA2-MoA13, 18
Jeong, B.H.: ALE-SuP14, 16
Jeong, J.: AA1-MoA4, 18; ALE-SuP12, 16
Jeong, J.Y.: EM-MoP15, **24**
Ji, H.: AF2-MoP18, 22
Ji, Y.J.: AF4-MoP11, 23
Jiang, Y.-S.: AA3-TuA14, 29
Jimenez, C.: AA4-TuP9, 34
~~Jõgiaas, T.~~: ~~EM-MoP7~~, 24
Johnson, A.: AA1-TuA7, 30
Johnson, N.: ALE2-MoA13, 21
Johnson, S.D.: AS2-TuA214, 31
Johs, B.: AF3-TuM13, 25
Jongen, R.: AS1-TuA5, 31
Joseph, E.A.: ALE2-WeM15, 39; PS2-MoM11, **17**
Journet, C.: NS-WeA7, 41
Jung, S.H.: AA2-TuP17, 33
Jung, Y.C.: EM-MoP5, 24
Junghans, T.: AA4-TuP6, 34
— K —
Kääriä, M.: AF5-MoP4, 23; AM-MoP9, 23
Kachian, J.: AA1-WeM6, **38**
Kagaya, M.: AF4-MoP6, 23
Kalaitzidou, K.: AA1-TuA4, 30
~~Kalam, K.~~: ~~EM-MoP7~~, **24**
Kalliomäki, J.: AF5-MoP4, 23; AM-MoP9, 23
Kaloyeros, A.: AS-TuP3, 34
Kanarik, K.J.: ALE1-MoA1, 21
Kang, D.: AA2-TuA12, **30**
Kang, E.H.: AA1-WeA3, 40
Kang, H.-K.: AA3-TuA16, 29
Kang, M.: AA2-TuP8, 33
Kanomata, K.: AA4-TuP3, 34; AA4-TuP5, 34; AF4-MoP1, 23
Kao, W.-C.: EM3-WeM15, **37**
Kar, G.S.: AA1-WeM5, 38
Karacaoglu, E.: AA1-WeA1, **40**
~~Karahashi, K.~~: AF4-MoP6, 23; ALE1-TuM1, 28; ~~ALE2-TuA15~~, 32; ~~ALE-SuP8~~, **16**
Karppinen, M.: AA2-TuA14, 30; EM2-WeM16, 36
~~Kasikov, A.~~: ~~EM-MoP7~~, 24
~~Katsman, A.~~: ~~AF5-MoP10~~, 23
Kazyak, E.: AA1-TuM7, 26; AA1-WeA2, 40; AA2-TuM12, 26; AA2-TuM13, 26; AA2-TuM15, 26; AS1-TuA7, 31
~~Kei, C.-C.~~: ~~AF2-MoP6~~, 22
Kelliher, A.: EM1-WeM4, 36
Kelliher, J.: AA4-TuP2, 34
Kemell, M.: AF2-TuM4, 27
Kenny, T.W.: AF5-MoP8, 23
Kessels, W.M.M.: AA1-TuM3, 26; AF1-TuM5, 25; **AF3-MoA12**, 19; AF-TuA2, 29; AS1-TuA5, 31; AS2-TuA111, 31; NS-WeA6, 41; PS1-MoM2, **17**
Khalil, G.: AA1-WeM5, 38
Khan, A.: AA3-TuA11, 29
Khan, S.: ALE1-TuA1, **32**
Khosravi, A.: AA3-TuA15, 29
Kia, A.M.: AF3-MoA13, 19
Killaire, G.: AA1-WeA5, 40
Killge, S.: AF1-TuM2, 25
Kim, B.: AA1-WeA6, **40**
Kim, B.J.: AA1-WeA3, 40
Kim, C.G.: AA2-MoA13, 18
~~Kim, C.-M.~~: ~~AA2-TuP7~~, 33
Kim, D.: AF1-MoP3, **22**; AF2-MoP1, 22
Kim, D.H.: AA2-MoA17, **18**; AF1-MoP7, **22**
Kim, D.S.: ALE-SuP14, **16**
Kim, G.J.: AA2-MoA13, 18
Kim, G.W.: AF4-MoP12, 23
Kim, H.: AA2-WeM14, 38; AA2-WeM15, 38; ~~AA5-TuP9~~, 34; AF2-MoP10, 22; AF2-MoP13, 22; AF2-MoP9, 22
Kim, H.J.: AF5-MoP8, 23; AM-MoP5, 23
Kim, H.-L.: AF1-MoP11, 22; AF2-MoP3, 22
Kim, H.S.: AA1-WeM3, **38**; AA3-TuA15, 29; AF4-MoP5, 23; AS-TuP4, 34
Kim, H.Y.: AA2-TuP17, **33**; AA4-TuP12, 34
Kim, J.: AA1-TuP17, **33**; AA1-TuP3, **33**; AA1-WeM3, 38; AA3-TuA15, 29; AF2-MoP3, **22**; AF3-MoP10, **23**; AF4-MoA17, 20; AF4-MoP5, 23; AF-TuA5, **29**; AS-TuP4, 34
Kim, J.E.: ALE-SuP14, 16
~~Kim, J.H.~~: ~~AF4-MoP8~~, **23**
Kim, J.-H.: AA2-TuP1, 33
Kim, J.Y.: AF4-MoP10, 23
Kim, K.H.: AF4-MoP11, **23**
Kim, K.Kim.: AA1-TuP10, **33**
Kim, K.S.: AF4-MoP11, 23
Kim, M.-S.: AF1-MoP1, 22; AF2-MoP2, **22**; AF4-MoP2, 23

Author Index

Kim, M.W.: AA4-TuP8, 34; AA5-TuP8, 34
Kim, S.: AF2-MoP14, 22; ~~AF2-MoP15~~, 22; AF2-MoP3, 22
Kim, S.G.: AA4-TuP8, 34
Kim, S.-H.: AA1-TuP7, 33; AF1-MoP7, 22; AF2-MoP10, 22; ~~AF2-MoP15~~, 22
Kim, S.J.: AA1-TuP3, 33
Kim, S.-J.: ALE1-MoA6, 21
Kim, S.Y.: EM-MoP5, 24
~~Kim, T.H.~~: ~~AF2-MoP15~~, **22**
Kim, W.-H.: AA2-WeM14, 38; AA2-WeM15, 38
Kim, Y.: AA3-TuA16, 29; ~~AA5-TuP9~~, 34; AF2-MoP14, 22; ALE-SuP9, **16**; EM-MoP14, **24**
Kim, Y.S.: ALE2-WeM12, 39; ALE-SuP13, 16
Kimes, W.: AF2-TuM1, 27
Kimmerle, B.: AM-MoP4, 23
Kimmerle, K.: AF2-TuM1, 27; AM-MoP4, 23
Kimmerle, W.: AF2-TuM1, 27
King, P.: NS-WeA5, 41
Kint, J.: **EM1-WeM7**, **36**
Kioussis, D.: AA1-WeM6, 38
Kishimoto, A.: AA2-TuA15, 30
Kisslinger, K.: EM2-WeM14, 36
Kivioja, J.: AF5-MoP4, **23**
Kiyono, H.: AA2-TuP19, 34; AF4-MoA16, 20
~~Kleinlein, J.~~: ~~AA2-TuP18~~, 33
Klement, P.: AS-TuP1, **34**
~~Klimin, V.~~: ~~ALE-SuP3~~, **16**
Knaut, M.: AF1-TuM2, 25
Knemeyer, K.: AF3-MoA11, **19**
~~Knez, M.~~: EM2-WeM12, **36**; ~~EM-MoP8~~, 24
Knoops, H.: AA2-TuP6, 33; AA5-TuP2, 34; AF-TuA2, 29
Ko, D.-H.: ALE-SuP12, 16
Kobayashi, A.: ALE1-MoA3, 21
Kobayashi, H.: ALE2-WeM13, 39
Kobayashi, N.: ALE1-MoA3, 21; ALE1-TuA3, 32; AM1-WeM7, 37
Koeck, F.: AF4-MoP4, 23
Koh, W.: EM-MoP14, 24
Koide, Y.: AA2-TuP19, 34
Komachi, J.: ALE1-TuA7, 32
Kondati Natarajan, S.: ALE1-TuA5, 32; ALE-SuP2, 16; ALE-SuP6, 16
Kondo, H.: ALE2-MoA17, 21
Kondusamy, A.L.N.: AF4-MoA17, **20**; AF4-MoP10, 23; AF4-MoP5, 23; AS-TuP4, 34
~~Kong, M.~~: ~~AA2-TuP20~~, 34
Konh, M.: ALE1-TuM4, 28; ALE-SuP1, **16**
Koo, J.: AA2-MoA17, 18; AA4-TuP7, 34
Korchnoy, V.: AA2-TuP5, **33**; AF3-TuM15, **25**
Kostamo, J.: AM-MoP9, **23**
Kozen, A.: AA5-TuP4, 34; ALE-SuP7, 16
Krahl, F.: EM2-WeM16, **36**
Krbal, M.: NS-TuP1, 35
Kreutzer, M.: AA1-TuM8, 26
Krick, B.: AA5-TuP4, 34
Kriegner, D.: AA3-TuA11, 29
Krishnamurthy, R.: AA1-WeM1, **38**
~~Krishtab, M.~~: ~~AS2-TuA113~~, **31**
Kropp, J.A.: AA1-TuA7, 30
Krüger, O.: AA2-TuP16, 33
Krumpolec, R.: AF2-MoP17, **22**
Krylov, I.: AF3-TuM15, 25
Kuboi, N.: ALE1-TuA7, **32**
Kubota, S.: AA4-TuP3, 34; AA4-TuP5, 34
Kubota, T.: AF-TuA1, 29
Kuech, T.F.T.: EM-MoP11, 24
Kuis, R.: AA1-TuA7, 30
~~Kukli, K.~~: ~~EM-MoP7~~, 24
Kulkarni, S.: ALE2-TuA13, **32**
Kumano, M.: AF3-MoP1, **22**
Kurek, A.: AA5-TuP2, **34**
Kurihara, H.: ALE2-TuM12, 28
Kuyel, B.: AF5-MoP7, **23**
Kwak, S.: AF1-MoA5, 20
Kwo, J.: AA2-TuP12, 33; **AA2-WeM16**, 38
Kwon, J.-D.: AA1-TuP2, **33**
~~Kwon, S. H.~~: ~~AA2-TuP7~~, 33; AA3-TuP1, 34; AA3-TuP5, 34
— L —
La Zara, D.: AA1-MoA1, **18**; EM-MoP2, **24**
Lai, S.: ALE1-WeM7, 39
Laiwalla, F.: AA1-MoA4, 18
Lam, D.V.: AA2-TuP1, 33
Lambert, D.: EM1-WeA8, 41
Lammel, M.: AA1-WeA8, **40**
Lancaster, A.: AF1-MoA1, 20
Land, M.: AF1-MoP4, **22**
Lange, A.: EM-MoP9, 24
Langeslay, R.: AA2-WeA6, 40
Larrabee, T.J.: AF3-MoP8, **23**
Lasso, J.: AA2-TuM12, 26
Lavrik, N.: EM2-WeM14, 36
Lawson, M.: NS-TuP5, **35**
Layne, B.: AA1-TuP14, 33
Lazzarini, L.: AA1-TuA3, 30
Le Roux, F.: ALE2-MoA14, **21**
Lee, B.: AA2-TuP8, 33
Lee, C.: AF1-MoP1, **22**; AF4-MoP10, 23; AF4-MoP2, 23
Lee, C.W.: AA2-WeM14, 38
Lee, H.B.R.: AF2-MoP9, 22
Lee, H.I.: AA3-TuA16, 29
Lee, J.: AA2-WeM15, **38**; AF1-MoP3, 22; AF2-MoP1, **22**; EM3-WeM13, 37; EM-MoP14, 24
Lee, J.-H.: EM1-WeM5, 36; EM1-WeM6, 36
Lee, J.-J.: ALE1-MoA6, 21
Lee, K.L.: ALE1-WeM1, 39
~~Lee, M.~~: ~~AA5-TuP9~~, **34**
Lee, M.Y.: AF2-MoP10, 22; ~~AF2-MoP15~~, 22
Lee, S.: AA1-TuM7, 26; AF2-MoP10, 22
Lee, S.D.: AA4-TuP8, 34
Lee, S.-H.: ALE1-MoA6, 21; EM1-WeM5, **36**; EM1-WeM6, 36
Lee, S.I.: AA4-TuP8, 34; AA5-TuP8, 34; AF1-MoP11, 22
Lee, S.-M.: AA2-TuP1, **33**
Lee, S.-W.: ~~AA2-TuP7~~, **33**; AF1-MoP1, 22; AF2-MoP2, 22; AF4-MoP2, **23**
Lee, T.: EM-MoP5, 24
Lee, W.-H.: EM3-WeM15, 37
Lee, W.-J.: AA1-TuP17, 33; AA3-TuP1, 34; AA3-TuP5, 34; AF1-MoP11, 22; AF2-MoP14, 22; ~~AF2-MoP15~~, 22; AF2-MoP3, 22; EM-MoP14, 24
Lee, W.O.: ALE-SuP14, 16
Lee, Y.: ALE2-MoA13, 21
~~Lee, Y.B.~~: ~~AF4-MoP8~~, 23
Lee, Y.-J.: ALE2-TuM12, 28
Lee, Y.K.: AA2-MoA13, 18
Lee, Y.-S.: ALE1-MoA6, **21**
Lefaucheux, P.: ALE1-MoA8, 21; ALE-SuP11, 16
Leff, A.: EM1-WeA2, 41
Lehto, T.: AF5-MoP4, 23; AM-MoP9, 23
Lei, X.: AF2-MoP8, 22; AF4-MoP2, 23
Leick, N.: AA2-MoA15, **18**; AA2-MoA16, 18
Leijtens, T.: AA2-MoA11, 18
Lemaire, P.C.: AS1-TuA3, 31
Lembesis, P.: ALE1-WeM8, 39
LePage, W.: AA1-WeA2, 40
Lesina, A.: AA1-WeA5, 40
Leskelä, M.: AF2-MoA7, 19; AF2-TuM2, 27; AF2-TuM4, 27; EM1-WeM2, 36; NS-WeA5, 41
Letourneau, S.: AF1-MoA1, 20; EM1-WeA1, 41; NS-WeA2, 41
Leusink, G.: AA2-WeM12, 38; AF2-MoP16, 22
Levrau, E.: EM1-WeA5, 41
Lezec, H.: AA1-WeA4, 40
Li, A.-D.: AA3-TuP7, 34; EM1-WeM1, 36
Li, C.: ALE2-WeM15, 39
Li, F.: AF3-MoP3, 22
Li, H.: AA1-WeA4, **40**; ~~AA3-TuP3~~, **34**; AF4-MoP6, **23**
Li, R.: AA2-TuM14, 26
Li, T.: AA1-TuM5, 26; AA2-TuP13, 33
Li, X.: AA2-TuP6, 33; ALE2-MoA11, **21**
Li, Y.: AA1-TuA4, 30; ALE2-TuM12, 28
Lim, E.T.: ALE-SuP10, **16**
Lim, H.-D.: AA4-TuP8, 34; AF1-MoP11, 22
Lim, H.-J.: AA3-TuA16, 29
Lim, T.: AA1-TuP12, **33**
Lin, B.-T.: AA1-WeA7, 40
~~Lin, C. L.~~: ~~AF2-MoP6~~, 22
Lin, H.-C.: EM3-WeM15, 37
Lin, K.-Y.: AA2-TuP12, 33; **AA2-WeM16**, **38**
Lin, K-Y.: ALE1-MoA5, 21; ALE2-WeM15, **39**
~~Lin, P.~~: ~~AA2-TuP9~~, 33; ~~AA4-TuP10~~, 34; ~~AM-MoP3~~, **23**
Lin, X.: ALE1-TuM4, 28
~~Lin, Y. C.~~: ~~AF2-MoP6~~, **22**
Lin, Y.-H.: AA2-TuP12, 33; **AA2-WeM16**, 38
Linford, M.: EM-MoP13, 24
~~Link, J.~~: AF2-TuM2, 27; ~~EM-MoP7~~, 24
Lisiansky, M.: AA2-TuP5, 33
Littau, K.: AA1-WeM4, 38; AF3-MoA16, 19
Liu, B.: AA2-TuP15, 33
~~Liu, B.-H.~~: ~~AF2-MoP6~~, 22
~~Liu, J.~~: ~~AA2-TuM16~~, 26; AA2-TuP12, 33; ~~EM1-WeA4~~, 41
Liu, M.: AA1-TuP14, 33
~~Liu, S.~~: AA5-TuP5, 34; ~~AF4-MoP9~~, **23**; AS1-TuA4, 31; ~~EM3-WeM16~~, 37
Liu, T.-L.: AS1-TuA1, 31; AS1-TuA2, **31**
Lively, R.: EM2-WeM13, 36
Lo, J.: ALE1-WeM8, 39
Long, N.V.: AA1-TuP15, 33; EM-MoP4, 24
Longo, E.: AA1-TuA3, **30**
Longo, M.: AA1-TuA3, 30
Losego, M.: AA1-TuA4, 30; AA1-TuA8, 30; AA1-WeA1, 40; EM2-WeM13, 36; EM2-WeM15, **36**; EM3-WeM12, 37
Lou, Q.: ALE1-WeM1, 39
Lu, Y.T.: ALE1-WeM1, 39
Lucero, A.T.: AF4-MoA17, 20; AF4-MoP10, 23
Ludwig, K.F.: AS2-TuA214, 31
Lushington, A.: AA2-TuM14, **26**
— M —
Ma, A.: AA2-TuP10, **33**
~~Ma, F.~~: ~~AA3-TuP6~~, 34
Ma, X.: AA2-TuP13, 33
Ma, Y.: EM2-WeM13, 36
Macak, J.: AA2-TuA16, **30**; NS-TuP1, 35
Mack, J.: AA2-TuP17, 33; AA3-TuA11, 29; AA4-TuP12, **34**
Mackus, A.J.M.: AS1-TuA5, 31; AS2-TuA111, 31
MacIsaac, C.: NS-WeA1, 41
Maeda, E.: AA2-TuP19, 34; AF4-MoA16, **20**
Maekawa, K.: ALE1-MoA8, 21; ALE-SuP11, 16
Maes, J.W.: AA1-WeM5, 38
Mahuli, N.: AF4-MoA15, **20**
Mai, L.: AF1-MoP12, **22**; AF1-MoP8, 22
Makarova, O.: AA5-TuP10, 34
Mallick, B.: AF2-TuM6, 27
Mallikarjunan, A.: AF2-MoP8, 22
Mameli, A.: ALE1-WeM3, **39**; AS1-TuA5, 31; AS-TuP5, **34**
Mandia, D.: AA1-TuP19, **33**; AS2-TuA215, 31; EM1-WeA1, 41; ~~EM1-WeA4~~, **41**
Mane, A.: AA1-TuP11, 33; AA1-TuP13, **33**; AA2-TuA11, 30; AA2-TuA12, 30; AA2-WeA6,

Author Index

40; AA4-TuP11, 34; EM1-WeA1, 41; NS-WeA2, **41**
~~Manc, A.U.~~: ~~EM1-WeA4~~, 41
Mannequin, C.: **ALE2-MoA16**, **21**
Manstetten, P.: ALE2-TuA12, 32
Mantovan, R.: AA1-TuA3, 30
Mäntymäki, M.: AM-MoP9, 23
Marichy, C.: NS-WeA7, **41**
Mariette, H.: **ALE2-MoA16**, 21
Marques, E.: AS-TuP6, 35
Marshall, C.: AA1-TuM5, 26
Marshall, J.: AF5-MoP7, 23
Martinez, M.: AA2-MoA16, 18
Martinson, A.: AA1-TuP19, 33; AS2-TuA215, 31
Masanobu, H.: ALE1-WeM1, 39
Maslar, J.: AF2-TuM1, **27**; AM-MoP4, 23
Masse de la Huerta, C.: AM1-WeM5, 37
Masuda, J.: AF2-TuM6, 27
Matsukuma, M.: AF4-MoP6, 23
Mattelaer, F.: AF1-TuM6, 25; **EM1-WeM7**, 36
Mattinen, M.: AF2-MoA7, 19; AF2-TuM2, 27; AF2-TuM4, 27; NS-WeA5, **41**
McBriarty, M.E.: AF3-MoA16, 19
McCarthy, M.: AA2-MoA12, 18
McFadden, A.: EM3-WeM13, 37
McGehee, M.: AA2-MoA11, 18
McGettigan, C.: AA1-TuA8, 30
McGuinness, E.: AA1-TuA8, 30; EM2-WeM13, **36**
McKee, T.: AA1-MoA4, 18
McKenzie, C.: AA5-TuP2, 34
~~Mei, Y.F.~~: ~~AA3-TuP6~~, **34**
Meng, X.: AF2-MoP12, **22**; AF4-MoA17, 20
Merkx, M.: AS1-TuA5, **31**
Messina, D.: AF4-MoP4, **23**; ALE2-MoA15, 21
Metzler, D.: ALE2-WeM15, 39
Mey-Ami, L.: AF3-MoP3, 22
Meyer, D.: AF-TuA7, 29
Meyler, B.: AA2-TuP5, 33
Meynaerts, B.: AS1-TuM16, 27
Michel, F.: AS-TuP1, 34
Miele, P.: AA1-MoA3, 18
~~Mikkor, M.~~: ~~EM-MoP7~~, 24
Miller, J.: EM-MoP9, **24**
Millward, A.R.: AF4-MoP10, 23
Min, S.H.: AA2-WeM14, **38**
Minjauw, M.: AF1-TuM7, 25; AF-TuA4, 29; **EM1-WeM7**, 36
Minot, M.: AA1-TuP13, 33
Mione, M.A.: AF1-TuM5, **25**
Mironov, A.: AF-TuA5, 29
Misra, V.: AA2-TuP8, 33
Mitschker, F.: AF1-MoP12, 22
Miura, M.: AA4-TuP3, 34; AA4-TuP5, 34; AF4-MoP1, 23
Miyoshi, N.: ALE2-WeM13, 39
Mizohata, K.: AF2-TuM2, 27; AF2-TuM4, 27; NS-WeA5, 41
Mizubayashi, W.: ALE2-TuM12, 28
Mizutani, F.: AF2-MoA8, **19**
Modreanu, M.: AA2-MoA12, 18; AA2-TuA15, 30
Mohammad, A.: AF3-MoP7, 23; AF3-TuM13, **25**; AF3-TuM16, 25; AF4-MoP3, 23; EM3-WeM14, 37
~~Mohammed, Y.~~: ~~AA4-TuP10~~, **34**
Mohan, J.: AA1-WeM3, 38; AA3-TuA15, **29**
Mokhtarzadeh, C.: ALE1-TuA5, 32; ALE-SuP2, 16
~~Molenkamp, L.~~: ~~AA2-TuP18~~, 33
Monaghan, S.: AA2-MoA12, 18
Moore, D.: AA2-MoA11, 18
Moran, D.: AA2-TuP6, 33; ALE2-MoA11, 21
Moret, J.: AA1-MoA2, 18
Mori, Y.: AA4-TuP5, **34**
Morisato, T.: AF1-MoA5, 20
Moriya, T.: AF4-MoP6, 23
~~Morrison, W.~~: ~~AF5-MoP3~~, 23
Motamedi, P.: AA1-TuP6, 33
Muckley, E.: EM2-WeM14, 36
Mudrick, J.: ALE-SuP4, **16**
~~Muenstermann, D.~~: ~~AA2-TuP11~~, 33
Mukherjee, N.: AA2-TuP17, 33; AA3-TuA11, **29**; AA4-TuP12, 34
Mullins, R.: ALE2-TuA14, 32; ALE-SuP6, **16**
Muneshwar, T.: AA2-TuP10, 33; AF1-MoA2, 20; EM-MoP12, **24**
Muñoz-Rojas, D.: AA4-TuP9, **34**; AM1-WeM5, **37**
Murdzek, J.A.: ALE1-TuM7, **28**
Mustard, T.: AF1-MoA5, **20**
Myers, T.: EM1-WeM8, **36**
— N —
Nabatame, T.: AA2-TuP19, 34; AF2-MoA8, 19; AF4-MoA16, 20
Naghibolashrafi, N.: AA2-TuP17, 33
Nakane, K.: ALE1-TuA3, 32
Nam, C.-Y.: AA1-TuP14, **33**; EM2-WeM14, **36**
Nam, S.W.: AA3-TuA16, 29
Nam, T.: AF2-MoP13, **22**; AF2-MoP9, 22
Nanayakkara, S.: AA2-MoA11, 18
Nandi, D.K.: AA1-TuP7, 33; AF1-MoP7, 22; ~~AF2-MoP15~~, 22
Narasimhan, V.K.: AF3-MoA16, **19**
Nardi, K.: AS1-TuA2, 31
~~Nassiri, A.~~: ~~EM1-WeA4~~, 41
Natarajan, S.K.: ALE1-TuM5, 28; ALE2-TuA14, 32
Nathan, S.: AA1-TuM6, **26**
Naumann d'Alnoncourt, R.: AF3-MoA11, 19
Naumann, F.: AA2-TuP16, 33; AM-MoP2, 23
Nelson, A.: EM-MoP9, 24
Nemanich, R.: AF4-MoP4, 23; ALE2-MoA15, 21
Nepal, N.: AF2-MoP11, 22; AF-TuA6, 29; AF-TuA7, 29; AS2-TuA214, 31
Ngoc Van, T.T.: EM1-WeM5, 36
Nguyen, C.T.: AF3-MoA14, **19**
Nguyen, N.D.: AA4-TuP9, 34
Nguyen, V.H.: AA4-TuP9, 34; AM1-WeM5, 37
Nicholas, C.: AA1-TuM5, 26
Nie, B.: AA2-TuP17, 33
Nielsch, K.: AA1-WeA8, 40
Niiranen, K.: AF3-TuM14, 25
Nilsen, O.: EM1-WeA6, 41
Nim, M.-H.: AF1-MoP6, 22; AF2-MoP14, 22
~~Nishida, A.~~: ~~AS1-TuM15~~, **27**
Noda, S.: ALE2-TuM12, 28
Noh, H.: EM-MoP15, 24
Noh, W.: AA2-WeM14, 38; AA2-WeM15, 38; AF1-MoP3, 22; AF2-MoP1, 22
Nolan, M.: ALE1-TuA5, 32; ALE2-TuA14, 32; ALE-SuP2, 16; ALE-SuP6, 16
~~Nowak, D.~~: ~~AF5-MoP3~~, 23
Nozawa, T.: AF-TuA1, 29
Nugteren, H.: AA1-TuM8, 26
Nurmikko, A.: AA1-MoA4, 18
Nyakiti, L.: AF-TuA7, 29
Nye, R.: EM1-WeM4, **36**
— O —
O'Brien, S.: AA2-MoA12, 18; AA2-TuA15, 30
Oehrlein, G.S.: ALE1-MoA5, 21; ALE2-WeM15, 39
Ogawa, Y.: EM1-WeA5, **41**
Oh, I.-K.: AA2-WeM14, 38; AA2-WeM15, 38; AS1-TuA1, **31**; NS-WeA1, 41
Oh, J.D.: AF1-MoP6, **22**
Oh, S.-J.: AA3-TuP1, 34; AA3-TuP5, **34**
Ohi, A.: AA2-TuP19, 34; AF4-MoA16, 20
Ohori, D.: AF-TuA1, 29; ALE2-TuM12, **28**
Okada, N.: AF1-MoP10, 22; ~~AS1-TuM15~~, 27
~~Okada, Y.~~: ~~ALE2-TuA15~~, 32
Okuno, H.: NS-WeA7, 41
Okuyama, Y.: AA2-TuP17, 33
Okyay, A.K.: AF3-TuM13, 25
O'Mahony, A.: AA2-TuP6, 33; AA5-TuP2, 34
Opila, R.: ALE1-TuM4, 28
Ostermay, I.: AA2-TuP16, 33
O'Tani, J.: EM-MoP13, 24
Overbeek, M.D.: AA1-TuA3, 30; EM-MoP10, **24**
Oyola-Reynoso, S.: ALE1-WeM1, 39
Ozaki, T.: AF-TuA1, 29; ALE2-TuM12, 28
Ozturk, E.: AA1-WeA1, 40
— P —
Paeng, D.: ALE2-WeM12, 39; ALE-SuP13, 16
Pakulski, R.: ALE1-WeM8, 39
Pallem, V.: ALE1-MoA7, 21; ALE1-TuM4, 28
Palmstrom, A.F.: AA2-MoA11, **18**
Palmstrom, C.J.: EM3-WeM13, 37
Palmstrøm, C.J.: AF1-TuM4, 25
~~Pan, D.~~: ~~AF3-MoP4~~, **23**
Pan, Y.: ALE1-MoA1, 21
Pandiyan, S.: AF1-MoA5, 20
Pannier, C.: AS1-TuA7, 31
~~Pantò, F.~~: ~~EM-MoP1~~, 24
Papanastasiou, D.: AA4-TuP9, 34
Parala, H.: AF1-MoP8, 22
Parise, R.: AM-MoP6, **23**
Park, B.-E.: AA2-WeM14, 38; AA2-WeM15, 38; AF2-MoP10, 22
Park, G.J.: AA4-TuP8, 34
Park, H.: ALE-SuP12, 16; EM-MoP15, 24
Park, H.-D.: AA1-WeA3, 40
Park, H.H.: AA2-MoA13, **18**
~~Park, H.S.~~: ~~AF4-MoP8~~, 23
Park, I.-S.: AF2-MoP18, 22; EM-MoP5, **24**
Park, J.: AA1-TuP15, **33**; ~~AA5-TuP9~~, 34; EM-MoP4, 24
Park, J.H.: AA2-MoA17, 18
Park, J.-H.: AA5-TuP8, 34
Park, J.J.: AA4-TuP8, **34**; AA5-TuP8, 34; AF1-MoP11, 22
Park, J.-R.: AF2-MoP14, 22
Park, J.S.: AA1-WeA3, **40**; AA4-TuP7, 34
Park, J.-S.: AA1-TuA1, **30**
Park, J.-S.: EM1-WeM5, 36
Park, J.-S.: EM1-WeM6, 36
Park, J.-W.: AF1-MoP6, 22; AF2-MoP14, 22
Park, J.Y.: AA3-TuP1, **34**; AA3-TuP5, 34
Park, K.-H.: AA1-WeA3, 40
Park, S.: AF2-MoP18, **22**; ~~AF5-MoP3~~, **23**
Park, S.-J.: AF-TuA5, 29
Park, S.M.: AF2-MoP10, **22**
Parsons, G.N.: ALE1-WeM5, 39; EM1-WeM4, 36
~~Patanè, S.~~: ~~EM-MoP1~~, 24
Patel, D.: EM-MoP13, 24
Pattison, T.: AS1-TuA6, 31
Pavlopoulos, D.: AA1-WeM6, 38
Pedersen, H.: AF1-MoA7, **20**; AF2-TuM3, 27
Peek, B.: AF1-MoP15, **22**; AF-TuA3, 29
Pelissier, B.: AS2-TuA112, 31
Pemble, M.: AA2-MoA12, 18
Peña, L.F.: AS-TuP4, 34
~~Peng, M.~~: ~~EM3-WeM16~~, 37
Pennachio, D.J.: AF1-TuM4, 25; EM3-WeM13, 37
Perng, T.-P.: AA1-TuM4, 26
Pesce, V.: AS2-TuA112, 31
Peterson, R.: AS1-TuA7, 31
Petersson, G.: AA1-MoA1, 18; EM-MoP2, 24
Pfeiffer, K.: AM-MoP2, 23
Phaneuf, R.: EM1-WeA2, 41

Author Index

Phillips, A.: AM1-WeM7, 37
Pi, T.-W.: **AA2-WeM16**, 38
Pidko, E.: AA1-MoA2, 18
Piercy, B.: EM3-WeM12, **37**
Piernavieja Hermida, M.: AF3-MoA11, 19
Pilvi, T.: AA1-MoA4, 18
~~Pinna, N.~~: AF2-TuM8, **27**; ~~EM-MoP1~~, 24
Poduval, G.K.: AA1-TuP18, **33**
~~Pokroy, B.~~: ~~AF5-MoP10~~, 23
Polakowski, P.: AA3-TuA13, 29
Polcawich, R.: EM1-WeA2, 41
Pollet, O.: ALE2-TuM14, 28
~~Ponti, A.~~: ~~EM-MoP1~~, 24
Poodt, P.: AA2-TuA13, **30**; ALE1-WeM3, 39; AS-TuP5, 34
Popecki, M.: AA1-TuP13, 33
Popov, G.: AF2-TuM4, **27**; NS-WeA5, 41
Popov, I.: AA2-TuP5, 33
~~Poruba, A.~~: ~~AF4-MoP8~~, 23
Posseme, N.: ALE2-MoA14, 21; ALE2-TuM14, 28
Possémé, N.: AS2-TuA112, 31
Potrepka, D.: EM1-WeA2, 41
Potter, R.: AF-TuA3, 29
Povey, I.: AA2-MoA12, 18; AA2-TuA15, **30**
~~Pradhan, A.~~: ~~AA2-TuP9~~, 33
Pranda, A.: ALE1-MoA5, **21**
Prasanna, R.: AA2-MoA11, 18
Pribil, G.: AA1-TuA6, 30
Prikryl, J.: NS-TuP1, 35
Prinz, F.: AF5-MoP8, 23
Provine, J.: AF3-TuM12, 25; AF5-MoP8, 23
Prunnila, M.: AA2-WeA4, 40
Pudas, M.: AA1-MoA4, 18
Pulskamp, J.: EM1-WeA2, 41
Pupek, K.: AA2-WeA6, 40
Puurunen, R.: **AF3-MoA12**, 19; AF3-MoA13, 19; AF3-MoA16, 19; AF5-MoP2, 23; AF-TuA2, 29
— Q —
Qadri, S.: AF-TuA7, 29
Qin, Y.: AF3-MoA17, 19
Qin, Z.: AF4-MoA17, 20
~~Qiu, P.~~: ~~EM3-WeM16~~, 37
Quayle, M.J.: AA1-MoA1, 18; EM-MoP2, 24
Quijada, M.: ALE-SuP7, 16
Quinn, B.: AM-MoP6, 23
— R —
Rabat, H.: AM1-WeM5, 37
Radue, E.: EM1-WeM4, 36
~~Rähn, M.~~: ~~EM-MoP7~~, 24
Rahul, R.: AA1-TuP7, 33
Räisänen, J.: AF2-TuM2, 27; AF2-TuM4, 27; NS-WeA5, 41
Rajbhandari, P.: AA1-TuP5, 33
Raley, A.: ALE1-WeM1, **39**
Ramachandran, R.: AF1-TuM7, 25
Ramos, C.: AM-MoP8, 23
Ramunno, L.: AA1-WeA5, 40
Rangelow, I.: ALE1-MoA4, 21
Ranjan, A.: ALE1-WeM1, 39; ALE2-TuA11, 32
Rao, M.: AF2-MoP8, 22
Rao, M.B.: AF2-MoA1, **19**
Rashkeev, S.: EM1-WeA8, 41
Rathi, S.: AA2-TuP17, 33; AA3-TuA11, 29; AA4-TuP12, 34
Ravikumar, V.: **AA1-TuA5**, 30
Raza, A.: AF-TuA4, 29
~~Raza, H.~~: ~~EM-MoP1~~, 24
Reeves, R.: EM-MoP9, 24
Reif, J.: AF1-TuM2, **25**
Resende, J.: AA4-TuP9, 34
~~Rezvan, A.~~: ~~ALE-SuP3~~, 16
Ricky, N.: NS-WeA1, 41
Riedl, T.: AF2-MoA5, 19; ALE2-TuM16, 28; AM1-WeM2, 37
Ritala, M.: AF2-MoA7, 19; AF2-TuM2, **27**; AF2-TuM4, 27; EM1-WeM2, 36; NS-WeA5, 41
Ritasalo, R.: AA1-MoA4, 18
~~Ritslaid, P.~~: ~~EM-MoP7~~, 24
Ritter, D.: AF3-TuM15, 25
Robertson, K.: AF1-MoP4, 22
Robinson, Z.R.: AF1-TuM4, 25; AS2-TuA214, 31
Rodin, D.: AA1-TuA8, 30
Rodriguez, M.: EM1-WeA7, 41
Roozeboom, F.: AF1-TuM5, 25; ALE1-WeM3, 39; AS-TuP5, 34
Rosenberg, S.G.: AF1-TuM4, **25**; AF-TuA6, 29; AS2-TuA214, 31; EM3-WeM13, 37
Rosowski, F.: AF3-MoA11, 19
Rozen, J.: EM1-WeA5, 41
Ruppalt, L.B.: AF3-MoP8, 23
Ryan, L.: AA2-MoA12, **18**
Ryu, J.S.: ALE-SuP10, 16
— S —
Sahota, A.: AA1-WeM3, 38; AA3-TuA15, 29
Saidjafarzoda, I.: EM3-WeM14, 37
Saito, K.: AA4-TuP3, 34; AF4-MoP1, **23**
Sakamoto, J.: AA2-TuM13, 26
Sakurai, A.: AF1-MoP10, **22**
Salami, H.: AA1-MoA5, 18; AA1-MoA8, 18; AA5-TuP7, **34**
Salmi, E.: AF3-TuM14, 25
Samukawa, S.: AF-TuA1, 29; ALE2-TuM12, 28
Sanchez, A.: AA2-TuM12, 26; AA2-TuM15, 26
Sandoval, T.: AS1-TuA1, 31
~~Santangelo, S.~~: ~~EM-MoP1~~, **24**
Saravade, V.: AA1-TuP16, 33
Sarnet, T.: AF5-MoP4, 23; AM-MoP9, 23
Sasaki, M.: **ALE2-MoA16**, 21
Sasao, N.: EM-MoP6, **24**
Sato, D.: ALE2-TuM12, 28
Sattelberger, A.: EM1-WeA1, 41
Sawant, S.Y.: AA1-TuP7, 33
Scanlan, D.: ALE1-TuA4, **32**
Schapmans, E.: AA1-WeM5, 38
Scheppe, A.: EM-MoP9, 24
Schierbaum, K.D.: AF1-TuM3, 25; AF2-MoA7, 19
~~Schlereth, R.~~: ~~AA2-TuP18~~, 33
Schlicht, S.: AA1-WeA8, 40
Schlitz, R.: AA1-WeA8, 40
Schlögl, R.: AF3-MoA11, 19
Schmidt, K.: EM1-WeA5, 41
Schnabel, H.-S.: AA4-TuP6, **34**
Schneider, J.: EM1-WeA3, 41
Schneidewind, J.: ALE2-TuM16, 28
Schörmann, J.: AS-TuP1, 34
Scowen, P.: AF4-MoP4, 23
~~Seemen, H.~~: ~~EM-MoP7~~, 24
Seidel, K.: AA3-TuA13, 29
Seidel, T.: AA1-TuP8, **33**; ALE1-WeM6, **39**
Sekine, M.: ALE2-MoA17, 21
Sekkat, A.: AM1-WeM5, 37
Selberherr, S.: ALE2-TuA12, 32
Seo, J.: AA2-MoA13, 18
~~Seo, K.~~: ~~AA2-TuP20~~, 34
Seo, S.: AF2-MoP9, **22**
Seok, J.-H.: AF1-MoP6, 22; AF2-MoP14, 22
Seong, I.-H.: ALE1-MoA6, 21
Seong, S.: EM-MoP5, 24
Shaffer, D.: AA1-TuP14, 33
Shah, D.: EM-MoP13, **24**
~~Shamim, S.~~: ~~AA2-TuP18~~, 33
Shamsi, Z.: AM-MoP8, 23
Sharma, K.: AS1-TuA3, 31
Sharma, V.: ALE1-TuM6, **28**
Shekhar, A.: **AA1-TuA5**, 30
~~Shekhar, P.~~: ~~AA2-TuP18~~, **33**
~~Sheng, Y.~~: ~~AA2-TuP11~~, 33
Shero, E.: AA2-WeA3, 40
Shi, J.: NS-WeA1, 41
Shi, Y.: ALE1-TuA6, 32
Shieh, J.: AA1-WeA7, 40; AA3-TuA14, 29
~~Shigeno, S.~~: ~~ALE2-TuA15~~, 32
Shigeru, K.: AF4-MoP1, 23
Shim, J.H.: AA1-WeA3, 40; AA2-MoA17, 18; AA4-TuP7, 34
Shimizu, M.: AF3-MoP1, 22
Shin, D.: ALE-SuP12, **16**
~~Shin, H.~~: ~~AS2-TuA216~~, **31**
Shin, J.W.: AM-MoP5, 23
Shin, S.S.: AA2-MoA13, 18
Shin, Y.: AF4-MoP12, 23
Shinoda, K.: ALE2-WeM13, **39**
Shkura, E.: ALE2-TuM16, **28**
Shong, B.: AF2-MoP9, 22; EM1-WeM5, 36
Shoute, G.: AF1-MoA2, **20**
Shu, Y.: AA5-TuP2, 34
Shukla, D.: AF3-MoP7, 23; AF3-TuM13, 25; AF3-TuM16, 25; AF4-MoP3, 23; EM3-WeM14, **37**
Shukla, S.: AM-MoP9, 23
Shul, R.: ALE-SuP4, 16
Shyue, J.-J.: EM3-WeM15, 37
Siebert, M.: ALE2-TuM16, 28
Siegel, D.: AA2-TuM12, 26
Sigurdsson, S.: AA1-MoA4, 18
Simbierowicz, S.: AA2-WeA4, 40
Singh, J.: AA1-TuM6, 26
Sippola, P.: AA3-TuA13, 29; AF2-TuM7, **27**
Smith, S.: EM1-WeA7, **41**
Sobell, Z.: AS1-TuM14, **27**
Soethoudt, J.: AS1-TuM16, 27; AS-TuP6, 35
Sohn, H.: EM-MoP15, 24
Solano, E.: AF1-TuM7, 25; AF3-MoA15, 19
Son, J.-P.: ALE1-MoA6, 21
Son, J.-W.: AA2-MoA17, 18
Song, C.: AF4-MoP12, **23**
Song, E.-J.: AA1-TuP2, 33
Song, H.: ALE-SuP12, 16
Song, S.H.: AA4-TuP4, **34**
Song, S.K.: ALE1-WeM5, **39**
~~Song, Y.~~: ~~EM3-WeM16~~, 37
Sønsteby, H.H.: EM1-WeA6, **41**
Sopha, H.: AA2-TuA16, 30
Sowa, M.: AA5-TuP4, **34**
Spampinato, V.: AS-TuP6, 35
Sperling, B.: AF2-TuM1, 27
Spiegelman, J.: AF2-MoP7, 22; AF4-MoA17, 20; AM-MoP8, **23**; AS-TuP4, 34
Sprey, H.: AA3-TuA13, 29
~~Sreenivasan, M.G.~~: ~~AA1-TuP1~~, 33
Sridhar, S.: ALE2-TuA11, 32
Stafford, N.: ALE1-MoA7, 21
Stan, L.: AA5-TuP10, 34
Stassen, I.: AM1-WeM8, **37**; EM1-WeM3, 36
Stephenson, D.: ALE1-TuA4, 32
~~Stern, R.~~: AF2-TuM2, 27; ~~EM-MoP7~~, 24
Stover, A.: ALE1-TuA4, 32
Strandwitz, N.: AA5-TuP4, 34
Strnad, N.: EM1-WeA2, **41**
Sugimura, S.: EM-MoP6, 24
Sumpter, B.: EM2-WeM14, 36
Sun, K.: AA1-TuM7, 26
Sun, P.: AF5-MoP1, 23; AM-MoP6, 23
Sun, Q.: AA2-TuM14, 26
Sun, Q.Q.: NS-TuP3, 35
Sun, X.: AA2-TuM14, 26; ALE1-WeM1, 39
Sunderland, T.L.: AF4-MoP10, 23
Sundqvist, J.: ALE1-TuA1, 32; AM1-WeM6, 37
Sung, T.: ALE1-WeM8, **39**

Author Index

Suyatin, D.: ALE1-TuA1, 32
Suzuki, K.: AF2-MoP7, 22
Sweet, W.: AA4-TuP2, 34
Szeghalmi, A.: AM-MoP2, 23
Szornel, J.: ALE1-MoA4, 21
— T —
Tadjer, M.: AF-TuA7, 29
~~Tak, Y.D.~~: ~~AF4-MoP8~~, 23
Takahashi, M.: AF4-MoA16, 20
Tamboli, A.: AF2-MoP4, 22
~~Tamm, A.~~: ~~EM-MoP7~~, 24
Tan, .: ALE1-MoA1, **21**
Tan, K.: AS-TuP4, 34
Tanaka, S.: AF3-MoP1, 22
Tang, C.-M.: AA5-TuP10, 34
Tanide, A.: ALE2-MoA17, 21
Tanimoto, Y.: ALE2-TuM12, 28
Tapily, K.: AA2-WeM12, 38
Tarafdar, R.: ALE1-WeM7, 39
Tasneem, N.: AA3-TuA11, 29
Tatsumi, T.: ALE1-TuA7, 32
Teeter, G.: AA2-TuM13, 26
Teplyakov, A.: ALE1-TuM4, **28**; ALE-SuP1, 16
Teramoto, T.: **ALE2-MoA16**, 21
Teranishi, T.: AA2-TuA15, 30
Tesfaye, A.: AA2-TuA16, 30
Teslich, N.: EM-MoP9, 24
Thakur, A.: AM1-WeM6, **37**
Thayne, I.: AA2-TuP6, 33; ALE2-MoA11, 21
Theirich, D.: AF2-MoA5, 19; ALE2-TuM16, 28; AM1-WeM2, 37
Theofanis, P.: ALE1-TuA5, **32**; ALE-SuP2, **16**
Thomas, A.: AA1-WeA8, 40
Thomas, O.: AA5-TuP2, 34
Thompson, T.: AA2-TuM12, 26
Thouless, M.D.: AA1-WeA2, 40
Thu, H.: AA1-TuP15, 33
Tillocher, T.: ALE1-MoA8, 21; ALE-SuP11, **16**
~~Tinacba, E.J.~~: ~~ALE2-TuA15~~, 32
Tompa, G.: AM1-WeM7, **37**
Tonner, R.: AS1-TuA1, 31
Torgesen, J.: AF3-TuM12, 25
Torres, A.: ALE2-MoA14, 21
Toyoda, N.: ALE2-TuM15, **28**
Tracy, R.: AA1-TuM5, 26
Tran Vo, H.C.: AA1-TuP3, 33
Tränkle, G.: AA2-TuP16, 33
Trejo, O.: AS1-TuA7, 31
~~Triolo, C.~~: ~~EM-MoP1~~, 24
Triyoso, D.: AA2-WeM12, **38**
Trunschke, A.: AF3-MoA11, 19
Tsai, Y.: ALE1-TuA6, 32
Tsampas, M.: AA1-TuM3, 26
Tsuchibuchi, G.: AF2-MoP7, 22
Tsutsumi, T.: ALE1-MoA3, **21**; ALE1-TuA3, 32; ALE2-MoA17, 21
Tulodziecki, M.: AA2-TuA13, 30
Tummala, R.: EM2-WeM15, 36
Tuominen, M.: ALE1-TuM6, 28
Tynell, T.: AA1-WeA8, 40
— U —
Uematsu, K.: ALE2-TuM15, 28
Unnikrishnan, S.: AA2-TuA13, 30
Utriainen, M.: **AF3-MoA12**, 19; AF3-MoA13, 19; AF3-MoA16, 19; AF-TuA2, 29
Utsuno, M.: AF-TuA1, 29
Uvarov, V.: AA2-TuP5, 33
Uy, A.: AA1-MoA5, 18; AA1-MoA8, **18**; AA5-TuP7, 34
Uyaner, M.: AA1-WeA1, 40
— V —
Vadapalli, A.: AA1-MoA8, 18; AA5-TuP7, 34
Vallée, C.: AA2-WeA7, 40; **ALE2-MoA16**, 21; AM1-WeM5, 37; AS2-TuA112, **31**
Van Daele, M.: AF1-TuM7, 25; AF-TuA4, **29**
van de Sanden, R.: AA1-TuM3, 26
van den Bruele, F.: AA2-TuA13, 30
Van Elshocht, S.: AS1-TuM16, 27
van Helvoort, A.T.J.: AF3-TuM12, 25
van Ommen, J.R.: AA1-MoA1, 18; **AA1-TuA5**, 30; AF5-MoP2, **23**; EM-MoP2, 24
van Ommen, R.: AA1-MoA2, **18**; AA1-TuM8, 26; AS-TuP6, 35
Varga, A.: AF2-MoA4, 19
Väyrynen, K.: AF2-TuM2, 27
Vehkamäki, M.: AF2-TuM4, 27; NS-WeA5, 41
Ventrice, Jr., C.A.: AF1-TuM4, 25
~~Ventzek, P.~~: ~~AF3-MoP5~~, 23; ALE1-WeM1, 39; ALE2-TuA11, 32
Vereecken, P.: **EM1-WeM7**, 36
Verheijen, M.: AS2-TuA111, 31; NS-WeA6, 41
Verni, G.: AF2-TuM7, 27
Vervuurt, R.: ALE1-TuA3, **32**
Vesterinen, V.: AA2-WeA4, 40
Veyan, J.: AS-TuP4, 34
Volk, A.: AF3-MoP10, 23
Vos, M.: AS2-TuA111, **31**
— W —
Waduge, W.L.I.: EM-MoP11, 24
Wajda, C.: AA2-WeM12, 38; AF2-MoP16, 22
Waldman, R.: AS2-TuA215, **31**
Wallace, R.: AA3-TuA15, 29
Wallas, J.: AF4-MoA15, 20
Walton, S.: AF-TuA6, 29; AF-TuA7, 29; ALE-SuP7, **16**
Wan, H.-W.: AA2-TuP12, 33; **AA2-WeM16**, 38
Wang, H.: AS1-TuA8, **31**
Wang, J.: AA1-WeA2, 40; AF3-MoP3, **22**
Wang, L.: AA1-TuP14, 33
Wang, M.: AF2-MoP8, **22**; ALE1-TuA6, 32
Wang, S.: ALE2-WeM16, 39
Wang, W.: AA2-TuP13, 33
Wang, X.: AA2-TuP13, 33; AF1-TuM1, **25**; AF2-MoP12, 22; ALE2-MoA15, 21
Wang, Y.: NS-TuP3, 35
Wang, Z.: AA3-TuA11, 29; ALE1-TuM4, 28
Warburton, R.F.: AA2-TuA12, 30
Weber, M.: AA1-MoA3, **18**; AA4-TuP1, **34**
Weck, A.: AA1-WeA5, 40
Wege, S.: AM1-WeM6, 37
~~Wei, H.~~: ~~EM3-WeM16~~, 37
Weimer, A.: AA2-MoA14, 18; AF1-MoA6, 20
Weinbub, J.: ALE2-TuA12, 32
Weinfeld, K.: AF3-TuM15, 25
Weinreich, W.: AF3-MoA13, **19**
Werbrouck, A.: AF1-TuM6, **25**
Wheeler, V.: AF2-MoP11, 22; AF-TuA6, 29; AF-TuA7, **29**
Wiemer, C.: AA1-TuA3, 30
Wilk, A.: AM-MoP1, **23**
Wilken, M.: AF1-MoP8, 22
Willis, B.: AF3-MoP7, 23; AF3-TuM13, 25; AF3-TuM16, 25; AF4-MoP3, 23; AM1-WeM1, 37; AS-TuP2, 34
Wilt, J.: AA2-TuP15, 33
Winter, C.H.: AA1-TuA3, 30; AF1-MoP2, 22; EM-MoP10, 24; EM-MoP11, 24
Winterkorn, M.M.: AF5-MoP8, **23**
~~Woehl, J.~~: ~~ALE-SuP5~~, 16
Woelk, E.: AF2-TuM1, 27; AM-MoP4, **23**
Wojtecki, R.: AS1-TuA6, **31**
Wollmershauser, J.: NS-TuP4, 35
Wolterbeek, B.: AA1-MoA2, 18
Woltersdorf, G.: AA1-WeA8, 40
Wood, K.: AA2-TuM13, 26
Wooding, J.: AA1-TuA4, **30**
Woodruff, J.H.: AA2-WeA5, 40
Woodward, J.M.: AF1-TuM4, 25; AF-TuA6, 29; AS2-TuA214, **31**
Wree, J.-L.: AF1-MoP8, 22; AF2-MoA7, **19**
Wright Jr., R.: AF1-MoP9, 22
Wright, R.: AF3-MoP2, **22**
Wu, J.: AA2-TuP15, 33
Würfl, J.: AA2-TuP16, 33
— X —
Xiang, J.: AA2-TuP13, **33**
Xiang, Q.: AA5-TuP1, 34
Xiao, M.: AF2-MoP8, 22
Xie, Q.: AF2-TuM7, 27
Xu, W.: AS1-TuA3, **31**
Xu, X.: AF3-TuM15, 25
— Y —
Yamakawa, S.: ALE1-TuA7, 32
Yamashita, A.: AF1-MoP10, 22; ~~AS1-TuM15~~, 27
Yamazaki, K.: ALE1-MoA8, 21; ALE-SuP11, 16
Yan, B.: AA5-TuP5, **34**
Yan, C.: ALE1-WeM8, 39
Yan, D.: AA1-TuP14, 33
Yang, B.C.: AM-MoP5, 23
Yang, B.-I.: AF1-MoP11, 22
Yang, H.: AF2-MoP18, 22
Yang, M.: ALE1-WeM8, 39
Yang, T.-Y.: AA2-MoA13, 18
Yang, W.: ALE1-MoA1, 21
Yanguas-Gil, A.: AF1-MoA1, **20**; EM1-WeA1, 41; ~~EM1-WeA4~~, 41
Yatsuda, K.: ALE1-MoA8, 21; ALE-SuP11, 16
Ye, X.: AA1-TuP14, 33; EM2-WeM14, 36
Yee, S.: AA1-TuA8, 30
Yeo, S.M.: AA2-MoA13, 18
Yeom, G.Y.: AF4-MoP11, 23; AF4-MoP12, 23; ALE-SuP14, 16
Yeom, W.K.: AF4-MoP12, 23
Yi, S.: AF4-MoP2, 23
Yi, S.-H.: AA1-WeA7, **40**
Yin, Y.-T.: AA3-TuA14, **29**; EM3-WeM15, 37
Ylivaara, O.: **AF3-MoA12**, **19**
Yoneda, M.: AA2-TuA15, 30
Yoo, S.-W.: ALE1-MoA6, 21
Yoon, H.: AF2-MoP10, 22
Yoon, H.R.: EM-MoP4, **24**
Yoon, S.: AF2-MoP18, 22
Yoshida, K.: AA4-TuP3, **34**; AA4-TuP5, 34
Yoshikawa, Y.: AA2-TuA15, 30
~~Yoshino, T.~~: ~~AS1-TuM15~~, 27
Yosida, K.: AF4-MoP1, 23
You, C.: **ALE2-MoA16**, 21
You, S-J.: ALE1-MoA6, 21
Young, E.C.: AF1-TuM4, 25
Young, L.B.: AA2-TuP12, **33**; **AA2-WeM16**, 38
Yu, S.: AA2-TuM12, 26
~~Yu, Y. S.~~: ~~AF2-MoP6~~, 22
Yuan, B.: ALE1-TuM4, 28
— Z —
Zafeiropoulos, G.: AA1-TuM3, 26
Zakaria, Y.: EM1-WeA8, 41
Zanders, D.: AF1-MoP8, 22; AF1-TuM3, **25**; AF2-TuM6, 27
Zazpe, R.: AA2-TuA16, 30; NS-TuP1, **35**
Zeng, D.: AM-MoP1, 23
Zeng, L.: NS-WeA1, **41**
Zeng, T.: AF2-TuM6, 27
Zhang, B.: AF3-MoA17, **19**
Zhang, C.: AA1-WeA4, 40; AS-TuP2, **34**; EM1-WeM2, **36**
Zhang, D.: AA1-MoA1, 18; ALE1-TuA6, **32**
Zhang, D.W.: NS-TuP3, 35
Zhang, F.: EM2-WeM13, 36
Zhang, H.: ALE2-WeM12, **39**; ALE-SuP13, **16**
~~Zhang, K.~~: ~~AA2-TuP9~~, **33**; ~~AA4-TuP10~~, 34; ~~AM-MoP3~~, 23
Zhang, T.: EM1-WeA8, 41
Zhang, Y.: AA4-TuP11, 34
Zhang, Z.: AS1-TuA4, **31**

Author Index

Zhao, Y.: AA2-TuM14, 26; AF1-MoP14, 22; ALE2-MoA15, 21
~~Zhao, Y.T.~~: ~~AA3-TuP6~~, 34
Zheng, L.: AA1-TuM5, **26**
~~Zheng, X.~~: ~~AF4-MoP9~~, 23; ~~EM3-WeM16~~, **37**
Zhiyang, Q.: AF4-MoP5, 23; AS-TuP4, 34
Zhou, B.: AA5-TuP1, 34
Zhou, C.: AA1-TuP16, 33
Zhou, L.: AA2-TuP13, 33
Zhou, X.: AF4-MoP10, **23**; AF4-MoP5, 23
~~Zhu, H.~~: ~~AA2-TuM16~~, **26**; NS-TuP3, 35
Zhu, K.: AA2-MoA11, 18
Zhu, W.: AA1-WeA4, 40
Zoubian, F.: AM1-WeM5, 37
Zuo, P.: EM-MoP11, 24
Zywitzki, D.: AF1-MoP8, 22; AF2-MoA6, **19**

Atomic Layer Etching
Evergreen Ballroom & Foyer - Session ALE-SuP
Atomic Layer Etching Poster Session

ALE-SuP1 Mechanistic Thermal Desorption Studies of Thermal Dry Etching Reactions for Cobalt and Iron Thin Films*, **Mahsa Konh**, A. Teplyakov,* University of Delaware

Atomic layer etching of cobalt and iron has a number of important applications. The mechanisms of thermal dry etching of thin films of these metals were investigated using temperature programmed desorption (TPD) to understand surface chemistry involved in each reaction step. X-ray photoelectron spectroscopy (XPS) and microscopic investigations were used to characterize the surfaces obtained as a result of the etching process. Diketones, such as 1,1,1,5,5,5-hexafluoro-2,4-pentanedione (hfacH) and 2,4-pentanedione (acacH), were tested as etchants. It was determined that in order for the volatile etching products to be formed, the films had to be oxidized or chlorinated, since clean surfaces resulted in decomposition of the diketonates. The oxidized surfaces were shown to evolve volatile transition metal-containing products at temperatures much higher compared to those on surfaces pre-exposed to Cl_2. However, the mechanism of the etching process appeared to be more complicated on chlorine-exposed surfaces. For example, a number of products of a general formula of $Co(hfac)_xCl_y$ were followed for hfacH reaction with cobalt films, and Co^{3+} was shown to participate in the process.

ALE-SuP2 Mechanistic Study of the Thermal Atomic Layer Etch of Tungsten Metal Using O_2 and WCl_6*, S. Kondati Natarajan, M. Nolan,* Tyndall National Institute, Ireland*; **Patrick Theofanis**, C. Mokhtarzadeh, S.B. Clendenning,* Intel Corp.

In semiconductor devices, the low electrical resistivity of tungsten coupled with its high resistance to electromigration have driven its use in contacts between transistor source/drains and higher layer interconnects. However, due to the diminishing dimensions of such devices, the need for precision controlled monolayer etch processes have become a necessity so as to enable current and future device architectures. Accordingly, Atomic Layer Etch (ALE) functions as a complementary process technique to well-established Atomic Layer Deposition (ALD) methodologies, such that sequential self-limiting etch processes can be targeted with the desired monolayer control for ultra-thin film material removal. Recently, thermal ALE processes for W have been reported by Parsons and co-workers[1,2] in which the W is first oxidized by a pulse of O_2 or O_3 gas and then the oxidized material is subsequently removed via gas phase pulses of WF_6 or WCl_6.

Herein, we present a first principles based computational analysis of this thermal ALE process for W metal using an oxidation step followed by introduction of WCl_6 as a co-reactant. We have investigated oxidants for the first pulse in the ALE sequence including O_2, N_2O and H_2O_2. It is shown that bulk oxidation of W is not spontaneous, but coverage of the W surface is dependent and subject to thermodynamic barriers of approximately 2 eV. The energetics associated with the removal of possible volatile etch species in the second ALE step such as $WOCl_4$ and WO_2Cl_2 will be presented. Additionally, the use of Cl_2 gas as an alternative to WCl_6 in the second ALE step has also been explored. A full reaction mechanism for these thermal atomic layer etch processes will be discussed.

1. Xie, W., Lemaire, P. C., Parsons, G. N. Thermally Driven Self-Limiting Atomic Layer Etching of Metallic Tungsten Using WF_6 and O_2. ACS Appl. Mater. & Interfaces, 2018, 10, 9147–9154.

2. Xie, W., Lemaire, P., Parsons, G.N. Self-Limiting Thermal Atomic Layer Etching of Tungsten Metal Using O_2 Oxidation and WCl_6 or WF_6: Role of Halogen Species in Temperature Dependence of ALE Reaction Rate. AVS ALE Workshop, 2018, Incheon, South Korea.

~~**ALE-SuP3 Using Etching of the Atomic Layer to Remove Damaged Layers Obtained by Plasma Chemical Etching with Subsequent Growth of GaAs Quantum Dots by the Method of Droplet Epitaxy***, **Victor Klimin**, A. Rezvan, O. Ageev,* Southern Federal University, Russia~~

~~The task of controlled synthesis of semiconductor self-organizing nanostructures - quantum dots, filamentous nanocrystals, metallic nanodroplets - is extremely important, first of all, to create effective sources of single and entangled photons - the basis of quantum cryptography systems, as well as functional elements based on filamentary nanocrystals, single quantum dots and / or their complexes with a given topology, on the basis of which cellular automata, memory elements, integrated photonics and functional blocks quantum computing systems [1-3].~~

~~At the same time, drip epitaxy, based on separate deposition of components of groups III and V, allows not only to significantly expand the range of structures formed (quantum dots, rings, disks and complex, hybrid structures based on them), but also to realize independent control of the density and size of quantum dots, as well as to use for their creation virtually any A3B5 system, which is inaccessible to techniques based on the Stranski – Krastanov mechanism.~~

~~The use of structured GaAs and Si substrates and the features of droplet epitaxy techniques will effectively localize epitaxial growth at given points on the surface, thereby ensuring precise positioning and control of the parameters of synthesized nanostructures — metal nanoscale droplets (catalytic centers) and quantum dots based on them (in the case of GaAs).~~

~~The structuring of the substrates was carried out by a combination of methods of focused ion beams and plasma chemical etching. However, after obtaining substrates with nanoscale relief, a broken layer was formed on the surface in the depressions caused by plasma and penetration of Ga ions after exposure to focused beams. To remove damaged layers, the best method is layer-by-layer etching of the GaAs surface [4].~~

~~To determine the penetration depth of gallium ions, a simulation was carried out and it was revealed that after treatment in chlorine plasma, 12 atomic disturbed layers remain, which were later removed using the atomic layer etching method. When using the "soft" etching mode, the angle of inclination of the nanoscale structures changed and the growth of quantum dots did not occur.~~

~~At the end of the experimental studies, samples were obtained with nanoscale surface profiling, a combination of methods of focused ion beams, plasma chemical etching, atomic layer etching, in which GsAs quantum dots were obtained by dropping epitaxy.~~

~~This work was carried out as part of a study conducted in the framework of the projects of the Russian Science Foundation No. 15-19-10006.~~

ALE-SuP4 Atomic Layer Etching of Silicon Using a Conventional ICP Etch Chamber for Failure Analysis Applications*, **John Mudrick**, R. Shul, K.D. Greth, R. Goeke, D. Adams,* Sandia National Laboratories

Silicon removal with true atomic fidelity has been shown to require fine control of reactant species concentrations, ion energies, and chamber conditioning. Such fine control of these process parameters is not straightforward to achieve, nor to verify, on legacy process equipment. This work highlights progress toward achieving atomic layer etching (ALE) of silicon wafers and packaged die in standard Cl_2/Ar plasma chemistry for failure analysis applications. Wafer-scale etch experiments show an etch rate decrease to below 1 nm/cycle with decreasing substrate temperature and Cl_2 surface modification step time, however the etch rate increases with the number of etch cycles due to insufficient control over Cl_2 reactant supply; this is especially problematic for silicon removal depths above a few hundred nm, required for failure analysis application. We will use time-resolved optical emission spectroscopy to demonstrate best-case reactant control in this system and suggest methods for achieving ALE-like etching. Furthermore, we observe that the D.C. voltage bias generated during the surface modification and sputter steps is significantly above target values during the first few seconds after plasma ignition for both steps. We have developed multi-step ignition schemes for both stages to ensure smooth transitions where the voltage bias remains very near zero during the Cl_2 plasma generation step and below the sputter threshold of the modified surface layer(s) during the sputter desorption step. For packaged die processing, we show that silicon removal is strongly dependent on both the carrier substrate type as well as die mounting scheme. Using the best developed method, we will present cross-section microscope images showing back-side handle silicon removal to within a few hundred nanometers of the still-functional active device area.

Sandia National Laboratories is a multimission laboratory managed and operated by National Technology & Engineering Solutions of Sandia, LLC, a wholly owned subsidiary of Honeywell International Inc., for the U.S. Department of Energy's National Nuclear Security Administration under contract DE-NA0003525.This paper describes objective technical results and analysis. Any subjective views or opinions that might beexpressed in the paper do not necessarily represent the views of the U.S. Department of Energy or the United States Government.

~~**ALE-SuP5 Study of the Chemical Fabrication Process of NSOM Probes and the Modification of its Surface for Sensing Applications**, ***Muhammad Nazmul Hussain**, J. Woehl,* University of Wisconsin-Milwaukee~~

~~Near-field scanning optical microscopy (NSOM) provides us with eyes for the nanoworld by combining the potentials of scanning probe technology with the power of optical microscopy. To acquire optical images beyond the diffraction limit, NSOM probes require a sub-wavelength optical aperture with wide cone angle of the probe for efficiently channeling the illumination light to the tip apex. Between the two NSOM aperture probe fabrication methods, chemical etching creates tips with wider cone angles of the probe. To determine the mechanism of probe formation and optimize the cone angle with the chemical etching method, different etching times were studied. Additionally, the NSOM probe surface was modified with different fluorescent compounds for high-resolution, fluorescence-based chemical sensing applications.~~

ALE-SuP6 A Mechanistic Study of the HF Pulse in the Thermal Atomic Layer Etch of HfO_2 and ZrO_2, ***Rita Mullins**, S. Kondati Natarajan, M. Nolan,* Tyndall National Institute, Ireland

Thermal atomic layer etching (ALE) of HfO_2 and ZrO_2 uses sequential and self-limiting fluorination reactions using HF as the reactant. This modern approach for ALE is the reverse of atomic layer deposition (ALD) and leads to isotropic etching that removes the modified layer. Each cycle of thermal ALE consists of two precursor pulses. In the first pulse the precursor reacts with the surface atoms of the substrate material and forms a stable and non-volatile layer, this surface modification is self-limiting in nature. We present a first principles study of the hydrogen fluoride pulse in the first step in thermal atomic layer etch of monoclinic hafnium dioxide and zirconium dioxide using density functional theory (DFT) calculations. HF molecules adsorb on the surfaces of these metal oxides by forming hydrogen bonds and may remain intact or dissociate to form, Hf-F and O-H for hafnium dioxide and Zr-F and O-H for zirconium dioxide. The adsorption of one HF molecule at the bare surface of both metal oxides results in dissociative adsorption at all binding sites. The adsorbed H atom can migrate to other O sites on the bare surface depending on energetic barriers. For multiple HF adsorption at coverages ranging from 1/16 to 1 monolayer we find mixed molecular and dissociative adsorption of HF molecules at the bare surfaces. The energetic barriers involved for the formation of H_2O from the HF pulse are estimated using the CI-NEB method.

ALE-SuP7 Atomic Precision Processing of Aluminum Mirrors for Enhanced Ultra-violet Optical Properties, ***Scott Walton**, A. Kozen,* U.S. Naval Research Laboratory*; J. del Hoyo, M. Quijada,* NASA Goddard Space Flight Center*; D. Boris,* U.S. Naval Research Laboratory

Astronomical measurements in the Far Ultra-violet (FUV, 90-200 nm) require the use of aluminum thin films due to aluminum's high reflectivity over this wavelength range. Unfortunately, the native aluminum oxide layer formed in atmosphere is strongly absorbing in this wavelength range, requiring that the aluminum films be passivated with a dielectric that inhibits oxidation. Due to the fast oxidation of aluminum, a simultaneous etch and deposition process is desirable to both eliminate the native aluminum oxide after growth and replace it with a different passivation coating layer. Optical measurements in the FUV range are some of the most challenging due to limited selection of low reflectivity coatings available for use on aluminum thin films. Typically magnesium fluoride (MgF_2) or lithium fluoride (LiF) coatings are used for these passivation purposes but each has its problems. MgF_2 has an absorption cutoff at 115 nm occluding a critical part of the FUV spectrum. LiF has a lower absorption cutoff at 102.5 nm, but is hygroscopic and thus susceptible to degradation in ambient conditions. A promising alternative to these coating materials is AlF_3, which theoretically can provide reflectivity greater than 50% down to 100 nm if the coating is sufficiently thin. In this work, we explore the use of electron beam generated plasmas to simultaneously etch the native oxide layer from aluminum thin films while depositing an AlF_3 capping layer to passivate the aluminum reflector. XPS measurements indicate that this approach is cable of producing very thin (<5 nm) AlF_3 films with some mild oxygen contamination. We will discuss the impact of plasma power, chemistry, and time on the composition and structure of the passivating layer and its subsequent optical properties. This work is supported by the Naval Research Laboratory base program and NASA Strategic Astrophysics Technology (SAT) grant No. NNH177ZDA001N.

~~**ALE-SuP8 Surface Reaction Analysis for Atomic-Layer Etching and Deposition by Means of Beam Experiments**, ***Kazuhiro Karahashi**, T. Ito, S. Hamaguchi,* Osaka University, Japan~~

~~As the sizes of semiconductor devices continue to diminish, atomically controlled damage-less selective etching processes are absolutely crucial for the fabrication of such devices. Ligand exchange processes of organic compounds deposited on metal surfaces, and low-energy ion or cluster beam processes are candidates for such highly selective precise etching processes. For the control of these processes, it is important to understand and control surface reactions of organic compounds and low-energy ions/clusters. Molecular beam experiments provide an understanding of the dynamics and kinetics of chemical interactions of gas molecules with solid surfaces. In this study, a new surface-reaction analysis system with molecular beams has been developed for the analyses of etching reactions. The system has differentially-pumped beam sources for low-energy ions, thermal-molecular and metastable radicals/clusters that independently irradiate the sample surface set in an ultra-high-vacuum (UHV) chamber. To study surface reactions, we detected the scattered species and desorbed products with a differentially pumped quadrupole mass spectrometer (QMS) and measured adsorbed chemical states on the surface during various beam irradiation by X-ray photoelectron spectroscopy (XPS). The QMS provided time-resolved measurements and could be synchronized with an ion or molecular beam. The system can experimentally simulate an atomically controlled process such as atomic layer etching (ALE) or atomic layer deposition (ALD). Also presented as sample experimental data obtained in this system are desorbed species, and surface chemical states during beam irradiation of transition metal (Ni, Cu etc.) surfaces with halogen and organic molecules (such as diketone).~~

ALE-SuP9 Atomic Layer Etching of SiO_2 and Si_3N_4 with Fluorocarbon, Hydrofluorocarbon and Fluoroether Compounds, *H. Chae,* ***Yongjae Kim**, T. Cha, Y. Cho,* Sungkyunkwan University (SKKU), Republic of Korea

Nanometer and angstrom scale etching is getting more critical as the critical dimension of semiconductor devices shrinks down to 10nm. Atomic layer etching (ALE) processes are being developed and studied to control etch depth in nanoscale and atomic scale by limiting the amounts of chemical reactants available on the surface with self-limited reactions. [1] With cyclic ALE processes, low surface roughness, high uniformity and high selectivity can be achieved with low damage to devices. [2-3]

In this work, cyclic plasma etching for SiO_2 and Si_3N_4 was developed and characterized with surface modification in an inductively coupled plasma (ICP) reactor with fluorocarbon, hydrofluorocarbon, and fluoro-ether plasmas. The process consists of two steps of surface modification and removal step. In the first step, thin fluoro- or hydrofluro-carbon layers are deposited on SiO_2 and Si_3N_4 surface with fluorocarbon, hydrofluorocarbon, and fluoroether plasmas. In the second step, the modified layers are removed with ions or radicals generated from Ar or O_2 plasmas. At the bias voltage increased, the incomplete etched region, the self-limiting etched region, and the sputtering region appeared, and lower etching rate was obtained using O_2 plasma than Ar plasma. Etching rate were compared at various conditions of reaction gases and plasma power and the rate could be controlled under 10 Å/cycle. Etching rate dependences are investigated on ion energy, etching time, FC film deposition, and precursor selection. Self-limited etching rate was obtained and higher selectivities of SiO_2/Si and Si_3N_4/Si etch rate were obtained with fluoroether.

References

[1] C. Li, D. Metzler, C. S. Lai, E. A. Hudson, and G. S. Oehrlein, J. Vac. Sci. Technol., A, 34, 041307 (2016)

[2] Y. Ishii, K. Okuma, T. Saldana, K. Maeda, N. Negishi, and J. Manos, Jpn. J. Appl. Phys., 56, 06HB07 (2017)

[3] K. Koh, Y. Kim, C.Kim, and H. Chae, J. Vac. Sci. Technol. A, 36, 01B106 (2018)

ALE-SuP10 Cyclic Etching of Copper Thin Films using Two Sequential Steps, ***Eun Tack Lim**, J.S. Choi, J.S. Ryu, M.H. Cha, C.W. Chung,* Inha University, Republic of Korea

Copper has been used as the interconnects in the semiconductor memory devices because it has many advantages such as low resistance and low diffusivity. In addition, the electromigration phenomenon which causes wire deformation and breakage occurs less on copper [1]. Currently, copper has been etched through a damascene process because direct dry etching process has not been developed. However, the damascene process reveals some limitations in achieving fine patterns of several nanometers [2]. To solve this issue regarding the damascene process, the intense studies on

copper patterning are being performed using conventional dry etching.Cyclic etching, as another approach to etch the copper films, can be a prospective etching technique. Cyclic etching including surface modification and its removal can provide the good etching performance of copper films by effectively inducing surface reaction and precisely controlling the etch depth. These results are attributed to the nature of self-limiting process and the removal of the film by layer-by-layer. There are possible various gas combinations in cyclic etching of copper films. In this study, cyclic etching with two sequential steps of surface modification and ion bombardment was performed. The surface modification and etch depth (etch rate) of copper film were confirmed using surface profilometer, scanning probe microscopy, and field emission scanning electron microscopy (FESEM) as a function of various parameters such as the time of surface modification (plasma exposure) and the bombardment energy of ions. Besides, the resultant etch profile and etch mechanism of copper film in the cyclic etching have been investigated by FESEM, X-ray photoelectron spectroscopy, and Raman spectroscopy.

Acknowledgments This research was supported by the MOTIE(Ministry of Trade, Industry & Energy (10080450) and KSRC(Korea Semiconductor Research Consortium) support program for the development of the future semiconductor device.

References[1] A. Strandjord, S. Popelar, C. Jauernig, Microelectron. Reliab. **42,** 265–283(2002) [2] H. Helneder, H. Ko¨rner, A. Mitchell, M. Schwerd, U. Seidel, Microelectron. Eng. **55**, 257–268 (2001)

ALE-SuP11 Analysis of Mechanisms Involved in Cryogenic ALE*, **Thomas Tillocher**, G. Antoun, P. Lefaucheux, R. Dussart,* GREMI Université d'Orléans/CNRS, France*; K. Yamazaki, K. Yatsuda,* Tokyo Electron Limited, Japan*; J. Faguet, K. Maekawa,* TEL Technology Center, America, LLC

Atomic Layer Etching (ALE) has been developed almost 40 years ago, but has gained interest these last years for micro and nanoelectronic processes where high precision patterning is required. ALE consists in a sequential process relying on the self-limited adsorption of precursor radicals on the first monolayer(s) of material to be etched. Then, under a low energy ion bombardment, the etch products form and desorb until the adsorbed layer is depleted. This self-limited reaction removes a few monolayers. By repeating the cycle, the material is etched a few monolayers by a few monolayers.

ALE of SiO_2 has been achieved with a 3-step process and reported in the literature [1]. The first step is an Ar/C_4F_8 plasma without any ion bombardment. The oxide surface is then coated with a very thin fluorocarbon layer. The second step is a pure Ar plasma still with no RF self-bias voltage where C_4F_8 is pumped out of the chamber. The third and final step is an Ar plasma with about 10V RF self-bias voltage. The ion energy must be kept below the sputtering threshold. If the thickness of the FC layer is accurately controlled, the etch step can be self-limited.

Although quasi-ALE of SiO_2 has been demonstrated with this process, fluorocarbon contamination of chamber walls is an issue. This affects the reproducibility of ALE processes and hence chamber cleaning is required. Cryogenic Atomic Layer Etching (Cryo-ALE) is proposed as a potential solution. In this new process, the substrate is cooled to very low temperature by liquid nitrogen. The plasma phase deposition step is replaced by a physisorption step consisting in exposing the cooled substrate to a fluorocarbon gas flow. Under such conditions, species are adsorbed only at the cooled surface and hence wall pollution is mainly suppressed. Cryo-ALE of SiO_2 has been shown to be effective at -120°C. The details regarding the overall process are presented in G. Antoun's abstract.

If the temperatures is raised of a few degrees (for instance to -110°C), no etching is observed since C_4F_8 does not significantly physisorb at such temperature. Therefore, understanding physisorption conditions as well as activation of etching using a physisorbed layer is relevant for a better control of the process. Desorption mass spectrometry experiments will be fully presented and discussed in this paper.

[1] Metzler et al., J. Vac. Sci. Technol. A 32(2), 020603-1 2014

Acknowlegment: The authors thank S. Tahara from Tokyo Electron Miyagi for helpful discussions.

ALE-SuP12 Study on Dry Etching Characteristics of Germanium Oxide by Atomic Layer Deposition*, **Donghyuk Shin**, J. Jeong, H. Song, H. Park, D.-H. Ko,* Yonsei University, Republic of Korea

While the Si-based electronics whose basis materials consisting of silicon substrate and silicon dioxide, have played a leading role in the semiconductor industry, germanium has also been receiving steady attention as a new channel material for its high carrier mobility. In particular, the studies on germanium oxide films of which the most are discussing mainly the Ge oxidation process on Ge substrates, have been conducted for several decades. However, the formation of GeO_2 film through the oxidation process restricts its own potential for utilization because it is only applicable on Ge substrates. Oxidation process conducted on the SiGe layer causes Ge condensation at its interface where Ge atoms remain nonbonded to oxygen due to the less negative Gibbs free energy to form the GeO_2 compared to SiO_2. In this context, the growth of GeO_2 film by the atomic layer deposition (ALD) enables its utilization to be enlarged even for use on Si substrate. For example, a literature examined the applicability of ALD GeO_2 film on Si substrate as a secure memory device employing its unusual film property of dissolving in water. However, the GeO_2 film inevitably exhibits unstable nature under the wet etching process, which means that the fundamental study on the GeO_2 film needs further explorations including dry etch characteristics.

In this talk, we discuss the growth and characterizations of GeO_2 film by ALD process. Film properties of ALD GeO_2 were evaluated using High-resolution X-ray photoelectron spectroscopy and Auger electron spectroscopy. We demonstrate the dry etch characteristics of ALD GeO_2 films. Dry etch test was performed in the reactive ion etching chamber equipped with a direct capacitive-coupled plasma, using C/F based dry etch chemistry. In addition, the dry etch mechanism of the ALD GeO_2 film was investigated in comparison with thermal oxide and silicon nitride. Basic dry etching selectivity mechanism between SiO_2 and Si_3N_4 lies on the different ability of each film to self-consume the polymer barrier layer which is formed during dry etching process using C/F based plasma. Our dry etch test results showing a faster dry etch rate for Si_3N_4 film against SiO_2 film during the reactive ion etching, are in good agreement with the exper imental results reported in literatures, while the ALD GeO_2 film reveals its dry etch characteristics which encompass the competing reaction between etching and polymerization.

ALE-SuP13 Laser Isotropic Atomistic Removal of Germanium*, D. Paeng, **He Zhang**, Y.S. Kim,* Lam Research Corp.

Pico second (ps) pulsed laser has been used to achieve isotropic atomistic removal of germanium (Ge). After hydrogen (H_2) plasma pre-treatment at room temperature, adsorption of O_2 or Cl_2 gas on the clean Ge surface is used to form germanium monoxide (GeO) or germanium chloride ($GeCl_x$) layer. Under laser irradiation, modified layer will heat up rapidly depending on the laser fluence. This surface oxide or halide desorbs thermally, and the short pulse of the ps laser suppresses heat diffusion into the material enabling surface-confined photo-thermal reactions on an ultrafast time scale without thermal budget issue. Etch rates (ER) of sub-nanometers per cycle have been achieved. We report on parametric studies showing how the laser parameters and process conditions affect the ER and the surface roughness after etching.

ALE-SuP14 Anisotropic Atomic Layer Etching of Tungsten using Reactive Ion Beam*, **Doo San Kim**, J.E. Kim, W.O. Lee, Y.J. Gill, B.H. Jeong, G.Y. Yeom,* Sungkyunkwan University, Republic of Korea

Atomic layer etching (ALE) is a next generation etching technique consisting of cyclic removal of a monolayer per cycle by repeating adsorption and desorption steps. ALE has advantages such as precise thickness control, high etch selectivity, surface smoothing effect, and minimization of the surface damage during the etching. For the fabrication of next generation nanoscale devices, both isotropic and anisotropic ALE techniques are required. In this study, anisotropic ALE of tungsten (W), which is used as an interconnect layer and the gate material of semiconductor devices, was investigated by sequentially exposing to F radicals by NF_3 plasma to form a tungsten fluoride layer followed by the exposure to an oxygen ion beam to remove the tungsten fluoride layer by forming volatile tungsten oxyfluoride (WO_xF_y) compound at room temperature. The result showed that, at optimized ALE conditions, a precise etch rate of ~ 2.6 Å/cycle was obtained while increasing the W etch depth linearly with increasing the number of etch cycles. And, the W ALE mechanism was investigated by analyzing the surface roughness and surface composition of W during the adsorption step and desorption step.

Plenary Session
Grand Ballroom A-G - Session PS1-MoM

ALD Plenary Session

Moderators: Sumit Agarwal, Colorado School of Mines, Dennis Hausmann, Lam Research Corp.

8:45am **PS1-MoM2 Atomic Scale Processing: From Understanding to Innovation***, **Erwin Kessels,*** Eindhoven University of Technology, Netherlands **INVITED**

Atomic scale processing is the collective term for processing methods that are currently more and more being explored – and industrially employed – to prepare thin films and nanostructures in a highly controllable way with atomic scale precision. Atomic layer deposition (ALD) and atomic layer etching (ALE) are two prominent examples but also state-of-the-art nanopatterning and area-selective deposition (ASD) approaches can in many cases be regarded as examples of atomic scale processing. In this presentation, I will address several recent and emerging trends in atomic scale processing and discuss how understanding of the underlying mechanisms has contributed to important innovations in the field, either in research or in industry. Application areas to be addressed are especially nanoelectronics and photovoltaics which I will discuss from my own experience and perspective. Topics to be discussed are: (i) the growing importance of plasma ALD, aspects such as conformality and the role (and control) of ions; (ii) the necessity of in situ metrology methods (e.g. in situ spectroscopic ellipsometry) for process monitoring and advanced surface spectroscopy for obtaining more quantitative insight into fundamental parameters; (iii) the use of ALD in nanopatterning and the interest in area-selective ALD including those combinations with intermediate etch steps; and (iv) the need for isotropic and anisotropic ALE, either thermal or plasma-based.

9:30am **PS1-MoM5 Elucidating the Mechanisms for Atomic Layer Growth through In Situ Studies***, **Jeffrey W. Elam,*** Argonne National Laboratory **INVITED**

Atomic Layer Deposition (ALD) provides exquisite control over film thickness and composition and yields excellent conformality over large areas and within nanostructures. These desirable attributes derive from self-limiting surface chemistry, and can disappear if the self-limitation is removed. Understanding the surface chemical reactions, i.e. the ALD mechanism, can provide insight into the limits of self-limitation allowing better control, successful scale up, and the invention of new processes. In situ measurements are very effective for elucidating ALD growth mechanisms. In this presentation, I will describe investigations into the growth mechanisms of ALD nanocomposite films comprised of conducting (e.g. W, Mo and Re) and insulating (e.g. Al_2O_3, ZrO_2 and TiO_2) components using in situ measurements. These ALD nanocomposites have applications in particle detection, energy storage, and solar power. We have performed extensive in situ studies using quartz crystal microbalance (QCM), quadrupole mass spectrometry (QMS), Fourier transform infrared (FTIR) absorption spectroscopy, and current-voltage measurements. These measurements reveal unusual ALD chemistry occurring upon transitioning between the ALD processes for the two components. This results in unique reaction products that affect the properties of the films in beneficial ways. The knowledge gained from our in situ studies of the ALD nanocomposite films has helped us to overcome problems encountered when we scaled up the ALD processes to large area substrates. Beyond fundamental understanding, in situ measurements are extremely effective in ALD process development and process monitoring. I will end my talk by describing our recent work combining in situ measurements and machine learning to accelerate ALD process development.

Plenary Session
Grand Ballroom A-G - Session PS2-MoM

ALE Plenary Session

Moderators: Craig Huffman, Micron Technology, Gottlieb S. Oehrlein, University of Maryland

11:00am **PS2-MoM11 Mapping the Future Evolution of Atomic Scale Processing to enable the World of Artificial Intelligence***, **Eric A. Joseph,*** IBM T.J. Watson Research Center **INVITED**

Advances in the semiconductor industry, historically based on Moore's Law and Dennard scaling, have become progressively challenging as device technology moves beyond the 7nm node. The ever-continuing trend to shrink device size, coupled with the introduction of novel materials, multi-component materials and/or nanoscale materials has driven the need for the ultimate solution: atomic scale precision. To meet this demand, considerable work has been underway to incorporate advances in atomic layer etching (ALE), atomic layer deposition (ALD), and area selective techniques to meet process requirements. However, as future technology undergoes a paradigm shift away from Moore's Law towards accelerator technologies for AI applications, the types of process driven challenges will also change. This transition will require a revised focus on process capability, expanding beyond traditional process enhancements, to minimizing process induced device performance degradation. Examples of this paradigm shift will be discussed in detail and a vision for the future challenges of atomic scale processes will be reviewed.

ALD Applications
Grand Ballroom A-C - Session AA1-MoA
ALD for Biological and Space Applications

Moderators: Elton Graugnard, Boise State University, Mato Knez, CIC nanoGUNE

1:30pm **AA1-MoA1 Atomic Layer Deposition on Pharmaceutical Particles for Inhaled Drug Delivery***, **Damiano La Zara**,* Delft University of Technology, Netherlands*; D. Zhang, M.J. Quayle, G. Petersson, S. Folestad,* AstraZeneca, Sweden*; J.R. van Ommen,* Delft University of Technology, Netherlands

Drug delivery by inhalation provides a targeted treatment for respiratory diseases such as asthma and chronic obstructive pulmonary disease. A growing amount of new inhaled active pharmaceutical ingredients (APIs) includes amorphous drugs, which are often very moisture-sensitive, as well as expensive and less potent drugs, which require improved flowability and aerosolization efficiency to meet the drug load requirements and to minimize their cost. Moreover, there is no commercially viable extended-release technique for inhaled drug particles. Therefore, there is an unmet need for novel solutions to provide surface modification of inhaled pharmaceutical powders that lead to improved processability and stabilization of solid state forms (e.g., amorphous, metastable, polymorphs, hydrates) and, most importantly, clinical benefits, e.g., controlled release of API from dosage forms.

In this work, we demonstrate the use of atomic layer deposition (ALD) as a route to modify the properties of inhaled pharmaceutical particles, namely (i) dispersibility, (ii) stability to moisture and (iii) dissolution rate. We deposit ultrathin oxide ceramic films, namely Al_2O_3, TiO_2 and SiO_2, on both API (e.g., budesonide and salbutamol) and excipient (i.e., lactose) particles, both crystalline and amorphous. The ALD process is carried out at ambient conditions in a fluidized bed reactor for a range of cycles from 10 to 50, using TMA/O_3, $TiCl_4$/H_2O and $SiCl_4$/H_2O as precursors for Al_2O_3, TiO_2 and SiO_2 ALD, respectively. The deposition strongly depends on the surface crystal structure of the particles. Time-of-flight secondary ion mass spectrometry and transmission electron microscopy reveal the deposition of uniform and conformal nanofilms on crystal surfaces, whereas uniform but non-conformal nanofilms are observed on amorphous surfaces. The dispersion properties are evaluated both in the liquid and dry state. The ALD-coated particles exhibit considerably higher dispersibility in both water and ethanol solutions, thus suggesting higher bioavailability, than the uncoated ones. In-vitro aerosolization testing by the next generation impactor shows improved fine powder delivery (<5 µm, i.e., particle size range relevant for inhalation) and greatly reduced powder retention in the inhaler for the ALD-coated particles. The dispersion and aerosolization properties are retained even upon different conditions of temperature (25-40 °C) and relative humidity (60-75 %) over 3 weeks. Finally, in-vitro dissolution tests and cell absorption studies reveal more sustained release with increasing film thickness.

1:45pm **AA1-MoA2 The Use of Atomic Layer Deposition to Increase the Availability of Medical Radio-Isotopes***, **Ruud van Ommen**, J. Moret, B. Wolterbeek, E. Pidko, A. Denkova,* Delft University of Technology, Netherlands

Since the first use of the radionuclide phosphorus-32 for treatment of haematological patients in the 1930s, the use of radioisotopes in medicine has expanded into a mainstream clinical speciality . It encompasses both diagnostic imaging (exploiting the tissue penetration of gamma rays released in nuclear decay) and targeted therapy (exploiting the cellular toxicity of beta minus and alpha particles) [1]. Radioisotopes are typically applied in single photon emission computed tomography (SPECT, e.g., ^{67}Ga, ^{99m}Tc, ^{111}In, ^{177}Lu) and positron emission tomography (PET, e.g., ^{68}Ga, ^{64}Cu, ^{44}Sc, ^{86}Y, ^{89}Zr), as well as in therapeutic applications (e.g., ^{47}Sc, ^{177}Lu, ^{90}Y, $^{212/213}$Bi, ^{212}Pb, ^{225}Ac, $^{186/188}$Re) [2].

In targeted radionuclide therapy a major hurdle is the dependence on a very limited number of nuclear reactors worldwide to produce these radioisotopes. Especially when some of these reactors are down due to unforeseen maintenance, critical situations for patients relying on the radionuclides can appear.

Atomic layer deposition (ALD) can provide a way to either exploit production in smaller nuclear reactors while still producing radionuclides of high specific activity (i.e. activity per unit of mass) or in some cases to prepare radionuclide generators, that can be placed in hospitals, providing on-site and on-demand supply [3]. In this presentation, we will compare the periodic table for medical radio-isotopes [1] with the periodic table for ALD precursors [4,5]. It will be discussed in which ways ALD can aid in the production of medical radio-isotopes . We will illustrate this by some examples, such as the production of ^{177}Lu and ^{99}Mo.

1. Blower, P. J. (2015). A nuclear chocolate box: the periodic table of nuclear medicine. *Dalton Transactions*, *44*(11), 4819-4844.
2. Price, E. W., & Orvig, C. (2014). Matching chelators to radiometals for radiopharmaceuticals. *Chemical Society Reviews*, *43*(1), 260-290.
3. Moret, J.L.T.M., Wolterbeek, H.T., Denkova, A.G., & van Ommen, J.R., (2016). Thin layer deposition of Lutetium on nano-particles. Presented at 16th International Conference on Atomic Layer Deposition (ALD 2016), Dublin, Ireland, 24–27 July 2016.
4. Puurunen, R. L. (2005). Surface chemistry of atomic layer deposition: A case study for the trimethylaluminum/water process. *Journal of applied physics*, *97*(12), 9.
5. Miikkulainen, V., Leskelä, M., Ritala, M., & Puurunen, R. L. (2013). Crystallinity of inorganic films grown by atomic layer deposition: Overview and general trends. *Journal of Applied Physics*, *113*(2), 2.

2:00pm **AA1-MoA3 Atomic Layer Deposition for Biosensing Applications***, O. Graniel, **Matthieu Weber**, S. Balme, P. Miele, M. Bechelany,* Institut Européen des Membranes, France

Atomic layer deposition (ALD) is a thin film deposition technique currently used in various nanofabrication processes for microelectronic applications. The ability to coat high-aspect-ratio structures with a wide range of materials, the excellent conformality, and the precise thickness control have made ALD an essential tool for the fabrication of many devices, including biosensors[1].

In this study, we combined ALD, nanosphere lithography (NSL), and electrodeposition to fabricate hollow ZnO urchin-like structures covered by a Au film for surface-enhanced Raman spectroscopy (SERS) applications. The morphology of the structures was investigated using scanning electron microscope (SEM) and transmission electron microscope (TEM). These three dimensional, high-aspect-ratio organized nanostructures enabled the detection of thiophenol with concentrations as low as $1x10^{-10}$ M. The impact of the gold layer thickness, and annealing conditions were investigated. Samples that were not annealed had a better overall reproducibility, whereas the ones annealed presented a stronger enhancement of the Raman signal due to the coalescence of Au into nanoparticles. Lastly, the biosensing capability of the urchin-like ZnO structures was demonstrated by successfully detecting adenine. These proof-of-concepts enabled for a better understanding of the properties of these peculiar nanostructures, and open prospects for the biosensing community.

1. Graniel, O., Weber, M., Balme, S., Miele, P. & Bechelany, M. Atomic layer deposition for biosensing applications. *Biosens. Bioelectron.* **122,** 147–159 (2018).

2:15pm **AA1-MoA4 Multi-layer Stacked ALD Coating for Hermetic Encapsulation of Implantable Biomedical Microdevices***, J. Jeong,* Pusan National University, Republic of Korea*; S. Sigurdsson, F. Laiwalla,* Brown University*; R. Ritasalo, M. Pudas, T. McKee, T. Pilvi,* Picosun Oy, Finland*; A. Nurmikko,* Brown University*; **Tom Blomberg**,* Picosun Oy/ASM, Finland

Introduction and Main Findings:

Implantable biomedical electronics are a promising technology for medical diagnosis and treatment if they can be made safe for chronic use. There is thus a growing need for compact-volume hermetic packaging methods for miniaturized biomedical implants. Here we describe the use of multi-layer ALD films comprising HfO_2 and SiO_2 (Picosun Oy, Finland) to hermetically encapsulate microscale wireless active electronic implants for use in the brain. The robustness of the 3-D conformal ALD coatings is validated using an accelerated aging test by application of thermal stress (87°C saline) and quantified in terms of water/ionic ingress (leakage currents) as well as overall device performance (the latter via wireless interrogation). ALD coated devices have an extrapolated physiologic temperature lifetime of > 10 years under active electric field stress. Failed devices maintain the layer integrity, and only show gross anomalies on SEM at sample edges likely consistent with handling stresses. This performance is not impacted by opening apertures in the coating (for fabrication of sensing/actuating interface electrodes).

Experimental:

All films were grown in Picosun™ R-200 advanced reactors using thermal ALD processes, and comprised alternating layers of HfO_2 and SiO_2 for a total thickness of 100 nm. The ALD temperature was varied between 150°C and 300°C. Samples were batch processed in a wire-mesh bag (Fig S2 (d)) for

full 3-D conformal multilayer encpasulation, and carefully poured on to Al foil and loosely packed for transportation. Sample handling was done using plastic-tip or vacuum tweezers. Three types of substrates were coated: 500 µm x 500 µm passive silicon die, active wireless microelectronic chiplets, and wired interdigitated electrodes. The substrates were subjected to an accelerated aging test by immersion in saline at 87 C. A subset of active microelectronic chiplets were constantly powered on using RF energy at 915 MHz. Failed samples were analyzed by scanning electron microscopy.

Results:

ALD-coated samples had an accelerated aging test survival time which can be extrapolated to > 10 years at physiologic temperatures (37°C) for passive as well as active samples (where the latter had continuous electric fields across the ALD films). Analysis of the failed samples shows areas of film breakdown at the edges, likely associated with post-encapsulation handling. There is no evidence of delamination of the ALD layer stack at the periphery of the failure, indicating that point-failure rather than a gradual degradation of the films.

Acknowledgements:

This work was supported by DARPA NESD Program Contract # N666001-17-C-4013)

2:30pm **AA1-MoA5 Modification of Spaceflight Radiator Coating Pigments by Atomic Layer Deposition for Thermal Applications***, **Vivek Dwivedi**,* NASA Goddard Space Flight Center*; R. Adomaitis, H. Salami, A. Uy,* University of Maryland*; M. Hasegawa,* NASA Goddard Space Flight Center

The optical and physical properties of spacecraft radiator coatings are dictated by orbital environmental conditions. For example, coatings must adequately dissipate charge buildup when orbital conditions, such as polar, geostationary or gravity neutral, result in surface charging. Current dissipation techniques include depositing a layer of ITO (indium tin oxide) on the radiator surface in a high temperature process. The application of these enhanced coatings must be such that the properties in question are tailored to mission-specific requirements.

The deposition of thin films by atomic layer deposition is a natural technological fit for manufacturing spacecraft components where weight, conformality, processing temperature, and material selection are all at a premium. Indium oxide (IO) and indium tin oxide (ITO) are widely used in optoelectronics applications as a high quality transparent conducting oxide layer. In this work, we present the thickness-dependent electrical and optical properties of IO thin-films synthesized by ALD with the aim of finding the optimum condition for coating a variety of substrates from Si(100) wafers, glass slides, and especially radiator pigments. Radiators are given surface finishes with high IR emittance to maximize heat rejection and low solar absorptance to limit heat loads from the sun. The surface finish is typically a white paint composed of nano/micron particle sized pigments with a silicate binder. It is the encapsulation of these particles that dictate the charge bleed off properties of the finished coating. Trimethylindium and ozone were used as precursors for IO, while a tetrakis(dimethylamino)tin(IV) source was used for Sn doping to produce ITO. As-deposited IO films prepared at 140 ° C resulted in a growth per cycle of 0.46 Å /cycle and relatively low film resistivity.

For the case of ITO thin-films, an ALD process supercycle consisting of 1 Sn + 19 In cycles was shown to provide the optimum level of Sn doping corresponding to the 10 wt.% widely reported in the literature. By using the inherent advantage of ALD in coating high aspect ratio geometries conformally, modification of these pigments can be accomplished during coating application preprocessing. The preprocessing is rendered directly on the dry pigment/particle before binding and not on the finished coated radiator geometry thus saving reactor volume.

Samples of our coating were recently launched into space and are currently onboard the International Space Station (ISS) as part of the one-year MISSE-10 materials test mission where the IO coated pigments are exposed to the harsh environment of space.

2:45pm **AA1-MoA6 Novel Atomic Layer Deposition Process/Hardware for Superconducting Films for NASA Applications***, **Frank Greer**, D. Cunnane,* Jet Propulsion Laboratory

Future sub-millimeter telescopes and spectrometers have the potential to revolutionize our understanding of the formation of the modern universe. Sub-millimeter astronomy can probe the fine structure of the cosmic microwave background, giving glimpses into the early universe immediately following the Big Bang. Recent advances in design have enabled the production of large arrays of cryogenically cooled superconducting detectors with sufficient sensitivity for photon counting applications. Transition edge sensors (TES) and other types of detectors, fabricated from thin films of metal nitrides and such TiN, NbN, TaN, VN, and their mixtures or high temperature superconductors like MgB2, are cryogenically cooled to just below their superconducting transition temperature. Atomic layer deposition is a chemical technique that can deposit extremely conformal and uniform films with angstrom level precision that would seem ideal for deposition of films of this type. However, one significant limitation of the technique is that it is often confined to those films that can be achieved through equilibrium processes. This is a significant limitation when the material of choice, such as MgB2, which is an excellent superconducting material, is Mg deficient as deposited by conventional chemical vapor deposition and only stoichometric MgB2 is a superconductor. Superconducting MgB2 thin films have been grown using hybrid physical/chemical vapor deposition when there is an excess of magnesium in the gas phase created by evaporation of elemental magnesium in the deposition chamber. The method for doing this is to have a charge of magnesium metal that is heated above its sublimation temperature in the very near vicinity of the substrate susceptor. Unfortunately, this method is currently only appropriate for small samples (1-2" in diameter) and for thick films (100nm or thicker). To overcome these limitations, we have built a custom lid for an existing atomic layer deposition reactor was machined to include a cavity to enable magnesium evaporation during deposition. We have subsequently used this approach to deposit MgB2 thin films detectors. This presentation will focus on our thin film results from both of the nitrides and MgB2 (composition, superconducting transition temperature, morphology, etc.) as well as the possible applicability of this generalized in situ thermal evaporation technology concept to other ALD materials.

3:00pm **AA1-MoA7 Fluoride-based ALD Materials System for Optical Space Applications***, **John Hennessy**,* Jet Propulsion Laboratory, California Institute of Technology

In this work we describe space technology applications that plan to utilize the recent development of atomic layer deposition (ALD) processes for metal fluoride materials like MgF_2, AlF_3, and LiF. These materials are valuable optical thin films in the deep ultraviolet, and are being used at NASA JPL to fabricate protected-aluminum mirror coatings, anti-reflection coatings, and detector-integrated filter coatings. Such systems are currently being implemented in a variety of sub-orbital missions including sounding rockets, cubesats, and high-altitude balloons that are relevant to astrophysics, heliophysics, and planetary science observations. We describe how ALD thin film properties may offer performance advantages over conventional methods with respect to film uniformity, microstructure, and integration with back-illuminated imaging sensors. We also describe the development of mitigating approaches to enhance the environmental stability of typically-hygroscopic fluoride materials through the use of ALD nanolaminates and mixed-composition fluorides. The same fluoride-based ALD approach has also been exploited to perform low-temperature atomic layer etching (ALE) to enhance the optical performance of some of these devices, and to pursue strategies for the development of protective coatings for lithium metal anodes relevant to future Li-ion battery applications.

3:15pm **AA1-MoA8 Atomic Layer Deposition of Aluminum Fluoride for use in Astronomical Optical Devices***, **Alan Uy**, H. Salami, A. Vadapalli, C. Grob, R. Adomaitis,* University of Maryland*; V. Dwivedi,* NASA Goddard Space Flight Center

Solid state metal halides typically have a high bandgap and low refractive index. Aluminum trifluoride (AlF_3) exhibits these properties, having a band gap greater than 10 eV and a refractive index of 1.35, making it an attractive material for thin film applications that include mirrors and optical devices [1]. Techniques to deposit thin films of AlF_3 include physical vapor deposition, sputtering, sol-gel, and atomic layer deposition (ALD) [2].

An important application of metal halides films in spacecraft missions has been for the protection of aluminum mirror from oxidation, which can severely affect overall reflectance in the far ultraviolet region. These coatings must maintain the underlying reflectivity of pure aluminum by having high transparency over the broad spectral range. To this end, AlF_3 stands out from other metal halide protective coatings, having higher transparency at the 100-200 nm wavelength region [1]. Due to long duration missions and the inability to service observatories in orbit, coatings of aluminum fluoride are also investigated for robustness and low interactions with potential foulers such as low earth orbit atomic oxygen. These thin coatings must be pinhole free to prevent access and reaction with underlying layers.

The highly conformal dense films and thickness control by ALD are attractive for this application. In this work, the growth of AlF_3 by ALD using precursors trimethyl aluminum (TMA) and titanium tetrafluoride (TiF_4) is investigated. Deposition of AlF_3 is performed in a custom hot-wall bench-scale reactor. We have shown that our deposition system can generate growth rates of ~0.5 Å/ALD cycle at relatively low temperatures of 180 ^oC. Varying ALD process parameters such as the exposure and purge times of precursor were found to have interesting effects to the film growth rate, especially those concerning the precursor TiF_4. These developments also give insight into potential reaction mechanisms between TMA and TiF_4, leading towards an overall hypothesized reaction mechanism for ALD process. Furthermore, optical properties, composition, and uniformity of film are analyzed. Lastly, the generated AlF_3 film quality over months under ambient conditions for robustness also is discussed.

[1] J. Hennessy, K. Balasubramanian, C. S. Moore, A. D. Jewell, S. Nikzad, K. France, M. Quijada, J. Astron. Telesc, Instrum. Syst. 2.4 (2016) 041206

[2] M. Mäntymäki, M. J. Heikkilä, E. Puukilainen, K. Mizohata, B. Marchand, J. Räisänen, M. Ritala, M. Leskelä, Chem. Mater. 2015, 27, 2, 604-611

ALD Applications
Grand Ballroom A-C - Session AA2-MoA
ALD for Solar Cells, Fuel Cells, and H_2 Storage

Moderators: Christophe Detavernier, Ghent University, Nicholas Strandwitz, Lehigh University

4:00pm **AA2-MoA11 Nucleation Layer for Atomic Layer Deposition Enabling High Efficiency and Flexible Monolithic All-Perovskite Tandem Solar Cells***, **Axel F. Palmstrom**, G. Eperon, T. Leijtens,* National Renewable Energy Laboratory*; R. Prasanna,* Stanford University*; S. Nanayakkara, S. Christensen, K. Zhu,* National Renewable Energy Laboratory*; M. McGehee,* University of Colorado Boulder*; D. Moore, J.J. Berry,* National Renewable Energy Laboratory

The emergence of metal halide perovskites as high efficiency, low-cost photovoltaic materials with a tunable band-gap has led to significant interest for perovskite-based tandems. Of existing perovskite-based tandem technologies, pairing wide-gap and low-gap perovskites in a monolithic all-perovskite tandem arguably offers the greatest potential by enabling efficiencies beyond the single-junction Shockley-Queisser limit with low-cost solution processing on a flexible, lightweight substrate. As of yet, efficiency of all-perovskite monolithic tandems has lagged behind perovskites paired with silicon or CIGS despite significant improvement to low-gap perovskite materials. A barrier to effectively combining state-of-the-art wide and low band gap perovskites in a monolithic tandem is the lack of a high-quality recombination layer that sufficiently protects an underlying perovskite thin-film to enable subsequent perovskite solution processing and minimal device shunting.

In this work, we aim to understand metal oxide growth by low-temperature atomic layer deposition (ALD) on C_{60} to develop improved recombination layers for all-perovskite 2T tandems. The effect of C_{60} surface modification with ultra-thin nucleophilic-containing materials is studied on ALD nucleation, growth, and film properties. We show, for multiple ALD systems, nucleophilic surface modification improves the water and dimethylformamide barrier properties of the grown oxide film. This strategy enables the fabrication of improved ALD recombination layers that are thinner and less laterally conductive (reduced shunting) than currently reported strategies. We demonstrate ALD-grown aluminum-doped zinc oxide (AZO) as an effective recombination layer for two-terminal all-perovskite tandems with efficiencies over 23% for rigid devices and 21% for flexible devices.

4:15pm **AA2-MoA12 Perovskite Solar Cells Fabricated using Atomic Layer Deposited Doped ZnO as a Transparent Electrode***, **Louise Ryan**, M. McCarthy, S. Monaghan, M. Modreanu, S. O'Brien, M. Pemble, I. Povey,* Tyndall National Institute, Ireland

Power conversion efficiencies of perovskite (PK) solar cells have rapidly improved in recent years obtaining efficiencies in excess of 20% [1]. Good absorption properties in the visible and infrared spectrum, high efficiencies and low fabrication costs have brought PK solar cells to the forefront. With single junction PK solar cells soon reaching theoretical efficiency limits a requirement for tandem cells, where materials of differing absorption characteristics convert a wider spectral range, is in demand. However, such tandem solar cells introduce fabrication complexities due to the thermal budget restrictions imposed by the complex layer structure [2].

Fluorine-tin oxide (FTO) and indium-tin oxides (ITO) are widely used transparent contacts in solar cells. However, the high deposition temperatures and energetic processes required for its production are detrimental to the fabrication of delicate perovskite based tandem solar cells and thus the need to find an alternative TCO is vital.

Here we have considered Ti-doped ZnO, produced by a ALD laminate doping method, as an alternative transparent contact and have incorporated it into perovskite solar cells in conjunction with an ALD-grown SnO_2 electron transport material. Detailed analysis of the influence of the growth process on the performance of the Ti-doped ZnO electrode is presented. Finally, the efficiency of the optimised perovskite solar cells are evaluated relative to the current state of the art.

[1] NREL: Efficiency Chart (2018). Https://www.nrel.gov/pv/assets/pdfs/pv-efficiencies-07-17-2018.pdf

[2] F. Sahli, et al., Nature Materials, 17(9) (2018) 820-826.

4:30pm **AA2-MoA13 Metal Oxide Barrier and Buffer Layers by Atomic Layer Deposition and Pulsed-Chemical Vapor Deposition for Semi-Transparent Perovskite Solar Cells***, **Helen Hejin Park**, T. Eom, R.E. Agbenyeke, S.M. Yeo, G.J. Kim, S.S. Shin, T.-Y. Yang, N.J. Jeon, Y.K. Lee, C.G. Kim, T.-M. Chung, J. Seo,* Korea Research Institute of Chemical Technology (KRICT), Republic of Korea

For *n-i-p* structured semi-transparent perovskite solar cells, thermal evaporation has been a common technique to deposit the sputter buffer material, such as molybdenum oxide and tungsten oxide, to protect the organic hole transporting layer (HTL) from damage due to sputtering of the transparent conducting oxide. However, thermal evaporation does not guarantee stoichiometric and uniform pinhole–free coverage of films, leading to inefficient protection against sputtering and poor air stability. While there have been well-established buffer materials by atomic layer deposition (ALD), such as SnO_2, for *p-i-n* structured semi-transparent perovskite solar cells, this is not the case for *n-i-p* structured devices. In addition, thermal evaporation has also been commonly used to deposit a barrier layer at the perovskite/HTL interface to improve the fill factor and open-circuit voltage, however, ALD can provide more precise control and conformal coverage for this layer. In this presentation, we demonstrate metal oxide deposition techniques by pulsed-chemical vapor deposition and ALD in perovskite solar cells for the sputter buffer and barrier layers, which result in efficiencies over 16% for semi-transparent devices. Effects of the optical and electrical properties of barrier/buffer layers on the performance of working devices will be addressed, and the mechanisms involved in the enhanced performance and stability will also be discussed.

4:45pm **AA2-MoA14 Particle Atomic Layer Deposition of Tungsten Nitride Environmental Barrier Coatings from Bis(t-butylimido)bis(dimethylamino) tungsten(VI) and Ammonia***, **Sarah Bull**, A. Weimer,* University of Colorado - Boulder

Ultra-thin tungsten nitride (WN) films were deposited by atomic layer deposition (ALD) on zirconia nanoparticles and yttria stabilized zirconia (YSZ) micropowders using a fluidized bed reactor. The film's intended use as a hydrogen barrier coating motivated the investigation of hydrogen diffusion in W using density functional theory (DFT) and differential thermal analysis (DTA). The lowest energy diffusion pathway was determined and the hydrogen charges at various sites along the pathway were calculated. DTA was used to investigate the efficacy of the W/WN films in preventing hydrogen attack. The temperature at which hydrogen reacted with the sample increased with film thickness, thereby indicating that the film inhibited this reaction. However, the existence of a hydrogen reaction peak in the thicker film indicated a material with greater than 2.0 eV energy barrier is necessary for a substantial decrease in hydrogen interaction with the substrate. This is the first study for ALD of WN on particles from bis(t-butylimido)bis(dimethylamino)tungsten(VI) and the use of ultrathin WN ALD films as environmental barrier coatings (EBCs) for high-temperature H_2 above 1000°C.

5:00pm **AA2-MoA15 Atomic Layer Deposition on $Mg(BH_4)_2$: A Route to Improved Automotive H_2storage***, **Noemi Leick**,* National Renewable Energy Laboratory*; K. Gross,* H₂ Technology Consulting LLL*; T. Gennett, S. Christensen,* National Renewable Energy Laboratory

In order to meet the U.S. Department of Energy requirements for on-board solid-state hydrogen (H_2) storage in fuel-cell powered vehicles, metal borohydrides are of particular interest. However, while materials such as magnesium borohydride, $Mg(BH_4)_2$, have a hydrogen capacity up to ~14wt%, challenges associated with hydrogenation-dehydrogenation cyclability need to be overcome. Specifically, improve the operating

temperatures for adsorption/desorption; increase the hydrogen absorption-desorption kinetics; and eliminate the formation of the toxic diborane (B_2H_6). Prior research has indicated that nano-encapsulation (*e.g.* through graphene nanosheets) and chemical additives (*e.g.* catalysts) are areas of significance to address these challenges.

This work is the first to approach these two strategies simultaneously using atomic layer deposition (ALD). ALD coatings have been shown to protect and enhance heterogeneous catalyized rates, as well as to precisely control the amount of chemical additive incorporated. In this project, metal-oxides (*e.g.* Al_2O_3, TiO_2, CeO_2), metal-nitrides (*e.g.* TiN, BN), pure metals (*e.g.* Ru, Pd) and combinations thereof were deposited by ALD on γ-$Mg(BH_4)_2$. We investigated how the deposition temperature, the use of water for some of these ALD processes and the composition of the additive affected the H_2storage properties of γ-$Mg(BH_4)_2$.

Compared to uncoated γ-$Mg(BH_4)_2$, we found that the ALD depositions lowered the H_2desorption temperature by 60–120 ˚C, doubled the desorbed gravimetric H_2capacity at temperatures below 250˚C, increased the desorption kinetics by a factor of ~6, and suppressed the formation of B_2H_6 substantially during the dehydrogenation step. The ALD-modified γ-$Mg(BH_4)_2$was also explored with respect to the structure, the effects of the total hydrogen capacity, and catalytic effects. In this presentation we will discuss data supporting these results from temperature programmed desorption, pressure composition temperature manometric measurements, inductively coupled plasma mass spectrometry, nitrogen physisorption measurements, nuclear magnetic resonance, transmission electron microscopy and diffraction spectroscopy.

5:15pm **AA2-MoA16 Plasmonic Mediated Hydrogen Desorption from Metal Hydrides***, **Katherine Hurst**, A. Gaulding, M. Martinez, N. Leick, S. Christensen, T. Gennett,* National Renewable Energy Laboratory

Excitation of plasmonic coatings deposited by atomic layer deposition (ALD) can provide important routes for tuning the performance of gas adsorption and desorption of hydrogen storage materials. Currently available hydrogen fuel-cell vehicles systems rely on hydrogen stored in compressed tanks at 700 bar. While this hydrogen storage system is partially fostering early-market deployment, the compressed gas system presents several practical challenges and expenses related to infrastructure and delivery that could limit widespread adoption. Metal hydrides are an important class of materials that can reach DOE system capacity targets for hydrogen storage. However, the gas uptake and release of hydrogen by metal hydrides requires high pressures and temperatures, and exhibits slow kinetics. It is well known that modification of a bulk hydride to the nanoscale phase, and the addition of catalyst additives can both greatly enhance the kinetics, lower operating temperatures, and increase cyclability. This work takes a unique route to alter the process of desorption through the incorporation of plasmonic materials into the hydride matrix. This allows for low-power-LED-illuminated systems to achieve the same rates of hydrogen desorption as radiative thermal heating

Specifically, recent work at the National Renewable Energy Laboratory has applied ALD to enable the use of plasmonic material coatings to alter the mechanism for hydrogen desorption. Through localized heating via surface plasmon excitation, the bulk thermal signature for hydrogen release can be significantly reduced. Furthermore, hydrogen desorption induced via plasmonic heating offers a completely new approach to using hydride materials. Temperature programmed desorption spectroscopy is used to monitor the kinetic changes associated with desorption by varying the conditions and type of plasmonic material introduced. The effects of partial coverages, ALD film thickness and crystallinity on the resonant plasmonic frequency are explored. This presentation will discuss advancements in enabling gas desorption via plasmonic excitation especially with respect to hydrogen carrier applications. These exciting results also point towards new applications for ALD in nano-scale photo-thermal processes.

5:30pm **AA2-MoA17 Surface Modification of Solid Oxide Fuel Cell Cathodes by Atomic Layer Deposition***, **Dong Hwan Kim**, H.J. Choi, J. Koo,* Korea University, Republic of Korea*; J.H. Park, J.-W. Son,* Korea Institute of Science and Technology (KIST), Republic of Korea*; J.H. Shim,* Korea University, Republic of Korea

Development of high-performance cathode is key to the commercialization of solid oxide fuel cells (SOFCs). Doped perovskite-type oxides including lanthanum strontium cobaltite (LSC) and lanthanum strontium cobalt ferrite (LSCF) are the most typical materials in practical SOFCs. However, degradation of LSC and LSCF from dynamic on-off operation at high temperature (600-1000 ºC) has been considered as the most serious technical obstacle. Many kinds of literature have reported that segregation of cations near the cathode surface leads to this degradation. Specifically, the A-site element of the cathode perovskite is subjected to electrostatic attraction to the surface due to excess oxygen vacancies on the cathode surface, which brings out the A-site element to segregate on the surface [1]. To solve this problem, we have proposed surface modification by atomic layer deposition (ALD) [2]. In this study, 1-4 cycles of ALD Al2O3 has been attempted on porous LSC to suppress the cation segregation and improve the surface redox kinetics. Performance of SOFCs with the ALD Al2O3-treated LSC cathodes has been evaluated in I-V-P and impedance. Finally, long-term stability at 500-600 °C has been examined in the potentio -static mode. In this presentation, the progress of this research will be shared in details.

[1] Cai et al. Chemistry of materials 24.6 (2012): 1116-1127.

[2] Choi et al. Advanced Energy Materials 8.33 (2018): 1802506.

ALD Fundamentals
Grand Ballroom H-K - Session AF1-MoA

ALD Growth Mechanisms I

Moderators: Simon Elliot, Schrödinger, Inc., Angel Yanguas-Gil, Argonne National Laboratory

1:30pm **AF1-MoA1 Hybrid Computational Fluid Dynamics / Machine Learning Approaches to Reactor Scale Simulations and Optimization of ALD, ALEt, and LPCVD Processes***, **Angel Yanguas-Gil**, S. Letourneau, A. Lancaster, J.W. Elam,* Argonne National Laboratory

As the range of potential applications of atomic layer deposition increases, it is becoming increasingly important to understand how processes scale up to large area substrates and complex substrate geometries. Compared to the number of processes available, there is still a scarcity of tools to explore the interaction between surface kinetics, gas phase transport, and thin film growth at a reactor scale. These tools can help us answer not only key questions regarding the economics or scalability of a given process in terms of throughput or precursor utilization, but they can help us develop a better understanding and intuition of processes and simulate the output of commonly used in-situ techniques such as quartz crystal microbalance or mass spectrometry.

In this work we describe an open source code developed at Argonne to simulate processes based on self-limited and non-self limited surface kinetics at a reactor scale. This code, which is freely available, is built on top of OpenFOAM, a free, open source Computational Fluid Dynamics software. In combination with open source mesh generators such as GMSH, our code provides a simple workflow to explore the role of surface kinetics and the scale up of ALD, ALEt, and LPCVD processes.

To validate our model, we have established a comparison between simulations and experimental results obtained at two different cross-flow ALD reactors. We have then used synthetic growth profiles as a starting point to explore the ability of machine learning approaches to extract relevant information from growth profiles and other experimental datasets. In particular, we have explored the use of artificial neural networks to extract relevant kinetic data from reactor profiles and extrapolate saturation profiles based on a reduced set of experiments.

1:45pm **AF1-MoA2 Scalable Kinetic Monte-Carlo Model for Parasitic Reactions in Silicon Nitride Growth using 3DMAS Precursor***, **Gem Shoute**, T. Muneshwar,* Synthergy Inc., Canada*; D. Barlage, K. Cadien,* University of Alberta, Canada

Atomic layer deposition (ALD) is a cyclical self-limiting reaction deposition technique that heavily depends on the characteristics of the chosen precursor. Currently, there are a limited number of ALD models that can give insight into key growth characteristics of a precursor such as ideal growth per cycle (GPC). Whether a self-limiting reaction can be achieved is determined by several factors related to the precursor itself, including its exposure and purge times and substrate temperature (T_{SUB}), all which affect the GPC of the desired material. For instance, the silicon nitride (Si_xN_y) precursor, tris[dimethylamino]silane (3DMAS), saturates at T_{SUB} up to ~150 °C but beyond this temperature window, it exhibits dependence on its exposure time resulting in a non-saturated growth. While saturation indicates ideal ALD behavior, the latter observation implies the presence of parasitic reactions that are concurrent with ALD reactions, resulting in non-ideal ALD growth. These non-idealities are especially prominent in aggressive topologies such as high aspect-ratio structures which are a

staple of numerous applications today. In this study, we will model the expected GPC of 3DMAS using a scalable kinetic Monte-Carlo approach (sKMC). The expected GPC vs. T_{SUB} relationship is compared to the experimental results of 3DMAS Si_xN_y. The discrepancies between the expected and experimental GPCs are attributed to additional parasitic reactions and interpreted through the lens of the sKMC model. Further developing these models is an important step towards rapid characterization of precursors and would serve as a useful tool for selecting the appropriate precursor for a given application.

2:00pm **AF1-MoA3 Diffusion and Aggregation in Island-Growth and Area-Selective Deposition***, **Fabio Grillo**,* ETH Zurich, Switzerland **INVITED**

Diffusion and aggregation phenomena play an essential role in many thin film processes [1]. Yet, their importance in atomic layer deposition (ALD) has been overlooked by most fundamental studies, which focus primarily on surface chemistry. This is not surprising because the latter governs the growth process when this proceeds in a layer-by-layer fashion, which is often the case. However, chemistry alone cannot account for the formation and growth of islands or nanoparticles during the so-called "nucleation delay". In this talk, I will present a theoretical framework that captures the kinetics of island-growth in ALD by accounting for diffusion and aggregation phenomena [2-4]. The framework is based on rate-equation and Kinetic-Monte-Carlo (KMC) models that build not only on the classic formulations of thin film nucleation kinetics but also on insights borrowed from research fields such as colloidal synthesis and catalyst sintering. These models describe the growth process as a balance between the cyclic generation of adatoms, arising from ALD surface reactions, and their aggregation due to non-equilibrium physical phenomena. The latter include: (1) adatom diffusion, (2) island formation by adatom aggregation, (3) island migration and coalescence (i.e., dynamic coalescence), (4) adatom attachment, and (5) inter-island exchange of atoms driven by the Gibbs–Thomson effect (i.e., Ostwald ripening). Throughout the talk I will demonstrate how these models can be used to relate the evolution of experimental observables such as the island-size distribution to well-defined growth mechanisms. For example, I will show how dynamic coalescence can govern nanoparticle growth during ALD of noble metals and how different surface diffusion rates can have a dramatic effect on the extent of the "nucleation delay". Finally, I will present KMC simulations showing how surface diffusion can induce topography-dependent growth in area-selective ALD.

[1] Venables, J. A., Philosophical Magazine 1973, 27 (3), 697–738.

[2] Grillo, F.; Van Bui, H.; Moulijn, J. A.; Kreutzer, M. T.; van Ommen, J. R., The Journal of Physical Chemistry Letters 2017, 8 (5), 975–983.

[3] Grillo, F.; Moulijn, J. A.; Kreutzer, M. T.; van Ommen, J. R., Catalysis Today 2018, 316, 51–61.

[4] Soethoudt, J., Grillo, F., Marques, E. A., van Ommen, J. R., Tomczak, Y., Nyns, L., Delabie, A., Advanced Materials Interfaces 2018, 5(24), 1800870.

2:30pm **AF1-MoA5 Surface Kinetics in ALD and ALE: Computing the Cooperative Effect by Automated Enumeration of Reaction Pathways with Spectator Adsorbates***, **Thomas Mustard**,* Schrödinger, Inc.*; S. Elliot,* Schrödinger, Inc.*; T. Hughes, A. Bochevarov, L. Jacobson, S. Kwak,* Schrödinger, Inc.*; T. Morisato,* Schrödinger K.K., Japan*; J. Gavartin,* Schrödinger, Inc., UK*; S. Pandiyan,* Schrödinger, Inc., India*; M. Halls,* Schrödinger, Inc.

The deposition or etching of solid films by ALD or ALE proceeds via reactions between gas-phase molecules and surfaces. The kinetics of such reactions have been previously computed to be strongly influenced by the local environment on the surface around the reaction site, which is called the 'cooperative effect' [1]. The activation energy at a reactive site has been shown to be affected by, or even dictated by, the presence of nearby co-adsorbed fragments or molecules, which otherwise take no part in the reaction and so may be termed 'spectators'. In the case of ALD, this means that previously-inert ligand remnants on the surface can become reactive once sufficient numbers of other ligands adsorb in their neighborhood. This has been experimentally verified in the case of low-temperature ALD of Al_2O_3 from TMA+H_2O [2].

Including a proper description of the cooperative effect is a serious challenge for first principles simulations of surface reactivity. One way forward is to sample the chemical space by automating the systematic investigation of the factors contributing to the cooperative effect. Specifically, we show how spectator Lewis acids and bases at various coverages and distances affect the activation energy for adsorption and proton transfer on the functionalized surfaces that are typically present during ALD of Al_2O_3.

To study the surface reactivity, we have generated an $(Al_2O_3)_{16}$-based cluster model of the (1 0 0) bilayer structure of q-Al_2O_3. We computed the activation energy for adsorption of H_2O onto an open Al site at the center of the cluster and for its dissociation into H+OH. The cluster is terminated with OH groups on its sides, but has space on top for up to 32 spectator molecules to surround the reactive site at distances ranging 2-6 Å. As spectator molecules we have considered various sizes of alkyl, alkoxyl, hydroxyl and halide groups, so as to probe both electronic and steric effects. All possible arrangements of spectator adsorbates were generated automatically with enumeration tools in the Schrödinger *Materials Science Suite* [3]. The reaction pathway for dissociative adsorption of H_2O was then re-computed for each new spectator environment revealing how the activation energy changes with spectator identity and proximity.

We discuss the importance of the results for our understanding of thin film deposition and related fields such as heterogeneous catalysis. We also look forward to the prospects for efficient and systematic computation of complex surfaces.

[1] M. Shirazi, S. D. Elliott, Nanoscale 7 (2015) 6311-6318

[2] V. Vandalon, W. M. M. Kessels, J. Vac. Sci. Techn. A 35 (2017) 05C313

[3] http://www.schrodinger.com/materials

2:45pm **AF1-MoA6 An Immiscible Fluids Approach for Correctly Predicting Agglomerate Dynamics during Particle Atomic Layer Deposition (Particle ALD)***, **Julia Hartig**, A. Weimer,* University of Colorado - Boulder

Particle agglomeration can significantly impact performance of fluidized bed reactors when running particle atomic layer deposition (Particle ALD). The fine powders frequently used in Particle ALD tend to agglomerate due to large interparticle forces, blocking surface sites and inhibiting surface coating uniformity. By modeling the agglomeration process during coating, steps can be taken to facilitate agglomerate breakup and mixing, thereby enhancing surface coating uniformity. However, current models of gas-solid flows which preserve the gas-solid interface, an important component for modeling ALD, have several limitations when incorporating agglomeration. Many of these approaches fail to address agglomerate size distributions or the dynamic formation and breakup process of fluidized agglomerates, shortcomings which remain a significant challenge to studying fluidized bed Particle ALD. In this work, we propose an alternative modeling approach which naturally accounts for the dynamic nature of fluidized agglomerates by treating the fluidizing gas and particles as two immiscible (non-interpenetrating) fluids. Agglomerates are modeled using dynamic "bubbles" whose interior consists of many primary particles from the solids phase. The position, shape and formation/breakup of these agglomerate "bubbles" are allowed to change with time as dictated by the corresponding transport equations. With this model, we can investigate the formation and breakup of agglomerates without prior knowledge of the agglomerate size characteristics. This study provides some preliminary agglomerate size distribution results from fluidized bed Particle ALD simulations and compares these results to experimental data from previous literature studies.

3:00pm **AF1-MoA7 The Time-Resolved Interface between ALD and CVD***, **Henrik Pedersen**,* Linköping University, Sweden **INVITED**

ALD (atomic layer deposition) is possibly the most important evolution of CVD (chemical vapor deposition). To a first approximation, ALD can be described as CVD where the precursor flows are separated in time. In other words, ALD is a time-resolved form of CVD. Despite this, CVD typically has a negative connotation in the ALD community. The phrase "CVD-component" is used to point to a process deviating from the idealized ALD behavior, where continual growth occurs.

The time-resolved precursor supply in ALD enables the self-limiting surface chemistry, rendering the very high degree of surface control which is the hallmark of ALD. However, CVD does not need to be time-resolved to have a very high degree of surface control. There are several examples in the literature of continuous CVD filling deep trench structures.[1,2] A time-resolved precursor supply without a self-limiting surface chemistry is another important evolution of CVD as it can be used for growing semiconducting nanowires on a patterned surface without the need for a catalyst[3] and can afford deposition of ternary or quaternary materials in some materials systems[4].

CVD can also be made time-resolved by controlling the amount of energy available to the process over time. While this is difficult to do with a thermally activated CVD process, a process driven by the energy provided

in a plasma discharge can easily be time-resolved in energy. This has allowed self-limiting processes with constant flow of precursors[5] and an enhanced ability to use ionic species for film deposition[6].

This talk will discuss the time-resolved interface between CVD and ALD but also how continuous CVD can outcompete time-resolved CVD for some films: a recent example is nearly conformal B-C films in a 2000:1 structure by continuous CVD at 700 °C and 5 kPa.[7] The talk will also seek to nuance the view of a "CVD-component" in ALD processes and discuss how the time component can be used as a process knob in ALD.

References:

1. Kumar, N.; Yanguas-Gil, A.; Daily, S. R.; Girolami, G. S.; Abelson, J. R. *J. Amer. Chem. Soc.***2008**, *130*, 17660-17661.

2. Wang. W. B.; Yang, Y.; Yanguas-Gil, A.; Chang, N. N.; Girolami, G. S.; Abelson, J. R. *Appl. Phys. Lett.***2013**, *102*, 101605.

3. Hersee, S. D.; Sun, X.; Wang, X. *Nano Lett.***2006**, *6*, 1808-1811.

4. Lindahl, E.; Ottosson, M.; Carlsson, J. O. *Chem. Vap. Deposition***2012**, *18*, 10-16.

5. Seman, M.; Robbins, J. J.; Agarwal, S.; Wolden, C. A. *Appl. Phys. Lett.***2007**, *90*, 131504.

6. Profijt, H. B.; van de Sanden, M. C. M.; Kessels, W. M. M. *J. Vac. Sci. Technol. A***2013**, *31*, 01A106.

7. Souqui, L.; Högberg, H.; Pedersen, H. ChemRxiv **2019**, https://doi.org/10.26434/chemrxiv.7663109.v1

ALD Fundamentals
Grand Ballroom E-G - Session AF2-MoA
ALD Precursors I

Moderators: Daniel Alvarez, RASIRC, Charles H. Winter, Wayne State University

1:30pm **AF2-MoA1 The Materials Supplier Challenge: Flawless Execution from Precursor Design to High Volume Manufacturing***, **Madhukar B. Rao,*** Versum Materials **INVITED**

Advancements in scaling and architecture in logic and memory devices are driving the development of new precursors which provide more precise control of film thickness, composition, morphology and electrical properties. The challenge for materials suppliers is to design new precursors that can meet the performance requirements, and scale-up the precursors to high volume, while meeting the cost of ownership targets. At Versum Materials, the process starts with defining technical requirements of the precursor through close collaboration with the customer and equipment vendor. We use our in-depth understanding of the structure-property relationships between precursor and final film to identify and synthesize promising new precursors on the laboratory scale and rapidly test new precursors using our in-house deposition capabilities to confirm the film performance. These results are validated with our collaboration partners and this defines the potential candidates for further scale-up.

Converting promising laboratory discoveries into viable commercial products is a complex and resource-intensive effort. The product development work must scale up and validate a low-cost synthetic route and purification methods, identify and quantify EH&S risks (e.g., toxicity, stability, reactivity), develop analytical methods to fingerprint incoming raw materials and ensure final product quality, design and validate suitable containers for delivery, ensure supplier quality and supply-chain readiness and prepare for container life-cycle management. This presentation highlights the key steps and technical challenges in the product development process and highlights the importance of close collaboration with customers, suppliers, and equipment manufacturers to make new products HVM ready.

2:00pm **AF2-MoA3 Precursor and Co-Reactant Selection: A Figure of Merit***, **Seán Barry**, M. Griffiths,* Carleton University, Canada

Developing novel precursors for atomic layer deposition (ALD) processes is a complicated task: the selected chemical compounds must be volatile and thermally stable, yet reactive with a surface, and perhaps even demonstrate selective reactivity among several different surfaces. Additionally, it is helpful if the precursors are liquid (for handling and to improve the kinetics of evaporation) and robust to a change in the chemical environment.

To initially study a compound for potential use as a precursor, one must understand both the volatility and thermal stability. We have recently established a Figure of Merit (FoM) for potential precursor compounds based on volatility and decomposition. Conceptually, this FoM alters the ratio in temperature between a judiciously chosen onset of decomposition and onset of thermolysis and modifies that with respect to the residual mass left behind in a standard thermogravimetric ramp experiment. In this way, the larger the value for the FoM, the better the precursor, with negative values representing compounds that decompose before acceptable volatility is achieved.

Selection of the onset of volatility and decomposition, as well as the construction of this Figure of Merit will be examined with respect to potential precursors for transition metals (Ni, Co, W, Mo, Au, Ag, Cu) as well as main group metals (Al, Ga, In, Sn, Pb) that are presently being developed in our group.

2:15pm **AF2-MoA4 Designing Thermal Atomic Layer Deposition Processes for Gold Metal using New Organogold Precursors and Co-reageants***, **Matthew Griffiths**, G. Bačić, A. Varga, S. Barry,* Carleton University, Canada

Gold nanoparticles have been studied extensively by virtue of their plasmonic properties and their ability to act as photocatalysts for CO_2 reduction and hydrogenation. In 2016, our group showed that $(PMe_3)AuMe_3$ would deposit gold nanoparticles by atomic layer deposition (ALD) using oxygen plasma and water as co-reagents. Recently, Van Daele et al. showed that the same compound could deposit gold with hydrogen plasma as a co-reagent at temperatures as low as 50 °C. The development of a process that uses thermal co-reagents is ongoing in our laboratory in order to circumvent the use of harsh co-reagents.

Bimolecular reductive coupling is believed to catalyze the on-surface decomposition of $(PMe_3)AuMe$ on Au. Thus, increasing the steric bulk of the alkyl ligand should increase the activation energy of this process and produce a surface species that resists decomposition to metallic gold. We synthesized a series of $(PMe_3)AuR$ compounds (R = Me, CH_2SiMe_3, $CH(SiMe_3)_2$, and $C(SiMe_3)_3$) with a stepwise increase in steric bulk. We then developed a screening process to test their ability to form self-limiting surface monolayers with an *in situ* quartz crystal microbalance (QCM). At equal vapour pressures and equal deposition temperatures, the rate of CVD decreased with increasing steric bulk, but was never fully prevented.

N-heterocyclic carbenes (NHCs) are ubiquitous ligands in modern chemistry, and they also form robust self-assembled monolayers on gold. We envisioned a second strategy where an NHC ligand bound to Au(I) in the general formula (NHC)AuR could play the role of the self-limiting ligand in an ALD process. All that would be needed is a co-reagent which could remove the NHC from the metallic gold surface to complete the cycle. A series of alkylgold(I) NHCs were synthesized and tested with a focus on small alkyl groups and stable, sterically unhindered NHCs to facilitate efficient packing on the surface. Using our QCM methodology, we compared the various compounds for their ability to form self-limiting monolayers, and we analyzed the gas-phase products of the ALD reactions using *in situ* quadrupole mass-spectrometry (QMS).

Finally, exploration of a third strategy was initiated by our discovery that a thermally stable *N*-heterocyclic silylene (NHSi) reacted with our previously reported and stubbornly inert gold ALD precursor $(PMe_3)AuMe_3$. We identified a highly reactive silylgold(I) silylene species by solution-phase NMR spectroscopy and set out to develop an ALD process using these two compounds. The surface chemistry was studied using our combined QCM and QMS methodology, and the final film properties were evaluated *ex-situ* by 4-point probe, XPS, and XRD.

2:30pm **AF2-MoA5 A New Carbene Based Silver Precursor Applied in APP-ALD Yielding Conductive and Transparent Ag Films: A Promising Precursor Class for Ag Metal ALD***, **Nils Boysen**,* Ruhr University Bochum, Germany*; T. Hasselmann, D. Theirich, T. Riedl,* University of Wuppertal, Germany*; A. Devi,* Ruhr University Bochum, Germany

The realization of transparent electrodes for solar cells and light-emitting devices based on metals like silver still remains a challenge due to a preferred Volmer-Weber growth mode in the initial stages of thin film growth. This results in a typically observed metal island formation with a high sheet resistance (R_{sh}) at a low film thickness. Atomic layer deposition (ALD) can be the method of choice to effectively lower the percolation threshold and to afford electrically conductive but at the same time optically transparent silver thin films. While the influence of different reducing agents in thermally- and plasma-activated silver ALD processes was studied in the past, the employment of different silver precursors and their influence on the growth behavior and percolation threshold of silver

thin films was not coherently studied before due to the limited number of volatile and thermally stable silver precursors. To overcome this issue and to set a starting point for further comprehensive studies, we herein report the synthesis and evaluation of a new fluorine-, oxygen- and phosphorous-free volatile N-heterocyclic carbene (NHC)-based silver precursor.[1] The successful synthesis of the new NHC-based silver amide compound 1,3-di-*tert*-butyl-imidazolin-2-ylidene silver(I) bis(trimethylsilyl)amide [(NHC)Ag(hmds)] was confirmed *via* ^{1}H- and ^{13}C-NMR spectroscopy, elemental analysis and EI-MS, while the thermal characteristics of the compound were determined *via* thermogravimetric and isothermal thermogravimetric analysis. Subsequently, the volatile silver precursor [(NHC)Ag(hmds)] was employed in spatial atmospheric plasma-enhanced ALD (APP-ALD) yielding high purity conductive silver thin films at temperatures as low as 100 °C and with a low resistivity of 10^{-5} Wcm utilizing an Ar/H_2 plasma. The growth characteristics were investigated, and the resulting thin films were analysed *via* SEM, XPS, optical transmittance (UV-Vis) and RBS. Compared to a nominally identical process employing the commercially available silver precursor [Ag(fod)(PEt_3)], [(NHC)Ag(hmds)] was able to considerably enhance the growth rate and prohibit unwanted contaminants like fluorine, oxygen and phosphorous. This renders the new precursor as a promising alternative to the currently established [Ag(fod)(PEt_3)]. The current study marks the first example of a carbene stabilized Ag complex that was successfully employed for ALD applications of Ag metal layers. In addition, these promising results create a basis for the development of new metal ALD precursors as there is only a very limited number of ALD precursors known, especially for silver metal ALD.

2:45pm **AF2-MoA6 Transition Metal β-ketoiminates: A Promising Precursor Class for Atomic Layer Deposition of Binary and Ternary Oxide Thin Films***, **Dennis Zywitzki**, A. Devi,* Ruhr University Bochum, Germany

Due to their abundancy in the earth's crust and promising characteristics in (photo-) electrocatalysis and energy storage devices, binary and ternary oxide films of first row transition metals such as Fe, Co, Ni, Zn have gained increasing attention in recent years. ALD is a promising technique for such applications, as it guarantees excellent interface quality to the underlying substrate and enables the conformal coating of large and nanostructured surfaces. Precursors for these metals however remain limited especially for water assisted processes. While ALD processes for ZnO are dominated by the pyrophoric alkyl compounds such as diethyl zinc, few other precursors were reported thus far. On the other hand, for Fe, Co and Ni, metal cyclopentadienyls and β-diketonates, which require strong oxidizing agents like ozone, have often been used. Water assisted process were realized by utilization of the amidinate ligand system for Fe, Co and Ni. In order to find a compromise between the stable but less reactive metal β-diketonates and the highly reactive metal β-ketiminates, metal β-ketoiminates have been found to be a promising precursor class, which can easily be tuned in terms of volatility and reactivity by employing different substitutions at the imino moiety.

A series of new β-ketoiminato precursors, suitable for ALD have been developed for transition metals. As representative examples, Fe, Co, Ni and Zn β-ketoiminates have been synthesized in good yields and were thoroughly characterized with regard to their purity, composition and molecular structure by NMR spectroscopy, elemental analysis, EI-MS and single crystal XRD. The spectroscopically pure and monomeric compounds were reactive toward water. Their volatility and decomposition behavior was evaluated by thermal analysis and were found suitable for ALD. The introduction of etheric sidechains led to lower melting points, ensuring a steady evaporation rate. Subsequently, water assisted ALD processes with Fe and Zn β-ketoiminate precursors were developed. The typical ALD characteristics were confirmed in terms of ALD window, saturation and thickness dependence. Lastly, the resulting films were analyzed for their structure, morphology, composition and the optical properties were investigated.

With the successful synthesis and characterization of transition metal β-ketominates, the library of potential precursors for first row transition metals was expanded. As representative examples, the successful development of water assisted ALD processes for iron and zinc oxide is demonstrated. The similarity in the physico-chemical properties of these precursors is an advantage to grow ternary metal oxides.

3:00pm **AF2-MoA7 A New and Promising ALD Process for Molybdenum Oxide Thin Films: From Process Development to Hydrogen Gas Sensing Applications***, **Jan-Lucas Wree**,* Ruhr University Bochum, Germany*; M. Mattinen,* University of Helsinki, Finland*; E. Ciftyürek, K.D. Schierbaum,* Heinrich Heine University Düsseldorf, Germany*; M. Ritala, M. Leskelä,* University of Helsinki, Finland*; A. Devi,* Ruhr University Bochum, Germany

The oxides of molybdenum are well known for their versatile properties and therefore serve as excellent materials for a wide range of applications like (photo)catalysis, optoelectronics, and gas sensors for a variety of gas species. Molybdenum oxide can occur in several oxidation states that exhibit very different properties. The different oxides can be distinguished by their crystalline structures as well as by their mechanical and electrical properties. While the different crystalline phases of MoO_3 (α, β, h) are semiconducting with wide band gaps between 2.7 eV and 3.5 eV, the less common suboxides such as Mo_4O_{11} exhibit higher electrical conductivity and the dioxide MoO_2 is even known as pure metallic conductor.[1] Recent studies have shown that α-MoO_3 is a promising material for gas sensing applications owing to its high activity towards gases such as ammonia, nitrogen dioxide and hydrogen at moderate temperatures.[2] Although various oxides of Mo have been tested for the sensing of hydrogen, which is an important source for clean energy, the suboxides of Mo are not well explored for hydrogen sensing.

In this study, we have investigated the feasibility of using the bis(tertbutylimido)bis(N,N'-diisopropyl-acetamidinato) compound of molybdenum [Mo(N^tBu)$_2$(dpamd)$_2$] as a potential precursor for atomic layer deposition (ALD) of MoO_x films. In the first part of the study, the focus was to optimize a new ALD process using this precursor together with ozone as the oxygen source. The phase and composition of the layers could be tuned by varying the process parameters which resulted in amorphous (≤250 °C), crystalline suboxide (275 °C), a mixture of suboxide and α-MoO_3 (300 °C), or pure α-MoO_3 (≥325 °C) films. The evaluation of the layers using synchrotron-based surface enhanced photoemission spectroscopy revealed a high amount of oxygen vacancies on the surface of MoO_x suboxide films deposited at 275 °C, which is relevant for sensing applications. Owing to the composition control that could be achieved, the second part of this study focused on evaluating the electrical properties of the MoO_x layers. The temperature dependent resistivity of the MoO_x films suggested them to be suitable for gas sensing applications. In this context, a simple hydrogen gas sensor device was built using 50 nm suboxide MoO_x films which showed reversible and fast response to hydrogen gas at low temperatures.[3] The results derived from this study are very encouraging and form a solid foundation for in-depth studies on tuning the crystallinity of the suboxides for applications beyond gas sensing such as catalysis and energy storage.

3:15pm **AF2-MoA8 Atomic Layer Deposition of Gallium Oxide Thin Films using Pentamethylcyclopentadienyl Gallium and Combinations of H_2O and O_2 Plasma***, **Fumikazu Mizutani**, S. Higashi,* Kojundo Chemical Laboratory Co., Ltd., Japan*; M. Inoue, T. Nabatame,* National Institute for Materials Science, Japan

Pentamethylcyclopentadienyl gallium (GaCp*) was synthesized as a new precursor for atomic layer deposition of Ga_2O_3 thin films. GaCp* has higher vapor pressure compared with ethylcyclopentadienyl indium (InEtCp), which we reported previously [1, 2]. GaCp* is a cyclopentadienyl compound having a pentahapto half-sandwich structure as well as the InEtCp. Therefore, Ga_2O_3 thin films could be deposited in a similar way. In this paper, we investigated the role of the combinations of oxidant gases, H_2O followed by O_2 plasma (WpO), H_2O followed by O_2 (WO), and solely O_2 plasma (pO), on deposition mechanism of Ga_2O_3 films by the ALD process with GaCp* precursor.

During WpO process at 200 °C, linear growth with no nucleation delay and with a growth rate (GPC) of approximately 0.06 nm/cycle was observed, when 0.1 s GaCp*, 3 s H_2O, and 50 s O_2 plasma pulse times were applied. For the WpO process, a self-limiting surface reaction occurred when an GaCp* pulse time of 0.1-0.3 s, a H_2O pulse time of 1-5 s and an O_2 plasma pulse time of 40-90 s were applied at 200 °C. At this time, with a short O_2 plasma pulse time of less than 40 s, the oxidation reaction insufficiently carried out and resulted in thinner Ga_2O_3 films.

To understand the role of the surface oxidation step in the ALD process on the GPC, GPCs at 200 °C for WpO process with shorter O_2 plasma pulse time of 14 s (0.1 s GaCp* and 3 s H_2O) and WO process (0.1 s GaCp*, 3 s H_2O, and 50 s O_2) were examined. The GPC for the WO and for the pO process were 0.04 nm/cycle and 0.003 nm/cycle, respectively. If the O_2 plasma pulse time is shortened for WpO process, the GPC becomes slightly

smaller. On the other hand, GPC becomes negligibly small without plasma (WO).

Next, the role of the H_2O step on the GPC was investigated. The GPC at 200 °C for pO process (0.1 s GaCp* and 50 s O_2 plasma) was 0.05 nm/cycle, indicating that the oxidation is insufficient compared with WpO process.

The Ga_2O_3 films by plasma-enhanced ALD using a new GaCp* precursor was demonstrated. Based on these experimental data, note that the Ga_2O_3 surface oxidation step is found to be extremely important.

References

[1] F. Mizutani, S. Higashi, and T. Nabatame, AF1-TuM6, 17th International Conference on Atomic Layer Deposition (2017)

[2] F. Mizutani, S. Higashi, M. Inoue, and T. Nabatame, AF2-TuM15, 18th International Conference on Atomic Layer Deposition (2018)

ALD Fundamentals
Grand Ballroom E-G - Session AF3-MoA

Growth and Characterization I

Moderators: Somilkumar Rathi, Eugenus, Inc., Sumit Agarwal, Colorado School of Mines

4:00pm **AF3-MoA11 Understanding Elemental Steps of ALD on Oxidation Catalysts***, **Kristian Knemeyer**, M. Piernavieja Hermida, R. Naumann d'Alnoncourt,* Technische Universität Berlin, Germany*; A. Trunschke, R. Schlögl,* Fritz Haber Institute of the Max Planck Society, Germany*; M. Driess,* Technische Universität Berlin, Germany*; F. Rosowski,* BASF SE, Germany

Since the invention in the 1970s, Atomic layer deposition (ALD) has been extensively studied. Over the course of 40 years, its benefits for the microelectronic industry have been spread to numerous different fields such as medicine, batteries and catalysts[1]. Despite being applied and investigated for such a long time the deposition mechanism is barely understood. Typically, ALD is applied by performing hundreds of cycles to grow layers in the range from nanometers to micrometers and most of the times the first cycles show different growth behavior than the following ones. The first cycles might not be of interest for depositing films but they are crucial for us, as our aim in catalyst synthesis and modification is a film thickness in the nm range which is achieved with only few cycles.

We focused on understanding the first cycles of ALD on vanadium pentoxide as oxidation catalyst. Phosphorous oxide ALD on V_2O_5 was conducted with two different precursors (P^{5+} and P^{3+}) and then compared to the highly investigated mechanism of TMA/H_2O. ALD was performed in a magnetic suspension balance to track the mass gain in situ[2]. Surface species were analyzed not only by ^{31}P-NMR but also by in-situ DRIFTS measurements of the second half cycle. XPS was conducted to determine oxidation states of bulk and surface species after each half cycle. STEM-EDX shows highly distributed P on the surface and no additional phases were found. With the combination of these analytics we will show that the ALD mechanism depends heavily on the substrate and that ALD on oxidation catalysts is clearly different than on typical catalyst supports, such as SiO_2 or Al_2O_3.

[1] J. Lu, J. W. Elam, P. C. Stair, Surf. Sci. Rep. **2016**, 71, 410

[2] V. E. Strempel, D. Löffler, J. Kröhnert, K. Skorupska, B. Johnson, R. Naumann D'Alnoncourt, M. Driess, F. Rosowski, *J. Vac. Sci. Technol. A Vacuum, Surfaces, Film.***2016**, *34*, 01A135.

4:15pm **AF3-MoA12 Advanced Lateral High Aspect Ratio Test Structures for Conformality Characterization by Optical Microscopy***, Oili Ylivaara, P. Hyttinen,* VTT Technical Research Centre of Finland Ltd, Finland*; K. Arts,* Eindhoven University of Technology, Netherlands*; F. Gao,* VTT Technical Research Centre of Finland Ltd, Finland*; W.M.M. Kessels,* Eindhoven University of Technology, Netherlands*; R. Puurunen,* Aalto University, Finland*; **M. Utriainen**,* VTT Technical Research Centre of Finland Ltd, Finland

Atomic Layer Deposition (ALD) is a key technology in 3D microelectronics enabling conformal coatings into deep microscopic trenches and high aspect ratio cavities. However, conformality characterization in 3D trench walls is challenging and requires sample preparation. The MEMS-based all-silicon Lateral High Aspect Ratio (LHAR) test structure, developed at VTT, named PillarHall® [1-3], provides a fast and accurate substrate and characterization concept for the thin film conformality analysis [4,5]. The most important outcome from the PillarHall® characterization is the film saturation profile, which provides valuable data for reaction kinetics modelling and quantifying conformality. Since the LHAR enables utilization of planar metrology instruments, multiple approaches are compatible.

In this study, we focus on characterization methods suitable to extract the saturation profile and show the advantage of simple optical microscopy image analysis. Studied material was prototypical ALD Al_2O_3 (40-50 nm thick layers) made in two separate research facilities. The study consisted of SEM/EDX planar view, micro-spot reflectometry and ellipsometry and optical microscopy image analyses. These experiments were carried out by two research labs and supported by leading edge optical metrology tool vendors, Semilab Ltd, JA Woollam and Filmetrics.

We also introduce advanced LHAR 4th generation design, which enables characterization of the penetration depth profile with distinct advantages. Namely, new pillar design enables employment of optical line scanners up to 50 µm spot sizes. Furthermore, internal distance indicators support positioning the characterization tools more accurately. These features are illustrated in Supplementary Material Fig S1.

The results show that the gray-scale optical microscopy image analysis with the thickness determination in opening area gives similar results as the reflectometry or ellipsometry line scans, within the accuracy limits. Optical thickness/λ of the film is a limitation for the image analysis, but designing the experiments properly, the grayscale optical micrograph can be a powerful, widely compatible and easy method for conformality analysis.

Support from Semilab Ltd is gratefully acknowledged.

References

[1] F. Gao et al., J. Vac. Sci. Technol. A Vacuum, Surfaces, Film.33, 010601 (2015).

[2] R. Puurunen and F. Gao, 2016. doi: 10.1109/BALD.2016.7886526

[3] M. Mattinen et al., Langmuir, 32, 10559 (2016).

[4] M. Ylilammi et al., J. Appl. Phys., 123, 205301 (2018).

[5] V. Cremers et al., Applied Physics Reviews, in press (2019).

4:30pm **AF3-MoA13 Dopant Concentration Analysis of ALD Thin Films in 3D Structures by ToF-SIMS***, A.M. Kia, **Wenke Weinreich**,* Fraunhofer-Institut fur Photonische Mikrosysteme (IPMS), Germany*; M. Utriainen,* VTT Technical Research Centre of Finland Ltd, Finland*; R. Puurunen,* Aalto University, Finland*; N. Haufe,* Fraunhofer-Institut fur Photonische Mikrosysteme (IPMS), Germany

Self-limiting nature of atomic layer deposition (ALD) proposes a unique deposition mechanism which can produce extremely good step coverage within high aspect ratio (HAR) structures. This layer-by-layer deposition method also provides fine control on different features of deposition techniques such as controlling the dopant distribution in the direction of growth.

The quantity of dopant per layer is controlled, by applying saturation coverage delivering adequate dose rate for each precursor/reactant mixture. There are different parameters that contribute to control the dopant concentration in both 2D and 3D structures. To understand the reasons and characterize the precursors' behavior in deep trench structures, we used dynamic SIMS. Time of flight secondary ion mass spectrometry (ToF-SIMS) is a well-known method due to high detection sensitivity for the measurement of concentration levels of the dopant materials. Nevertheless, due to the geometry of the vertical HAR structures, it is challenging to characterize samples by ToF-SIMS. The absence of a simple and immediately available 3D structure for analyzing thin films produced by ALD has led most studies being made on flat surfaces.

A potential approach to circumvent the challenges is a MEMS-based all-silicon lateral high aspect ratio (LHAR) test structure, PillarHall® developed at VTT[1-2]. After removal of the top membrane (Fig.a-c) the LHAR test chip enables utilization planar characterization tools to examine the properties of deposited thin film on the 3D trench wall. This study focuses on semiquantitative characterization of different doping concentrations of La-doped HfO_2 with using LHAR. The LHAR Test Chips (LHAR3-series, AR2:1-10000:1, 500nm gap height) were used on carrier wafers in a 12 in wafer ALD process (Jusung Eureka 3000).

The findings show that the main difficulties with respect to the geometry for elemental analysis in non-planar structures can be resolved with LHAR. In particular, with the power of ToF-SIMS in data imaging (Fig.d) and integrating of data point from interested area (Fig.e), we are able to quantify doping profile along with understanding the properties of the trench wall in depth penetration.

REFERENCES

[1] Gao et al., J. Vac.Sci.Technol. A,33(2015) 010601.

[2] Puurunen et al., AF-SuA15,ALD 2017,Denver,USA.

4:45pm **AF3-MoA14 Metallic Ruthenium Coating on SiO_2 Powder by Atomic Layer Deposition using H_2O Reactant.***, **Chi Thang Nguyen**,* Incheon National University, Republic of Korea

Ruthenium has been many times studied by atomic layer deposition (ALD) for various applications, such as metal-insulator-metal capacitors (MIMCAP), diffusion barriers, and electrodes for dynamic random access memory (DRAM), due to its good thermal and chemical stability, high conductivity (resistivity of Ru ~ 7.4 μΩ.cm) and high work function (4.7 eV). Most of the ALD Ru films reported were deposited by the oxidants such as O_2 and O_3, and the main mechanism of Ru deposition was combustion reactions by the oxidant. So, Ru oxide phases were unintentionally formed under overexposure condition of oxidant. In this study, we used H_2O as a reactant to deposit metallic Ru film by ALD. We proposed an abnormal reaction mechanism between H_2O and the new beta-diketonate Ru precursors (5-methyl- 2,4- hexanediketonato) Ru(II), Carish, $C_{16}H_{22}O_6Ru$) led to the formation of Ru metallic film without the appearance of oxide phase under overexposure condition of the reactant. The formation of metallic Ru film by H_2O was analyzed with experimental and theoretical approaches, including the X-ray diffraction (XRD), X-ray photoelectron spectroscopy (XPS), transmission electron microscopy (TEM) and Density functional theory (DFT). Also, the cyclic voltammetry (CV) testing was performed on ALD Ru on SiO_2 powders.

5:00pm **AF3-MoA15 Low Energy Ion Scattering Study of Pt@Al_2O_3 Nanoparticle Coarsening***, **Philipp Brüner**,* IONTOF GmbH, Germany*; E. Solano,* ALBA Synchrotron Light Source, Spain*; C. Detavernier, J. Dendooven,* Ghent University, Belgium

Coarsening of dispersed Pt nanoparticles has been shown to occur at elevated temperatures [1], leading to the formation of larger particles, and consequently a reduction of the total number of particles. This has important consequences in real-world applications of Pt nanostructures, such as heterogeneous catalysis, where a high number of small, highly dispersed particles are desirable to maintain high catalytic activity.

One attempt to prevent coarsening is to coat the Pt nanoparticles by a thin Al_2O_3 shell deposited by atomic layer deposition (ALD). Advanced surface analytical techniques are required to study the resulting complex structures. In this study, low energy ion scattering (LEIS) is used to support existing data obtained by grazing incidence small angle X-ray scattering applied to Pt nanoparticle model systems prepared by ALD [1]. In LEIS, the energy spectrum of noble gas ions scattered from the sample surface is recorded. The evaluation of elemental peaks in the resulting spectra allows the quantification of the elemental composition of the first atomic layer [2]. This extreme surface sensitivity of just a single atomic layer, combined with composition analysis, is unique to LEIS and makes it especially useful in the study of nanoscale systems. In addition, sub-surface scattering signal from deeper layers gives information about sample composition and layer thickness up to depths of 10 nm.

We show how the monolayer surface sensitivity of LEIS enables the precise determination of the areal density of the deposited nanoparticles and the particle surface coverage of sub-monolayer Al_2O_3 shells. Furthermore, cracking of the shells by annealing has been observed. By measuring layer thickness values, average particle sizes are determined, which give insight into coarsening processes. The thickness of Al_2O_3 shells can be determined precisely over a wide range of values, including ultra-thin sub-monolayer shells after just five cycles of Al_2O_3 deposition.

The results demonstrate that the effectiveness of the Al_2O_3 shell depends on the process conditions during the deposition of the Pt nanoparticles. $MeCpPtMe_3$ was used as a precursor, with either O_2 gas or N_2 plasma as reactants [3]. In the former case, even a sub-monolayer Al_2O_3 shell can completely prevent particle coarsening. In the latter case, the N_2 plasma based Pt process results in a denser collection of smaller Pt nanoparticles and stabilization with an Al_2O_3 overcoat is proven to be more difficult.

[1] Nanoscale, 2017, 9, 13159-13170

[2] "Low-Energy Ion Scattering" in Characterization of Materials - Second Edition ISBN 978-1-118-11074-4 - John Wiley & Sons.

[3] Nat. Commun. 8 (2017) 1074

5:15pm **AF3-MoA16 Physical and Electrical Characterization of ALD Chalcogenide Materials for 3D Memory Applications***, **Vijay K. Narasimhan**, V. Adinolfi, L. Cheng, M.E. McBriarty,* Intermolecular, Inc.*; M. Utriainen, F. Gao,* VTT Technical Research Centre of Finland Ltd, Finland*; R. Puurunen,* Aalto University, Finland*; K. Littau,* Intermolecular, Inc.

In three-dimensional memory integration schemes, like those used for current NAND Flash memory technologies, the active layers of the memory devices are filled into vias with aspect ratios of 40:1 or greater. It is important for the deposited films to demonstrate consistent properties all the way through the depth of the via. Recently, novel ALD chalcogenide materials have emerged [1-3] that could be used as phase-change memory (PCM) and ovonic threshold switch (OTS) selectors. ALD chalcogenides are attractive because they could be compatible with 3D integration schemes; however, the properties of these films in high-aspect ratio structures have not been extensively investigated.

In this study, we use PillarHall® Lateral High Aspect Ratio (LHAR) test chips [4-6] to elucidate the properties of ALD chalcogenides on a trench wall using standard in-plane metrology techniques without fabricating full device stacks. The PillarHall all-silicon LHAR test chip includes multiple trenches in the aspect ratio range 2:1 - 10000:1 with constant 500 nm gap height [6]. LHAR chips are used as substrates for ALD binary and ternary chalcogenide films using $HGeCl_3$, $[(CH_3)_3Si]_2Te$, $[(CH_3)_3Si]_2Se$, and $(C_2H_5O)_4Te$ as precursors. Using optical microscopy, scanning electron microscopy with energy-dispersive x-ray spectroscopy, and scanning-probe techniques, we describe the chemical, physical, mechanical, and electrical properties of these films. We show that the thickness and atomic composition of certain chalcogenide films changes dramatically inside of high-aspect ratio features (Fig. S1). Furthermore, we perform optical profilometry on silicon micro-membranes on the PillarHall test chips (Fig. S2) to rapidly estimate the ALD film stress on the microscopic level, which is not directly measurable in devices today despite its importance in 3D architectures. We use these results to comment on the ALD reaction kinetics and discuss implications for future research on ALD chalcogenide films.

Combining high-aspect ratio and stress measurements on a single test chip can accelerate R&D of ALD chalcogenides for applications in PCMs and OTSs as well as other microscopic 3D applications of ALD thin films.

References

[1] T. Gwon *et al.*, *Chem. Mater.* 29, 8065 (2017).

[2] W. Kim *et al.*, *Nanotechnology*, 29, 36 (2018).

[3] L. Cheng, V. Adinolfi, S. L. Weeks, Sergey V. Barabash, and K. A. Littau, *J. Vac. Sci. Technol. A.* ALD2019, 020907 (2019).

[4] F. Gao, S. Arpiainen, and R. L. Puurunen, *J. Vac. Sci. Technol. A.* 33, 010601 (2015).

[5] M. Ylilammi, O. M. E. Ylivaara, and R. L. Puurunen, *J. Appl. Phys.* 123, 205301 (2018).

[6] O.M.E Ylivaara *et al.*, *Proc. 18th Int. Conf. At. Layer Depos.* (2018).

5:30pm **AF3-MoA17 The Tailoring of the Single Metal Atom-Oxide Interface***, **Bin Zhang**, Y. Qin,* Institute of Coal Chemistry, Chinese Academy of Sciences, China

The metal-oxide interface plays important roles in the metal-based heterogeneous catalyst. By sample tailoring the types of interface, size and crystal structure of metal and oxides, etc, the catalytic performance of the catalyst changes dramatically. Thus, the preciously tailoring the metal-oxide interface in atomic scale is a key and most important strategy to design an effective metal-based catalyst. Atomic layer deposition (ALD) is a promising and controllable approach to precisely design and tailor the metal-oxide interface because of its atom-level thickness control, excellent uniformity and conformality and good repeatability in film or particle deposition. Recently, we have developed new strategies for the tailoring of the interface structure by building a serial of nanostructures, such as the core-shell structures, inverse oxide/metal structure, porous sandwich structure, multiple confined metal nanoparticles in oxide nanotubes, and tube-in-tube structure with multiple metal-oxide interfaces. In many case, the metal–oxide interface forms at the cost of metal surface sites through ALD overcoating or modification. In order to increse the ratio of metal-oxide interface and utilization of metal, the building of single metal atom-oxide interface with high loading of metal is a good but challenge strategy since the unstability of single atoms. We have realized this in many ways, such as developing new ALD deposition approachs, depositing oxide site in advance, and changing the deposition dynamic conditions etc. Pt/FeO_x, Cu-

TiO_2, and Pt-CeO_2 single metal atom-oxide interface showed high catalytic performance in selecitive hydrogenation with high efficiency.

References

1. H. Ge, B. Zhang, X. Gu, H. Liang, H. Yang, Z. Gao, J. Wang, Y. Qin, *Angew. Chem. Int .Ed.* 2016, **55**: 7081-7085.

2. Z. Gao, M. Dong, G. Z. Wang, P. Sheng, Z. W. Wu, H. M. Yang, B. Zhang, G. F. Wang, J. G. Wang, and Y. Qin, *Angew. Chem. Int .Ed.* 2015, **54**: 9006-9010.

3. J. K. Zhang, Z. B. Yu, Z. Gao, H. B. Ge, S. C. Zhao, C. Q. Chen, S. Chen, X. L.Tong, M. H.Wang, Z. F., and Y. Qin, *Angew. Chem. Int .Ed.* 2017, **56**: 816–820.

4. B. Zhang, Y. Qin, *ACS Catal.* 2018, 8, 10064-10081.

ALD Fundamentals
Grand Ballroom H-K - Session AF4-MoA

Growth Mechanisms II

Moderators: Viljami Pore, ASM, Mikko Ritala, University of Helsinki

4:00pm **AF4-MoA11 Monolithic Integration of Single Crystal Perovskites on Semiconductors with ALD*, John Ekerdt,*** University of Texas at Austin **INVITED**

The semiconductor industry faces new challenges in the sub-10 nm era as scaling will no longer dominate performance improvement. New materials provide opportunity to improve performance with minimal architectural overhaul. For example, high-mobility channels of Ge and III-V semiconductors can provide both lower power consumption and faster computing speeds. In certain applications significant advantages are gained by monolithic integration of the oxides directly on the substrates that will host other devices/components. Perovskite oxides offer a wide range of properties from high-k to multiferroic affording the device designer a suite of possibilities and are particularly important due to their common structure and lattice-matching with common semiconductors.

Here, we report the fabrication of monolithically integrated, single crystal, metal-ferroelectric-semiconductor structures. This talk demonstrates the possibilities through the monolithic integration of perovskite oxides on Si(001) for applications in silicon nanophotonic devices and low-power transistors. Barium titanate (BTO) films, and BTO/$La_xSr_{1-x}TiO_3$ ($x \leq 0.15$) perovskite heterostructures are grown on strontium titanate (STO)-buffered Si(001) using atomic layer deposition at 225 °C. Film strain and *c*-axis orientation are manipulated by growth and annealing conditions. Piezoresponse force microscopy (PFM), electrical and electro-optic measurements establish BTO film ferroelectric (FE) behavior at the µm-scale. The $La_xSr_{1-x}TiO_3$ ($x \leq 0.15$) perovskite heterostructures sandwiched between Si(001) and BTO permits examination of a quantum metal between Si and a FE film.

It is possible to grow crystalline perovskites directly on Ge(001) by ALD and we have used this to deposit STO, BTO, $SrHfO_3$, $Sr(HfTi)O_3$, $SrZrO_3$, and $SrSnO_3$ directly on Ge(001). We will also present the growth and properties of theses perovskite layers directly on Ge(001) and will discuss the how the interface chemistry and structure control the interfacial reactions that allow for crystalline film formation during ALD, and how they affect film properties.

~~4:30pm **AF4-MoA13 Introducing the Concept of Pulsed Vapor Phase Copper-free Surface-Click chemistry using the ALD Technique*, Iva Šarić, R. Peter, M. Kolympadi Markovic, I. Jelovica Badovinac,*** University of Rijeka, Croatia*; C. Rogero,* Materials Physics Center (CSIC-UPV/EHU), Spain*; M. Ilyn,* Donostia International Physics Center (DIPC), Spain*; M. Knez,* CIC nanoGUNE, Spain*; G. Ambrozic,* University of Rijeka, Croatia~~

~~While ALD allows deposition of a broad variety of inorganic materials, MLD typically relies on very few basic organic reactivity concepts and therefore is not yet as versatile as it could or should be. Given the great promise of ALD/MLD, it is highly demanded to extend the choice of available chemistries, providing a greater choice of suitable organic precursors. The idea behind our work is to extend the range of possible surface chemical reactions by introducing click chemistry as an additional option into the organic chemical vapor phase deposition concept. Click chemistry, initially developed for drug delivery, has recently gained increasing attention in surface patterning with important applications in biotechnology and in development of nanomaterials. Here we report for the first time on a model gas phase copper-free azide-alkyne click reaction performed in an ALD instrumentation [1]. The newly developed process is based on an *in situ* two-step pulsed vapor phase sequence consisting of initial exposure of ZnO to propiolic acid as the first precursor, followed by gas phase click chemistry coupling of benzyl azide as the second precursor. The organic phase compositions were analyzed by XPS and FTIR, while the preservation of ZnO surface morphology was investigated by SEM and STEM. When compared to known state-of-the-art *ex-situ* gas phase click reactions [2,3], the ALD/MLD processing conditions ensure reproducibility and improve the time and surface coverage efficiency. The resulting hybrid material exhibits no surface contaminations with physisorbed organic precursors and/or by-products deriving from organic precursor degradation. This study offers great potential toward the development and fabrication of complex functional organic layers on metal oxide surfaces by selective azide-alkyne cycloadditions performed in an ALD/MLD instrument and broadens the variation range of applicable chemistry in MLD. Variation of the functionalities of the organic precursors will allow MLD type of polymer growth based on click chemistry and add degrees of freedom for the design of functional polymeric coatings.~~

~~[1] I. Saric, R. Peter, M. Kolympadi Markovic, I. Jelovica Badovinac, C. Rogero, M. Ilyn, M. Knez and G. Ambrozic, *ChemComm*, 2019, DOI: 10.1039/C9CC00367C.~~

~~[2] F. Gao, S. Aminane, S. Bai and A. V. Teplyakov, *Chem. Mater.*, 2017, 29, 4063-4071.~~

~~[3] M. Konh, C. He, Z. Li, S. Bai, E. Galoppini, L. Gundlach and A. V. Teplyakov, *J. Vac. Sci. Technol. A*, 2018, 36, 041404.~~

4:45pm **AF4-MoA14 Surface Enhanced Raman Spectroscopy Studies of Aluminum ALD Precursors for Al_2O_3 Growth*, Michael Foody,*** Illinois Institute of Technology

Trimethylaluminum (TMA) is perhaps the most widely employed and emblematic ALD precursor – mainly for its robust reactivity with hydroxyl surface species and well-behaved ALD growth. Although one would expect other alkyl aluminum compounds to have similar properties, we have found the highly pyrophoric compound triisobutylaluminum (TiBA) does not grow alumina under similar ALD-like conditions. Unlike many other thin-film deposition techniques, ALD is driven by the reactivity at the vapor-substrate interface, and the stark divergence between these chemically similar precursors offers insight into the fundamental principles of ALD.

In this work, we use surface enhanced Raman spectroscopy (SERS) to show the limited reactivity between surface alkyl groups and water. SERS shows when TiBA is exposed to a 3-mercaptopropionic acid surface, only small signals corresponding to Al-C and isobutyl bond modes appear. The small signal corresponding to isobutyl peaks remains even after treatment with water indicating no reactivity between the isobutyl alkyl surface and water. These measurements suggest a mechanism in which proton transfer acts as the limiting step.

This knowledge informed the design of new precursors to test the structural and electronic effects of Al precursors. As a comparison, two additional aluminum precursors were synthesized, and used to grow alumina thin films by ALD. The two new precursors have varying alkyl groups – analogous to TMA and TiBA – as a way to compare the proton transfer reactivity to a methyl group and an isobutyl group at the vapor-substrate interface. Measurements were made using QCM and SERS, and were found to be consistent with our findings of the reactivity profiles of TMA and TiBA. The methyl aluminum complex was found to be a robust precursor for alumina deposition with water, while the isobutyl analogue did not deposit any mass or show films by ellipsometry on silica. All depositions were done under 200C, and SERS measurements were made at 100C, thus demonstrating the relatively low-temperature deposition conditions of these compounds. The SERS measurements presented here are among the first reports using SERS to evaluate ALD systems. They provide powerful insights into deposition mechanism by measuring bond vibrational modes over a much larger range of frequencies than more common methods (FTIR). The measurements (along with QCM) provide a new understanding of the reactivity of alkyl aluminum precursors, which have broader implications for general precursor design.

5:00pm **AF4-MoA15 Atomic Layer Deposition of Aluminum, Hafnium and Zirconium Oxyfluoride Films with Tunable Stoichiometry*, Neha Mahuli,*** *J. Wallas, S.M. George,* University of Colorado - Boulder

The reactivity of metal oxide films with halogen chemistries can be reduced by incorporating fluorine into the metal oxide during film deposition. This study explored the atomic layer deposition (ALD) of various metal oxyfluorides such as aluminum oxyfluoride (AlO_xF_y), hafnium oxyfluoride

(HfO_xF_y) and zirconium oxyfluoride (ZrO_xF_y). Techniques were developed to obtain tunable stoichiometry of the metal oxyfluoride films.

The metal oxyfluoride ALD films were deposited at 150˚C. H_2O and HF-pyridine were used as the oxygen and fluorine sources. $Al(CH_3)_3$ was used as the Al source and Hf and Zr amidinates precursors were used as the Hf and Zr metal sources. The metal oxyfluorides were deposited using either (1) the halide-exchange method (see Supplemental Figure 1) or (2) the nano-laminate method (see Supplemental Figure 2). Both methods were evaluated using *in situ* quartz crystal microbalance (QCM) measurements and *ex situ* X-ray photoelectron spectroscopy (XPS) analysis.

The halide-exchange method is based on the facile exchange of oxygen by fluorine from HF. HF exposures after deposition of the metal oxide easily replaced oxygen with fluorine. In addition, the fluorine also diffused into the underlying metal oxide film. The oxygen/fluorine exchange and fluorine diffusion complicates the control of the stoichiometry of the metal oxyfluoride film.

Compositional control was achieved by the halide-exchange mechanism using either metal oxide layers with various thicknesses or different HF pressures. The stoichiometry could also be tuned using the nano-laminate methods with different numbers of metal oxide ALD and metal fluoride ALD cycles. These two methods gave rise to tunable stoichiometry from pristine metal oxide to adjustable oxyfluoride to pristine metal fluoride.

5:15pm **AF4-MoA16 Fundamental Study on the SiO_2 Growth Mechanism of Electronegativity Difference of Metal-O in the High-*k* Underlayers by PE-ALD Method***, **Erika Maeda,*** Shibaura Institute of Technology, Japan*; T. Nabatame,* National Institute for Materials Science, Japan*; M. Hirose,* Shibaura Institute of Technology, Japan*; M. Inoue, A. Ohi, N. Ikeda,* National Institute for Materials Science, Japan*; M. Takahashi, K. Ito,* Osaka University, Japan*; H. Kiyono,* Shibaura Institute of Technology, Japan

To fabricate silicate films such as $HfSiO_x$ and $AlSiO_x$ as gate insulator of GaN power devices, the HfO_2/SiO_2 and Al_2O_3/SiO_2 laminates was initially deposited by atomic layer deposition (ALD) process [1]. Understanding the SiO_2 growth mechanism on HfO_2 and Al_2O_3 layers is an important in terms of the design of the $HfSiO_x$ and $AlSiO_x$ formation. In this study, we systematically investigate the growth rate of SiO_2 film on various high-*k* underlayers (Metal-O) by plasma-enhanced ALD (PEALD) using Tris(dimethylamino)silane (TDMAS) precursor and O_2 plasma gas, and we also discuss about role of the electronegativity difference in Metal-O on the SiO_2 growth mechanism.

At first, 30-nm-thick HfO_2, TiO_2, and Al_2O_3 layers and 5-nm-thick SiO_2 layer on Si substrates were prepared as Metal-O. The thicknesses of the SiO_2 films were varied on Metal-O by changing ALD cycles during PEALD at 300 °C. The thickness of the SiO_2 film was estimated using spectroscopic ellipsometry and Si_{2p} intensities of XPS.

All data of the SiO_2 thickness on HfO_2, TiO_2, Al_2O_3, and SiO_2 layers as a function of ALD cycle satisfied the linear relationship. The growth per cycle (GPC) value of the SiO_2 film was increased in the following order: SiO_2 (0.036 nm/cycle) < Al_2O_3 (0.090) < TiO_2 (0.11) < HfO_2 (0.13). Here, we pay attention to the electronegativity values of the Si, Al, Ti, Hf, and O atoms of Metal-O. Note that the GPC increased as the difference of electronegativity such as Si-O (1.76), Al-O (2.03), Ti-O (2.18), and Hf-O (2.27) in the Metal-O increased [2]. Based of these experimental data, we proposed one idea of the SiO_2 growth mechanism. In the TDAMS precursor supply step during PEALD, the adsorption of TDMAS precursor on the surface of Metal-O must be strongly influenced by the difference of electronegativity. This is because Si atom of the TDMAS precursor is easily attracted to oxygen atoms having a large electron density of Metal-O. Therefore, the adsorbed amount of the TDMAS precursor increases as the electron density of oxygen atoms becomes higher in the following order: Si-O < Al-O < Ti-O < Hf-O. This behavior was observed up to ALD 10 cycles. When the ALD cycle increases more than 10 times, the GPC became the same value (0.036 nm/cycle) as SiO_2 regardless of underlayer materials. This suggests that the adsorption amount of the TDMAS is similar to that of SiO_2 because the 1.2-nm-thick SiO_2 layer covered on the underlayer materials. To understand the SiO_2 growth mechanism, we should pay attention to the difference of electronegativity of Metal-O in underlayer.

[1] T. Nabatame et al., Appl. Phys. Express 12, 011009 (2019).

[2] A. L. Allred et al., J. Inorg. Nucl. Chem., 5, 264 (1958).

5:30pm **AF4-MoA17 Low Temperature Aluminium Nitride Deposition: Comparing Hydrazine and Ammonia***, **Aswin L.N. Kondusamy**, S.M. Hwang, A.T. Lucero, Z. Qin, X. Meng,* The University of Texas at Dallas*; D. Alvarez, J. Spiegelman,* RASIRC*; J. Kim,* The University of Texas at Dallas

Aluminium nitride is a wide bandgap material having high thermal conductivity [1]. Depositing thin films of high thermal conductivity such as Aluminium nitride as a capping layer or a passivation layer by a CMOS compatible method is a viable approach to tackle the heat management issue that arises with scaling down of devices. Compatibility demands lower deposition temperature (<300 °C) and improved conformality over high-aspect ratio structures. AlN_x ALD using low reactive NH_3 results in incomplete reaction below 300 °C [2], resulting in carbon and hydrogen impurities and Plasma enhanced ALD (PEALD) frequently exhibits poor conformality. Thermal ALD (t-ALD) with a more reactive nitrogen precursor such as hydrazine is expected to overcome these problems. Newly available ultra-high purity hydrazine sources have been successfully used to deposit metal nitrides at low temperature [3]. In this work we study the low temperature t-ALD growth characteristics of aluminium nitride using hydrazine and trimethylaluminium (TMA) and evaluate the properties of the films. t-ALD results with hydrazine will be compared to films grown by t-ALD with NH_3 and PEALD with NH_3 plasma, all using the same ALD reactor in the same temperature range.

AlN_x films were deposited using a custom-made ALD reactor from 175-350 °C. Hydrazine is supplied from a BRUTE hydrazine source. Growth with hydrazine shows saturation behavior, with growth per cycle (GPC) saturating at hydrazine exposure as low as 0.1 s (~10^4 L). High GPC of 2.8-3.2 Å/cycle is observed at 300 °C with refractive index of 1.890 whereas t-ALD with NH_3 shows lower GPC (1.1 Å/cycle) for similar exposure, which is expected due to superior reactivity of hydrazine. AlN_x growth using hydrazine shows high temperature dependence in the range 175-300 °C. X-ray photoelectron spectroscopy is used to confirm film stoichiometry: films with low carbon (1%) impurities can be achieved. Films deposited below 250 °C get oxidized easily under air due to low film density. A novel densification method is proposed to obtain denser films at these temperatures to overcome this problem. The denser films are expected to have higher thermal conductivity. The detailed experimental results will be presented.

[1] G. A. Slack, R. A. Tanzilli, R. O. Pohl, J. W. Vandersande, J. Phys. Chem. Solids, 48 (1987) 641-647

[2] R. L. Puurunen, M. Lindblad, A. Root, A. O. I. Krause, Phys. Chem. Chem. Phys., 3 (2001) 1093-1102

[3] D. Alvarez, J. Spiegelman, R. Holmes, K. Andachi, M. Raynor, H. Shimizu, ECS Transactions, 77 (2017) 219-225

Atomic Layer Etching
Regency Ballroom A-C - Session ALE1-MoA

Energy-enhanced ALE

Moderators: Keren J. Kanarik, Lam Research Corp., Harm Knoops, Oxford Instruments Plasma Technology

1:30pm **ALE1-MoA1 Atomic Layer Etching – Advancing Its Application with a New Regime***, **Samantha Tan**, W. Yang, K.J. Kanarik, Y. Pan, R. Gottscho,* Lam Research Corp. **INVITED**

Continued shrinking of device dimensions has placed extreme requirements on plasma etching technology, making it increasingly challenging to faithfully transfer patterns with nanometer-sized features. To address this nanoscopic challenge, atomic layer etching (ALE) has been successfully used to extend conventional etch technology and some critical processes have been implemented in high-volume manufacturing (HVM) [1]. To be adopted for more applications, ALE must further overcome both productivity and technical limitations. Directional ALE typically operates in a low energy (< 100 eV) regime which results in relatively low etch rates (~5 Å /cycle). Productivity can be improved by engineering hardware to increase switching speed – but there is room for improvement. In addition, ALE faces technical limitations in applications where synergy is < 100 % which can result in sidewall etching. This is particularly problematic for maintaining a directional etch profile in high aspect ratio features. In this talk, we will present results obtained using a new operating regime that has the potential to meet the productivity and technical challenges for ALE while retaining its inherent benefits: low damage, smoothing, aspect ratio independence, and selectivity [2, 3].

[1] Lam Research Corporation, September 2016. [Online]: https://investor.lamresearch.com/news-releases/news-release-details/lam-research-introduces-dielectric-atomic-layer-etching. >

[2] K. Kanarik, S. Tan, and R. A. Gottscho, J. Phys. Chem. Lett. 2018, 9, pp. 4814–4821>

[3] Michael Koltonski, Wenbing Yang, Craig Huffman, Mohand Brouri and Samantha Tan, "Opportunities and Challenges Utilizing Atomic Layer Etch for Lead Edge Technology Metal Line Widths", SPIE Advanced Lithography Conference, San Jose, CA, Feb 24-28, 2019>

2:00pm **ALE1-MoA3 Control of the Interface Layer in ALE Process by Alternating O_2 Plasma with Fluorocarbon Deposition for High Selectivity Etching***, **Takayoshi Tsutsumi**, A. Kobayashi,* Nagoya University, Japan*; N. Kobayashi,* ASM Japan K.K., Japan*; M. Hori,* Nagoya University, Japan

Our research group developed a process for atomic layer etching of an SiO_2 film using alternating nanometer-thick fluorocarbon film deposition and O_2 plasma irradiation [1]. This process allows the atomic scale etching of SiO_{-2} with high reproducibility because of removing extra carbon on surface and cleaning chamber walls by O_2 plasma. The ALE process could have benefits for etching SiO_2 selective to Si_3N_4 if we actively control the chemistry in the mixture region between Si-compounds and fluorocarbon, and suppress the oxidation of Si_3N_4 by O_2 plasma.

In this time, the ALE process was performed to a SiO_2 and Si_3N_4 deposited by ALD process in a capacitively coupled plasma (CCP) reactor. A 100-MHz electrical power of 100 W was applied to the upper electrode at a pressures of 2.0 Pa. The wafer temperature was set at 20°C. For the deposition process, C_4F_8/Ar plasma was used to form a fluorocarbon film. Figure 1 shows the C 1s spectra of a SiO_2 and Si_3N_4 after the deposition processes. The C 1s spectrum of SiO_{-2} after the deposition process exhibits C-C, C-CF_x, CF, CF_2, and CF_3 peaks. On the other hands, the spectrum of Si_3N_4 shows an increased in the fraction of the C-C bond and exhibits the Si-C bond. Higher fraction of the C-C and forming Si-C and C-N bonds in the mixture regions lead to etching SiO_{-2} selective to $Si_{-3}N_4$. Higher F/C ratio in fluorocarbon film is required for etching SiC compared to SiO_2 and Si_3N_4 because of etching products of SiF_4 with very little SiF and SiF_2[2]. Moreover, higher bond energies of CN, which are C-N of 305 kJ/mol, C=N of 615 kJ/mol and C≡N of 887 kJ/mol, could suppress oxidation of SiN by control of ion energy and wafer temperature. If the oxidation by O_2 plasma is suppressed, our ALE by alternating fluorocarbon deposition and O_2 plasma could apply to industry process for next-generation devices due to high controllability and reproducibility. We analyze the depth profiles of atomic concentrations in the mixture regions for a SiO_2 and Si_3N_4 by angle resolved X-ray photoelectron spectroscopy (XPS) to control chemistry of the mixture regions by some knobs such as ion energy and surface temperature.

[1] T. Tsutsumi et al., J. Vac. Sci. Technol. A **35**, 01A103 (2017)

[2] H. Winters et al., J. Vac. Sci. Technol. B **1**, 927 (1983)

2:15pm **ALE1-MoA4 Self-limiting Atomic Layer Etching of SiO_2 using Low Temperature Cyclic Ar/CHF_3 Plasma***, **Stefano Dallorto**,* Lawrence Berkeley National Laboratory*; A. Goodyear, M. Cooke,* Oxford Instruments Plasma Technology, UK*; S. Dhuey,* Lawrence Berkeley National Laboratory*; J. Szornel,* Lawrence Livermore National Laboratory*; I. Rangelow,* Ilmenau University of Technology, Germany*; S. Cabrini,* Lawrence Berkeley National Laboratory

Single digit nanometer semiconductor manufacturing is increasingly demanding atomic scale process controllability to further decrease critical dimensions and pitches. High etching precision and material selectivity become essential in the atomic scale era. Plasma based atomic layer etching (ALE) shows promise to attain atomic etch precision, enhancing energy control and reaction chemistry control.

Here we study a Fluorocarbon(FC)-based ALE process for controlling the etching of silicon dioxide at the atomic level. Figure 1 shows the schematic of atomic layer etching process using Ar plasma and CHF_3 gas. In this technique, an Ar plasma is maintained continuously through the process, below the energy threshold for SiO_2 sputtering. A fluorocarbon chemistry is then introduced via CHF_3 pulsing to provide the reactant absorption. Subsequently, once the gas pulse has concluded, bias power is introduced to the Ar plasma, to provide enough energy to initiate reaction of the FC with the SiO_2. In ideal ALE, each of the steps is fully self-limiting for over exposure to increase uniformity on the microscale (wafer) and atomic scale.

With the goal of achieving self-limiting FC-based ALE, we investigated the etch step using low energy Ar ion bombardment. By carefully tailoring the energy of ion bombardment, it is possible to control the etching depth to approach a self-limiting behavior. The impact of various process parameters on the etch performance is established. We demonstrated that the SiO_2 amount etched per cycle (EPC) is strongly affected by the forward bias plasma power, as well as the substrate temperature (Figure 1(a)). The substrate temperature has been shown to play an especially significant role, at -10 °C the contributions to chemical etching coming from fluorine and fluorocarbon compounds from chamber walls are minimized and a quasi-self-limiting behavior ALE is observed.

Figure 1(b)-(f) showed the Cr features after being etched for 60 ALE cycles with the optimal ALE self-limiting conditions. Feature trenches vary from 20-200 nm and were defined using metal lift-off. Overall, using the cyclic CHF_3/Ar ALE at -10 °C, we reduced geometric loading effects during etching and reached aspect ratio independent etching, with great potential for significant improvement in future etching performances.

2:30pm **ALE1-MoA5 Evolution of Photoresist Layer Structure and Surface Morphology in a Fluorocarbon-Plasma-Based Atomic Layer Etching Process***, **Adam Pranda**, K-Y. Lin, S. Gutierrez Razo, J. Fourkas, G.S. Oehrlein,* University of Maryland

The impact of continuous-wave plasmas in realizing a pattern transfer process with a Ar/fluorocarbon composition on photoresist etching behavior and surface roughness development has been extensively studied.[1] However, the characteristics of photoresists under atomic layer etching (ALE) processes have not been well established. Specifically, the structure and morphology of the photoresist layer is dependent on the interplay between energetic ion bombardment and the diffusion of reactive species at the surface. For evaluating these photoresist properties, we used an ALE process with an Ar carrier gas and a fluorocarbon (FC) precursor gas, for example C_4F_8.[2]

For sample characterization, we utilized a combination of real-time, *in situ* ellipsometry and post-process surface roughness and surface chemistry analysis using atomic force microscopy (AFM) and x-ray photoelectron spectroscopy, respectively. The AFM characterization provided information on both the surface roughness magnitude as well as the distribution via a power spectral density analysis. Both an industry-standard 193 nm photoresist and an extreme ultraviolet (EUV) photoresist were evaluated.

Based on the ellipsometric characterization, we find that the 193 nm photoresist initially develops a surface dense amorphous carbon (DAC) layer from Ar ion bombardment of both the native photoresist and deposited FC, which contributes additional carbon to the DAC layer, increasing its thickness. Upon the FC deposition step in the ALE process, the refractive index of the DAC layer decreases due to fluorine diffusing into the layer structure. Corresponding AFM analysis shows a reduction in the surface roughness. Once the DAC layer becomes saturated with fluorine, a discrete FC layer forms on the surface. Subsequently, in the etching step, the discrete FC layer is removed, the DAC layer recovers its thickness, and the cycle repeats.

The authors gratefully acknowledge Eike Beyer for assistance with the experimental setup, R. L. Bruce, S. Engelmann, and E. A. Joseph for supplying the EUV materials, and financial support of this work by the National Science Foundation (NSF CMMI-1449309) and Semiconductor Research Corporation (2017-NM-2726).

[1] S. Engelmann et al., J. Vac. Sci. Technol. B Microelectron. Nanom. Struct. **27**, 1165 (2009).

[2] D. Metzler et al., J. Vac. Sci. Technol. A **32**, 020603 (2014).

2:45pm **ALE1-MoA6 Optimized Radical Composition of C4F8/Ar Plasma to Improve Atomic Layer Etching of SiO_2***, **Young-Seok Lee**, J.-J. Lee, S.-W. Yoo, S.-H. Lee, I.-H. Seong, C.-H. Cho, S.-J. Kim, J.-P. Son, S-J. You,* Chungnam National University, Korea

For the last decade, there was a big step in atomic layer etching (ALE) of SiO_2 with fluorocarbon plasma. After a computer simulation suggested a surface modification method via fluorocarbon film deposition on SiO_2 and its atomically thin removal, ALE of SiO_2 was demonstrated experimentally using an inductively coupled fluorocarbon plasma. Ever since, there have been a lot of research trying to improve the ALE of SiO_2. Meanwhile, it was also found that a fluorocarbon film deposited during deposition-based SiO_2 ALE is formed from fluorocarbon neutral radicals as well as low-energy ions. Their compositions therefore are expected to play a significant role to determine characteristics of the deposited fluorocarbon film and, in the end, the result of ALE of SiO_2. For an investigation into an optimized composition of the fluorocarbon plasma components, we measured neutral radical densities under various conditions using a quadrupole mass

spectrometer and monitored SiO_2 thickness changes during ALE in real time with in situ multi-wavelength ellipsometer. An improved SiO_2 ALE process and possible improvement mechanisms will be presented.

3:00pm **ALE1-MoA7 Atomic Layer Etching of Silicon Nitride with Ultrahigh Etching Selectivity over Silicon and Oxide Materials by Utilizing Novel Etch Gas Molecule***, **Xiangyu Guo**,* American Air Liquide*; N. Stafford,* Air Liquide*; V. Pallem,* American Air Liquide

Silicon nitride etching with high selectivity over silicon and silicon oxide material, without or with minimal damage to the exposed surfaces, is one of the most critical processes in the fabrication of complementary metal-oxide-semiconductor (CMOS) devices. In this work, the authors propose a novel hydrofluorocarbon etch gas molecule for Si3N4 etching with ultrahigh etching selectivity over Si materials (p-Si, SiO2, SiON, SiCN, etc) based on atomic layer etching (ALE) cyclic process. Each cycle of the ALE process consists two independent unit process reactions: step A - polymer deposition and step B - removal step. The process was conducted in a home-built capacitively coupled plasma (CCP) chamber and was optimized on planar thin films first. CH3F was used as the process baseline. The authors show that novel gas molecule demonstrates significant improved performance in several aspects comparing to CH3F - ultrahigh selectivity, minimal damage, smoother surface after etching, higher ALE synergy, etc. The new molecule was also evaluated on patterned structure - Si3N4 gate spacer. The authors demonstrate the ALE process utilizing proposed novel hydrofluorocarbon molecule outperforms typical spacer process, in particular, with better etch profile control - the spacer footing can be reduced more than 70%, and with minimal nitride sidewall thinning. The authors also show that due to the ultrahigh etch selectivity, damages to Si substrate was minimized, as evidenced by further surface elements characterization - no formation of Si-C/SiO. Surface smoothing effect was also observed after the etch process with the novel gas molecule. Because of these advantages, the proposed novel hydrofluorocarbon etch gas is a very promising candidate for spacer patterning, to enable further CD and pitch downscaling of the CMOS device.

3:15pm **ALE1-MoA8 Atomic Layer Etching at Low Substrate Temperature***, **Gaëlle Antoun**, T. Tillocher, P. Lefaucheux, R. Dussart,* GREMI Université d'Orléans/CNRS, France*; K. Yamazaki, K. Yatsuda,* Tokyo Electron Limited, Japan*; J. Faguet, K. Maekawa,* TEL Technology Center, America, LLC

Semiconductor industry has followed Moore's law through years. Nowadays, industry and researchers are trying to reach nanoscale dimensions to continue the trend "beyond Moore's Law".

In this framework appeared atomic layer etching (ALE) where self-limited etching is performed, for instance, on SiO_2, using C_4F_8/Ar plasma [1]. In this process, CF_x monolayers are deposited on the surface before etching.

In order to perform ALE cycles without reactor wall contamination by CF_x species, ALE process is proposed at low substrate temperature. In our experimental protocol, fluorocarbon gas such as C_4F_8, is physisorbed at the sample surface in a first step. Then, in a second step, etching is performed by Ar plasma.

The experiments were carried out in an inductively coupled plasma reactor. Tests were performed on three different samples (SiO_2, Si_3N_4, and a-Si) that were glued on a carrier wafer. Then, they were cooled down to very low temperature by liquid nitrogen. In-situ spectroscopic ellipsometry was used to follow the layer thickness evolution of the central sample. The other samples were characterized ex-situ after the experiment. Surface roughness evolution before and after etching was checked by performing atomic force microscopy (AFM).

Finally, Langmuir probe and Quadrupole Mass Spectrometry (QMS) were used to better understand the involved mechanisms.

The aim of the first tests was to prove that etching occurs only at low temperature when using fluorocarbon gas flow. For that, the same etching test was performed at -120°C and few degrees above. At -110°C, etching is very limited, which shows that physisorption is not as significant as at -120°C. However, at –120°C, a few monolayers of C_4F_8 can be physisorbed and etching with Ar plasma has been observed thereafter.

Then, the main goals of this research was to reach self-limited etching regime and get an identical etching rate through cycles. To this end, the influence of various parameters of the process were examined. Different step times and pressures were studied to understand physisorption mechanisms. Temperature effect on species residence time was also evaluated using in-situ ellipsometry and QMS. In order to limit physical sputtering by ion bombardment and reach self-limited etching, different plasma parameters , such as self-bias, ICP power and step time, were studied. The etch per cycle is typically between 0.2 and 0.5 nm depending on the process parameters. The different steps of deposition, purge and etching can be clearly identified by ellipsometry.

Acknowledgments

The authors gratefully thank S.Tahara for his helpful discussions.

1. Metzler et al., J. Vac. Sci. Technol. A 32(2), 020603-1 2014

Atomic Layer Etching
Regency Ballroom A-C - Session ALE2-MoA

ALE of Compound Semiconductors

Moderators: David Boris, U.S. Naval Research Laboratory, Ishii Yohei, Hitachi High Technologies

4:00pm **ALE2-MoA11 Developments of Atomic Layer Etch Processes and their Applications in Fabricating III-V Compound Semiconductor Devices***, **Xu Li**, Y.-C. Fu, S.-J. Cho, D. Hemakumara, K. Floros, D. Moran, I. Thayne,* University of Glasgow, UK **INVITED**

In recent years, atomic layer etch (ALE) to precisely remove very thin layers of materials using sequential self-limiting reactions has attracted extensive attention in semiconductor processing. Our work has indicated that ALE processes have versatile potential in the fabrication of III-V compound semiconductor devices, a number of which will be discussed in this presentation. One example is the use of an ALE process for precise control of the threshold voltage of GaN-based power transistors. This enables both normally off and normally on devices to be realised on the same wafer, which a vital for the realisation of an integrated cascode transistor (Fig 2). Another application example is the realisation of III-As and III-Sb nanowires and finfets for low power logic applications using a lateral ALE process to minimize the wire diameter and fin width. A further example is using a lateral ALE process to selectively etch gate metal stacks to form nanometer scale T-gates required for low noise for RF devices (Fig 3). This has been achieved using Si industry compatible subtractive processes and without the need for complicated resist stacks.

In our ALE processes, Cl_2, HBr, and SF_6 have been used as the reactive gases for surface modification, with the details depending on the etched materials and target applications. The etching chemistries are based on the formation of self-limited Ga, In, Al, and Sb halides in the case of III-V materials or Mo, W and Pt in the case of T-gate metal stacks. The modified surfaces are then removed using an Ar plasma formed with optimized RF and/or ICP power. The impact of all ALE process parameters on etch induced electrical damage has been an important aspect of our work (Fig 4)

To gain insight into the etching mechanisms, in-situ surface analyses have been carried out using Auger spectrometry and XPS techniques. The ALE processes and surface analyses which will be described in this presentation are carried out in a cluster tool from Oxford Instrument Plasma Technology, which includes an ICP etching chamber with repeat loop function and a Scienta Omicron NanoSAM surface analysis tool with Auger spectrometer and XPS (Fig 1). The clustered arrangement enables samples to be subjected to plasma processing and then transferred, under vacuum, into the analysis chamber. This flexibility enables each step of the ALE cycle to be evaluated (Figs 5&6).

4:30pm **ALE2-MoA13 GaN and Ga_2O_3 Thermal Atomic Layer Etching Using Sequential Surface Reactions***, N. Johnson, Y. Lee, **Steven M. George**,* University of Colorado - Boulder

Atomic layer etching (ALE) of GaN and Ga_2O_3 is important for the fabrication of power electronics devices. Thermal ALE of GaN and Ga_2O_3 was performed using sequential, self-limiting surface reactions. The thermal ALE was accomplished using fluorination and ligand-exchange reactions. XeF_2 and HF were used as the fluorination reactants. BCl_3 was the main metal precursor for ligand-exchange. Ga_2O_3 was also etched using $Al(CH_3)_3$, $AlCl(CH_3)_2$, $TiCl_4$ or $Ga(N(CH_3)_2)_3$ as the metal precursors for ligand-exchange.

Crystalline GaN samples prepared using MOCVD techniques were etched with sequential XeF_2 and BCl_3 exposures. GaN etch rates varied from 0.18 to 0.72 Å/cycle at temperatures from 170 to 300°C, respectively (see Supplemental Figure 1). Because the GaN etch rates were self-limiting versus BCl_3 exposure and BCl_3 pressure, the GaN etching mechanism is believed to involve XeF_2 fluorination of GaN to GaF_3 and then ligand-exchange between BCl_3 and GaF_3 to yield volatile BCl_wF_x and GaF_yCl_z species. GaN fluorination using a NF_3 plasma was also successful for etching crystalline GaN at 250°C.

Ga_2O_3 samples deposited using ALD techniques were etched with sequential HF and BCl_3 exposures. Ga_2O_3 etch rates varied from 0.59 to 1.35 Å/cycle at temperatures from 150 to 200°C, respectively. The Ga_2O_3 etch rates were self-limiting versus HF and BCl_3 exposure. Ga_2O_3 ALE was also performed using HF for fluorination and a variety of metal precursors for ligand-exchange. Ga_2O_3 etch rates at 250°C were 0.2, 0.8, 1.1 and 1.2 Å/cycle for $Ga(N(CH_3)_2)_3$, $TiCl_4$, $Al(CH_3)_3$ and $AlCl(CH_3)_2$ as the metal precursors, respectively (see Supplemental Figure 2). The wide range of metal precursors that can etch Ga_2O_3 argues that the ligand-exchange reaction with GaF_3 is facile

4:45pm **ALE2-MoA14 Selective GaN Etching Process using Self-limiting Cyclic Approach for Power Device Applications***, **Frédéric Le Roux**, N. Posseme, P. Burtin, S. Barnola, A. Torres,* Univ. Grenoble Alpes, CEA, LETI, France

Formation of the two-dimensional electron gas (2DEG) in AlGaN/GaN heterostructrures is the key-point for successful development of GaN-based power-electronics such as High Electron Mobility Transistors (HEMT) and diodes. Plasma-etching steps are considered as critical in fabrication for such devices. Indeed standard chlorine plasma[1] can lead to surface roughness degradation[2] and surface state modifications (non-stoichiometric layers, surface potential modifications and dangling bonds)[3–5]. This is why Atomic Layer Etching (ALE) and Digital Etching (DE) are developed to limit the material degradations and to have a better etch depth control[6]. The aim of this study is first to evaluate a self-limited GaN etching process using DE for power devices. This DE consists in two steps. First an O_2 plasma oxidizes the GaN surface. Then, the oxidized layer is removed using BCl_3 plasma selectively to the non-oxidized GaN.

Experiments have been carried out on 200mm wafer using the following stack: GaN (80 or 20nm)/$Al_{0,22}Ga_{0,78}N$ (24nm)/AlN (<1nm)/GaN (1,8µm)/buffer layers/Si substrate.

The development and optimization of the DE process will be presented. The etch mechanism of the self-limited process has first been understood thanks to XPS analyses performed on blanket wafers. It will be demonstrated that the O_2 plasma oxidizes the surface until a saturation level, which enable the self-limitation. Then the BCl_3 plasma removes the oxidized film selectively to the non-oxidized GaN film. This selectivity has been explained by the deposition of B_xCl_y layer on non-oxidized GaN. Small amount of boron oxide by-products is also detected at on the surface after the DE.

Then DE O_2/BCl_3 cyclic process has been compared to standard chlorine based plasma. It will be shown that the roughness and the uniformity are similar for both processes, while the cyclic process present better performances in term of electrical and material degradation. The benefit of the self-limited GaN etching process has finally been validated on patterned wafers for power device integration.

In the second part of this study, the first results of a Cl_2/Ar ALE process for GaN etching will be presented and compared to the DE O_2/BCl_3 cyclic process.

1. Pearton, S. J. *et al.J. Appl. Phys.***86**, 1–78 (1999).

2. Li, X. *et al.J. Semicond.***39**, (2018).

3. Eddy, C. R. *et al.J. Electron. Mater.***28**, 314–318 (1999).

4. Pearton, S. J. *Appl. Surf. Sci.***117**–**118**, 597–604 (1997).

5. Tripathy, S. *et al.J. Vac. Sci. Tech. Part Vac. Surf. Films***19**, 2522–2532 (2001).

6. Kanarik, K. J. *et al.J. Vac. Sci. Tech. Vac. Surf. Films***33**, (2015).

5:00pm **ALE2-MoA15 ALE of GaN (0001) by Sequential Oxidation and H_2/N_2 Plasma***, **Kevin Hatch**, D. Messina, H. Fu, K. Fu, X. Wang, M. Hao, Y. Zhao, R. Nemanich,* Arizona State University

Atomic layer etching of GaN may be used to reduce the high surface defect concentrations produced during inductively coupled plasma (ICP) etching and other processing methods. We have demonstrated a new method for plasma enhanced atomic layer etching (PEALE) of GaN (0001) using sequential surface modification by remote O_2 plasma, followed by removal of the surface oxide through H_2/N_2 plasma etching. The efficacy of etching the surface oxide via H_2/N_2 plasma exposure was confirmed by deposition and removal of several nm of plasma enhanced atomic layer deposited (PEALD) Ga_2O_3 epilayers on GaN. The composition of the H_2/N_2 plasma was investigated, and a H_2:N_2 volumetric flow ratio of 2:1 was found to produce sufficient etch rates at 500°C. An etch per cycle (EPC) of 2 nm was achieved and is attributed to the oxidation rate of GaN. This PEALE process was performed on "as-grown" unintentionally doped GaN (UID-GaN) deposited on a GaN substrate by metalorganic chemical vapor deposition (MOCVD), which also underwent Ar/Cl_2/BCl_3 ICP etching prior to the PEALE process. Application of several PEALE cycles resulted in improved surface stoichiometry, which was attributed to removal of Ga-rich layers created during ICP etching. After the PEALE process the N:Ga ratio increased from 0.5 to 0.8, and the surface roughness improved from R_{RMS} = 0.3 nm to R_{RMS} = 0.2 nm, as measured by AFM. This ALE process has been performed on ICP etched samples prior to regrowth and the I-V characteristics have been measured, showing improved voltage breakdown observed.

Research supported by the ARPA-E PNDIODES program through grant DE-AR0001691.

5:15pm **ALE2-MoA16 Comparative Study of Two Atomic Layer Etching Processes for GaN***, Cédric Mannequin, **C. You**,* University of Tsukuba, Japan*; G. Jacopin, T. Chevolleau, C. Durand,* University Grenoble-Alpes, France*; **C. Vallée**,* LTM-UGA, France*; C. Dussarat, T. Teramoto,* Air Liquide Laboratories, Japan*; H. Mariette,* University Grenoble-Alpes, France*; K. Akimoto, M. Sasaki,* University of Tsukuba, Japan*; E. Gheeraert,* University Grenoble-Alpes, France

Drastic reduction of defect density after etching in nitride semiconductor-based devices becomes a pressing requirement to improve further device performances. Defects introduced by etching process during the formation of the recess gate at AlGaN/GaN or during the fabrication process of GaN displays based on µ-Light Emission Diodes are the main sources issues of devices reliability degradation. Atomic Layer Etching (ALE) processes relying on two times separated half reactions: adsorption step and activation step are of great interests for solving these issues.

In this work, we propose a comparative study of two ALE processes for undoped *c*-oriented Ga-polar GaN, relying both on Cl_2-based plasma for the absorption step but using two different gases for the activation step. The two ALE processes were developed in an Inductively Coupled Plasma etcher (RIE-200iP from SAMCO). In-situ Optical Emission Spectroscopy (OES) was used to monitor gas dissociation for the adsorption, activation and purge steps, allowing identification of active species. Additionally, OES monitoring were used to calibrate Cl_2 dosing time and purging time to ensure complete separation of the Cl_2 dissociation by-products and the gas used for the activation step. The ICP source power (RF_{source}) and pressure for the adsorption step were varied in the 5—120 W range and 0.65—2 Pa range, respectively. For set adsorption step conditions, the self-bias (V_{DC}) of the activation step was varied in the range of 11—40 V by changing the ICP Bias power (RF_{bias}). For each condition, the Etching rate Per Cycle (EPC) was estimated from the etched depth of GaN submitted to 200 ALE cycles using Scanning Electron Microscopy images and reported as a function of V_{DC} (from the activation step).

In the case of the first activation gas, we report an ALE mode with an EPC of 0.276 nm, corresponding to 1.3 monolayer (ML) of the GaN wurtzite structure in the *c*-direction. For this first activation gas, a constant EPC were observed for V_{DC} in the 15—17 V range consistent with ALE process. For higher V_{DC}, the EPC continuously increase with V_{DC}. For the second activation gas, we report an ALE mode presenting an EPC of 0.567 nm corresponding to 2 ML. A constant EPC for V_{DC} in the 16—22 V range were observed. From Atomic Force Microscopy observations of 500 x 500 nm^2, we report significant decrease of the Rms roughness from 0.18 nm for as-deposited GaN surface to 0.07 nm after ALE processing.

Finally, we will discuss and tentatively propose mechanisms to explain the significant differences observed between our two ALE approaches.

5:30pm **ALE2-MoA17 Chlorinated Surface Layer of GaN in Quasi Atomic Layer Etching of Cyclic Processes of Chlorine Adsorption and Ion Irradiation***, **Masaki Hasegawa**, T. Tsutsumi,* Nagoya University, Japan*; A. Tanide,* SCREEN Holdings Co., Ltd.*; H. Kondo, M. Sekine, K. Ishikawa, M. Hori,* Nagoya University, Japan

In fabrication of the next-generation power electronic devices of gallium nitride (GaN), an atomic layer etching (ALE) technique with cyclic processes of ion irradiation and Cl adsorption steps has been attracted for reduction of plasma induced damage. To control the ALE of GaN, we have studied the chlorinated surface layer of GaN at each Ar and Cl reaction step using the beam experiments with *in situ* X-ray photoelectron spectroscopy (XPS).[1,2]

Samples were GaN films grown on sapphire substrate by Hydride Vapor Phase Epitaxy (HVPE) method. Prior to the beam experiments, native oxide on GaN surface was removed by wet cleaning (5% HF) and Ar ion sputter. The as-cleaned surface was exposed by Cl radicals with a dosage of 10^{19} cm^{-2} generated in Cl_2 gas (flow rate 0.5 sccm) plasma by application of RF power of 400 W. Next, Ar ions with a dosage of 10^{16} cm^{-2} and the

accelerating voltage of 100 V or 200 V. The one cycle consisted of these Ar ion irradiation and Cl radical exposure. To stabilize the GaN surface, five cyclic processes were carried out. Then, the GaN surface at each step was analyzed by angle-resolved XPS with take-off-angles of 20, 30, 40, 60, and 90 degrees with respect to the wafer plane. Depth profiles were analyzed by the maximum entropy method.

The Ar ion bombardments change the GaN surface to Ga-rich. Subsequently, as the ion-bombarded Ga-rich surface exposes to the Cl adsorption step, the surface stoichiometry recovers to high N/Ga ratio, resulting to form Ga chlorides as a volatile. The depth profiles obtained from XPS data after the 7th Cl radical exposure were compared with the different Ar ion energies. In the depth profiles of Cl concentration after Cl radical exposure after irradiation with 100-eV-ion (a) and 200-eV-ion (b), the Cl amount and penetration with a depth of approximately 2 nm during the Cl radical exposure were in details observed quantitatively. In the Ar ion bombardments, the formation of non-bonded Ga (dangling bond) and disordered structure was dominated by the ion energies. The resultant etching depth per cycle and the surface stoichiometry were depended on the non-bonded Ga amounts that resulted to desorb Ga chlorides during the Cl radical exposure. This indicates that the surface chlorination layer determined the ALE-properties of real layer-by-layer etching and self-limiting reaction. Not only the ion energy but also the chlorination layer depths should be taken account for the ALE cyclic processes.

[1] T. Takeuchi et al., J. Phys. D: Appl. Phys. 46, 102001 (2013).

[2] Y. Zhang et al., J. Vac. Sci. Technol. A 35, 060606 (2017).

ALD Fundamentals
Evergreen Ballroom & Foyer - Session AF1-MoP
Precursor Synthesis and Process Development Poster Session

AF1-MoP1 Atomic Layer Deposition of Molybdenum Films from Molybdenum Pentachloride Precursor*, **Changwon Lee**, S.-W. Lee, M.-S. Kim,* Versum Materials, Republic of Korea*; S. Ivanov,* Versum Materials, Inc.

The lower resistivity WL (Word Line) material is very attractive to the 3DNAND device makers, because they could reduce the cell stack height while maintaining the device speed. Current POR material of 3DNAND WL is tungsten made by tungsten hexafluoride ALD. However, it is well-known that fluorine results in fatal defects in the device critical layer. Fluorine free tungsten precursors such as tungsten pentachloride has been evaluated recently worldwide not only for 3DNAND application but also other memory and logic devices application. Molybdenum is considered as an attractive WL material for next generation 3DNAND devices. Molybdenum has almost same level of low bulk resistivity comparing to tungsten, but it has smaller EMFP (Electron Mean Free Path), so the effective resistivity, a product of bulk resistivity and EMFP, is expected to be lower compare to tungsten for films less than 10nm. Molybdenum chlorides are considered as potential precursors for deposition of molybdenum films from fluorine free precursors.

Here, we report thermal ALD of molybdenum films on PVD titanium nitride substrates up to 500°C from heated solid high-purity molybdenum pentachloride precursor. Hydrogen was used as a reactant gas under cyclic CVD and ALD conditions. Thickness of molybdenum and titanium nitride films was measured with XRF. Sheet resistance of molybdenum films was measured using 4-point probe technique. The films have been also characterized with TEM and XPS for conformality at aspect ratio 15 trench pattern and impurity depth profile in the film.

We've found that the etching of titanium nitride could be controlled lower than 0.5nm during the molybdenum deposition by variation of molybdenum pentachloride delivery rate. Molybdenum GPC was 0.06 nm per cycle at 500°C wafer temperature. The dependence of step coverage on deposition conditions was investigated and will be discussed. The properties of molybdenum films deposited from molybdenum pentachloride will be compared to properties of tungsten films deposited from similar tungsten pentachloride precursor. Preliminary results suggest that resistivity of the molybdenum films is lower compare to resistivity of tungsten films at 10-15 nm of film thickness. Rapid thermal annealing at 700°C further reduced the sheet resistance of the films.

In this paper, we demonstrated thermal molybdenum ALD with fluorine free molybdenum precursor, which shows low etch of titanium nitride substrate and relatively low resistivity compared to tungsten; which is important for next 3DNAND's WL forming application. Details of the deposition study and properties of the molybdenum films will be presented.

AF1-MoP2 Atomic Layer Deposition of Silver Metal Films: Synthesis and Characterization of Thermally Stable Silver Metal Precursors*, **Harshani J. Arachchilage**, C.H. Winter,* Wayne State University

Silver metal has the lowest resistivity (1.59 μΩ cm) of all metals and has applications in plasmonic devices. Growth by thermal atomic layer deposition (ALD) has been hampered by the low thermal stabilities of virtually all silver precursors. The low precursor thermal stabilities is complicated by the positive electrochemical potential of the silver(I) ion (E° ($Ag^+ + e^- \leftrightarrow Ag$) = 0.7996 V). Herein, we will describe volatile and highly thermally stable silver pyrazolate precursors. The silver pyrazolates $[Ag(3,5\text{-}(CF_3)_2pz)]_3$ and $[Ag(3\text{-}^tBu\text{-}5\text{-}(CF_2CF_2CF_3)pz)]_3$ were synthesized and their volatility thermal stabilities were evaluated by sublimation studies, solid-state thermal decomposition experiments, and thermogravimetric analysis (TGA). $[Ag(3,5\text{-}(CF_3)_2pz)]_3$ was used with 1,1-dimethylhydrazine to deposit silver metal films on SiO_2 substrates at 180 °C with a growth rate of 0.82 Å/cycle. A plot of growth rate versus substrate temperature showed an ALD window of 170 to 220 °C. Saturative self-limited growth was demonstrated in both $[Ag(3,5\text{-}(CF_3)_2pz)]_3$ and 1,1-dimethylhydrazine at 180 °C. The as-deposited films were crystalline. We will also describe the synthesis and characterization of silver pyrazolate complexes containing N-heterocyclic carbene (NHC) ligands. Treatment of $[Ag(3,5\text{-}(CF_3)_2pz)]_3$ and $[Ag(3\text{-}^tBu\text{-}5\text{-}(CF_2CF_2CF_3)pz)]_3$ with three equivalent of the NHC ligands afforded complexes afforded new monomeric complexes of the formula $Ag(R_2pz)(NHC)$. X-ray crystal structures, sublimation data, and the thermal stability of these complexes will also be presented.

AF1-MoP3 Atomic Layer Deposition of Lanthanum Oxide Using Heteroleptic La Precursors*, **Daehyeon Kim**, J. Lee, W. Noh,* Air Liquide Laboratories Korea, South Korea

Rare earth-based oxides are of interest for their potential application in future logic and memory technologies, and lanthanum oxide (La_2O_3) is a well known high-k material for metal gate transistors and a dopant for high-k materials. In past studies, heteroleptic precursors which have alkylcyclopentadienyl and amidinate ligands, $La(RCp)_2$(R'-amd), have been developed to aim to be liquid and to enhance volatility and thermal stability. In this work, three heteroleptic precursors, $La(MeCp)_2$(iPr-amd), $La(EtCp)_2$(iPr-amd), $La(iPrCp)_2$(iPr-amd), were synthesized, and their physical properties were compared. $La(EtCp)_2$(iPr-amd) and $La(iPrCp)_2$(iPr-amd) were liquid at RT, and very thermally stable. ALD evaluation of $La(EtCp)_2$(iPr-amd), which is more promising than $La(iPrCp)_2$(iPr-amd) in terms of the vapor pressure and the viscosity, was performed with O_3 and H_2O as a co-reactant. Both processes had two plateaus in the ALD windows which were at low and high temperature, respectively. The desired ALD window will be the plateau at higher temperature (>350 ℃), because of low C impurity. The plateau at lower temperature might be useful for another processes. Carbon impurity at the low temperature was drastically decreased below detection limit, after post annealing in N_2 atmosphere. In case of ozone process, the cubic phase was observed at 400 ℃ while all films with water process showed amorphous phase even at 400 ℃.

AF1-MoP4 Synthesis and Thermal Characterization of New Molybdenum Precursors for Atomic Layer Deposition of Molybdenum Metal*, **Michael Land**,* Carleton University, Canada*; K. Robertson,* Saint Mary's University, Canada*; S. Barry,* Carleton University, Canada

To keep pace with "Moore's Law" (i.e., the number of transistors in an integrated circuit doubles every 18 months), the size regime of high-performance transistors has now shrunk to ≤ 10 nm. With this decrease of size, traditional metallization materials (e.g., Cu, Al) begin to fail. When microelectronic interconnects – the wiring of integrated circuits – become smaller than 10 nm, the resistivity of the material increases due to electromigration of the metal atoms within the interconnect. Promising metals to replace copper are molybdenum, osmium, iridium, ruthenium, rhodium, and tungsten, because they all have high melting temperature and relatively low bulk resistivities (~4-10 μΩ.cm), leading to lower electromigration.

A method of choice that can be used for the preparation of these small interconnects is atomic layer deposition (ALD). The goal of this project is to develop a chemical precursor compound for the ALD of molybdenum metal. To date, there has only been one reported ALD process for molybdenum metal, however that process utilized harsh co-reagents, and the resulting films had high resistivities. We have chosen the known *bis*(*tert*-butylimido)molybdenum(VI)dichloride as a synthetic starting material, and it has been derivatized with various neutral coordinating ligands, such as ethers, phosphines, amines, and carbenes The ligands were found to have varying effects on the thermal stability of the precursors (up to 300 ºC for the 2,2'-bipyridine adduct), which sometimes came at the cost of poor volatility. However, complexes incorporating less Lewis basic ligands, such as the 1,2-dimethoxyethane adduct, was found to have a large thermal range, with an onset of volatilization of 80 ºC and thermal decomposition at 180 ºC.

These compounds have been characterized in the condensed state, using traditional spectroscopic techniques, and their solid-state structures have been determined using single crystal X-ray diffraction. Their mechanisms of volatilization will also be proposed, based on results from thermal gravimetric analysis (TGA), differential scanning calorimetry (DSC), and the resulting sublimation products. Finally, the thermal stabilities of these compounds have been studied using DSC and thermolysis in flame-sealed NMR tubes, and non-volatile decomposition products were characterized using a scanning electron microscope (SEM) with energy-dispersive X-ray spectroscopy (EDS). From these results, mechanisms of thermal decomposition will also be proposed, including methods to prevent low temperature decomposition pathways and furnish viable vapour deposition precursors.

AF1-MoP6 A Novel Hf Precursor with Linked Cyclopentadienyl-Amido Ligand for Thermal Atomic Layer Deposition of HfO_2 Thin Film*, **Jeong do Oh**, M.-H. Nim, J.-S. An, J.-H. Seok, J.-W. Park,* Hansol Chemical, Republic of Korea

HfO_2 thin film has been widely used as gate oxide layer in the complementary metal oxide semiconductor (CMOS) device as well as dynamic random access memory (DRAM) due to suitable band offset with Si, high thermodynamic stability on Si, and high permittivity [1].

In this study, we investigated a novel Hf precursor, CMENHa, which is coordinated by cyclopentadienyl-amido ligand. The physical characteristics of precursor and film properties of the ALD HfO_2 thin films were analyzed via TGA, viscometer, XPS, XRD and TEM. As compare to widely applied CpTDMAH precursor, CMENHa precursor showed higher thermal stability due to chelate effect of bidentate ligand, lower residue (0.6%) and lower viscosity. In addition, CMENHa was observed wide ALD window range up to 400 with low carbon impurity contents and good electrical properties such as high dielectric constant and low leakage current density. Base on excellent step coverage, purity and thermal stability, the CMENHa precursor has demonstrated potential as dielectric material for use in CMOS device and DRAM capacitor.

Reference [1] J. Robertson et al., *Rep. Prog. Phys.* **69**, 327−396. (2006).

AF1-MoP7 Atomic Layer Deposition of WS_2 using a New Metal-Organic Precursor and H_2S Molecules*, **Deok Hyun Kim**, D.K. Nandi, S.-H. Kim,* Yeungnam University, Republic of Korea

Transition metal dichalcogenides (TDMCs) are exntesively researched in past few years due to their 2D layerd structure similar to graphne . This group of materials offer tunable opto-electronic properties depending on the number of layers and therefore have wide range of applications. Tungten disulfide (WS_2) is one of such TMDCs that has relatively less studied compared to MoS_2. WS_2 has an indirect bandgap of 1.3–1.4 eV in bulk, which have trigonal prismatic coordination around tungsten. The bandgap of WS_2 increases with decreasing thickness and, intriguingly, becomes direct at monolayer thickness with a magnitude of approximately 2.3 eV for the optical bandgap. Such tunability of WS_2 makes it suitable for many semiconductor applications such as field-effect transistors, photodetectors, and photocatalysis, while other promising applications include electrocatalysis and electrochemical energy storage. Atomic layer deposition (ALD) can be adopted very efficiently to control the thickness of WS_2 and hence its properties. Therefore, in this study is WS_2 thin films are grown on several types of substrates by ALD using a new metal-organic precursor [tris(hexyne) tungsten monocarbonyl, $W(CO)(CH_3CH_2C{\equiv}CCH_2CH_3)$ and H_2S at a relatively low temperature of 300°C.The typical self-limiting film growth (growth rate of 0.13 nm/cycle) is clearly observed with both the precursor and reactant pulsing time. The as-grown films are amorphous with considerable S-deficiency but can be crystallized as WS_2 film with (002) preferential orientation by post-annealing in H_2S/Ar atmosphere at 800 °C. Moreover, the post-annealing helps to reduce the C and O content in the film signififcantly as confirmed by the X-ray photoelectron spectroscopy. Further characterizations of the as-deposited and annealed films are perfomed using several other spectroscopic measurements like Raman, Rutherford backscattering, and UV-vis spectroscopy. The current study thus establishes a new and efficient route to obtain WS_2 thin films which could find several potential applications in future.

Acknowledgements

This work was financially supported by the Ministry of Trade, Industry & Energy (MOTIE; #10080651) and Korea Semiconductor Research Consortium (KSRC) support program for the development of the future semiconductor device. The precursor used in this study was provided by UP Chemical Co. Ltd., Korea.

AF1-MoP8 Recent Advances in the Development of Metal Organic Precursors for Atomic Layer Deposition*, **Anjana Devi**, L. Mai, D. Zywitzki, S.M.J. Beer, N. Boysen, D. Zanders, J.-L. Wree, M. Wilken, H. Parala,* Ruhr University Bochum, Germany

Atomic layer deposition (ALD) has gained significant attention from the research community and industry due to the distinct advantages in terms of uniform and conformal coating with precisely tunable stoichiometry and thin film thickness. Since ALD is a chemical vapor phase technique, one of the important parameters governing the process is the precursor employed, which most often is in the form of a metal organic complex. The precursor must be volatile and at the same time it must possess a certain thermal stability to avoid decomposition. Furthermore, due to the surface driven reactions the precursor has to be reactive toward the reactive surface sites and in the second reaction step toward co-reactants to achieve a self-limiting behavior to obtain the desired material. However, the library of precursors for various material systems is not very large and for certain metals there are limited precursors commercially available.

This prompts researchers to develop new precursors or fine tune the characteristics of the already adopted precursors to improve upon the properties relevant for ALD. Over the years, our research group focused on developmental precursor chemistry spanning the periodic system and identified several ligand systems bound to the metal center that are well suited for ALD conditions. Herein, we present an overview of our research work including the synthetic strategies for various ligands, namely guanidinates, amidinates, b-ketoiminates, cyclopentadienyls, diazadienes, N-heterocyclic carbenes and alkylamines. Potential precursor solutions for group III, IV, V and VI transition metals as well as lanthanides are presented employing guanidinates and amidinates among which Y, Hf, Mo, W, Gd and Er were already successfully used in ALD processes. For the fourth period transition metals ranging from Fe to Zn, employing b-ketoimines and diazadienes resulted in promising precursors. Noble metals like Cu and Ag can be deposited using N-heterocyclic carbene complexes. Precursors for main group III metals such as Al, Ga and In, were fine tuned for both, low and high temperature ALD processes employing either alkylamines, amidinates or guanidinates. Furthermore, we identified and developed ligand systems which were combined with Sn, Pb for main group IV metals and Sb for main group V, resulting in potential ALD precursors.

In this presentation, precursor systems covering a range of metals will be presented alongside representative examples for the application in ALD processes. We will also demonstrate that this large library is not only suitable for inorganic oxides, or nitrides but also compatible with organic co-reactants in ALD/MLD processes.

AF1-MoP9 Synthesis of Group VI Oxyhalide Adducts and Mo Metal Film Growth on TiN Surfaces*, **David Ermert**, R. Wright Jr., T. Baum,* Entegris, Inc.

Molybdenum and tungsten metal films are being widely considered for logic and memory (DRAM/NAND) devices, a result of their low-resistivity and high melting points (low electromigration). Challenges to more widespread adoption of group VI film growth using chemical vapor deposition (CVD) and atomic layer deposition (ALD) stem, in part, from the availability of suitable metal-containing precursors. When considering materials for CVD/ALD applications, halide-saturated MX_n species (e.g. $MoCl_5$, WF_6) offer suitable volatility and can deposit high-quality metal films, but may not be compatible with neighboring films within the device. For example, the resulting HCl or HF byproducts may be detrimental to diffusion barrier performance within the device.

Zero-valent metal carbonyls are logical choices for metal deposition as they display suitable vapor pressures and do not require chemical reduction during thermal decomposition on a surface. Barriers to adoption of these precursors include prohibitively high decomposition temperatures, the formation of metal carbides via incorporation of carbon in the films, and the release of toxic carbon monoxide by-products. In general, volatile organometallic precursors that can be deposited at low temperatures offer attractive alternatives for film deposition provided the deposited films are carbon-free.

Here, we describe a general approach to CVD/ALD precursor design and subsequent growth of molybdenum metal films, at moderate surface temperatures, using a molybdenum oxyhalide species and H_2 co-reactant. Group VI oxychloride adducts of the general formula $MO_2Cl_2L_n$ (where M = Mo, W with L = Lewis base adduct and n = 1, 2) are prepared and screened as potential ALD candidates. Precursor characterization and use in thermal deposition studies will be described. Deposited metal film resistivity approaching 50 µΩ-cm were observed at temperatures below 500 °C. Film composition studies, carried out by XRF spectroscopy, demonstrated a strong substrate temperature-dependence on film identity.

AF1-MoP10 Gallium Precursor Development for ALD Film Applications*, **Atsushi Sakurai**, M. Hatase, N. Okada, A. Yamashita,* ADEKA Corporation, Japan

Gallium-based films such as gallium oxide and gallium nitride have been attracting the world's attention of those who are looking at future power electric devices with high power, high breakdown voltage, and energy-saving benefit. Although ALD process could be useful for producing many kinds of metal oxide, nitride, carbide thin films with execellent quality and conformality, many studies have not yet been done regarding gallium precursor screening for ALD applications.

Trimethylgallium (TMG) is the well-known gallium precursor to make various kinds of Ga-based thin films such as gallium nitride and gallium arsenide. However, TMG with remote oxygen plasma ALD process still left over some carbon impurity in the gallium oxide film [1]. Furthermore, it has been pointed out that TMG has undesirable pyrophoric nature when exposed to air.

We are looking for various kinds of gallium precursors which have non-pyrophoric nature, good volatility, enough thermal stability, and high ALD reactivity to produce gallium-based thin film even with gentle ALD process conditions. Fig.1 indicates that our new precursor of GNP-7 has the highest vapor pressure of several kinds of N-based gallium molecules. Thermal ALD process using GNP-7 and H_2O co-reactant produced the amorphous gallium oxide film with good ALD process window at low temperature domain (Fig.2). We are also demonstrating gallium nitride films using GNP-7 and NH_3, whose results will be shown in our presentation then.

[1] Xiao Chen et al., ALD 2018 technical program & abstract book, p128, AA3+AF+EM-WeM6

AF1-MoP11 Design and Optimization of Heteroleptic Zirconium Precursors by Density Function Theory Calculation*, **Romel Hidayat**,* Sejong University, Republic of Korea*; J.-H. Cho, H.-D. Lim, B.-I. Yang, J.J. Park, W.-M. Chae,* DNF Co. Ltd, Republic of Korea*; H.-L. Kim,* Sejong University, Republic of Korea*; S.I. Lee,* DNF Co. Ltd, Republic of Korea*; W.-J. Lee,* Sejong University, Republic of Korea

The stack capacitor of DRAM is continuously developed by decreasing the horizontal dimension, increasing the aspect ratio, and adopting dielectric materials with higher dielectric constants (k). Zirconium oxide (ZrO_2) is a high-k material currently in use in dynamic random access memory (DRAM) devices. The deposition of high-k dielectric materials with excellent conformality and accurate thickness control is required, and the atomic layer deposition (ALD) technology is the best choice. The high-temperature ALD process is desirable for the high dielectric constant and low leakage current density of the deposited film, so the thermal stability of the precursor should be excellent. The reactivity of the precursor is an essential factor to obtain a better conformal film. Also, the precursors must have excellent reactivity for conformal deposition of the film on high-aspect-ratio patterns. A new heteroleptic zirconium precursor for ALD of ZrO_2 has been developed to meet these requirements, and the deposition process and thin film properties using this precursor were presented [1]. The result showed a wide ALD temperature window and excellent step coverage. In the present work, we present the design and optimization of the zirconium precursors by using density functional theory (DFT) calculations. We compared zirconium compounds with different numbers of triamine and dimethylamine ligands to determine the most stable structure. Then, we optimized the alkyl groups in triamine ligand in terms of thermal stability, reactivity, and viscosity. The optimized zirconium compound with a triamine ligand showed better reactivity and stability as compared with the cyclopentadienyl tris-dimethylamine zirconium [$CpZr(N(CH_3)_2)_3$], which is in a good agreement with deposition experiments. DFT calculation is a powerful tool for designing new precursors for ALD process to obtain the desired thermal stability, reactivity, and viscosity.

Figure 1. Lewis base indices and zirconium charge densities of triamine-type zirconium compounds with different combinations of alkyl groups.

[1] H.-D. Lim *et al*., ALD 2018, AF2-TuA13.

AF1-MoP12 Low Temperature Plasma-Enhanced Atomic Layer Deposition of ZnO from a New Non-Pyrophoric Zn Precursor*, **Lukas Mai**, F. Mitschker, P. Awakowicz, A. Devi,* Ruhr University Bochum, Germany

With its high transparency to visible light and tunable conductivity, zinc oxide (ZnO) is a transparent conductive oxide (TCO) and promising candidate for microelectronic applications such as thin film transistors (TFTs), solar cells or chemical sensors. Furthermore, with a direct band gap of E_g= 3.37 eV it can not only be used for electrical but optical applications e.g. in UV-light emitting diodes (LEDs), too. Owing to its high density, ZnO layers can be employed as protective coating as well and could serve as conductive and protective gas barrier layer (GBL) at the same time on polymers in flexible electronics. For high quality GBLs, the thin films should be very uniform, dense and conformal over the whole surface. With atomic layer deposition (ALD), it is possible to fabricate such thin films at low temperatures with a precise thickness control. For the ALD of ZnO, diethylzinc ([$ZnEt_2$], DEZ) is the most commonly used precursor. Despite the inherent advantages of DEZ in terms of high volatility and reactivity toward a range of co-reactants at low temperatures, there are certain issues with DEZ such as its pyrophoric behavior and not well-defined ALD window. Thus, we attempted the synthesis of an alternative Zn precursor.

Here, we present the synthesis and detailed characterization of bis-3-(dimethylamino)propyl zinc, [$Zn(DMP)_2$] as an alternative precursor for ALD of ZnO. As already demonstrated for aluminum precursors,[1] the DMP ligand stabilizes the zinc center atom by a dative bond from the amine to the metal. This yields a favored 18 electron complex, causing a thermally stable, non-pyrophoric solid compound with a melting point at only 46 °C. The thermal properties are thoroughly characterized showing a high evaporation rate at only 55 °C. Using this precursor, a new plasma enhanced (PE)ALD process employing O_2 plasma was developed. The process is self-limiting at substrate temperatures between 60 °C and 140 °C on Si(100) with growth rates of 0.44 Å $cycle^{-1}$at 60 °C and 0.72 Å $cycle^{-1}$at 140 °C. The resulting ZnO thin films are conformal, uniform, smooth, dense and of high purity even at low deposition temperatures and were analyzed regarding their optical and electrical properties. For the investigation of the ZnO films as GBL, thin films of various thicknesses were deposited on PET substrates at 60 °C and the improvement of the gas barrier of the PET by a factor of 60 for a 10 nm thin film obtained by oxygen transmission rate (OTR) measurements. The thin film properties are of the same quality as for layers obtained from DEZ, rendering the new intramolecular stabilized precursor to be a promising and safe alternative for ALD of ZnO coatings.

AF1-MoP13 Homoleptic and Heteroleptic Yttrium Precursor: Tuning of Volatility, Reactivity and Stability for ALD Applications*, **Sebastian Markus Josef Beer**, A. Devi,* Ruhr University Bochum, Germany

Rare-earth (RE)-based materials in the form of thin films have gained significant attention due to their unique functional properties rendering them suitable for a broad variety of applications. Especially yttrium oxide (Y_2O_3) has been intensively studied for optics, protective coatings or high-k dielectrics. Furthermore, the ability to dope Y into other oxide material systems opens up new avenues for the development of high–performance materials as for instance yttrium doped zinc oxide (Y:ZnO), yttria stabilized zirconia (YSZ) or yttrium doped $SrSnO_3$.[1-3]

Atomic layer deposition (ALD) serves as a superior thin film processing technique enabling precise layer thickness control paired with conformal growth and uniformity fulfilling the main requirements for the fabrication of high-quality thin films. However, ALD processes strongly depend on the performance of the applied precursors. Therefore, the rational design and development of metalorganic compounds comprising optimal physico-chemical characteristics remains a key factor for ALD-based research. Over the years, various Y metalorganic precursors have been developed for ALD processes mainly focusing on homoleptic complexes such as β-diketonates [$Y(thd)_3$], silylamides [$Y(tmsa)_3$], amidinates [$Y(dpamd)_3$], guanidinates [$Y(dpdmg)_3$] or cyclopentadienyls [$Y(Cp)_3$]. Some of these compounds have high melting points, low volatility, reactivity or thermal stability which, in most cases, can be tuned through side-chain variations of the ligand moieties.

Another promising approach is to employ mixed ligand systems to form heteroleptic substituted compounds, ideally combining the characteristics of the respective homoleptic analogues. In earlier reports, RE precursor systems with combination of ligands were demonstrated by Leskelä *et al*[4] and Lansalot-Matras *et al*[5] where liquid precursors were successfully employed for RE oxide thin films. These approaches encouraged us to design and develop new metalorganic Y complexes with advantageous physico-chemical properties such as a high volatility, reactivity and stability thus ensuring applicability in ALD processes.

In our study, we focused on the guanidinate and amidinate ligand classes which provide pronounced reactivity toward co-reactants such as water through their Y-N bonds in combination with the cyclopentadienyl ligand, possessing good thermal stability due to the formation of robust leaving groups. Herein, we present a rational development and detailed characterization of new, spectroscopically pure heteroleptic and monomeric yttrium cyclopentadienyl guanidinate and yttrium cyclopentadienyl amidinate precursors for ALD processes of Y-based thin film materials.

AF1-MoP14 Gallium ALD Precursor Development based on Mechanistic Study*, M. Foody, Y. Zhao, **Adam Hock**,* Illinois Institute of Technology

Low temperature deposition of Ga_2O_3 remains a challenge, particularly in the absence of energetic oxygen sources (e.g. plasma or ozone). This is somewhat surprising given the close chemical relationship of aluminum to gallium. For example, trimethylaluminum is an incredibly well-behaved ALD precursor combined with a variety of oxygen sources, trimethylgallium requires the energetic reagent ozone as an ALD partner. We have synthesized a variety of gallium precursors that span the potential chemical space for gallium, e.g. 4, 5, and 6-coordinate complexes, alkyl, amide, and

other ligands, etc. and conducted in depth mechanistic analyses of the potential ALD chemistry.

In this talk we discuss the effect of ligand coordination number, identity (N vs C, etc), and ALD partner reagent on nucleation and growth of gallium oxides. This includes QCM measurements under ALD conditions, solution model reactions, and synchrotron studies conducted at the Advanced Photon Source (APS) located at Argonne National Laboratory. The surface reaction of Ga precursors and half-reaction with oxygen sources were also observed by X-ray absorption spectroscopy (XAS). We have found that nucleation of GaOx growth can be achieved on a variety of substrates, however sustained growth of Ga_2O_3 requires forcing conditions for some precursors. The results of these studies were applied to improved gallium oxide processes, including doping strategies. Film characterization will also be discussed as time allows.

AF1-MoP15 Fluorine Doping of Aluminium Oxide Through In-situ Precursor Synthesis: Theory, Design and Application.*, **Ben Peek**,* University of Liverpool, UK

Fluorine doped metal oxides are technologically important as conducting thin films, for applications in photovoltaics, flat panel displays, mem resistive devices and power semiconductors. Conventional precursor sources for F-doping involve the use of harmful or toxic reagents such as hydrofluoric acid. Use of these precursors presents challenges in terms of handling and disposal.

Here we report a novel method to synthesise a fluorine precursor, $FAl(CH_3)_2$ in-situ, using mechanisms like those found in atomic layer etching. The method involves a pre-reaction between $Al(CH_3)_3$ and AlF_3 powder to generate the $FAl(CH_3)_2$ immediately before it is injected into the ALD reactor chamber. The intermediate fluorine product has been isolated and analysed using ^{19}F NMR. The effects of key process parameters, including the $Al(CH_3)_3$ dosing and AlF_3 powder bed temperature have been assessed and optimised. The design and fabrication of a system to generate the precursor is presented.

We demonstrate how the precursor has been exploited for the fluorine-doping of aluminium oxide grown by atomic layer deposition. The F-doped Al_2O_3 films have been characterised using low energy ion scattering as a probe of the surface and through-thickness distribution of fluorine in the doped films. This approach is used to elucidate the incorporation mechanisms and the composition of deposited materials.

This in-situ precursor generation technique, potentially opens new routes to doping of a wider range of ALD thin film materials. The full potential of the approach is discussed and other doped systems are considered.

ALD Fundamentals
Evergreen Ballroom & Foyer - Session AF2-MoP
Precursor Selection and Growth Optimization Poster Session

AF2-MoP1 Atomic Layer Deposition of Cyclopentadienyl Based Hf Precursor With Various Oxidants*, **Jooho Lee**, D. Kim, W. Noh,* Air Liquide Laboratories Korea, South Korea

In electronic devices, a hafnium based oxide film has drawn a lot of attention, because it is a potential High-k material that can replace SiO_2 in a conventional transistor. Recently, hafnium based oxide films can be used for other applications, such as next generation DRAM capacitors and NAND flash memories. HfCl4 was one of the best precursor candidates for a HfO_2 film, however, there are some issues related to corrosive halide ligands, low vapor pressure, difficulty in delivering a solid precursor. In order to solve those issues, $Hf(RCp)(NMe_2)_3$ (R = H, Me), which are chlorine free precursors, were proposed. In this work, these precursors were evaluated for physical properties and ALD processes. Both precursors showed high thermal stability and clean evaporation in TG. $Hf(Cp)(NMe_2)_3$ and $Hf(MeCp)(NMe_2)_3$ have high vapor pressure (1 Torr at 90□) and low viscosity (9 cP at 30□). According to ALD evaluation, both precursors obtained high ALD windows up to 360 - 370□ with a growth rate of 0.9 - 1.0 Å/ cycle with ozone and a growth rate of around 0.5 Å/ cycle with water. X-ray photoelectron spectroscopy (XPS) showed that deposited thin films were pure, carbon and nitrogen impurities were below the detection limit. Step coverage of the film was excellent (~100%, AR= 1:40) at 360□.

AF2-MoP2 Atomic Layer Deposition of Magnesium Oxide Thin Films by using Bis(ethylcyclopentadienyl)Magnesium Precursor and H_2O, O_2 Plasma and O_3 Reactants*, **Moo-Sung Kim**, S.-W. Lee,* Versum Materials Korea, Republic of Korea*; S. Ivanov,* Versum Materials, Inc.

Since MgO has high temperature stability, wide band gap, insulating, and diffusion barrier properties, it has been studied to use as a cathode coating layer in Li-ion battery, buffer layer for superconductors, high-k gate dielectric and ferroelectric non-volatile memory, a dopant for High K capacitors, etc.

In this work, deposition of magnesium oxide (MgO) thin films was conducted with liquid precursor Bis(ethylcyclopentadienyl) magnesium ($Mg(EtCp)_2$) and various reactants such as H_2O, O_2 plasma and O_3 by using atomic layer deposition (ALD) method. The MgO films were analyzed by ellipsometry, transmission electron microscopy (TEM), X-ray photoelectron spectroscopy (XPS), X-ray diffraction (XRD) and X-ray reflectivity (XRR) to compare step coverage, chemical composition, crystallite orientation as well as film density of the films deposited with three different reactans.

ALD characteristic saturation behavior was observed for H_2O and O_2 plasma processes between 200 and 300°C with Mg saturation pulse time 1 sec and 1.5 sec, respectively. GPC of MgO at 250°C was 1 A/cy with H_2O and O_2 plasma processes. In the case of O_3 process, however, ALD characteristic saturation behavior was only observed above 250°C. MgO deposition rate was constant between 200°C and 300°C for O_2 plasma process only. MgO deposition rate was decreased with temperature in the case H_2O process, and was increased with the temperature in the case of O_3 process.

MgO films deposited with water thermal ALD and O_2 PEALD exhibited good stoichiometric composition about Mg:O = 1 : 1 with low carbon content and excellent step coverages at the deposition temperatures between 200 and 300°C. MgO film density with XRR was ~3.6g/cc at most deposition conditions. However, in O_3 process at 200°C, a large amount of carbon (~ 13%) was detected, which also led to poor step coverage (~ 68%). XRR density was less than 2.5g/cc, lower than other deposition conditions. In addition, it showed no MgO XRD peak suggesting deposition of amorphous film. On the contrary, O_3 process at 300°C showed sharp and strong MgO XRD peak with (200) dominant orientation, and film density was ~3.5g/cc, similar to H_2O and O_2 plasma processed MgO films.

In summary, we have demonstrated MgO ALD with $Mg(EtCp)_2$ and 3 types of reactants, H_2O, O_2 plasma, and O_3. Most conditions showed stoichiometric film composition, and good step coverage. Only O_2 plasma process showed constant ALD rate between 200 and 300°C. O_3 process below 250°C showed high carbon and oxygen content in the film, lower film density and poor step coverage. However, at 300°C, similar films were deposited with all three reactants.

AF2-MoP3 Comparative Study between $CpTi(OMe)_3$ and $CpTi(NMe_2)_3$ for Atomic Layer Deposition of Titanium Oxide*, **Jaemin Kim**, S. Kim, R. Hidayat, Y. Choi, H.-L. Kim, W.-J. Lee,* Sejong University, Republic of Korea

Titanium oxide (TiO_2) and titanium-based perovskites have been attracting attention as capacitor dielectric materials for the next-generation DRAM. Atomic layer deposition (ALD) is used as a deposition method because it can prepare conformal films over high-aspect-ratio capacitor structures. Titanium precursors capable of high-temperature ALD process were studied to produce high-quality TiO_2 films with excellent step coverage. The most common ALD precursors, tetrakis(dimethylamino)titanium and titanium tetraisopropoxide, showed low ALD temperatures due to their insufficient thermal stability. Heteroleptic titanium precursors having a cyclopentadienyl (Cp) ligand that binds strongly to titanium have been reported to increase the ALD process temperature [1]. There are two types of the titanium precursors with a Cp ligand: alkylamines having dimethylamino (NMe_2) ligands and alkoxides having methoxy (OMe) ligands. However, no direct comparison between two types of precursors and ALD processes using them has been reported. In the present study, an alkylamine-type heteroleptic precursor, tris(dimethylamino) cyclopentadienyl titanium [$CpTi(NMe_2)_3$], and an alkoxide-type heteroleptic precursor, trimethoxy cyclopentadienyl titanium [$CpTi(OMe)_3$], were comparatively studied. Ozone was used as an oxidizing agent for ALD TiO_2. The saturation doses of both precursors were measured at different temperatures to determine the ALD temperature window. The results showed that $CpTi(OMe)_3$ has better reactivity and thermal stability compared to $CpTi(NMe_2)_3$., which is explained by density functional theory calculations. Both precursors showed excellent step coverage and relatively wide bandgap at the temperature at which the thin film grows only by the ALD reaction. However, the poor step coverage and narrow bandgap were

observed at temperatures at which the CVD reaction occurred due to the thermal decomposition of the precursor. Therefore, a titanium precursor capable of a high-temperature ALD process is essential, and the alkoxide-type titanium precursor is superior to the amine-type titanium precursor.

[1] R. Katamreddy, et al., in: ECS Trans., ECS, 2009: pp. 217–230. doi:10.1149/1.3205057.

AF2-MoP4 Tin Nitride Atomic Layer Deposition using Hydrazine*, **Ann Greenaway**, A. Tamboli, S. Christensen,* National Renewable Energy Laboratory

There is substantial lag in the development of atomic layer deposition (ALD) processes for nitridescompared to the high-quality, conformal oxides for which ALD has become the standard. A major factor in this disparity is the ready availability of highly reactive oxygen sources (mainly H_2O, O_2, and H_2O_2). High-energy nitrogen precursors are similarly required for the efficient incorporation of nitrogen in a film. Ammonia has often been used in conjunction with metal chlorides but requires relatively high temperatures for thermal ALD. Plasma-enhanced ALD can utilize molecular nitrogen as a precursor but can reduce film conformality on complex supports and damage the underlying substrate.

Hydrazine (N_2H_4) is an alternative precursor which has been rarely explored for the fabrication of nitrides in ALD, but which is experiencing a surge in popularity due to its high reactivity, which enables the deposition of nitrides as-yet undemonstrated by ALD.[1] The added reactivity and volatility of liquid hydrazine may enable new reaction mechanisms, lower deposition temperatures, and conformality for high aspect ratio applications.

Sn_3N_4 is a metastable semiconductor which shares a crystal structure with its analog, Si_3N_4; unlike Si_3N_4, Sn_3N_4 has only recently been grown by ALD,[2] being synthesized much more often through reactive sputtering.[3] As a binary, Sn_3N_4 has applications as a battery anode material, for photoelectrochemistry, and optoelectronic devices. We will report progress on the deposition of Sn_xN_y films from tetrakis(dimethylamido) tin (TDMASn) and N_2H_4. Growth per cycle of this material (determined by x-ray reflectivity) is 0.4 Å at 200 °C, similar to the sole report of Sn_3N_4 from PE-ALD,[5] despite films being substantially Sn-rich. Identification of ALD growth window and self-limiting deposition characteristics are underway; initial testing indicates a competing chemical vapor deposition process which can be eliminated with adequate tuning of pulse/purge characteristics. A comparison of film conductivity and optical absorption at different growth temperatures will be presented. General issues of N_2H_4 purity and routes to prevent or control oxynitride formation will be discussed.

(1) Du, L., *et al*. The First Atomic Layer Deposition Process for Fe_xN Films. *Chem. Comm.*, **2019**,*ASAP.* DOI: 10.1039/C8CC10175B [https://doi.org/10.1039/C8CC10175B].

(2) Stewart, D. M., *et al*. Tin Oxynitride Anodes by Atomic Layer Deposition for Solid-State Batteries. *Chem. Mater.* **2018**, *30*, 2526–34.

(3) Caskey, C. M., *et al*. Semiconducting Properties of Spinel Tin Nitride and Other IV3N4 Polymorphs. *J. Mater. Chem. C* **2015**, *3*, 1389–96.

~~**AF2-MoP5 Growing Polycrystalline Indium Oxide Film by Atomic Layer Deposition***, **Chien-Wei Chen**,* ITRC, NARL, Republic of China~~

~~In light-emitting diode (LED) and thin film transistors (TFT) displays industry, In_2O_3 could be a high quality transparent conducting oxide (TCO) layer for enhancing the optical and electrical properties. Therefore, thickness control and uniformity of the film is important in the preparation of ultra-thin In_2O_3 film. In this study, the uniform polycrystalline In_2O_3 films were successfully grown on the 4" silicon(100) substrate at 300℃. Trimethylindium (TMI) and water were chosen as the metal and non-metal precursors, respectively. The In_2O_3 growing temperature is between 100℃ to 300℃ and the growth rate per cycle (GPC) increases and the surface roughness reduces with the temperature increasing. The GPC of In_2O_3 film grown at 300°C is 0.5Å and the refractive index n is found to be 1.98 at the wavelength of 632 nm which is close to the bulk. The linear growth rate of In_2O_3 and saturation behavior of TMI with different pulse time is shown in Fig.1 and Fig.2, respectively. Fig.3 (a) shows the TEM cross sectional image of In_2O_3 grown at 300°C. The lattice stacking shown in Fig.3 (b) presents the formation of poly crystalline In_2O_3 film.~~

~~**AF2-MoP6 Low Temperature Tin Oxide by Atomic Layer Deposition***, **Yu-Chiao Lin**, B. H. Liu, Y. S. Yu, C. C. Kei, C. L. Lin,* National Applied Research Laboratories, Republic of China~~

~~Tin oxide (SnO_2) has attracted lots of attention because of its excellent chemical, electrical, and optical properties. SnO_2 films were deposited on Si(100) substrates by home-build atomic layer deposition (ALD) using tetrakis dimethylamino tin (TDMASn) as metal precursor and H_2O as oxidant at low substrates temperature. Low temperature SnO_2 ALD process is especially important due to low thermal budget consideration for thermally sensitive materials such as organic light emitting diodes and photovoltaic cells. Thickness and refraction index of SnO_2 films were determined by ellipsometry. The surface morphology and cross-sectional image were observed by scanning electron microscopy (SEM) and transmission electron microscopy (TEM), respectively. As shown in Fig. 1, the growth rate of SnO_2 thin film at 150 ℃ was saturated about at 1.65 Å/cycle when TDMASn pulse time is larger than 0.7 s. The growth rate of SnO_2 thin film increased to about 2.55 Å/cycle as the substrate temperature was decreased to 50 ℃. Top-view SEM image in Fig. 2 shows uniform SnO_2 thin films were deposited on Si wafer. Cross section HRTEM image in Fig. 3 shows that the dense and continuous SnO_2 thin films of 32.4 nm at very low substrate temperature (50 ℃).~~

AF2-MoP7 Dielectric ALD with Hydrogen Peroxide: Comparitive Study of Growth and Film Characteristics for Anhydrous H_2O_2, H_2O_2/H_2O Mixtures and H_2O*, **Daniel Alvarez**,* RASIRC*; K. Andachi, G. Tsuchibuchi, K. Suzuki,* Taiyo Nippon Sanso Corporation*; J. Spiegelman,* RASIRC

ALD of dielectrics requires new precursor chemistries. Development efforts have focused on new Organometallic, Organosilicon and Organoaluminum precursors. Our research focus has been on oxidants, and specifically hydrogen peroxide reactivity. Due to this reactivity, hydrogen peroxide use may allow lower deposition temperatures and achieve distinct properties in the resulting film when compared to other oxidants. Our research study uses:

- Gas-phase hydrogen peroxide, delivered from an anhydrous, ampoule-based formulation by use of a membrane delivery system.
- High concentration H_2O_2/H_2O delivery by *in situ* concentration methods and use of a membrane vaporizer as a gas generator.

Initial results for ALD growth of ZrO_2 from anhydrous H_2O_2 and $CpZr(N(CH_3)_3)$ exhibit high quality growth of film at 260° C. Minimal saturation delay and a linear growth curve were observed. XPS and XRR were used to characterize ZrO_2 composition, showing significant similarities to films grown using ozone. Subsequently, films grown using ALD and H_2O_2 were placed into MIMCAP structures, which had high k values measured at 35. This was a slight improvement over films grown with 20% ozone concentration which had high k values of 32.

Novel Gas Generator

Our approach involved development of a novel gas generator that delivers H_2O_2/H_2O mixtures. A carrier gas is connected to this generator, which delivers up to 5% H_2O_2/21% H_2O gas by volume from 30wt% H_2O_2 liquid solution (H_2O/H_2O_2=4.2). This gas mixture enables SiO_2 films to be grown at highly reduced temperature compared to water. Testing was done with tris(dimethylaminosilane) $(N(CH_3)_2)_3SiH$ and H_2O_2/H_2O. SiO_2 was deposited at temperatures at least 200° C lower with the hydrogen peroxide mixture than with water.

For Al_2O_3 ALD, initial results show that anhydrous H_2O_2 generates higher density films with better initial nucleation as measured by *in situ* XPS. The presentation will compare Al_2O_3 film characterization for anhydrous H_2O_2, H_2O_2/H_2O mixtures and water. Data will be reported on wet etch rates, refractive index and capacitance.

AF2-MoP8 Atomic Layer Deposition of Carbon Doped Silicon Oxide and Effect of Thermal Treatment or Hydrogen Plasma Treatment on The Films*, **Meiliang Wang**, H. Chandra, X. Lei, A. Mallikarjunan, K. Cuthill, M. Xiao, M. Rao,* Versum Materials, Inc.

Atomic Layer Deposition (ALD) of silicon oxide is commonly used in the semiconductor industry for its excellent thickness control and conformality. For some applications, films deposited at low temperatures with low wet etch rate or low dielectric constant (k) are required. Carbon doping is a known method to reduce the wet etch rate as well as the k value of the silicon oxide film. In this paper, ALD SiO_xC_y films were studied. The impact of oxidant concentration and deposition temperature on the carbon content, WER, k value and other properties of the deposited film, with and without post deposition annealing and post deposition hydrogen plasma treatment is discussed.

In ALD conference 2017[1], the impact of the precursor design for the number of $Si-CH_3$, Si-N and Si-H bonds on the reactivity, carbon content, and dHF WER of the deposited films were reported. It was demonstrated that precursors with only one $Si-CH_3$ bond substitution, eg. di-iso-propylaminomethylsilane (DIPAMS), could deposit silicon oxide film with a relatively high GPC and carbon doping up to 10 at. %. In this report, a new

organosilane precursor "Precursor V" is designed and it provides higher reactivity and higher carbon content and lower WER than DIPAMS, films with up to ~20 at. % C are obtained. With thermal annealing at 600 ℃, film k value reduced from ~6 to < 4, almost no etch after 10min in 0.5% dHF dip, while film carbon content showed no change, and film shrinkage was < 2%. FTIR spectra show decreased Si-OH peak, and increased Si-O-Si network peak, indicating that Si-OH to Si-OH crosslinked to form Si-O-Si linkage at 600 ℃. In contrast, by annealing at 800 ℃, the film carbon content is reduced significantly, from 17 at. % to 6 at. %, and the film density is increased from 1.5 g/cm^3 to 2.0 g/cm^3. A high shrinkage of ~25% was also observed from the 800 °C anneal, indicating a significant densification of the film with carbon removal. Direct hydrogen plasma treatment on the film was also studied. The film k value reduced from around 6 to < 4. The film develops a dense surface layer with higher WER, between 10-40 ℃. However, WER of the bulk film remains unchanged compared to as-deposited film. Corresponding to this observation, the film surface carbon is reduced, but the bulk film carbon content is kept constant. FTIR shows Si-OH decrease, Si-O-Si increase, and Si-H increase, indicating crosslinking of Si-OH bonds to form Si-O-Si network and generation of Si-H bonds during H_2 plasma treatment. The hydrogen plasma treatment forms a densified SiO_2 layer with removal of carbon near surface region and protecting the bulk film from carbon depletion.

[1] M. Wang, *et al.* ALD 2017

AF2-MoP9 DFT Study on Atomic Layer Deposition of Al_2O_3 with Various Oxidants*, **Seunggi Seo**, T. Nam,* Yonsei University, Republic of Korea*; H.B.R. Lee,* Incheon National University, Republic of Korea*; B. Shong,* Hongik University, Republic of Korea*; H. Kim,* Yonsei University, Republic of Korea

Atomic layer deposition (ALD) is a vapor phase thin film deposition technique, which enables deposition of thin films with high material quality, good uniformity, high conformality, and sub-nanometer thickness controllability. Therefore, ALD has been regarded as one of the most suitable deposition technologies for semiconductor device fabrication. Since ALD is based on sequential self-limited reactions on surfaces, understanding the surface chemical reaction mechanism is crucial for development of ALD process.

ALD of Al_2O_3 has been widely investigated owing to its wide ALD temperature window, high vapor pressure of Al precursors such as trimethylaluminum (TMA), and wide applicability of Al_2O_3. It is known that the reaction between surface adsorbed precursors and reactants, and the resulting material properties of deposited Al_2O_3, are affected by the type of the oxidant. However, relatively small research effort has been focused on the chemical reaction mechanisms of each oxidants during ALD.

In this study, we investigate the reaction mechanism of various oxidants such as H_2O, H_2O_2 and O_3 during ALD of Al_2O_3 with TMA. Density functional theory (DFT) calculations at B97D3/6-311+G* level of theory were performed using Gaussian 09 suite of programs. Our results show that the methyl groups adsorbed on the surface can be oxidized into hydroxyls with all considered oxidants with ease. The number of oxidant molecules required for the reaction is one for H_2O, and two for O_3 or H_2O_2. According to the activation energy of the considered reactions, it is suggested that O_3 is the most reactive oxidant for Al_2O_3 ALD with TMA.

AF2-MoP10 Effect of Heteroleptic Structure on Atomic Layer Deposited HfO_2 Using $Hf(N(CH_3)_2)_4$ and $CpHf(N(CH_3)_2)_3$ Precursors*, **Sungmin Park**, B.-E. Park, S. Lee, H. Yoon,* Yonsei University, Republic of Korea*; M.Y. Lee, S.-H. Kim,* Yeungnam University, Republic of Korea*; H. Kim,* Yonsei University, Republic of Korea

With scaling down of complementary metal-oxide semiconductor (CMOS), atomic layer deposition of HfO_2 is a key technology for ultra-thin and high-*k*gate dielectrics. To obtain high-quality HfO_2 and good devices performances, various Hf precursors, such as Hf halides, alkylamides, and alkoxides, have been employed. However, these precursors have clear limitations such as low reactivity of halides and alkoxides and poor thermal stability of alkylamids. Recently, heteroleptic precursors have been investigated as alternatives to the existing homoleptic precursors. Among them, partial substitution with a cyclopentadiene (Cp)-based ligand has been reported to control volatility and thermal stability of the precursor. Despite of the promising usages, there is still lack of systematic studies on the film properties associated with growth characteristics of ALD HfO_2 using Cp-containing precursors.This could be due to the complexity of the Cp-containing precursors, which makes difficult to conduct theoretical studies to support the growth mechanism.

In this study, we investigated the effects of substituting Cp ligands for high-*k*properties of ALD HfO_2 by using $Hf(N(CH_3)_2)_4$ and $CpHf(N(CH_3)_2)_3$. The Cp ligand improved the thermal stability of precursor to withstand thermal decomposition up to 350 °C, but decreased the saturated GPC in the ALD window. The growth characteristics were discussed with the theoretical calculations utilizing geometrical information on the precursor and density functional theory. In addition, we analyzed the chemical composition such as C impurities and oxygen vacancies through XPS and the microstructure such as crystallinity, density, and interlayer through XRD, XRR and TEM. These results were comparatively studied in relation to the electrical properties of ALD HfO_2. This study can provide researchers with a broad insight to select proper precursor for the fabrication of high quality dielectric layer in future nanoscale devices.

AF2-MoP11 Effect of Co-Reactant on the Atomic Layer Deposition of Copper Oxide*, **Jason Avila**, N. Nepal, V. Wheeler,* U.S. Naval Research Laboratory

Atomic layer deposition (ALD) of copper oxide presents a powerful opportunity to grow p-type semiconductor material for a wide variety of applications such as transparent conducting oxide, solar fuels catalysis, and power devices. There are, however, very few ALD processes to facilitate the growth of copper oxide. Cu(II) bis(dmiethylamino-2-propoxide) (Cudmap) has previously been used to grow copper metal using a reducing source such as tertiary butyl hydrazine.[1,2] Cudmap has also been demonstrated to grow Cu_2O using water as a co-reactant, self-reducing from Cu(II) to Cu(I) in the presence of water.[3] This study will examine the effect of ALD co-reactants, ozone and water, on the copper oxidation state of copper oxide films grown using Cudmap.

Copper oxide films were grown in a Veeco Savannah ALD reactor using Cudmap and ozone or water at 150 °C on Si and c-plane sapphire. This is the first experimental demonstration of CuO films using Cudmap and ozone. Using ozone, a growth rate of 0.18 Å/cycle was achieved at 150 °C, far higher than the measured growth rate of 0.04 Å/cycle when growing with water. Additionally, XPS was able to confirm only the Cu(II) oxidation state with a Cu/O ratio of 1 verifying CuO films. For comparison, films grown with water show the presence of only Cu(I) oxidation state and have a nearly stoichiometric with a Cu/O ratio of 2:1. AFM also indicated uniform film growth as low as 2 nm independent of co-reactant, with CuO films grown with ozone being rougher than Cu_xO films grown with water. Initial optical and electrical properties of the films will be examined for p-type semiconductor applications.

References

(1) Väyrynen, K.; Mizohata, K.; Räisänen, J.; Peeters, D.; Devi, A.; Ritala, M.; Leskelä, M. , , 6502.

(2) Kalutarage, L. C.; Clendenning, S. B.; Winter, C. H. , , 3731.

(3) Avila, J. R.; Peters, A. W.; Li, Z.; Ortuno, M. A.; Martinson, a. B. F.; Cramer, C. J.; Hupp, J. T.; Farha, O. , , 5790.

AF2-MoP12 A Systematic Study on Atomic Layer Deposition of ZrO_2 Thin Films*, X. Wang, J. Cai, **Xiangbo Meng**,* University of Arkansas

Zirconium oxide (ZrO_2) is an attractive material with many applications because of its excellent mechanical, thermal, optical, and electrical characteristics [1-3]. ZrO_2 can present three crystalline structures, i.e., monoclinic (below 1170 °C), tetragonal (1170-2370 °C), and cubic (above 2370 °C) [1]. To synthesize ZrO_2 nanomaterials, there have to date many methods developed. ALD is a unique thin-film technique, featuring its tremendous capabilities for depositing conformal and uniform thin films with the atomic preciseness [4, 5]. Using Tetrakis(dimethylamido)zirconium and water as precursors, previous studies [6, 7] have deposited ZrO_2 on carbon substrates in the range of 100 – 250 °C. However, these studies have not fully investigated the growth mechanism and film characteristics of the ALD ZrO_2. Applying *in situ* quartz crystal microbalance (QCM), in this study we optimized growth parameters and then further studied the growth characteristics in the range of 50 – 275 °C. We found that the growth rate of the ALD ZrO_2 decreases with increasing temperature in the range of 50 – 225 °C, but the growth of the ALD ZrO_2 at 250 and 275 °C terminated after the first several ten cycles. Furthermore, we applied synchrotron-based techniques to study crystallinity and film thickness of the ALD ZrO_2 deposited at different temperatures, including X-ray diffraction and X-ray reflectivity. In addition, we studied the films' composition using X-ray photoelectron spectroscopy, observed the films' morphology using scanning electron microscopy, and analyzed the films' structure using transmission electron microscopy. These studies provided

us an integral understanding on the growth mechanism and films' characteristics of ALD ZrO_2.

1. O. S. Abd El-Ghany and A. H. Sherief, *Future Dental Journal*, 2016, **2**, 55-64.

2. S. Kouva, K. Honkala, L. Lefferts and J. Kanervo, *Catalysis Science & Technology*, 2015, **5**, 3473-3490.

3. L. Yin, Y. Nakanishi, A.-R. Alao, X.-F. Song, J. Abduo and Y. Zhang, *Procedia CIRP*, 2017, **65**, 284-290.

4. X. Meng, X. Wang, D. Geng, C. Ozgit-Akgun, N. Schneider and J. W. Elam, *Materials Horizons*, 2017, **4**, 133-154.

5. X. Meng, X.-Q. Yang and X. Sun, *Adv Mater*, 2012, **24**, 3589-3615.

6. J. Liu, X. B. Meng, M. N. Banis, M. Cai, R. Y. Li and X. L. Sun, *J Phys Chem C*, 2012, **116**, 14656-14664.

7. J. Liu, X. B. Meng, Y. H. Hu, D. S. Geng, M. N. Banis, M. Cai, R. Y. Li and X. L. Sun, *Carbon*, 2013, **52**, 74-82.

AF2-MoP13 Hydrophobic SiO_x Thin Film Deposition using Low-Temperature Atomic Layer Deposition*, **Taewook Nam**, H. Kim,* Yonsei University, Republic of Korea

A hydrophobic coating has been widely used in various applications from passivation coating on electronics to medical or even pharmaceutical devices. In many applications, organic material coatings such as fluorocarbon or hydrocarbon compounds have been used for hydrophobic coating due to their low material cost, simple coating process, and chemical stability. However, organic coatings have several disadvantages in practical applications, chiefly their inherently poor mechanical durability and thermal stability. Hydrophobicity was also found in a few inorganic metal oxides. However, hydrophobicity using inorganic metal oxide was not retained after high-temperature annealing or UV exposure because of the generation of the surface hydroxyl group. To overcome these problems, hydrophobic coating using rare-earth oxide (REO) was reported. Although its superior thermal and chemical stability, however, REO is expensive because of its scarcity and has some deleterious effects on the human body. In addition, the relatively high process temperature is an obstacle for coating on a thermally fragile substrate, such as fabric or polymer substrate. Therefore, it is highly required to fabricate a hydrophobic surface with low cost and safety material at low temperature.

Silicon oxide (SiOx) is a well-known material in semiconductor industries. Since it can be easily formed by using vapor deposition, exhibiting good chemical, mechanical, and electrical properties, it has been greatly investigated for various applications. SiOx is inherently hydrophilic material because of the presence of silanol (Si-OH) groups on the surface. Therefore, it is hard to make a hydrophobic surface of SiOx without surface treatment or functionalization.

In this study, hydrophobic ALD SiOx was obtained at the low growth temperature without any post-treatment. The water contact angle of ALD SiOx grown at 50 °C is 94 °. However, when the growth temperature is 100 and 150 °C, the water contact angles were decreased to 74 and 53 °, respectively. This hydrophobic characteristic of ALD SiOx was retained after the annealing at 300 °C. To analyze this phenomenon, various analysis including XPS and AFM had proceeded. To obtain superhydrophobicity, ALD SiOx was coated on the silicon nanowire (SiNW) at 50 °C. On SiOx-coated SiNW, superhydrophobicity is observed for water, blood, and 10 wt% ethanol solution. Owing to its low process temperature, hydrophobic SiOx can be also coated on the thermally fragile cloth, cotton or spandex, for instance, enhancing the waterproof characteristics. The detailed experimentation and origin of hydrophobicity of low-temperature ALD SiOx will be discussed.

AF2-MoP14 Characteristics of High-temperature ALD SiO_2 Thin Films Using a Si Precursor with Excellent Thermal Stability*, **Jae-Seok An**, J.-R. Park, M.-H. Nim,* Hansol Chemical, Republic of Korea*; Y. Kim, J. Gu, S. Kim,* Sejong University, Republic of Korea*; J.-H. Seok, J.-W. Park,* Hansol Chemical, Republic of Korea*; W.-J. Lee,* Sejong University, Republic of Korea

In recent years, technologies for stacking semiconductor devices in three dimensions have been introduced as a method for overcoming the limitations of the two-dimensional scaling of devices. Thus, there is an increasing interest in atomic layer deposition (ALD) which can deposit thin films with excellent conformality in high-aspect-ratio three-dimensional patterns. In particular, SiO_2 and SiN thin films used as tunneling oxide, trap layer, and blocking oxide in 3-dimensional vertical NAND devices must have excellent step coverage in channel hole as well as good physical and electrical characteristics. In the conventional ALD processes of silicon oxide, the physical and electrical properties of the deposited thin film are improved as the deposition temperature increases, however, at high temperatures above 500°C, the thermal decomposition the Si precursor occurs, resulting in poor step coverage and film properties [1]. In the present work, we developed an ALD process using a Si precursor with excellent thermal stability, which does not cause a step coverage degradation due to thermal decomposition up to 750°C. The thermal decomposition of the Si precursor was evaluated by examining the growth rate change with the feeding time of Si precursor at 600°C or higher temperatures. The step coverage, composition, density, and leakage current of silicon oxide films deposited at different temperatures were investigated and compared with thermal oxide. The effects of the oxidizing agent on the deposition kinetics and the film properties were also investigated and discussed.

References [1] S.-W. Lee et al., *Electrochem. Solid-State Lett.,* **11**, G23 (2008).

~~**AF2-MoP15 Developing Routes Toward Atomic Layer Deposition of Tungsten using Fluorine Free W Precursor and Various Reactants with Density Functional Theory***, **Tae Hyun Kim**, D.K. Nandi, M.Y. Lee,* Yeungnam University, Republic of Korea*; R. Hidayat, S. Kim, W. J. Lee,* Sejong University, Republic of Korea*; S. H. Kim,* Yeungnam University, Republic of Korea~~

~~The W ALD process using WF_6 is applied to the fabrication of the nucleation layer for W plug and W gate or bit line in the current semiconductor device manufacturing. However, the highly corrosive nature of the F contained in the precursor, damages the underlying oxide and metal film, and degrade the electrical characteristics and reliability of the device. Therefore, it is necessary to develop an ALD process with F free W (FFW) precursor. In this study, $EtCpW(CO)_3H$ is selected as a FFW metal organic precursor, while suitable reactants (reducing agents) among various ones, molecular H_2, H_2 plasma (which provides highly reactive H radical), trimethyl aluminum triethyl aluminum, TBH (tert butyl hydrazine), diethylamineborane (DEAB), dimethylamineborane (DMAB) NH_3 etc. are adopted based on the density functional theory (DFT) calculation. Following the DFT predictions, successful ALD W films are prepared using the reducing agents diethylamineborane (DEAB) and H_2 plasma at a deposition temperature of 325°C. The growth rate observed using DEAB reactant is ~1.3Å /cycle. On the other hand, H_2 plasma, as a reactant, offers relatively lower growth rate of ~ 0.4 Å/cycle. The crystalline and amorphous phase of the as-deposited W films are confirmed using X-ray diffraction (XRD) for H_2 plasma and DEAB, respectively, Furthermore, the XRD reveals a mix-phase of β-W and tungsten carbide (WC) for the films grown by H_2 plasma and the X-ray photoelectron spectroscopy analyses confirm considerable impurities (Boron, Carbon, Nitrogen, Oxygen) in the films grown by DEAB. However, a post annealing could further improve the properties of these films.~~

AF2-MoP16 ALD HfO_2 with Anhydrous H_2O_2 in a 300 mm Cross-flow Reactor – Comparison with H_2O and O_3 Oxidants*, **Steven Consiglio**, R. Clark, C. Wajda, G. Leusink,* TEL Technology Center, America, LLC

HfO_2-based dielectrics deposited by ALD have been utilized in CMOS manufacturing since the 45 nm node [1]. In addition to applications of ALD HfO_2-based dielectrics in CMOS and DRAM, the recent discovery of ferroelectricity in HfO_2-based dielectrics [2] shows promise for applications in emerging non-volatile memory [3] and neuromorphic computing [4]. Thus, improving and modifying the growth of ALD HfO_2 is of significant industrial interest.

For ALD growth of HfO_2, H_2O and O_3 are the most commonly used oxidants. The drawbacks of H_2O include low oxidative reactivity and strong adsorption to surfaces in the deposition chamber which requires long purge times. Although the use of the strong oxidant O_3 in ALD typically uses reduced cycle times compared to H_2O, O_3 exposure can lead to unwanted oxidation of the underlying substrate which can significantly impact final device properties. In this regard, H_2O_2, which has an oxidation potential greater than H_2O but less than O_3, is an attractive candidate as an alternative oxidant for ALD growth of metal oxides.

In this study we evaluated a source for anhydrous H_2O_2 delivery which overcomes some of the drawbacks of H_2O_2/H_2O solutions, which have a low concentration of H_2O_2 in the vapor phase. The novel source and delivery system (RASIRC® BRUTE™ Peroxide) consists of > 99% H_2O_2 dissolved in non-volatile solvent passed through a tubular membrane which is selective to H_2O_2.[5-7]

By optimizing the hardware and delivery setup to minimize vapor phase H_2O_2 decomposition and depletion effects, we were able to demonstrate uniform ALD HfO_2 growth across a 300 mm wafer in a cross-flow deposition

chamber. In order to compare the performance of H_2O_2 with the other commonly used oxidants, we compared ALD HfO_2 growth with well-established processes using H_2O and O_3 [8]. Dose dependence of H_2O_2 was investigated to determine reactant saturation. Using a saturated H_2O_2 pulse we obtained > 50% increase in growth-per-cycle compared to both H_2O and O_3 while also significantly improving within-wafer-uniformity. Further optimization of purge times and carrier Ar flow rate achieved a reduced cycle time for H_2O_2 process which was > 50% less than the cycle time required for H_2O process and approaching the optimized cycle time for the O_3 process.

References

1) M. T. Bohr et al., *IEEE Spectr*. **44**, 29 (2007)

2) T. S. Böscke et al., *Appl. Phys. Lett*.**99**, 102903 (2011)

3) T. Mikolajick et al., *MRS Bull*. **43**, 340 (2018)

4) H. Mulaosmanovic et al. *Nanoscale***10**, 21755 (2018)

5) D. Alvarez, Jr. et al., *ALD 2014*

6) D. Alvarez, Jr. et al., *AVS 2015*

7) www.rasirc.com/product-brute-peroxide.html

8) R. D. Clark et al., *ECS Trans.* 16(4), 291 (2008)

AF2-MoP17 Atomic Layer Deposition of Copper (I) Chloride using Liquid 1-Chlorobutane Precursor*, **Richard Krumpolec**, D. Cameron, D. Bača, J. Humlíček, O. Caha,* Masaryk University, Czech Republic

Zinc blende-structure γ-copper (I) chloride is a wide, direct bandgap semiconductor with the potential for applications in UV optoelectronics. Atomic layer deposition has previously been applied to deposition of copper chloride CuCl thin films and nanocrystallites [1,2]. The ALD-like process was reported using solid precursors [Bis(trimethylsilyl)acetylene]-(hexafluoroacetylacetonato)copper(I) and Pyridine HCl [3]. In this paper, we worked with anhydrous 1-Chlorobutane as a Cl precursor for deposition of CuCl thin films. The advantage of this liquid precursor is high vapour pressure enabling short pulsing times. The CuCl films were deposited on crystalline silicon with different pretreatment protocols and also on flexible polyimide polymeric substrates. The structural, chemical, optical and photoluminescent properties of CuCl thin films were studied by SEM, XRD, AFM, XPS, optical reflectance and photoluminescence. Figure 1 shows the SEM images of a layer of CuCl crystallites on a silicon substrate cleaned by RCA protocol and deposited using liquid 1-Chlorobutane. The deposition using a liquid 1-chlorobutane precursor is compared to the process using previously reported solid Pyridine hydrochloride precursor.

Figure 1: SEM images of a layer of CuCl crystallites on a silicon substrate cleaned by RCA protocol.

References:

[1] G. Natarajan, P.S. Maydannik, D.C. Cameron, I. Akopyan, B. V. Novikov, Atomic layer deposition of CuCl nanoparticles, Appl. Phys. Lett. 97 (2010) 241905. doi:https://doi.org/10.1063/1.3525929.

[2] P.S. Maydannik, G. Natarajan, D.C. Cameron, Atomic layer deposition of nanocrystallite arrays of copper(I) chloride for optoelectronic structures, J. Mater. Sci. Mater. Electron. 28 (2017) 11695–11701. doi:10.1007/s10854-017-6973-8.

[3] R. Krumpolec, T. Homola, D. Cameron, J. Humlíček, O. Caha, K. Kuldová, et al., Structural and Optical Properties of Luminescent Copper(I) Chloride Thin Films Deposited by Sequentially Pulsed Chemical Vapour Deposition, Coatings. 8 (2018) 369. doi:10.3390/coatings8100369.

AF2-MoP18 Number Effect of Si Atoms Contained in Precursor for SiN Atomic Layer Deposition*, **Seungbae Park**, H. Ji, H. Yang, S. Yoon,* DUKSAN Techopia company, Republic of Korea*; I.-S. Park,* Hanyang University, Republic of Korea

Silicon nitride (SiN) films have been widely applied to the in solid-state devices as functional and process layers. The examples include charge trap layer in flash memory, gate dielectric layer in thin film transistors. gate spacer in FinFET transistor, etch stop layer in CMP, and capping layers in interconnection. The requirements of thin and smooth film, its uniform thickness and composition distribution, and high conformal coating on complicated structure have allowed ALD method to be widely introduced to make SiN films. In SiN-ALD process, the selection of Si precursor is significant because of the variability of film characteristics such as growth rate and material/dielectric/electrical properties. In this work, the number of Si atoms in precursor has focused on fabricating SiN-ALD films to investigate its linkage to growth and materials properties of SiN films. Three precursors of SiCl4, Si2Cl6, and Si3Cl8 were used as Si source for ALD for the model materials with the 1, 2, and 3 Si atoms. The ALD-SiN were performed at plasma system with NH3 reactant. For the growth rate of SiN, Si2Cl6 has the highest value of 1.44 A/cycle at the deposition temperature of 400 C. The Si : N ratio of all SiN films was analyzed by using XPS measurement, was the same with 1 : 1.16 near the surface, and kept constant with depth. The contamination of Cl and C was under the limit of XPS resolution. With the increase of Si number in precursor, the oxygen content in SiN was apparently reduced. The increased Si number make the SiN film much dense, and hence their wet etch rate against diluted HF solution was reduced from 0.55 A/sec to 0.36 A/sec for SiCl4 to Si3Cl8. The SiN film properties compared with Si numbers in precursor presented in this work will be useful for the fast and robust film formation.

ALD Fundamentals
Evergreen Ballroom & Foyer - Session AF3-MoP
Growth Mechanisms and In Situ Studies Poster Session

AF3-MoP1 Langasite Crystal Microbalance (LCM) for In-situ Process Monitoring of ALD up to 440 º C*, **Masafumi Kumano**,* Tohoku University, Japan*; K. Inoue,* Piezo Studio, Japan*; K. Hikichi,* Technofine co. Ltd, Japan*; M. Shimizu, S. Tanaka,* Tohoku University, Japan

A quartz crystal microbalance (QCM) is often used as an in-situ monitoring tool for ALD process. The piezoelectric constant of quartz crystal starts to decrease at 300 º C and disappears at 573 º C . In addition, it's temperature coefficient of frequency (TCF) around the turn over temperature increases above 300 . Therefore, QCM is generally limited in use under 300 º C . In a higher temperature range, $GaPO_4$ is only a material practically used for a microbalance[1)]. However, the crystal growth of $GaPO_4$ is not industrially established like quartz, and the crystal size is limited.

Langasite $Ca_3TaGa_3Si_2O_{14}$ is a new candidate for a high temperature microbalance. It keeps piezoelectricity in a wide temperature range without any phase transition, and a large crystal can be potentially grown in an industrial scale. Around the turnover temperature range, a Langasite crystal microbalance (LCM) shows a much smaller TCF than the conventional QCM (Fig. 1).

The Langasite has a dielectric constant about 5 times as larger as that of quartz. This must be taken into account of to use an available QCM oscillator circuit. As shown in Fig. 2, the active area of the LCM, i.e. the center part where the electrodes on both sides overlap, is smaller than that of the QCM. Fig. 3 shows the resonance impedance characteristic of the LCM. The resonance frequency is 6 MHz, and the electromechanical coupling factor is 2.6%. A weak spurious mode remains in Fig. 3, but it can be swept out by polishing the crystal surface to a convex shape.

The LCM was applied for TMA/H_2O cycle up to 440º C. The inside of a LCM holder is purged by pulsed pressure synchronized to the ALD cycle to avoid internal deposition. Transient temperature fluctuation is repetitive and reproducible over the ALD sequence and can be separated from a mass change by averaging over sequence numbers. The measured LCM frequency change by a mass change of each cycle is 1.6 Hz at 395º C and 2.2 Hz at 280º C, which is smaller than that of the QCM (3.5 Hz/cycle at 285 º C). The sensitivity is improved using a larger active area of LCM in conjunction with a dedicated oscillator circuit.

1) J. W. Elam and M. J. Pellin, Anal. Chem. 77 (2005) 3531-3535

AF3-MoP2 In-Situ Process Monitoring of Precursor Delivery Using Infra-Red Spectroscopic Method*, **Robert Wright**, T. Baum,* Entegris, Inc.

ALD processing is an increasingly critical deposition method for conformally coating high-aspect ratio features in advanced logic and memory devices. Accurate, consistent and controllable delivery of precursor materials to the deposition system is a necessity. To achieve reliable, low-cost deposition processes, *a sensitive and non-destructive real-time method for monitoring the precursor concentration is increasingly important. A*n IR method offers chemical specific information for both the reactant and the reaction by-products. An IR based system was developed and used to measure the 'direct' flux from a solid source in real time. The real-time measurement of precursor concentrations in the gas-phase can be applied to process monitoring, process control and towards the detailed characterization of key variables in the precursor delivery. Further, this method can be used to characterize ampoule performance under different pressure, temperature and flow conditions for a specific chemical precursor.

AF3-MoP3 Quantitative Analysis of High-k ALD Precursors for Trace Elemental Impurities by Inductively Coupled Plasma – Mass Spectrometry (ICP-MS)*, **Jinjin Wang**, L. Mey-Ami, F. Li,* Air Liquide Electronics – Balazs NanoAnalysis

The scaling of logic technology node following Moore's law has reached <10 nm. Consequently, high-k dielectrics are prevalent in modern microelectronic devices. They are insulating thin films of metal oxides, metal nitrides or other types of metallic compounds with much higher dielectric constant k ranging from 8 to 32, in contrast to SiO_2 with 3.9. These thin films are deposited from high-k dielectric precursors, which are organometallic or inorganic compounds, via atomic layer deposition (ALD) technology. The ALD allows growth of thin films of high conformity and uniformity downscaled to single nm. In order for these thin films to function in micro devices, the films must be free of contamination that causes defects of microelectronic devices. Therefore, for quality control of the ALD process, all high-k precursors used must be completely free of elemental impurities. As a result, each batch of high-k precursors is now analyzed for elemental impurities before it can be used in the ALD process.

ICP-MS is the preferred technique for analysis of high-k precursors for trace metals at sub ppb and ppt level. High-k dielectric precursors generally contain a metal atom bound to a ligand or other organic components, and often react violently with water and moisture in atmosphere. Both metal and organic components create various matrix effects and mass interferences, both of which affect the accuracy of the precursor analysis. One of the matrix effects is known as "space-charge-effects" due to high metal concentration present in the precursor sample. The "space-charge-effects" suppresses the signal of many elements of interest and causes low spike recovery and poor analytical accuracy. In addition, there are two other types of mass interferences that can be formed due to high concentration of metal and organic components. These mass interferences generally exist in the form of polyatomic molecular ions and isobaric ion species. The polyatomic molecular ions include and are not limited to metal oxide, metal argide and metal carbide, formed by high concentration metal ions reacting with organic components and other species in the plasma. Doubly charged ions are another form of mass interferences that affect the analysis.

ICP-MS methods have been developed to reduce and eliminate all these matrix effects and mass interferences. The method development strategy enables us to develop low detection limits, which allow process engineers to set lower quality control specification limits for their process. Our method capability analysis (MCA) shows the low detection limits that we have achieved, excellent repeatability and accuracy as demonstrated by spike recovery experiments. The MCA also shows that the matrix effects and the mass interferences have significantly been reduced or eliminated.

~~**AF3-MoP4 Numerical Studies of the Fluid Dynamics and Chemical Kinetics of Spatial Atomic Layer Deposition of Al_2O_3***, **Dongqing Pan**,* University of North Alabama~~

~~Low throughput is a major limitation for industrial level atomic layer deposition (ALD) applications. Spatial ALD is regarded as a promising solution to this issue. With numerical simulations, this paper studies an in-line spatial ALD reactor by investigating the effects of gap size, temperature, and pumping pressure on the flow and surface chemical deposition processes in Al_2O_3 ALD. The precursor intermixing is a critical issue in spatial ALD system design, and it is highly dependent on the flow and material distributions. By numerical studies, it's found that bigger gap, e.g., 2 mm, results in less precursor intermixing, but generates slightly lower saturated deposition rate. Wafer temperature is shown as a significant factor in both flow and surface deposition processes. Higher temperature accelerates the diffusive mass transport, which largely contributes to the precursor intermixing. On the other hand, higher temperature increases film deposition rate. Well maintained pumping pressure is beneficial to decrease the precursor intermixing level, while its effect on the chemical process is shown very weak. It is revealed that the time scale of in-line spatial ALD cycle is in tens of milliseconds, i.e., 15 ms. Considering that the in-line spatial ALD is a continuous process without purging step, the ALD cycle time is greatly shortened, and the overall throughput is shown as high as 4 nm/s, compared to several nm/min in traditional ALD.~~

~~**AF3-MoP5 Mechanistic Understanding of Dicholosilane Thermal Decomposition during Atomic Layer Deposition of Silicon Nitride***, **Gyeong Hwang**, G. Hartmann,* University of Texas at Austin*; P. Ventzek,* Tokyo Electron America Inc.*; T. Iwao, K. Ishibashi,* Tokyo Electron Ltd.~~

~~Silicon nitride (SiN) thin films have been widely employed for various applications including microelectronics, but their deposition presents a challenge especially when highly conformal layers are necessary on nanoscale features with high aspect ratios. Plasma-enhanced atomic layer deposition (PEALD) has been demonstrated to be a promising technique for controlled growth of SiN thin films at relatively low temperatures (< 400 °C), in which thermal decomposition of Si-containing precursors on a N-rich surface is a critical step. In this talk, we will present our recent findings regarding potential underlying mechanisms leading to facile thermal decomposition of dicholosilane (DCS, SiH_2Cl_2) on the N-rich SiN surface, based on periodic density functional theory calculations. Our study highlights the importance of high hydrogen content on the N-rich surface, rendering primary and secondary amine groups. When the N-rich SiN surface is fully hydrogenated, the molecular adsorption of DCS is predicted to be exothermic by 0.6 eV. In this case, DCS decomposition appears to be initiated by nucleophilic attack by an amine lone-pair on the electrophilic Si, leading to the formation of a DCS-amine adduct intermediate followed by release of a Cl- anion and a proton. The predicted activation barrier for the DCS decomposition reaction is only 0.3 eV or less, depending on its adsorption configuration. We will also discuss the formation and role of HCl, the subsequent formation and nature of Si-N bonds, and the interaction between adsorbed DCS molecules. While clearly demonstrating advantageous features of DCS as a Si precursor, this work suggests that thermal decomposition of Si precursors, and in turn the ALD kinetics and resulting film quality, can be strongly influenced by surface functional groups, in addition to product accumulation and precursor coverage.~~

AF3-MoP6 New Challenges of the Channeled Spectroscopic Ellipsometry for ALD Applications*, **Gai Chin**,* ULVAC Inc., Japan

The channeled spectroscopic ellipsometry is a snapshot method for the spectrally resolved polarization analysis. Two high-order retarders are utilized to generate a channeled spectrum carrying information about the wavelength-dependent multiple parameters of polarization of light. This method does not requires mechanical or active components for polarization-control, such as a rotating compensator and electro-optic modulator. It can measure the thickness and optical constants of thin films at an ultra-high speed. Its data acquisition time is as short as 10 ms per measurement.

This innovative technology created great opportunities for new applications of the spectroscopic ellipsometry in which the compactness, the simplicity and the rapid response are extremely important. It can be integrated into many kind of deposition tools and successfully measured thin films in-situ and ex-situ. Obviously, ALD is one of the promising applications for this novel spectroscopic ellipsometry.

This paper describes the principle, system configuration and new challenges on developing this compact high-speed spectroscopic ellipsometry to satisfy daily increasing in-situ monitoring requirements from the ALD industrial and R&D users.

Some of the successful ALD applications will be introduced, such as measurement data obtained on Al_2O_3, HfO_2, TiO_2, Ta_2O_5 and TiN thin films etc. By acquiring thickness and optical constants data from this spectroscopic ellipsometry, the layer by layer growth and material properties of the films can be studied in detail. The growth rate per cycle was determined directly, and an automatic process control can be realized by feedback and feed-forward approach on the ALD tools.

AF3-MoP7 ***In-situ Ellipsometric Analysis of the Plasma Influence on Atomic Layer Deposited AlN Thin Films***, **Necmi Biyikli**, *S. Ilhom, D. Shukla, A. Mohammad, B. Willis,* University of Connecticut

In this report we have carried out real-time process monitoring to understand the impact of RF-plasma power and plasma exposure time on aluminum nitride (AlN) growth and film properties via *in-situ*ellipsometry. AlN thin films were grown on Si(100) substrates with plasma-enhanced atomic layer deposition (PE-ALD) using trimethyl-aluminum (TMA) as metal precursor and $Ar/N_2/H_2$plasma as co-reactant. Saturation experiments have been employed in the range of 25-200 W plasma power and 30-120 s plasma exposure time within 100 - 250 °C substrate temperature. *In-situ*multiwavelength ellipsometry provided the necessary sensitivity to identify single chemical adsorption (chemisorption) and plasma-assisted ligand removal events, as well as changes in growth-per-cycle (GPC) with respect to plasma power. Our real-time dynamic *in-situ*monitoring study

revealed mainly the following insights about the plasma power influence on AlN growth: GPC and TMA chemisorption amount exhibited plasma-power dependent saturation behavior at 30 seconds of plasma duration. The amount of chemisorption saturated at ~2.25 Å for higher RF-power levels, while for 25 and 50 W it went to below 1 Å, which was attributed to insufficient ligand removal. Besides *in-situ*characterization, ex-situ measurements to identify optical, structural, and chemical properties were also carried out on 500-cycle AlN films as a function of plasma power. AlN samples displayed single-phase hexagonal crystal structure with (002) preferred orientation for 150 and 200 W, while the dominant orientation shifted towards (100) at 100 W. On the other hand, 50 and 25 W resulted in films with amorphous character with no apparent crystal signature. Furthermore, it was found that when the plasma exposure time was increased from 30 to 120 s for 25 and 50 W, the amount of chemisorption exceeded the thickness gain values recorded for 150-200 W: ~2.4Å . However, such a recovery in chemisorption did not reveal crystalline material as the AlN films grown at sub-50 W both showed amorphous character.

AF3-MoP8 Reaction Mechanisms of Thermal and Plasma-Modified ALD Growth Studied by *In-Situ* Mass Spectrometry*, **Thomas J. Larrabee,** L.B. Ruppalt,* U.S. Naval Research Laboratory

Mechanisms of gas-surface chemical reactions, and reactions caused by plasma-surface interactions, have been studied to understand different aspects of the atomic layer deposition (ALD) of zinc oxide (ZnO) and niobium oxide (NbO_x) using a differentially-pumped, highly-sensitive *in-situ* quadrupole mass spectrometer to detect reactant and product gas species. Examination and comparison of the gaseous reaction products of these two ALD processes aid our understanding of how to use plasmas to modify ALD oxide growth, generally.

In some of these cases, the ALD process was modified by inserting argon/hydrogen plasma steps, which has been shown to alter the stoichiometry of ZnO and NbO_x (*i.e.* Nb_2O_5 to NbO_2), driving metal-enriched films and lower oxidation states. To date, it has been unclear what the mechanism of the plasma-surface reactions is in these processes or precisely how the thermal ALD growth has been altered by the insertion of argon/hydrogen plasma steps. By examining the reactant and product gas species detected by the *in-situ* quadrupole mass spectrometer, we are able to investigate the chemical reactions that occur during the ALD process, uncovering information not only about the impact of the plasma steps, but also the underlying mechanism of the thermal growth process, itself. Reagents used were diethylzinc for ZnO and (t-butylimido)tris(diethylamino)niobium(V) for NbO_x, repectively, and water as the oxidant. In plasma experiments, capacitively-coupled plasmas of H_2/Ar and Ar alone were used to alter surface chemistry.

Comparison was made between thermal reactions, and inserting plasma steps at different parts of an ALD sequence. Evidence for a mechanism involving metal-organic ligand desorption and possible further reaction with the plasma is to be presented for both the Zn and Nb precursors. No evidence demonstrating removal of oxygen atoms from the growing film, either by O_2 or H_2O gas evolution was found for ZnO. The chemistry of the NbO_x growth, both for thermal and plasma-modified reactions will also be presented. Results are relevant for the nearly ubiquitous alkyl-amino transition metal precursors.

Metal precursor saturation has been investigated, from which inference about physisorption vs. chemisorption may be gleaned. Relative abundances and the dynamics of reactant and product peaks are explored to clarify the problem of peaks appearing both as reactants and as products, which has previously obfuscated interpretation of mechanisms by examining QMS data alone.

AF3-MoP10 In-situ Quartz Crystal Microbalance Study of Poly(3,4-ethylenedioxythiophene) (PEDOT) by Oxidative Molecular Layer Deposition (o-MLD)*, **Jungsik Kim**, A. Volk,* North Carolina State University

Molecular Layer Deposition (MLD) has emerged as a promising vapor-phase deposition technique due to its self-limiting reactions and conformal film growth. This work investigates oxidative MLD (o-MLD) of poly(3,4-ethylenedioxythiophene) (PEDOT) by using a volatile liquid oxidant agent and 3,4-ethylenedioxythiophene monomer (EDOT). Traditionally, PEDOT growth has been synthesized through solution-based processes involving oxidation and deprotonation steps. Despite its simplicity, poor solubility of PEDOT requires a water-soluble polyanion, poly(styrenesulfonate) (PSS), often increasing the film resistivity. Alternative vapor-phase methods such as oxidative chemical vapor deposition (o-CVD) have been reported, but chemical additives/post treatments are necessary to obtain high conductivity. Previously, Atanasov et al.has reported an o-MLD process of PEDOT using molybdenum(V) chloride oxidant ($MoCl_5$) and EDOT [1]. However, the low vapor pressure of $MoCl_5$ limits deposition temperature and facile dosing. Moreover, few basic growth analyses such as in-situ quartz crystal microbalance (QCM) have been carried out to understand PEDOT growth by o-MLD.

In this work, in-depth PEDOT growth behavior during o-MLD has been studied. The relationship between the film growth and various deposition conditions such as precursor dose/purge time, working pressure, and chamber/precursor temperature was investigated. The mass change per cycle is linear with the number of cycles for two different oxidant dose times. However, much longer purge times are required for the longer oxidant dose to remove the byproducts. QCM, X-ray photoelectron spectroscopy (XPS), spectroscopic ellipsometry (SE), and scanning electron microscopy (SEM) show that PEDOT film has been uniformly deposited at 100 ℃, with a growth rate of ~1.5 ℃/cycle. At higher chamber temperature, the growth rate decreases; above 150 ℃, PEDOT growth is hindered by decomposition of precursors and monomer limited adsorption, resulting in rapid decrease of film growth. These QCM studies will play a pivotal role for understanding nucleation and growth mechanism of PEDOT via o-MLD and developing area selective MLD processes.

[1] S.E. Atanasov et al., Chem. Mater. 26, 3471−3478(2014)

ALD Fundamentals
Evergreen Ballroom & Foyer - Session AF4-MoP
Plasma Enhanced ALD Poster Session

AF4-MoP1 Low-temperature Atomic Layer Deposition of Yttrium Oxide using tris(butylcyclopentadienyl)yttrium and a Plasma-Excited Humidified Argon*, **Kentaro Saito**, K. Yosida, K. Kanomata, M. Miura, B. Ahmmad, K. Shigeru, F. Hirose,* Yamagata University, Japan

Yttria (Y_2O_3) is attracting much attention since it has a high dielectric constant and it is expected to be used as an oxide insulator in the field of large scale integration. Conventionally Y_2O_3 film has been deposited by chemical vapor deposition (CVD) and atomic layer deposition (ALD). These require heating at 200 °C or higher. This high temperature process is not suitable for the fabrication of flexible electronics. To decrease the process temperature, we developed a low-temperature ALD of Y_2O_3 using tris(butylcyclopentadienyl)yttrium ($(BuCp)_3Y$) as the Y precursor and a plasma-excited humidified argon as an oxidizer.

We used a double-side polished p-type Si (100) with a size of 20 × 20 mm^2 as a sample. Y_2O_3 ALD was performed by introducing a precursor from the heated container at 140 °C and the oxidizer alternately into a cumber at 80 °C. We designed the process condition of ALD as follows, $(BuCp)_3Y$ injection of 300 sec and plasma excited humidified argon of 600 sec. The evacuation times after the $(BuCp)_3Y$ and plasma excited humidified argon are 30 sec and 90 sec, respectively. We measured chemical status of Y_2O_3 films by X-ray photoelectron spectroscopy (XPS) to confirm the presence of Y_2O_3. We extracted a growth per cycle of ALD by spectroscopic ellipsometry. In fig. 1, we show a wide scan XPS spectrum obtained from the 80 °C grown Y_2O_3 film. Fig. 2 shows Y_2O_3 thicknesses as a function of ALD growth cycles. We estimated the growth per cycle of 0.084 nm/cycle.

In this work, we succeeded in 80 °C ALD of Y_2O_3. It must be possible to form Y_2O_3 films on most of flexible substrates by this process, because the process temperature was limited below 80 °C in this ALD process. In the conference, we show the related results and discuss the reaction mechanism.

AF4-MoP2 Plasma Enhanced Atomic Layer Deposition of Silicon Nitride Thin Film by Organosilane Precursor and Process Engineering*, **Se-Won Lee**, C. Lee, M.-S. Kim,* Versum Materials Korea, Republic of Korea*; S. Yi, X. Lei,* Versum Materials, Inc.

In this study, we demonstrated that a multi chloride ligand organosilane precursor with no oxygen content, designated as Precursor T to deposit SiN film at the identical deposition temperature for a possible low thermal budget and reliable device operating in industrial applications. Precursor T was used as a Si precursor, and NH3 and N2 were used as the reactants. Ar gas was used as a main and a carrier gas. Plasma enhanced ALD (PEALD) method was conducted to obtain SiN film at 300 oC wafer temperature. SiN PEALD deposition conditions with two different reactants are as follows; Precursor T/purge/NH3*/purge (process A,* denotes plasma use), Precursor T/purge/N2*/purge (process B), Precursor T/purge/NH3*/

purge/N2*/purge (process C, applied additional N2 plasma after NH3 plasma) and Precursor T/purge/N2*/purge/NH3*/purge (process D, applied additional NH3 plasma after N2 plasma).

Deposited SiN film with process A and process C exhibited good stoichiometric film compositions at about Si : N ratio of 3 : 4 with low oxygen and carbon contents and excellent SC of more than 95 %. SiN film with process D also showed good stoichiometric characteristic but, SC was ~ 65 % which is not good property than the above two methods. SiN film with process B showed a higher level of impurities over 3 % carbon and chlorine and 20 % oxygen contents, and a poor SC less than 20 % was found. Consistent with the above results, the XRR results also differed significantly from the other three process in SiN film with process B. The film density from process A to D were 2.65, 2.44, 2.73, and 2.73 g/cm3, respectively, which show that the film density of process B are not perfect SiN film.

For the WER performance with 0.1% HF solution, SiN with process C shows the lowest WER of 10 A/min among the four conditions. (WERs of process A, process B and process D SiN films were 88, 187 and 15 A/min, respectively.) It is demonstrated that WER is improved with combinatorial deposition with NH3*/N2* compared to the deposition with NH3* or N2* alone.

In summary, we have deposited SiN film by using a multi chloride ligand organosilane precursor and ALD process design. SiN film was deposited with NH3 and N2 reactant gases by PEALD. Excellent SC and WER results were obtained for SiN film deposited with Precursor T/NH3*/N2* PEALD process. These results would be able to be applied to spacers or passivation layer, etc. by depositing SiN films with process engineering and would be expected to reduce thermal budget or to obtain reliable device operation.

AF4-MoP3 Understanding the Effect of Plasma Gas Chemistry and Reactor Pressure on the Crystallinity of AlN Films Grown via Plasma-Assisted Atomic Layer Deposition*, **Saidjafarzoda Ilhom**, D. Shukla, A. Mohammad, N. Biyikli, B. Willis,* University of Connecticut

In this study we investigate the correlation between the structural properties of AlN thin films and the plasma gas composition as well as the ALD reactor pressure. Towards this aim, AlN films were grown on Si(100) substrates via hollow-cathode plasma-assisted atomic layer deposition (HCPA-ALD) using trimethyl-aluminum (TMA) and $Ar/N_2/H_2$plasma as metal precursor and co-reactant, respectively. Growth saturation experiments have been carried out within 0-100 sccm range for each co-reactant gas, at 100W RF-plasma power and 200°C substrate temperature. *In-situ*ellipsometry was utilized to monitor the growth-per-cycle (GPC) characteristics and real-time surface reactions including chemisorption and plasma-assisted ligand removal and nitrogen incorporation events. GPC values showed a fairly constant behavior at lower pressures followed by a considerable decrease at ~1 Torr. Our real-time dynamic *in-situ*monitoring suggests that the decline in GPC at higher pressures, and thus higher co-reactant gas flow rates, is mainly due to incomplete removal of surface ligand groups. Each of the plasma gas content was decoupled by keeping two of the co-reactants at an optimal flow rate and changing one over the range of 5-100 sccm in order to observe the GPC behaviour. In general, decoupling of N_2 and H_2 showed that the GPC is reduced at lowest and highest flow rates with rather a higher and fairly constant value in between. On the other hand, for Ar the GPC increased under low flow rates followed by a decay at higher flow rates. Moreover, N_2 and H_2 plasma gas mixture were also decoupled in time domain to investigate the GPC behavior in such a regime. We have observed that GPC was reduced for shorter H_2 plasma exposure times of 5 and 10 seconds followed with higher and constant value for longer durations, which was correlated to the incomplete ligand removal at the shorter H_2 plasma exposure that was supported by the single-cycle real-time *in-situ*measurements data. Also, extended 500-cycle long runs of AlN growth were carried out as a function of different plasma gas content and pressure. All AlN samples displayed single-phase wurtzite polycrystalline character, which exhibited preferred (002) crystalline orientation with peak intensity values changing as a function of Ar flow rate.

AF4-MoP4 Plasma Enhanced Atomic Layer Deposition of Aluminum and Aluminum Fluoride*, **Daniel Messina**, Z. Haung, B. Eller, F. Koeck, P. Scowen, R. Nemanich,* Arizona State University

Plasma enhanced atomic layer deposition (PEALD) is an emerging energy enhanced ALD technique that utilizes plasma radicals to drive surface reactions rather than thermal energy, as in traditional ALD. PEALD allows for lower impurities, increased growth rates, improved stoichiometry, and lower deposition temperatures, which are essential for the development of high reflectivity VUV structures and multilayer Fabry-Perot bandpass filters. The goal of this project is to develop an oxygen and nitrogen free ALD process to grow both aluminum and AlF_3 in the same chamber to enable UV optical filters that can be operated at <120 nm. The system is designed to deposit aluminum on a hydrogen terminated Si substrate, by sequential exposures of trimethylaluminum (TMA), an Ar purge, and a hydrogen plasma. The deposition of metal fluorides has been limited by difficulty in handling, and storing, anhydrous HF. The use of Pyridine-HF as the fluoride source reduces the risk for deposition of UV fluoride layers including AlF_3 and MgF_2. The process designed for the growth of AlF_3 layers proceeds by exposing the fresh PEALD Al to HF followed by an Ar purge. The process is designed for growth of Al and AlF_3 at 100-300° C. The PEALD system is connected to an X-ray photoelectron spectroscopy (XPS) system for elemental analysis and a UV spectrometer for far UV optical properties. *Ex-situ* characterization was conducted using atomic force microscopy (AFM), Rutherford backscattering (RBS), UV-VIS ellipsometry, and X-ray topography (XRT).

Research supported by NASA through grant NNX16AC30G.

AF4-MoP5 High-temperature Hollow Cathode Plasma Enhanced Atomic Layer Deposition of Silicon Nitride (SiN_x) Thin Films using Hexachlorodisilane (HCDS)*, **Su Min Hwang**, A.L.N. Kondusamy, Q. Zhiyang, H.S. Kim, J. Kim,* University of Texas at Dallas*; X. Zhou, B.K. Hwang,* Dow Chemicals

Recently, plasma enhanced atomic layer deposition (PEALD) is expected to overcome the limitation of conventional LPCVD and PECVD processes and could be used to deposit conformal thin films in convoluted high aspect ratio structures with thickness scalability.[1] A number of studies on PEALD SiN_x process have been reported and mostly capacitively coupled plasma (CCP), inductively coupled plasma (ICP) or microwave (MW) plasma source was employed.[2] The characteristics of the plasmas, such as low plasma density in CCP, high plasma damage in ICP and high oxygen contamination in MW, etc., can be problematic for film properties, especially wet etch resistance. On the other hand, hollow cathode plasma (HCP) can be applied for high-quality silicon nitride films due to its lower oxygen contamination, higher plasma density and lower plasma damage. Inspired by the unique characteristics of HCP, we proposed to explore the feasibility of high-quality PEALD-SiN_x films by improving the films properties with HCP. Additionally, the relationship between plasma source and PEALD-SiN_x films properties has rarely been studied.

In this work, we not only clarified the effect of plasma source on the oxygen contamination of PEALD SiN_x films, but also achieved high-quality SiN_x films using hollow cathode PEALD. PEALD system with ICP or HCP source was employed to study SiN_x films comprehensively. Hexachlorodisilane (HCDS, Si_2Cl_6) was used as the silicon precursor due to its higher reactivity than $SiCl_4$ and SiH_2Cl_2 while exhibiting a distinct self-limiting growth behavior. We explored the effect of process temperature (310−570 °C), precursor exposure, and plasma gas composition (NH_3/N_2 or NH_3/Ar) on the film properties. Within a range of process temperature window (310−480 °C), the combination of Si_2Cl_6 and NH_3 plasma showed the distinct self-limiting growth behavior at a low precursor exposure (5×10^2 L). In plasma source comparison, the SiN_x films deposited with ICP source showed higher oxygen contamination (> 7.0 at%) than the HCP-PEALD SiN_x films (> 3.5 at%). Particularly, the HCP-PEALD SiN_x film deposited at 480 °C had the wet etch resistance in HF acid (> 0.4 nm/min, 200:1 HF) and film density (2.9 g/cm^3) comparable to the LPCVD SiN_x films. These result could pave the way for achieving high-quality SiN_x films using the unique HCP source.

[1] H.S. Kim, X. Meng, S.J. Kim, A.T. Lucero, L. Cheng, Y.-C. Byun, J.S. Lee, S.M. Hwang, A.L.N. Kondusamy, R.M. Wallace, G. Goodman, A.S. Wan, M. Telgenhoff, B.K. Hwang and J. Kim, ACS Appl. Mater. Interfaces **10**, 44825 (2018).

[2] X. Meng, Y.C. Byun, H.S. Kim, J.S. Lee, A.T. Lucero, L. Cheng, and J. Kim, Materials (Basel). **9**, 1007 (2016).

AF4-MoP6 Effects of Ion Bombardment in Plasma Enhanced Atomic Layer Deposition Processes*, **Hu Li**,* Tokyo Electron Technology Solutions Ltd., Japan*; T. Ito,* Osaka University, Japan*; M. Kagaya, T. Moriya,* Tokyo Electron Technology Solutions Ltd., Japan*; K. Karahashi, S. Hamaguchi,* Osaka University, Japan*; M. Matsukuma,* Tokyo Electron Technology Solutions Ltd., Japan

Plasma enhanced technology has been widely used in the fabrication of thin films. In an atomic layer process, for example in a plasma enhanced atomic layer deposition (PEALD) process, chemically reactive plasma is expected to achieve high growth per cycle (GPC) at relatively low process

temperature. A typical PEALD process may also be used in multiple patterning. In such patterning processes, much more precise resolution of film patterning is highly required for the nanoscale pattering. However, the film surfaces suffer the bombardment of energetic ion species, which are generated in the plasma. In such processes, film properties are affected. Therefore, the goal of this study is to clarify the effects of ions or radicals in the plasma enhanced atomic layer processes and gain a further understanding of deposition mechanisms.

In this study, we have estimated the sputtering yields of a SiO_2 film deposited by a PEALD process, by an oxygen ion (O^+) beam as well as inert gas species with the use of a mass-selected ion beam system. We have also examined the effects of low-energy ion bombardment on a precursor-absorbed SiO_2 or Si surface. After precursor exposure, the surface was exposed to energetic argon ions (Ar^+). The surface chemical compositions after ion bombardment were analyzed by *in-situ* X-ray Photoelectron Spectroscopy (XPS). From the XPS observations, it has been found that impurities, such as nitrogen (N) and carbon © originating from the organic precursor molecules, remain in the surface region even after Ar^+ ion bombardment. We have also examined the effects of oxygen, which will be discussed in the presentation.

~~**AF4-MoP8 Microwave Generated Plasma Enhanced Atomic Layer Deposition of Oxides***, **Ji Hye Kim**, Y.D. Tak, Y.B. Lee,* ISAC Research Inc., Republic of Korea*; A. Poruba, J. Dolak,* SVCS Process Innovation s.r.o., Czech Republic*; H.S. Park,* ISAC Research Inc., Republic of Korea~~

~~With the continued down-scaling of devices and structure changed to 3-dimensional, new ALD processes are in great demand. Microwave surfatron plasma is considered new plasma source because it enables very low-temperature deposition and good film quality due to its low electron temperature and higher plasma density.~~

~~In this work, surfatron plasma source was incorporated to ALD reactor. We studied the characteristics of oxide films grown by microwave plasma enhanced ALD in the reactor. The films had high growth rate and low impurities, and they grew conformally on 6 inch Si wafer. The successful incorporation of surfatron plasma source to ALD reactor encourages the study of challenging ALD processes.~~

~~**AF4-MoP9 Epitaxial Growth of GaN by Plasma-Enhanced Atomic Layer Deposition***, **Sanjie Liu**, X. Zheng,* University of Science and Technology Beijing, China~~

~~In this work, the epitaxial growth of single crystalline GaN films on sapphire substrate is realized by plasma enhanced atomic layer deposition (PEALD) at a growth temperature of 350 ℃. The XRD patterns show that the GaN films are single crystalline and display a single hexagonal (002) phase. The high-resolution transmission electron microscopy reveals a nanoscale single crystal GaN heteroepitaxy and a sharp interface. The full width at half-maximum of the X-ray rocking curve of the GaN epilalyers is 709 arcsec. The hetero-epitaxial GaN thin films have broaden its application in photovoltaic area, such as improving the performance of the solar cells.~~

AF4-MoP10 Improving Plasma Enhanced Atomic Layer Deposition of Silicon Nitride with A Halodisilane*, B.K. Hwang, C. Lee,* ***Xiaobing Zhou****, A.E. Foss,* DuPont*; T.L. Sunderland, A.R. Millward,* Dow Chemicals*; S.M. Hwang, J.Y. Kim, A.T. Lucero, A.L.N. Kondusamy,* University of Texas at Dallas

In our continuous evaluation of disilane compounds as silicon source precursors for plasma enhanced atomic layer deposition of silicon nitride films (PEALD SiN), a halodisilane is found to give a superior film-forming performance and film properties. The halodisilane having 99% purity was evaluated with ammonia plasma on a PEALD tool with a remote hollow cathode plasma source. SiN films were deposited at about 1 Å/cycle growth rate within the ALD window up to about 450 °C. This growth rate represents a 20% improvement over the growth rate of hexachlorodisilane (HCDS). The wet etch rate (WER) of the PEALD SiN films of the halodisilane is 50% lower than that of HCDS in 200:1 HF. The step coverage is comparable to that of HCDS in high aspect ratio trenches. The PEALD SiN film results of this precursor including saturation behavior, ALD window, composition, refractive index, uniformity, density, wet etch rate and step coverage are summarized and compared with those of HCDS and pentachlorodisilane (PCDS) in this presentation.

AF4-MoP11 Characteristics of Silicon Nitride Film Deposited by Multi-electrode VHF (162 MHz)-PEALD*, **Ki Hyun Kim**, K.S. Kim, Y.J. Ji, J.Y. Byun,* Sungkyunkwan University, Republic of Korea*; A.R. Ellingboe,* Dublin City University*; G.Y. Yeom,* Sungkyunkwan University, Republic of Korea

Silicon nitride (SiN_x) thin films are used as passivation layers, diffusion barrier materials, and structural materials for various micro-electro-mechanical systems (MEMS) due to their excellent chemical and mechanical properties. The conventional plasma enhanced chemical vapor deposition (PECVD) process couldn't meet recent stringent requirements such as high conformality on a high aspect ratio pattern, high chemical stability, and high film density at low temperatures. To overcome these limitations, recently, atomic layer deposition (ALD) has received widespread attention as an alternative process for PECVD. In this study, a very high frequency (VHF, 162 MHz) multi-tile push-pull plasma source was applied to plasma enhanced atomic layer deposition (PEALD) of silicon nitride. As the silicon precursor and nitrogen atomic source, Di-isopropylamino Silane (DIPAS) and nitrogen (N_2) plasma were used, respectively, and the characteristics of silicon nitride deposited by the 162MHz VHF PEALD were investigated. XPS data showed that the silicon nitride film deposited by 162MHz VHF PEALD has a high nitrogen percentage in the SiN_x film which is close to the stoichiometric silicon nitride possibly due to a high dissociation rate of nitrogen at 162MHz VHF. Furthermore, a uniform step coverage of silicon nitride over a high aspect ratio trench (> 25 : 1) was confirmed by cross-sectional scanning electron microscope (SEM).

AF4-MoP12 Characteristics of Low Damage Cobalt Films Deposited by Very High Frequency Plasma Enhanced Atomic Layer Deposition*, **Changhoon Song**, W.K. Yeom, Y. Shin, G.W. Kim, G.Y. Yeom,* Sungkyunkwan University, Republic of Korea

In this study, to improve the properties of thin films deposited by plasma enhanced atomic layer deposition (PEALD), two different very high frequency (VHF) plasmas (60MHz, 100MHz)were used for the deposition of cobalt film by PEALD and, the characteristics of plasmas and cobalt films deposited by different frequencies were investigated. For the characterization of VHF plasmas, ion density and electron temperature were measured using a Langmuir probe. It is found that the higher frequency showed a higher plasma density with a lower electron temperature at the same rf power. When the NH radicals, which are required to remove the ligands of the cobalt precursor during the plasma exposure step in the ALD cycle, w ere measured by OES, the intensity of NH peak at 100 MHz was higher than that at 60 MHz, indicating that more NH_3 plasma dissociation at the higher frequency. The composition and the RMS surface roughness of the deposited cobalt films were measured by XPS and AFM, respectively. AFM data showed the lower RMS surface roughness value at the higher frequency possibly indicating denser films due to more active surface reactions at the higher frequency. As a result, it is expected that the cobalt thin films deposited by the higher VHF PE-ALD will improve the characteristics of deposited thin films.

Keywords : Very high frequency (VHF) plasma, Atomic layer deposition (ALD), Cobalt, dissociation, radical

ALD Fundamentals
Evergreen Ballroom & Foyer - Session AF5-MoP
Characterization of ALD Films Poster Session

AF5-MoP1 Film Thickness and Trace Metal Analysis of Compound Semiconductor Stacks through Direct Film Stripping (DFS) followed by ICP-MS/OES*, **Vijay (Jaya) Chowdhury**, J. Huang,* ChemTrace*; P. Sun,* UCT - ChemTrace*; E. Appiah,* ChemTrace

Advances in the deposition of thin film and heterojunctions have revolutionized the photonics and LED markets. Promising gate dielectric deposition techniques such as atomic layer deposition (ALD) on compound semiconductors such as Sapphire and Gallium Nitride (GaN) have accelerated the scalability and high yield manufacturability. Deposition of high quality and scalable thin films through ALD involve some sequential use of gaseous precursors introduced to the substrate surface within a reaction chamber. In order to achieve ultra-high purity products, essentially free from trace metals and organic impurities, the film precursors need to be fully qualified and the deposited films require full characterization for process optimization to eliminate device critical contaminants in the mature process. Several techniques are available for the analysis of film thicknesses and impurity levels on the surface and bulk of the stacks keeping in view the precision and accuracy requirements. One of the technical challenges for in-film trace metal contamination analysis is the lack of selective film stripping sample preparation methods.

In this paper, we will discuss the direct film stripping (DFS) technique developed for top metal oxide film analysis on Sapphire/GaN substrates with minimal etching of the substrate. Using the optimized direct film stripping sample preparation method followed by ICP-MS/OES, trace

metals in a single film layer can be analyzed with minimum etching of the substrate below. Efficient film removal selectivity and satisfactory method detection limits are achieved. We will also share a film depth study done on HfO_2/Al_2O_3 stack on silicon wafers using ICP-OES. The study results provided an excellent stoichiometric quantification of the Al and Hf elements and good correlation with a beam based technique, Rutherford Backscattering (RBS). A combination of the two techniques can be useful for the study of thin film analysis. The direct film stripping technique developed in this study can be expanded for trace metal analyses of other films stacks.

Keywords: *Direct film stripping (DFS), Inductively Coupled Plasma Mass Spectrometry (ICP-MS), Inductively Coupled Plasma Optical Emission Spectroscopy (ICP-OES), trace metals, Gallium Nitride (GaN)*

AF5-MoP2 Overview of Doctoral Theses on Atomic Layer Deposition Worldwide - Outcome of the Virtual Project on the History of ALD*,* *J. Aarik,* University of Tartu, Estonia*; J. Aav, E. Ahvenniemi,* Aalto University, Finland*; A.R. Akbashev,* Stanford University*; S. Ali,* Aalto University, Finland*; M. Bechelany,* Institut Européen des Membranes, France*; M. Berdova,* Aalto University, Finland*; I. Bodalyov,* St. Petersburg State Institute of Technology, Russian Federation*; S. Boyadjiev,* Bulgarian Academy of Sciences, Bulgaria*; D. Cameron,* Masaryk University, Czech Republic*; N. Chekurov,* Oxford Instruments Analytical Oy, Finland*; R. Cheng,* Huazhong University of Science and Technology, China*; M. Chubarov,* The Pennsylvania State University*; V. Cremers,* Ghent University, Belgium*; A. Devi,* Ruhr University Bochum, Germany*; V.E. Drozd,* St. Petersburg State Institute of Technology, Russian Federation*; L. Elnikova,* Institute for Theoretical and Experimental Physics, Russian Federation*; G. Gottardi,* Fondazione Bruno Kessler, Center for Materials and Microsystems, Italy*;* ***J. Ruud van Ommen****,* Delft University of Technology, Netherlands*; R. Puurunen,* Aalto University, Finland

Atomic Layer Deposition (ALD) is a materials growth technique that has become globally important during the past decades. In 2018 the Finnish inventor of ALD, Tuomo Suntola, received the Millennium Technology Prize.

ALD has been discovered independently twice, under the names Molecular Layering (ML) in the 1960s in the USSR and Atomic Layer Epitaxy (ALE) in 1974 in Finland. The Virtual Project on the History of ALD (VPHA) is a volunteer-based Open Science effort set up in 2013 [2] to clarify the early days of ALD. Especially the ML path has remained poorly known and acknowledged until recently. The core activity of VPHA is to overview early ALD publications up to 1986. VPHA has already resulted in four scientific journal articles [2-5] and several presentations at international conferences.

This poster will overview doctoral theses worldwide related to ALD up to year 2018. The doctoral thesis list has been built by combining the lists of Ref. 4 and the exhibition material 40 Years of ALD in Finland - Photos, Stories (FinALD40) [6], and allowing volunteers to enter missing information (open list in http://vph-ald.com/VPHAopenfiles.html). At the time of writing the abstract, the doctoral thesis collection contains close to 500 entries. The list is likely not yet complete and more entries are welcome. More volunteers are also still welcome to join and contribute in the VPHA.

Acknowledgements: R.L.P. thanks Tuomo Suntola for his support during the VPHA. Aziz Abdulagatov and Annina Titoff are acknowledged for significant help during the initiation of VPHA. The authors are grateful for all volunteers, who in addition to the current authors have shared at least one comment in the ALD-history-evolving-file during VPHA (as of Feb. 11, 2019): S.D. Elliott, D.C. Smith. The author list is intentionally in alphabetical order.

References:

[1] https://en.wikipedia.org/wiki/Millennium_Technology_Prize (accessed 11.2.2019)

[2] E. Ahvenniemi et al. (62 authors), Journal of Vacuum Science & Technology A 35 (2017) 010801, https://doi.org/10.1116/1.4971389

[3] R. L. Puurunen, Chemical Vapor Deposition 20 (2014) 332–344, https://doi.org/10.1002/cvde.201402012

[4] A. A. Malygin, V. E. Drozd, A. A. Malkov, and V. M. Smirnov, Chemical Vapor Deposition, 21 (2015) 216–240, https://doi.org/10.1002/cvde.201502013

[5] R. L. Puurunen, ECS Transactions, 86, (2018) 3–17, https://doi.org/10.1149/08606.0003ecst (open access: https://ecsarxiv.org/exyv3/)

[6] 40 Years of ALD in Finland - Photos, Stories (FinALD40). Materials via http://www.aldcoe.fi/events/finald40.html and http://vph-ald.com/ALD-history-publications.html

~~**AF5-MoP3 Nanoscale Chemical Characterization of Ultrathin Films via PiFM***, **Sung Park**, D. Nowak, W. Morrison,* Molecular Vista~~

~~Chemical analysis of ultrathin films with nanometer scale lateral spatial resolution remains a challenge for the nanotechnology community. In this poster, we introduce a new nanoscale and non-destructive chemical imaging technique called photo-induced force microscopy (PiFM) where the dipole-dipole force due to optical response of the sample is measured by an atomic force microscope (AFM) along with the standard AFM topography [1]. This dipole-dipole optical force interaction between the AFM tip and the sample is strongly enhanced at the apex of the metal-coated tip due to the antenna effect and leads to a routine spatial resolution that is better than 10 nm. Since both the optical excitation and detection are accomplished in near-field, the optical information can be acquired without the far-field background interference, making the technique easy-to-use compared to other near-field techniques. PiFM can be coupled with a tunable infrared (IR) light sources to probe the IR absorption of various organic and inorganic materials for identification of molecular materials and their relationship to local topography. PiFM is surface sensitive due to the short interaction range of the measured dipole-dipole force and can detect monolayer of materials with good sensitivity, making it an ideal tool for characterizing ultrathin films.~~

~~PiFM works equally well with both organic and inorganic materials and lends itself as an excellent analytical to characterize ALD, molecular layer deposition, and organic-inorganic hybrid materials.~~

~~1. Nowak, D., et al., "Nanoscale chemical imaging by photoinduced force microscopy," Sci. Adv. 2 (2016), e1501571.~~

AF5-MoP4 The Effect of Impurities on Film Properties in the $Y(MeCp)_3/O_3$ Process*,* *J. Kalliomäki, T. Lehto, M. Kääriä, T. Sarnet,* ***Jani Kivioja****,* Picosun Oy, Finland

Y_2O_3 thin films are utilized as insulating materials in electronic devices, hydrophobic layers and corrosion inhibiting coatings. Several different yttrium ALD precursors have been demonstrated in the literature, from β-diketonates to heteroleptic cyclopentadienyls. When the deposition temperature is below 300 °C, authors usually report deterioration of film properties, such as crystallinity and density, with increasing impurity levels. [1,2] Nevertheless, further studies on the impurities are often outside the scope of the research found in literature.

The cyclopentadienyl-based ligands are commonly used in rare earth metal precursors, and the reaction mechanisms for them are proposed in literature. [3] However, the effect of deposition temperature over the full available range is not as widely researched.

This work focuses on the effects the reaction mechanism of the $Y(MeCp)_3/O_3$ process has on the type of carbon-based impurity species that result in the deposition temperature range 150-425 °C. The change in coordination/bonding of the impurities, and associated effect on film properties, is considered.

The experiments were made with a PICOSUN™ R-200 Advanced hot-wall ALD system. Si wafers with native oxide layers were used as substrates.

According to the results, the deposition temperature range can be divided into three regions that produce films with notably different materials properties (Figures 1-2). Each region is categorized by its distinct type of carbon-based impurity content, and the effect on optical, structural and electrical film properties will be discussed.

Understanding the underlying mechanism of growth, and how it can change and shape the process and the properties of the resulting films, is one key factor to widen the effective deposition temperature range of known oxide processes. Knowing the impact of the reaction mechanisms on the film properties allows more accurate process controls for specific applications and ultimately will help to create more high-quality end products.

[1] S. Seppälä, J. Niinistö, T. Blanquart, M. Kaipio, K. Mizohata, J. Räisänen, C. Lansalot-Matras, W. Noh, M. Ritala, M. Leskelä. Chem. Mater., 28 (2016) 5440–5449

[2] J. Niinistö, M. Putkonen, L, Niinstö. Chem. Matter, 16 (2004) 2953-2958

[3] M. Nolan, S. Elliot Chem. Mater. 22 (2010) 117–129

AF5-MoP6 Internal Photoemission Spectroscopy Measurement of Barrier Heights between ALD Ru and Al_2O_3, ***Melanie Jenkins**, M.H. Hayes, K. Holden, J.F. Conley, Jr.,* Oregon State University

ALD metals are of growing interest for applications that require conformal, pinhole free conductive films, particularly for high aspect-ratio structures. Ru, due to relatively low bulk resistivity, high work-function, a conductive oxide (RuO_2), and ease of etching, is of interest as a gate electrode for MOS transistors, metal-insulator-metal (MIM) capacitors, RRAM, and tunnel diodes, and well as a conductive Cu diffusion barrier/liner for Cu interconnects. A recent ALD process for Ru using $Ru(DMBD)(CO)_3$ and O_2 shows near zero nucleation, low roughness, and low resistivity.[1] The electrode performance depends strongly on the effective work function ($\Phi_{M,eff}$) or barrier height (ϕ_{Bn}) of the metal in direct contact with an insulator. Although capacitance-voltage (C-V) measurements may be used to estimate $\Phi_{Ru,eff}$ using MOS devices with a series of insulator thicknesses, this procedure is not possible in MIM devices. Internal photoemission (IPE) spectroscopy is the only analytical technique capable of directly determining metal-insulator ϕ_{Bn} in device structures.[2-5] To date, little IPE work has been reported on ALD metals. In this work, we use IPE to directly measure the ϕ_{Bn} between ALD dielectrics and ALD Ru.

10 nm ALD Al_2O_3 was deposited at 300 °C using TMA and H_2O in a Picosun Sunale R-200, immediately followed by 12 nm of ALD Ru at 260 °C using $Ru(DMBD)(CO)_3$ and O_2.[1,2] TaN and TiN were used for bottom metal electrodes in MIM devices. For direct comparison to C-V extracted $\Phi_{Ru\text{-}eff}$, MOS devices were also measured. Some devices were annealed at 500 °C for 60 min in H_2/N_2.

Representative (IPE yield)$^{1/2}$ vs. photon energy (2-5 eV) plots (Fig. 1) under negative and positive polarity allow extraction of voltage dependent spectral thresholds for the (a) Ru/Al_2O_3 interface and (b) TaN/Al_2O_3 interface, respectively. Schottky plots of spectral thresholds vs. field$^{1/2}$ reveal ϕ_{Bn} of 3.7 eV and 2.9 eV for as-deposited Ru and TaN, respectively (Fig. 2). Using an electron affinity of 1.4 eV for Al_2O_3, we estimate $\Phi_{M,eff}$ at 5.1 eV and 4.3 eV for Ru and TaN, respectively, both consistent with reports for sputtered films.[5]

ALD Ru and RuO_2 ϕ_{Bn} with Al_2O_3 and HfO_2 in MIM and MOS devices before and after annealing in H_2/N_2 will be reported and compared to $\Phi_{Ru\text{-}eff}$ extracted using C-V techniques as well as IPE results on amorphous metals[3,4] and reported values for sputtered Ru.

[1] D.Z. Austin *et al.*, Chem. Mater. **29**, 1107 (2017).

[2] N.V. Nguyen *et al.*, AIP Conf. Proc. **931**, 308 (2007).

[3] M.A. Jenkins *et al.*, J. Appl. Phys. **125**, 055301 (2019)

[4] M.A. Jenkins *et al.*, Phys. Status Solidi RRL **12**(3), 1700437 (2018).

[5] Afanas'ev *et al.*, Phys. Status Solidi (a) **13**(6), 1700865 (2017).

AF5-MoP7 Growth and Characterization: Low Temperature ALD, ***Birol Kuyel**, A. Alphonse, K.P. Hong, J. Marshall,* Nano-Master, Inc.

Growth and film deposition characteristic in a downstream ICP PEALD reactor are studied using a unique new process called Continuous Flow Process* that cuts the cycle time in half. This process is implemented in a PEALD reactor where uniform variable density O_2 and N_2 or H_2 plasmas are produced but any contact of the plasma with the substrate is prevented. Precursors are not allowed to enter the plasma production region making it possible to obtain repeatable operation free of deposits or plasma instabilities. This Continuous Flow Process is used for depositing PEALD GaN, Al_2O_3, and AlN films on Si substrates. It is shown that with this process ultra-smooth and uniform films with thickness linearly proportional to the number of cycles are deposited. Then it is applied to low temperature deposition of Si_3N_4 and SiO_2 films on Si wafers. The film surface roughness, thickness, uniformity, index of refraction, composition, and stress are studied down to room temperature depositions. Results are compared to thermal deposition in the same reactor and others' reported findings.

*US Patent # 9,972,501 B1 May 15, 2018

AF5-MoP8 Etch Rate Characterization of Oxide ALD Films, ***Martin M. Winterkorn**, H.J. Kim, J. Provine, F. Prinz, T.W. Kenny,* Stanford Univ.

For designing any kind of nanofabrication process, knowing the etch rates of available thin films, as well as their compatibility with commonly used processing chemicals is crucially important. Previous work by Williams et al. [1][2] tabulating rates for large numbers of film-etchant combinations has gained great popularity in the nanofabrication community, but does not include any ALD films. While there have been examinations [3] for select ALD processes and etchants since, the etch rates of ALD films have not yet been studied in comprehensive fashion.

We report on the characterization of the etch rates of 9 oxide ALD films in 20 different wet and vapor etchants, which include many commonly used silicon etchants, oxide etchants and metal etchants, as well as solvents, cleaning solutions and photoresist strippers. Each of the 180 etch rates is based on data from a minimum of 4 separate etches, with a total of over 1500 thickness measurements performed by ellipsometry. To allow efficient coverage of such a large scope, a high-throughput sample fabrication and measurement workflow was developed and successfully employed. Extension of the work to nitride ALD films is currently underway.

All oxide films were deposited at 200°C in Veeco / Cambridge Nanotech Fiji F202 ALD reactors, employing both thermal and plasma-enhanced ALD (PEALD), when available. To achieve representative results, standard deposition recipes were used, which are not optimized for low etch rates or any other specific metric, but have been developed for general purpose use. Chemicals were freshly poured for all wet etching. Film compositions as deposited were characterized using X-ray photoelectron spectroscopy (XPS).

References

[1] K. Williams, and R. Muller, Etch Rates for Micromachining Processing, *JMEMS* 5 (**1996**) 256.

[2] K. Williams, K. Gupta, and M. Wasilik, Etch Rates for Micromachining Processing - Part II, JMEMS 12 (**2003**), 761.

[3] J Provine, P. Schindler, Y. Kim, S. Walch, H.J. Kim, K.H. Kim, and F. Prinz, Correlation of film density and wet etch rate in hydrofluoric acid of plasma enhanced atomic layer deposited silicon nitride, *AIP Advances* 6 (**2016**).

~~**AF5-MoP10 Structural Aspects of Nanometer Size Amorphous Materials**, ***Yael Etinger-Geller**, A. Katsman, B. Pokroy,* Technion – Israel Institute of Technology, Israel~~

~~Crystallization in the course of biomineralization, often occurs via an amorphous precursor phase, allowing additional control over the mineralization process. One of the main advantages of this method is that it enables organisms to exert control over the resulting polymorph, which is not necessarily the thermodynamically stable one, by manipulating the short-range order of the amorphous phase.~~

~~Although many aspects of science and technology rely on amorphous materials, considerably less research focuses on the structure of amorphous materials as compared to their crystalline counterparts. In this research, we draw inspiration from nature and study the ability to control the short-range ordering in amorphous materials via nanometer size effects. We chose atomic layer deposition (ALD) to deposit thin amorphous oxides since this a technique that can provide extremely precise, sub-nanometric, thickness control and can deposit conformal and pinhole-free amorphous films of various materials.~~

~~Amorphous thin films of Al_2O_3, deposited by ALD, were characterized by EELS, AR-XPS, SS-NMR and GI-XANES at SOLEIL synchrotron and found to vary structurally as a function of size. Moreover, it was shown that these films exhibit surface layer of a different short-range ordering, in comparison to its "bulk". We explain this effect from a thermodynamic point of view and relate it to surface reconstruction that occurs, in order to reduce the energy of the system. The structural variations were expected to cause a change within the density of the thin film and indeed, it was experimentally found the amorphous thin film's average density changes with size, as well as other density related properties. Similar finding were obtained for other systems as well, meaning that this effect is not restricted to the Al_2O_3 case but may exist in different amorphous materials. We believe that the ability to tune one property or another solely by size, can open new possibilities for materials selections and applications, in science and technology.~~

~~1. Y. Etinger-Geller et al., Chem Mater, 2017, 29~~

~~2. Y. Etinger-Geller et al., J Appl Phys, 2019, 125~~

ALD for Manufacturing
Evergreen Ballroom & Foyer - Session AM-MoP
ALD for Manufacturing Poster Session

AM-MoP1 Cobalt Precursor Supply Chain - Ethics and Risks, ***Andreas Wilk**, A. Frey, O. Briel,* Umicore AG & Co. KG, Germany*; D. Zeng,* Umicore AG & Co. KG

Cobalt precursors are being used as lining and capping materials since a while. The use is beneficial to limit diffusion of copper into the dielectric

layer. Additionally deposited cobalt (and longer term ruthenium) metal will displace copper and tungsten because of lower resistivity and these materials require no liner or barrier when used as an interconnect.

Unfortunately, there are significant uncertainties in the supply chain.

Ethical sourcing of Cobalt: While Cobalt is not yet listed as a conflict material like gold, tantalum, tungsten and others, articles published by Amnesty International in Jan 2016 (https://www.amnesty.org/en/latest/news/2016/01/child-labour-behind-smart-phone-and-electric-car-batteries/) and Nov. 2017 (https://www.amnesty.org/en/latest/news/2017/11/industry-giants-fail-to-tackle-child-labour-allegations-in-cobalt-battery-supply-chains/) alerted end users and Semiconductor companies alike about child labor and artisanal mining being used to produce cobalt minerals. Umicore is worldwide one of the largest users of cobalt and has taken significant measures to ensure that cobalt sourced and downstream products supplied by Umicore don't come from unethical sources. This has been audited and certified by an independent firm. Our poster contains more details on these issues.

The manufacture of cobalt precursors requires access to an intermediate called dicobaltoctacarbonyl. This material is currently only manufactured by two minor companies with limited production resources, one of these company is even located in a geographical area, which may add to the supply complexity. The poster details how Umicore plans to overcome this bottleneck and ensure sufficient supply for future growth of the industry.

Cobalt is also a raw material for Lithium batteries. This application is forecasted to grow significantly in future because of the electrification of the automobile. This raises questions about future price development and availability of cobalt raw materials. Our poster reviews the impact on the electronics industry, the impact on the electronics industry and possible solutions.

In addition, we will introduce the latest Co metal precursors as potential candidates for ALD and MOCVD applications.

AM-MoP2 Homogeneous and Stress Controlled PEALD Films for Large Optics*, **Hassan Gargouri**, F. Naumann, S. Golka,* SENTECH Instruments GmbH, Germany*; K. Pfeiffer,* Fraunhofer Institute for Applied Optics and Precision Engineering IOF, Germany*; V. Beladiya,* Friedrich Schiller University, Germany*; A. Szeghalmi,* Fraunhofer Institute for Applied Optics and Precision Engineering IOF, Germany

The deposition of homogenous conformal films with a precise thickness control on structured surfaces is essential for numerous applications for semiconductors, sensors and optics. Atomic Layer Deposition (ALD) is the key technology to fulfill the high requirements of such devices e.g. DRAM, MEMS, gratings. Plasma Enhanced Atomic Layer Deposition (PEALD) is an extension of ALD that opens up new possibilities such as an increased choice in materials and precursors, extended process region, and processing at reduced substrate temperatures. The new SILAYO ALD system of SENTECH Instruments GmbH with Planar Triple Spiral Antenna (PTSA) as large planar inductively coupled (IC) plasma source promises highly uniform and conformal ICPEALD deposition. Furthermore, the SILAYO system is equipped with substrate bias to control film stress during the deposition process.

ICPEALD Al_2O_3, SiO_2 and TiO_2 films were deposited on 8-inch silicon (Si) substrates. Trimethylaluminium (TMA), bis(diethylamino) silane (SAM.24) and tetrakis(dimethylamino) titan (TDMAT) were used as metal organic precursors and oxygen plasma was applied as oxygen source for the ICPEALD processes. Due to the low vapor pressure of the Si- and Ti-precursor, the material containers were heated to 70 °C. During the deposition process the substrate temperature of 250 °C was kept constant. Nitrogen (N_2) was used as carrier gas for the precursors and a constant flow of oxygen was applied through the plasma source.

The Al_2O_3 process exhibits a growth rate of 1.4 Å/cycle and an excellent non-uniformity of ± 0.3 % over the 8-inch Si wafer. The 66 nm Al_2O_3 film shows a refractive index of 1.64 with also an excellent non-uniformity of ± 0.08 %. The SiO_2 and TiO_2 processes show a growth rate of 1.1 Å/cycle and 0.6 Å/cycle, respectively. The two processes reveal an excellent non-uniformity of ± 0.7 % or ± 0.8 % over the 8-inch Si wafer. Furthermore, ICPEALD Al_2O_3 films were deposited with substrate bias. Standard Al_2O_3 film shows 97 MPa tensile stress. Applying a bias voltage during the deposition process, the Al_2O_3 film shows compressive film stress between -109 MPa and -144 MPa, depending on the set bias voltage.

~~**AM-MoP3 Sensing Response of ZnO Nanotube Gas Sensor Synthesized on Porous Substrate by Atomic Layer Deposition***, **Pengtao Lin**, K. Zhang, H. Baumgart,* Old Dominion University~~

~~Among various Metal Oxide Semiconductor (MOS) gas sensor, gas sensors based on ZnO nanostructures have been widely used due to its large exciton binding energy, wide band gape of 3.37 eV, good electrical conductivity, low cost, and high mechanical stability. In this work, ZnO nanotube nanostructure was introduced into the gas sensor application to ethanol vapor concentration due to its high electrochemical stability, nontoxicity, and, especially, high surface-to-volume ratio. Several coaxial ZnO nanotubes were synthesized on porous substrate to further enhance the sensing response to ethanol vapor with increased reaction surfaces.~~

~~In this study, ZnO nanotubes were synthesized by Atomic Layer Deposition (ALD) on Anodic Aluminum Oxide (AAO) with sacrificial Al_2O_3 layers. The Al_2O_3 sacrificial layer was synthesized on AAO by ALD with TMA (Al2(CH3)6) and DI water as precursors. Then ZnO thin films were deposited on the surface of the sacrificial layer with precisely controlled thickness by ALD. The whole procedure is considered as one super cycle. More super cycles were applied to synthesize additional coaxial ZnO nanotubes. To eliminate the sacrificial layer, Precision Ion Polishing System (PIPS) was used to remove the top cover as shown in Figure 1. Therefore, the Al_2O_3 sacrificial layers were exposed for Sodium Hydroxide (NaOH) etching. After the sacrificial layers were removed by NaOH, ZnO nanotube gas sensors were synthesized as shown in Figure 1 (b).~~

~~To investigate the sensing performance of ZnO nanotube gas sensors to ethanol vapor, a gas sensor testing system was developed with a sealed reaction chamber and control system with stable temperature control and accurate concentration control. The sensing performance of one ZnO nanotube, two coaxial ZnO nanotubes, and three coaxial ZnO nanotubes to ethanol vapor were measured and analyzed under various ethanol vapor concentrations at different temperatures.~~

AM-MoP4 Temperature-based Control of Liquid Precursor Delivery for ALD Processes*, **Egbert Woelk**,* CeeVeeTech*; K. Kimmerle, B. Kimmerle,* NSI*; J. Maslar,* National Institute of Standards and Technology

Liquid precursors for ALD processes are commonly delivered in an inert carrier gas from a bubbler (an ampoule with a dip tube) or a vapor draw ampoule (an ampoule with no dip tube: the gas in and gas out ports open directly into the ampoule headspace). Compared to some other delivery methods, the use of such ampoules for precursor delivery is relatively straight-forward. However, a potential drawback of using such ampoules is that evaporative cooling of the precursor can lead to a reduction in the amount of precursor delivered over time, i.e., cooling reduces the water vapor pressure and hence the amount of material entrained in the carrier gas. For example, the vapor pressure of water changes 5% per Kelvin at 20°C, while that of trimethylaluminum changes 6% per Kelvin at 20°C. For ALD processes that involve a chemical vapor deposition component, a decrease in the amount of water delivered can be detrimental to deposited film properties. To overcome this drawback, a device has been developed that controls the amount of precursor delivered based upon the precursor temperature. The concept is as follows. A temperature sensor is inserted into a thermowell on the ampoule to below the liquid level. Then, a target temperature is selected that would result in the desired amount of precursor being delivered based on the vapor pressure at this temperature. When flow is initiated through the ampoule, evaporative cooling of the precursor results in a decrease in precursor temperature which is measured with the temperature sensor. To compensate for this decrease, the amount of precursor delivered is increased in one of two ways: (1) the carrier gas flow rate is increased in a flow control mode or (2) the system pressure is decreased in a pressure control mode. In both modes, the amount of precursor is increased to compensate for the decrease in vapor pressure. To demonstrate the performance of this control device, the precursor partial pressure was measured with and without active control using custom-built optical gas sensors. The time-dependent partial pressure was converted to precursor flow rate assuming that the ratio of the precursor to carrier gas partial pressures equals the ratio of the respective flow rates. A five-element temperature sensor array was used to measure temperature. Flow control was demonstrated by controlling the set point of the carrier gas mass flow controller. Pressure control was demonstrated by controlling the set point of a downstream pressure controller. Water and hexane were utilized to investigate the impact of precursor vapor pressure on controller performance. In addition, both bubblers and vapor draw ampoules were investigated.

AM-MoP5 Design and Manufacturing of ICP-Type Remote Plasma ALD*, **Dohyun Go**, J.W. Shin, B.C. Yang, H.J. Kim,* Seoul National University of Science and Technology, Republic of Korea

Plasma-enhanced ALD (PEALD) is a type of ALD, which utilizes ions and radicals in plasma as oxidants which have higher reactivity than conventional oxidants. Plasma can not only effectively eliminate ligand of precursors but also possibly reduce deposition temperature. While the system of commercial PEALD usually adopt capacitively coupled plasma (CCP) or inductively coupled plasma (ICP), it is usually complicated regardless of plasma generating method; such complexity of system may increase the system cost and hamper the process flexibility.

In this presentation, we show the design and manufacturing of fully functioning compact size PEALD station using ICP plasma chamber. Systematic mechanical design process was applied including quality function deployment (QFD), fluid/thermal analysis, and 3D modeling. In the system manufacturing process, gate valve and stop valve have been modified to increase the versatility of the process conditions as well as the possible deposition of many more materials. In addition, the electrical biasing table was added to the system to control the characteristics of the plasma such as the density and flux of ions, and therefore the crystallinity of the film. Furthermore, the biasing table can be further applied for selectively functionalizing the 2-dimensional materials, e.g., graphene, on metal-patterned substrate, and accordingly selectively depositing ALD films on them. As a result, PEALD station that we have designed and manufactured can provide economic options for researchers who want to explore PEALD processes for novel applications.

AM-MoP6 ACS™ (Atomically Clean Surface™) Cleaning and Analytical Validation of Recycled ALD Chamber Parts for the Semiconductor Industry*, **Russell Parise**, I. Iordanov, B. Quinn,* UCT - QuantumClean*; P. Sun,* UCT - ChemTrace

ALD deposition has enabled the semiconductor industry to deposit thin, highly conformal films. Foundational to delivering the consistent film quality is managing the quality of the parts within the chamber, especially the recycled parts sent offsite for cleaning. It is an under-recognized challenge to reliably produce "certifiably" clean chamber parts. The highly conformal, high step coverage nature of ALD process results in surface deposits on the parts that are tightly adhered. Additional considerations include: parts fragility, part size, high number of ALD film chemistries, and maintaining tight dimensional tolerances.

To address these challenges, recycled part cleaning processes and metrology validation methods have been developed. The processes are non-destructive and provide for an Atomically Clean Surface™ (ACS™) that meets the micro contamination requirements of the most stringent processes. The validation scope spans impurities identification (e.g. trace metals, particles, and trace impurities) and dimensional measurements (e.g. surface roughness, defects, flatness) via use of equipment such as ICP-MS and CMM. Handling systems to provide for employee ergonomics and to protect the parts will also be discussed with regard to the multi-wafer equipment.

In addition, there is smaller demand to refurbish of valves, fittings, and other parts external to the process chamber that may become coated or damaged. Processes have been adapted to address these components as well as ensuring critical dimensions and surface roughness of mating surfaces is maintained.

This paper will review the technologies developed to clean, rinse, dry, and validate that the recycled parts meet performance requirements for various ALD processes.

Keywords: ACS™, ICP-MS, surface cleanliness, micro contamination, non-destructive, CMM

AM-MoP8 Process Control and Mass Delivery Optimization from Low Vapor Pressure Precursors*, **Jeffrey Spiegelman**, C. Ramos, D. Alvarez, Z. Shamsi,* RASIRC

Continual device shrinkage and incorporation of new alloy materials has led to difficult thermal constraints for ALD in microelectronic applications. Process temperatures are now required to be to less than 350° C where sub-300° C is desired. PEALD has successfully been used in some applications, but has difficulty for 3D structures and aspect ratios greater than 50.

Therefore more reactive oxidant precursors for thermal ALD have been sought where water and ammonia no longer have sufficient reactivity at reduced temperatures. Examples include anhydrous Hydrogen Peroxide and Hydrazine, which exist as low vapor pressure liquids at room temperature. Delivery of a controlled and stable vapor from a liquid source is more challenging than delivering compressed gases with a mass flow controller. Due to the complex nature of chemical liquid-vapor equilibrium, it is difficult to accurately predict the vapor mass output of a liquid precursor for the wide range of ALD operating conditions when solely relying on theoretical models. The liquid phase is in constant equilibrium with its vapor phase counterpart. Slight changes in one, strongly affect the other. Transformation of a liquid to a vapor depends on:

- Ampoule headspace pressure
- Carrier gas flow rate
- Liquid precursor temperature
- ALD precursor pulsing recipe
- Saturation efficiency of the carrier gas with the precursor vapor
- Intermolecular forces and binary interactions for multicomponent liquids
- System heat transfer
- Ampoule design

A liquid precursor ALD simulation manifold was built to re-create typical ALD conditions. The system is composed of mass flow and pressure flow controllers, pressure sensors, metering valves, vapor mass flow sensors, and several pneumatic valves. Automated test programs control the valves and sensors to simulate custom ALD process recipes. Data collected from the test fixture can quantify liquid precursor/ampoule vapor mass flow rates at different process pressures, carrier gas flow rates, precursor liquid temperatures, and different pulsing recipes. Mass delivery parameters can thus be optimized for process control and material utilization.

Anhydrous hydrogen peroxide gas can be precisely delivered in the range of 20-300 mg/min at moderate temperatures and pressures. Optimized delivery for several recipes will be presented as a function of pressure and liquid temperature. Conclusions pertinent to several low vapor pressure materials will be discussed.

AM-MoP9 Scaling Low-temperature Thermal ALD of SiO_2 to Batch*, J. Kalliomäki, M. Mäntymäki, T. Lehto, S. Shukla, M. Kääriä, T. Sarnet,* ***Juhana Kostamo,*** Picosun Oy, Finland

Silicon dioxide has become an integral part of the microelectronics industry, due to the abundance of silicon, and the convenient electrical properties of the thermally formed native oxide. As a thin film, SiO_2 can also be used to tailor the mechanical properties of film stacks, act as an etch stop layer or prevent gas diffusion. In industrial manufacturing, the rate of thin film deposition is crucial. Additionally, a low temperature SiO_2 process is desirable to minimize any effect the deposition process will have on other device materials or the substrate itself.

In ALD, SiO_2 has many available chemistries, each with its own pros and cons. The chlorides and chlorosilanes require a deposition temperature of >300°C and can cause particles and chloride impurities in the films. Since these are unacceptable in industrial applications, many amine chemistries have become available. They can fulfil the growth rate, if not always the temperature requirements, required for industrial production.

In general, lower temperature processes is needed as interlayer diffusion must be avoided and the substrates are becoming more sensitive – e.g. organic or polymer substrates might require <200°C thermal budget. The simplest solution, PEALD [1], can however result in sacrificing the higher throughput possibilities that thermal batch ALD can provide. Plasma processes also exhibit limited applicability on higher aspect ratio samples, due to the short lifetime of radical species.

Achieving industrially feasible growth rates at low temperatures with thermal processes is challenging. For example, with a commonly used process such as bis(diethylamino) silane and ozone, the growth rate at 100°C is only < 0.1Å per cycle [2]. Most results in literature are also only on single wafers.

We present a reliable low temperature SiO_2 process with growth rates in excess of 1Å per cycle from 60 to 350°C, on single wafers (Figure 1) and in batches, using a precursor with 3 Si atoms and an amine group. While the film thickness increases linearly with the number of cycles, other properties will need to be a compromise between film quality and deposition temperature – a feature common to many ALD processes. In our example, the impurity content was lower at higher deposition temperatures.

The experiments were made with PICOSUN™ R-200 Adv, P-300B and P-1000 hot-wall ALD systems. Si wafers with native oxide layers were used as substrates. The ALD process, its scalability to larger batches, and various properties of the resulting thin films were evaluated in this study.

[1] Won et al. (2010), IEEE Electron Device Lett. 31 (2010)

[2] Hirvikorpi et al., Appl. Surf. Sci. 257 (2010)

Emerging Materials
Evergreen Ballroom & Foyer - Session EM-MoP
Emerging Materials Poster Session

~~**EM-MoP1 Structure and Magnetism of Electrospun α-Fe_2O_3 Nanofibers SiO_2 Coated by ALD**, *F. Pantò,* CNR-Istituto di Tecnologie Avanzate per l'Energia (ITAE), Italy; *H. Raza,* Humboldt Universität zu Berlin, Germany; *A.M. Ferretti,* CNR-Istituto di Scienze e Tecnologie Molecolari (ISTM), Italy; *C. Triolo,* Università di Messina, Italy; *A. Ponti,* CNR-Istituto di Scienze e Tecnologie Molecolari, Italy; *S. Patanè,* Università di Messina, Italy; *N. Pinna,* Humboldt Universität zu Berlin, Germany; ***Saveria Santangelo,*** Università Mediterranea, Italy~~

~~In the last years, thanks to its appealing properties (high abundance, low-cost, environmental friendliness, good chemical stability, small energy band gap) hematite has attracted considerable attention as a photocatalyst for the H_2 production. Electrospun α-Fe_2O_3 nanofibers (NFs) have been evaluated in other energy related applications potentially benefiting from their high porosity and large surface area and could also be utilized in less common ones, e.g., as a theranostic agent [1]). Besides, magnetism of nanohematite is a current topic in fundamental research. [2] A study focused on the magnetic properties of electrospun α-Fe_2O_3 NFs has shown that the fiber diameter strongly controls the magnetic behaviour [3]. Coating elongated α-Fe_2O_3 nanoparticles (NPs) by silica via sol-gel chemistry allows controlling the saturation magnetisation, remanent magnetisation and coercivity through the thickness of the coating layer [4]. ALD offers the possibility to coat NPs with well-calibrated and conformal thin films, thus in principle enabling the fine-tuning of the magnetic properties. This contribution focuses on SiO_2-coated electrospun α-Fe_2O_3 NFs and their nanostructure. The changes of the magnetic properties, with respect to pristine hematite, due to the SiO_2 coating are discussed as a function of the number of ALD cycles (10–100) and of the sequence of the production steps (i.e. calcination of the electrospun NFs followed by SiO_2-ALD or vice versa). SiO_2-ALD prior to calcination results in fibers formed by smaller α-Fe_2O_3 grains and by a higher structural disorder. Regardless of the sequence of production steps, ALD coating brings about a local rearrangement process in the oxide lattice with gradual surface defects suppression. These structural changes reflect on the magnetic NF properties, especially coercivity and remanence (Morin temperature).~~

~~[1] Chem. Mater. 26 (2014) 2105~~

~~[2] J. Magn. Magn. Mater. 475 (2019) 611~~

~~*[3] J. Phys. Chem. C 115 (2011) 17643*~~

~~[4] *Mater. Lett. 61 (2007) 5268*~~

EM-MoP2 Fluidized Bed Molecular Layer Deposition of Ultrathin Poly(ethylene terephthalate) Films on TiO_2 P25 Nanoparticles*, **Damiano La Zara**, M. Bailey, D. Benz,* Delft University of Technology, Netherlands*; M.J. Quayle, G. Petersson, S. Folestad,* AstraZeneca, Sweden*; J.R. van Ommen,* Delft University of Technology, Netherlands

Molecular layer deposition (MLD) is a vapour phase technique allowing the controlled, layer by layer growth of purely organic thin films on a wide range of substrates. To date, most MLD studies have focused on coating flat substrates, but MLD also holds significant promise for application to particles. In particular, the inherent biocompatibility of organic coatings is of interest to passivate the surface of pigment particles and to tailor the dissolution profile of drug particles. Of the organic coatings produced thus far, polyimide and polyurea coatings predominate, whereas polyester polymerisation chemistry has received considerably less attention. Amongst this class of polymers, Poly(ethylene terephthalate) (PET) is of particular interest due to its widespread industrial usage, thermal stability, and gas and moisture barrier properties stemming from the terephthalate group. The use of conventional deposition reactors operating at vacuum conditions, reported in nearly the entirety of MLD literature, hinders facile and low cost up-scaling. Therefore, the development of processes with better scale-up potential is crucial when aiming for commercial applications, especially when it concerns high-surface area powders.

In this work, we deposit ultrathin PET films on gram-scale batches of TiO_2 P25 nanoparticles (NPs) using terephthaloyl chloride and ethylene glycol as precursors. The MLD process is carried out in an atmospheric-pressure fluidized bed reactor at 150-160 °C for a broad range of growth cycles (i.e., from 5 to 50). Ex-situ diffuse reflectance infrared fourier transform spectroscopy (DRIFTS-FTIR) shows the presence of the characteristic C=O stretch of ester groups in the range 1730-1750 cm^{-1}, thus demonstrating the successful MLD reaction. DRIFTS-FTIR and thermogravimetric analysis (TGA) confirm the self-saturating behaviour of the precursors, and the linear increase in mass with the number of cycles. Moreover, TGA highlights the good thermal stability of the PET films, which are stable up to ~225 °C. Transmission electron microscopy (TEM) enables the visualization of uniform PET films on the surface of TiO_2 NPs. Preliminary TEM observations suggest a low PET growth per cycle (GPC), around 0.03-0.04 nm. This value seems also in agreement with the GPC estimated by the amount of deposited material on TiO_2 NPs measured by TGA as well as with the GPC of PET on SiO_2 wafers measured by spectroscopic ellipsometry. Finally, ultrathin PET films are effective in suppressing the photocatalytic activity of the TiO_2 P25 NPs, without affecting its absorptive properties in the UV-vis spectrum.

~~**EM-MoP3 Fabrication and Characterization of Organic-Inorganic Hybrid Thin Films***, **Chu Huong**,* Hanyang University, Republic of Korea~~

~~Currently, the next generation of electronic devices requires new materials that have great properties. The straight way to fabricate new materials is the hybridization of existing materials having different properties. The hybrid materials mixed by organic and inorganic components are expected to have combined properties both of inorganic parts, such as stability and high electrical or optical performance and organic parts with great flexibility and functionality. Furthermore, the hybrid materials are expected to have synergic effects which are not shown in just one component.~~

~~In this report, we fabricated new types of organic-inorganic hybrid thin films by molecular layer deposition. The hybrid thin films were made by sequential surface reactions of metal alkyls and bifunctional monomers. Diethylzinc and 2,4-hexadiyne-1,6-diol are used as an inorganic precursor and an organic precursor, respectively, in order to fabricate poly(zinc diacetylene). Some methods are used to characterize the microstructure and composition of the hybrid films such as Raman, XPS and TEM analysis. And, the electric and optical properties were analyzed by a TFT fabrication and photoluminescence spectroscopy, respectively. The high performance of TFTs, on/off ratio of over 10^7 and saturation electron mobility of over 10 cm2/V·s. The molecular layer deposition process can proceed under the low temperature condition that indicates the possible use of hybrid films to flexible devices.~~

EM-MoP4 High Performance Encapsulation Polymer-Al_2O_3 Hybrid Thin Layer by Atomic Layer Infiltration*, **Hong Rho Yoon**, J. Park, N.V. Long, C. Huong,* Hanyang University, Republic of Korea

Encapsulation is an important technology for isolating and protecting air-sensitive materials and is key in the development of new generation flexible electronic devices. Here we report an extremely high performance encapsulation hybrid thin layer prepared by filling the free volume of the polymer with Al2O3 using gas-phase atomic layer infiltration. The high density polymer−inorganic hybrid thin layer shows extremely low gas transmission rate, below the detection limit of the Ca corrosion test (water vapor transmission rate <10^(−7) g/m^(−2) day^(−1)). Furthermore, because of the remarkable nanometer-scale thinness of the complete polymer−inorganic hybrid, it is highly flexible, which makes it useful for encapsulation technology of new generation flexible devices.

EM-MoP5 ALD of Metal Oxides Fabricated by using $La(NO_3)_3{\cdot}6H_2O$ Oxidant and their Applications*, **In-Sung Park**, S.Y. Kim, T. Lee, S. Seong, Y.C. Jung, J. Ahn,* Hanyang University, Republic of Korea

The oxide films with high-k including Al_2O_3, HfO_2, and ZrO_2 have been widely applied to dielectric of capacitor devices in fabrication of semiconductor memory. Recently, ALD method has been widely spreading to making the ultra-thin, dense, conformal, and widely-uniform deposition areas in spite of its very low productivity. In ALD process, the selection of oxidant is very important because of the variability of film characteristics such as growth rate, ALD temperature window, crystalline structure, contamination, and dielectric/electrical properties.

In this work, the using of $La(NO_3)_3{\cdot}6H_2O$ catalytic oxidant will be focused to fabricate HfO_2 films for insulator of resistor and dielectric of capacitor. The H_2O oxidant was used to make above films for the comparison. The devices with metal-insulator-metal structure were prepared and their electrical properties were also compared.

HfO_2 films were synthesized by ALD method using $Hf(NCH_3C_2H_5)_4$ precursor and $La(NO_3)_3{\cdot}6H_2O$ solution, which is catalyst and oxidant. The growth rate of HfO_2 film made with $La(NO_3)_3{\cdot}6H_2O$ solution is approximately three times faster than that with H_2O oxidant. The $La(NO_3)_3{\cdot}6H_2O$ solution effectively altered the surface roughness, crystalline status, and resistive switching properties of HfO_2 films. In spite of the same crystalline structure of both HfO_2 films made with $La(NO_3)_3{\cdot}6H_2O$ and H_2O, the surface roughness of

HfO_2 film grown by using $La(NO_3)_3 \cdot 6H_2O$ solution oxidant is smoother than that using H_2O. Moreover, resistive switching characteristics of HfO_2 grown using $La(NO_3)_3 \cdot 6H_2O$ was enhanced not only uniformity of switching parameters but also endurance.

EM-MoP6 Bringing Higher Etch-resistance to Metal-infiltrated Polymer*,* ***Norikatsu Sasao****, K. Asakawa, S. Sugimura,* Toshiba Memory Corporation

Infiltration synthesis is an emerging technology that enables to realize organic-inorganic hybrid materials. The gaseous metal precursors penetrate into polymers followed by oxidation process, which stabilizes the metal derivatives into the polymer-matrix. Up to date, many fundamental studies have been carried out on the infiltration of trimethylaluminum(TMA) into polymethylmethacrylate(PMMA) thin films[1][2]. There has also been reported that TMA is selectively infiltrated to PMMA phase of the phase-separated block copolymer of PMMA and polystyrene, where etch-resistance of infiltrated PMMA is remarkably increased[3].

Although literatures show that TMA readily coordinates onto carbonyl group of the acrylate unit, the density of the resulting aluminum derivatives in PMMA is eliminated to the density of carbonyl groups. By increasing the carbonyl density in the monomeric unit of the polymer, we can expect to have higher aluminum content in the polymer after the infiltration process which could result in higher etch-resistance.

Recently we have synthesized a polymer having two or more carbonyl groups branched on the main-chain to increase carbonyl density compared to PMMA. Evidences show that TMA was infiltrated into the polymer at a higher density compared to that of PMMA and the etch-resistance increased as the aluminum content increased. Our novel strategy shows further pathways for future applications.

[1] M. Biswas, J. A. Libra, S. B. Darling, and J. W. Elam, "New Insight into the Mechanism of Sequential Infiltration Synthesis from Infrared Spectroscopy," *Chem. Mater*., 2014, 26, 6135

[2]E. C. Dandley, C. D. Needham, P. S. Williams, A. H. Brozena, C J. Oldham and G. N. Parsons, "Temperature-dependent Reaction Between Trimethylaluminum and Poly(methyl methacrylate) during Sequential Vapor Infiltration: Experimental and *abinitio* Analysis," *J. Mater. Chem. C.*, 2014, 2, 9416

[3] R. Ruiz, L. Wan, J. Lille, K. C. Patel, E. Dobisz, D. E. Johnston, K. Kisslinger and C. T. Black, " Image Quality and Pattern Transfer in Directed Self Assembly with Block-selective Atomic Layer Deposition," *J. Vac. Sci. Technol. B*, 2012, 30(6), 06F202

~~**EM-MoP7 Magnetic and Electric Properties of Atomic Layer Deposited ZrO_2-based Thin Films***, **Kristjan Kalam**, H. Seemen, P. Ritslaid, T. Jõgiaas, M. Rähn, A. Kasikov, A. Tamm, K. Kukli, M. Mikkor,* University of Tartu, Estonia*; J. Link, R. Stern,* National Institute of Chemical Physics and Biophysics, Estonia*; S. Dueñas, H. Castán,* University of Valladolid~~

~~Multiferroic materials of simple stoichiometry may have prospective applications in memory and sensor technologies, especially if they could be produced at low temperatures over large-area substrates by ALD. Tetragonal or cubic sputtered ZrO_2 has found to be ferromagnetic [1], and, when combined with HfO_2 by ALD, behaved as a ferroelectric material [2]. Therefore, it is of interest to investigate if ZrO_2 coupled with another metal oxide would exhibit both ferroelectric and ferromagnetic hysteresis behavior in the same material sample.~~

~~We have studied, for instance, ZrO_2-Fe_2O_3 [3], ZrO_2-HfO_2 [4] and ZrO_2-Co_2O_3 [5] mixed layers or nanolaminates grown by ALD from $ZrCl_4$, $FeCp_2$, $HfCl_4$, $Co(acac)_3$, H_2O and/or O_3 mostly at 300 °C. The composition of the films could be controlled by varying the ratio of constituent metal oxide cycles. Structural evaluation revealed dominantly tetragonal or cubic ZrO_2. All oxides, as deposited, exhibited magnetization field behavior characteristic of that in ferromagnetic materials. Most of the films in as-deposited states also showed certain remnant charge polarization in their charge field dependences. The behavior could be strongly influenced by the charge transport and interfacial charge trapping. Certain ferroelectric component contributing to the polarization could not be neglected, although the charging was probably overwhelmed by leakage currents. Nonetheless, in some films, in particular ZrO_2-HfO_2, hysteresis loops implying both ferromagnetic and ferroelectric components in the materials could be observed. In this presentation, performance of different oxides as potential multiferroic host materials will be comparatively discussed.~~

~~[1] S. Ning and Z. Zhang, RSC Adv. 5 (2015) 3636.~~

~~[2] S. L. Weeks *et al*. ACS Appl. Mater. Interfaces, 9(15), 13440 (2017).~~

~~[3] K. Kalam *et al*., Beilstein J. Nanotech. 9 (2018) 119.~~

~~[4] K. Kalam, et al, ECS J. Solid State Sci. Technol. 7.9 (2018): N117-N122.~~

~~[5] K. Kalam, et al., Thin Solid Films 669 (2019) 294-300.~~

~~**EM-MoP8 Vapor Phase Infiltration as a New Approach in the Fabrication of Advanced Hybrid Thermoelectric Materials***, **Jaime DuMont**, M. Knez,* CIC nanoGUNE, Spain~~

~~Hybrid organic-inorganic materials are rising stars in the field of thermoelectrics (TE), whose principal aim is to salvage the rejected heat of energy conversion processes by directly converting waste heat into electricity. With two-thirds of the 160 TWh required for global power consumption lost to the environment each year, the development of flexible, non-toxic, inexpensive and scalable TE materials would be of great economic and environmental interest. Realizing this ambition will require a new approach that can break away from the rare, toxic and expensive materials that have dominated the field until now.~~

~~This next generation of hybrid TE materials will require a synthesis strategy which 1) functions at temperatures low enough to not destructively act on the polymer 2) can tune the electrical and thermal conductivity of the hybrid material for optimal TE performance 3) maintain a strong chemical binding between the organic and inorganic components for long term stability and operational efficiency and 4) can be easily scaled for large-area applications. Vapor phase infiltration (VPI) is a technique primed to meet these requirements. In this work we will survey VPI processes of various transition metal compounds as a tool for the top-down fabrication of metal-poly(3-hexyl)thiophene (P3HT) hybrids as promising candidates for advanced TE materials. By monitoring the electrical conductivity and thermopower of these novel hybrid materials, we will show how the VPI process can be used to generate and optimize a new set of thermoelectric materials.~~

EM-MoP9 Low-temperature Atomic Layer Deposition of Aluminum Oxide on Polymeric Powder Feedstocks for Improved Powder Rheology*,* ***John Miller****, C. Gillespie, J. Chesser,* Lawrence Livermore National Laboratory*; A. Scheppe,* United States Air Force Academy*; A. Nelson, N. Teslich, A. Lange, S. Elhadj, R. Reeves,* Lawrence Livermore National Lab

Some organic materials of interest in the additive manufacturing industry require inkjet/colloid based processes to avoid degrading the properties of the material of interest. Some of these organic feedstocks are cohesive in nature and tend to form agglomerates in suspensions, making them undesirable for use in additive manufacturing printing processes. Atomic Layer Deposition (ALD) can be used as a technique used to change the surface property of the material without changing the property of the bulk material of interest. ALD sequentially pumps reactive precursors into and out of a reactor vessel, which react on the surface of a desired substrate to form films with sub-nm level control. This paper studies the reduced temperature ALD deposition of aluminum oxide on polyimide/Si reference flats and melamine and nylon organic powder feedstocks for coating quality and its effect on the powder rheology and cohesivity. The result is a mixed amorphous phase aluminum oxide-hydroxide coating that is both highly uniform and conformal on the powder's surface. Alumina coatings on the nylon powders did not produce a significant change in the flow properties of the powder, due to the initial low cohesivity of nylon. The melamine however experienced significant improvements to flowability due to a reduction in cohesivity of the melamine feedstocks from the surface coating. Results show that thin coatings of 20 nm or less on these feedstocks can remarkably improve their surface chemistry for use in additive manufacturing processes.

IM Release Number: LLNL-ABS-767926

EM-MoP10 Atomic Layer Deposition of Molybdenum Oxide Carbide and Molybdenum Carbide Films*,* ***Michael D. Overbeek****, C.H. Winter,* Wayne State University

The atomic layer deposition (ALD) of Mo(O,C) and MoC films is described using $MoCl_5$ and the co-reactants oxalic acid or formic acid. Self-limited ALD growth was demonstrated at 350 °C for $MoCl_5$ and oxalic acid, however, the growth rate decreased at long $MoCl_5$ doses, consistent with etching. The growth rate of the $MoCl_5$ and oxalic acid process was 0.18 Å/cycle within an ALD window of 325-400 °C. The resistivities of the films decreased with increasing deposition temperature and was 366 μΩ cm for an 18 nm thick film grown at 400 °C. A plot of thickness versus number of cycles was linear with no nucleation delay. X-ray diffraction of the as-deposited films was consistent with nanocrystalline Mo(O,C). Atomic force microscopy of 18 nm thick films grown with $MoCl_5$ and oxalic acid in the ALD window gave RMS roughnesses of 0.49-0.56 nm, indicating very smooth surfaces. X-ray photoelectron spectroscopy (XPS)

showed Mo, O, and C in the films, with low levels of other elements. The films obtained using $MoCl_5$ and oxalic acid are thus Mo(O,C). Formic acid was also used with $MoCl_5$ as a co-reactant, since oxalic acid decomposes thermally at high temperatures to formic acid and CO_2. A plot of growth rate versus pulse length showed self-limited growth at 400 °C, but a plot of growth rate versus deposition temperature did not show an ALD window between 400-450 °C. Films grown with formic acid at 400 and 450 °C with thicknesses of 28.5 and 48.1 nm, respectively, showed RMS roughnesses between 0.55 and 0.88 nm. XPS of a film grown using $MoCl_5$ and formic acid at 450 °C showed a composition of MoC, with low oxygen and chlorine levels. The resistivity of a 48 nm thick MoC film grown at 450 °C with 1000 cycles was 177 μΩ cm.

EM-MoP11 Solid Phase Epitaxy of ALD-Grown $PrAlO_3$ Films*, **Navoda Jayakodiarachchi**, W.L.I. Waduge,* Wayne State University*; Y. Chen, P. Zuo, T.F.T. Kuech, S.E. Babcock, P.G. Evans,* University of Wisconsin-Madison*; C.H. Winter,* Wayne State University

An atomic layer deposition (ALD) process is reported for the growth of PrAlO3 thin films using tris(isopropylcyclopentadienyl)praseodymium (Pr(C5H4iPr)3), trimethylaluminum (AlMe3), and water. Pr(C5H4iPr)3 was chosen as a precursor because of its good volatility, high thermal stability, and high reactivity with water. Pr(C5H4iPr)3 was first evaluated as a precursor for the formation of Pr2O3 films using water as the co-reactant. Self-limited growth was demonstrated for pulse lengths of ≥3 s, with a growth rate of ~0.85 Å/cycle. An ALD window was observed between 275 and 350 °C, and the as-deposited Pr2O3 films were crystalline. The ALD growth PrAlO3 films was examined next on Si(100) and SiO2 substrates. Self-limited growth was demonstrated for Pr(C5H4iPr)3), AlMe3, and water at 300 °C using a 1:1 ratio of Pr(C5H4iPr)3) and AlMe3 pulses. An ALD window was observed from 275 to 325 °C with a growth rate of ~1.7 Å/cycle. The increase in film thickness as a function of the number of cycles at 300 °C was linear and showed a small nucleation delay. The as-deposited PrAlO3 films were amorphous, had smooth surfaces, and contained <0.5% carbon and chlorine, as analyzed by grazing incidence wide-angle X-ray scattering, X-ray reflectivity and atomic force microscopy, and X-ray photoelectron spectroscopy, respectively. The films grown with a 1:1 ratio of Pr(C5H4iPr)3) and AlMe3 pulses were slightly aluminum-rich (Pr:Al ~1.2-1.4) by electron probe microanalysis. As deposited PrAlO3 films grown on single crystal (100) SrTiO3 substrates at 300 °C were amorphous and annealing at 800 °C for 3 h resulted in fully crystallized PrAlO3 films. The crystallized PrAlO3 films were highly (001)-orientedwith a small population of polycrystalline grains with other orientations. The PrAlO3 00L and SrTiO3 00L reflections appeared on the same rod of reciprocal space, further indicating that the amorphous PrAlO3 film transforms into an epitaxial layer. The rocking curve width of the PrAlO3 (001) reflection was 9°. By contrast, PrAlO3 films deposited on Si(100) substrates with native SiO2 remained amorphous after annealing at 1000 °C for 8 h. The difference in the crystallization between PrAlO3 layers deposited on crystalline SrTiO3 and amorphous native SiO2 substrates indicates that PrAlO3 on SrTiO3 crystallized by solid phase epitaxy, in which the nucleation and orientation of the crystallized layer is set by the substrate.

EM-MoP12 Homogenous Distribution of Dopants in ALD Films: Tin-Doped Zinc Oxide (ZTO) Case Study*, **Triratna Muneshwar**, D. Barlage, K. Cadien,* University of Alberta, Canada

ALD is a well-established thin film deposition technique where the material growth stems from the stacking of partial atomic monolayer in each surface reaction step. Being a bottom-up approach, doping of ALD could be readily achieved from introduction of dopant species during growth. For example, the most common approach for deposition of B-doped AO oxide growth, is to periodically deposit oxides AO with n_1 cycles and BO with n_2 cycles (super-cycle: $n_1 \cdot AO + n_2 \cdot BO$). Although the relative A/B content is precisely controlled with n_1 and n_2, the resulting multilayered structure would have a non-homogeneous dopant-B distribution (hence may require additional processing steps like annealing, ion bombardment, etc.). To overcome this limitation we demonstrate a method for homogeneously doped ALD films with BAOBAO… pulsing sequence. We show that the choice of dopant precursor, process parameter and also the sequence (ABO… or BOA…) are critical in controlling dopant concentration. As example we report our early results on tin-doped zinc oxide (ZTO) ALD films grown at 50 °C substrate temperature using tetraallyltin (TASn), diethyl zinc (DEZ), and a remote ICP O-plasma. We show that the pulsing sequence Sn/Zn/O gives a better control over Sn-content in ZTO films. With increasing Sn-content, measured room temperature electrical resistivity (ρ^{ele}) of as-grown ZTO films (each ~24 nm thick) was found to systematically decrease from 450 Ω-cm for ZnO, to 19.72 Ω-cm, 5.7×10^{-1} Ω-cm, and 2.8×10^{-2} Ω-cm for samples ZTO#1, ZTO#2 and ZTO#3 respectively.

EM-MoP13 Uniform, Thermal ALD of Al_2O_3 and ZnO on Zirconia Particles*, **Dhruv Shah**, D. Patel, J. O'Tani, M. Linford,* Brigham Young University

The technical literature contains relatively little on the topic of atomic layer deposition (ALD) on particles. Here we report thermal ALD of thin films of alumina and zinc oxide on zirconia powder substrates from trimethylaluminum and water, and diethylzinc and water, respectively. Very similar growth was obtained when ozone was substituted for water in these depositions. Depositions were optimized by varying the dose and purge times for the precursors with an aim to obtain uniform film thickness and growth per cycle (GPC). X-ray photoelectron spectroscopy (XPS) clearly showed an increase in surface aluminum and zinc with increasing numbers of ALD cycles. Transmission electron microscopy (TEM) showed uniform film growth and particle coverage. Film thicknesses were also measured on planar witness shards by spectroscopic ellipsometry (SE). Ultimately, up to 10 nm films of alumina and zinc oxide were grown on zirconia particles via 100 ALD cycles.

EM-MoP14 Composition Control of Ge-Sb-Te Film by Supercycles of ALD GeSb and ALD Sb Followed by Tellurization Annealing*, **Yewon Kim**, J. Lee,* Sejong University, Republic of Korea*; S.J. Baik,* Hankyong National University, Republic of Korea*; W. Koh,* UP Chemical Co., Ltd., Republic of Korea*; W.-J. Lee,* Sejong University, Republic of Korea

Phase change random-access memory (PCRAM) is getting attention as storage class memory (SCM) which is can fill the performance and cost gap between DRAM and NAND flash. Ge-Sb-Te (GST) compounds have been extensively studied due to their fast switching speed and high data retention. The GST thin films were prepared by physical vapor deposition, chemical vapor deposition and atomic layer deposition (ALD) techniques. As the mushroom structure changes to confined cell structure because of thermal interference, ALD technique is needed in order to deposit a thin film in a nano-size hole. Conventional ALD GST film was prepared with ALD GeTe and ALD Sb2Te3 supercycle. This method is complicated and deposited as amorphous during deposition, resulting in void formation during repeated PCRAM operation. In previous work, we prepared GST film by tellurization of ALD Ge-Sb. This process simplifies the supercycle ALD GST process and can form a crystalline GST thin film. Also, the incorporation of Te improves the gap fill characteristic by expanding the volume. Tellurization of the ALD Ge-Sb film could control the composition of Te by the tellurization temperature or the number of cycles, however it cannot control the composition ratio of Ge to Sb. Since the switching speed and durability of the phase change memory cell depend on the composition of the GST film, a method of controlling the composition ratio of Ge and Sb in the GST film is also required. In the present work, GST films with different compositions were prepared by ALD super-cycle process consisting of ALD Ge-Sb and ALD Sb. The composition ratio of Ge to Sb was controlled by changing the ratio of the sub-cycles. The temperature window and growth rate of ALD Ge-Sb and ALD Sb were investigated to determine the temperature and sub-cycle ratios of the super-cycle process. Ge-Sb films of different compositions were prepared by ALD super-cycle processes and then annealed in a tellurium atmosphere. The composition and phase transition temperature of the GST thin films were examined before and after the tellurium annealing. The phase transition temperature was tunable by controlling the subcycle ratio or tellurization conditions. Step coverage and gap filling characteristics were also investigated.

EM-MoP15 Study on The Crystallinity and The Dielectric Constant of $Zr_xGe_{1-x}O_2$ Films using Mixed Zr - Ge Precursor by Atomic Layer Deposition*, **Ju Young Jeong**, Y. Han, H. Sohn,* Yonsei University, Korea*; H. Noh, H. Park,* SK Hynix Inc

Scaling of Dynamic Random Access Memory(DRAM) requires high k dielectric materials for data storage capacitor. ZrO_2 is favorite material for storage capacitors becasue of large band gap, low leakage current, good thermal stability. Dielectric constant of ZrO_2 depends on the crystal structure (monoclinic =19.7, cubic = 36.8, tetragonal=46.6). It was reported that doping of ZrO_2 with elements such as Mg, Ca, Y, La, and Ge enhances tetragonal phase of ZrO_2. In general, such elements are incorporated in ZrO_2 using laminated growth structure.

In this study, Ge-doped ZrO_{-2} films were fabricated using mixed Zr-Ge precursor ($CpZr[N(CH_3)_2$

ALD Applications
Grand Ballroom E-G - Session AA1-TuM
ALD for Catalysts, Electrocatalysts, and Photocatalysts

Moderators: Jeffrey W. Elam, Argonne National Laboratory, Parag Banerjee, University of Central Florida

~~8:00am **AA1-TuM1 ALD for Solar Fuels: Rendering Halide Perovskites Acid-Compatible + Precision Cluster Electrocatalysts***, Alex Martinson, I.S. Kim, M. Pellin,* Argonne National Laboratory **INVITED**~~

~~Although solution-processable halide perovskite semiconductors exhibit optoelectronic performance comparable to the best photoabsorbers for solar fuel production, halide perovskites rapidly decompose in the presence of water or even humid air. We show that a hybrid electron transport layer, a $PC_{61}BM$ + TiO_2 film (18–40 nm thickness) grown over the sensitive absorber by atomic layer deposition, enables photo-assisted proton reduction without further encapsulation. These semitransparent photocathodes, when paired with a Pt catalyst, display continuous reduction of H^+ to H_2 for hours under illumination, even while in direct contact with a strongly acidic aqueous electrolyte (0.5 M H_2SO_4). More affordable and active catalysts for more challenging solar-to-fuels reactions (e.g. N_2 or CO_2 reduction) will require catalysts with exquisite precision. The bottom-up, selective ALD synthesis of controlled-atom-number clusters will also be discussed as a potentially powerful route to designer solar fuels catalysts.~~

8:30am **AA1-TuM3 Plasma-Assisted ALD of Cobalt Phosphate: Process Development and Electro-Catalytic Activity Towards Oxygen Evolution Reaction***, V. Di Palma,* Eindhoven University of Technology, Netherlands*; G. Zafeiropoulos, R. van de Sanden,* Dutch Institute for Fundamental Energy Research*; W.M.M. Kessels,* Eindhoven University of Technology, Netherlands*; M. Tsampas,* Dutch Institute for Fundamental Energy Research*; **Mariadriana Creatore,*** Eindhoven University of Technology, Netherlands

Water splitting is a viable approach to enable storage of renewable energy in the form of fuels. Major issues hampering the development and implementation of this technology, are: the high cost associated with the use of noble-metal-based electro-catalysts; the sluggish kinetics of the oxygen evolution reaction (OER). Cost-effective, transition metal- based electro-catalysts [1], e.g. cobalt phosphate (CoPi), show promising results in terms of performance towards OER. So far, CoPi has been synthesized by electro-deposition with severe limits in the control of layer thickness and chemical composition, the latter being highly influenced by the choice of precursors, electrolyte and pH. Instead, a higher level of control in terms of layer thickness and tunable stoichiometry is expected when adopting ALD.

In the present work we synthesize CoPi thin films by plasma-assisted ALD [2]. The process is based on an ABCD scheme, where A and C are the cobaltocene (CoCp) and trimethylphosphate (TMP) exposure steps. B and D correspond to O_2 plasma steps. CoPi layers, characterized by a stoichiometry of $Co_{3.2}(PO_{4.3})_2$, are deposited at 300°C with a growth per cycle of 1.1 Å, as determined by *in-situ* spectroscopic ellipsometry. Cyclic voltammetry shows that the ALD CoPi layer exhibits a current density peak of 1.8 mA/cm^2 at 1.8 V vs. Reversible Hydrogen Electrode (RHE). This value is comparable to those reported in literature for electro-deposited CoPi. Since cobalt is recognized in literature as reactive center governing the electrocatalytic activity [3], we also investigate the effect of Co-to-P concentration ratio on the OER. The deposition process is then based on a $(AB)_x(CD)_y$ supercycle. For just 1 extra AB cycle, accompanied by 11 cycles of CoPi (x= 12; y= 11), a Co-rich stoichiometry ($Co_{3.8}(PO_{4.7})_2$) is achieved. The latter leads a higher current density peak (2.9 mA/cm^2 at 1.8 V vs RHE) than the earlier addressed CoPi sample. When comparing the performance of the ALD Co-rich CoPi layer with electro-deposited CoPi [4] in terms of current density, the former exhibits superior OER performance. These results highlight the role that stoichiometry of cobalt phosphate has on its OER activity, suggesting that tuning the Co-to-P ratio can be adopted as approach to design efficient Co-based electro-catalysts for OER.

[1]M.W. Kanan, D.G. Nocera, *Science* 321, 1072 (2008)

[2] V. di Palma *et al*., Electrochemistry Communications 98, 73 (2019)

[3] J. Surendranath *et al*., *J. Am. Chem. Soc*., 132, 13692 (2010)

[4] K. Klingan *et al*., ChemSusChem 7, 1301 (2014)

8:45am **AA1-TuM4 Improved Electrochemical Activity of Pt Catalyst Fabricated by Vertical Forced-Flow Atomic Layer Deposition***, **Tzu-Kang Chin**, T.-P. Perng,* National Tsing Hua University, Republic of China

Currently, carbon black is the most commonly used support material for depositing platinum (Pt) nanoparticle catalyst by wet chemical reduction of Pt salts in aqueous solution. However,oxidation of carbon black occurs under highly humid atmosphere and corrosive operating condition of proton exchange membrane fuel cell (PEMFC), which results in agglomeration of Pt nanoparticles, leading to degradation of catalytic performance. In addition, Pt nanoparticles fabricated by wet chemical reduction require additional steps to purify, such as removing the residual capping agent, and post-treatment to increase the crystallinity of Pt. Consequently, it is urgent to develop a novel support material with high electrical conductivity and electrochemical stability and a more facile fabrication method for Pt catalyst. Titanium oxynitride (TiO_xN_{1-x}) is an intermediate phase which is regarded as a solid solution of titanium nitride (TiN) and the cubic titanium oxide (TiO). It has been reported that the Pt deposited on TiO_xN_{1-x} results in significant enhancements of specific activity, mass activity, and corrosion resistance compared to that deposited onto carbonous support material. Atomic layer deposition (ALD) is a dry process that is able to deposit materials without contamination from capping ligands and residual organic compounds. Pt catalyst prepared by ALD has advantages of high activity and precise particle size control. However, the uniformity and conformity of the coating by conventional ALD equipment on high aspect-ratio or porous substrate is still a great challenge to overcome. To solve this problem, a novel forced-flow configuration was designed recently by our group, i.e., vertical forced-flow ALD. In this study, conductive TiO_xN_{1-x} nanoparticles were fabricated and investigated for the potential application in PEMFC as a catalyst support material. Vertical forced-flow ALD was utilized to deposit Pt nanoparticles with very small particle size uniformly on TiO_xN_{1-x}. The electrochemical activities were examined by cyclic voltammetry and oxygen reduction reaction. The Pt nanoparticles deposited on TiO_xN_{1-x} with 30 cycles show 2-3 times higher electrochemical surface area and also larger half-wave potential of oxygen reduction reaction than those of Pt prepared by conventional wet chemical reduction and commercial E-tek electrocatalyst.

9:00am **AA1-TuM5 Improved Catalyst Selectivity and Longevity using Atomic Layer Deposition***, C. Marshall,* Argonne National Laboratory*; A. Dameron, R. Tracy,* Forge Nano*; C. Nicholas, L. Abrams, P. Barger,* Honeywell UOP*; T. Li, **Lu Zheng**,* Argonne National Laboratory

Introduction

Many important industrial scale chemical reactions rely on catalysts and require high temperatures to achieve commercially viable product yields. However, catalysts deactivate over time and lose surface area due to thermal degradation (sintering), fouling, and poisoning. Decreased catalytic activity results in lower selectivity and higher yields of unwanted byproducts. In many cases, the remedy for sintering of metals is to raise the reactor temperature and thus increase energy consumption, or to remove and replace the spent catalyst, which is expensive and leads to loss in productivity.

This project is overcoming catalyst degradation issues via an ALD overcoating technology that deposits protective layers around the active metal, preserving catalyst integrity under reaction conditions. The ALD overcoating technique applies one or more protective layers to the catalyst to inhibit metal sintering. Channels introduced into the ALD layers provide reactants with access to the catalyst's active metal and improve reaction selectivity. This project is applying the overcoating technology to extruded platinum-based catalysts used in the propane dehydrogenation (PDH) to propylene. Improvements in both the efficiency and selectivity reduce the energy required for the process.

Materials and Methods

Alumina extrudates were synthesized by peptizing Versal-251 and extruding it into 1/16" cylinders. The dried extrudates are calcined at temperatures ranging from 500ºC to 1185ºC to generate Al_2O_3 bases with varying surface area and porosity. Pt is impregnated via standard incipient wetness techniques.

ALD is performed in fixed bed reactors typically at 200 °C during all depositions. Precursors for Al_2O_3 were TMA and H_2O, while for TiO_2 they were $TiCl_4$ and H_2O. Depositions are monitored in situ by measuring the reaction composition downstream of the reactor with a quadrupole mass spectrometer.

Results and Discussion

The project team applied overcoatings with different shell thicknesses and compositions. Initial investigations were carried out with $TiCl_4$ to distinguish overcoated layers from the catalyst base. The growth rate of TiO_2 measured by ellipsometry is 0.4Å/cycle, which is similar to previously reported studies. The $TiCl_4$ dose and soak time were then increased simultaneously until the Ti loading reached saturation on 1/16" Al_2O_3 extrudates. We report that loading of Ti after one cycle is 4.5%. No crystalline TiO_2 phase is visible in XRD.

We investigated, and report on, the effect of these overcoated layers on the propane dehydrogenation reaction rate, selectivity and catalyst deactivation.

9:15am **AA1-TuM6 Enhancing Co_2C Activity for C_{2+} Oxygenate Production from Syngas using ALD Promoters***, **Sindhu Nathan**, J. Singh, A. Asundi, S.F. Bent,* Stanford University

Residential, transportation, and industrial needs have led to a reliance on nonrenewable energy sources, which has contributed to the rising greenhouse gas concentration in the atmosphere and a subsequent rise in global temperature.The scarcity of nonrenewable fossil fuels and the continually growing demand for energy necessitates the search for renewable and carbon neutral energy sources. One promising pathway is to catalytically convert molecules like CO and H_2 (syngas), which can be generated renewably, to fuels like ethanol or other higher oxygenates which produce fewer emissions than traditional fossil fuels.

Modified cobalt nanoparticle catalysts are of interest for this reaction. Cobalt, a prevalent Fischer-Tropsch catalyst, readily converts syngas to linear hydrocarbons. Much work has been done to direct the selectivity of cobalt towards higher oxygenate production, but there has been little success in engineering a practically useful catalyst. Nanoparticle catalyst activity and selectivity are influenced by interaction with the support and any other metal or metal oxide promoters that interact with the metal surface. Atomic layer deposition (ALD) offers the capability of depositing precise amounts of modifying material on catalyst nanoparticles, allowing atomic-level control over surface composition, which in turn enables better understanding of the catalyst surface.

Prior work has shown that modifying Co with ZnO ALD (using diethylzinc and water) causes restructuring of metallic Co to Co_2C on SiO_2-supported catalysts, and further modifies the carbide, resulting in enhanced oxygenate selectivity but significantly lowered activity [1]. In this work, we investigated whether Co/Co_2C activity towards higher oxygenates could be enhanced by varying the support of ZnO-modified Co. The modified Co on most of the tested supports also showed restructuring to Co_2C. However, these alternate support materials did not enhance the oxygenate activity compared to the ZnO-modified Co/SiO_2. In contrast to the other materials, we found that ZnO-modified Co/Al_2O_3 did not carburize, but that the activity of the catalyst was much greater than Co/SiO_2. To combine this activity improvement with the selectivity of Co_2C, Al_2O_3 ALD (using trimethylaluminum and water) was applied to ZnO-modified Co/SiO_2. The additional Al_2O_3 ALD enhanced the activity of the Co/Co_2C catalysts, and an Al_2O_3 ALD support modifier improved the turnover frequency of ZnO-modified Co/SiO_2 by four times. By using ALD modifying layers, the activity of Co/Co_2C catalysts towards higher oxygenates can be improved while retaining enhanced selectivity.

[1] J. A. Singh et al., *ChemCatChem*. **2018**, 10, 799.

9:30am **AA1-TuM7 Atomic Layer Deposition of Bismuth Vanadate Core-Shell Nanowire Photoanodes***, **Ashley Bielinski**, S. Lee, J. Brancho, S. Esarey, A. Gayle, E. Kazyak, K. Sun, B. Bartlett, N.P. Dasgupta,* University of Michigan

Photoelectrochemical (PEC) water splitting is a direct route for capturing solar energy and storing it in the form chemical bonds. Bismuth vanadate (BVO) is one of the most promising photoanode materials for water oxidation. It has a bandgap of 2.4 eV, which enables visible light absorption and its bands are favorably positioned for water oxidation. BVO has demonstrated potential for high anodic photocurrents, but it is limited by electron-hole separation, charge transport, and water oxidation kinetics. The development of an ALD process for BVO enables core-shell architectures that help address the charge transport and carrier separation challenges by decoupling carrier diffusion and light absorption lengths.

In this study we demonstrate the deposition of ALD BVO using $Bi(OCMe_2{}^iPr)_3$ as the bismuth source, vanadium(V) oxytriisopropoxide as the vanadium source, and water as the oxidant [1]. The choice of this Bi precursor provides full control of Bi:V stoichiometry. The BVO films were deposited as a nanolaminate of binary bismuth and vanadium oxides and then post-annealed to achieve the photoactive monoclinic $BiVO_4$ phase. Film composition and photocurrent were investigated as a function of deposition pulse ratio and film thickness. Additionally, we demonstrate 3D nanostructured BVO photoanodes by depositing the BVO on ZnO nanowires with an ALD SnO_2 interlayer.

The photoactivity of the ALD BVO photoanodes was measured in a three-electrode cell under simulated AM1.5G illumination. A planar photoanode of 42 nm thick BVO produced a photocurrent density of 2.24 mA/cm^2 at 1.23 V vs. RHE (reversible hydrogen electrode) and the application of a ZnO nanowire substrate provided a 54% increase in photocurrent to 3.45 mA/cm^2 at 1.23 V vs. RHE. These values are the highest reported to date for any photoanode using an ALD film as the primary light absorber.

[1] A. R. Bielinski, S. Lee, J. Brancho, S. L. Esarey, A. J. Gayle, E. Kazyak, K. Sun, B. M. Bartlett, N. P. Dasgupta *Submitted*

9:45am **AA1-TuM8 Improved Photocatalytic Efficiency by Depositing Pt and SiO_2 on TiO_2 (P25) using Atomic Layer Deposition in a Fluidized Bed***, **Dominik Benz**, H. Nugteren, H. Hintzen, M. Kreutzer, R. van Ommen,* Delft University of Technology, Netherlands

Photocatalysts for water cleaning typically lack efficiency for practical and economical applications. Here we present a new material that was developed using knowledge of working mechanisms of catalysts and the abilities of Atomic Layer Deposition (ALD). The deposition of ultrathin SiO_2 layers on TiO_2 nanoparticles, applying ALD in a fluidized bed reactor, showed in earlier studies in our group their beneficial effects for the photocatalytic degradation of organic pollutants. There we assume that due to the surface modification with SiO_2 the surface becomes more acidic which benefits the hydroxyl radical generation. Furthermore, we have investigated the role of Pt on P25 as an improved photocatalyst. There we found the main reason for the catalytic improvement is adsorbed oxygen on the Pt particles, which is an important reactant in the photocatalytic degradation process of organic pollutants. Having recognized, that the two independent materials, SiO_2:P25 and Pt:P25, have different mechanisms improving the photocatalytic activity gave us the opportunity to combine these two materials into a new material, where we deposited SiO_2 onto P25 followed by deposition of nanoclusters of Pt. Indeed, this new material exceeded the performance of the individual SiO_2:P25 and Pt:P25 catalysts. This unconventional approach shows that by understanding the individual materials' behavior and using ALD as an appropriate deposition technique, new materials can be developed, further improving the (photo-)catalytic activity and moving one step closer to implementation. We will demonstrate that ALD is an attractive technology to produce the catalysts developed by this approach in a precise and scalable way.

ALD Applications
Grand Ballroom E-G - Session AA2-TuM

ALD for Batteries I

Moderators: Neil P. Dasgupta, University of Michigan, Noemi Leick, National Renewable Energy Laboratory

10:45am **AA2-TuM12 Atomic Layer Deposition of Glassy Lithium Borate-Carbonate Electrolytes for Solid-State Lithium Metal Batteries***, E. Kazyak, A. Davis, S. Yu, K.-H. Chen, A. Sanchez, J. Lasso, T. Thompson, A. Bielinski, D. Siegel, **Neil P. Dasgupta**,* University of Michigan

Solid electrolytes could enable significant improvements in the energy density, cycle life, and safety of next-generation battery chemistries. The ability to fabricate thin electrolyte films with high ionic conductivity and electrochemical stability on complex architectures has been a bottleneck to realizing a wide range of 3D structured thin-film and bulk batteries. Recent progress in ALD for solid electrolytes has shown great promise, and there is significant interest in realizing materials with even higher conductivities and stability with Li metal anodes in order to dramatically enhance the energy density of ALD-based batteries. In addition, ALD films with high ionic conductivity and good stability could be used for interfacial engineering of bulk-type solid and liquid based batteries to improve stability and safety.

This work demonstrates a novel ALD process for glassy lithium borate-carbonate thin films with ionic conductivities above 10^{-6} S/cm at 298K [1]. This is the highest reported value to date for any ALD-deposited solid electrolyte. The composition, structure, and stability of the films are characterized with X-ray photoelectron spectroscopy and a range of electrochemical measurements. These experiments are compared with

those calculated with Density Functional Theory and Molecular Dynamics to elucidate the origins of the high ionic conductivity and excellent stability. The film properties are studied as a function of ALD deposition temperature, showing tradeoffs between process conditions and performance, and demonstrating the precise control afforded by the ALD process. The optimized film remains an ionic conductor when in contact with metallic Li, with no measurable changes after several weeks, and displays stable cycling when paired with a thin-film cathode and Li metal anode. This new ALD material and process represents a pathway towards interfacial engineering of both thin-film and bulk solid-state batteries, enabling stable cycling against Li metal anodes.

1) Kazyak, E.; Chen, K. H.; Davis, A. L.; Yu, S.; Sanchez, A. J.; Lasso, J.; Bielinski, A. R.; Thompson, T.; Sakamoto, J.; Siegel, D. J.; Dasgupta, N. P. *J. Mater. Chem. A* **2018**, *6*, 19425–19437.

11:00am **AA2-TuM13 ALD Interlayers for Stabilization of $Li_{10}GeP_2S_{12}$ Solid Electrolytes Against Li Metal Anodes***, **Andrew Davis,*** University of Michigan*; K. Wood,* National Renewable Energy Laboratory*; R. Garcia-Mendez, E. Kazyak, K.-H. Chen, J. Sakamoto,* University of Michigan*; G. Teeter,* National Renewable Energy Laboratory*; N.P. Dasgupta,* University of Michigan

Solid-state batteries based on high-ionic-conductivity solid electrolytes are a promising technology to increase battery lifetime and capacity, and reduce safety concerns associated with flammability. In recent years, sulfide solid electrolytes such as $Li_{10}GeP_2S_{12}$ (LGPS) have achieved ionic conductivities comparable to or higher than that of traditional liquid electrolytes. Despite these promising breakthroughs, realization of sulfide solid-state batteries with high capacities and energy densities has proved elusive. This can be attributed to the narrow electrochemical stability window of sulfide electrolytes, which leads to undesirable reactions at the electrode/electrolyte interface against both high voltage cathode materials and Li metal anodes. This forms an unstable solid electrolyte interphase (SEI), which dramatically degrades battery performance. Artificial SEIs made of ALD interlayers have recently been explored as a method of increasing stability of the Li metal/solid electrolyte interface. ALD allows for conformal, pinhole free coating of the LGPS which protects the surface from direct contact with lithium metal while facilitating Li-ion transport across the interface.

In this study, we explore the impact of ALD interlayers at the LGPS-Li metal interface, in order to gain a deeper fundamental understanding of the dynamic evolution of the SEI. A multi-modal characterization approach was performed that combined electrochemical measurements*, operando* X-ray photoelectron spectroscopy (XPS), *in-situ* auger spectroscopy, scanning electron microscopy (SEM), and optical microscopy. This allowed for quantitative evaluation of the time-dependent degradation of the interface, which occurs due to the evolution of a variety of decomposition by-products. ALD coated samples exhibited significantly less decomposition of the LGPS interface. *Operando* XPS was used to correlate the distinct decomposition products that correspond to increases in overpotential [1]. Auger, SEM and optical mapping of the surface shows spatial inhomogeneities that lead to preferential Li plating and corresponding $Li_{10}GeP_2S_{12}$ breakdown. These observations were rationalized in the context of bulk solid-state batteries employing Li metal anodes, demonstrating the advantages and challenges associated with ALD modification of solid-state battery interfaces.

K. N. Wood, K. X. Steirer, S. E. Hafner, C. Ban, S. Santhanagopalan, S.-H. Lee, G. Teeter, *Nature Communications* **9**, 2490 (2018).

11:15am **AA2-TuM14 ALD and MLD on Lithium Metal – A Practical Approach Toward Enabling Safe, Long Lasting, High Energy Density Batteries***, **Andrew Lushington,*** Arradiance*; Y. Zhao, L. Goncharova, Q. Sun, R. Li, X. Sun,* University of Western Ontario, Canada

Global warming and rising levels of atmospheric CO_2 have resulted in a rapid search for alternative energy sources. Among the possible portable energy storage systems available, lithium-based batteries have the highest theoretical energy density. Unfortunately, current battery technology is approaching its limits and research toward alternative battery chemistries with higher energy density, such as Li-S, Li-O_2 and all solid-state batteries, is required to meet future energy storage demands. However, these next-generation batteries require the use of a pure Li-metal anode .[1] Li-metal has a high specific capacity of 3860 mAh g^{-1}, a value 10x greater than the standard graphite anode (370 mAh g^{-1}) used today. Unfortunately, Li-metal is highly reactive and forms a high surface area mossy-like reaction product with the electrolyte, known as the solid electrolyte interface (SEI). The uncontrolled growth of this SEI rapidly consumes liquid electrolyte, drying up the battery and causing it to quickly fail. This problem is further exacerbated by dendrite growth which can short circuit the battery, posing a significant safety threat.[2] One effective strategy for mitigating these problems is to use Atomic layer deposition (ALD) and molecular layer deposition (MLD) to coat the surface of electrodes. This strategy has been shown to help form a stable SEI layer and improve battery longevity.[3]

Herein we compare the stripping and plating behavior of Li-metal coated using 3 different ALD and MLD films. Galvanostatic cycling revealed that MLD coated electrodes vastly outperform ALD coated ones. We use Gravimetric Intermission Titration Technique (GITT) to carefully analyze the voltage behavior of coated electrodes and disseminate the key MLD film properties that enable the formation of a stable SEI layer. Additionally, electrode morphology was examined using scanning electron microscopy along with Rutherford backscattering spectroscopy to reveal the composition of the SEI. To further demonstrate the practicality of MLD coated Li-metal, full cell batteries using lithium iron phosphate and carbon-sulfur as a cathode was performed. This presentation provides the necessary fundamental understanding of the hurdles that face the commercialization of lithium metal anodes and how ALD/MLD can be used to address these challenges.

1. Lin, D., Liu, Y. & Cui, Y. Reviving the lithium metal anode for high-energy batteries. *Nat. Nanotech.* **12**, 194–206 (2017).

2. Palacín, M. R. & De Guibert, A. Batteries: Why do batteries fail? *Science.***351**, (2016).

3. Zhao, Y. et al. Robust Metallic Lithium Anode Protection by the MLD Technique. *Small Methods.***2(5)**, 1700417 (2018).

11:30am **AA2-TuM15 Synergistic Effect of 3D Current Collectors and ALD Surface Modification for High Coulombic Efficiency Lithium Metal Anodes***, **Kuan-Hung Chen**, A. Sanchez, E. Kazyak, A. Davis, N.P. Dasgupta,* University of Michigan

Improving the performance of Li metal anodes is a critical bottleneck to enable next-generation battery systems beyond Li-ion. However, stability issues originating from undesirable electrode/electrolyte interactions and Li dendrite formation have impaired long-term cycling of Li metal anodes. In this work, we demonstrate a bottom-up fabrication process using templated electrodeposition of vertically aligned Cu pillars, which are subsequently coated by an ultrathin layer of ZnO by atomic layer deposition (ALD) to form a to form core-shell geometry with precise thickness control [1]. Transmission electron microscopy (TEM) analysis was performed to show the uniform thickness and core-shell geometry on the pillar surface. We demonstrate the application of these core-shell 3-D architectures as an efficient current collector for Li metal electro-deposition and dissolution. By rationally tuning geometric parameters of the 3D current collector architecture, including pillar diameter, spacing, length, and ALD shell thickness, the morphology of Li plating/stripping upon cycling can be controlled.

We further demonstrate the mechanistic role of the ZnO shell on current collector surface, which facilitates the initial Li nucleation, and influences the morphology and reversibility of subsequent cycling. The improved nucleation is correlated with increased wettability of molten Li metal, which is quantitively evaluated using a sessile drop test inside of an argon glovebox. The resulting core-shell pillar architecture allows for the geometry and surface chemistry to be decoupled and individually controlled to optimize the electrode performance. Leveraging the synergistic effects of the optimized 3D geometry and ALD surface modification, we have demonstrated cycling of Li metal anodes with Coulombic efficiency of 99.5%, which is among the highest reported values to date for any Li metal anode. The results from this work thus provide a pathway toward high-efficiency and long-cycle life Li metal batteries with reduced excess Li loading.

[1] K.-H. Chen, A. J. Sanchez, E. Kazyak, A. L. Davis, N. P. Dasgupta, *Adv. Energy Mater*. **9**, 1802534 (2019).

~~11:45am **AA2-TuM16 Atomic Layer Deposition FeS@CNT from Elemental Sulfur as an Electrode for Lithium-Ion batteries***, **Hongzheng Zhu**, J. Liu,* University of British Columbia, Canada~~

~~Iron sulfide (FeS) is regarded as an attractive anode material for high-performance LIBs because of its high lithium storage capability, natural abundance, and ecofriendly. However, FeS suffer from low reversible capacity and large volume change (200%) during charging and discharging process, resulting in mechanical degradation of cracking and loss of electrical connection with current collectors and then rapid capacity loss [1]. In order to overcome these problems, we choose ALD (Atomic Layer~~

~~Deposition) method to deposit a controllable thin layer on CNT to building 3D nanostructured electrode for Li ion batteries [2-3]. In this work, ALD method are chosen to realize thickness and size control of FeS, and CNTs are applied for replacing traditional carbon black to further improve the electrical conductivity and excellent physical support for the electrodes. In most of the metal sulfide ALD processes, film was deposited by using H_2S as the source of sulfur. However, H_2S is a flammable, corrosive, and highly toxic gas, and its incorporation in the ALD technology presents several serious technical challenges. Therefore, the aspiration for a new route of FeS by ALD process seems particularly strong. It is known that sulfur-based ALD processes have been reported for copper sulfide thin films recently [4]. But there is no report on FeS sulfur-based ALD process.~~

~~Here, we present a simple ALD process for the deposition of FeS thin films by using elemental sulfur as sulfur source, and test its performance in Li-ion batteries, as a highly viable solution to the challenges discussed above. The XPS spectra of the Fe 2p and S 2p regions are shown in figure a and b for FeS thin film with ALD deposited temperature at 180 °C. The Fe 2p3/2 peaks located at 710.6 and 713.0 eV belong to Fe^{2+} of FeS, which is a solid evidence for the existence of FeS. However, the FeS might partially be oxidized to $FeSO_4$. From the S 2p region in figure b, S 2p3/2 at binding energies 169.1 and 170.2 eV are belonging to SO_4^{2-}, which is the proof of FeS oxidation. Figure c shows the growth rate of FeS is ≈5.2 Å per cycle. The cyclic voltammograms (CVs) of the FeS electrode are shown in Figure d. The strong peak at 0.7 V is attributed to the decomposition of the electrolyte and formation of a solid electrolyte interlayer (SEI) in the first cathodic scan. The peak at 1.7 V in the second cathodic scan is related to the reversible interaction of Li^+ with FeS: $2FeS + 2Li + 2e^- = Li_2FeS_2 + Fe$. In the anodic sweep, the oxidation peak appear obviously at 2.5 V is attributed to the oxidation of Fe and the delithiation process of Li_2FeS_2 to form $Li_{2-x}FeS_2$.~~

ALD Fundamentals
Grand Ballroom A-C - Session AF1-TuM

In-Situ Characterization of ALD Processes

Moderators: Christophe Vallée, LTM-UGA, Erwin Kessels, Eindhoven University of Technology

8:00am **AF1-TuM1 Surface Chemistry during ALD of Nickel Sulfide***, **Xinwei Wang**,* Peking University, China

ALD of metal sulfides has recently aroused great interest, and many new sulfide ALD processes have emerged during the past several years. Surface chemistry plays a key role in ALD, but it remains yet to be investigated for many recently developed sulfide ALD processes. In this representation, I will report our study on the surface chemistry of the ALD of nickel sulfide (NiS) from a Ni amidinate precursor ($Ni(amd)_2$) and H_2S, using the in situ characterization techniques of X-ray photoelectron spectroscopy (XPS), low-energy ion scattering (LEIS), quartz crystal microbalance (QCM), and quadrupole mass spectrometry (QMS). The surface chemistry is found to deviate from the conventional ligand-exchange ALD scheme, and a formation of a nonvolatile acid-base complex from acidic surface sulfhydryl and basic amidine is suggested during the H_2S half-cycle [1]. We further investigate the initial ALD growth of NiS on a SiO_x surface, and the initial growth mechanism is found to be rather different from that in the later steady film growth. In the initial ALD cycles, the XPS results show a drastic cyclic variation of the signals for the Ni–O bonds, with prominently observable Ni–O signals after each $Ni(amd)_2$ dose but almost negligible after the subsequent H_2S dose. These results suggest that the Ni–O bonds are first formed on the surface in the $Ni(amd)_2$ half-cycles and then mostly converted to NiS in the following H_2S half-cycles. To describe this initial ALD growth process, a reaction-agglomeration mechanistic scheme is proposed [2].

References

[1] R. Zhao, Z. Guo, X. Wang, *J. Phys. Chem. C* (2018) 122, 21514.

[2] R. Zhao, X. Wang, *Chem. Mater*. (2019) 31, 445.

8:15am **AF1-TuM2 In situ and In vacuo Studies on Plasma Enhanced Atomic Layer Deposited Cobalt Films***, **Johanna Reif**, M. Knaut, S. Killge, N.A. Hampel, M. Albert, J.W. Bartha,* Technische Universität Dresden, Germany

Outstanding properties like high thermal and electrical conductivity as well as an unique magnetic behavior make cobalt thin films suitable for demanding applications in modern microelectronic devices. With physical vapor deposition (PVD) and chemical vapor deposition (CVD) techniques, it is already possible to deposit such films with high quality. However, cobalt metal film growth by atomic layer deposition (ALD) is required to satisfy conformality and thickness requirements in nanoscale devices.

In this report we will present experiments and results on the deposition of cobalt films with various plasma enhanced ALD (PEALD) processes using different standard cobalt precursors (e.g., cyclopentadienylcobalt dicarbonyl ($CpCo(CO)_2$), cobaltocene ($CoCp_2$) and tricarbonylnitrosylcobalt ($Co(CO)_3NO$)) combined with hydrogen, nitrogen, ammonia and argon based plasma gases. All our experiments were performed in a cross-flow ALD reactor, which is equipped with a capacitively coupled hallow-cathode plasma source, specially designed for the deposition of conductive films. In situ and in real-time highly sensitive quartz crystal microbalances (QCM) measurements allowed a rapid and low-cost process development. The utilized ALD reactor was clustered to an ultra-high vacuum analytic system for direct surface analysis like X-ray photoelectron spectroscopy (XPS) and scanning probe microscopy (SPM). The combination with a non-destructive analytic system enabled a sample transfer without vacuum break and thereby a direct qualification and quantification of the chemical surface composition under quasi in situ conditions. The high sensitivity of these measurements allowed investigations of interface reactions for a single PEALD pulse as well as initial film growth mechanism on different substrate materials. Furthermore we studied the impact of various cobalt precursors combined with different plasma gas compositions on the resulting film properties. The influence of process parameters (e.g., pulse times, plasma power, pressure and substrate temperature) on the film composition and film properties was also investigated. Cobalt films grown using the precursor $CpCo(CO)_2$ and H_2/N_2 plasma as coreactant showed a stable film composition of 75 at.% cobalt, 4 at.% carbon and 21 at.% nitrogen. Using scanning electron microscopy and four point probe measurements a moderate electrical resistivity of about 80 µΩcm is calculated for a 14 nm thick film.

Beyond those results in our publication we will discuss the suitability of the precursors for the deposition of high-quality cobalt films as well as the occurrence of sputtering and temperature effects due to high plasma powers.

8:30am **AF1-TuM3 Investigation of PEALD Grown HfO_2 Thin Films via Near Ambient Pressure XPS: Precursor Tuning, Process Design and a New In-situ Examination Approach for Studying Film Surfaces Exposed to Reactive Gases***, **David Zanders**,* Ruhr University Bochum, Germany*; E. Ciftyurek,* Heinrich Heine University Düsseldorf, Germany*; C. Bock, A. Devi,* Ruhr University Bochum, Germany*; K.D. Schierbaum,* Heinrich Heine University Düsseldorf, Germany

Hafnium (IV) oxide (HfO_2) is a high-k dielectric whose thin films have become a fundamental part of electronics since their commercial usage in CMOSFETs in 2008.[1] Furthermore, interest in orthorhombic HfO_2 is arising owing to the discovery of its ferroelectric nature in 2011,[2] which may lead to electronics beyond present limits.[3] Atomic layer deposition (ALD) and plasma enhanced (PE)ALD are favorable for such applications due to the low processing temperatures, precise control of thickness as well as dense and conformal coverage over complex device geometries. Furthermore, it must be ensured that films exhibit the desired stoichiometries with only low surface defect densities as the presence of surface defects, allows interactions with reactive gases and moisture that can initiate surface degradation of the dielectric, having a negative effect on its electrical properties.[4]

We report on the development of a promising PEALD process employing a precursor originating from the novel mono-guanidinato tris-alkylamido class. Four variants were subjected to thermal and chemical analysis proving their tunable volatility and thermal stability (Fig. 1). Typical ALD growth characteristics in terms of saturation, ALD window and linearity were confirmed and the growth behaviour upon variation of plasma pulse lengths was studied (Fig. 2). The obtained HfO_2 layers exhibited high quality evidenced by XRR, AFM, RBS/NRA and XPS investigations. Selected films were exposed to reactive gases such as H_2, O_2 and H_2O vapor at different temperatures and *in-situ* characterized by near ambient pressure (NAP)-XPS. Surface compositional changes and responses were monitored in a new methodical approach that has not been reported so far for thin films to the best of our knowledge. Finally, metal-insulator-semiconductor (MIS) capacitors were fabricated using HfO_2 as dielectric layer to assess its performance in device structures. This is a first report on a highly promising PEALD process for HfO_2 in a broad temperature range (60 – 240) °C developed from a new Hf precursor exhibiting optimal properties for ALD. Employing NAP-XPS is shown to be a promising development as investigations of surfaces during exposure to defined reactive gas

atmospheres leads to new in-sights into stability or triggered changes of composition and states indicating either presence, absence or formation of surface defects which strongly influence the functional properties of the layers.

[1] Ahvenniemi, E.;*et al.*; *JVST A*:**2017**, *35*, 10801.

[2] Park, M. H.; et al.;*MRC***2018**, *8*, 795–808.

[3] Hoffmann, M.; et al.;*Nature***2019**, *565*, 464–467.

[4] Wen, L.; Doctoral dissertation. Hdl.handle.net/1969.1/3225.

8:45am **AF1-TuM4 Surface Science Studies of GaN Substrates Subjected to Plasma-Assisted Atomic Layer Processes***, **Samantha G. Rosenberg**,* ASEE*; D.J. Pennachio,* University of California, Santa Barbara*; E.C. Young, Y.H. Chang, H.S. Inbar,* University of California Santa Barbara*; J.M. Woodward,* U.S. Naval Research Laboratory*; Z.R. Robinson,* SUNY College at Brockport*; J. Grzeskowiak,* University at Albany-SUNY*; C.A. Ventrice, Jr.,* SUNY Polytechnic Institute*; C.J. Palmstrøm,* University of California Santa Barbara*; C.R. Eddy, Jr.,* U.S. Naval Research Laboratory

III-N semiconductors are well suited for applications in several important technological areas, including high current, normally-off power switches.[1,2] Such devices require heterostructures not readily achievable by conventional growth methods. Therefore, we have developed a technique adapted from ALD, called plasma-assisted atomic layer epitaxy (ALEp).[2] Using surface science techniques, we strive to develop not only a fundamental understanding of the ALEp growth process but also complimentary atomic level processes (ALPs) that will result in the best preparation method for a pristine GaN starting surface for ALEp.

Here we employ *in-situ* and *in-vacuo* surface studies of GaN substrate preparation to advance fundamental understanding of the ALEp process. Having optimized our GaN surface preparation process (gallium flash off ALP),[3] we conduct *in-vacuo* X-ray photoelectron spectroscopy (XPS), reflection high-energy electron diffraction (RHEED), and scanning tunneling microscopy (STM) studies conducted at the Palmstrøm Lab at UCSB to further refine both our process and our understanding. Preliminary XPS results show that a GFO ALP conducted at 250°C for 12 cycles reduces the oxygen content by 5% but shows no reduction in the carbon content, while a GFO ALP conducted at 400°C for 30 cycles reduces the carbon content by 60% but shows no reduction in the oxygen content. In addition, we conducted comparable temperature program desorption (TPD) and low energy electron diffraction (LEED) experiments at SUNY Polytechnic Institute to correlate structural and chemical changes that occur on the GaN surface during our GFO ALP. TPD shows that NH_3 is released from GaN surfaces not subjected to GFO ALP as it is heated past 150°C, while GFO ALP GaN surfaces show no NH_3 release upon subsequent TPD experiments. Both GaN surfaces show an unreconstructed 1x1diffraction pattern in LEED.

1. N. Nepal, et al., Appl. Phys. Lett. 103, 082110 (2013)

2. C. R. Eddy, Jr, et al., J. Vac. Sci. Technol. A 31(5), 058501 (2013)

3. S. Rosenberg, et. al., J. Vac. Sci. Technol. A 37, 020908 (2019)

9:00am **AF1-TuM5 Infrared and Optical Emission Spectroscopy on Atmospheric-Pressure Plasma-Enhanced Spatial ALD of Al_2O_3***, **Maria Antonietta Mione**, R. Engeln, W.M.M. Kessels,* Eindhoven University of Technology, Netherlands*; F. Roozeboom,* Eindhoven University of Technology and TNO, Netherlands

In the past decade, atmospheric pressure spatial atomic layer deposition (AP-SALD) has gained momentum as a fast deposition technology for functional thin layers. The unparalleled merits of conventional ALD, such as superior control of layer thickness, conformality and homogeneity, joined with the high throughput offered by the spatially separated half-reactions and the cost-effectiveness of vacuum technology free systems, make AP-SALD well-suited for industrial large-area applications. Additionally, the use of atmospheric pressure plasmas as co-reactants enables to rapidly deposit high-quality, dense films at relatively low temperatures. [1]

Despite its industrial relevance, the chemistry at the base of the atmospheric pressure plasma-enhanced spatial ALD processes largely remains unaddressed. Effective ALD metrology techniques are of great importance to gain detailed insight into the nature of the process as well as to improve its perfomance thus opening the way to its wide industrial implementation. However, due to the dynamic nature of the spatial concept, monitoring AP-SALD processes can be rather challenging, especially in the case of close-proximity systems where the substrate is at ~100 micrometer distances from the gas injection head.

In this work, we employed optical emission spectroscopy (OES) and infrared spectroscopy on effluent plasma gasses as diagnostic tools to study the underlying chemistry of the AP-SALD process of Al_2O_3 films prepared using $Al(CH_3)_3$ and Ar-O_2 plasma. We identified the main reaction products and studied their trend as a function of the exposure time to the precursor to verify the ALD layer-by-layer growth characteristic. Findings show that the spatial separation of the ALD half-reactions and the use of an atmospheric pressure plasma as the reactant give rise to a complex underlying chemistry. Infrared absorbance spectra show CO, CO_2, H_2O and CH_4 as the main ALD reaction byproducts originating from 1) combustion-like reactions of the methylated surface with oxygen plasma radicals and ozone, and 2) a concurrent latent thermal component due to surrounding substrate. In addition, CH_2O and CH_3OH are identified as ALD reaction byproducts either formed at the surface or in the plasma by electron-induced dissociation. Furthermore, the investigated trends in CO_2, CO and CH_4 formed as a function of the exposure time confirmed self-limiting ALD behavior. Finally, OES results corroborated that, as soon as the plasma-enhanced SALD process takes place, emission from OH and CH arises while excited oxygen species are consumed.

[1] Mione *et al.*, ECS J. Solid State Sci. Technol. **6**, N243 (2017), and references therein.

9:15am **AF1-TuM6 Fingerprinting of ALD Reaction Products with Time-Resolved In situ Mass Spectrometry***, **Andreas Werbrouck**, F. Mattelaer, J. Dendooven, C. Detavernier,* Ghent University, Belgium

The importance of in-situ process monitoring during atomic layer deposition has been highlighted extensively by, among others, the review of Knapas and Ritala [1]. However, the examination of ALD processes via quadrupole mass spectrometry (QMS) is especially hard (compared to other fields where it is employed) since there is only a limited amount of reaction products, which are present in the chamber for only a fleeting moment. This shows the need for time-resolved measurements. However, most commonly available equipment is limited to a real-time resolution of only a few ion/radical masses. In QMS measurements, incoming molecules are cracked and ionized into a composite 'fingerprint' spectrum of several mass-to-charge (m/z) ratios. Thus, it is very likely that information is lost if only a few individual masses are tracked, in particular because the decision on which mass-over-charge ratios have to be measured usually depends on preliminary assumptions, knowledge of the precursor ligands and gut feeling. This limits the practical use of QMS to the detection of simple reaction products and may introduce a bias towards certain reaction chemistries. A novel data acquisition method is described which allows for time-resolved measurements of full m/z-spectra. This allows for 'fingerprinting' molecules present at a certain time instead of using a priori assumptions to decide which m/z ratios have to be monitored.

ALD processes have the exploitable advantage that they are of cyclic nature. Hence after the first cycles where initial growth effects could be of importance, the chemistry of each cycle should be identical and can be repeated as often as necessary to obtain data with good signal-to-noise ratio. In this work, we combine data from several ALD cycles to construct a time-resolved m/z spectrum of one cycle, over the full relevant range of the process, measured with a standard quadrupole mass spectrometer (Hiden HPR-30). As such, complete time-resolved mass spectrum analyses of ALD reaction chemistries is enabled.

A proof of concept is delivered with the standard TMA-H_2O chemistry, before we move on to the reaction mechanism of a more complex process. Lithium hexamethyl disilyl azide (LiHMDS) and trimethyl phosphate (TMP) can be combined to grow a crystalline lithium phosphate. As is shown in the accompanying figure, time-resolved measurements offer a unique and unbiased insight in the growth mechanism of this process.

[1] Kjell Knapas & Mikko Ritala (2013) In Situ Studies on Reaction Mechanisms in Atomic Layer Deposition,

Critical Reviews in Solid State and Materials Sciences, 38:3, 167-202, DOI: 10.1080/10408436.2012.693460

9:30am **AF1-TuM7 Studying Pt and Pd Nanoparticle ALD through X-ray based In situ Characterization***, **Jolien Dendooven**, J.-Y. Feng,* Ghent University, Belgium*; E. Solano,* ALBA Synchrotron Light Source, Spain*; R. Ramachandran, M. Minjauw, M. Van Daele,* Ghent University, Belgium*; D. Hermida-Merino,* ESRF European Synchrotron, France*; A. Coati,* Synchrotron SOLEIL, France*; C. Detavernier,* Ghent University, Belgium **INVITED**

The performance of supported nanoparticles (NPs) in heterogeneous catalysis is closely related to their size, shape and interparticle distance. Tailoring the structural properties of noble metal NPs is attractive to elucidate performance-structure relationships and tune the catalytic

activity, selectivity and stability. In this regard, there is an increasing interest in ALD to conformally deposit noble metal NPs with atomic-scale control over the metal loading (atoms per cm^2) and NP size. Here, we aim to demonstrate that in situ X-ray fluorescence (XRF) and grazing incidence small angle X-ray scattering (GISAXS) can offer unique insights in the ALD growth and thermal stability of metal NPs, offering approaches towards superior size and coverage control, and improved stability.

In a first study, the $Me_3(MeCp)Pt$ precursor is combined with either O_2 gas or N_2 plasma to grow Pt NPs on planar SiO_2 surfaces, and in situ XRF and GISAXS measurements provide the evolution of Pt loading, NP dimensions and spacing. It is found that O_2 induces atom and cluster surface diffusion and promotes the ripening of the Pt NPs, while diffusion phenomena seem to be suppressed during N_2 plasma-based ALD. This insight inspired a tuning strategy that combines both processes and offers independent control over NP size and coverage [Nat. Comm. 8, 1074 (2017)]. Next, in situ GISAXS is used to investigate the coarsening behavior of the Pt NPs [Nanoscale 9, 13159 (2017)] and probe the influence of stabilizing Al_2O_3 overcoats. The overcoat thickness required to stabilize the NPs is investigated for different Pt NP coverages and sizes, revealing that one single ALD cycle is sufficient to stabilize widely spaced NPs, while it is challenging to avoid NP coarsening for closely packed Pt NPs.

A second case study concerns plasma-enhanced ALD of Pd NPs on planar Al_2O_3 surfaces with the $Pd(hfac)_2$ precursor at 150°C, comparing a purely reducing chemistry (H_2 plasma as reactant) with three-step processes that include an oxidizing agent (sequential dosing of H_2 plasma and O_2 plasma or vice versa). The choice of reactant and reactant sequence has a clear impact on the initial nucleation density. The highest areal density is obtained for the three-step process that uses H_2 plasma followed by O_2 plasma, explained by the cleaning role of O radicals towards poisoning hfac ligands on the Al_2O_3 surface. Finally, the use of TMA to clear the surface from site-blocking species [APL 95, 143106 (2009)] is systematically investigated on planar SiO_2 using in situ GISAXS, providing a way to control the Pd NP coverage.

ALD Fundamentals
Grand Ballroom H-K - Session AF2-TuM
ALD Precursors II

Moderators: Jin-Seong Park, Hanyang University, Seán Barry, Carleton University

8:00am **AF2-TuM1 Characterizing Water Delivery for ALD Processes***, **James Maslar**, B. Sperling, W. Kimes,* National Institute of Standards and Technology*; W. Kimmerle, K. Kimmerle,* NSI*; E. Woelk,* CeeVeeTech

Water is utilized as the oxygen source for many metal oxide ALD processes. Water is commonly delivered in an inert carrier gas from a bubbler (an ampoule with a dip tube) or a vapor draw ampoule (an ampoule with no dip tube: the gas in and gas out ports open directly into the ampoule headspace). While it is relatively simple to implement a delivery system based on such ampoules, it can be difficult to reproducibly deliver water from such ampoules. This is at least in part due to evaporative cooling, i.e., cooling reduces the water vapor pressure and hence the amount of material entrained in the carrier gas. For an ideal ALD process, irreproducible water delivery may not lead to undesirable changes in the deposited film properties (unless the dose is insufficient to saturate the reactive surface sites). However, if the ALD process involves a chemical vapor deposition component, irreproducible water delivery can result in undesired film properties. The goal of this work is to obtain a better understanding of the factors influencing water delivery from bubblers and vapor draw ampoules. To achieve this goal, both the amount of water delivered from an ampoule and the temperature distribution of the water in the ampoule were measured under a range of process conditions, in bubblers and vapor draw ampoules. The amount of water delivered and the water temperature vertical distribution in the ampoule were measured using a tunable diode laser spectroscopy system and a five-element temperature sensor array, respectively. These data were used determine the degree to which the amount of water delivered was correlated to evaporative cooling in the ampoule. For bubblers, this determination was relatively straight-forward as bubbling tended to homogenize the water temperature. For vapor draw ampoules, however, this determination was complicated by a temperature gradient that existed during flow. The focus of this investigation was on commercial 1.5 L ampoules (with a maximum fill of 1.2 L), although different ampoule designs were examined. The results from this work could facilitate development of ALD process recipes, delivery control methods, and improved ampoule designs.

8:15am **AF2-TuM2 A Nickel Chloride Adduct Complex as a Precursor for Low-Resistivity Nickel Nitride Thin Films with Tert-butylhydrazine as a Coreactant***, K. Väyrynen, T. Hatanpää, M. Mattinen, M.J. Heikkilä, K. Mizohata, J. Räisänen,* University of Helsinki, Finland*; J. Link, R. Stern,* National Institute of Chemical Physics and Biophysics, Estonia*; M. Leskelä, **Mikko Ritala**,* University of Helsinki, Finland

From the very beginning of ALD, metal chlorides have been extensively used precursors because of their high thermal stability and reactivity as well as low cost. However, not all metal chlorides are volatile enough to be used in ALD. Cobalt and nickel chlorides for example have a polymeric structure and therefore low volatility. To circumvent this limitation, we have recently explored a strategy of adducting these chlorides with chelating ligands. With properly selected diamines the adduct complexes are monomeric and thermally stable enough to be volatilized and used in ALD. These compounds have been earlier been used for deposition of CoO [1] and intermetallics Co_3Sn_2 and Ni_3Sn_2 as a novel class of ALD materials [2].

Herein, we have studied ALD of nickel nitride and nickel thin films using $NiCl_2(TMPDA)$ (TMPDA = *N,N,N′,N′,*-tetramethyl-1,3-propanediamine) as the metal precursor and tert-butylhydrazine (TBH) as a nitrogen containing reducing agent. The films were grown at low temperatures of 190–250 °C. This is one of the few low-temperature ALD processes that can be used to grow Ni_3N and Ni metal on both insulating and conductive substrates. X-ray diffraction showed reflections compatible with either hexagonal Ni or Ni_3N. ToF-ERDA analyses showed that the films were close to stoichiometric Ni_3N. Upon annealing the films at 150 °C in 10% forming gas their nitrogen content lowered down to 1.2 at.%, and the nonmagnetic nitride films were converted to ferromagnetic Ni metal.

[1] K. Väyrynen, K. Mizohata, J. Räisänen, D. Peeters, A. Devi, M. Ritala, M. Leskelä, *Chem. Mater.* **2017**, *29*, 6502.

[2] K. Väyrynen, T. Hatanpää, M. Mattinen, K. Mizohata, K. Meinander, J. Räisänen, J. Link, R. Stern, M. Ritala, M. Leskelä, *Adv. Mater. Interfaces* **2018**, *12*, 1801291.

8:30am **AF2-TuM3 Simple, Rationally Designed Aluminum Precursors for the Deposition of Low-impurity AlN Films***, **Sydney Buttera**, S. Barry,* Carleton University, Canada*; H. Pedersen,* Linköping University, Sweden

Main group chemistry has been integral in the field of ALD since its inception, particularly concerning the extensive work on the most fundamental ALD process: the deposition of aluminum oxide from trimethylaluminum (TMA) and water. It is surprising that strategically functionalized analogues to this fundamental precursor have not been more extensively studied in order to optimize subsequent deposition processes. A simple, rationally designed precursor can regulate surface chemistry and limit decomposition pathways, permitting straightforward reactivity. Our focus is to enable the deposition of low-impurity aluminum nitride by ALD.

This presentation will describe the study of a set of simple molecules that are novel as ALD precursors, based on a substituted TMA framework (Figure 1a-c). Tris(dimethylamido)aluminum(III) is a direct analogue of TMA with methyl groups replaced by dimethylamido ligands. It demonstrates excellent ALD precursor behaviour with a 1 Torr temperature of 67 °C and no decomposition visible by TGA, likely attributed to the stabilization of the Al centre by the coordinative donation from the bridging NMe_2. This precursor deposited aluminum oxide and aluminum oxy-nitride films with carbon impurities lower than those reported using TMA.[1] From this, it was deduced that metal-nitrogen bonds in precursor design were beneficial to stabilizing the metal centre, and importantly, in lowering carbon contamination in deposited films by eliminating direct Al-C bonds.

Using the same TMA framework, $AlH_x(NMe_2)_{3-x}$ (x = 1, 2) compounds were prepared due to the potential for the reducing ability of the hydride ligand and a maintained absence of metal-carbon bonds. These compounds were also found to be volatile and thermally stable, and thus suitable as potential AlN precursors.

This led to the study of further nitrogen-containing ligands: the family $Al(^{Me}NacNac)_x(NMe_2)_{3-x}$ (x = 1, 3) similarly showed excellent volatility and thermal stability. Interestingly, an Al species with one monoanionic and one doubly anionic $^{Me}NacNac$ ligand was discovered (Figure 1d) and presented this novel reduced ligand for potential use in ALD precursors. This compound was synthesized via reduction of the $^{Me}NacNac$ ligand, and its thermal characterization and reactivity, as well as that of contrarily

unsuitable ALD candidates using these ligands, will also be discussed in this presentation.

[1] Buttera, S. C.; Mandia, D. J.; Barry, S. T. Tris(dimethylamido) aluminum(III): An Overlooked Atomic Layer Deposition Precursor. *J. Vac. Sci. Technol. A Vacuum, Surfaces, Film.* **2017**, *35* (35), 1–128.

8:45am **AF2-TuM4 Atomic Layer Deposition of Lead(II) Sulfide at Temperatures Below 100 °C***, **Georgi Popov**,* University of Helsinki, Finland*; G. Bačić,* Carleton University, Canada*; M. Mattinen, M. Vehkamäki, K. Mizohata, M. Kemell,* University of Helsinki, Finland*; S. Barry,* Carleton University, Canada*; J. Räisänen, M. Leskelä, M. Ritala,* University of Helsinki, Finland

Lead(II) sulfide (PbS) is one of the oldest known semiconductors. It has a narrow band-gap of 0.4 eV that can be widened by quantum confinement effects. Owing to these properties, PbS is a recognized material in IR detection and quantum dot (QD) based devices such as light emitting diodes (LEDs) and photovoltaics. Photovoltaics are also central to our study. The aim is to develop an ALD PbS process that can be applied in halide perovskite solar cells.

ALD processes for PbS exist at least since 1990[1], however we discovered that known ALD PbS processes are incompatible with halide perovskites such as $CH_3NH_3PbI_3$ due to their extremely low thermal budget[2]. To our knowledge the lowest temperature at which PbS can be deposited with existing ALD processes is 130 °C.[3] $CH_3NH_3PbI_3$ film degrades completely at that temperature in our ALD reactors. Thus, we set out for a new PbS process that would work at even lower temperatures. From our previous studies on ALD of PbI_2 we already knew one lead precursor suitable for low temperature ALD: lead(II) bis[bis(trimethylsilyl)amide] or $Pb(btsa)_2$.[4] Recently Bačić et al. reported another suitable candidate: lead(II) *rac*-N^2,N^3-di-*tert*-butylbutane-2,3-diamide or Pb(dbda).[5] With these lead precursors and H_2S as a co-reactant we developed two new processes capable of depositing PbS even below 100 °C.

$Pb(btsa)_2$-H_2S process produces uniform, high-quality, crystalline PbS films in the 65 – 155 °C range. TOF-ERDA composition analysis revealed exceptionally high purity for such low deposition temperatures. The process exhibits two regions with temperature independent growth per cycle values (GPC) of 0.50 Å and 0.15 Å at 65 – 80 °C and 115 – 155 °C, respectively. The GPC saturates rapidly with respect to both precursor pulses and is independent of the purge duration and number of deposition cycles. $CH_3NH_3PbI_3$ films survive the PbS deposition at the lowest deposition temperatures and studies of perovskite stability after PbS deposition are ongoing.

With Pb(dbda) film deposition occurs in an even wider temperature range of 45 – 155 °C. However, XRD measurements show that at 95 °C and above, the films contain crystalline impurities. Nevertheless, high-quality polycrystalline PbS films can be deposited at temperatures as low as 45 – 75 °C. We are currently conducting studies on the influence of process parameters on the PbS film properties.

[1] Leskelä et al. *Vac.* **1990**, 41, 1457–1459.

[2] Zardetto et al. *Sustain. Energ. Fuels* **2017**, 1, 30-55

[3] Nykänen et al. *J. Mater. Chem.* **1994**, 4, 1409.

[4] Popov et al. *Chem. Mater.* **2019,** Article ASAP. DOI: 10.1021/acs.chemmater.8b04969

[5] Bačić et al. *Inorg. Chem.* **2018**, *57*, 8218-8226.

9:00am **AF2-TuM5 Development and Characterization of a Novel Atomic Layer Deposition Process for Transparent p-Type Semiconducting Nickel Oxide using $Ni(^{tBu2}DAD)_2$ and Ozone***, **Konner Holden**,* Oregon State University*; C.L. Dezelah,* EMD Performance Materials*; J.F. Conley, Jr.,* Oregon State University

Nickel oxide (NiO), a wide band gap p-type oxide semiconductor, is of interest for applications in solar energy conversion,[1] electrocatalysis,[2] and as a tunnel barrier for metal/insulator/metal (MIM) diodes for infrared energy harvesting.[3] ALD is an ideal technique for the highly conformal, uniform thin films needed for these applications. We develop a new process for ALD of NiO using $Ni(^{tBu2}DAD)_2$ and O_3-.

ALD growth of metallic Ni was demonstrated recently using $Ni(^{tBu2}DAD)_2$ and *tert*-butylamine.[4] ALD of metallic Co and cobalt oxide have been reported using $Co(^{tBu2}DAD)_2$ with formic acid and O_3, respectively.[5,6] Taking a similar approach, we deposit NiO in a Picosun Sunale R-150 using N_2-purge-separated cycles of $Ni(^{tBu2}DAD)_2$ held at 150°C and an O_3/O_2 mixture of ~10%. NiO films were characterized using grazing-incidence x-ray diffraction (GIXRD), x-ray photoelectron spectroscopy (XPS), atomic force microscopy (AFM), variable angle spectroscopic ellipsometry (VASE), and p-NiO/n-Si heterojunction diodes.

A plot of GPC vs. temperature for depositions using a 5/30/4/30 s $Ni(^{tBu2}DAD)_2/N_2/O_3/N_2$ pulse sequence shows a clear ALD "window" of constant GPC = 0.12 nm/cycle from 185-200 °C (Fig. 1) in which $Ni(^{tBu2}DAD)_2$ and O_3 pulses saturate after ~5 s and ~4 s, respectively (Fig. 2). Below the temperature window, condensation of $Ni(^{tBu2}DAD)_2$ occurs resulting in uncontrolled growth with 1.2% C and 0.7 % N impurities (XPS) at 150 °C. Above the window, from 200-230 °C, desorption of $Ni(^{tBu2}DAD)_2$ occurs, followed by decomposition of $Ni(^{tBu2}DAD)_2$ above 230 °C on the chamber walls upstream of the wafer, both contributing to decreased GPC. Inside the temperature window, for saturating films deposited at 200 °C, GIXRD shows randomly-oriented polycrystalline cubic NiO (Fig. 3), consistent with XPS elemental analysis showing a Ni:O ratio near unity, without any detectable C or N impurities. VASE reveals that refractive index (~2.4) and band-gap (~3.8 eV) are close to bulk values while AFM RMS roughness was 0.6 nm for an 18 nm thick film (Fig. 4). p-NiO/n-Si diodes show highly asymmetric ($I_+/I_{-,MAX} \approx 10^4$) behavior. All results point towards an as-deposited transparent p-type semiconducting NiO. Further growth studies, characterization, and electrical measurements will be discussed at the meeting.

6. S. Seo et al., Nanoscale 8, 11403 (2016).
7. K. L. Nardi et al., Adv. Energy Mater. 5 (2015).
8. N. Alimardani et al. Appl. Phys. Lett. 105, 082902 (2014).
9. M. M. Kerrigan et al., ACS Appl. Mat. & Interfaces. 10, 14200 (2018).
10. J. P. Klesko, M. M. Kerrigan, and C. H. Winter, Chem. Mater. 28, 700 (2016).
11. J. Kim et al., Chem. Mater. 29, 5796 (2017).

9:15am **AF2-TuM6 Blocking Thermolysis in Diamido Plumbylenes***, **Goran Bacic**,* Carleton University, Canada*; D. Zanders,* Ruhr University Bochum, Germany*; I. Frankel,* Carleton University, Canada*; J. Masuda,* Saint Mary's University, Canada*; T. Zeng,* Carleton University, Canada*; B. Mallick, A. Devi,* Ruhr University Bochum, Germany*; S. Barry,* Carleton University, Canada

Lead-containing nanomaterials like PbS quantum dots and $CH_3NH_3PbI_3$ perovskite films have received a frenzy of attention because of their unique optoelectronic properties. Atomic layer deposition (ALD) is an especially attractive method for their fabrication as it can deposit uniform, conformal films over large areas at low temperatures with subnanometer thickness control. However, current lead-containing ALD processes have rarely been adopted due to their poor thermal budget, the low volatility of known precursors, and the small library of thermally robust lead complexes. Our interest in the deposition of lead-containing materials prompted us to study amido ligands because of their low cost, flexibility, and proven effectiveness of other group 14 diamido complexes as precursors for ALD.

In a pilot study,[1] we identified the thermally stable (dec. >100 °C) and highly volatile (subl. 40 °C/0.01 Torr) 5-membered *N*-heterocyclic plumbylene *rac*-N^2,N^3-di-*tert*-butylbutane-2,3-diamido lead(II) (**1**), however it failed to cleanly react with our sulfur-source *tert*-butylthiol below its decomposition temperature. To explore safe (i.e., less reactive) co-reagents for ALD, we needed to push the thermal stability even higher through a mechanistic understanding of the decomposition pathways of diamido plumbylenes. With few reports on the mechanisms of their thermolysis, we decided to undertake a combined synthetic and theoretical approach to this problem. The two most promising examples in the literature, **1** and $Pb[N(SiMe_3)_2]$, suggested both cyclic and acyclic scaffolds were viable.

We postulated two dominant thermolysis pathways for plumbylenes: formation of metallacycles by π-overlap of *N*-substituents and the $6p^0$ orbital of lead (**A**); and concerted pericyclic cycloreversion reactions (**B**). We found experimentally that known acyclic complexes were dominated by **A,** and 5-membered cyclic derivatives were found to be dominated by pathway **B** so we designed bespoke ligands to block thermolysis through two strategies: coordinatively saturating lead with a Lewis base to hinder **A**, and rigid ligands to block **B**. *Ab initio* calculations were performed on a model set of plumbylenes to help reveal the way forward to indefinitely robust and volatile plumbylenes for deposition, and provide a better understanding of the unique ligand-metal cooperation required for lead.

[1] Bačić, G., Zanders, D., Mallick, Devi, A., Barry, S.T.Designing Stability into Thermally Reactive Plumbylenes. *Inorg. Chem.* **2018**, *57* (14), pp 8218-8226.

9:30am **AF2-TuM7 ALD of Sc_2O_3 with $Sc(cp)_3$ and a Novel Heteroleptic Precursors***, T. Ivanova,* ***Perttu Sippola,*** ASM, Finland*; G. Verni, Q. Xie,* ASM, Belgium*; M. Givens,* ASM, Finland

The deposition and the properties of rare earth oxide thin films have been extensively studied for applications as protective coatings, optics and microelectronics. Sc_2O_3 thin films have recently attracted a strong interest for application as gate dielectrics for metal-oxide-semiconductor field-effect transistors (MOSFET) because they have a dielectric constant of 14, a band gap of 6.3 eV and excellent thermal stability. Despite its advantages, very few studies have investigated Sc_2O_3 on Si. We therefore investigated growth characteristics of Sc_2O_3 films deposited by atomic layer deposition (ALD) from $Sc(cp)_3$ and a novel liquid heteroleptic cyclopentadienyl containing Sc precursor, which are thermally stable (>300 ˚C), volatile, with a good reactivity to H_2O. The depositions were done in a hot-wall cross-flow-type ASM Pulsar® 3000 reactor connected to a Polygon 8300 platform.

The film growth properties, such as growth per cycle, impurity concentrations, and thickness uniformity on 300 mm Si (100) wafers were studied. A growth rate per cycle of 0.46 Å/ cycles and 0.52 Å/cycle was obtained at 225 ˚C with novel Sc based precursor and $Sc(cp)_3$, respectively. The Sc_2O_3 film non-uniformity was about 1 % and 5 % with novel Sc heteroleptic precursor and $Sc(cp)_3$, respectively. Sc_2O_3 films based on the novel Sc precursor were stoichiometric, with a low C impurity content of <1%, while films based on $Sc(cp)_3$ precursor exhibited ~4.5 % of residual carbon impurity level under similar processing conditions.

Electrical measurements were done on planar TiN gated MOS capacitor (MOSCAP) with high k thickness ~8 nm. $Sc(cp)_3$ based Sc_2O_3 exhibited a leakage current density of 1.5 x 10^{-4} A/cm^2 and an effective work function (eWF) of 4.05 eV for an equivalent oxide thickness (EOT) of 3.43 nm at 1.0 V, which is significantly lower than TiN eWF (~4.8 eV) indicating considerable positive fixed charges incorporated in deposited Sc_2O_3 film. While novel heteroleptic Sc based Sc_2O_3 films exhibited much lower leakage current density of 1.0 x 10^{-8} A/cm^2 and close to TiN eWF of 4.77 eV for an EOT of 3.15 nm at 1.0 V. It was shown that good quality and low defects Sc_2O_3 films can be obtained by using the novel heteroleptic Sc precursor.

9:45am **AF2-TuM8 A Novel Self-limited Atomic Layer Deposition of WS_2 based on the Chemisorption and Reduction of bis(t-butylimido)bis(dimethylamino) Complexes***,* ***Nicola Pinna,*** Humboldt-Universtät zu Berlin, Germany

A novel self-terminating chemical approach for the deposition of WS_2 by atomic layer deposition based on chemisorption of bis(t-butylimido)bis(dimethylamino)tungsten(VI) followed by sulfurization by H_2S is reported. A broad spectrum of reaction parameters including temperatures of the reaction chamber and the precursor and durations of every ALD step are investigated and optimized to reach a high growth per cycle of 1.7 Å and a high quality of the deposited thin films. The self-terminating behaviour of this reaction is determined by the variation of the dose of the precursors. The physical, chemical and morphological properties are characterized by a combination of analytical techniques. XRD, XPS and Raman prove that highly pure and well-defined WS_2 layers can be synthesized by ALD. TEM and AFM images show that WS_2 grows as platelets with a thickness of 6^{-10} nm and diameter of 30 nm, which do not vary dramatically with the number of ALD cycles. A low deposition temperature process followed by a post annealing under H_2S is also investigated in order to produce a conformal WS_2 film. Finally, a reaction mechanism could be proposed by studying the chemisorption of bis(t-butylimido)bis(dimethylamino)tungsten(VI) onto silica, and the thermal and chemical reactivity of chemisorbed species by ^{1}H NMR, GC-MS and FT-IR.

ALD Fundamentals
Grand Ballroom A-C - Session AF3-TuM
Growth and Characterization II

Moderators: Jolien Dendooven, Ghent University, Henrik Pedersen, Linköping University

10:45am **AF3-TuM12 Enabling Nucleation Phenomena Studies of ALD Deposited Films by In-situ High-Resolution TEM***,* ***Stephanie Burgmann,*** *A. Dadlani, A. Bin Afif,* Norwegian University of Science and Technology, Norway*; J. Provine,* Aligned Carbon*; A.T.J. van Helvoort, J. Torgesen,* Norwegian University of Science and Technology, Norway

Understanding the nucleation stage and growth characteristics of atomic layer deposition (ALD) is indispensable for the fabrication of quantum dots or very thin films of just a few nanometers thickness. The tools for analyzing such small features and films are limited and often include post deposition characterization failing to capture the initial nucleation step. Enabling ALD processes in a closed gas-cell system inside a transmission electron microscope (TEM) allows manufacturing and characterization during film evolution at working conditions, a significant component in optimizing the nucleation phase.

In-situ characterization of deposition processes could be performed in an environmental TEM (ETEM) or a separated closed gas-cell holder system in a TEM preserving all analytical signals and TEM imaging capabilities as well as possible. A gas-cell reactor promises benefits in terms of versatility, controllability, and a defined deposition area. A successful implementation of ALD in a closed gas-cell system necessitates a gas-cell rector, a microscale heating system, a heated gas injection system, and an evacuation system to be placed into the limited space of a TEM holder.

An *in-situ* gas-cell holder system allowing deposition of different materials in a TEM has to be tailored to the delicate temperature sensitive ALD processes. To avoid contamination due to outgassing of sealing components, a gas-cell is designed based on a single wafer process, using the "Sandbox" process as basis. A layered structure employing ALD Al_2O_3 as etch stop layer and window material gives the opportunity to create a buried channeling system. Precursor gases will be injected from the back side of the chip using the two outer openings as inlet and exhaust. The central opening is the area where the electron beam is transmitted through the chip for imaging purposes. Al_2O_3 layers are used as functional windows with only a few atomic layers in thickness to achieve best possible high-resolution imaging and serve as a substrate for deposition. The design of the gas cell on a single wafer enhances the possibility to use characteristic x-ray signals for compositional analysis due to higher signal yield and simplifies the preparation for TEM studies involving environmental conditions.

The *in-situ* gas-cell reactor system is currently prototyped and will be tested thoroughly before its application inside the TEM. Ultimately, we envision that it enables controlled deposition inside any TEM, opening up new opportunities in nucleation studies for various researchers working on functional thin films around the world, opportunities not necessarily limited to ALD only.

11:00am **AF3-TuM13** ***In-situ*** **ellipsometric analysis of plasma assisted ALD grown- stoichiometric and crystalline AlN films***,* ***Adnan Mohammad,*** *D. Shukla, S. Ilhom, B. Willis,* University of Connecticut*; B. Johs,* Film Sense LLC*; A.K. Okyay,* Stanford University*; N. Biyikli,* University of Connecticut

The self-limiting aluminum nitride (AlN) plasma-assisted ALD (PA-ALD) growth process is monitored in dynamic real-time mode by in-situ multi-wavelength ellipsometry. AlN thin films are deposited on Si(100) substrates by PA-ALD reactor featuring a capacitively-coupled hollow-cathode plasma source and using trimethyl-aluminum (TMA) and Ar/N2/H2 plasma as metal precursor and coreactant, respectively. The temperature range for the saturation experiments is 100 – 250 °C, while each growth parameter variation is carried out for 10-cycle sub-runs. The sensitivity of the multi-wavelength ellipsometry has provided sufficient resolution to capture not only the subtle changes in the growth-per-cycle (GPC) parameter, but as well the single chemical surface reactions including precursor adsorption and plasma-assisted ligand removal and nitrogen incorporation. GPC values showed a slight increase with temperature slope within 100 – 200 °C, followed by a stronger surge at 250 °C, signaling the onset of thermal decomposition of TMA. The real-time dynamic in-situ monitoring depicted mainly the following perceptions into the HCPA-ALD process of AlN: (i) The GPC and TMA chemisorption amount showed plasma-power dependent saturation behavior which was also correlated with the substrate

temperature; (ii) The cycle dependent refractive index profile shows a faster increase

within the first ~100 cycles followed by a slower increase as the AlN film gets thicker; (iii) The crystallinity is improved particularly when substrate temperature exceeded 200 °C. In terms of additional materials characterization, optical, structural, and chemical properties are studied via ex-situ measurements on 500-cycle grown AlN films as a function of substrate temperature. The single-phase wurtzite polycrystalline character was confirmed for all AlN samples with no detectable carbon and relatively low (< 5%) oxygen content within the bulk of the films. Moreover, the highly stoichiometric (~1:1) elemental composition was also noticed as well for all AlN samples, regardless of the substrate temperature. A detailed comparative analysis with previously published reports on PA-ALD grown AlN will be presented.

11:15am **AF3-TuM14 Film Properties of ALD SiNx Deposited by Trisilylamine and N_2 Plasma***, **Markus Bosund**, E. Salmi, K. Niiranen,* Beneq Oy, Finland

Silicon nitride is a widely used material in semiconductor applications, such as gate dielectrics, III/V surface passivation and etch stop layer.

PEALD SiNx films have been previously grown using aminosilanes like BTBAS with N_2 plasma [1]. These processes generally have a relatively low growth rate of 0.15 - 0.21 Å/cycle and high film quality can only be reached at above 300 °C deposition temperatures. Trisilylamine (TSA) has been previously combined with N_2/H_2 plasma at 300–400 °C [2], NH_3 plasma at 50–400 °C [3] and N_2 plasma at 250 – 350 °C [4] to grow PEALD SiNx films. However, in these works the low temperature range has remained either inaccessible or uncharted.

In this work we explored the PEALD TSA-N2 plasma process with a wide deposition temperature range from 50 to 350 °C. Focus was given to the electrical and optical properties of the films. A Beneq TFS 200 capacitively coupled hot wall plasma ALD reactor was used at direct plasma mode. It was found that reactor temperature, and plasma power and time had the highest impact on the film properties. Film deposition was observed at temperatures as low as 50 °C. Metal insulator semiconductor (MIS) structures were used to determine the breakdown field and leakage current at different temperatures. Films were dipped in 1 % HF solution for etch rate determination.

[1] KNOOPS, Harm CM, et al. Atomic layer deposition of silicon nitride from Bis (tert-butylamino) silane and N2 plasma. ACS applied materials & interfaces, 2015, 7.35: 19857-19862.

[2] TRIYOSO, Dina H., et al. Evaluation of low temperature silicon nitride spacer for high-k metal gate integration. ECS Journal of Solid State Science and Technology, 2013, 2.11: N222-N227.

[3] JANG, Woochool, et al. Temperature dependence of silicon nitride deposited by remote plasma atomic layer deposition. physica status solidi (a), 2014, 211.9: 2166-2171.

[4] WEEKS, Stephen, et al. Plasma enhanced atomic layer deposition of silicon nitride using neopentasilane. Journal of Vacuum Science & Technology A: Vacuum, Surfaces, and Films, 2016, 34.1: 01A140.

11:30am **AF3-TuM15 Comparison of Properties of Conductive Nitride Films Prepared by PEALD using Quartz and Sapphire Plasma Sources***, I. Krylov, X. Xu, K. Weinfeld, **Valentina Korchnoy**, D. Ritter, M. Eizenberg,* Technion - Israel Institute of Technology, Israel

We report on the properties of various conductive nitrides (TiN, ZrN, TaN) prepared by PEALD using either quartz or sapphire inductively coupled plasma (ICP) sources. Quartz and sapphire are two commonly used ICP source materials. The films were deposited at 300°C in Ultratech/Cambridge Fiji G2 PEALD system using metal-organic precursors and plasma half-cycles, separated by a purge period. Different reactive gases (N2, NH3, and H2) and various pressures during the plasma half-cycle were examined. All deposited films were ~ 30nm thick. TiN deposition rates are higher for the processes with the sapphire ICP source compared to those with the quartz source (Fig.1). The difference in deposition rates increases if the hydrogen based reactive gases are used for deposition. The low deposition rates of H2 plasma-grown TiN obtained using the quartz source may indicate a significant chemical etch of the quartz source by H radicals. Quartz tube etching is manifested by oxygen contamination in the deposited films, especially at processes with high H_2 flow (Fig.2). All deposited TiN films were found crystalline with a strong preferential orientation (XRD data is shown in Fig.3). The ICP source material has a significant role on film morphology if a H_2 plasma is used for deposition. Films deposited using the quartz source consist of small (a few nm size) grains. Deposition using the sapphire ICP source results in films with large (20nm size) columnar grains (Fig.4). The most technologically important parameter of conductive nitrides is film resistivity. At thicknesses significantly higher than the electron mean free path film resistivity is increased due to scattering at grain boundaries and point defects. Therefore, the main parameters determining film resistivity of the deposited 30nm thick TiN films are the grain size and the oxygen contamination. For all examined nitrides, the lowest film resistivity and the highest film density was obtained for the H2 plasma-grown films deposited using the sapphire based ICP source (Fig.5,6). Sapphire source enabled higher deposition rates, better crystallization, lower film resistivity, and lower oxygen contamination. This indicates a superior chemical resistivity of sapphire to etching by hydrogen radicals compared to that of quartz. The advantage of the sapphire based ICP source is pronounced when a H_2 plasma and/or at high reactive gas flow are used for nitride deposition. The influence of ICP source material choice on the nitride film quality may be minimized if nitrogen based reactive gases and low flow conditions are used for nitride deposition. Optimal deposition conditions for both ICP source materials are determined.

11:45am **AF3-TuM16 Role of Hydrogen Radicals in the Surface Reactions of Trimethyl-Indium (TMI) with Ar/N_2 Plasma in Hollow-Cathode Plasma-Assisted ALD***, **Saidjafarzoda Ilhom**, A. Mohammad, D. Shukla, N. Biyikli, B. Willis,* University of Connecticut

In this work we investigate the surface reactions of trimethyl-indium (TMI) with varying nitrogen plasma compositions. Extended 600-cycle long runs were carried out to grow thin films on Si(100) substrates via hollow-cathode plasma-assisted atomic layer deposition (HCPA-ALD). TMI and variants of $Ar/N_2/H_2$ plasma (N_2-only, Ar/N_2, and $Ar/N_2/H_2$) were utilized as metal precursor and nitrogen co-reactant, respectively. Growth experiments have been performed within 50 - 200 W plasma power range and 120 - 240 °C substrate temperature. Dynamic *in-situ*ellipsometry was employed to monitor the growth-per-cycle (GPC) characteristics and real-time growth behavior. In addition to *in-situ*analysis, *ex-situ*characterizations were done to identify structural, chemical, and optical properties of the grown InO_xN_yfilms. It was found that samples displayed polycrystalline single-phase hexagonal InN only when Ar/N_2-plasma was utilized. However, introducing H_2gas to the nitrogen plasma led to the growth of crystalline indium oxide (In_2O_3) films. In general, all In_2O_3samples displayed polycrystalline character, which exhibited preferred (222) crystalline orientation with peak intensity values changing as a function of RF-plasma power and substrate temperature. Interestingly, in the film grown at 160 °C the dominant crystal orientation shifted towards (321) with additional appearance of two metallic indium crystalline peaks. The role of H_2in possible reaction mechanisms resulting in the replacement of nitrogen with oxygen will be discussed based on the correlation of XRD and XPS results. The analysis of *in-situ*and *ex-situ*ellipsometry data will provide additional insight into the optical properties of the films as well as how the single chemisorption, ligand removal, and nitrogen/oxygen incorporation events possibly occur along the ALD cycles.

Atomic Layer Etching
Regency Ballroom A-C - Session ALE1-TuM
ALE: Gas-phase and/or Thermal ALE

Moderators: Steven M. George, University of Colorado - Boulder, Venkateswara Pallem, American Air Liquide

8:00am **ALE1-TuM1 Analyses of Hexafluoroacetylacetone (Hfac) Adsorbed on Transition Metal Surfaces***, **Tomoko Ito**, K. Karahashi, S. Hamaguchi,* Osaka University, Japan **INVITED**

Transition metals are known as hard-to-etch materials for reactive ion etching (RIE) processes. Although Ar milling processes are now widely used for such metal etching, physical sputtering processes with high energy ions have problems of low selectivity and poorly controlled etched profiles. Surface damages induced by energetic ion bombardment may also cause degradation of the material surface properties. Therefore alternative transition-metal etching processes with high selectivity and low damage, rather than physical sputtering, have been sought after in the industry. In recent years, atomic layer etching (ALE) by the formations of volatile organic metal complexes has attracted much attention as a means to achieve atomically controlled and low damage etching. ALE reactions may be considered as reverse reactions of atomic layer deposition (ALD). For example, metal beta-ketoenolate complexes are often used as precursors for ALD, so stable adsorption of beta-ketones on a metal surface and the

formation of metal beta-ketoenolates thereon are crucial steps for the development of corresponding ALE processes. In this study, we have examined surface reactions of transition metals or their oxides with hexafluoroacetylacetone (hfac) [1] and demonstrated that such reactions can be used to develop ALE processes for some transition metals. Experiments were performed in what we call the "Atomic-Layer-Process (ALP) Surface Analysis System," which consists of ALP reaction chambers and an *in-situ* high-resolution X-ray photoelectron spectroscopy (XPS) system. In the reaction chamber, the substrate temperature can be controlled by a ceramic heater, which is installed on the back side of the sample. After exposure to reactive gases, the sample can be transferred from the reaction chamber to the XPS chamber without being exposed to ambient air for *in- situ* surface chemical analysis. Ion irradiation effects on an hfac adsorbed metal surface may be studied with the use of low energy Ar^+ ion beam of the XPS system. We used Ni and Co substrates in this study. It has been found that hfac molecules adsorbed on a metal oxide surface are less likely to be decomposed at room temperature than those on a metal surface and, at an elevated temperature, a metal oxide surface is preferentially etched by hfac than a metal surface.

[1] H. L. Nigg and R. I. Masel, J. Vac. Sci. Technol. A, 17, 3477 (1999).

8:30am **ALE1-TuM3 Thermal Atomic Layer Etching of Silicon Nitride using an Oxidation and "Conversion-Etch" Mechanism***, **Aziz Abdulagatov**, S.M. George,* University of Colorado - Boulder

The thermal atomic layer etching (ALE) of silicon nitride was demonstrated using an oxidation and "conversion-etch" mechanism (see Supplemental Figure 1). In this process, the silicon nitride surface was oxidized to a silicon oxide layer using O_2 or ozone. The silicon oxide layer was converted to an Al_2O_3 layer using trimethylaluminum (TMA). The Al_2O_3 layer was fluorinated by HF to an AlF_3 layer prior to the removal of the AlF_3 layer by ligand-exchange using TMA. Silicon nitride ALE was studied using Si_3N_4 films deposited using low pressure chemical vapor deposition (LPCVD). *In situ* spectroscopic ellipsometry was employed to monitor the thickness of both the Si_3N_4 and the silicon oxide layer during ALE. These studies observed that the silicon nitride film thickness decreased linearly with number of reaction cycles while the silicon oxide thickness remained constant.

Using an O_2-HF-TMA reaction sequence, the Si_3N_4 ALE etch rate was 0.26 Å/cycle at 290°C. This etch rate was obtained using static reactant pressures of 250, 0.65 and 1.0 Torr, and exposure times of 10, 5 and 5 s, for O_2, HF and TMA, respectively. Employing similar dosing conditions, the process using O_3 yielded a higher Si_3N_4 etch rate of 0.47 Å/cycle (see Supplemental Figure 2). The Si_3N_4 etch rates remained the same for O_3 pressures from 30-250 Torr. The order of the reactant sequence affected the Si_3N_4 etch rate. Changing the reactant sequence from O_3-HF-TMA to O_3-TMA-HF reduced the Si_3N_4 etch rate from 0.47 to 0.20 Å/cycle at 290°C. The Si_3N_4 ALE etch rate was also reduced at lower temperatures. Using the O_3-HF-TMA reaction sequence, the Si_3N_4 etch rate was reduced from 0.47 Å/cycle at 290°C to 0.07 Å/cycle at 210°C.

Si_3N_4 ALE also decreased the roughness of the Si_3N_4 surface. The RMS roughness of the initial Si_3N_4 films was 4.7 Å measured using atomic force microscopy (AFM). The RMS roughness decreased to 3.1 Å after 80 ALE cycles. An SiO_2 oxide thickness of ~10-15 Å remained after Si_3N_4 ALE at 290°C. This oxide could be removed by 15 sequential TMA and HF exposures after the Si_3N_4 ALE. Thermal Si_3N_4 ALE should be useful in advanced semiconductor fabrication. Thermal Si_3N_4 ALE could also find applications in optoelectronics, photonics and MEMS fabrication.

8:45am **ALE1-TuM4 Thermal Dry Atomic Layer Etching of Cobalt with Sequential Exposure to Molecular Chlorine and Diketones***, M. Konh, C. He, X. Lin,* University of Delaware*; X. Guo, V. Pallem,* American Air Liquide*; R. Opila,* ***Andrew Teplyakov****, Z. Wang, B. Yuan,* University of Delaware

The mechanism of thermal dry etching of cobalt films is discussed for a thermal process and a sequential exposure to chlorine gas and a diketone (either 1,1,1,5,5,5-hexafluoro-2,4-pentanedione (hexafluoroacetylacetone, hfacH) or 2,4-pentanedione (acetylacetone, acacH)). The process can be optimized experimentally to approach atomic layer etching (ALE), and a sequential exposure to Cl_2 and hfacH dry etchants at 140°C is shown to proceed efficiently. The use of acacH as a diketone does not result in ALE with chlorine even at 180°C; however, the decrease of surface chlorine concentration and chemical reduction of cobalt is noted. Thermal desorption analysis suggests that the reaction of chlorinated cobalt surface exposed to the ambient conditions (oxidized) with hfacH does produce volatile Co-containing products within the desired temperature range and the products contain Co^{3+}. The effect of ligands on the energy required to remove surface cobalt atoms is evaluated using density functional theory and the findings are consistent with the experimental observation of surface smoothing during atomic layer etching.

9:00am **ALE1-TuM5 Spontaneous Etching of B_2O_3 and TiO_2 by HF: Removal Reaction in WO_3 ALE and TiN ALE***, **Austin Cano**,* University of Colorado - Boulder*; S.K. Natarajan,* Tyndall National Institute, Ireland*; J. Clancey,* University of Colorado - Boulder*; S. Elliot,* Schrödinger Inc*; S.M. George,* University of Colorado - Boulder

Thermal atomic layer etching is typically based on two sequential surface reactions. The first reaction activates the surface layer and the second reaction leads to material removal by the desorption of volatile etch products. The surface activation can be halogenation, conversion to a different material, or oxidation of the initial material. For example, BCl_3 is able to convert the WO_3 surface to a B_2O_3 surface layer during WO_3 ALE. The B_2O_3 surface layer is then spontaneously removed by etching using HF. In another example, O_3 is able to oxidize the TiN surface to a TiO_2 surface layer during TiN ALE. The TiO_2 surface layer is then spontaneously removed by etching using HF.

This study explored the spontaneous etching of B_2O_3 and TiO_2 with HF using Fourier Transform Infrared (FTIR) spectroscopy and quadrupole mass spectrometry (QMS) analysis. The initial B_2O_3 films were grown using B_2O_3 ALD with BCl_3 and H_2O as the reactants. The initial TiO_2 films were grown using TiO_2 ALD with $TiCl_4$ and H_2O as the reactants. FTIR measurements observed the growth of the B_2O_3 films and TiO_2 films by monitoring the absorbance of the B-O and Ti-O stretching vibrations, respectively, versus number of ALD cycles. FTIR experiments also observed the spontaneous etching of B_2O_3 and TiO_2 with HF by measuring the loss of the absorbance of the B-O and Ti-O stretching vibrations, respectively (See Supplemental Figure 1).

QMS studies were also able to monitor the volatile etch products during the spontaneous etching of B_2O_3 nanopowder with HF. The expected reaction products are BF_3 and H_2O based on the reaction $B_2O_3 + 6HF \rightarrow 2BF_3 + 3H_2O$. In comparison, the QMS detected $B(OH)F_2$, BF_3 and H_2O as the main etch products (See Supplemental Figure 2). In addition, the QMS also revealed species at higher masses that were consistent with six-member ring species, such as $B_3O_3F_3$.

The reaction of HF with B_2O_3 and TiO_2 was also examined using a density functional theory (DFT) based computational approach. By comparing the thermodynamic free energy profiles of competing self-limiting surface and bulk reactions, the DFT calculations predicted the spontaneous etching of B_2O_3 by HF above -160°C and of TiO_2 (but not TiN) above 90°C, in agreement with the experimental findings.

9:15am **ALE1-TuM6 Thermal Based Atomic Layer Etching of Aluminum Oxide and Titanium Nitride***, **Varun Sharma**,* ASM, Finland*; T. Blomberg,* Picosun Oy/ASM, Finland*; M. Tuominen, S. Haukka,* ASM, Finland

Thermal based Atomic Layer Etching (th-ALEt) has opened a new horizon and triggered an increased interest in the Semiconductor Industry for the fabrication of sub-10 nm as well as complex 3D nano-devices. In the th-ALEt technique, a material is chemically etched from thermally activated surface by sequence of one or more reactants each separated by purge steps. Unlike the conventional anisotropic plasma etching, th-ALEt is isotropic, selective and its slow etch rate may possess excellent atomic-scale control. Most of the reported th-ALEt chemistries utilize hydrogen fluoride (HF from HF-pyridine) as one of the reactants. However, due to some safety concerns associated with the use and handling of HF, we have considered other fluorine donating compounds. In this work, we report niobium pentafluoride (NbF_5) as an alternative to HF. Carbon tetrachloride (CCl_4) is used as a co-reactant with NbF_5 to etch aluminum oxide (Al_2O_3) as well as titanium nitride (TiN). The various attributes of the etching process like etch rates, selectivity and post-etch surface roughness were studied. It was found that NbF_5 promotes the fluorination of Al_2O_3 and the fluorinated Al_2O_3 surface can be etched away by a subsequent exposure of CCl_4 gas. TiN can be etched in continuous pulsed mode just by CCl_4, while adding NbF_5 to the process enables etch-rate control. The etch results and proposed reaction pathway for the etching of Al_2O_3 and TiN will be discussed in the presentation.

9:30am **ALE1-TuM7 Thermal Atomic Layer Etching of Amorphous and Crystalline Hafnium Oxide, Zirconium Oxide and Hafnium Zirconium Oxide***, **Jessica A. Murdzek**, S.M. George,* University of Colorado - Boulder

Thermal atomic layer etching (ALE) can be achieved with sequential surface reactions using the fluorination and ligand-exchange mechanism. For metal oxide ALE, fluorination converts the metal oxide to a metal fluoride. The ligand-exchange reaction then removes the metal fluoride by forming

volatile products. Previous studies have demonstrated the thermal ALE of amorphous HfO_2 and ZrO_2 ALD films. No previous investigations have explored the differences between the thermal ALE of amorphous and crystalline films. The thermal ALE of crystalline films is important because amorphous films may not crystallize easily when they are too thin. Consequently, amorphous films may have to be grown thicker, crystallized, and then etched back to obtain the desired ultrathin crystalline film thickness.

This study explored the thermal ALE of amorphous and polycrystalline films of hafnium oxide, zirconium oxide, and hafnium zirconium oxide. HF was used as the fluorination reactant. Dimethylaluminum chloride (DMAC) or titanium tetrachloride was employed as the metal precursor for ligand-exchange. The amorphous films had a much higher etch rate per cycle than the crystalline films. The differences were most pronounced for hafnium oxide. At 250 °C with HF and DMAC as the reactants, the etch rate was 0.03-0.08 Å/cycle for crystalline HfO_2 and 0.68 Å/cycle for amorphous HfO_2 (See Supplemental Figure 1).

Under the same conditions at 250 °C with HF and DMAC as the reactants, the etch rate was 0.60-0.82 Å/cycle for crystalline ZrO_2 and 1.11 Å/cycle for amorphous ZrO_2. In comparison, the etch rate was 0.16-0.26 Å/cycle for crystalline $HfZrO_4$ and 0.69 Å/cycle for amorphous $HfZrO_4$. The etch rates for $HfZrO_4$ were between HfO_2 and ZrO_2 for both the amorphous and crystalline films. When HF and $TiCl_4$ were used as the reactants at 250 °C, the etch rates were smaller than the etch rates with HF and DMAC as the reactants for every material. The etch rates also increased with temperature for both the amorphous and crystalline films. The differences between amorphous and crystalline HfO_2 are sufficient to obtain selective thermal ALE of amorphous HfO_2.

9:45am **ALE1-TuM8 Isotropic Atomic Layer Etching of Cobalt with Smooth Etched Surfaces by using Cyclic Repetition of Plasma Oxidation and Organometallization***, **Sumiko Fujisaki**,* Hitachi R&D Group, Japan

Isotropic atomic layer etching (ALE), which produces atomically precise, conformal removal, will have an important role in semiconductor manufacturing. This is because highly selective ALE has become necessary to deal with processing of new materials with the advances in minitualization of devices such as 3D structures. In the past several years, isotropic ALE of various materials has been reported which includes thermal ALE for metal oxides and thermal-cyclic ALE for nitride films [1]. To meet the requirements concertning the variety of materials to be etched, isotropic ALE of cobalt must be developed. In 2018, thermal ALE of cobalt has been reported by using treatment with formic acid and ligands to produce volatile cobalt complexes [2]. In this paper, the authors successfully demonstrate isotropic ALE of cobalt film with smooth etched surfaces, which is important issue in the development of ALE of cobalt.

The experimental apparatus used in this study is 300-mm ALE tool equipped with inductively-coupled plasma source and infrared lamps. The cyclic ALE process is composed of three step repetitions: oxidation of cobalt surface with oxygen plasma, organometallization of the cobalt oxide with a low acidity ligand vapor, and sublimation of the organemetallic cobalt by thermal annealing.

The etching depth of cobalt increased with increasing the number of repetitions of the cycle. For one cycle of etching, it was 1 nm high. The root-mean-square (RMS) roughness of etched cobalt surface was estimated to be 0.8 nm. It was found that formation of homogeneous CoO (II) was important because compound oxide such as Co_3O_4 (II & III) resulted in rough etched surfaces with columnar morphology. Furthermore, controllability of etching amount was substantially improved by using low reactivity ligands compared to high-reactivity ligands. These results implied that the combination of homogenious CoO formation, low-reactivity ligands, and sublimation was essential for achieving smooth etched surfaces and excellent controllability of etching amount.

In conclusion, we have obtained well-controlled etch front roughness and etching depth of cobalt, which can be applied to semiconductor process, by controlling reactions of both oxidation and metal complex formation using the 300-mm ALE apparatus.

[1] K. Shinoda et al., J. Phys. D: Appl. Phys. 50, 194001 (2017).

[2] C. Winter, AVS 65th, PS+EM+TF-ThM5 (2018).

Atomic Layer Etching
Regency Ballroom A-C - Session ALE2-TuM

Alternative Methods to ALE

Moderators: Jean-François de Marneffe, IMEC VZW, Satoshi Hamaguchi, Osaka University

10:45am **ALE2-TuM12 Atomic Layer Etching for Germanium using Halogen Neutral Beam =Comparison between Br and Cl Chemistry=***, T. Fujii, **Daisuke Ohori**,* Tohoku University, Japan*; S. Noda,* National Institute of Advanced Industrial Science and Technology, Japan*; Y. Tanimoto, D. Sato, H. Kurihara,* Showa Denko K.k.*; W. Mizubayashi, K. Endo,* National Institute of Advanced Industrial Science and Technology, Japan*; Y. Li,* National Chiao Tung University*; Y.-J. Lee,* National Nano Device Laboratories*; T. Ozaki, S. Samukawa,* Tohoku University, Japan

Recently, 3D Fin field-effect transistors (FETs) have been developed for breaking through limitations of the short-channel effect for highly scaled metal-oxide-semiconductor (MOS) FETs. However, the Ge channel formation for Fin FET has not been deeply investigated since the Ge etching reaction is not known well compared to the Si etching reaction. As a result, the carrier mobility degradation was observed by electron scattering due to surface roughness and defects on the channel sidewall surface etched by conventional plasma etching (PE). In the PE, energetic ion bombardment and ultraviolet (UV) light irradiation cause a large side-etching, sidewall surface defects, and sidewall surface roughness. These lead to the degradation of carrier mobility and I-V characteristics [1]. To realize higher performance electrical characteristics without compromising the intrinsic high carrier mobility of Ge, atomic layer defect-free, roughness-free, and profile-controlled etching must be accomplished for future sub-10 nm Ge Fin FET. In this work, we demonstrated atomically flat, extremely high selective and defect-free etching with the hydrogen bromide (HBr) neutral beam etching, and investigated the mechanism compared with the Cl_2 NBE.

We investigated Ge etching rate dependence on the substrate temperature from -20 to 150 ºC by using HBr and Cl_2 neutral beam. Sample structure was p-type Ge (100) wafer with SiO_2 line pattern mask of 150 nm in width of a nanoimprint.

We carried out the cross-sectional SEM observation and ellipsometer measurement for checking the Ge etching rate and SiO_2 etching rate, respectively. For the HBr NBE, the Ge etching rate was almost constant at 35 nm/min from -20 to 90 ºC. On the other hand, for the Cl_2 NBE, the Ge etching rate linearly increased from 38 to 45 nm/min from -20 to 150 ºC. SiO_2 etching rate for HBr and Cl_2 NBE were 0.3 nm/min and 2.8 nm/min at any substrate temperature, respectively. The HBr NBE could realize almost 10 times higher etching selectivity as compared with Cl_2 NBE. Moreover, the sidewall etching for HBr NBE was perfectly eliminated from -20 to 90 ºC. In contrast, the sidewall etching for Cl_2 NBE occurred at more than 90 ºC. It is considered that non-volatile Bromide protected layer, such as $GeBr_4$ and $Si_xBr_yO_z$was formed on the Ge sidewall and SiO_2 top surface in case of using HBr. HBr NBE could perfectly eliminate the sidewall etching and obtain extremely high etching selectivity to SiO_2 even at more than 90 ºC . In conclusion, we succeeded to fabricate the Ge Fin structure of highly anisotropic and extremely high selectivity with HBr NBE.

[1] W. Mizubayashi, et al., Appl. Phys. Express, 10, 026501 (2017).

11:15am **ALE2-TuM14 A New Etching / Passivation Process in Cyclic Mode for Spacer Etching in 3D CMOS Integrations***, O. Pollet,* CEA-LETI, France*; N. Posseme,* Univ. Grenoble Alpes, CEA, LETI, France*; V. Ah-Leung, **Valentin Bacquie**,* CEA-LETI, France

With ever-decreasing gate length in CMOS technology, integrations have changed from planar to 3D architectures, such as FinFET or stacked nanowires, where the channel is a tall and narrow structure protruding from the surface, thereby providing a better electrostatic control and reduced leakage. However from an etch standpoint this raises new challenges particularly for spacer formation since the stopping layer has become a structured surface instead of being flat, which induces the formation of parasitic spacers on channel sidewalls. To overcome this issue overetch must be significatively lengthened, from 30-50% in planar CMOS to 200-300% in 3D CMOS. Considering other requirements such as no CD loss, no channel material loss or damaging, spacer etching has turned into a very challenging process.

Conventional processes based on fluorocarbon chemistries like $CH_3F/CH_4/O_2$ do not provide sufficient selectivity to silicon to enable long overetch required to get rid of spacers on channel sidewalls without considerably consuming or damaging the channel material. To improve

selectivity a new process was proposed recently, that contains $SiCl_4$ in addition to fluorocarbon in the etching chemistry.

XPS analyses showed that this specific gas composition leads to the deposition of SiO_xF_y, which acts as a passivation layer on silicon, instead of the usual carbon-rich organic film deposited with CH_zF_w/O_2 chemistries. Ellipsometry measurements highlighted that SiO_xF_y passivation grows preferentially on silicon than on silicon nitride, which allows etching to carry on this material while silicon is passivated. Less than 1nm of silicon consumption is consistently measured even for long process times while at the same time silicon nitride is etched linearly providing a selectivity up to 40:1 between nitride and silicon.

To further improve process performance this $SiCl_4$-containing process was combined in a cyclic mode with a non-selective CHF_3 step. The $SiCl_4$ step function is to etch silicon nitride while depositing passivation on silicon. During the CHF_3 step both silicon nitride and passivation on silicon are etched and respective step times were set up in such way that silicon nitride is linearly etched at a rate of 7.3nm/cycle while the silicon surface is permanently covered by the SiO_xF_y layer. This ALE-inspired process was demonstrated on a stacked nanowires integration: a 12.5nm thick SiN IRAD spacer was etched with very limited CD bias on the gate while parasitic spacers formed on 36nm high active area sidewalls were thoroughly removed without inducing more than 1.5nm silicon consumption.

11:30am **ALE2-TuM15 Atomic Layer Etching of Transition Metals with Gas Cluster Ion Beam Irradiation and Acetylacetone***, **Noriaki Toyoda**, K. Uematsu,* University of Hyogo, Japan

Atomic layer etchings (ALE) of transition metals with gas cluster ion beam (GCIB) and acetylacetone were investigated. In general, the ion energy in the removal step in ALE is several tens of eV, which is higher than the sublimation energy of the surface layer (several eV). These excess energies might be the origin of the damages on the target materials. We have investigated the feasibility of GCIB as energetic ions in the removal steps of ALE process. Since GCIBs are aggregates of thousands of gas atoms or molecules, the energy/atoms or energy/molecules can be easily reduced to several eV even though the total energy of GCIB is several keV. In additions, since GCIB induce dense energy deposition without severe damage, the bombarded area experiences transient high-temperature and high-pressure conditions. As a result, chemical reactions are enhanced at low-temperature. In the previous study, ALE of Cu films was demonstrated successfully using O_2-GCIB and acetic acid.

In this study, we have investigated ALE process for transition metals (Cu and Ni) using acetylacetone. We separated each etching step as following; (1) adsorption of acetylacetone on metal oxide, (2) evacuation of residual acetylacetone vapor, (3) irradiation of O_2-GCIB to remove metal oxide. Effects of the following etching parameters on ALE were investigated from real-time thickness on a quartz crystal monitor; acceleration voltage of oxygen GCIB, irradiation time of GCIB, exposure time of acetylacetone.

When the acceleration voltage of O_2-GCIB is 20 kV, very thin layer of nickel oxide with adsorbed acetylacetone is removed quickly, however, Ni atoms are physically sputtered. Consequently, the etching process with 20 kV oxygen GCIB is not self-limiting. On the contrary, surface nickel oxide with adsorbed acetylacetone are removed by 5 kV O_2-GCIB and there is no physical sputtering. Since the average cluster size of O_2-GCIB is 3000 molecules/ion, the energy/molecule is below 2 eV. By using 5 kV O_2-GCIB, self-limiting removal step is realized.

11:45am **ALE2-TuM16 Atomic Layer Etching at Atmospheric Pressure***, **Eugen Shkura**, D. Theirich, K. Brinkmann, T. Haeger,* University of Wuppertal, Germany*; J. Schneidewind, M. Siebert,* SENTECH Instruments GmbH, Germany*; T. Riedl,* University of Wuppertal, Germany

Atomic Layer Etching (ALE) is a cyclic process which is based on sequential surface reaction of two or more reactants and ideally provides control on the monolayer level. In the last decade the main focus was on two types of ALE. The first approach relies on the chlorination and sometimes fluorination to initially create metal-halide species at the surface which are subsequently removed by a plasma [1,2]. Another approach is thermally driven ALE, e.g. by using HF and $Sn(acac)_2$ to etch metal oxides [3]. More recent reports indicated isotropic etching by using radically driven, plasma enhanced ALE [4]. In all these examples, the ALE process is vacuum based and as such provides some limitations towards high throughput and low manufacturing costs. Here, we introduce a novel process for Atomic Layer Etching at atmospheric pressure (AP-ALE). As a case study, we investigate the etching of ZnO by AP-ALE and spatial AP plasma enhanced-ALE by using Hacac at substrate temperatures in the range of 80-140 °C. Ozone as well as an atmospheric pressure dielectric Ar/O_2 barrier discharge is used for AP-ALE and spatial AP Plasma Enhanced-ALE, respectively. In-situ quartz crystal microbalance as well as ex-situ spectroscopic ellipsometry were used to characterize the etching process. Depending on the processing conditions, an etch per cycle of 0.5 to 5 Å is found. Ex-situ AFM measurements before and after ALE show a modification of ZnO-Surface and a decrease in film thickness. Furthermore, growth characteristics in dependence of process parameters like substrate velocity and substrate temperature were investigated. We discuss the prospects to use spatial AP-ALE for materials other than metal oxides, such as III-V semiconductors like GaN or AlGaN.

[1] K.J. Kanarik et al. Solid State Technology 56(8) 14-17 (2013).

[2] S. Rauf et al. J. Appl. Phys. 101, 033308 (2007).

[3] Y. Lee et al., ACS nano, 9(2), 2061-2070. (2015).

[4] A. Mameli et al., ACS Applied Mater. & Interfaces 10, 38588-38595 (2018).

Area Selective ALD
Grand Ballroom H-K - Session AS1-TuM

Area-Selective ALD Techniques

Moderator: Adrie Mackus, Eindhoven University of Technology

10:45am **AS1-TuM12 Overview of Wet And Dry Selective Processes Driven by Area Activation or Deactivation Down to Below 20nm Critical Dimensions***, **Silvia Armini**,* IMEC, Belgium **INVITED**

Area selective deposition (ASD) is proposed as a method for preferentially depositing a material on a specific area on the surface while the remainder is left uncoated, providing spatial control over a deposited thin film. In the context of downscaling microelectronics components below 1x nm of critical dimension, ASD by Atomic Layer Deposition (ALD), Chemical Vapor Deposition (CVD) or Electroless Deposition (ELD) offers the potential to relax downstream processing steps by enabling self-aligned patterning processes, such as self-aligned vias and tone reversal, or bottom-up metallization schemes, such as supervia or via prefill. Due to the limitations of inherent ALD selectivity, we focus our work on material surface functionalization by selective grafting thin organic films both in ALD activation and passivation mode or by plasma exposure.

For ASD ALD processes which relies on delayed nucleation on a non-growth area, defectivity and the lack of a wide portfolio of application-relevant materials are two of the main concerns for the adoption of this technology in nanofabrication. Among the strategies addressing the defectivity issue, repetitive refreshment of the non-growth surface and selective etching of undesired nuclei are particularly promising.

In this study, we review our current understanding of the relationship between structure and properties of the inhibiting/activating materials and the correspondent surface dependence of different ALD processes. Nucleation and growth behaviour of ALD on different surfaces functionalized by organic films deposited from the liquid and vapor phase on 300mm wafers or by plasmas will be analyzed and wet depassivation processes with be investigated in the attempt of removing the defects formed on top of the inhibition films.

In an attempt to understand the interaction between the ALD conditions (i.e. temperature, coreactants...) to the decomposition and modification of the organic films, in-situ XPS is exploited such as high sensitivity characterization techniques such as Secondary Ion Mass Spectrometry (SIMS).

Finally, the selectivity of the passivation and subsequent ASD process will be evaluated as a function of the patterned pitch size down to 16nm half-pitch structures. We aim at building some understanding about the relationship between the changes in surface composition due to the patterning, pitch variation and/or due to diffusion (in case of mobile species such as metals) and the ASD performance.

11:15am **AS1-TuM14 Electron-Enhanced Atomic Layer Deposition (EE-ALD) of Cobalt Metal Films at Room Temperature***, **Zach Sobell**, A. Cavanagh, S.M. George,* University of Colorado - Boulder

Electron-enhanced atomic layer deposition (EE-ALD) is possible at room temperature by using electrons to stimulate the desorption of surface species. The electron stimulated desorption (ESD) process opens up free surface sites that enable the adsorption of reactants. ALD can be achieved by sequential application of electron and reactant exposures. A variety of materials have been deposited using EE-ALD at room temperature

including GaN, Si and BN. Because EE-ALD is dependent on the electron flux, EE-ALD films are deposited only on surface areas illuminated by the electron beam.

In this study, Co EE-ALD was performed using sequential, self-limiting cobalt tricarbonyl nitrosyl [$Co(CO)_3NO$ (CTN)] and low energy electrons exposures at room temperature. The electron energies were varied from 75 to 175 eV. In the Co EE-ALD process, the CTN molecules first adsorb on the substrate. The electrons then induce ESD of the carbonyl (CO) and nitrosyl (NO) ligands from the adsorbed CTN. The ESD produces reactive surface sites. Subsequent CTN exposures react with the reactive surface sites and add Co to the substrate. The consumption of the reactive surface sites produces self-limiting Co EE-ALD.

In situ ellipsometry measurements observed a maximum growth rate of 0.5 Å per cycle at an electron energy of 125 eV. The in situ ellipsometry measurements also could monitor the CTN adsorption and the desorption of CO and NO ligands (see supplemental Figure 1). Quadrupole mass spectrometer (QMS) measurements confirmed the desorption of CO and NO during electron exposures. The spatial profile of the Co EE-ALD film resulting from the finite surface area illuminated by electrons was mapped by ex situ ellipsometry. This spatial profile was used to calculate an ESD cross section of $\sigma = 1x10^{-16}$ cm^2. This ESD cross section is close to the electron dissociation cross section for CTN observed in the gas phase.

There are many applications for EE-ALD because the ESD process is topographically selective. This area selectivity comes from the directionality of the electron flux. Surfaces normal to the incident electrons receive the full electron flux, whereas surfaces parallel to the incident electron path receive no electron flux. EE-ALD should be useful for the bottom-up fill of high aspect ratio structures like trenches and vias. EE-ALD may also be important for depositing ALD films on thermally-sensitive substrates. In addition, EE-ALD could be valuable for enhancing the nucleation of ALD films by creating reactive surface species on the initial substrate.

~~11:30am **AS1-TuM15 Area Selective Atomic Layer Deposition on Molecular Design,** ***Akihiro Nishida,*** *T. Yoshino, N. Okada, A. Yamashita,* ADEKA Corporation, Japan~~

~~Area-selective atomic layer deposition (AS-ALD) is promising as a self-aligned fabrication method and has become more important in recent years. Several types of AS-ALD precursors and processes have been developed all over the world so far. We recognize the importance of AS-ALD technology as well and have studied it for many years. However, it is challenging to achieve a high selectivity and hence investigation of molecule design and surface chemistry are essential factors to clarify the mechanism of selective deposition and film growth.~~

~~In this study, we have carried out the investigation on the effect of surface selectivity using several types of Co ALD precursors, and found that selectivity was affected by high steric hindrance structure, chemical surface characteristics and so on. Based on the results, new Co ALD precursors having a good selectivity have been developed. As an example, Bis(N-tert-butyl-N'-1-methyl-2-dimethylaminoethyl acetamidinato)cobalt (II) [CBPA-1] has high selectivity and is liquid at room temperature. CBPA-1 showed a very clean TG curve without decomposition and residue at 10 Torr. Additionally, thermal ALD of thin Co metal film was demonstrated using CBPA-1 and hydrogen as the co-reactant on Ru and SiO_2 substrates, and succeeded in making shiny metallic Co films at 150-300 °C only on the Ru substrate. Regarding film quality, X-ray photoelectron spectroscopy (XPS) shows that high purity Co film was deposited. As a comparison, we also carried out thermal ALD using reference precursor Bis(N, N'-di-tert-butyl-acetamidinato)cobalt (II). However, Co was detected on both Ru and SiO_2 substrates over 275 °C by X-ray fluorescence (XRF) measurement. As a conclusion, CBPA-1 is better suited for Co AS-ALD process compared to conventional precursors such as dicobalt hexacarbonyl tert-butylacetylene (CCTBA) and Co amidinates complex. On top of that, a reducing method of isolated particles growth on SiO_2 substrate by using aminosilane was found out so it will be reported likewise.~~

11:45am **AS1-TuM16 From Surface Dependence in Atomic Layer Deposition to Area-Selective Deposition of TiN in Nanoscale Patterns***,* ***Annelies Delabie,*** IMEC, Belgium*; D. Carbajal,* UNAM*; J. Soethoudt, B.T. Chan, E. Altamirano Sanchez, B. Meynaerts, J.-W. Clerix, S. Van Elshocht,* IMEC, Belgium

Area-selective deposition (ASD) holds potential for nano-electronic device manufacturing for bottom-up deposition in small trenches or holes, or to create nanoscale structures with great precision by self-alignment. Under certain surface and deposition conditions, material can grow selectively on a predefined pattern, while the rest of the surface remains unaffected. Nevertheless, ASD by atomic layer deposition (ALD) has been studied only for a limited number of materials. In addition, defectivity in the non-growth area is a challenge as inhibition in ALD is associated with island growth [1]. Insight into the surface dependence and growth mechanisms is needed to design highly selective ASD processes for relevant materials for nano-electronic devices.

First, we compare the inherent selectivity for a range of thermal ALD processes for oxides, nitrides and metals by investigating the surface dependence on blanket substrates. OH-terminated SiO_2 is the growth surface as all ALD processes considered here show linear growth on this surface, while CH_3-terminated SiO_2 is the non-growth surface. Both precursor and co-reagent affect selectivity (figure 1a). The selectivity for H_2O based ALD depends on the precursor in the order $TiCl_4$ > $HfCl_4$ > $Al(CH_3)_3$. The selectivity is higher for $TiCl_4/NH_3$ ALD than for $TiCl_4/H_2O$ ALD in spite of the higher deposition temperature.

In view of the high inherent selectivity of $TiCl_4/NH_3$ ALD, we investigate TiN ASD in nanoscale patterns consisting of Si_3N_4 spaces and amorphous carbon (aC) lines with a critical dimension (CD) of 45nm. This material system is relevant for a tone inversion application of ASD for line-space patterning [2]. A H_2 plasma pretreatment enables ASD by passivating the aC surface by formation of methyl groups [2,3]. The selectivity for Si_3N_4 versus aC is 0.94 for 6.4 nm TiN, even higher than for OH- versus CH_3-terminated SiO_2 (blankets). The selectivity is maintained for ALD temperatures between 250 and 390° C. However, in nanoscale patterns, the selectivity is affected by impurities due to patterning. By considering surface cleans before ASD, we demonstrate ASD of 7.5nm TiN on the 45nm CD line-space patterns, with little to no TiN detected on the aC top surface and sidewalls by transmission electron microscopy (Figure 1b).

[1] J. M. Mackus et al, Chem. Mater. 2019, 31, 2

[2] E. Stevens et al, Chem. Mater. 2018, 30, 3223

[3] I. Zyulkov et al, ACS Appl. Mater. Interfaces 2017, 9, 31031

ALD Applications
Grand Ballroom E-G - Session AA1-TuA

Emerging Applications I

Moderators: Anjana Devi, Ruhr University Bochum, Han-Bo-Ram Lee, Incheon National University

1:30pm **AA1-TuA1 Atomic Layer Deposition of Indium Gallium Zinc Oxide (IGZO) Semiconductor Thin Films: From Precursor to Thin Film Transistor Application***, **Jin-Seong Park,*** Hanyang University, Republic of Korea**INVITED**

Oxide semiconductor thin film transistors (TFTs) have been extensively researched as a switching device in display industry. Also, the amorphous indium gallium zinc oxide (a-IGZO) have been already adopted for the mass-production of OLED TVs because it showed remarkable performances such as high mobility (>10cm^2/V. sec), low process temperature (<350°C), optical transparency (>3eV) and low-cost fabrication process. Recently, there are a few efforts to fabricate atomic layer deposited (ALD) IGZO thin films and demonstrating their device properties. However, ALD IGZO systems are quite difficult to understand their electrical and chemical properties because each precursor is affected to growth mechanism, crystallinity, and electrical performance.

In this talk, I will show key properties (growth behavior, electrical/chemical properties, and device performances) of indium gallium oxide (IGO) and indium gallium zinc oxide (IGZO) thin films depending on a few In and Ga precursor species. There films are deposited using the concept of "super-cycle" – IGO (n cycle InO_x – m cycle GaO_x) and IGZO (n cycle of InO_x – m cycle of GaO_x – k cycle of ZnO). Then, the bottom gate-top contact (inverted staggered structure) thin film transistors were fabricated by ALD processes. The devices with IGO and IGZO active layers are named Device A (IGO TFT using Indium A precursor), Device B (IGZO TFT using indium B precursor), Device C (IGZO TFT using Indium B precursor), Device D (IGZO TFT using indium B' precursor).

The representative transfer curves and performance parameters are shown in Figure 1 and Table 1. The IGZO device D exhibited boost mobility of 74.4 cm^2/V.sec. but the IGZO device B and C with different Indium precursors showed different mobilities of devices. It may result from a different growth rate and film composition. Thus, it is believed that ALD IGZO TFT will be very promising for the next generation switching transistor beyond the low-temperature poly-silicon (LTPS) thin film.

2:00pm **AA1-TuA3 ALD Growth of Ultra-thin Co Layers on the Topological Insulator Sb_2Te_3***, **Emanuele Longo**, R. Mantovan, R. Cecchini,* CNR-IMM Unit of Agrate Brianza, Italy*; M.D. Overbeek,* Wayne State University*; M. Longo,* CNR-IMM Unit of Agrate Brianza, Italy*; L. Lazzarini,* CNR-IMEM, Italy*; M. Fanciulli,* Università degli Studi di Milano-Bicocca, Italy*; C.H. Winter,* Wayne State University*; C. Wiemer,* CNR-IMM Unit of Agrate Brianza, Italy

The coupling between ferromagnetic thin films (FMs) and topological insulators (Tis) is nowadays one of the hottest topics in the context of spintronics. The presence of Dirac-like dispersed surface states in the TI, jointly with the presence of a large spin-orbit coupling, is expected to favor a super-efficient (i.e. low-power) FM's magnetization manipulation through a large *spin orbit torque* (SOT). The role of the interface between Co and TI is fundamental in driving SOT functionalities, making the choice of the deposition technique crucial and itself often responsible of low-quality interfaces formation. The high conformality, excellent low thickness control and its low energetic character make atomic layer deposition (ALD) an appealing technique for spintronic applications. We present here a pure ALD process to grow few nm-thick Co metal films in direct contact with a granular-TI Sb_2Te_3 thin film grown by Metal Organic Chemical Vapor Deposition (MOCVD). The ALD of Co metal films was performed by alternating a saturative pulsing sequence of bis(1,4-di-tert-butyl-1,3-diazadienyl)cobalt (Co(^{tBu2}DAD)$_2$) (4 s), N_2 purge (10 s), *tert*- butylamine ($tBuNH_2$) (0.1 s) and N_2 purge (10 s) at 180°C. In order to compare the Co growth on the Sb_2Te_3 substrate, we performed simultaneous Co depositions on sputtered Pt substrates (conventionally used as a SOT material), maintaining the same number of cycles. We conducted a thorough chemical-structural characterization of the Co/Sb_2Te_3 and Co/Pt heterostructures by employing X-Ray Diffraction (XRD), X-Ray Reflectivity, Scanning Electron Microscopy (SEM) and Transmission Electron Microscopy (TEM). The results demonstrated the possibility to synthesize Co thin films from several tens, down to 4 nm, forming uniform and high-quality Co thin films characterized by a stable and sharp interface with the Sb_2Te_3 substrate. Indeed, XRR showed that the thinner Co films replicate the surface roughness of the Sb_2Te_3 buried layer, proving their conformal growth. The growth rate was found to be higher on Sb_2Te_3 than on Pt. XRD evidenced the substrate selectivity of this growth process, showing the structural continuity of the grown Co layer on the underlying substrate. On Pt, the Co grains were found to adapt to the [111] textured substrate by developing a strained cubic structure. On Sb_2Te_3, Co was shown to grow with hexagonal structure, with out-of-plane grains oriented along the [00l] direction, as the rhombohedric Sb_2Te_3 layer. The distinct magnetic ordering of cubic and hexagonal Co polymorphs, with the possibility to selectively grow Co with different magnetic properties, pave the way towards novel applications in spintronics.

2:15pm **AA1-TuA4 Modifying Interfacial Chemistry of Cellulose-Reinforced Epoxy Resin Composites using Atomic Layer Deposition (ALD)***, **Jamie Wooding**, Y. Li, K. Kalaitzidou, M. Losego,* Georgia Institute of Tech

Automotive and aerospace industries require new lightweight materials that enhance payload and improve efficiency via vehicle weight reduction. Employing composites, such as fiber-reinforced polymer resins, is a common approach to light-weighting these vehicles. In this talk, we will examine the use of ALD to modify the surface chemistry of cellulosic reinforcements to improve the interfacial adhesion in polymer resin composites. Cellulosic reinforcements offer advantages in sustainable materials sourcing, lower density, and lower cost. However, raw cellulosics are hydrophilic and are immiscible with most non-polar thermosetting polymer resins. In this study, a variety of ALD-derived surface modification schemes are discussed as a means to improve resin permeation within the fibrous structure and to establish better adhesion at the cellulose – polymer matrix interface. Specifically, we consider surface modification with the ALD-precursors trimethylaluminum (TMA) and titanium tetrachloride ($TiCl_4$), as well as with vapor-delivered carboxylic acids and silanes. Surface modification is confirmed with XPS studies and contact angle measurements. All are found to make the cellulose prepreg more hydrophobic, but the $TiCl_4$ – H_2O treatment demonstrates the best permeability for the polymer resin. Composites treated with low cycles of $TiCl_4$ – H_2O are found to have a 30% improvement in the modulus of elasticity and a 38% increase in the tensile strength compared to untreated cellulose – resin composites. Furthermore, the $TiCl_4$ – H_2O surface treatment results in a composite tensile strength equal to that of a 3-aminopropyltriethoxysilane, a widely-used surface modifying agent, treatment while avoiding the disadvantages of using wet chemistry. The structural enhancements in the cellulose – resin composite, as demonstrated via wicking studies and scanning electron microscopy (SEM), inform these improvements in mechanical properties.

2:30pm **AA1-TuA5 Atomic Layer Deposition of Au Nanoparticles on Titania***, Fatemeh S.M. Hashemi,* Delft University of Technology, Netherlands*; F. Grillo,* ETH Zurich, Switzerland*; V. Ravikumar, **D. Benz**, A. Shekhar,* Delft University of Technology, Netherlands*; M. Griffiths, S. Barry,* Carleton University, Canada*; J.R. van Ommen,* Delft University of Technology, Netherlands

Nanoparticles of Au supported on TiO_2 have various applications in photocatalysis, plasmonics and photovoltaics. These supported materials are commonly synthesized using liquid-based techniques such as sol-gel and deposition-precipitation. These methods, while being low-cost, result in high level of impurities and formation of Au particles with inhomogeneous size and composition. Here we present a vapor-based approach via atomic layer deposition (ALD) for controlled deposition of Au nanoparticles on TiO_2. We also use the designed structures for photocatalytic degradation of pollutants.

We perform a low temperature (105 °C) thermal ALD process using Trimethylphosphino-trimethylgold (III) and two oxidizers (ozone and water) in a fluidized bed reactor under atmospheric pressure condition. While plasma-assisted ALD of Au using Trimethylphosphino-trimethylgold (III) has been previously reported (Griffiths et al., Chemistry of Materials 2016), no studies have looked into the thermal deposition process for this precursor. We investigate the effects of Au precursor saturation and oxidizing reactants on controlling the nucleation, particle size distribution and composition of the Au nanoparticles.

Our studies suggest that ozone and water have an opposite effect on Au particle size distribution. While longer ozone pulse time results in the deposition of smaller Au particles, larger particles are formed when water pulse time is increased. TiO_2 nanoparticles have a high surface area of about 50 m^2/g, thus achieving precursor saturation on them requires long precursor dosage times. However, we show that the growth properties can also be controlled in the under-saturation regime. We also investigated the effects of Au loading and particle size on the photocatalytic activity of

Au/TiO_2 nanoparticles. A 3 fold enhancement in the photocatalytic activity of TiO_2 is achieved when Au/TiO_2 nanoparticles are used for degradation of the model pollutants (Acid Blue 9 and Rhodamine B). This all vapor process provides a highly controlled and efficient method for producing Au/TiO_2 particulates that meet the criteria for various applications.

2:45pm **AA1-TuA6 Multi-layer Protective Coatings on Silver for Protection of Historic Silver Artifacts***, E. Breitung,* Metropolitan Museum of Art*; S. Creange,* Rijks Museum, Netherlands*; G. Pribil,* J.A. Woollam*; A. Bertuch,* ***Ritwik Bhatia,*** Veeco-CNT

Historic silver artifacts are usually protected from tarnish by polymer-based coatings such as nitro-cellulose lacquer [1]. These coatings can be problematic because of uneven application, incomplete coverage and yellowing due to age. This has led to investigation of atomic later deposition of oxide layers as a possible alternative to lacquer based protective coating. It is important that the ALD coatings do not change the appearance (color, luminance) of the artifact. This is particularly challenging since historic silver can have bulk compositional variability as well as differences in surface composition [2].

In this work we start with substrates of silver content between 75% - 99.9% with copper as the major impurity. These substrates are characterized by variable angle spectroscopic ellipsometry to obtain their optical properties across the visible spectrum. It is found that (a) optical properties of the silver substrates depend significantly on composition and surface finish, and (b) a thin (2-11nm) interface layer is required to adequately model the ellipsometric data.

The optical model of the substrates obtained by ellipsometry is used to obtain the reflection spectrum and color of the substrates when coated with various ALD films such as SiO2, Al2O3 and TiO2. The modeled color of the coated substrate is compared to an uncoated substrate using the color difference metric (ΔE_{00}) [3]. Consistent with previous findings [4], we show that pure silver (99.99%) can be coated with SiO2 and Al2O3 without a perceptible color difference ($\Delta E_{00} < 1$) for a wide angle of incidence range (AOI = 0-75°). However, for silver alloys (80-95% silver) there is no coating thicker than 10nm that results in $\Delta E_{00} < 1$. [Figure-1]

The need to find a film stack that worked not just for pure silver but for silver alloys led to a multi-objective optimization problem – minimizing ΔE_{00} for silver substrates of different composition and AOI in 0-60°. A multi-layer film stack was found that showed $\Delta E_{00} < 1.25$ for all substrates for AOI=0-70°.

In addition to the optical characterization, modelling and optimization work mentioned above, we will report on the deposition and color measurement of the ALD films stacks on the silver substrates.

References:

[1] Grabow, Nicole et al. Metal 07: Interim meeting of the ICOM-CC Metal WG, Amsterdam, 17-21 September 2007, Amsterdam: Rijksmuseum, 2007, pp. 44-50.

[2] Mass, Jennifer and Matsen, Catherine. Handheld XRF for art and archaeology, Leuven: Leuven University Press, 2012, pp. 215-248.

[3] CIE Improvement to industrial color-difference evaluation. CIE 142-2001 ISBN: 978 3 901906 08 4

[4] Makela M et al. USPTO: 20090004386A1

3:00pm **AA1-TuA7 Nonlinear Optical Properties of TiO_2-Based ALD Thin Films***, **Theodosia Gougousi**, R. Kuis, I. Basaldua, P. Burkins, J.A. Kropp, A. Johnson,* University of Maryland, Baltimore County

Nonlinear materials in thin film form are highly desirable for the development of ultrafast all-optical system on-a-chip platforms, optical frequency converters and optical limiting applications. Conventional nonlinear optical (NLO) materials are usually cut from bulk crystals or are liquids that are not suitable for integration with the contemporary semiconductor industry process flow. The third order nonlinear response of ALD TiO_2-based films is investigated using thermally managed Z-scan technique. Some of the as-deposited films exhibit very high nonlinear response which is orders of magnitude higher than conventional nonlinear optical materials such as silica fibers and CS_2. Thermal treatment of the films at 450°C for 3 hours in an oxygen rich atmosphere affects the films' optical properties and results in the loss of the high nonlinear optical response. TiO_2 films deposited by Physical Vapor Deposition (PVD) from a 99.9% TiO_2 target at room temperature are used as control samples and their nonlinear optical response is found below the detection limit of the Z-scan setup. This extraordinary nonlinear optical behavior of the TiO_2 ALD films is linked to the presence of a very small at. % of TiN bonding in the film. We will present detailed characterization of these films by x-ray photoelectron spectroscopy, x-ray diffraction and UV-Vis absorption. The high level of control of the nonlinear index of refraction, n_2, using the deposition process coupled with the ability of ALD to coat non-planar geometries with atomic level precision and the fact that these processes are CMOS compatible have the potential to provide a breakthrough in optical device design and applications.

3:15pm **AA1-TuA8 Atomic Layer Deposition to Alter the Wetting and Thermal Properties of Lumber***, **Shawn Gregory**, C. McGettigan, E. McGuinness, D. Rodin, S. Yee, M. Losego,* Georgia Institute of Technology

This talk will discuss the use of atomic layer deposition (ALD) to modify the surface chemistry of bulk wood to alter its wettability and thermal conductivity. Wood blocks were ALD treated with three different metal oxide chemistries: $TiCl_4$-H_2O, $Al(CH_3)_3$-H_2O, and $Zn(C_2H_5)_2$-H_2O. All treatments consisted of only 1 ALD cycle. The resulting chemical modification of the wood with TiO_2, Al_2O_3, and ZnO was confirmed with energy dispersive X-ray (EDX) spectroscopy. All ALD chemistries made the wood hydrophobic with contact angles ranging from 90° to 130°. However, upon water submersion, it was found that TiO_2 coated wood had the least water uptake. While untreated wood absorbed up to 70 wt% water, the optimized TiO_2 treatment exhibited only a 10 wt% water uptake after 60 minutes. To understand these differences, we have considered the effective Fickian diffusion kinetics in the high-aspect ratio porosity of the wood structure. Measured pressure changes fit to Fickian diffusion models suggest that $Al(CH_3)_3$, and $Zn(C_2H_5)_2$ follow diffusion limited kinetics while $TiCl_4$ follows reaction limited kinetics. The apparent faster gas diffusion of $TiCl_4$ presumably results in more conformal coverage of the wood's structure. These models also suggest that $TiCl_4$ reacts to a greater extent than either Al or Zn precursor in this study. Because water content contributes significantly to the thermal transport of wood, we also measured thermal conductivity using the hot disc technique. Under dry conditions, untreated and TiO_2 coated wood have approximately the same thermal conductivity (~0.2 $W \cdot m^{-1}K^{-1}$). However, whereas the thermal conductivity of untreated wood increases by 50% in our tested wet environments, the thermal conductivity of $TiCl_4$ treated lumber remains nearly constant.

ALD Applications
Grand Ballroom E-G - Session AA2-TuA

ALD for Batteries II

Moderator: Yong Qin, Institute of Coal Chemistry, Chinese Academy of Sciences

4:00pm **AA2-TuA11 Tunable Electrical Properties of Lithium Fluoride Thin Films using Different Fluorine Sources***, **Devika Choudhury**, A. Mane, J.W. Elam,* Argonne National Laboratory

Considering that it has one of the largest optical bandgaps, lithium fluoride is probably the most popular material of choice for ultraviolet coatings today, as compared to other metal fluorides like MgF_2 and AlF_3. The low refractive index of 1.39 (at 580nm) also makes it useful as a window material in the UV-region of electromagnetic radiation.[1] Other utilities of LiF include thermoluminescent detector layers for X-rays and extreme UV sensor applications, electron injection layers in LED or photovoltaics etc.[2] Apart from optical applications, LiF may be useful as a protective coating on the cathodes of Li-ion batteries due to its chemical stability and wide electrochemical window. In this regard, LiF can be mixed with other metal fluorides to improve the lithium-ion conductivity while maintaining the chemical stability. Lithium ion conductivities of order 10^{-6} S/cm at room temperature have been reported for Li_3AlF_6 and Li_2NiF_4.[3]

LiF thin films grown by atomic layer deposition have been reported earlier using lithium tert-butoxide and HF-pyridine resulting in a room temperature ionic conductivity of 10^{-14} S/cm.[4] In this work we explore the possibility of growing LiF films with alternate sources of fluorine, WF_6 and MoF_6. *In-situ* quartz crystal microbalance and fourier transform infrared spectroscopy studies are carried out to obtain the growth characteristics of the films. Compositional analysis is obtained from XPS measurements. Impedance spectroscopy measurements are performed to evaluate the effect of LiF concentration in mixed metal fluoride coatings.

References:

1. Miia Matymaki et al., Chem. Mater. 2013, 25, 1656.

2. John Hennessy et al., Inorganics 2018, 6, 46.

3. T. Oi et al., Mater. Res. Bull. 1981, 16, 1281.

4:15pm **AA2-TuA12 The Role of Al_2O_3 ALD Precursor Chemistry on the Electrochemical Performance of Lithium Ion Battery Cathode Mmaterials***, **Donghyeon Kang**, A. Mane, J.W. Elam,* Argonne National Laboratory*; R.F. Warburton, J.P. Greeley,* Purdue University

Al_2O_3 coatings prepared by atomic layer deposition (ALD) using trimethyl aluminum (TMA) and H_2O on lithium metal oxide cathode surfaces have been shown to enhance the performance of lithium ion batteries. However, the effects depend on the choice of cathode material. For example, 1-2 TMA/H_2O cycles on lithium cobalt oxide (LCO) dramatically improves cyclability and slightly decreases capacity [1]. In contrast, the same treatment on lithium manganese oxide (LMO) improves capacity but has little effect on cyclability [2]. Furthermore, the TMA surface reactions on LMO are unusual in that they do not involve hydroxyls, ethane is released, and the Mn undergoes redox chemistry. Density functional theory (DFT) calculations reveal that this unique mechanism is driven by the large free energy changes upon methyl loss from TMA [2]. This leads us to speculate that the surface reactions and subsequent electrochemistry might also depend on the choice of Al precursor. To evaluate this hypothesis, we are exploring a range of aluminum precursors including trimethyl aluminum (TMA), tris(dimethylamido) aluminum (Al-TDMA), aluminum trichloride ($AlCl_3$), dimethyl aluminum isopropoxide (DMAI), and aluminum triisopropoxide (ATIP) on a variety of cathode materials such as LCO, LMO, and nickel manganese cobalt (NMC) materials. Our initial results suggest a correlation between cation reduction on the cathode surface and the relative Lewis acidity of the Al precursor ligands. We will elaborate on these findings using results from XPS measurements, DFT calculations, and coin cell cycling studies.

[1] Y. S. Jung et. al., *J. Electrochem. Soc.***157** (1) A75-A81, (2010).

[2] L. Chen et. al., *Chem***4** 2418-2435 (2018).

4:30pm **AA2-TuA13 Spatial Atomic Layer Deposition of Hybrid Nanolaminates for High Capacity Li-ion Battery Electrodes***, E. Balder, L. Haverkate, M. Tulodziecki, F. van den Bruele, S. Unnikrishnan, **Paul Poodt**,* TNO/Holst Center, Netherlands

Lithium-ion batteries have become the dominant battery technology in many applications. For future applications, there are still several challenges that need further development, including increasing the energy- and power density, reducing charging time, increasing the lifetime and improving the safety of operation. Solutions to these challenges can be found in combinations of new battery architectures, high performance materials and manufacturing methods.

ALD could be one of these new manufacturing methods, because of its unique characteristics in terms of film quality, uniformity and step coverage. For that reason, ALD is being explored for a wide variety of functional layers inside battery devices. One main drawback of ALD is its low deposition rate, limiting throughput and thereby leading to high manufacturing costs. Atmospheric pressure Spatial ALD could be a solution to this challenge, as it combines all the benefits of ALD with high deposition rates and scalability to large areas. Spatial ALD technology has already been developed for high performance applications in e.g. photovoltaics, roll-to-roll SALD for barrier foils and large-area SALD for OLED displays. This technology can potentially also be used as future manufacturing method of next generation solid state (3D) lithium ion batteries.

A material that is receiving considerable attention as an electrode for lithium-ion batteries is TiO_2, since it offers a potentially cheap, environmentally friendly and stable alternative to the current electrode materials. However, due to its low electronic conductivity and poor Li-ion conductivity it has a poor rate performance. The rate performance of TiO_2 films can be increased by decreasing the thickness, which comes at a cost of capacity. Nanolaminates of TiO_2 films can be used to maximize both the capacity and rate performance, where a stack of a number of thin TiO2 films will have a higher capacity than a monolithic film with the equivalent thickness. We have used Spatial ALD to make a hybrid nanolaminate film composed of thin TiO_2 layers separated by decoupling layers made by Spatial MLD of aminophenol-based titanicones. These decoupling layers have both a sufficient electrical conductivity and ionic conductivity in order for Li ions to penetrate in the underlying TiO_2 layers. When tested in a coin cell configuration, these nanolaminate electrodes demonstrate a 2-3 higher capacity than the reference, bulk TiO_{-2} electrodes of the same thickness, a high Coulombic efficiency and a good cycling stability.

These results demonstrate the potential of nano-scale engineered high performance electrodes made by high throughput Spatial ALD.

4:45pm **AA2-TuA14 Lithium Organic Thin Films for Various Battery Components***, **Juho Heiska**, M. Karppinen,* Aalto University, Finland

The field of energy storage is constantly evolving and facing new challenges. The next-generation batteries should be cheap, constitute of abundant elements only, and show electrochemical performances at least on par with the current state-of-the-art lithium-ion batteries. One of the promising new material families is the organic electrode materials; they are composed of light elements and thus possess high gravimetric capacities. Organic electrode materials do however suffer from low electronic conductivity and solubility issues when applied with a liquid electrolyte. Coating the organic materials with a thin passivation or solid-electrolyte layer is an effective way to suppress the dissolution without dramatically affecting the electrochemical properties. An attractive way to deposit these layers in a controlled manner is the atomic/molecular layer deposition (ALD/MLD) method. When organic electrodes are deposited with ALD/MLD the redox mechanisms are easy to experiment on since the system works as such without any conducting carbon or binder making it a simple model system. The deposition of solid electrolytes or protective coatings is also a highly feasible application for ALD/MLD.

In this research, a new ALD/MLD processes were developed for promising organic electrode materials and novel Li-organic coatings. The experimented molecules are related on the known electrode material lithium terephthalate with additional functional groups which alter the electrochemical properties. Since the bulk electrode composition is not standard in literature the comparison of the materials is difficult and prone to error. When the thin films of lithium-2-aminoterephthalate and lithium-2,5-dihydroxyterephtalate (Li_2DHTP) are compared with lithium terephthalate (Li_2TP) the direct comparison of electrochemical performance is possible. We find that both of the films do decrease the redox voltage as expected but also the flat discharge plateau of Li_2TP is lost. In addition, the rate capability and the cycling life of the films were negatively affected. We propose that the functional groups that donate electron density to the π-conjugated system are causing π-π repulsion between adjacent molecules. In addition, it was found hydroxyl groups of Li_2DHTP are lithiated at low potentials vs. Li^+/Li. Also, a novel lithium ethylene glycol ALD/MLD process was developed showing promising properties as a coating material for lithium-ion batteries. This and previous studies demonstrates the feasibility of this approach for developing better batteries and battery materials and highlights the potential of ALD/MLD technique for actual battery applications.

5:00pm **AA2-TuA15 ALD Infiltration of $LiCoO_2$ for High Rate Lithium Ion Batteries***, **Ian Povey**, M. Modreanu, S. O'Brien,* Tyndall National Institute, Ireland*; T. Teranishi, Y. Yoshikawa, M. Yoneda, A. Kishimoto,* Okayama University, Japan

Atomic layer deposition (ALD) was selected to deposit Al_2O_3 on cathode active material, $LiCoO_2$, to create a protective barrier layer [1], supress the high potential phase transition and thus reduce the subsequent Co dissolution [2]. However, surprisingly in this study it was found that it also resulted in the reduction of the charge transfer resistance at the cathode-electrolyte interface, thus enhancing the performance of the battery and not just its robustness. Energy-dispersive X-ray spectroscopy, in conjunction with transmission electron microscopy, shows that a discrete Al_2O_3 shell was not formed under the selected growth conditions and that the Al diffused into the bulk $LiCoO_2$ [3]. The resulting active oxide material, which was significantly thicker than the nominally Al_2O_3 ALD growth rate would predict, is proposed to be of the form $LiCoO_2$: Al with amorphous and crystalline regions depending on the Al content. Cells fabricated from the modified electrodes were found to have good cycling stability and discharge capacities of ~110 $mAhg^{-1}$ and ~35 $mAhg^{-1}$ at 50C and 100C respectively. Here we discuss the reasoning behind these observations and through a series of electrode treatments prior to ALD tune the behaviour.

[1] I.D. Scott, Y.S. Jung, A.S. Cavanagh, Y. Yan, A.C. Dillon, S.M. George, S-H. Lee, Nano Lett. 11 (2011) 414-418

[2] J.H. Woo, J.J. Travis, S.M. George, S-H. Lee, J. Electrochem. Soc. 162 (2014) A344-A349

[3] T. Teranishi, Y. Yoshikawa, M. Yoneda, A. Kishimoto, J. Halpin, S. O'Brien, M. Modreanu, I. M. Povey, ACS Appl. Energy Mater. 1 (2018), 3277-3282

5:15pm **AA2-TuA16 ALD Al_2O_3 and MoS_2 Coated TiO_2 Nanotube Layers as Anodes for Lithium Ion Batteries***, H. Sopha,* University of Pardubice, Czech Republic*; A. Tesfaye,* Ecole Nationale Supérieure des Mines de Saint-Etienne, France*; R. Zazpe,* University of Pardubice, Czech Republic*; T. Djenizian,* Ecole Nationale Supérieure des Mines de Saint-Etienne, France*; **Jan Macak**,* University of Pardubice, Czech Republic

The miniaturization of Lithium ion batteries (LIBs) as a power source to drive small devices such as smartcards, medical implants, sensors, radio-frequency identification tags etc. has been continuously developed to meet the market requirements of portable applications.[1] In this direction, 3D microbatteries have been considered to satisfy the requirements of these portable devices. Anodic TiO_2 nanotube layers (TNTs) have been recently explored as anodes for LIBs due to their high surface area, low volume expansion, short diffusion lengths for Li^+ ion transport and good capacity retention even at faster kinetics.[2,3]

Recently, various coatings produced by Atomic Layer Deposition (ALD) on electrode materials have been explored extensively in LIBs. For example, Al_2O_3 and TiO_2 coatings act as a protective layer for the suppression of the solid electrolyte interphase (SEI) in various electrode materials.[4,5] But their influence on increasing the electronic conductivity of the electrode material has not been explored in details. In addition, it is also possible to synthesize using ALD the main electrode materials, such as oxides[6] and sulphides.[7] However, high surfacearea and sufficiently conducting support would be beneficial for these ALD derived materials to support an excellent performance of the batteries. The door for various one-dimensional nanomaterials, such as TNTs, is therefore open

In this presentation, we will show ALD synthesis of Al_2O_3[8] and MoS_2[9] coatings on TNTs as new electrode material for lithium-ion batteries. We show an influence of different coating thicknesses on the battery performance, in particular on the charging and discharging capacity.

References

1) B.L. Ellis, P. Knauth, T. Djenizian, Adv. Mater. 26 (2014) 3368-3397.

2) G. F. Ortiz et al., Chem. Mater. 21 (2009), 63–67.

3) T. Djenizian et al., J. Mater. Chem. 21 (2011) 9925-9937.

4) Y. S. Jung et al., Adv. Mater. 22 (2010) 2172−2176.

5) E. M. Lotfabad et al., Phys.Chem. Chem. Phys., 2013, 15, 13646

6) M. Y. Timmermans et al., J. Electrochem. Soci., 164 (2017) D954-D963.

7) D. K. Nandi et al., Electrochim. Acta 146 (2014) 706–713.

8) H. Sopha et al., ACS Omega 2 (2017) 2749-2756.

9) H. Sopha et al., ACS Applied Energy Materials, submitted.

ALD Applications
Grand Ballroom A-C - Session AA3-TuA

ALD for Memory Applications I

Moderators: Scott B. Clendenning, Intel Corp., Adrien LaVoie, Lam Research Corp.

4:00pm **AA3-TuA11 Doped Hi-K ALD Films of HfO_X and ZrO_X for Advanced Ferroelectric and Anti-Ferroelectric Memory Device Applications:***, **Niloy Mukherjee**, J. Mack, S. Rathi,* Eugenus, Inc.*; Z. Wang, A. Gaskell, N. Tasneem, A. Khan,* Georgia Institute of Technology*; M. Dopita, D. Kriegner,* Charles University **INVITED**

The discovery of ferroelectricity in doped hafnium oxide has generated excitement in the solid-state device community in recent years since hafnium oxide is a relatively simple oxide compared to traditional perovskite-based ferro-/anti-ferroelectric materials, and hafnium oxide is already used widely in the semiconductor industry. The discovery has inspired many researchers to study the system in further detail in the past few years. Recently, this group has discovered the ability to obtain anti-ferroelectric ZrOx in as-deposited ALD films alone, without the need for capping metallic electrodes or any post-deposition/post-metallization annealing. Tunability of the anti-ferroelectric behavior of ZrOx is also demonstrated using lanthanum doping and is co-related to changes in unit cell tetragonality with lanthanum doping. Process methods, including precursor delivery schemes and ALD deposition schemes, used to deposit doped HfOx and ZrOx-based ferroelectric and anti-ferroelectric films will be described in detail. Structural and electrical properties of such films will be described in detail and co-related.

4:30pm **AA3-TuA13 ALD of La-Doped HfO_2 Films for Ferroelectric Applications***, **Tatiana Ivanova**, P. Sippola, M. Givens,* ASM, Finland*; H. Sprey,* ASM, Belgium*; T.M. Büttner, P. Polakowski, K. Seidel,* Fraunhofer IPMS-CNT, Germany

Ferroelectric (FE) HfO_2 and its doped compounds [1] have received increasing interest for potential to harness these materials for non-volatile memory applications. ALD HfO_2-based ferroelectrics can provide smooth process integration to silicon based semiconductor technology in contrast to e.g., perovskite FE materials. Especially, La-doped HfO_2 films have been shown to exhibit superior ferroelectric responses with the so far highest reported remanent polarization for doped FE-HfO_2 [2]. Nevertheless, a comprehensive in depth study of this promising material system has not been done.

This research covers highlights of the growth and FE properties of La-doped HfO_2 ALD films. The 10 nm La-doped HfO_2 films were deposited on 300 mm Si wafers in an ASM Pulsar® 3000 ALD reactor over a temperature range of 200-300 ° C. The La-doped HfO_2 ALD process utilized $HfCl_4$ and a novel lanthanum precursor with co-reactant oxidants. Spectroscopic ellipsometer and x-ray photoemission spectroscopy were used to study the film growth and composition properties, respectively. In addition, La-doped HfO_2 crystallization kinetics were studied with in-situ x-ray diffractometry (IS-XRD). The FE properties were studied via fabrication and electrical characterization of planar metal-ferroelectric-metal capacitors (MFMCap).

Control of La-doped HfO_2 in the range of [La] ~ 1-10 % (based on 100*[La]/([La] + [Hf])) was studied by varying the ratio of LaO_x:HfO_2 subcycles during the ALD process. The La-doped HfO_2 growth rate and residual C and Cl impurity concentrations were studied as a function of LaO_x:HfO_2 subcycle ratio and temperature for as-deposited films. IS-XRD analysis during high temperature annealing revealed the presence of the desired high symmetry phase of FE hafnium oxide for low [La] (1-5 %) and lower temperature (200-250 ° C) deposited samples, while samples with higher [La] showed an even stronger stabilization of the film which showed electrically no FE behavior. Crystallization temperatures increased with increasing La content, while it decreased with increasing deposition temperature: e.g. [La]~2 % samples deposited at 200-300 ° C crystallized at 615-470 ° C, respectively. The MFMCap studies confirmed the presence of strong FE responses for the low La content films exhibiting maximum remanent polarization of 26.5 $\mu C/cm^2$ (post cycle conditioning) for [La]~2 % films deposited at 250 ° C.

[1] T. S. Böscke, et al., Applied Physics Letters 99, 102903 (2011)

[2] J. Müller et al., IEEE International Electron Devices Meeting (2013)

4:45pm **AA3-TuA14 Characterization of Multi-Domain Ferroelectric ZrO_2 Thin Films for Negative Capacitance and Inductive Responses***, **Yu-Tung Yin**, P.-H. Cheng, Y.-S. Jiang, J. Shieh, M.J. Chen,* National Taiwan University, Republic of China

By using a specific plasma-enhanced atomic layer deposition (PEALD) process, an as-deposited nanoscale ferroelectric ZrO_2 (nano-*f*-ZrO_2) thin film has been prepared. A unique periodically arranged crystalline has been observed under nano-beam electron diffraction (EBED) and dark field TEM images, indicating the presence of multi-domain structure in nano-*f*-ZrO_2. From the large-signal RLC oscillations in time domain analysis, the existence of positive imaginary part of the impedance, enhancement of small-signal capacitance of the series-connected capacitances, and the sub-60mV/dec subthreshold swing in nanoscale transistors, the multi-domain nano-*f*-ZrO_2 has provided the experimental observation for the inductive behavior and negative capacitance induced by the net polarization switching. According to the theoretical calculation, the net polarization switching of multi-domain nano-*f*-ZrO_2 produces an effective electromotive force which is similar in behavior with Lenz's law, leading to the inductive responses and the negative capacitance effect. Since the as-deposited multi-domain nano-*f*-ZrO_2 thin film provides a significant inductance behavior compared to conventional inductors, the PEALD deposited nano-*f*-ZrO_2 would become a promising material in a variety of applications including nanoscale transistors, filters, oscillators, and radio-frequency integrated circuits.

5:00pm **AA3-TuA15 Scaling Ferroelectric $Hf_{0.5}Zr_{0.5}O_2$ on Metal-Ferroelectric-Metal (MFM) and Metal-Ferroelectric-Insulator-Semiconductor (MFIS) Structures***, **Jaidah Mohan**, H. Hernandez-Arriaga, H.S. Kim, A. Khosravi, A. Sahota,* The University of Texas at Dallas*; R. Wallace,* University of Texas at Dallas*; J. Kim,* The University of Texas at Dallas

Ferroelectricity in Hafnium Zirconate (HZO) has recently garnered interest due to the possibility of achieving sub-60mV/decade Subthreshold swing

(SS) at room temperatures [1]. Such steep slope behavior could lead to various advantages like reducing static power dissipation and lowering operating voltages. "Negative Capacitance" is the currently proposed mechanism for such behavior but substantial claims and controversies are still being reported. Big mystery questions remain unsolved, (i) can hysteresis free switching continue to get steeper even at GHz frequencies? (ii) Can negative capacitance really be stabilized Nevertheless, various observations of sub-60 SS swing have been reported using a ferroelectric material as the gate dielectric [2][3]. In this work, we study scaling of HZO on Metal-Ferroelectric-Metal (MFM) and Metal-Ferroelectric-Insulator-Semiconductor (MFIS) structures which can further aid in reducing the operating voltages.

In this study, the ferroelectric properties of HZO was studied on MIM and MFIS structures, scaling down to 3nm. HZO was deposited using TDMA-hafnium ($Hf[N(CH_3)_2]_4$), TDMA-zirconium ($Zr[N(CH_3)_2]_4$), and O_3 as the Hf-precursor, Zr-precursor and oxygen source respectively at 250°C. Blanket TiN (90 nm thick) electrodes were deposited after the HZO deposition as the stress given by the TiN electrode helps in crystallizing HZO into the ferroelectric phase. Then, rapid thermal annealing was done at 450°C in an N_2 atmosphere for 60s to crystallize the HZO films. A conventional photolithography/etching process was used to make capacitors of different diameters. Grazing Incidence X-ray Diffraction (GIXRD) confirms that the ferroelectric orthorhombic phase is stable for HZO deposited on top of HF treated Silicon. The ferroelectric HZO film was scaled up to 5nm on top of Silicon and showed significant ferroelectric properties while 4nm and 3nm HZO showed very high leakage properties. Effects or reannealing to increase the grain size and hence the ferroelectric behavior was also studied. It was also observed that as the ferroelectric thickness decreases or the SiO_2 thickness increases, there is an increase in the ferroelectric dipole relaxation, i.e. the ferroelectric domains are naturally tend to orient themselves in a particular direction.

REFERENCES:

[1] S. Salahuddin et al, *Nano Lett.*, vol. 8, no. 2, pp. 405–410, 2008.

[2] S. Dasgupta, et al, *IEEE J. Explor. Solid-State Comput. Devices Circuits*, vol. 1, pp. 43–48, 2015.

[3] A.I. Khan *et al.*, *IEEE Electron Device Lett.*, vol. 37, no. 1, pp. 111–114, 2016.

5:15pm **AA3-TuA16 Interface Characteristics of MIM Capacitors using Vanadium Nitride Electrode and ALD-grown ZrO_2 High-k Dielectric Film***, **Jae Hyoung Choi**, Y. Kim, H.I. Lee, H.-J. Lim, K. Hwang, S.W. Nam, H.-K. Kang,* Samsung Electronics, Republic of Korea

One of the most critical challenges for DRAM (Dynamic Random Access Memory) downscaling is cell capacitor technology, and so far ZrO_2 and TiN film have been adopted as a high-k dielectric and an electrode material respectively, for the capacitor application [1]. ZrO_2 film has been spotlighted in TiN/Insulator/TiN (TIT) capacitor due to its high dielectric constant, wide band gap, and thermal stability [2].

A wide variety of DRAM capacitor electrodes are currently being evaluated as replacements for TiN including VN, HfN, and Ru. Ru-base electrode has advantage of high work function but also has cost and integration problem. Thermally robust HfN/HfO_2 gate stack structure was reported with scaling down of equivalent oxide thickness (Toxeq.) less than 10Å and several attempts to prepare HfN films by metal organic chemical vapor deposition (MOCVD) have been continued [3,4]. Even though Vanadium Nitride (VN) exhibits high melting point, chemical inertness, low resistivity, and high work function from 5.05 to 5.15eV, very little is known about its qualities as DRAM capacitor electrode [5].

In this study, we fabricated new MIM (Metal/Insulator/Metal) capacitor using VN electrode and ALD-ZrO_2 dielectric for DRAM capacitor. VN films (100~1,000Å) were deposited at different temperatures ranging from 25 to 500°C by reactive magnetron sputtering. ZrO_2 films were used as a dielectric by atomic layer deposition (ALD) method with Tetra-Ethyl-Methyl-Amino-Zirconium (TEMAZ) liquid precursor and O_3 reactant at the temperature of 250□. ALD-ZrO_2 films were progressed to post deposition anneal (PDA) in N_2 atmosphere to crystallize the dielectric layer. Electrical properties of MIM capacitor with VN/ZrO_2 combination such as capacitance, leakage current density and dielectric constant were compared with TiN/ZrO_2 stack. Resistivity, composition, interfacial reaction, and crystalline structure of VN and ZrO_2 films were analyzed by 4-point probe, Rutherford backscattering spectroscopy (RBS), X-ray photoelectron spectroscopy (XPS), X-ray diffraction (XRD), and transmission electron microscopy (TEM). Furthermore, the VN/ZrO_2 interface effects on the electrical properties will be discussed in detail.

REFERENCES

1. S.K. Kim and C.S. Hwang, *Electrochem. Solid-State Lett.***11**(3), G9 (2008).

2. C. W. Hill et al., *J. Electrochem. Soc.*, **152**(5), G386 (2005).

3. H.Y. Yu, et al., *IEEE Electron Device Lett.*, **25**, 70 (2004).

4. Y. Kim, et al., *Proc. 15th EUROCVD, ECS* **9**, 762 (2005).

5. R. Fujii et al., Vacuum, **80**(7), 832 (2006).

6. K. Yoshimoto et al., *Jpn. J. Appl. Phys.***45**(1A) 215 (2006).

ALD Fundamentals
Grand Ballroom A-C - Session AF-TuA

Plasma ALD: Growth and Characterization

Moderators: Hyeongtag Jeon, Hanyang University, Jiyoung Kim, The University of Texas at Dallas

1:30pm **AF-TuA1 Low Temperature High Quality Silicon Dioxide by Neutral Beam Enhanced Atomic Layer Deposition***, **Hua-Hsuan Chen**, D. Ohori, T. Ozaki,* Tohoku University, Japan*; M. Utsuno, T. Kubota, T. Nozawa,* ASM Japan K.K., Japan*; S. Samukawa,* Tohoku University, Japan

Atomic layer deposition (ALD) has shown to have high control of conformality on thin films in recent decades. Instead of conventional deposition technique, such as physical vapor deposition and plasma-enhanced chemical vapor deposition, it is usually used to deposit thin layers on complex structures due to its thickness control ability. Plasma-enhanced ALD (PEALD) and thermal ALD are the examples. However, there are some serious problems. For instance, plasma irradiation and charge accumulation existed in PEALD [1] can cause defects in thin films; high temperature is also needed in thermal ALD. In previous studies, neutral beam technology has shown advantages on depositing high quality films, such as low-k SiOCH film [2] and nitrogen doping diamond-like carbon film [3]. Here, we demonstrated the atomic layer growth of SiO_2 film on Si using novel neutral beam-enhanced deposition (NBEALD) technique, which was deposited at room temperature, and serves as an important material in various applications.

Neutral beam enhanced atomic layer deposition system consists of a large-radius ALD process chamber and an inductively coupled plasma source. We used Aminosilane as the precursor and O_2 as the neutral beam source to deposit films on the Si substrate. The stage temperature was controlled at 30□. After the ALD cycle which was composed of: precursor feed, precursor purge, O_2 injection, neutral beam irradiation and O_2 purge, the SiO_2 film was grown on silicon wafers. We used spectroscopic ellipsometry to measure film thickness; the atomic force microscope was used to investigate the surface morphology; the X-ray photoelectron spectroscopy (XPS), X-ray reflectivity (XRR) and secondary ion mass spectrometry (SIMS) were used to analyze the chemical composition of the films for investigating the SiO_2 film quality.

The ALD cycle shows the thickness is linearly dependent on the number of cycles with growth per cycle comparable to that of PEALD [4]. The uniformity of the film was obtained by measuring thickness on different places of 8 inch wafer, and the result shows the film has good uniformity. For the XPS, XRR and SIMS results, high quality and high density SiO_2 film composition was confirmed. Furthermore, the excellent surface morphology could be seen on SiO_2 films as no difference for thickness discrepancy. Therefore, we succeeded to make high quality SiO_2 films using NBEALD technique under room temperature.

[1] H. B. Profijt et al, *J. Vac. Sci. Technol. A* 29, 050801 (2011)

[2] Y. Kikuchi et al, *J. of Phys. D: Appl. Phys.* Vol. 46 (2013)

[3] S. Yasuhara et al, *J. of Phys. D: Appl. Phys.* Vol. 43 (2010)

[4] S. J. Won et al, *IEEE Elec. Dev. Lett*. Vol. 31, No. 8 (2010)

1:45pm **AF-TuA2 Radical Surface Recombination Probabilities during Plasma ALD of SiO_2, TiO_2 and Al_2O_3 Determined from Film Conformality***, **Karsten Arts**,* Eindhoven University of Technology, Netherlands*; M. Utriainen,* VTT Technical Research Centre of Finland, Finland*; R. Puurunen,* Aalto University, Finland*; W.M.M. Kessels,* Eindhoven University of Technology, Netherlands*; H. Knoops,* Oxford Instruments Plasma Technology, UK

This work addresses the growth of conformal films on high aspect ratio (AR) structures by plasma ALD, which can be challenging due to loss of the

reactive radicals through surface recombination. Using plasma ALD of SiO_2, TiO_2 and Al_2O_3 as case studies, we show that the AR up to which film growth is achieved gives quantitative insight into the recombination probability *r* of plasma radicals on given material surfaces. Such quantitative information on *r* is often not available in the literature and difficult to obtain by conventional methods, while it is essential for predicting and understanding the conformality achieved by plasma ALD. Applications of plasma ALD such as the conformal growth of SiO_2 spacers for self-aligned patterning can thus benefit from this work.

In this study we use microscopic lateral-high-aspect-ratio structures[1] supplied by VTT (PillarHall® LHAR4) to assess the conformality of plasma ALD processes. As these chips have extremely high AR trenches (AR<10000) deposition is typically limited up to a certain penetration depth. For the first time, we demonstrate that this penetration depth can be used to quantify *r* during plasma ALD.

By carrying out plasma ALD of SiO_2 using $SiH_2(N(C_2H_5)_2)_2$ and different O_2/Ar plasma exposure times, we have observed that the penetration depth increases logarithmically with the plasma time used in the ALD cycle. This relation is well described by a simple analytical model which can be used to calculate *r*. For plasma ALD of SiO_2 this gives $r=(6\pm3)\cdot10^{-5}$, which compares well to reported literature values.[2] Using a long plasma exposure, deposition of SiO_2 is achieved up to an AR as high as 900. Similarly, growth of TiO_2 using $Ti(N(CH_3)_2)_4$ reaches AR>250. In contrast, plasma ALD of Al_2O_3 using $Al(CH_3)_3$ shows a surprisingly low penetration (AR~80) compared to the thermal ALD process, even with long plasma exposure, which indicates the impact of a relatively high surface recombination probability. Estimations of the corresponding values of *r* and additional insights will be provided in this contribution. These results demonstrate that our method is a powerful and straightforward way to gain knowledge on surface recombination during plasma ALD and its strong effect on film conformality.

1. Arts, Vandalon, Gao, Utriainen, Puurunen, Kessels and Knoops, 18th Int. Conf. At. Layer Depos. ALD 2018 – Proc., (2018)

2. Kim and Boudart, Langmuir 7, 2999 (1991)

2:00pm **AF-TuA3 A Robust Method for In-situ Gas Monitoring of ALD Processes using Optical Emission Spectroscopy of a Pulsed Remote Plasma***, **Joe Brindley**, B. Daniel, V. Bellido-Gonzalez,* Gencoa Limited, UK*; R. Potter, B. Peek,* University of Liverpool, UK

Effective and robust monitoring of individual gas concentrations during the ALD processes offer a unique insight into the process behavior as well as being an important step in the eventual wide-spread industrialization of the ALD technique.

Conventional quadrupole residual gas analyzers have difficulty monitoring ALD processes due to the high process pressures and the presence of contaminating hydrocarbons contained within many ALD precursors. For these reasons monitoring of precursor gas concentrations during the ALD process is not often undertaken, especially at the production stage.

An alternative gas sensing technique that operates directly at pressures above $1E^{-4}$ mbar has been built around remote plasma emission monitoring. This technique involves the generation of a small, remote plasma using an inverted magnetron placed within the ALD vacuum system. Consequently, species that are present within the vacuum become excited in the sensor's plasma, emitting a spectrum of light, which can then be used to identify and monitor the emitting species. Importantly, this plasma, generated inside the sensor, has a sole function as a gas detector and does not affect the ALD process itself.

This work will demonstrate that the sensing method is robust when exposed to the ALD processing environment. Previous work had demonstrated the usefulness of this technique but limitations were encountered when using a DC voltage to generate the sensor's plasma as contamination and reduced sensitivity developed when used with certain precursors. This work will describe a novel method of generating the detector plasma using a high peak power, low duty cycle pulsed voltage. It will be demonstrated that the pulsed power technique is more effective than DC in preventing contamination of the sensor's electrodes as well as improving the detection sensitivity of common ALD precursors and their reaction by-products.

Examples of this sensing technique's practical uses for Al_2O_3 and TiO_2 ALD processes are discussed; this includes detection of contaminants, optimizing purge cycle length and monitoring the reaction dynamics in terms of precursor gas consumption and reaction by-products.

2:15pm **AF-TuA4 Near Room Temperature Plasma Enhanced Atomic Layer Deposition of Gold Metal***, **Michiel Van Daele**,* Ghent University, Belgium*; M. Griffiths,* Carleton University, Canada*; A. Raza,* Ghent University - IMEC, Belgium*; M. Minjauw,* Ghent University, Belgium*; S. Barry,* Carleton University, Canada*; R. Baets,* Ghent University - IMEC, Belgium*; C. Detavernier, J. Dendooven,* Ghent University, Belgium

Currently only two Au ALD processes exist, using two different precursors. The first Au ALD process, reported by Griffiths et al. [1], is a three step process using Me_3AuPMe_3 as the precursor in combination with an oxygen plasma and water vapour as the reactants. The deposition of metallic gold was reported at a deposition temperature of 120°C, with only some carbon and oxygen impurities present in the film (6.65% C and 1.83% O). A growth per cycle of 0.05 nm per cycle was achieved. The Au ALD process, reported by Mäkelä et al. [2], uses $Me_2Au(S_2CNEt_2)$ as the precursor and ozone as the reactant. Deposition between 120-180°C was reported with self-limiting growth at 180°C and a growth rate of 0.09 nm per cycle. The deposited films had low resistivity values (4-16μΩ cm) and were chemically pure with few impurities, O (2.9%), H (0.9%), C (0.2%), and N (0.2%).

A new plasma enhanced ALD process has been developed using Me_3AuPMe_3 and H_2 plasma as the precursor and reactant, respectively. Both precursor and reactant exhibit saturating behaviour, with a growth per cycle of 0.03 nm per cycle. A temperature window between 50°C and 120°C is achieved, with decomposition of the precursor above 120°C. The as-deposited gold films are polycrystalline and pure, with no phosphorous present in the film and very few carbon impurities (0.3%). Measured resistivity values (5.85μΩ cm) were close to the expected bulk value of gold (2.44 μΩ cm).

The surface chemistry and growth mechanism were investigated using in-situ RAIRS measurements, optical emission spectroscopy, and mass-spectrometry, pointing to an abbreviated growth cycle, instead of a complete one [3]. The initial growth starts off with the nucleation of gold particles on the surface. The formed gold nanoparticles grow and coalesce during the ALD process, as characterized using SEM measurements. The spacing of the gold particles makes this process interesting for surface enhanced Raman spectroscopy (SERS). Free space Raman measurements were performed on some of the samples and these showed excellent surface enhancement of the Raman signal. As far as we know this is the first report of an ALD gold film that shows SERS properties. In contrast to other SERS substrate fabrication methods, often involving lithography, this ALD process provides a direct way to fabricate SERS substrates without the need for a lot of process steps.

[1] M. B. E. Griffiths, P. J. Pallister, D. J. Mandia, and S. T. Barry, Chem. Mater. 28(1) (2016) 44-46

[2] M. Mäkelä, T. Hatanpää, K. Mizohata, J. Räisänen, M. Ritala, and M. Leskelä, Chem. Mater. 29(14) (2017) 6130-6136

[3] S. Elliott, G. Dev, and Y. Maimaiti, J. Chem. Phys. 146(5) (2017) 052822

2:30pm **AF-TuA5 Low-Temperature Deposition of Gallium Oxide and Aluminum Oxide with Arrays of Microcavity Plasma Enhanced Atomic Layer Deposition***, **Jinhong Kim**, A. Mironov, S.-J. Park, J.G. Eden,* University of Illinois at Urbana-Champaign

A new atomic layer deposition (ALD) technology has been developed with an array of microcavity plasma devices which enable to grow the atomic layers at low temperature and enhance the growth rate with less defects and contamination. Confining low temperature plasmas to an array of microcavities yields uniform, glow discharges operating at pressures of 1 atmosphere and beyond. Not only are electron densities above 10^{16} cm^{-3} now routine, but the plasma electron temperature (T_e) and the ratio of the local electric field strength to the gas number density (E/N) are also increased significantly relative to conventional (macroscopic) plasmas. All of these characteristics are ideal for plasma chemical processing to generate oxidants efficiently compared to conventional RF or others existing source technology. A compact ALD system of which volume reduced by at least a factor of five was realized thanks to the minizturized microplasma source operating in lower frequency ac waveform. The uniform and conformal gallium oxide (Ga_2O_3) and aluminum oxide (Al_2O_3) thin films were deposited at low temperatures (< 50 °C) on silicon, quartz, and even polyethylene terephthalate (PET). Due to the complete reaction between precursors, the stoichiometric value of films presents ~ 1.5 in crystalline state, indicating the presence of negligible levels of impurities. MOSCAP was fabricated to analyze the electrical characteristic of 30 nm thickness of Al_2O_3 film. This MOSCAP exhibits higher breakdown electric field of 6.1 MV than conventional Al_2O_3 thin film . Hysteresis width from the sweep bias voltage was measured to less than 1 mV which is close to ideal

MOSCAP electrical characteristics. In addition, Ga_2O_3 films deposited on PET were used to fabricate for transparent and flexible solar-blind photodetector with metal-semiconductor-metal junction structure. The crystallinity of films was analyzed using Transmission electron microscope (TEM) and X-ray diffraction (XRD). Post annealing (> 800 C) with argon environment was essential to produce polycrystalline β-Ga_2O_3. Bandgap was calculated by optical characteristics of the films from UV spectrophotometer. The photoresponse properties of photodetectors were investigated by the current-voltage characteristics and time-dependent photoresponse curves. Various thin film grown by microplasma enhanced ALD demonstrates improved optical and electrical properties. The scientific inspiration of this new deposition technology as well as the prospect for commercial application will be discussed in this presentation.

2:45pm **AF-TuA6 The Effects of Varying Plasma Conditions on Plasma Assisted Atomic Layer Epitaxy***, **David Boris**, V. Wheeler, N. Nepal, S.G. Rosenberg, J. Avila, J.M. Woodward, V. Anderson, S. Walton, C.R. Eddy, Jr.,* U.S. Naval Research Laboratory

Plasma assisted atomic layer deposition (PA-ALD) is a low temperature, conformal, layer-by-layer deposition technique that is based on a pair of self-terminating and self-limiting gas-surface half-reactions, in which at least one half-reaction involves species from a plasma. This approach generally offers the benefit of substantially reduced growth temperatures and greater flexibility in tailoring the gas phase chemistry to produce varying film characteristics. The flexibility and lower growth temperatures that plasmas provide come at the cost of a complex array of process variables that often require great care on the part of the user.

In response to this challenge, this work focuses on the use of plasma diagnostics to inform the choice of process conditions for PA-ALD systems. In this work we employ VUV-NIR spectroscopy, charged particle collectors near the substrate, and spatially resolved Langmuir probe measurements to characterize the inductively coupled plasma source used in a Fiji 200 (Ultratech/CNT) PA-ALD tool. In particular, we assess the total ion flux reaching the substrate surface, spatial variation of plasma properties, and the relative fractions of atomic and molecular species generated in the plasma under a variety of pressures and gas input flow fractions in context of PA-ALD of AlN, InN, TiO_2 and Ga_2O_3 films. Changes in plasma parameters are then linked with changes in film characteristics.

3:00pm **AF-TuA7 Plasma-Enhanced Atomic Layer Epitaxy of Ultra-wide Bandgap Ga_2O_3 and $(Al_xGa_{1-x})_2O_3$ Films***, **Virginia Wheeler**, N. Nepal, D. Boris, S. Walton, S. Qadri, J. Avila, D. Meyer, B. Downey, V. Gokhale,* U.S. Naval Research Laboratory*; L. Nyakiti,* Texas A&M University*; M. Tadjer,* U.S. Naval Research Laboratory*; M. Goorsky,* University of California Los Angeles*; C.R. Eddy Jr.,* U.S. Naval Research Laboratory **INVITED**

Ga_2O_3 has emerged as a promising material for next generation power electronics. While β-Ga_2O_3 (monoclinic) is the most stable and studied of five Ga_2O_3 polymorphs, the slightly less energetically favorable α- and ε-Ga_2O_3 phases have unique characteristics that can be exploited. α -Ga_2O_3 (rhombohedral, corundum) has the largest bandgap of 5.3 eV and can be alloyed with α-Al_2O_3 and α-In_2O_3 for bandgap engineering. ε-Ga_2O_3 phase (hexagonal, wurtzite) is polar, with a predicted polarization strength that is 10 and 3 times larger than that of GaN and AlN, respectively. Like the III-N system, polarization induced charges can lead to higher charge densities and mobilities in two-dimensional electron channels formed at heterojunctions, which would improve the viability of Ga_2O_3 electronic devices. Plasma-enhanced atomic layer deposition (PEALD) is a popular, conformal, energy-enhanced synthesis method for thin films due to its many advantages, including: deposition at reduced growth temperatures, access to metastable phases and improved crystallinity, and increased growth rates. In this work, we use PEALD to produce high-quality heteroepitaxial Ga_2O_3 and $(Al_xGa_{1-x})_2O_3$ (AlGO) films, and investigate phase selectivity as a function of substrate, growth temperature (T_g), plasma gas phase chemistry and gas pressure.

All Ga_2O_3 films were deposited in a Veeco Fiji G2 reactor equipped with a load lock and turbo pump using trimethygallium and O_2 plasma. Initial studies on c-plane sapphire substrates at 350°C and 8 mTorr, show the phase could be altered from β to α by a varying the O_2 flow during plasma pulse from 5-40 sccm. Optical emission spectroscopy indicate that the O^*/O_2 ratio is crucial for phase selectivity while the high ion flux to the surface can contribute to the crystallinity at low T_g. To grow ε-Ga_2O_3 on c-plane sapphire required going to much higher temperature (500°C), pressure (100's mTorr), and O_2 flow (100sccm) . Under no conditions was pure ε-Ga_2O_3 on sapphire achieved. Using optimum growth conditions for the three phases on sapphire, films were deposited on GaN and diamond to determine the effect of substrate structure. While films on diamond resulted in mixed β/ε phases, pure ε-phase films were attained on GaN and the strain varied with pressure and T_g. To investigate favorable heterojunctions for 2DEG formation, AlGO films were developed. While the full stoichiometric range could be reached using a PEALD digital alloying method, crystallinity was lost above ≈30 %Al, independent of phase. Initial electrical results on breakdown voltage and heterojunctions will be shown in order to establish the feasibility of these films in device applications.

Atomic Layer Etching
Regency Ballroom A-C - Session ALE1-TuA

Modeling & Instrumentation I

Moderators: Ankur Agarwal, KLA-Tencor, Alok Ranjan, Tokyo Electron America Inc.

1:30pm **ALE1-TuA1 Atomic Layer Etching of Nanostructures***, **Sabbir Khan**,* Niels Bohr Institute, University of Copenhagen, Denmark*; D. Suyatin,* Lund University, Sweden*; J. Sundqvist,* Fraunhofer Institute for Ceramic Technologies and Systems IKTS, Germany **INVITED**

Progress in modern electronics demands atomic precision-controlled fabrication of devices and atomic layer etching (ALE) provides etch processes which can assist device trimming with atomic precision. ALE is now becoming a key technique for nanofabrication and the semiconductor industry. In this talk we will demonstrate ALE of thin film Ga-polar GaN (0001) where surface modification is done by Cl_2 adsorption and later modified chlorinated layer is removed by low energy Ar ions in plasma environment using standard reactive ion etching (RIE) system (Oxford Plasmalab 100) [1]. Further, using a similar system, Cl_2 and Ar based highly anisotropic ALE on crystalline Si (100) with good etch selectivity for SiO_2 masks will be discussed. This high material selectivity enables nano-patterning of different geometries on Si wafer and post-ALE patterns inspection allows us to understand different effects (such as, trenching and sidewall tapering etc.) and limitations of the process. We also demonstrate that the ALE processed patterned substrates can be used as molds for high resolution nanoimprinting of features size down to 30 nm [2]. Finally, ALE on semiconductor nanowires will be shown, indicating that the process can be used for damage free processing of semiconductor nanowire devices and precise nanofabrication below 20 nm [3].

Reference:

1. Christoffer Kauppinen, Sabbir Ahmed Khan, Jonas Sundqvist, Dmitry B. Suyatin, Sami Suihkonen, Esko I. Kauppinen and Markku Sopanen. Atomic Layer Etching of Gallium Nitride (0001). Journal of Vacuum Science & Technology A, 35, 6, 060603 (2017).

2. Sabbir Khan, Dmitry B. Suyatin, Jonas Sundqvist, Mariusz Graczyk, Marcel Junige, Christoffer Kauppinen, Anders Kvennefors, Maria Huffman, Ivan Maximov. High-Definition Nanoimprint Stamp Fabrication by Atomic Layer Etching. ACS Applied Nano Materials, 1, 6, 2476–2482 (2018).

3. Sabbir Khan, Dmitry B. Suyatin, Jonas Sundqvist, A Method for Selective Etching of Nanostructures. WO2017157902A1, Patent Application (2017).

2:00pm **ALE1-TuA3 Selectivity during Plasma ALE of Si-Compounds: Reaction Mechanism Studied by in-situ Surface Spectroscopy***, **René Vervuurt**,* ASM*; K. Nakane, T. Tsutsumi, M. Hori, N. Kobayashi,* Nagoya University, Japan

Plasma atomic layer etching (ALE) processes based on plasma modification and modification layer removal by fluorine radicals have recently been reported, for the etching of SiN and SiC [1-3]. The proposed processes offer advantages in terms of etch process control, uniformity and etch selectivity versus SiO_2 compared to more conventional etching techniques.

In this contribution the selective ALE of Si-compound films is investigated and the reaction mechanism behind the etch selectivity between compounds is discussed. H_2, He and N_2 plasma modification and the subsequent etching of the modified layer by F-radicals are studied by *in-situ* Fourier Transform Infrared Spectroscopy (FTIR) and spectroscopic ellipsometry (SE) for several Si-compounds (SiN, SiC, SiCOH, and SiO_2).

in-situ SE measurements show that the selectivity of the ALE process can be controlled by the modification plasma; H_2 plasma can be used for the selective etching of SiN, SiC and SiCOH versus SiO_2, whereas a N_2 plasma makes the selective etch of SiC and SiCOH versus SiN and SiO_2 possible. He plasma modification on the other hand did not result in etching by F-radicals.

The origin of the selectivity and underlying reaction mechanism is discussed on the basis of *in-situ* FTIR measurements. These show that H_2 plasma modification of SiN, creates a H-rich modification layer containing Si-H and N-H groups. Both Si-H and N-H group formation saturate with exposure time. The created Si-H and N-H groups are removed by the subsequent F-radical exposure resulting in the net removal of SiN. The reaction mechanism for H_2 plasma ALE of SiC and SiCOH is found to be similar; a H-rich layer is formed on top of the sample which can be etched using F-radicals, while SiO_2 is not modified. This makes it possible to selectively etch SiN, SiC and SiCOH versus SiO_2.

N_2 plasma can be used to selectively modify SiC versus SiO_2 and SiN by creating a Si-H and C=N rich layer. The Si-H groups are created by the restructuring of the hydrogen already present in the SiC film in the form of C-H bonds. The modified layer can be removed using F-radicals allowing for the selective etch of SiC.

He plasma exposure of SiN, SiC and SiCOH creates a Si-O rich modification layer. This layer cannot be removed by F-radicals and therefore does not result in etching.

The obtained results indicate that the formation of a Si-H rich layer is essential for the plasma ALE of SiN, SiC and SiCOH. By tuning the plasma conditions the formation of this layer can be controlled allowing for the selective ALE between SiN, SiC, SiCOH and SiO_2.

[1] Sherpa et al. *JVSTA* 35,1, 2016

[2] Kumakura et al. *DPS 2018*, Nagoya

[3] Vervuurt et al. *DPS 2018*, Nagoya

2:15pm **ALE1-TuA4 Chamber Vacuum Strategies to Enable High Productivity ALE***, **Declan Scanlan**, D. Stephenson, A. Stover,* Edwards Vacuum, Ireland

As device lateral dimensions shrink with each successive technology node, the semiconductor industry is now poised to transition from the nanoscale era to the atomic scale era, and must now turn to atomic scale processing techniques.

Analogous to atomic layer deposition (ALD), Atomic Layer Etch is a technique for removing thin layers of material using sequential reaction steps that are either fully or quasi self-limiting. While this technique has shown extremely promising on-wafer results for a variety of etch applications, the transition into high volume manufacturing has been relatively restricted, since the productivity penalty, particularly wafer throughput, is still a major limiting factor. These sequential reaction steps typically require a full and complete exchange of the reactive gas chemistry within the chamber, and therefore a very high-flow, sequentially intermittent, gas purge step is often deployed. To improve the efficiency of this total gas exchange, equipment manufacturers have developed novel fast gas ***delivery*** hardware capability, but the complementary rapid gas ***evacuation*** capability remains largely overlooked. Chamber pumping strategies that can improve the efficiency of this rapid switching between very different flow volume regimes will be presented.

Apart from this extended pumping time requirement, these high-flow steps present other productivity challenges to the vacuum system. Historically, the chamber vacuum system was relied upon to deliver a low pressure using turbomolecular pumps (TMPs). These pumps operate spinning rotors at very high speeds to propel gases down and out of the pump. In general, the higher the gas flow rate, the more heat that is imparted to the TMP rotor and the higher the rotor temperature. However, a hot rotor poses two challenges: creep and corrosion, the rates of both are increased at higher temperatures. Rotor creep is deformation due to sustained stress and temperature and increases exponentially with temperature (See Figure 1). Furthermore, condensable etch by-products need to be managed by controlling the internal pump temperature profile to ensure that surfaces in the gas path are hot enough to keep the by-product in the vapour phase. In addition, the adoption of specific surface passivation and protection techniques, utilising precursor deposition chemistry, (e.g. in-situ ALD / ALE) intensifies this challenge of by-product management within the vacuum system.

This paper will not only discuss how internal pump technology can help address these challenges, but also how different chamber pumping strategies can be deployed to this end.

2:30pm **ALE1-TuA5 Mechanistic Study of the Thermal Atomic Layer Etch of Cobalt Metal Using Propene and CO***, S. Kondati Natarajan, M. Nolan,* Tyndall National Institute, Ireland*; **Patrick Theofanis**, C. Mokhtarzadeh, S.B. Clendenning,* Intel Corp.

Due to the possibility of improved electromigration properties and lower resistivity at decreased critical dimensions, Co has been identified as a candidate to replace Cu and potentially W in future semiconductor devices. To enable the use of Co at such small dimensions, monolayer control in processing is desirable. Accordingly, Atomic Layer Etch (ALE) functions as a complementary process technique to well-established Atomic Layer Deposition (ALD) methodologies, such that sequential self-limiting etch processes can be targeted with monolayer control for ultra-thin film material removal.

Herein, we present a theoretical analysis using first principles simulations of a thermal ALE process for cobalt metal utilizing a sequential thermal-chemical etch cycle employing propene and carbon monoxide (CO). It is shown that ALE can be achieved via the oxidative addition-H_2 elimination of propene to the Co surface followed by the introduction of CO to generate $(\eta^3\text{-}C_3H_5)Co(CO)_3$ as a volatile etch product at process conditions. It was found that the generation of $(\eta^3\text{-}C_3H_5)Co(CO)_3$ is thermodynamically favourable and necessitates a high CO step coverage. A full proposed mechanism for this potential thermal atomic layer etch process will be discussed.

2:45pm **ALE1-TuA6 Selective Quasi-ALE of SiO_2 over Si_3N_4 via Bottom-up Si_3N_4 Passivation: A Computational Study***, **Du Zhang**, Y. Tsai, Y. Shi, M. Wang,* TEL Technology Center, America, LLC

Selective SiO_2/Si_3N_4 atomic layer etching (ALE) has broad applications in both logic and memory device fabrication. Conventional methods of achieving SiO_2/Si_3N_4 selectivity generally employ a preferential top-down carbon-based polymer passivation on Si_3N_4. However, achieving a highly preferential passivation of Si_3N_4 only is challenging in this top-down carbon polymerization approach. To overcome these limitations, we propose a two-step selective SiO_2/Si_3N_{-4} ALE method that utilizes bottom-up Si_3N_{-4} passivation. In the first step, the formation of an ammonium (NH_4^+) salt blocking layer on the Si_3N_4 surface is enabled in a plasma containing H_2 and HF via surface conversion, with its feasibility and reaction pathways demonstrated with thermodynamics and quantum chemistry calculations. The SiO_2 substrate, by contrast, undergoes a partial surface reduction by the H radicals, demonstrated with molecular dynamics simulations. In the second step, the partially reduced SiO_2 surface can be volatilized in a plasma containing fluorine and/or other halogens, leaving the Si_3N_4 underneath the NH_4^+ salt layer intact. This new approach provides a promising solution toward infinite SiO_2/Si_3N_4 selectivity, thanks to the N atoms for the NH_4^+ salt passivation layer provided by the Si_3N_4 substrate alone. Moreover, the bottom-up passivation also translates into better pattern fidelity due to precise etch control, which is essential for the ever-shrinking CD of devices.

3:00pm **ALE1-TuA7 Insights of Different Etching Properties between CW and ALE Processes using 3D Voxel-Slab Model***, **Nobuyuki Kuboi**, T. Tatsumi, J. Komachi, S. Yamakawa,* Sony Semiconductor Solutions Corp., Japan **INVITED**

Atomic layer etching (ALE) processes have attracted considerable attention to realize high control etching (layer-by-layer) and very low damage (defect creation) caused by ion bombardment from plasma [1]. To use ALE as a practical process in mass production of semiconductor devices, it is necessary to know how to control process nobs along with the mechanism. To obtain such knowledge in the view point of numerical simulations, we modeled the ALE process of SiO_2 and Si_3N_4 films and simulated etching properties in the cases of conventional continuous-wave (CW) etching and ALE.

We propose a surface reaction model for the ALE process which consists of a deposition step by $C_4F_8/O_2/Ar$ plasma and etch step by Ar plasma for SiO_2 and Si_3N_4 film etching. This is based on the slab models of SiO_2 [2] and Si_3N_4 [3], which can give not only the etch rate and thickness of the C-F polymer layer but also the damage distribution described by Si dangling bond density on the etched layers. he surface layer is assumed to consist of two layers: a reactive layer divided by several thin slabs of lattice size order and a deposited C-F polymer layer on the reactive layer. We considered not only outflux of O and N from the reactive layer described previously [2][3] but also the enhancement effects of F from the deposition step and the etched polymer layer by an Ar^+ ion on the etch yields of SiO_2 and Si_3N_4 films by the Ar^+ ion. To analyze the 3D etched profile for the self-aligned contact (SAC) process, we developed a 3D simulation technique using an advanced

voxel model (called "smart voxel"), which also includes the slab model with the above surface reactions.

From the simulations for blanket film wafer and SAC etching compared with CW and ALE processes using our 3D voxel-slab model, we found that the use of monochromatic ion energy improve the controllability of surface layer thickness (polymer layer and reactive layer) and that quantitative control of the time variation of both the polymer layer thickness and ion penetration depth are necessary for low damage. Furthermore, relatively high SiO_2 etch rate (~ 40 nm/min) with high selectivity (> 100) can be obtained after optimizing polymer layer thickness, ion energy, and cycle time. For realizing higher performance of ALE, accurate prediction of the surface reaction and further quantitative control of the plasma parameters are necessary.

References

[1] J. K. Keren *et al*., JVST A**35** 05C302 (2017).

[2] N. Kuboi *et al*., JJAP **50**, 116501 (2011).

[3] N. Kuboi *et al*., JVST A**33**, 061308 (2015).

Atomic Layer Etching
Regency Ballroom A-C - Session ALE2-TuA

Modeling & Instrumentation II

Moderators: Dmitry Suyatin, Lund University, Tetsuya Tatsumi, Sony Semiconductor Solutions Corp.

4:00pm **ALE2-TuA11 First-principles Understanding of Atomic Layer Etching of Silicon Nitride using Hydrofluorocarbons***, **Gyeong Hwang**, E. Cheng,* University of Texas at Austin*; S. Sridhar,* TEL Technology Center, America*; P. Ventzek, A. Ranjan,* Tokyo Electron America Inc.

The removal of thin layers of material with atomic-scale precision and spatial control (area selectivity) is critical for advanced device fabrication, making atomic layer etching (ALE) more attractive due to its ability to tightly control etch rates and to achieve wafer scale uniformity without physical damage. While ALE processes have been widely used to remove Si, Ge, compound semiconductors, and various oxides, only a few studies on ALE of Si_3N_4 films have been reported despite its technological importance. Recent experimental investigations have demonstrated that ALE of Si_3N_4 can be achieved via sequential exposure of hydrogen and fluorinated plasma or a cyclic process involving two alternating CH_3F gas adsorption and Ar^+ bombardment steps. Both methods are avenues for area selective etch and isotropy control. However, the fundamental mechanisms by which the etching occurs are poorly understood. In this talk, we will present our recent findings regarding underlying mechanisms leading to facile ALE of Si_3N_4 using hydrofluorocarbons, based on periodic density functional theory calculations. Our study highlights the important role of adsorbates and surface functional groups. For CH_3F chemisorption on a N-rich Si_3N_4 surface, we have found a trimolecular process to be the thermodynamically most favorable pathway for initiation of the process, consisting of a nucleophilic attack of a primary amine site, if available, on CH_3F, followed by a stabilization of the fluoride leaving group by an adjacent primary amine site. While this mechanism as is has a relatively high activation energy (~0.9 eV), the presence of products from other reactions on the surface such as HF, F^-, and H^+ have been demonstrated to lower this activation energy significantly. Furthermore, we find that it is not the methylation of the surface that facilitates etching, but rather the production of H^+/F^- that helps facilitate formation of volatile N-containing species and Si-F bonds. More importantly, our study also suggests that the surface reaction mechanism responsible for Si_3N_4 ALE may be altered when CH_3F is replaced by CHF_3 or CF_4.

4:15pm **ALE2-TuA12 An Extended Knudsen Diffusion Model for Aspect Ratio Dependent Atomic Layer Etching***, **Luiz Felipe Aguinsky**, P. Manstetten,* TU Wien, Austria*; A. Hössinger,* Silvaco Europe Ltd., UK*; S. Selberherr, J. Weinbub,* TU Wien, Austria

Atomic layer etching (ALE) is a fundamental part of semiconductor processing as device critical dimensions must be controlled to the order of nanometers [1]. One known issue in ALE, as in other etching processes, is aspect ratio dependent etching (ARDE) [2], which is the reduction of etch rates as the aspect ratio of a feature increases. One of the mechanisms linked to ARDE is the depletion of neutral species towards the bottom of a feature. This phenomenon has been investigated using a three-dimensional Monte Carlo method [3]. However, this method requires a complex setup and it is computationally expensive. For deposition processes, Knudsen diffusion [4] models provide analytical results and are actively developed. These models have been used for estimating surface parameters in some atomic layer deposition processes [5]. The Knudsen diffusion approach arises from physical considerations to the mass balance at each volume element. Alternatively, given isotropic reflections and particle source, the fluxes can be calculated exactly over the whole domain via the radiosity equation [6]. The radiosity approach requires the assembly and inversion of a matrix describing the exchanges, being notably unsuitable for low sticking regimes.

We propose a model extending the standard deposition Knudsen diffusion approach by including the direct flux from a particle source and a geometric factor to enable a more rigorous picture of ARDE in ALE. The inclusion of the direct flux is motivated by the radiosity equation, while avoiding the costly matrix inversion step. The geometric factor enables a more accurate description of the geometry by integrating over the whole feature at each volume element. We compare our extended Knudsen diffusion model against a reference radiosity model [6], achieving good agreement. Our results highlight one shortcoming of the standard Knudsen diffusion model: The flux near the bottom of a high aspect ratio feature is underestimated. We also show that the geometric factor describes the particle transport more accurately near the extremities of finite cylinders.

The financial support by the Austrian Federal Ministry for Digital and Economic Affairs and the National Foundation for Research, Technology and Development is gratefully acknowledged.

[1] K. Ishikawa et al., Jpn. J. Appl. Phys. **56**, 06HA02 (2017).

[2] C.G.N. Lee et al., J. Phys. D: Appl. Phys. **47**, 273001 (2014).

[3] C. Huard et al., J. Vac. Sci. Technol. A **35**, 05C301 (2017).

[4] A. Yanguas-Gil, Growth and Transport in Nanostructured Materials (Springer, 2017).

[5] M. Ylilammi et al., J. Appl. Phys. **123**, 205301 (2018).

[6] P. Manstetten et al., Solid-State Electron. **128**, 141 (2017).

4:30pm **ALE2-TuA13 Thermodynamics-Based Screening Approach for Atomic Layer Etching***, **Nagraj Kulkarni**,* Consultant

A thermodynamics-based approach for screening directional or thermal Atomic Layer Etching (ALE) processes is discussed for the purpose of achieving high synergies close to unity. The Ta-Cl system was selected as a test case for this analysis. Reaction equilibria for over 30 condensed-gas species were computed from available thermodynamic data in this system. Suitable process conditions for the formation of stable reaction products or compounds and the corresponding partial pressures of known gas species were first obtained with the aid of volatility diagrams that were calculated using thermodynamic data for all known solid-gas reactions. For optimum conditions during the first stage of a typical ALE process (passivation step), the selection of suitable metal-gas compound/s that have very low vapor pressures and hence negligibly low etch rates was made. For optimum conditions during the second stage (inert ion sputtering) of a directional ALE process, an assessment of the potential for selective sputtering of the selected compound/s relative to the base metal was made from knowledge of the surface binding energies of the base metal and relevant compound/s that are usually considered to be the enthalpy changes of the relevant solid-gas sputtering reactions at room temperature. In the case of an isotropic, thermal ALE process, the selection of suitable temperatures for the direct volatilization of the reaction product layer during the second stage of ALE is also discussed.

4:45pm **ALE2-TuA14 Always in Competition: Self-limiting Versus Continuous Reactions in ALD and ALEt***, **Simon D. Elliott**,* Schrödinger, Inc.*; S.K. Natarajan, R. Mullins, M. Nolan,* Tyndall National Institute, Ireland*; A. Cano, J. Clancey, S.M. George,* University of Colorado - Boulder

One of the main challenges in designing novel atomic layer deposition (ALD) and atomic layer etch (ALEt) processes is to ensure the self-limiting (SL) nature of reactions during the individual precursor pulses at the target temperature of interest. It is important to establish a SL temperature window to ensure that the precursors will not produce chemical vapour deposition (CVD) or chemical vapour etching (CVE). To that end, we have developed a first principles based computational methodology to study the competition between continuous and SL reactions when a material surface is exposed to precursor gases.

ALEt processes for oxides have been reported using sequential fluorination by HF and ligand exchange reactions at elevated temperatures.[1] Herein, we investigate the nature of the HF pulse when treating a range of materials including B_2O_3, TiO_2, HfO_2, ZrO_2, Al_2O_3 and TiN by comparing the free energy

profiles of the potential CVE and SL reactions computed with density functional theory (DFT). In general, elevated temperatures favour CVE of these materials, whereas fluorination of the surface is self-limiting at lower temperatures. HF was computed to continuously etch B_2O_3 and TiO_2 even at temperatures below 100°C by forming volatile fluorides. This is in good agreement with experimental FTIR, where the onset of continuous etching of TiO_2 by HF was found at 80°C – 90°C and where etching of B_2O_3 proceeded even more rapidly than that of TiO_2. However, in another example, HF is predicted to preferably etch HfO_2 above 160°C, whereas experiment[1] shows the process to be still self-limiting at 200°C. Therefore, this simple thermodynamic analysis, which does not include reaction kinetics, is only able to provide a lower threshold temperature at which a CVE reaction may become favourable, subject to overcoming any kinetic barrier. We also computed that Al_2O_3 resists continuous etching up to 340°C while TiN can not be etched until temperatures exceed 1300°C.

This methodology is also used to understand the competing CVD and SL reactions in the ALD of Ru using the RuO_4 precursor and H_2.[2] The DFT calculations show that RuO_4 undergoes an SL decomposition into RuO_2 on electron-rich surfaces and that this is in competition with CVD.

These examples illustrate that this relatively quick computational approach can be effectively used to screen candidate precursor molecules to be selected for material processing.

1. Y. Lee et al., *Chem. Mater.28*, 7657-7665 (2016).

2. M. M. Minjauw et al., *J. Mater. Chem. C3*, 132-137 (2015).

~~5:00pm **ALE2-TuA15 Variation of Etched Depth per Cycle and Removal of Reactive Species in Atomic-Layer Etching (ALE) : Molecular Dynamics Study**, ***Satoshi Hamaguchi,*** *E.J. Tinacba, S. Shigeno, Y. Okada, M. Isobe, T. Ito, K. Karahashi,* Osaka University, Japan~~

~~Alternating application of reactive species from a plasma with no bias energy and Ar plasma with low bias energy to a Si based film (such as Si, SiO2, and SiN) can cause atomic layer etching (ALE) of its surface. In this process, the initial application of reactive species to the surface will leave a sufficient number of reactive species (e.g., Cl atoms) bonded with the surface atoms (e.g., Si, forming Si-Cl bonds) and, in the second step where low energy Ar+ ions irradiate the surface, a thin mixed layer of the reactive species and surface atoms is formed and volatile molecules (e.g., SiCl4) desorb from the surface. Since the incident energy of Ar+ is too low to physically sputter surface atoms, etching or desorption of volatile species ends as soon as reactive species are exhausted from the surface - even if Ar+ ions continue to bombard the surface with low incident energy. This self-limited etched depth of a single cycle (i.e., application of reactive species and application of low-energy ions) allows "nearly" layer-by-layer etching of the material surface. At the end of each cycle, where self-limited etching takes place, some reactive species tend to remain on the surface or in the subsurface region, causing surface roughness. Depending on how deep such reactive species diffuse into the subsurface region or how thick the formed mixed layer becomes, the etched depth per cycle changes. In this study, etched depth per cycle and remaining reactive species are discussed based on the results of molecular dynamics (MD) simulation of single cycles of various ALE processes. Example considered here include Si ALE by fluorine reactions, SiO2 ALE by fluorocarbon reactions,~~

~~And SiN etching by hydrofluorocarbon or hydrogen reactions.~~

Area Selective ALD
Grand Ballroom H-K - Session AS1-TuA
Area-Selective ALD by Area-Deactivation

Moderators: Rong Chen, Huazhong University of Science and Technology, Jessica Kachian, Intel Corp.

1:30pm **AS1-TuA1 Elucidating Mechanisms of Selective ALD of Al_2O_3 by a Comparative Study of Precursors**, ***Il-Kwon Oh,*** *T.-L. Liu,* Stanford University*; T. Sandoval,* Technical University Federico Santa Maria*; R. Tonner,* Philipps-Universität Marburg, Germany*; S.F. Bent,* Stanford University

Area-selective atomic layer deposition (AS-ALD) may allow a reduction in the number of lithography and etch steps, resulting in lowering of errors in the patterning process as well as a decrease in manufacturing costs. For example, a self-aligned hard mask fabricated by AS-ALD can guide etching of via holes and deposition of metal wires in the metallization process to avoid shorts between metal layers.

Several metal oxide systems, such as Al_2O_3, TiO_2, ZnO, and HfO_2, have been explored for AS-ALD processes. For a hard mask, Al_2O_3 possesses advantages over other metal oxides due to its high hardness as well as chemical inertness for etching selectivity. However, despite extensive studies on ALD Al_2O_3, there are few studies on AS-ALD of Al_2O_3. Furthermore, literature suggests that Al_2O_3 may be comparatively difficult to block; for example, the blocking selectivity of Al_2O_3 is limited to only ~6 nm whereas ZnO can be blocked for over ~30 nm.[1] The difference in blocking highlights the importance of precursor chemistry for AS-ALD, which motivates the current study to elucidate the mechanism of Al_2O_3 AS-ALD based on a comparative study of Al precursors.

In this work, we study the growth mechanism of $Al_2O_3$with four Al precursors; trichloroaluminum (TCA), dimethylaluminum chloride (DMACl), trimethylaluminum (TMA), and triethylaluminum (TEA). They offer a comparative study of precursor ligand properties (reactivity, polarity, and geometric factors) by changing both the number of methyl (Me) and chloride (Cl) group in $AlMe_xCl_{3-x}$(x=0, 1, and 3) and the chain length of alkyl ligands in AlC_nH_{2n+1}(n=1 and 2). Results of quantum chemical calculations of the reaction pathways show product energetics that are strongly correlated with experimental observations. For example, with increasing number of Cl ligands, the growth rate is found experimentally to increase at low temperature, consistent with a large initial adsorption energy of TCA on Si .Interestingly, although they have similar geometrical factors, the precursors exhibit different ALD growth rates (0.75, 1.0, and 1.2 Å/cycle for for TCA, DMACl, and TMA respectively) corresponding to the calculated trend in activation energies as the Cl number increases. AS-ALD of Al_2O_3 using octadecyltrichlorosilane SAMs as an inhibitor is also investigated; the blocking properties of the four Al precursors will be compared and the results discussed based on the growth mechanism. By pursuing first principles design of selective ALD processes, this work may enable new methods for additive nanoscale patterning.

(1) Bobb-Semple, D. et. al., *Chem. Mater.***2019**, acs.chemmater.8b04926. https://doi.org/10.1021/acs.chemmater.8b04926.

1:45pm **AS1-TuA2 Area-Selective Atomic Layer Deposition using Dodecanethiols: Comparison of Monolayer versus Multilayer**, ***Tzu-Ling Liu,*** Stanford University*; K. Nardi, N. Draeger, D. Hausmann,* Lam Research Corp.*; S.F. Bent,* Stanford University

As the size of transistors continues downward scaling, more difficulties are introduced into traditional top-down semiconductor fabrication processes, such as edge placement errors and two-dimensional overlay control. In addition, the number of processing steps and cost are becoming significant. To overcome these challenges, it is necessary to develop new techniques, and selective deposition is one promising solution to reduce patterning errors and process complexity. Atomic layer deposition (ALD) is considered to be well suited for selective deposition because of its self-limiting reactions between precursors and specific functional groups at the substrate surface. By manipulating the surface functional groups with self-assembled monolayers (SAMs), area-selective ALD has been successfully demonstrated on technologically-important metal/dielectric (Cu/SiO_2) patterns. In recent years, using alkanethiols as the inhibition layer has received much attention because they can be deposited onto metal surface via a vapor-phase approach that can be readily incorporated into industrial semiconductor fabrication processes.

Despite the apparent simplicity of the alkanethiolate SAM system for AS-ALD, recent studies have shown that either a monolayer or multilayers of the thiols can form on Cu depending on the preparation details, including a dependence on the oxidation state of the Cu surface. However, the effect of having multilayer versus monolayer thiols on the blocking ability in AS-ALD of metal oxides has not been reported.

In this work, we compare the ALD blocking ability of multilayer and monolayer dodecanethiols (DDT) deposited from the vapor phase. The results show that monolayer DDT films are better than multilayer DDT films at inhibiting Al_2O_3 ALD. In contrast, the multilayer DDT films show better blocking performance against ZnO ALD. The influence of monolayer and multilayer DDT on area selective deposition of ALD films onto Cu/SiO_2 patterns is also studied. On the multilayer DDT-coated Cu/SiO_2 patterns, we show that there is a nucleation delay for ZnO ALD on SiO_2 near its interface with Cu, resulting in a thinner ZnO film at the edge of the SiO_2 region, an effect which is pitch dependent. The possible mechanism underlying this phenomenon will be discussed.

2:00pm **AS1-TuA3 Mechanism for Breakdown in Selectivity During Area-Selective Atomic Layer Deposition of ZrO_2 on a SiO_2 Surface Functionalized with a Blocking Layer***, **Wanxing Xu**,* Colorado School of Mines*; P.C. Lemaire, K. Sharma, D. Hausmann,* Lam Research Corp.*; S. Agarwal,* Colorado School of Mines

The conventional lithography is becoming increasingly challenging due to continued downscaling of modern semiconductor devices. Area-selective deposition of dielectrics and metals can simplify patterning for next-generation devices. Atomic layer deposition (ALD) has emerged as a very promising technique for achieving selective deposition because film growth during ALD is highly sensitive to the surface functionalization of the underlying substrate. In this study, we focus on the area-selective ALD of ZrO_2 on metals while inhibiting growth on SiO_2 by terminating the surface with fluorocarbon or hydrocarbon ligands.

The starting SiO_2 surface was functionalized with the inhibitor molecules: nonafluorohexyldimethyl(dimethylamino)silane (NHDDAS) , *n*-octyldimethyl(dimethylamino)silane (ODDAS), or *n*-octadecyltrichlorosilane (ODTS). The aminosilanes were attached to –OH-terminated SiO_2 either through the vapor phase or in solution, while ODTS was attached to surface through the solution phase. The functionalized SiO_2 surfaces were characterized by Fourier transform infrared (FTIR) spectroscopy, ellipsometry, and water contact angle measurements. We show that aminosilane and chlorosilane precursors react with almost all of the surface –SiOH groups forming ºSi–O–Si–R bonds on the surface (see Figure 1). This surface functionalization is stable over the temperature range of 200–300 °C.

ZrO_2 was grown by ALD on the passivated SiO_2 surfaces using either tetrakis(ethylmethylamino)zirconium(IV) (TEMAZ) $[Zr(NCH_3C_2H_5)_4]$ or zirconium(IV) tert-butoxide (ZTB) $[Zr(OC(CH_3)_3)_4]$, and H_2O over a temperature of 200–250 °C. While no ZrO_2 growth was detected during the initial few cycles, *in situ* four–wavelength ellipsometry showed that growth inhibition breaks down after an increased number of cycles. We recorded the corresponding surface reactions during ZrO_2 ALD using *in situ* attenuated total reflection FTIR spectroscopy, which allows us to identify the surface reaction sites and adsorbed surface species. Surprisingly, after repeated exposure of the functionalized SiO_2 surface to TEMAZ and ZTB, these precursors reacted with Si–O–Si bonds in the absence of surface –SiOH groups (see Figure 2). This suggests that while ALD of ZrO_2 may proceed through reaction with surface –OH groups, other reactions with a higher activation energy barrier become important as these surface reactive sites are removed through surface functionalization. These results highlight the importance of steric blocking of the substrate surface as an additional requirement for growth inhibition during ALD.

2:15pm **AS1-TuA4 Area Selective Chemical Vapor Deposition of Co from the Co (CO) Precursor: Use of Ammonia to Afford Dielectric-Dielectric Selectivity***, **Zhejun Zhang**, S. Liu, G. Girolami, J. Abelson,* University of Illinois at Urbana-Champaign

We previously reported the area selective chemical vapor deposition of MoC_xN_y thin films on metal substrates using $Mo(CO)_6$ precursor with a coflow of NH_3 inhibitor: at temperatures of 150-210 °C, film grows readily on metal or metal nitride surfaces but nucleation and growth are suppressed on all oxide surfaces. This was attributed to the site-blocking of hydroxyl groups or a reduction in the acidity of the surface by NH_3.

Here, we demonstrate chemical vapor deposition of cobalt thin films that is *area-selective between oxide surfaces* using $Co_2(CO)_8$ precursor with a coflow of NH_3 inhibitor at 70 °C: growth is suppressed on acidic oxides such as SiO_2 and WO_3 during experiments lasting up to 60 minutes, but proceeds unimpeded at rate of 0.6 nm/min on basic oxides such as Al_2O_3, HfO_2 and MgO. Selectivity of > 99% between SiO_2 and Al_2O_3 can be obtained. In the absence of ammonia, nucleation occurs readily on all oxide substrates but the area density of nuclei, and consequently the film smoothness, are better on Al_2O_3 than on SiO_2. Cobalt films grown with and without ammonia have a resistivity ranging from 15–25 μΩ·cm and 11–20 μΩ·cm, respectively. Surprisingly, in the presence of a very small partial pressure of NH_3, growth can proceed on SiO_2 and the area density of nuclei is *increased*. To account for these observations, we propose that ammonia reduces the surface diffusion of adsorbed precursor. Under this hypothesis, for small NH_3 pressure, adsorbates may react to form new nuclei instead of being transported to, and incorporated into, existing nuclei; but at high NH_3 pressure, adsorbate-adsorbate interaction may be suppressed, such that the rate of desorption outpaces that of nucleation.

2:30pm **AS1-TuA5 Area-Selective ALD of Silicon Oxide using Inhibitors in Four-step Cycles for Metal/Dielectric Selectivity***, **Marc Merkx**, R. Jongen,* Eindhoven University of Technology, Netherlands*; A. Mameli,* TNO/Holst Center, Netherlands*; D. Hausmann,* Lam Research Corp.*; W.M.M. Kessels, A.J.M. Mackus,* Eindhoven University of Technology, Netherlands

The fabrication of nanoelectronics at sub-5 nm dimensions using conventional top-down fabrication schemes is becoming more and more difficult due to the increasingly straining requirements in alignment. Area-selective ALD allows for deposition of material in a self-aligned fashion and thereby enables more reliable device fabrication. In our previous work, area-selective ALD of ~1 nm SiO_2 was demonstrated using three-step (ABC) ALD cycles consisting of acetylacetone (Hacac) inhibitor (A), $H_2Si[N(C_2H_5)_2]_2$ precursor (B), and an O_2 plasma co-reactant (C) doses.[1] In this contribution, the reaction mechanisms involved in cyclewise removal and reapplication of inhibitor molecules will be described. Based on the acquired insights, new opportunities and challenges for this approach will be discussed.

The reapplication of the inhibitor allows for the use of ozone or plasmas as the co-reactant, which is one of the merits of the approach. However, using in situ infrared spectroscopy it was found that the Hacac molecules are not completely removed during the O_2 plasma exposure. Remaining Hacac fragments hinder the Hacac adsorption in the subsequent ALD cycle, and thereby decrease the selectivity. The challenge of reapplying the inhibitor molecules every cycle is therefore to ensure that the non-growth area is returned to its original state before the next inhibitor dose. In order to completely remove all Hacac species, a four-step (ABDC) ALD cycle was developed which employs a H_2 plasma step prior to the O_2 plasma exposure. The added H_2 plasma, significantly improves the selectivity, such that ~2.5 nm SiO_2 can be deposited selectively in the presence of an Al_2O_3 non-growth area.

In general it is challenging to use an O_2 plasma on structures with metal areas, due to potential oxidation of the metal during the plasma exposure which reduces the conductivity. However, the H_2 plasma in the ABDC cycle was found to largely remove the precursor ligands, and therefore only a very mild O_2 plasma exposure is required for SiO_2 deposition. In this way, area-selective ALD was achieved relative to Co as the non-growth area without significant damage to the Co substrate. The application possibilities of this ABDC-type ALD process for reliable interconnect fabrication (i.e. self-aligned VIA) will be discussed.

[1] A. Mameli, M.J.M. Merkx, B. Karasulu, F. Roozeboom, W.M.M. Kessels, A.J.M. Mackus, ACS Nano **11**, 9303-9311 (2017)

2:45pm **AS1-TuA6 Selective Area Growth of Deactivating Polymers***, **Rudy Wojtecki**,* IBM Research - Almaden*; T. Pattison,* University of Melbourne, Australia*; A. Hess, N. Arellano, A. Friz,* IBM Research - Almaden

As the semiconductor community continues scaling, area selective atomic layer deposition (ASD) offers the potential to relax down-stream processing steps by enabling self-aligned strategies (e.g. self-aligned via). ASD can be achieved under a variety of conditions and, with the use of organic inhibiting materials, exhibit high levels of selectivity during depositions. However, the organic materials exploited are generally relegated to small molecules and may require multiple cycles of etch-back processes followed by renewal of the surface protection coating. Recent work has shown that a variety of polymeric materials offer the potential to broaden the number and film compositions that can be selectively deposited. However, an attractive ASD approach requires the directed grafting of polymers to a surface using selective adhesion groups, for instance. Inhibiting polymers could be functionalized with metal binding ligands and the resulting polymer brushes retain their inhibiting properties on blanket films. On patterned surfaces though, brushes exhibit poor selectivity, adhering to both metal and dielectric surfaces and resulting in high defectivity after a subsequent atomic layer deposited (ALD) film (polymer particles were observed on both a metal and dielectric). An alternative approach is a grafting from strategy where a low molecular weight monomer, containing a diphosphonic acid binding group, enables area selective grafting on a prepatterned surface containing copper lines and silicon spaces. Subsequent treatment of these surfaces with a catalyst and introduction of a norbornene monomer in the vapor phase allows the area selective growth of polynorbornene (PNB) producing films with thicknesses between 10-100nm. The surface grown PNB films shows excellent inhibitory properties against the ALD deposition of metal oxides, TiO_2 and ZnO, where only trace metal concentrations are observed on the polymer surfaces even after a long number of ALD cycles. This area selective surface grown polymer strategy offers the potential to address several challenges in ASD

such as: (i) lateral overgrowth of an ALD film once film thickness exceeds that of the inhibiting material. A polymer strategy offers the potential to control the polymer film thickness and thus the desired ALD film thickness (ii) On patterned surfaces line edges and corners are sites for significant defectivity in ASD. The surface growth of a polymer readily covers these corners and edges to ensure these features are protected during the ALD process.

3:00pm **AS1-TuA7 Area-Selective ALD of ZnO Films Patterned by Electrohydrodynamic Jet Printing of Polymers with Sub-Micron Resolution***, **Tae Cho**, N. Farjam, C. Pannier, C. Huber, O. Trejo, C. Allemang, E. Kazyak, R. Peterson, K. Barton, N.P. Dasgupta,* University of Michigan

An increasing demand for customization in manufacturing of integrated nanosystems has motivated the development of printable electronics that can be adapted to the unique requirements of an end-user. The current state-of-the-art in nanofabrication of functional devices involves multiple lithographic patterning steps, combined with thin-film deposition and top-down etching processes. While this has led to tremendous advances in spatial resolution and process reliability, lithographic processes are inherently parallel processes, and not easily customizable. In contrast, additive manufacturing processes enable rapid prototyping of 3-D structures that can be easily tuned, and multiple layers of dissimilar materials can be integrated in a bottom-up manner. Therefore, combining a 3-D printing technology with area-selective ALD could enable a new paradigm in customizable nanomanufacturing.

Area-selective ALD has been previously demonstrated with patterns printed by ink-jet printing, micro-contact printing, directed self-assembly of templates, and a variety of other methods. However, there have been few techniques with the ability to directly 3-D print customizable patterns with sub-micron resolution, as traditional ink-jet printing is limited to a spatial resolution of ~20 microns. In this study, we demonstrate the use of electrohydrodynamic jet (e-jet) printing of polymers with sub-micron resolution [1], which can act as either inhibitors or promotors of ALD growth. The e-jet system allows for 3-D printing of polymers that pattern the surface chemistry by thermodynamically / kinetically activating or passivating local regions to nucleation of inorganic layers by ALD [2]. This enables bottom-up patterning of ALD growth, which can be integrated into 3-D nanosystems without the need for lithography or etching.

A variety of polymers were tested, demonstrating the ability to inhibit or promote the growth of ALD ZnO coatings on the surface by additive and subtractive printing approaches. Auger electron spectroscopy (AES), atomic force microscopy (AFM), transmission electron microscopy (TEM), and x-ray photoelectron spectroscopy (XPS) were used to perform compositional and elemental analysis of the patterned materials. After thin-film deposition by ALD, the electronic properties of the patterned films were characterized, demonstrating a pathway towards additive 3-D nanomanufacturing of customizable electronic devices.

1) M. S. Onses, E. Sutanto, P. M. Ferreira, A. G Alleyne, J. A. Rogers, *Small* **2015**, *11*, 4237–4266.

2) S. F. Nelson, C. R. Ellinger, D. H. Levy, *ACS Appl. Mater. Interfaces* **2015**, *7*, 2754–2759.

3:15pm **AS1-TuA8 Selective Deposition of Silicon Nitride***, **Han Wang**, B. Hendrix, T. Baum,* Entegris Inc.

Atomic layer deposition of SiN using SiI_4 and NH_3 was studied. The growth per cycle and initial nucleation of SiN films were analyzed as a function of the deposition temperatures and precursor pulse times on different substrates. The sequential reaction of SiI_4 and NH_3 showed longer nucleation delay on silicon oxide surfaces (native and thermal SiO_2) when compared to metal oxide (ZrO_2 and Al_2O_3) surfaces. This nucleation delay decreased with the increased deposition temperature. By pretreating metal and silicon oxide surfaces with an NH_3 plasma, SiI_4 and NH_3 process showed no nucleation delay on the pretreated silicon oxide surfaces, while a significant delay was observed on the pretreated metal oxide surfaces. By using the definition of selectivity developed by Gladfelter [Chem. Mater. 5, 1372 (1993)], we have achieved $t_{S=0.90}$ = 18 Å for the process without NH_3 plasma pretreatment and $t_{S=0.94}$ = 74 Å for the process with NH_3 plasma pretreatment. This selectivity was not observed for pretreatment using H_2, N_2, or N_2-H_2 mixtures (50% N_2) plasma. Ex-situ XPS was used to determine the surface species with and without plasma pretreatments.

Area Selective ALD
Grand Ballroom H-K - Session AS2-TuA1

Area-Selective ALD: Combinations with Etching

Moderators: Silvia Armini, IMEC, Dennis Hausmann, Lam Research Corp.

4:00pm **AS2-TuA111 Area-Selective Deposition and Smoothing of Ru by Combining Atomic Layer Deposition and Selective Etching***, **Martijn Vos**, Eindhoven University of Technology, Netherlands; S. Chopra,* University of Texas at Austin*; M. Verheijen,* Eindhoven University of Technology, Netherlands*; J. Ekerdt,* University of Texas at Austin*; S. Agarwal,* Colorado School of Mines*; W.M.M. Kessels, A.J.M. Mackus,* Eindhoven University of Technology, Netherlands

Area-selective ALD is expected to become a key technology for fabrication of nanoelectronics with sub-5 nm dimensions. The technology is nevertheless in an early stage of development, and one of the main challenges is to obtain a high selectivity.[1] The selective window can however be extended by introducing periodic etch steps that remove defects or nuclei from the non-growth area.[2]

In this work, it is demonstrated that Ru can be grown selectively on top of Pt or Ru (metal-on-metal), by integrating etch cycles into an ALD-etch supercycle. Furthermore, it is shown that this supercycle recipe simultaneously leads to smoothing of the Ru film on the growth area. Area-selective ALD of metal-on-metal is interesting for applications in semiconductor devices, and Ru is specifically relevant since Ru is being considered for the replacement of Cu in small dimension interconnects.

The optimal deposition temperature for the thermal Ru ALD process (without etching) was determined, by maximizing the difference in growth per cycle between growth on Pt and SiO_2. Even for the optimized temperature, the ALD process demonstrated a limited growth-selectivity between the two areas. A periodic etch cycle, consisting of an O_2 plasma exposure and a reducing H_2 dose, was therefore introduced to remove unwanted Ru nucleation from the SiO_2, allowing for area-selective deposition with improved selectivity. Both the etch time and frequency were varied to optimize the net growth rate on Pt, while maintaining a clean SiO_2 non-growth area. Using an etch cycle performed after every 100 ALD cycles, 8 nm was deposited with high selectivity on patterned Pt lines, demonstrating the potential of the approach. In addition, it is shown that the inclusion of etch cycles also has the benefit of smoothing of the Ru film, resulting in a lower surface roughness than for the ALD recipe itself. Finally, some guidelines will be discussed for extending the ALD-etch supercycle approach to other material systems.

[1] Mackus *et al*., Chem. Mater., 31, 1, 2019.

[2] Vallat *et al*., J. Vac. Sci. Technol. A., 35, 01B104, 2017.

4:15pm **AS2-TuA112 Single Batch Strategies for the Development of an Area Selective Deposition Process with the Deposition/Etch Approach***, **Christophe Vallée**, M. Bonvalot,* LTM-UGA, France*; R. Gassilloud,* CEA-Leti, France*; V. Pesce, A. Chaker, S. Belahcen,* LTM-UGA, France*; N. Possémé,* CEA-Leti, France*; B. Pelissier, P. Gonon, A. Bsiesy,* LTM-UGA, France

Several approaches are currently being investigated for the development of Area Selective Deposition (ASD) processes. For instance, the use of self-assembled monolayers (SAM) or block copolymers, processing temperatures promoting inherent selectivity, spatial ALD or selective ALD based on ABC-type cycles are common routes under study for this purpose [1-3]. The original approach developed in our group consists in taking benefit from an *in situ* etching step in a standard ALD cycle [4]. This deposition/etch approach is a simple and effective strategy and recently, two selective depositions have been obtained for two different plasma etching chemistries:

- First, selective deposition on metallic surfaces versus silicon-based surfaces (SiN, SiO_2 and Si) has been demonstrated in the case of Ta_2O_5 and TiO_2 by the application of an extra NF_3 plasma etching step to standard PEALD cycles [4-5];

- Second, geometric selective deposition (also called Topographically Selective Deposition) has been achieved on trench walls by the application of an extra Ar^+ sputtering step to standard PEALD cycles [6].

In this work, advantages and drawbacks of this deposition/etch approach to ASD processes will be discussed. The following issues will be addressed:

- What is the impact of the extra etching step on the material properties and on the overall throughput of the process? Are there any etching-induced damages to the substrate (etching, roughness…)?

- Does the deposition temperature have to be determined according to the boiling temperature of etching by-products?

- May the etching step induce any drift of the process?

By addressing these questions, the need for an appropriate specific design of the PEALD reactor will be emphasized so as to provide an efficient strategy for a precise control of plasma parameters. Special attention will be devoted to the role of medium energy ions in the plasma, as illustrated by the following two examples:

- At first, a new route for topographically selective deposition on top and bottom only of trenches will be discussed;

- Second, a surface selective deposition on SiO_2 surfaces versus metallic surfaces using the alternating PEALD/Atomic Layer Etching (ALE) approach will be shown.

[1] A. J. M. Mackus et al, *Chem. Mater.* **31** (2019) 2-12

[2] G. N. Parsons, J. Vac. Sci. Technol. A 37 (2019) 020911

[3]R. Chen, H. Kim, P. C. McIntyre, and S. F. Bent, Appl. Phys. Lett. 84 (2004) 4017

[4] R. Vallat *et al*, *J. Vac. Sci. Technol. A* **35** (2017) 01B104

[5] R. Vallat *et al*, *J. Vac. Sci. Technol. A* **37** (2019) 020918

[6] A. Chaker *et al*, *Appl. Phys. Lett*. **114** (2019)

~~4:30pm **AS2-TuA113 Surface Halogenation of Amorphous Carbon for Defect-free Area Selective Deposition of Metal Oxides***, Mikhail Krishtab,* KU Leuven, Belgium*; S. Armini,* IMEC, Belgium*; S. De Gendt,* KU Leuven/IMEC, Belgium*; R. Ameloot,* KU Leuven, Belgium~~

~~The area-selective deposition (ASD) processes gained recently a lot of attention from the microelectronics industry as a potential solution for the issues associated with top-down pattern formation at nanoscale. As the critical dimensions approach few tens of nanometers, the precise positioning of a pattern becomes essential for reliably functioning devices or connections between them. The area-selective atomic layer deposition (ALD) guided by the contrast in surface functionality allows to circumvent some of the lithography-related issues by introducing self-alignment of adjacent layers. However, the defectivity of typical ASD ALD processes relying on delayed nucleation on a non-growth area is one of the key concerns for the adoption of this technology. Among the strategies addressing the defectivity issue, repetitive refreshment of the non-growth surface and selective etching of undesired nuclei are particularly promising.~~

~~In this study, we examined the possibility to combine the two defect-reduction strategies by employing low-power Cl_2 or CF_4 plasmas for both surface functionalization/re-functionalization and for removal of nuclei from a non-growth layer represented by amorphous carbon. We employed prototypical water-based metal oxide processes such as ALD ZnO (DEZ/H2O) and ALD TiOx (TiCl4/H2O) to demonstrate area-selective deposition on top of silicon oxide using both blanket films and patterns of amorphous carbon landing on a layer of thermal silicon oxide. At first, the plasma parameters were optimized to minimize etching of amorphous carbon and silicon oxide. Then the selectivity of the ALD processes under study was checked on the plasma-halogenated amorphous carbon films using a standard ALD sequence and a sequence interrupted by the appropriate plasma treatment steps. While CF_4 plasma showed better performance in etching of metal oxide nuclei on top of amorphous carbon, the more hydrophobic fluorinated films exhibited inferior selectivity as compared to chlorinated amorphous carbon films for both types of ALD processes. In turn, Cl_2 plasma treated films of amorphous carbon demonstrated outstanding ALD ZnO growth inhibition along with lower tendency to formation of nucleation defects during ALD ZnO and ALD TiOx. The origin of the defects and of the observed differences in selectivity is discussed in the context of detailed surface composition analysis of the halogenated amorphous carbon films.~~

Area Selective ALD
Grand Ballroom H-K - Session AS2-TuA2

Late Breaking Abstracts

Moderators: Silvia Armini, IMEC, Dennis Hausmann, Lam Research Corp.

4:45pm **AS2-TuA214 Real-time Grazing Incidence Small-angle X-ray Scattering Studies of Indium Aluminum Nitride Growth***, **Jeffrey M. Woodward**, S.G. Rosenberg,* ASEE (residing at U.S. Naval Research Laboratory)*; S.D. Johnson, N. Nepal,* U.S. Naval Research Laboratory*; Z.R. Robinson,* SUNY College at Brockport*; K.F. Ludwig,* Boston University*; C.R. Eddy,* U.S. Naval Research Laboratory

Indium aluminum nitride (InAlN) is an attractive material for power electronic applications. However, conventional methods of epitaxial growth of InAlN are challenged by a large miscibility gap and the significant differences in optimal growth conditions for the constituent aluminum nitride (AlN) and indium nitride (InN) binary compounds. Despite these challenges, the epitaxial growth of InAlN alloys throughout the entire compositional range has been demonstrated using plasma-assisted atomic layer epitaxy (ALEp)[1], a variant of atomic layer deposition in which relatively higher temperatures are utilized. In the ALEp growth of InAlN, the desired alloy compositions are achieved by forming ultra-short period superlattices of alternating InN and AlN layers, referred to as digital alloys (DA). In order to further advance these empirical efforts, significant research is needed to better understand the nucleation and growth kinetics of ALEp DA growth. To this end, we employ *in situ* grazing incidence small angle X-ray scattering (GISAXS) for the real-time study of the evolving ternary InAlN surfaces as has been done previously for binary InN[2] and AlN[3].

Here we present *in situ* GISAXS studies of ALEp growth of InN, AlN, and a range of InAlN DAs on GaN (0001) substrates, which were performed at Brookhaven National Laboratory's NSLS-II using a custom reactor. The InAlN DAs studied include $In_{0.19}Al_{0.81}N$ (3 AlN cycles and 2 InN cycles per supercycle), $In_{0.5}Al_{0.5}N$ (1 AlN cycle and 3 InN cycles per supercycle), $In_{0.64}Al_{0.36}N$ (1 AlN cycle and 5 InN cycles per supercycle) and $In_{0.83}Al_{0.17}N$ (1 AlN cycle and 14 InN cycles per supercycle). Preliminary analysis of the data suggests that while the pure InN and AlN grew in 3D and 2D modes, respectively, the InAlN growth mode did not follow a simple trend as the nominal composition was tuned from InN to AlN. Instead, select compositions (50% and 83% In) exhibited predominantly 3D growth, while others (19% and 64% In) exhibited 2D growth. *Ex situ* X-ray reflectivity data show evidence of phase separation in the 83% In DA.

[1] N. Nepal, V.R. Anderson, J.K. Hite, and C.R. Eddy, Thin Solid Films **589**, 47 (2015)

[2] J.M. Woodward, S.G. Rosenberg, A.C. Kozen, N. Nepal, S.D. Johnson, C. Wagenbach, A.H. Rowley, Z.R. Robinson, H. Joress, K.F. Ludwig Jr, C.R. Eddy Jr, J. Vac. Sci. Technol. A **37**, 030901 (2019)

[3] V.R. Anderson, N. Nepal, S.D. Johnson, Z.R. Robinson, A. Nath, A.C. Kozen, S.B. Qadri, A. DeMasi, J.K. Hite, K.F. Ludwig, and C.R. Eddy, J. Vac. Sci. Technol. A **35**, 031508 (2017)

5:00pm **AS2-TuA215 Expanding the Materials Library of Sequential Infiltration Synthesis: Conductive Indium and Gallium Oxides Grown in Polymers***, **Ruben Waldman**,* University of Chicago*; N. Jeon, D. Mandia, O. Heinonen, S. Darling, A. Martinson,* Argonne National Laboratory

Over the past decade, researchers have developed a deeper understanding of how the chemistry of ALD can be applied to polymeric substrates. Polymers are fundamentally unlike traditional ALD substrates in that precursors diffuse through the polymer and associate with functional groups that are distributed throughout the volume of polymer, rather than on a two-dimensional surface.

In one implementation of ALD in polymers called sequential infiltration synthesis (SIS), very long static exposures of precursors are used to enable diffusion into the polymer bulk. The published SIS materials library is quite limited compared to the broad ALD materials library. Aluminum oxide (Al_2O_3), as synthesized via SIS with trimethylaluminum (TMAl) and water, is by far the most studied system and has been utilized in applications ranging from lithography to oil sorption. Prior attempts to expand this library build upon on a primary SIS cycle of Al_2O_3 to act as a scaffold for subsequent synthesis of other materials. However, the insulating Al_2O_3 is detrimental to the properties of optoelectronically interesting materials. A detailed understanding of the physical and chemical processes of solvation, diffusion, and complexation between ALD precursors and polymer

functionalities is required to engineer hybrid polymer-metal oxide devices and to develop a broader library of SIS materials.

Through a combined experimental and first principles computational study we have developed primary SIS processes for two previously unreported materials – indium oxide (In_2O_3) and gallium oxide (Ga_2O_3) – using congeners to TMAl (TMIn, TMGa) and water. Through Fourier transform infrared spectroscopy and density functional theory, we elucidate the binding configuration and affinity of TMAl, TMIn, and TMGa for the carbonyl functional groups in polymethylmethacrylate (PMMA). We find that the three form isostructural adducts, though TMAl binds three times more strongly, and observe that the kinetics of adduct formation/dissociation for TMAl are more than ten times slower than for TMIn or TMGa.

With detailed knowledge of the TMIn reaction kinetics we designed an SIS recipe with exposure and purge durations tuned to the time-scales of vapor diffusion in and out of the polymer film. This led to the templated synthesis of In_2O_3/PMMA hybrid films which are readily converted upon annealing to crystalline, conductive In_2O_3 films. Notably, we observe substantial SIS growth rates of In_2O_3 at 80 °C, well below what is possible with these precursors in ALD. This suggests that complexation with polymers can catalyze reactions, opening routes for further exploration of low temperature deposition processes.

~~5:15pm **AS2-TuA216 Highly Efficient and Stable Organic – Inorganic Halide Perovskite Solar Cells with ALD-grown Charge Transport Layers,** ***Hyunjung Shin,*** Sungkyunkwan University, Republic of Korea~~

~~$CH_3NH_3PbI_3$ with perovskite crystal structure has attracted considerable interest for high power conversion efficiency. Metal oxide grown *via* ALD provides pinhole free uniform and dense films which are suited to function as passivation layer since ALD is deposited by self limiting sequential chemical reaction. ALD chemistry for TiO_2, SnO_2, and ZnO are well known and the process requires relatively low deposition temperature as much as ~ 100 °C, which is applicable to deposit onto halide perovskite materials. In this presentation, we report highly efficient perovskite solar cells having a long-term stability that adapts uniform and dense inorganic charge transport layer (TiO_2, SnO_2, Al:ZnO, and NiO) grown by atomic layer deposition (ALD) at relatively low temperature. Ultra-thin un-doped NiO films were prepared by ALD with a highly precise control over the thickness. Thin enough (5 ~ 7.5 nm in thickness) NiO films with the thickness of few times of Debye length (1 ~ 2 nm for NiO) show enough conductivities achieved by overlapping space charge regions, which finally exhibited a highest PCE of 17.40 % with a negligible current-voltage hysteresis. Furthermore, highly dense inorganic electron transport layer (ETL) has been deposited onto perovskite using ALD process at relatively low temperature (100 °C). The devices shows excellent water-resistant properties and long term stability at 85 °C under illumination compared to devices without ETL grown by ALD.~~

~~**References**~~

~~[1] H. Shin, et. al. "Perovskite Solar Cells with Inorganic Electron and Hole Transporting Layers Exhibiting Long – Term (≈ 500 h) Stability at 85 ° C under Continuous 1 Sun Illumination in Ambient Air", Adv. Mater., (2018)~~

~~[2] H. Shin, et. al., "Atomic Layer Deposition of SnO Electron Transporting Layer for Planar Perovskite Solar Cells with a Power Conversion Efficiency of 18.3 %" , Chem Comm (2019)~~

~~[3] **Shin, H.** et. al. "Atomic Layer Deposition for Efficient and Stable Perovskite Solar Cells" *ChemComm* (2019)~~

ALD Applications
Evergreen Ballroom & Foyer - Session AA1-TuP
Energy Harvesting and Storage Poster Session

~~**AA1-TuP1 Study on Atomic Layer Deposited Al_2O_3, TiO_2 and ZnO for the Application in Silicon Photovoltaics**, ***Arun Haridas,*** *M.G. Sreenivasan,* Hind High Vacuum Company Pvt. Ltd., India*; A. Antony,* Indian Institute of Technology Bombay, India~~

~~We have fabricated a thermal atomic layer deposition (ALD) system with a substrate size of 150 mm diameter. Non uniformity of 95 nm Al_2O_3 films deposited over polished (100) Si substrate at a temperature of 200°C is ± 0.41 % over 150 mm diameter as measured using ellipsometry. The optical properties, i.e. n & k values were found to be very uniform indicating the uniformity of the growth and the quality of the layer over large area. Passivation quality of the Al_2O_3 films over the Silicon substrate is studied by measuring the minority carrier life time and photoluminescence. Application possibility of ALD grown TiO_2 and ZnO films have been examined as carrier selective layer for Silicon.~~

~~Highly uniform Atomic layer deposition of Al_2O_3 thin film using trimethyl Aluminium and H_2O as counter reactant has been achieved. Surface recombination is a major loss factor in the Si solar cells. These losses can be reduced with good quality chemical passivation or field effect passivation. Al_2O_3 is a promising high quality passivation material for p-type Si, because of its ability to act as a field effect passivator for the charge carriers. Crucial parameter of this layer is thickness and uniformity that can be precisely controlled using ALD.~~

~~The material quality and doping level by the oxygen vacancies of the metal oxide layer plays a crucial role in the performance of the carrier selective silicon solar cells. High quality films of TiO_2 using Titanium isopropoxide and H_2O, as well as ZnO using diethyl Zinc and H_2O are investigated for carrier selectivity. ALD has very good potential as effective tool for depositing ultra thin carrier selective layers for solar cells.~~

~~In this work we are exploring the advantages of the ALD technique to grow pinhole free, conformal and extremely uniform films for improving the performance of Silicon solar cells.~~

AA1-TuP2 Nitrogen-Doped TiO_2 Film Deposited using Plasma-Enhanced Atomic Layer Deposition to Improve the Electrical Conductivity for Surface Passivation of Crystalline Silicon*, E.-J. Song,* Korea Institute of Materials Science, Republic of Korea*; J.-H. Ahn,* Korea Maritime and Ocean University, Republic of Korea*;* ***Jung-Dae Kwon,*** Korea Institute of Materials Science, Republic of Korea

For surface passivation with improved electrical conductivity, we investigate nitrogen doped TiO_2 film by combining the TiO_2, TiN sub-cycles using plasma-enhanced atomic layer deposition. For composition control of the TiON films, a super-cycle was adopted which was composed of one cycle of TiO_2 and x-cycles of TiN. The thickness of the TiON films as the nitrogen doping concentration linearly increases with the number of super-cycles. We confirm the chemical states, crystalline phase and interface characteristics of these TiON films through the XPS, XRD and C-V analysis. When the nitrogen was doped in the TiO_2 thin film, the carrier lifetime was increased from 30 to 243 µs and the resistivity decreased from 3.1E+08 to 7.1E-01 Ω·cm for the TiO_2:TiN=1:20 film.

AA1-TuP3 Multilayer Encapsulation for Highly Stable Perovskite Solar Cells with Atomic Layer Deposited Al_2O_3 and Chemical Vapor Deposited Flowable Oxide*,* ***Jungwoo Kim****, H. Hwangbo, S.J. Kim, J.H. Jang, H.C. Tran Vo, H. Chae,* Sungkyunkwan University (SKKU), Republic of Korea

Perovskite solar cells (PVSCs) are known to be easily deteriorated in atmospheric environment. Many researchers have studied encapsulation technique to protect PVSCs. However, few researchers reported long term stability under severe conditions such as 85 °C with 85% relative humidity (RH). Atomic layer deposited metal oxides are considered to be effective to thin film encapsulation. However, PVSCs can be easily damaged by oxygen radicals during the metal oxide deposition process. In this work, we introduced flowable oxide inter layer for the cell protection before spatially-resolved plasma atomic layer deposition (ALD) process. The flowable oxide layer prevent oxygen radicals generated in N_2O plasma during Al_2O_3 process and the power conversion efficiencies (PCEs) of PVSCs were almost preserved. With flowable oxide and Al_2O_3 double layer, 45% in efficiency drop was observed after 1000 hours in 85 °C/35% RH condition. The PSVCs with multiple stacked flowable oxide/Al_2O_3 layer with glass encapsulation showed less than 10% of efficiency degradation after 1000 hours in 85 °C/85% RH. The multilayer with flowable oxide protection layer and Al_2O_3 moisture barrier layer structure is expected to provide long term stability in ambient condition.

AA1-TuP5 Oxide Buffer Layers for Perovskite Solar Cells Grown with a 200 mm Commercial ALD System Using Low-Temperature Process*, P. Rajbhandari,* ***Tara Dhakal,*** Binghamton University

Organic materials provide a very small thermal budget for any post-fabrication treatment or for a subsequent layer in device fabrication. The demand for the low-temperature process has driven the focus of our study to obtain atomic layer deposited oxide buffer layer at temperatures suitable for a perovskite solar cell. The buffer layer will assist in blocking holes, effectively extract electrons, provide better shunt protection and act as a sputter protection layer covering the organic perovskite films from sputter damage from a subsequent layer, such as a transparent conductor. Three different oxide layers, Al_2O3, ZnO, and TiO_2 are grown at 100°C and studied for this purpose using **Synchronous Modulated Flow Draw ALD (SMFD-ALD)** technology optimized in commercial 200 mm ALD reactor from Sundew Technologies. It allows greater precursor utilization and shorter deposition cycle times that in turn reduces thermal processing time compared to traditional ALD processes. These thin films have shown to enhance the fill factor (FF) and high charge extraction from the solar cell. Three oxides are compared on all aspect, among which ZnO (4 nm) along with Al_2O_3 (1 nm) as a buffer layer has shown excellent performance improvement in the device up to 20% power conversion efficiency. In this presentation, ALD growth details of the oxide layers and the resulting perovskite solar cell results will be discussed.

AA1-TuP6 Ultra-thin Nickel Films for Energy Harvesting Applications*,* ***Ken Bosnick****, P. Motamedi,* National Research Council Canada, Canada*; K. Cadien,* University of Alberta, Canada*; K. Harris, J.-Y. Cho,* National Research Council Canada, Canada

The harvesting of ambient heat and light could potentially lead to useful power for driving off-grid, internet-of-things sensors. Recent theoretical predictions suggest that ultra-thin Ni films can show thickness dependent optical properties that can lead to enhanced solar absorptance. The maximum solar absorptance is predicted to occur at a very thin layer thickness of ~12 nm and is attributed to an impedance matching effect [N. Ahmad, *et. al, Nano Energy* **1**, 777 (2012)]. Light absorptance in ultra-thin Ni films can be further enhanced by patterning the Ni films and depositing multi-layer structures. Atomic layer deposition (ALD) produces conformal films with a high level of control and uniformity with respect to the film thickness. While ALD is most widely known for depositing ultra-thin dielectric materials for advanced electronics applications, we have successfully used the technique to deposit ultra-thin Ni films [P. Motamedi, *et al., ACS Appl. Mater. Interfaces* **9**(29), 24722 (2017); P. Motamedi, *et al.*, *Adv. Mater. Interfaces* **5**(24), 1800957 (2018)].

In this study, ALD Ni films are deposited with varying thicknesses onto fused silica and sapphire substrates. Structural characterization indicates that the films are continuous, polycrystalline Ni films with a relatively low degree of roughness and are suitable for comparison with the theoretical predictions. Optical absorptance is measured using an integrating sphere as a function of film thickness and compared with theory. An optimum thickness is found but the experimentally determined absorptance maximum is less significant than theoretically predicted. Possible explanations include surface roughness or deviations from the refractive index of bulk Ni. Nevertheless, the thickness for optimum absorptance is found to be around 10 nm for planar ALD Ni films.

Glancing angle deposition (GLAD) is used to produce quasi-periodic silica pillars on fused silica wafers and ALD Ni films are deposited conformally onto the GLAD pillars. It is hypothesized that the GLAD films with ultra-thin ALD Ni coatings will act similarly to lithographically patterned gratings and lead to enhanced optical absorptance. Optical absorptance measurements reveal a low reflectance at all wavelengths, but an extremely high absorptance in the UV / visible range that decreases to very low values in the NIR. The spectra are seen to have a strong dependence on the ALD Ni thickness but to be less sensitive to changes in the GLAD deposition parameters. Structural characterization, further control experiments, and theoretical modeling are planned to understand these optical results.

AA1-TuP7 MoNx-Deposited on High-surface N-doped Carbon Coated-Carbon Cloth Substrates: The Best Possible Option for ALD in View of Energy Storage Application*, S.Y. Sawant, D.K. Nandi, R. Rahul, S.-H. Kim,* ***Moo Hwan Cho,*** Yeungnam University, Republic of Korea

Molybdenum [https://www.sciencedirect.com/topics/chemistry/nitride] (MoN_x) was directly grown on 3-dimensional nitrogen doped-carbon coated

carbon cloth (NC-CC) at a relatively low temperature of 250 °C by atomic layer deposition (ALD) and then tested as an electrode for supercapacitive charge storage. The charge storage performance of NC-CC and MoN_x deposited CC have also been evaluated for the comparative studies. The successful formation of MoN_x@NC-CC and MoN_x@CC composite was confirmed by several characterization techniques. The scanning and [https://www.sciencedirect.com/topics/chemistry/transmission-electron-microscopy] analyses showed the extremely uniform and conformal coating of the MoN_x on NC-CC. The 3D and porous texture of NC provided the excessive surface area for MoN_x coating and also granted easy access for the electrolyte penetration. The high areal capacitance of 911 mF/cm^2 was achieved at a current density of 4 mA/cm^2 which is 1.3 times higher than that of NC-CC. The negligible charge storage capacity of 7 mA/cm^2 obtained for MoN_x@CC highlighted the significance of NC deposition on CC prior to the loading of MoN_x. The ultra -high stability of MoN_x@NC-CC (108% capacity retention after 50,000 cycles) further confirmed its exceptional supercapacitive charge storage performance.

AA1-TuP8 ALD Coatings for Nano Imprint Masks*, **Thomas Seidel**,* Seitek50

Nano Imprint Lithography (NIL) usage has been limited by mask defects during fill and release process steps. Additionally, as for any process step, it is desirable to improve throughput. The optical intensity in the features of quartz imprint masks with high index conformal coatings was simulated using Maxwell solver software.[1] The index of refraction of the coatings, exposure wavelength, aspect ratio, film thickness and feature size were varied parameters. The simulations indicate the optical intensity may be increased within the mask features using coatings of higher index films relative to the uncoated reference quartz mask for physical feature sizes below 7nm, indicating the possibility of improved productivity.[2] Defectivity is proposed to be addressed by the application of *fractional* fluorine terminated monolayers of a fluro-hydrocarbon (FHC) film at the mask feature surface. This approach is intended to address the dichotomy of fill and release type defects in the imprint feature.[1,2] In addition, ALD conformal films may be used to reduce the critical feature size below that achievable with the state-of-the-art electron beam processes. A matrix of candidate ALD precursors and processes for higher index coating films (Al_2O_3, TiO_2 and Si) relative to quartz, as well as monolayer FHC precursors are reviewed with considerations of quality and throughput. Various ALD wafer systems are considered for process deposition for square mask quartz plates of 6in. x 6in. x 0.25in. geometry.

The support of Nayoa Hayashi and Nobuhito Toyama of Dia Nippon Printing is acknowledged for the simulations.

1. T. E. Seidel, A. Goldberg and M. D. Hall; "Optical Simulations for Fractional Fluorine Terminated Coatings on Nanoimprint Lithography Masks," *Proc. SPIE* 9635, Photomask Technology 2015, paper 96350S (October 23, 2015)

2. Thomas E. Seidel US 10,156,786B "Method and Structure for Nanoimprint Lithography Masks using Optical Film Coatings," Dec 18, 2018

AA1-TuP9 The Investigation of Al_2O_3 Passivation Characteristics in the Condition of Growth Temperature and Ozone Concentration*, **Young Joon Cho**, H.S. Chang,* Chungnam National Univ., Republic of Korea

The surface passivation for high efficiency c-Si solar cell is a prerequisite for the achievement of high efficiency solar cell. The capability of Al_2O_3 passivation using trimethlyaluminium(TMA, $Al(CH_3)_3$) precursor and H2O oxidant was presented. Aluminum oxide (Al_2O_3) grown by atomic layer deposition (ALD) was showed excellent passivation performance as good as obtained by thermally grown SiO_2. A superior property of the ALD- Al_2O_3 film appeared to be the field-effect passivation induced by negative fixed charges and the high level of chemical passivation resulting from a low interfacial defect density. ALD- Al_2O_3 film using ozone oxidant showed better thermal stability and no-blistering because of excluding hydroxyl group in ozone oxidant. Therefore, more detail study is required about the effect of growth temperature and ozone concentration on ALD- Al_2O_3 passivation.

Al_2O_3 were deposited on 8 inch p-type crystalline semiconductor Si(100) wafers of 10 Ω-cm resistivity and 710 ~ 740 µm wafer thickness. Al_2O_3 films of about 20 nm thickness were deposited in the range of 150°C and 300°C with trimethlyaluminium ($Al(CH_3)_3$) (TMA) precursor and ozone oxidant at the concentraion of 200g/Nm^3 and 330g/Nm^3 after RCA cleaning. Comparing H_2O oxidant, ozone oxidant has several advantages, such as its higher activity for ligand elimination relative to H_2O, significantly less amount of defect states like Al–Al and OH bonds compared with those prepared with H_2O. Ozone concentration was controlled by MKS ozone generator at 150g/Nm3 (~10wt%) and 330g/Nm3(~20wt%).

As a result, the lifetime and implied Voc for the as-deposited Al_2O_3 shows the maximum at growth temperature 250°C and for both of ozone concentration 200g/Nm^3 and 330g/Nm^3. After annealing, the lifetime and implied Voc has a similar tendency with the as-deposited Al_2O_3. We investigated the reason that the lifetime and implied Voc have a maximum at 250°C before and after annealing through SIMS(secondary ion mass spectroscopy), XPS(X-ray photoelectron spectroscopy), TEM(tunneling electron microscopy), etc.

AA1-TuP10 Effect of Al2O3 Passivation on n-type Si Solar Cell with Passivated Emitter and Rear Cell (PERC)*, **Kiryun Kim**, H.S. Chang,* Chungnam National University, Republic of Korea

N-type solar cells are immune to LID (Light Induced Degradation) effect, because of the absence of the boron-oxygen defect. However, The fabrication process of n-type PERC includes more steps and makes a solar cell more expensive. Therefore, newer technologies will be needed efficient process steps and structures.

In this study, we investigated n type-PERC cell formed by double-sided Al2O3 deposition using ALD. Al2O3 films as a passivation layer were grown by ALD at 300℃. After double-sided Al2O3 deposition, UV laser ablation with ns pulse performed to make a electrode contact-patterning. Finally, we evaluated passivation performance as a function of emitter sheet resistance and electrode open ratio. In addition, we have evaluated the passivation characteristics affected by electrode materials such as Cu and Al.

The passivation performance of the Al2O3 layer was compared with the emitter saturation current (J0) and the implied Voc through Quasi-Steady-State Photoconductance (QSSPC). As a result, We have achieved iVoc of 680 mV through the optimization process.

AA1-TuP11 High Quality CaF_2 from a New ALD Process: Enabling New Approaches in Battery Technology and Optical Applications*, **Max Gebhard**, A. Mane, J.W. Elam,* Argonne National Laboratory

Calcium fluoride (CaF_2) is highly transparent over a broad range of the electromagnetic spectrum, covering ultra-violet (UV), visible, and infrared (IR) wavelengths. Its high transparency between 150 nm – 12,000 nm and its extremely low refractive index *n* (~1.43 at λ = 500 nm - 600 nm) makes it a well-known candidate for optical applications. In combination with materials exhibiting a higher refractive index, CaF_2 coatings find application in anti-reflective coatings and band pass filters. Like other fluorides, such as MgF_2 and LaF_3, the ionic bonding situation in CaF_2 enables applications even below 200 nm (*e.g.* photolithography). Recently, metal fluoride materials were also suggested to be incorporated in Lithium-Ion-Batteries, acting either as the solid electrolyte or electrode material.[1]

In both cases, *i.e.* optical applications (such as lenses and three-dimensional structures for optical filters) and coatings in Li-ion batteries, the respective thin film must be of high purity and thickness control is of utmost importance. In consequence, the fabrication of CaF_2*via* ALD is the method of choice. Different ALD processes for CaF_2 have been reported in the past, using $Ca(thd)_2$[2,3] and $Ca(hfac)_2$[4] as metal source and NH_4F,[2] TiF_2,[3] and Hhfac[4] as fluorine precursor.[2] These processes showed best results at temperatures around 300 °C.

Herein, we present a new and straight-forward ALD process for CaF_2 thin films using the $[Ca(amd)_2]_2$–dimer and HF-pyridine as precursor, working at temperatures as low as 175 °C. The process was monitored and optimized employing *in-situ* diagnostics such as FTIR and QCM, and thin films were characterized in terms of their composition (XPS), structure (TEM, XRD, PDF) and optical properties (UVVis, ellipsometry). The process was applied to cathode powers used in Li-ion-batteries and the performance of the respective materials was investigated.

[1] M. Mäntymäki, M. Ritala and M. Leskelä, *Coatings***2018**, 8, 277

[2] M. Ylilammi and T. Ranta-aho, *J. Eletrochem. Soc.* **1994**, 141 (5), 1278

[3] T. Pilvi, K. Arstila, M. Leskelä and M. Ritala, *Chem. Mater.***2007**, 19, 3387

[4] M. Putkonen, A. Szeghalmi, E. Pippel and M. Knez, *J. Mater. Chem.***2011**, 21, 14461

AA1-TuP12 Properties of Molybdenum Oxide Deposited by Plasma Enhanced Atomic Layer Deposition for High Efficiency Solar Cells*, **Taewan Lim**, H.S. Chang,* Chungnam National University, Republic of Korea

Transition Metal Oxides (TMO) are applied as a carrier selective contact layer in silicon hetero junction (SHJ) solar cells. MoO_x has high work function (> 6 eV) and wide band gap (~ 3 eV). It is well known that molybdenum oxide exhibits good optical and electrical properties when deposited on Crystalline Silicon (c-Si). But, MoO_x is sensitive to

temperature, plasma, and air exposure, and for this reason the work function of MoO_x is degraded and its properties are reduced.

In this study, MoO_x is deposited by plasma-enhanced atomic layer deposition (PE-ALD)using Molybdenum hexacarbonyl ($Mo(CO)_6$) is selected as precursor for Mo and O_2 is adopted as precursor for plasma. Argon was used as a carrier gas of $Mo(CO)_6$ and the gas line and canister temperature was maintained to 40˚C and 45˚,respectively. To obtain the best passivation performance, the plasma power was varied between 10W and 500W at PE-ALD process. To investigate the effect of temperature, the sample was annealed at temperature range from 250 ˚C to 500 ˚C.

X-ray photoelectron spectroscopy (XPS) analysis confirmed the chemical state of the MoO_x film. The growth per cycle(GPC) of MoO_x film and MoO_x/c-Si interface was investigated by transmission electron microscopy (TEM). The GPC of MoO_x film deposited by PE-ALD was found to be 0.25 Å. The life time and V_{oc} were measured by quasi steady state photoconductivity (QSSPC).

AA1-TuP13 Understanding and Mitigating F Migration in ALD Nanocomposite Coatings*, **Anil Mane**, M. Gebhard, J.W. Elam,* Argonne National Laboratory*; M. Popecki, T. Cremer,* Incom Inc.*; M. Minot,* incom

We have developed atomic layer deposition (ALD) processes to synthesize metal-dielectric oxide nanocomposite coatings comprised of conducting, metallic nanoparticles (M) embedded in an amorphous dielectric matrix, nominally Alumina (Al_2O_3), and where the metallic component is selected from either tungsten (W) or molybdenum (Mo). The nanocomposite layers are prepared using alternating exposures to trimethyl aluminum (TMA) and H_2O for the Al_2O_3 ALD and alternating metal hexafluoride / disilane (MF_6/Si_2H_6) or metal hexafluoride TMA (MF_6/TMA) exposures for the metal ALD component. By varying the ratio of M:Al_2O_3 ALD cycles and the order of precursor dosing for the two components, we can tune the composition enabling a wide range of mechanical, electrical, and optical properties of these nanocomposites. We have applied these nanocomposites to a variety of applications, but I will focus this presentation on their use as resistive layers for glass capillary array microchannel plates (GCA-MCPs). These ALD nanocomposite coatings contain residual fluorine (F) from the metal hexafluoride precursor in the form of AlF_3. Although we can modulate the F content by adjusting the W nucleation conditions, it is not possible to eliminate the F and this can introduce challenges for device fabrication and integration. For instance, we often deposit ALD magnesium oxide (MgO) following the ALD resistive coating to improve the secondary electron emission (SEE) of the surface. In these cases, we find that residual F can diffuse from the resistive layer into the MgO forming MgF_2 and affecting MCP performance. In this presentation, I will describe several strategies we have developed to minimize F migration. I will conclude by showing the enhanced performance and stability of ALD-GCA-MCPs achieved with this technology.

AA1-TuP14 Ultrathin Metal Oxide Passivation by Atomic Layer Deposition Enhances Stability and Performance of Visible Solar Water Splitting on Solution-Processed Organic Semiconductor Thin Films*, L. Wang, D. Yan,* Stony Brook University*; D. Shaffer,* Brookhaven National Laboratory*; X. Ye,* Stony Brook University*; B. Layne, J. Concepcion, M. Liu, **Chang-Yong Nam**,* Brookhaven National Laboratory

Solution-processable organic semiconductors have potentials for visible photoelectrochemical (PEC) solar water splitting because of their tunable small band gaps and electronic energy levels. However, the poor stability and photocatalytic activity of organic semiconductors have been posing persistent challenges. Here, we demonstrate that the application of ultrathin metal oxide passivation by low-temperature atomic layer deposition (ALD) enables the direct, visible PEC water oxidation on solution-processed organic semiconductor thin films with enhanced stability and performance. N-type fullerene-derivative thin films passivated by sub-2 nm ALD ZnO allowed the visible PEC water oxidation at wavelengths longer than 600 nm in harsh alkaline electrolyte environments with up to 30 μA/cm^2 photocurrents at the thermodynamic water-oxidation equilibrium potential, which is accompanied by the photoanode half-lifetime extended to ⍰1000 s. The investigation shows that the enhanced water oxidation catalytic activity is afforded by the ALD ZnO passivation, and the hole transfer through the passivation layer governs the charge collection process. Further improved PEC water splitting performances were realized by improving the bottom ohmic contact to the organic semiconductor, again via the ZnO interlayer implemented by ALD, ultimately achieving ⍰60 μA/cm^2 water oxidation photocurrent at the equilibrium potential, the highest value reported for organic semiconductor thin films to our knowledge. The results not only highlight the significant utility of ALD on improving the stability and performance of organic-semiconductor-based solar water splitting but also provide important design guidelines for optimal ultrathin passivation on organic semiconductor photoelectrodes.

AA1-TuP15 Enhancement of Photovoltaic Efficiency using a Novel Nickel-4 Mercaptophenol Hybrid Interfacial Layer*, **Jinseon Park**, N.V. Long, H. Thu,* Hanyang University, Republic of Korea

In this work, we introduced a novel Ni-4 mercaptophenol (Ni4MP) as an interfacial layer in Sb_2S_3-sensitized mesoporous TiO_2 solar cells. Ni4MP thin films with controllable thickness were prepared by an integrated approach via atomic/molecular layer deposition techniques and were systematically characterized. Introduction of the Ni4MP interlayer significantly enhanced the photovoltaic performance and the interfacial charge transfer kinetics of Sb_2S_3-sensitized solar cells. The augmentation of open circuit voltage and short circuit density due to the insertion of a Ni4MP interlayer enhanced the power conversion efficiency of the solar cells from 2.07% to 2.79%, corresponding to a 35% increase in efficiency. This improvement in device performance was discussed based on the energy band diagram. We found that the Ni4MP interlayer can effectively extract the photo-generated holes from the Sb_2S_3 sensitizer due to the excellent band matching and hole scavenging characteristics, thus enhancing the charge transport and suppressing the recombination.

AA1-TuP16 Enhancement of Photovoltaic Properties of Metal/III-V Schottky Solar Cells using Al2O3 Anti-Reflection and Passivation Layer*, A. Ghods, V. Saravade, C. Zhou, **Ian Ferguson**,* Missouri University of Science and Technology

The metal-semiconductor (M-S) Schottky junction structure is gaining traction in photovoltaic device applications compared to *p-n* junction structure, due to simplicity in device processing, possibility of development of high efficiency multi-junction structures, and also cost-effective large-scale device fabrication[1]. III-V compound semiconductors with direct bandgap and short absorption depth are suitable candidates for fabrication of high efficiency solar cells. Schottky solar cells based on Au/$Al_{0.3}Ga_{0.7}As$/GaAs heterostructure have been designed and fabricated, resulting into short-circuit current density and power conversion efficiency of 20.46 mA/cm^2 and 4.84%, accordingly[2].

One of the main issues regarding the M-S structures for solar cells remains about the high reflectivity from the top metal surface. This leads to significant reduction in photon absorption in the active layer of solar cell and, therefore, lowered photo-generated current. Graphene and indium-tin-oxide (ITO), with transmission of more than 80% in the visible region, have been used in conjunction with *n*-GaAs to create Schottky solar cells, leading to short circuit current density and power conversion efficiency of up to 19 mA/cm^2 and 11.1%, respectively[3,4].

Anti-reflection coating (ARC), such as aluminum oxide (Al_2O_3), has been used to reduce the reflection from top surface of M-S Schottky solar cells, and enhance the photovoltaic properties of these devices. In this work, an 80 nm Al_2O_3 has been grown on the whole top surface of the Ag/*n*-GaAs Schottky solar cell using atomic layer deposition (ALD) technique at 200˚C, Figure 1 (attachment). The initial optical measurements show the reduction of reflection from the solar cells from 48% (without ARC) to 16% (with ARC), indicating the improvement in photon absorption, Figure 2. *J-V* and EQE measurements will be performed to extract the photovoltaic properties of these devices and investigate the effect of ARC on M-S structure.

Moreover, the effect of Al_2O_3 as passivation layer will be studied in the full paper. Initial measurements have indicated a decrease in leakage current between the metal contacts, leading to enhancement of shunt resistance from 3×10^4 W to 1×10^5 W. This will be further investigated, and changes in photovoltaic properties of the solar cells, including filling factor, reverse saturation current, and power conversion efficiency, will be reported.

[1] X. J. Jun et al., *Chin. Phys. Lett.*, **26**, 098102 (2009).

[2] Y. D. Shen and G. H. Pearson, *Sol. Ener. Mater.*, **2**, 31 (1979).

[3] L. Wen et al., *J. Mater. Chem. A*, **6**, 17361 (2018).

[4] H. S. Kim et al., *Thin Solid Films*, **604**, 81 (2016).

AA1-TuP17 Investigation of ALD-grown i-ZnO Buffer Layer Properties for CIGS Solar Cell Application*, **Jeha Kim**, V. Arepalii,* Cheongju University, Republic of Korea*; W.-J. Lee, Y.-D. Chung,* Electronics and Telecommunications Research Institute, Republic of Korea

Zinc oxide (ZnO) is a wide bandgap (3.4 eV) n-type semiconductor material that can be mostly used in various optoelectronic applications from thin

film transistors (TFTs) to solar cells due to its excellent optical and electrical properties [1]. In the CIGS solar cell device structure, the i-ZnO thin film acts as a buffer layer that reduces the leakage of shunt current paths and also it improves p-n hetero-junction quality. In the present study, we deposited the i-ZnO thin films from 80°C to 180°C onto both Si (100) and soda lime glass (SLG) by using atomic layer deposition (ALD) method. The as-grown films were characterized by scanning electron microscopy (SEM), energy dispersive spectroscopy (EDS), X-ray diffraction, UV-Vis-NIR spectroscopy, and Hall effect measurements. The thickness of as-grown ZnO films is independent of the growth temperatures from 100°C to 180°C. All samples exhibit the optimal bandgap of 3.24 eV. The ZnO buffers show the electrical resistivity of 6 Ω×cm, 0.29 Ω×cm, and 0.0058 Ω×cm for the films-grown at 80°C, 100°C, and 150°C, respectively. In addition, we investigated the J-V characteristics of the fabricated CIGS solar cells using ALD-grown i-ZnO buffers prepared at 80°C, 100°C, and 150°C. The solar cell fabricated with i-ZnO buffer grown at 100°C exhibits the best power conversion efficiency (η) of 8.59% with V_{oc} of 470 mV, J_{sc} of 28.84 mA/cm^2, and *FF* of 63.48%.

References: [1] T. Tynell and M. Karppinen, Atomic layer deposition of ZnO: a review, Semicond. Sci. Technol. 29 (2014) 043001.

Acknowledgment:

This research was supported by the Technology Development Program to Solve Climate Changes of the National Research Foundation (NRF) funded by the Ministry of Science, ICT & Future Planning (NRF-2017M1A2A2087577) and (NRF-2016M1A2A2936759), also, this research was financially supported by the Ministry of Trade, Industry and Energy (MOTIE) and Korea Institute for Advancement of Technology (KIAT) through the National Innovation Cluster R&D program (P0006704).

AA1-TuP18 Atomic Layer Deposited Zirconium-doped ZnO Transparent Conductive Oxides for Silicon Solar Cells*, **Geedhika Kallidil Poduval**, M.A. Hossain, B. Hoex,* University of New South Wales, Australia

Transparent conductive oxides (TCOs) are intensively investigated due to their ability to conduct charge carriers and transparency in the visible light in various fields ranging from large scale displays to photovoltaic devices. Currently, the most widely used TCO is indium tin oxide (ITO) which simultaneously offers high optical transparency and high electrical conductivity. Limited reserves, increasing indium prices, and free carrier absorption due to relative high carrier concentration have been the motivation to explore other TCO materials. Some of the alternatives to ITO are, doped ZnO, SnO_2, Cu_2O, and TiO_2.

Among the various kinds of silicon solar cell architectures, heterojunction (HET) silicon solar cells consisting of crystalline silicon absorber and amorphous silicon (a-Si) surface passivation and doped a-Si as the electron and hole selective layers implement TCOs to improve the lateral conductivity of collected carriers. As a-Si degrades at temperatures >200°C and sputtering of ITO damages the interface, leading to increased absorption and recombination, a surface sensitive low-temperature self-limiting process such as atomic layer deposition is very appealing.

In this work, Zr is used as a dopant to increase the mobility and reduce parasitic absorption of earth-abundant ZnO. The recipe for ZrO_2 growth using Tetrakis(dimethylamido) zirconium(IV) (TDMAZ) was developed and optimized on a Fiji G2 plasma enhanced ALD tool. The growth properties were studied by *in-situ* spectroscopic ellipsometry. The effects of doping (0-29 at.% Zr) were investigated for 40 nm thick films. ZnO and ZrO_2 supercycles at different ratios were carried out, and their influence on optical and electrical properties was investigated. A slight increase in mobility of ~5% up to 19 cm^{2}V^{-1}s^{-1} was observed by doping ZnO with 2.4% Zr, and the mobility reduces with increased doping. The optical band gap of ZnO increases with doping level up to a value of 3.42 eV at 10% Zr and reduces for higher Zr concentrations. First-principles density functional theory (DFT) calculations reveal the formation of defects states in the conduction band resulting from the substitutional replacement of Zn by Zr. XPS results indicate that the Zr ions in ZnO are in the Zr^{+4} oxidation state thereby contributing two additional electrons to the lattice. This results in an increase in carrier concentration from 2x10^{19} cm^{-3} to 1.2x10^{20} cm^{-3}. Elemental depth profiling using Tof-SIMS is currently ongoing and will be shown at the time of the conference. The improvement in TCO properties of ZnO upon doping with Zr opens the possibility for applications in silicon solar cells as well as thin film solar cells.

AA1-TuP19 Atomic Layer Deposition of Few-Atom Cluster Arrays for Solar Fuel Catalysis*, **David Mandia**, N. Guisinger, A. Martinson,* Argonne National Laboratory

Solar fuels catalysis is vital to developing new technologies for creating value-added products from alternative feedstocks, such as carbon dioxide and water. Inhomogeneities in typical "state-of-the-art" synthesis techniques for heterogeneous catalysts severely limit the accuracy of determining the chemical composition of active sites and elucidating mechanistic details for catalysis. In the present work, we synthesize discrete, few-atom metal oxide cluster arrays to gain insight into the relationship between cluster size/shape and catalytic activity/efficiency. Clusters are synthesized with exquisite synthetic control via atomic layer deposition (ALD) on chemically modified epitaxial graphene (EG) on SiC. Metal oxide/nitride/sulfide ALD thin film growth is strongly inhibited on graphene. Understanding the factors contributing to unintentional and intentional nucleation and growth on EG will benefit from the use of an accurate, precise imaging technique such as STM. Furthermore, we employ an *in-situ* plasma treatment (H_2, N_2, O_2) of EG to create attachment points for intentional cluster nucleation via ALD. Discrete, few-atom clusters will be synthesized and cluster size, morphology, distribution, and density of states will be determined via STM/XPS/AFM/Raman mapping. We will correlate these parameters to catalytic activity and efficiency for solar fuels catalysis.

ALD Applications
Evergreen Ballroom & Foyer - Session AA2-TuP
Microelectronics Poster Session

AA2-TuP1 Chemically and Mechanically Activated Carbonaceous Materials for Supercapacitor*, D.V. Lam, J.-H. Kim, **Seung-Mo Lee**,* Korea Institute of Machinery and Materials, South Korea

Carbothermic reduction in the chemistry of metal extraction (MO(s) + C(s) → M(s) + CO(g)) using carbon as a sacrificial agent has been used to smelt metals from diverse oxide ores since ancient times. Here, we paid attention to a new aspect of the carbothermic reduction remained unnoticed till now to prepare activated carbon textile for high rate-performance supercapacitors. On the basis of thermodynamic reducibility of metal oxides reported by Ellingham, we employed not carbon, but metal oxide as a sacrificial agent in order to prepare activated carbon textile. We conformally coated ZnO on bare cotton textile using atomic layer deposition (ALD), followed by pyrolysis at high temperature (C(s) + ZnO(s) → C'(s) + Zn(g) + CO(g)). We figured out that it leads to concurrent carbonization and activation in a chemical as well as mechanical way. Particularly, the combined effects of mechanical buckling and fracture occurred between ZnO and cotton were turned out to play an important role in carbonizing and activating cotton textile, thereby significantly increasing surface area (nearly 10 times) compared with the cotton textile prepared without ZnO. The carbon textiles prepared by carbothermic reduction showed impressive combination properties of high power and energy densities (over 20 times increase) together with high cyclic stability.

~~**AA2-TuP2 Diamond Field Effect Transistors with Different Gate Lengths of HfO_2 Deposited by Atomic Layer Deposition***, **Changzhi Gu**,* Institute of Physics, Chinese Academy of Sciences, China~~

~~The single crystal diamond was treated in hydrogen plasma formed by microwave plasma chemical vapor deposition equipment, and the normally off hydrogen terminal diamond field effect transistors with different gate lengths were prepared by atomic layer deposition of HfO_2 as gate oxide. We studied the effect of hydrogen treatment time and HfO_2 gate oxide on hydrogen terminal diamond field effect transistor. The experimental results showed that the HfO_2 gate oxide was suitable to fabricate hydrogen terminal diamond field effect transistor and exhibited a normally off characteristic, which is advantageous for the fabrication of power devices. Furthermore, with increasing the gate length, the drive current density, threshold voltage and transconductance of the diamond device decreased.~~

AA2-TuP3 Atomic Layer Deposition of IGZO Thin Films for BEOL Applications*, **Shóna Doyle**,* Tyndall National Institute, Ireland

In the drive for scaling of electronic devices one approach has been the integration of functionality into the back end of line (BEOL). Thin film transitors (TFT) are one such component with high quality devices being realised by PVD indium-gallium-zinc oxide (IGZO). However, the limitations of the PVD deposition process in terms of reliability and coverage in

complex 3D topologies is of concern, where uniform sub nanometre films that demonstrate high mobility are required.

Here we have used atomic layer deposition (ALD) to deposit both nano-crystalline/amorphous ZnO and IGZO based laminate structures to generate high mobility thin film materials with sub-nm thickness control. Materials were grown using both thermal and plasma processes on a 200 mm Picosun R200 ALD system. Characterisation, in terms of morphology and composition, were achieved through electron microscopy, x-ray diffraction and x-ray photoelectron spectroscopy. Electrical properties were assessed via 4-point probe and both AC and DC Hall measurements.

AA2-TuP5 High Voltage MIM Capacitor based on ALD Deposited Crystalline $HfAlO_x$ Film*, **Valentina Korchnoy**,* Technion - Israel Institute of Technology, Israel*; M. Lisiansky,* Tower Semiconductor Ltd., Israel*; I. Popov, V. Uvarov,* The Hebrew University of Jerusalem, Israel*; B. Meyler,* Technion - Israel Institute of Technology, Israel

MIM capacitor was developed herein with ALD-fabricated $HfAlO_x$ dielectric layer. MIM capacitor is a key building element in modern CMOS platforms. It may occupy a significant part of the chip area. The high-k dielectric materials were introduced in the advanced production to minimize the footprint area of MIM: HfO_2-based materials grown by ALD replaced conventional dielectrics SiO_2 and Si_3N_4. To prevent the uncontrolled crystallization of amorphous HfO_2 film in a monoclinic phase that degrades its electrical parameters, some dopants (i.e. alumina) are introduced in deposited HfO_2 layer: the composite HfO_2/Al_2O_3 remains amorphous at deposition and during BEOL annealing processes.[1] Thus, amorphous materials are usually used in MIM capacitors located in BEOL. Hafnia doping enhances the composite crystallization (T≥600˚C) into metastable phases of higher symmetry having significantly higher k-value (30-40).[2] Crystalline HfAlOx dielectric has been employed in low voltage capacitors used in DRAM. Some CMOS applications (RF, CIS) require HV MIM capacitor (operating voltage 2.5-3.3V) located as DRAM in IMD0, to benefit from the attractive properties exhibited by crystalline HfAlOx. The increased operational voltage of HV MIM entails thicker dielectric layers compared to those used in DRAM. To take advantage of crystallinity of the HfAlOx film, engineering of the film growth and its crystallization parameters should be optimized for the required film thickness of the HV MIM capacitor. The developed capacitor with EOT≤2nm shows excellent dielectric integrity (V_{BVD}≥8V) along with the low leakage current.

Table 1 presents the plan of experiment where HfO_2-Al_2O_3 laminated stack (12:1) was deposited by ALD in the same run on two types of substrates: Si/SiO2/TiN(70nm) – structure A (MIM) and p-Si/thermal SiO_2(6.4nm) – structure B (MOS). The stack thickness is 14nm. Both pre-deposition (PreDA) and post-deposition (PDA) annealing were performed at the same conditions (T>600˚C). The RTA processing of structure A samples (MIM) was applied in three different flows to distinguish between the effects produced by RTA on the TiN bottom electrode and on the $HfAlO_x$ dielectric layer. Fig.1 shows the scheme of MIM capacitor. The results of electrical characterization are presented in Fig.2 and Table 2. The difference in electrical parameters of MIM capacitors were compared with the detailed structural study of samples 1, 2 and 3 performed by XRD (Fig.3) and TEM/STEM (Fig.5) techniques. Surface characteristics of the TiN electrode was shown in Fig.4. PreDA process allows to prevent the void formation at the TiN/HfAlOx interface and to improve electrical integrity of sample 2.

AA2-TuP6 Improved Performance of GaN Metal-Oxide-Semiconductor Capacitors byPplasma ALD of AlN Interlayer*, **Dilini Hemakumara**, X. Li, K. Floros, S. Cho,* University of Glasgow, UK*; I. Guinney, C. Humphreys,* University of Cambridge, UK*; I. Thayne,* University of Glasgow, UK*; A. O'Mahony,* Oxford Instruments Plasma Technology*; H. Knoops,* Oxford Instruments Plasma Technology, UK*; D. Moran,* University of Glasgow, UK

High quality metal-oxide-semiconductor (MOS) gate stacks with stable threshold voltage are required for future GaN-based power transistors [1]. Here, we report a route to the realization of GaN MOS-capacitors (MOSCAPs) with an ALD AlN interlayer between GaN and Al_2O_3 using a FlexAL ALD system. AlN was grown using plasma enhanced ALD at 300^0C using TMA and N_2 and H_2 plasma. The GaN samples were first exposed to an N_2 150W 5min plasma pre-treatment followed by in-situ ALD of approximately 2nm of AlN. A 20nm Al_2O_3 was then deposited in-situ using thermal ALD at 200^0C using TMA and H_2O. The results from these samples were then compared with MOSCAPs that had only an N_2 150W 5min plasma pre-treatment followed by a 20nm thermal ALD Al_2O_3 layer.

20nm Pt/ 200nm Au contacts were deposited ex-situ as the gate contact and the MOSCAPs were measured at room temperature using capacitance-voltage (C-V) and current-voltage (I-V) measurements. The C-V measurements were used to calculate the hysteresis and frequency dispersion of these samples. The hysteresis included the flat band voltage difference between the forward and backward sweep of the C-V curve when swept from -5 to +5V and back to -5V at 1MHz. The frequency dispersion gives the maximum difference in the flat band voltage for C-V curves measured at various frequencies ranging from 1MHz to 1kHz (1MHz, 500kHz, 100kHz, 10kHz and 1kHz).A flat band voltage hysteresis and a frequency dispersion of 200mV was observed for samples that only had an Al_2O_3 gate dielectric while the insertion of an AlN interlayer resulted in a hysteresis and a dispersion of 50mV.

The I-V measurements produced a leakage of 0.016mA/cm^2 at 1V for the sample with only Al_2O_3 while the one with the interlayer produced a leakage of 0.0096 mA/cm^2 at 1V. These positive improvements with the insertion of an AlN interlayer could result due to the prevention of GaO_x sub-oxide formation at the GaN-Al_2O_3 interface [2].

In summary, the insertion of a PE-ALD AlN interlayer between an N_2 plasma treated GaN surface and ALD Al_2O_3 gate dielectric reduces the C-V hysteresis and frequency dispersion by 75% and decreases the leakage current by 40%. Both of these are encouraging for the realisation of high performance GaN power transistors.

1. Fiorenza, P., et al, "Slow and fast traps in metal-oxide-semiconductor capacitors fabricated on recessed AlGaN/GaN heterostructures" . *Appl. Phys. Lett.***106,** 1–5 (2015).

2. Liu, S. *et al.*, "Interface/border trap characterization of Al2O3/AlN/GaN metal-oxide-semiconductor structures with an AlN interfacial layer.", *Appl. Phys. Lett.***106,** 2–6 (2015).

~~**AA2-TuP7 2-Dimensional Perovskite Oxide Thin Films Deposited by ALD for High-k Application***, **Seung-Won Lee**,* Korea Maritime and Ocean University, Republic of Korea*; C.-M. Kim, S.-H. Kwon,* Pusan National University, Republic of Korea~~

~~As the size of the DRAM is scaled down, the new high-k dielectric materials have received considerable attention. Among high-k materials, the dielectrics based on Zr and Hf have extensively been used in semiconductor industry. However, there is a limitation to obtaining an equivalent oxide thickness of under 0.5nm. Therefore, to replace the high-k material based on Zr- or Hf-, new high-k materials, such as rutile-TiO_2 and perovskite oxide, have attracted a candidate in next generation DRAM devices. Meanwhile, 2-D perovskite oxide films made by Langmuir-Blodgett method were reported that the permittivity was measured over 200.[1] However, Langmuir-Blodgett method can't be applied to electronic applications, especially on the substrate with a high aspect ratio.~~

~~Therefore, in this paper, $Sr_xNb_yO_z$ (SNO) thin films with 2-D perovskite structure were deposited on TiN and $SrRuO_3$ substrate using atomic layer deposition (ALD). Then, rapid thermal annealing and laser annealing were performed for crystallization of thin films. Finally, we analyzed physical and electrical properties by RBS, TEM, XRD and semiconductor parameter analyzer.~~

AA2-TuP8 High Performance Atomic Layer Deposition (ALD) of Gate Dielectrics for 4H-SiC Power Device Application*, B. Lee, M. Kang,* North Carolina State University*; **Adam Bertuch**,* Veeco-CNT*; V. Misra,* North Carolina State University

Silicon carbide is one of most promising substrates for the power Metal Oxide Semiconductor Field Effect Transistor (MOSFET) and other power electronic devices. Due to high density of interface states (D_{it}) at SiO2/SiC interface, the mobility of Si-face (0001) 4H-SiC MOSFETs remains extremely low. Incorporations of nitrogen and phosphorous into the thermal oxide through a high temperature anneal are proven to be effective to suppress the D_{it}. Although the presence of nitrogen or phosphorous improves the mobility, achieved mobility values remain low when compared to the bulk SiC mobility. Additionally, nitrogen and phosphorous incorporations lead to negative threshold voltage (V_T) shift and makes even normally on devices. A positive enough threshold voltage is necessary for safe and reliable operation of power devices. Therefore, to deal with this trade-off between mobility and threshold voltage, deposited dielectrics on 4H-SiC have attracted more research interest to replace the thermal oxide. With deposited gate dielectrics, the substrate consumption is minimized and thus the carbon related defects associated with thermal oxidation can be avoided. Using deposited dielectrics also enables interface engineering to control interface properties independently. Among various deposition method, the atomic layer deposition (ALD) technique has proven to provide good film quality, low substrate damage, precise thickness control, and low temperature processing. This work first evaluates device electrical

characteristics and reliability of SiO_2grown by either thermal or plasma ALD. $SiO_2$is the most suitable dielectric due to its large bandgap as well as a high conduction band offset to SiC resulting in suppression of electron tunneling current in SiC MOS devices. It was found that the channel mobility is similar between thermal and plasma ALD SiO_2but thermal ALD oxide shows lower threshold voltage compared to the plasma ALD oxide. Although ALD SiO_2provides positive threshold voltage and good gate insulating property, the SiC/SiO_2interface requires further treatment to enhance the mobility. We have recently demonstrated a novel interface engineering technique to improve the MOSFET mobility by combining ultrathin lanthanum oxide (LaO) at the SiC/dielectric interface and ALD SiO_2. In this study, we deposited ultrathin 1nm LaO followed by 30nm SiO_2using ALD tool without breaking the vacuum. It was found that the channel mobility is enhanced with the incorporation of 1nm LaO between SiC and SiO_2as compared to the device without LaO layer. This combination of ultrathin LaO and SiO_2provides an effective solution to challenges of SiC MOSFETs for power applications.

~~AA2-TuP9 Atomic Layer Deposted TiO_2-Based Memristors using In-situ Fabricated Al-Doped ZnO Thin Film as Electrodes~~*~~, Kai Zhang,~~ P. Lin,* ~~Old Dominion University; A. Pradhan,~~ Advance Material Solution LLC~~; H. Baumgart,~~ Old Dominion University

~~Memristor is a nonlinear and two-terminal passive device, which has ability to change the resistance between high resistive states and low resistive states by applying bias voltage. This property called resistive switching makes the memristors suitable for a wide range of applications in nonvolatile random access memory, dynamic random access memory and flash memory. In recent years, Metal-oxide-based memory devices have drawn significant attention due to their high density integration, high endurance, fast switching behavior, low power consumption and simple structure. In addition, among the promising binary transition metal oxide materials, such as nickel oxide, zirconium oxide, zinc oxide, hafnium oxide, and titanium oxide, TiO_2 films are extensively used to fabricate the nonvolatile memristor devices due to its simple structure and compatible with CMOS integration process. Recently, ZnO has been widely used for various applications due to its good electrical conductivity, wide band gape (3.37 eV), high exciton binding energy (~60 meV), low cost, nontoxicity, high mechanical and thermal stability. When doped with Aluminum ZnO grown via atomic layer deposition (ALD) has been reported to show resistivity values ranging from insulating to on the order of 10^{-3} Ω·cm, which is suitable for memory device electrodes.~~

~~Currently, the most common methods used were magnetron sputtering, pulsed laser deposition, thermal oxidation, electrodeposition, chemical vapor deposition, sol-gel chemical reaction, and atomic layer deposition. The ALD is a self-limiting technique that allows atomic layer growth each time. ALD can precisely control the film layer thickness, stoichiometry, composition, uniformity, and sharp interface. ALD also shows perfect conformal coverage when it deposits thin film on complex surface structures. Therefore, ALD is considered as a novel and competitive method to deposit MIM memory structures. To create such devices, transparent Al:ZnO film was grown on Si wafers as an transparent electrode followed by an active layer of TiO_2 film, then the other layer of Al:ZnO was deposited *in-situ* on the TiO_2 layer to form memristor structures. All the thin films in the structures were synthesized by the ALD system sequentially.~~

~~Several physical characterization techniques have been employed to determine the ALD films of memory devices. The crystal structure was analyzed by X-ray diffraction. The film morphology was determined by field emission scanning electron microscopy. The surface roughness was analyzed by atomic force microscopy. The electric properties were measured by semiconductor analyzer. The results demonstrate a fairly good memristive device.~~

AA2-TuP10 Homogeneously Doped Atomic Layer Deposition Zinc Tin Oxide Thin Films for Improving Contact Resistance in Semiconductor Device Applications*, **Alex Ma,*** University of Alberta, Canada*; T. Muneshwar,* Synthergy Inc., Canada*; D. Barlage, K. Cadien,* University of Alberta, Canada

For thin film semiconductor device applications, the formation of high quality contacts is critical. Currently, it is difficult to realize ohmic contacts on zinc oxide (ZnO) thin films especially for applications that require more resistive active layers e.g. thin film transistors (TFTs) and Schottky diodes. In this work, we investigate the contact resistance in thin film devices that employ ZnO active layers grown by low temperature plasma-enhanced atomic layer deposition (ALD) with the gated transmission length method (TLM). The contact performance in intrinsic ZnO devices are compared to identical devices but with a homogeneously doped ALD zinc tin oxide (ZTO) interlayer inserted between the semiconductor body and metal contact. By incorporating a small percentage of tin (Sn) in the ZnO during ALD growth, we observed an increase in the film's electron concentration resulting in lowered contact resistance.

~~AA2-TuP11 AlGaN/GaN Layers Obtained by Atomic Layer Deposition Targeting Thin Film HEMT~~*~~, Joaquin Alvarado, M. Chávez,~~* ~~Benemérita Universidad Autónoma de Puebla, Mexico; S. Gallardo,~~ ~~CINVESTAV-IPN, Mexico; Y. Sheng, D. Muenstermann,~~ ~~Lancaster University, UK~~

~~$Al_xGa_{1-x}N$ and GaN films were obtained using Plasma enhanced Atomic Layer Deposition (PE-ALD) at 300 °C, we study the effect of Al content variation on the optical and structural and electrical performance. XRD measurements show the hexagonal structure, SIMS profile signals reveals the main components of $Al_xGa_{1-x}N$.~~

~~Experimental~~

~~AlGaN thin films were deposited on silicon wafers via atomic layer deposition using a mega cycle which consists of sub cycles of AlN and GaN to obtain the $Al_xGa_{1-x}N$ alloy. The AlN sub cycle consist of (1) pulse of Trimethyl Alluminium (TMA), (2) Ar purge, (3) H_2/N_2 plasma and (4) Ar purge, the growth ratio is (0.5Å/cycle) at 300°C, the total number of megacycles were 215. GaN sub cycles consist of (1) pulse of Trimethyl Galliu (TMGa), (2) Ar purge, (3) H_2/N_2 plasma and (4) Ar purge, the growth ratio is (0.2Å/cycle) at 300 °C, the total number of megacycles were 131. The number of megacycles were calculated in order to obtain ~20 nm.~~

~~Results~~

~~The XRD patterns of $Al_xGa_{1-x}N$ on silicon substrates growth with 0.3 and 0.6 Al content were performed. Two peaks were observed in the sample $Al_{0.3}Ga_{0.7}N$ the peak located at 2θ=34.5° (002) is assigned to hexagonal phase of GaN and a second peak at 2θ=32.3° (100) correspond to the hexagonal phase of AlN. The sample $Al_{0.6}Ga_{0.4}N$ show peaks at 2θ=32.3° , 34.3° ,37.0° assigned (100), (002), (100) AlN. Furthermore, from photoluminescence characterizations it is possible to observe in the $Al_{0.3}Ga_{0.7}N$ sample a yellow luminescence band situated at 2.32 eV, which is related to Gallium and N vacancies, carbon defects, as well as to the high concentrations carriers 10^{19} cm^{-3} [1]. The peak observed at 2.2 eV is associated to dislocations defects [2]. However, a sample which contains higher content of Al didn't show PL signal.~~

~~On the other hand, by SIMS sputtering time profile it is possible to observed that the sample with $Al_{0.3}Ga_{0.7}N$ show a non-uniform Al content, although $Al_{0.6}Ga_{0.4}N$ show a better Al distribution film. Electrical characterizations of the deposited films will be also included.~~

AA2-TuP12 High-Temperature Thermal Stability of ALD-TiN Metal Gate on *In-situ* Al_2O_3/Y_2O_3/(In)GaAs(001): Toward the Self-Aligned Gate-First Process*, **Lawrence Boyu Young**, H.-W. Wan, J.-H. Huang, K.-Y. Lin, J. Liu, Y.-H. Lin,* National Taiwan University, Republic of China*; J. Kwo,* National Tsing Hua University, Republic of China*; M. Hong,* National Taiwan University, Republic of China

High-k metal gate (HKMG) technology has been introduced since the 45-nm node complementary metal oxide semiconductor (CMOS). The gate-first process was replaced by the gate-last process because of the threshold voltage pinning caused by the subsequent high-temperature process[1]. The gate-first process provides a capability to reduce the process complexity, and is more economic than the gate-last process. To realize high-performance MOS field-effect transistors (MOSFETs) using self-aligned gate-first process, the thermal stability of MOS structure must be excellent to sustain the subsequent high temperature process. With the higher electron mobility, GaAs-based III-V semiconductors have potential to replace the current Si-based CMOS technologies. However, the reported thermal stability between high-k/III-V was limited to 500~600°C caused by the inter-diffusion. In our previous study, ultra-high thermal stability above 850°C between in-situ grown oxide/III-V interface was attained[2,3], critical for the present study of atomic layer deposition (ALD)-TiN/oxide/(In)GaAs thermal stability at temperatures ranging from 850 to 950°C. Here, we have studied the samples with different post-metallization annealing (PMA) using transmission electron microscopy (TEM), J-E, and C-V characteristics of the MOS capacitors (MOSCAPs). The samples were prepared in a ultra-high vacuum (UHV) multi-chamber growth/analysis system (Fig. 1). The detailed fabrication process and the schematic structure of the MOSCAPs are shown in Fig. 2 . The TEM shows the smoothness in an atomic scale of the ALD-TiN/high-k/(In)GaAs interfaces. The interface remained intact without degradation after 800°C 5s in He ambient (Fig. 3). From the J-E

curves (Fig. 4), the leakage current densities of the MOSCAP with different PMA in N_2 show no degradation after 900°C annealing for 10s. The leakage current density of the MOSCAPs maintained below 10^{-7} A/cm^2 at electric fields of ± 4 MV/cm, which is the same with that of the MOSCAP without PMA. A different behavior was found in the MOSCAP with PMA in He. The leakage current density raised sharply in the negative bias region, probably resulted from the generation of nitrogen vacancies during the high temperature annealing in He. Similar features were found in the C-V characteristics (Fig. 5). With the PMA in N_2, the C-Vs showed no degradation after 900-950°C annealing, while the MOSCAP was too leaky to measure the C-Vs for the MOSCAP with PMA in He with temperatures above 900°C. The excellent electrical and thermal stability of the MOS structures with TiN gate are vital to realize high performance GaAs inversion channel MOSFETs using a gate-first process.

AA2-TuP13 Identification of Interfacial Defect in ALD Grown Al_2O_3/GeO_x/Ge Gate Stack*, **Jinjuan Xiang**, L. Zhou, X. Wang, X. Ma, T. Li, W. Wang,* Institute of Microelectronics of Chinese Academy of Sciences, China

Germanium (Ge) has attracted tremendous interest as a channel material for high performance complementary metal-oxide-semiconductor (CMOS) devices. The interfacial cfixed charges are detrimental to the performance promotion of Ge MOSFET devices as they can form Coulomb scattering center to reduce channel carrier mobility and device reliability. Thus we experimentally investigate the interfacial defect in the GeO_x/Al_2O_3 gate stack grwon by ALD using X-ray photoelectron spectroscope (XPS) and electrical charateristics by capacitance-voltage (*C-V*) measurement. For GeO_x interlayer by ozone oxidation, oxygen vacancies exist and show positive charges at the Ge/GeO interface. The O_2 annealing is helpful to decrease the oxygen vacancy defect. For the GeO_x/Al_2O_3 interface, oxygen dangling bonds exist, and show negative charges. This work can be effectively applied to engineer the interface promotion and enhance the performance of Ge-based devices.

AA2-TuP15 Effect of Metal-insulator Interface on Dielectric Properties of Ultrathin Al_2O_3 and MgO Fabricated using *In-situ* Sputtering and Atomic Layer Deposition*, **Jagaran Acharya**, J. Wilt, R. Goul, B. Liu, J. Wu,* The University of Kansas

We have investigated the properties of ultrathin $Al_2O_3$and MgO in metal-insulator-metal (M-I-M) trilayers fabricated using *in situ* integrated sputtering and atomic layer deposition (ALD). The quality of ultrathin Al_2O_3 was found to be significantly dependent on the pre-ALD conditions which lead to extremely different M-I interface. After optimization of ALD processing parameters, M-I interfacial layer (IL) was reduced to a negligible level obtaining a dielectric constant (ε_r) up to 8.9 on the Al_2O_3films in a thickness range between 3.3-4.4 nm, corresponding to an effective oxide thickness (EOT)~1.4-1.9 nm respectively comparable to high-K dielectrics. While ε_r decreases at a smaller Al_2O_3 thickness, the hard-type dielectric breakdown 32 MV/cm and in situ scanning tunneling spectroscopy (STS) revealed band gap ~2.63 eV confirming high quality dielectric as good as an epitaxial Al_2O_3 film. This result suggests that the IL is unlikely a dominant reason for the reduced ε_r at the Al_2O_3 thickness of 1.1-2.2 nm and is due to electron tunneling as supported by transport current-voltage measurement. However, non-optimal conditions result in the growth of significant IL with drastically reduced ε_r~0.5-3.3. The properties of MgO with and without 5C-ALD Al_2O_3 studied in the thickness range 2.5-5 nm point out significance of seed layer in fabrication of high-quality dielectrics, approaching ε_r~9 for 5C-ALD-Al_2O_3/ALD-MgO at thickness 3.8-4.9 nm corresponding to EOT~1.6-2.1 nm respectively. But, 40C-ALD MgO without seed layer has unexpectedly lower ε_r~3-4 possibly due to poor nucleation forming an interfacial layer, and correspondingly increase in the leakage current. The similar decreasing trend in ε_r with decrease in MgO thickness is observed but at thickness greater than that of Al_2O_3, due to higher leakage current observed for MgO dielectrics and also confirmed by in situ STS analysis. Our results demonstrate the significance of controlling the nucleation in ALD to achieve better M-I interface in order to fulfill the demand for leak-free and defect-free high-quality ultrathin dielectrics an alternative for low-cost gate dielectric for CMOS, and tunnel junction for quantum computing and memory applications.

AA2-TuP16 Thermal and Plasma ALD Al_2O_3 Gate Insulator for GaN Electronic Devices Characterized by CV-Stress Measurements*, **Nicole Bickel**, E. Bahat Treidel, I. Ostermay, O. Hilt, O. Krüger,* Ferdinand-Braun-Institut, Germany*; F. Naumann, H. Gargouri,* SENTECH Instruments GmbH, Germany*; J. Würfl, G. Tränkle,* Ferdinand-Braun-Institut, Germany

The technology of atomic layer deposited (ALD) Al_2O_3 films is ideally suited for fabrication of high quality GaN MISFET's gate insulator especially in vertical GaN n-channel transistor technology (Fig. 1). The gate oxide technology is a very crucial process step as it influences transistor functionality such as normally-OFF operation, hysteresis and low positive threshold voltage drift. Furthermore, dependent on the transistor design the gate oxide/channel interface may also determine ON-OFF-ratio. For qualifying and characterizing the gate insulator film technology, circular-planar MIS-capacitors were formed on a *n*-GaN layer (Fig. 2). The 25 nm thick Al_2O_3 films were deposited by plasma enhanced atomic layer deposition (PEALD) and thermal atomic layer deposition (ThALD) in SENTECH ALD system SI PEALD. Different in-situ surface pre-treatment conditions such as NH_3-plasma, NH_3-flow and without any pre-treatment were tested to optimize the GaN/Al_2O_3 interface. After top electrode metallization the capacitors were annealed at 350°C in N_2-ambient to achieve a large $\Delta C_{ON\text{-}OFF}$. Accumulated capacitance-voltage-(CV)-scans were performed to evaluate the insulator charging effects, to identify possible shifts in the CV-profile and to gain insight into bulk and interface charging phenomena (see Figs. 3 and 4). While measuring the accumulated bidirectional scans the maximum positive stress bias voltage was increased in 2 V steps from 0 V to 16 V after each bias sweep. The capacitance was measured at 1 MHz and 1 V AC amplitude. According to Figs. 3 and 4 a negative bias down to -15 V has turned out to be sufficient to empty the interface traps. PEALD and NH_3-plasma treated samples show a significant broadening of the positive bias stress CV-profile. Furthermore the flat band voltage shifts up to 7.2 V (Fig. 5). In contrast, the ThALD films with NH_3-plasma pre-treatment show a reduced broadening with a flat band voltage shift of only 2.9 V. When using NH_3-plasma pre-treatment, the calculated maximum negative fixed-oxide charges are less for ThALD ($-\Delta N_{OX}$ 5.1 × 10^{12} cm^{-2}) as compared to PEALD ($-\Delta N_{OX}$ 1.1 × 10^{13} cm^{-2}), see Fig. 6. Therefore thermal ALD in combination with NH_3-plasma pre-treatment is very suitable for GaN MISFET technology.

AA2-TuP17 Variable Morphology Highly-Conformal Diffusion Barriers for Advanced Memory and Logic Applications*, **Hae Young Kim**, S. Rathi, B. Nie, N. Naghibolashrafi, Y. Okuyama, S. Chugh, J. Heo, S.H. Jung, J. Mack, N. Mukherjee,* Eugenus, Inc.

Atomic layer deposition (ALD) of metallic ternary TiSiN films is associated with a variety of morphological and structural variations. Among these phenomena are the thickness and stoichiometric-dependent amorphous to crystalline phase transitions, film density changes, surface roughness and film resistivity variations. In the case of TiSiN films deposited via thermal ALD at temperatures of about T<600° C, using chlorine-based Si precursors, titanium tetrachloride and ammonia, the film structure is highly dependent on the total Si incorporated in the film. In this work, we demonstrate the tunability of crystalline phase in highly conformal TiSiN films with varied Si content. TiSiN films were deposited on high aspect ratio structures using a Eugenus 300mm commercial QXP mini-batch system. Film thickness and Si content were varied, and corresponding structural analysis was performed using multiple characterization techniques. X-ray diffraction and reflectivity studies of these films showed a reduction in film density and transition from nano-crystalline to pure amorphous phase with increase in Si fraction. Cross-section high resolution transmission electron microscopy (HRTEM) and selected area electron diffraction (SAED) pattern analyses corroborates with the X-ray analysis that high-Si TiSiN films exhibit a fully amorphous structure. Moreover, control of Si fraction in the film enables tuning of the morphology from polycrystalline to fully amorphous; in all cases, excellent step coverage on high aspect ratio structures were obtained.

~~**AA2-TuP18 Room Temperature Deposition of Hafnium Oxide by Atomic Layer Deposition for Gating Applications***, **Pragya Shekhar**, S. Shamim, S. Hartinger, J. Kleinlein, R. Schlereth, H. Buhmann, L. Molenkamp,* University of Wuerzburg, Germany~~

~~The advancement of fabrication techniques for nanostructures devices has led to technological breakthrough in semiconductor industries. Apart from the lithographic developments, high κ materials like ZrO_2 and HfO_2 have been employed as gate dielectric for efficient control of the carrier density. In this regard, atomic layer deposition (ALD) has been used to grow these insulators as it produces highly uniform and conformal layer with precise thickness. Previous works to grow HfO_2 by ALD require higher temperature (>100 °C) for microelectronic devices has been done. However, many~~

~~devices and materials have additional constraints that their properties degrade at higher temperatures. This limits the operating temperature at which the various fabrication processes can be carried out. For our research in the field of topological physics, mercury telluride (HgTe) topological insulators (Tis) are significant due to its versatility and tunability from trivial to 2D TI to 3D TI to Weyl by tuning the thickness and applied strain (compressive or tensile). However, the transport properties degrade when the HgTe wafer are heated above 80 ºC . To overcome this problem, we have developed a room temperature ALD process for growing HfO_2. A comprehensive study of structural and transport properties of devices containing HfO_2 gate dielectrics was carried out and results has been compared to device containing coventional SiO_2/ Si_3N_4 multilayers insulator films grown by plasma enhanced chemical vapour deposition (PECVD).This comparison demonstrates that our ALD grown insulator is superior in terms of structural properties. We have already shown that microstructures fabricated with ALD grown insulator shows quantum spin hall effect for 2D HgTe based devices. This capability is critical for understanding the properties of microscopic devices and may provide new insights in the field topological insulators. Our process is not just limited to HgTe (e.g. we use Si for process control) but can be easily adapted to other material systems which also require low temperature lithography process in order to retain the intrinsic property of material.~~

AA2-TuP19 Influence of Surface Cleaning Process on Initial Growth of ALD-Al_2O_3 and Electrical Properties of Pt/Al_2O_3/*β*-Ga_2O_3 MOS Capacitors*, **Masafumi Hirose,*** Shibaura Institute of Technology, Japan*; T. Nabatame,* National Institute for Materials Science, Japan*; E. Maeda,* Shibaura Institute of Technology, Japan*; A. Ohi, N. Ikeda, Y. Irokawa, Y. Koide,* National Institute for Materials Science, Japan*; H. Kiyono,* Shibaura Institute of Technology, Japan

β-Ga_2O_3 power device with metal-oxide-semiconductor (MOS) structure have been widely investigated. Al_2O_3 is the leading candidate as gate insulator because of relatively stable amorphous structure, a high dielectric constant (*k*) of 8 - 9 and a large bandgap of 6.5 - 6.8 eV. Al_2O_3 films are generally formed by atomic layer deposition (ALD). However, it remains big issues such as an abnormal flatband voltage (V_{fb}) shift and a large interface state density (D_{it}). To improve these electrical properties, various surface cleaning techniques of the substrate have been considered. In this study, we investigate how the surface cleaning technique affects to morphology of the surface of *β*-Ga_2O_3 and electrical properties of Pt/Al_2O_3/*β*-Ga_2O_3 MOS capacitors.

At first, n-*β*-Ga_2O_3 epilayer (2.0×10^{16} cm^{-3}) / n^+-*β*-Ga_2O_3 (3.7×10^{18} cm^{-3}) substrates (n-*β*-Ga_2O_3) were cleaned under four conditions: just a SPM for 5min, and SPM for 5 min (SPM), followed by BHF for 1 (BHF1), 10 (BHF10), and 30 min (BHF30). 25-nm-thick Al_2O_3 films were deposited on n-*β*-Ga_2O_3 substrates by ALD at 300 °C using TMA precursor and H_2O gas. Finally, Pt gate electrodes and Ti/Pt ohmic electrode were deposited.

The minimum root mean square (RMS) value (0.36 nm) of the n-*β*-Ga_2O_3 substrate was observed after SPM treatment. The RMS values (~ 0.6 nm) increased drastically when BHF treatment carried out even for 1 min and the value was unchanged even if treatment time was longer. In addition, the n-*β*-Ga_2O_3 substrate was etched by 0.9 nm for the BHF30. This is because the increase of the surface roughness is due to the heterogeneous etching of the n-*β*-Ga_2O_3 substrate. The Al_{2p} XPS intensities of the Al_2O_3 films after ALD 5 cycles for the BHF10 and BHF30 decreased by about 25 % compared to the SPM and BHF1, suggesting that the surface roughness affects to the initial growth of the Al_2O_3.

The MOS capacitor exhibited similar *J-V* properties regardless of the surface treatment techniques, indicating that the characteristic of the Al_2O_3 films was unchanged. On the other hand, the V_{fb} hysteresis ($V_{fb\ hys}$) due to the trapped/detrapped electrons increased as the BHF treatment time increases. The D_{it} energy distribution due to the fixed charge, which was calculated using conductance method, increased with increasing the BHF treatment time. These $V_{fb\ hys}$ and D_{it} behaviors are in good agreement with the data of the surface roughness of the n-*β*-Ga_2O_3 substrate. Considering to these data, note that the fixed charge and trapped/detrapped electrons occur at the Al_2O_3/n-type *β*-Ga_2O_3 interface. Therefore, the BHF surface treatment technique is not necessary promising from the viewpoint of the interface characteristics.

~~**AA2-TuP20 Reliable Gate Stack Development Employing Plasma Assisted Atomic Layer Deposited HfO_xN_y on InGaAs Substrate***, **Sukeun Eom,** M. Kong, K. Seo,* Seoul National University, Republic of Korea~~

~~We developed an advanced plasma-assisted atomic-layer-deposited (PA-ALD) HfO_xN_y process targeted on InGaAs substrate. The developed ALD process is consisted of isopropyl oxidant precursor and in situ cyclic N2 plasma nitridation that improves both interface and dielectric bulk quality as well. The interface chemistry and capacitance voltage characteristics of HfO_xN_y / InGaAs MOS devices are investigated. Clear oxide related elements were eliminated using our ALD process confirmed by XPS and STEM measurements. The IPA-based HfO_xN_y/n-$In_{0.53}Ga_{0.47}As$ MOS capacitor exhibited a significant decrease of interface trap density, D_{it}, of 4.5×10^{11} $eV^{-1}cm^{-2}$ at $E_c - E_t = 0.3$ eV and outstanding inversion behaviors. Morevover, substantial improvement was found not only in n-type substrates but also in p-type substrates as well. The significant mid-gap D_{it} decrease is responsiblefor this inversion behavior. The improvement mechanism of the proposed technology is assumed to be that nitrogen incorporation reduces oxygen vacancies which act as oxygen diffusion paths and with the use of IPA oxidant the interface would be strongly protected during pre- and post-dielectric deposition. Detailed electrical characteristics such as positive-bias temperature instabiltiy characteristics were investigated.~~

ALD Applications
Evergreen Ballroom & Foyer - Session AA3-TuP
Catalysis and Sensor Applications Poster Session

AA3-TuP1 Highly Dispersed Uniform Pt Catalysts on Carbon Support by Atomic Layer Deposition with Fluidized Bed Reactor(FBR)*., **Jung-Yeon Park,** W.P. Hong, S.-J. Oh,* Hyundai Motor Group, Republic of Korea*; W.-J. Lee, S.-H. Kwon,* Pusan National University, Republic of Korea

One of the key issues for fuel cell study is to increase the active surface area by controlling the size of Pt catalyst and reduce Pt loading to achieve high performance and cost savings. Atomic layer deposition (ALD) has recently received attention as an effective method for synthesis of nano catalyst since it allows precise control at the atomic level. In this study, Pt catalyst is synthesized using ALD directly on the surface of porous carbon support floated by fluidizing bed reactor (FBR). The oxygen functional group introduced on carbon surface through acid solution treatment provides reaction site of Pt precursor. In initial cycle, nucleation occurs on carbon surface, and high density 1-2 nm size uniform nanoparticle is formed. The Pt precursor adheres to the surface of already generated Pt and grows the Pt nanoparticle. Because of this growth mechanism, the size distribution of the particle is slightly wider at high cycles, but the size of the particle is controlled by the cycle and grows up to about 4 nm in 30 cycles. About 1 nm size particles have the highest active surface area, but in terms of catalyst performance, about 3 nm size particles show the best results under the Pt loading fixed condition. When the size of particle is not less than 3 nm, Pt exhibit physical properties as a catalyst and agglomeration of particles can be suppressed. To evaluate the catalyst performance of new processes , MEA optimization is important and this remains as a future plan.

~~**AA3-TuP3 Stabilizing Ultrasmall Colloidal Platinum Diphosphide (PtP_2) Nanocrystals with Atomic Layer Deposition Oxide for Neutral H_2O_2 Electrosynthesis***, **Hui Li,** S. Geyer,* Wake Forest University~~

~~Despite recent demonstrations of various electrocatalysts for small amount hydrogen peroxide (H_2O_2) production with rotating ring-disk electrode technique, it is still a great challenge to develop an efficient, selective, and stable O_2-to-H_2O_2 electrocatalyst for realizing continuous on-site production of neutral hydrogen peroxide. Here we synthesize ultrasmall and monodisperse colloidal PtP_2 NCs which achieves nearly zero-overpotential and unit H_2O_2 selectivity at 0.27 V vs. RHE for ORR. DFT calculation suggests that the P play a key role in promoting associative hydrogenation of OOH* to H_2O_2 and suppressing the dissociative OOH* to O*. With precise ALD Al_2O_3 overcoat and activation, the proton exchange membrane fuel cell (PEMFC) with $42Al_2O_3/PtP_2$-600 catalyst achieves a maximum r(H_2O_2) of 2.26 mmol h^{-1} cm^{-2} and a highest current efficiency of 78.8% for 120 h. Under recycle mode, the accumulated neutral H_2O_2 concentration reaches up to 3wt% for 65 h and 1.21 mol L^{-1} for 120 h, and which can be readily used for medical, food, and environmental applications.~~

AA3-TuP5 Synthesis of Core Shell Nanocatalysts using Atomic Layer Deposition with Fluidized Bed Reactor for PEMFC*, **Seung-Jeong Oh,** W.P. Hong, J.Y. Park,* Hyundai Motor Group, Republic of Korea*; W.-J. Lee, S.-H. Kwon,* Pusan National University, Republic of Korea

Proton Exchange Membrane Fuel Cells(PEMFC) have attracted significant interest as sources of renewable energy due to higher energy conversion efficiency than conventional internal combustion engines and zero-

emission characteristics. Despite its great advantages, it is difficult to commercialize due to high stack cost. Among the parts, Platinum(Pt) catalyst is expensive and scarce, so it is important to maximize the catalyst activity with minimal usage. Many researchers have significantly focused on core shell nanocatalysts due to their great activity, selectivity and stability with reducing the Pt loading. To optimize the characteristics of core shell nanocatalysts, it is necessary to precisely control shell composition and thickness. With the Atomic Layer Deposition(ALD) process, the size of nanocatalysts and shell thickness could be finely tuned at atomic scale. In order to uniformly deposit the nanocatalysts on the porous carbon support with large surface area, ALD with Fluidized Bed Reactor(ALD-FBR) offers the solution. By dispersing the carbon powder in the chamber, particle agglomeration is prevented and nanocatalysts can be uniformly deposited.

In this work, we synthesized core shell nanocatalysts using ALD-FBR. We utilize Nickel(Ni), Ruthenium(Ru) for the core materials, and Pt for the shell material. Ni(1-dimethylamino-2-methyl-2-butanolate)$_2$, η^4-1,3-cyclohexadiene ruthenium tricarbonyl, and Trimethyl (methylcyclopentadienyl)platinum(IV) are used as Ni, Ru and Pt precursor, respectively. The size of nanocatalysts and shell thickness is controlled by changing each ALD cycles. TGA, XRD and HRTEM are used to examine the structural and chemical properties of core shell nanocatalysts. From EDX line profile analysis, shell material(Pt) is preferentially deposited on core nanoparticles(Ni, Ru). Electrochemical Surface Area(ECSA) and cell performance were measured by Cyclic Voltammetry(CV) and MEA test. Core shell nanocatalysts by ALD-FBR show higher ECSA and cell performance than commercial catalyst.

~~AA3-TuP6 Porous Nanomembranes Grown by Atomic Layer Deposition: Self-Rolling in Solvent and their Sensing Applications~~*~~, F. Ma, Y.T. Zhao, G. Huang,~~* ***~~Yong Feng Mei~~***~~,~~ Fudan University, ~~China~~

~~Tubular microstructures of various materials have emerged as active agents for large-scale detoxification, sensing, and many other promising applications [1]. Generally, for sensing application, binding of specific recognition sites on tubular structures for targets molecule is engaged to achieve capture and detection of certain molecular [2]. The rolled-up technology [3,4] provide the possibility of producing microtubular structures with desired geometries and surface decoration on surface, which should be of great importance for real-time bio-sensing. In this study, porous nanomembranes were fabricated with high productivity by depositing active material on the surface of 3D polymer porous template with rough surface via atomic layer deposition technique [5]. The free-standing porous ZnO nanomembranes were obtained after the sacrificial template was removed at high temperature in oxygen. The rough surface of the template and the high temperature treatment make the surface of the nanomembrane with porous microstructure. Self-rolled porous ZnO nanomembranes were then prepared by sonication in chemical solvent. The porous surface was used as cysteine recognition sites for effective and selective binding of neurotransmitter compounds like dopamine (DA). Such selective binding is significantly enhanced by the high surface to volume ratio of the porous structure . For sensing applications, dispersion solution containing rolled-up structures was dropped on the surface of glassy carbon electrode, and then cysteine recognition sites was self-assembled on porous ZnO nanomembrane to capture target DA molecules which induces concentration-dependent electrical signals. Detailed analyses demonstrate that increased mass transfer leads to the enhanced sensitivity for DA. The current strategy provides an opportunity to develop 3D biosensor for high-affinity capture-based detection of nerve agents and can be extended to environmental contamination field.~~

~~References:~~

~~[1] B. Esteban-Fernández de Ávila, et al. *Acc. Chem. Res.* 2018, **51**, 1901.~~

~~[2] E. Karshalev, et al. 2018, , 3810.~~

~~[3] G. S. Huang, et al. 2009, , 263.~~

~~[4] B. R. Xu, et al. *Sci. Adv.* 2018, **4**, eaap8203.~~

~~[5] Y. T. Zhao, et al. 2018, , 22870.~~

AA3-TuP7 Fabrication and Characterization of Atomic Layer Deposited ZnO-based Ultra-thin Films for Hydrogen Sensing*, **Yan-Qiang Cao**, A.-D. Li,* Nanjing University, China

As a high-energy density, non-polluting renewable energy source, hydrogen is widely used in many fields such as industrial synthesis, fuel cells, and rocket propulsion. It is of great importance to develop reliable, fast, and precise hydrogen sensors so as to avoid possible explosion risks and harm. Due to the low cost, chemically and thermally stability, extremely abundant nanostructures and simple fabrication technique, ZnO as n-type semiconductor is widely used to detect reductive gases, such as hydrogen. Usually thin film-based sensor is more effective for improved gas sensing performance due to its small size, larger surface to volume ratio, and feasibility in integrated circuits. To date, research on ZnO ultra-thin film-based H_2 sensor is still lacking.

In this work, the ZnO ultra-thin films with varied thicknesses from 5 nm to 30 nm were grown on SiO_2 substrate at 200 ℃ using diethyl zinc (DEZ) and H_2O by atomic layer deposition (ALD), which could precisely control the thickness of the films down to values comparable to the Debye length. The effect of ZnO thickness and post-anneal on H_2 sensing, such as detection concentration, work temperature, and sensitivity has been carefully investigated. It is found that H_2 sensor based on 10 nm-thick ZnO ultrathin film exhibits better room temperature sensing performance with R_{air}/R_{gas} of 29 in 4000 ppm H_2. We also attempted to prepare Pt nanoparticles-decorated ZnO ultra-thin films by ALD. The impact of Pt NCs size and areal density on enhanced H_2 sensing of ZnO film sensor has been evaluated. The improved mechanism has been proposed.

ALD Applications
Evergreen Ballroom & Foyer - Session AA4-TuP
Protective Coatings, Barrier Films, Membranes and Flexible Substrates Poster Session

AA4-TuP1 ALD for Membrane Applications*, **Matthieu Weber**, M. Bechelany,* Institut Européen des Membranes, France

Atomic layer deposition (ALD) is a technology allowing for the preparation of conformal ultrathin films with a sub-nanometer thickness control, a unique capability. Therefore, this route is particularly suited for the structural modification and pore tailoring of porous structures. ALD can be advantageously applied to the area of membranes by fine-tuning their surface properties, and by controlling the diameter and the aspect ratio of the pores with (sub)nanometer precision. The precise control over the chemical and physical nature of the pore surface provided by ALD makes this route extremely valuable for membrane science. Thus, ALD coatings have been prepared on a wide variety of membrane substrates, from inorganic templated substrates to porous polymers.

This presentation aims to provide a summary of the advances of ALD applied to membranes. Based on a wide literature data survey including some of our recent data,[1–3] the application of ALD for different types of membranes will be described and illustrated using relevant examples, and the main challenges and opportunities of the ALD route will also be assessed.

(1) Weber, M.; Koonkaew, B.; Balme, S.; Utke, I.; Picaud, F.; Iatsunskyi, I.; Coy, E.; Miele, P.; Bechelany, M. Boron Nitride Nanoporous Membranes with High Surface Charge by Atomic Layer Deposition. *ACS Appl. Mater. Interfaces***2017**, *9* (19), 16669–16678.

(2) Weber, M.; Iatsunskyi, I.; Coy, E.; Miele, P.; Cornu, D.; Bechelany, M. Novel and Facile Route for the Synthesis of Tunable Boron Nitride Nanotubes Combining Atomic Layer Deposition and Annealing Processes for Water Purification. *Adv. Mater. Interfaces***2018**, *5* (16), 18–56.

(3) Weber, M.; ALD for membranes: Basics, Challenges and Opportunities. *Chem. Mater.***2018**, 30, 21, 7368-7390.

AA4-TuP2 Nano-Hardness of ALD Films*, **James Daubert**, W. Sweet, J. Kelliher,* Northrop Grumman

In this presentation, we will explore different films (Al_2O_3, ZrO_2, Ta_2O_5) deposited using atomic layer deposition (ALD) to compare how the processing conditions (i.e. deposition temperature, material interfaces, and annealing temperatures) effect hardness. The mechanical and electrical performance of materials used in microelectronics are often dependent on the processing conditions of material, but extensive testing after device manufacturing is often required to determine these relationships. Bulk, macroscale measurements, such as thickness, index of refraction, and sheet resistance can easily be measured, but often do not translate well to the performance of the final device, because the devices are often dependent on nanoscale properties of the materials (i.e. defects). If the nanoscale properties of the materials can be measured before final device fabrication, then correlations can be established linking material processing conditions with device performance.

One method to measure nanoscale properties of materials is through nano-identation. Nano-indentation is a method to measure the hardness of

materials using atomic force microscopy (AFM) that allows one to see differences in hardness on the nanoscale. Measuring the hardness of a material on the nanoscale allows you to elucidate variations in hardness that results from polycrystallinity of the material. We report on how the hardness is impacted by film thickness (50-1000 Å) and the underlying material. We also show how crystallinity produced by deposition or anneal temperature influences hardness of ALD films.

AA4-TuP3 High Acid Corrosion Resistance of Nb_2O_5 Thin Film Deposited by Room Temperature ALD*, **Kazuki Yoshida**, K. Saito, M. Miura, K. Kanomata, B. Ahmmad, S. Kubota, F. Hirose,* Yamagata University, Japan

Metal oxide thin films like aluminum oxide (Al_2O_3), silicon oxide (SiO_2), and titanium oxide (TiO_2) have been well known as gas barrier materials for moisture. For acid corrosion, Al_2O_3 exhibits a slight deliquescence against hydrochloric acid. On the other hand, niobium pentoxide (Nb_2O_5) has been studied as a cathode protective layer of a fuel cell and a corrosive barrier film for metal. By laminating Nb_2O_5 on Al_2O_3 using thermal ALD, the corrosion resistance was enhanced to a certain degree. However, the deposition temperature was over 200℃ although the high-temperature process is not acceptable for not heat-tolerant flexible electronics. In this study, a laminated film of Al_2O_3 and Nb_2O_5 was deposited by room temperature atomic layer deposition (RT-ALD) and we report the improved acid corrosion resistance.

We used plasma excited humidified Ar as an oxidizing gas, trimethylaluminum (TMA) and tert -butylimidotris-(ethylmethylamido) niobium (TBTEMN) as precursors of Al_2O_3 and Nb_2O_5, respectively. The RT-ALD system is shown in Figure 1. We prepared SUS 304 plates with a size of 20 × 50 mm^2 as samples. The SUS plates were cleaned by ultrasonic cleaning with using acetone, isopropyl alcohol, and deionized water to remove organic impurities. The surface was slightly etched with dilute hydrochloric acid to remove the surface scratches, For the corrosion resistance test, we immersed substrates into the concentrated hydrochloric (36 wt%).

Figure 2 shows the anti-corrosion film coated substrate immersed in concentrated hydrochloric acid for 30 minutes. Al_2O_3 thin films were deposited 30 nm both (a) and (c). The Nb_2O_5 was deposited with a thickness of 5nm both the substrate(b) and (c). The substrate (c) is laminated Nb_2O_5 on Al_2O_3. As we can see from Fig.2, the corrosion resistance for hydrochloric acid is clearly improved by laminating Nb_2O_5. We consider the RT deposited Nb_2O_5 is applicable for not heat tolerant flexible and MEMS application.

AA4-TuP4 Effects of Composition Ratios on Mechanical and Electrical Properties of AZO – Zincone Composite Thin Film Deposited on Transparent Polyimide Film Using Atomic and Molecular Layer Depositions.*, **Seung Hak Song**, B.-H. Choi,* Korea University, Republic of Korea

The combination of ALD and MLD techniques enables the fabrication of various functional organic – inorganic composite thin film structures. It is possible to fabricate thin films with various mechanical and electrical properties by adjusting the ratio of organic / inorganic components. In this study, a composite thin film composed of Al-doped zinc oxide (AZO) and the zincone organic film were deposited on a transparent polyimide substrate using diethylzinc (DEZ) with H_2O and hydroquinone (HQ) precursors. The characteristics of the hybrid thin film are varied significantly with the change of composition ratios, so the change of mechanical and electrical properties of the thin films according to the ratio of zincone organic film were measured. Various nano-structures of hybrid thin film were fabricated by controlling the composition ratio and process conditions, and their morphology and characteristics were analyzed. To investigate the ratio of thin films with high durability and electrical conductivity, the variation of electrical resistivity of thin films according to bending was measured.

AA4-TuP5 Room-temperature Atomic Layer Deposition of Aluminosilicate Thin Film on Flexible Films*, **Yoshiharu Mori**, K. Yoshida, K. Kanomata, M. Miura, B. Ahmmad Arima, S. Kubota, F. Hirose,* Yamagata Univ., Japan

In recent years, aluminosilicate thin films are applied in various fields such as ion absorbers. Aluminosilicate is generally prepared by hydrothermal synthesis. However, it is based on high temperature and pressure processes. It is also not suited for the fabrication on electronic devices. To solve these problems, we newly developed room temperature ALD of aluminosilicate using tris [dimethylamino] silane (TDMAS), trimethylaluminum (TMA) and plasma excited humidified argon. We realized deposition of aluminosilicate on flexible films at room temperature as shown in Fig.1. Fig.2 shows a wide scan XPS spectrum measured from the RT grown aluminosilicate on a PEN film. We confirmed significant peaks of Si, Al and O. The aluminosilicate film thickness was measured by spectroscopic ellipsometry that exhibited the growth per cycle of 0.16 nm/cycle at room temperature. This suggest the possibility of the film thickness control with a precision of nanometer. We confirmed the ion absorption ability of the film. It was confirmed that Na and K cations were effectively absorbed on the film. The ion exchange properties from Na to K was also confirmed. The present RT-ALD offers the ion exchange function on flexible films. This research is expected to be applied as heavy metal ion filters and ion sensitive field effect transistors.

AA4-TuP6 ALD Layers for Reduced Wear on Micro Cutting Tools*, T. Junghans, **Hans-Dieter Schnabel**,* Westsächsische Hochschule Zwickau, Germany

In modern life, the usage of electronics is increasing day by day. Therefore, many circuit boards need to be machined. One of the major problems in circuit board manufacturing is the wear of micro cutting tools used for it. Hard and corrosion resistant coatings might be a good opportunity to reduce the wear of these tools [1,2]. Due to the small size of the tools, with diameters of 300 µm and 3 mm, most traditionally used coating techniques are unable to produce conformal coatings on them [3]. This is why the works presented in a poster aimed for thin wear reducing films generated with atomic layer deposition.

The materials used were Al_2O_3 and TiN in various thicknesses from 20 nanometer to 150 nanometer. Those were used because of their properties, like hardness and corrosion resistance [1,4] and the well-established ALD-processes. In order to achieve dense films and low deposition temperatures the processes were plasma enhanced. Al_2O_3 was deposited with TMA as precursor in combination with an oxygen-argon plasma. The TiN films were generated by reacting TDMAT with an ammonia-argon plasma.

The poster shows that Al_2O_3 and TiN do not differ in wear behavior. Therefore, the focus is on Al_2O_3, due to the more stable and less time-consuming process. As the film thickness becomes bigger than 50 nm the Al_2O_3-layers are spalling off of the tools. Therefore, a lower or none reduction of wear was achievable with films as thick as or thicker than 50 nm. The work also shows that especially thin films of about 20 nm thickness achieved high reduction in tool wear. This shows that ALD-layers have promising properties in the field of wear reducing coatings for micro cutting tools.

[1] Y.L. Su and W.H. Kao; Journal of Materials and Performance: 7 (5), 1998

[2] Bull, S.J. et al.; Surface and Coatings Technology: 36, 1988

[3] Mayer, T.M. et al.; Applied Physics Letters, Vol. 82, No. 17, 2003

[4] Arslan E. et al.; Surface and Coatings Technology: 204, 2009

AA4-TuP7 Fabrication of Atomic Layer Deposited Alumina as Protective Coating of Silver*, **Gwon Deok Han**, J.S. Park, J. Koo, J.H. Shim,* Korea University, Republic of Korea

Silver is one of the precious metals widely used in human life. Silver has the disadvantage of being easily corroded or discolored when exposed to moisture and oxygen. Protective coatings of thin oxide films are effective in preventing corrosion and discoloration of silver products such as cookware, coins and jewelry. It is especially important to make a thin, uniform protective coating to protect the silver products from external environments. In this respect, atomic layer deposition (ALD) is considered the best technique for forming a protective oxide layer. ALD has an excellent function to form a uniform film without pinholes even in a complex three-dimensional (3D) structure with a high aspect ratio.

In this study, we evaluated the anti-corrosion performance of ALD alumina coatings for silver products [1]. The protection stability of the alumina coating layer was tested using an artificial sweat solution. The stability of the protective layer was evaluated by depositing alumina layers of changing thicknesses of 20-80 nm on silver samples and immersing the coated samples in artificial sweat solutions. We have demonstrated that a relatively thick alumina layer is effective in protecting the original properties of silver samples. In this meeting, we will discuss the protection performance of ALD alumina including its microstructure, optical properties and corrosion resistance.

[1] Park, S. W., Han, G. D., Choi, H. J., Prinz, F. B., & Shim, J. H. Evaluation of atomic layer deposited alumina as a protective layer for domestic silver articles: Anti-corrosion test in artificial sweat. *Applied Surface Science*, *441*, 718-723 (2018).

AA4-TuP8 Characterization of Laminated Thin Films for Encapsulation using Single Si Precursor by PEALD*, **Joong Jin Park**, S.D. Lee, H.-D. Lim, S.J. Jang, S.G. Kim, G.J. Park, S.I. Lee, M.W. Kim,* DNF Co. Ltd, Republic of Korea

OLEDs(Organic Light-Emitting Diodes) are used in display devices such as mobile and TV, and next-generation OLED displays should be flexible and foldable. Flexible and foldable OLED displays require curvature radius less than 2.5R. In addition, a good encapsulation property is required in a thin thickness. Therefore, it is essential for OLED to realize these characteristics through laminated thin film rather than single thin film. The laminated thin film can reduce the diffuse reflection by generating the antireflection film effect due to the difference of the refractive index of each single layer film. It is also effective in reducing stress in the film and blocking ultraviolet rays. [1, 2]

Recently, the ALD process has been applied as a method of depositing thin films with excellent film quality. These ALD methods are used to develop thin film encapsulation technology because of the self-limiting surface reaction and the advantages of the reaction fraction.

In this paper, structure of the SiO2 / SiNx stack films were fabricated by using PEALD(Plasma Enhanced Atomic Layer Deposition) method at low temperature (90 ℃) using a single precursor, NSi-01. The thickness and refractive index of the thin film were measured using a Woollam M2000D spectroscopic ellipsometer. In addition, WVTR (Water Vapor Transmission Rate) was measured by using MOCON Aquatran 2 for thin films deposited on polyethylene naphthalate (PEN). In the structure of the SiO2 / SiNx stack film, the refractive index was measured to be 1.47 / 1.85, confirming the possibility of antireflection effect through the multilayer. The WVTR characteristics were measured over 100 hours according to the thickness of the thin film. At a thickness of less than 150 Å, the SiO_2 thin film or SiNx thin film had poor WVTR characteristics. In order to overcome this problem, SiO2 / SiNx structure was deposited. It is also expected that 2 to 3% of carbon in the deposited SiNx film will lower the film stress and maintain the flexibility of the entire film (Figure 1). The SiO2/SiNx/SiO2 laminated thin films exhibited excellent WVTR characteristics with the prevention of destruction of the encapsulation characteristics at a thin thickness(Figure 2). From this work, we confirmed the possibility of a laminated thin film consisting of a silicon oxide film and a nitride film by PEALD in one chamber using one precursor. In particular, the production of a laminated thin film can prevent both reflection and moisture absorption, and it is expected that the next generation OLED encapsulation will be applicable.

AA4-TuP9 Low-cost Fabrication of Flexible Transparent Electrodes based on Sprayed Nanocomposites Silver Nanowires and Al Doped ZnO Deposited by Spatial ALD*, V.H. Nguyen, J. Resende, D. Papanastasiou, C. Jimenez, D. Bellet,* LMGP Grenoble INP/CNRS, France*; S. Aghazadehchors,* LMGP, France*; N.D. Nguyen,* Université de Liège*; **David Muñoz-Rojas**,* LMGP Grenoble INP/CNRS, France

We report the study of nanocomposite transparent electrodes based on Aluminium doped Zinc Oxide (ZnO:Al) thin films and silver nanowire (AgNW) networks. The electrodes are fully fabricated by low-cost, open-air techniques, namely, atmospheric pressure spatial atomic layer deposition and spray coating. We show that the transparency and the conductivity of the ZnO:Al/AgNW nanocomposites can be tuned by controlling the AgNW network density. We also demonstrate that the thermal, electrical and mechanical stabilities of the composites are superior to those of AgNW networks or ZnO:Al thin films separately. We have also developed a theoretical model to explain the relationship between the conductivity of the composites and the AgNW network density. Our results provide a means to predicting the physical properties of such nanocomposites for applications in solar cells and other optoelectronic devices. Finally, the deposition methods used open the way towards stable, low-cost flexible and transparent electrodes for industrial application.

~~**AA4-TuP10 Nanomechanical Properties of Crystalline Anatase Titanium Oxide Films Synthesized using Atomic Layer Deposition***, **Yousuf Mohammed**, P. Lin, K. Zhang, H. Baumgart, A. Elmustafa,* Old Dominion University~~

~~Titanium dioxides (TiO_2) thin films have received significantly attentions due to their remarkable biocompatibility, stability, nontoxicity, and excellent photocatalytic properties. TiO_2 films are used in artificial heart valves, photocatalyst in solar cells. The photocatalytic activity of titanium dioxide is exhibited in both the anatase and the rutile phases. Likewise, the photocatalytic properties of TiO_2 thin film coatings are noticeable in medical applications in bactericidal coatings of wound care gauze or in coatings of surgical instruments to be sterilized and for antimicrobial surfaces in hospitals. Fabrication of TiO_2 films has intensified in the last two decades due to their notable optical and electronic properties and their excellent potential applications for gas sensing. Another application for anatase TiO_2 in photovoltaics, when their team realized impressive photovoltaic performance advances with perovskite/ TiO_2 heterojunction solar cells, which were fabricated with pure phase anatase TiO_2 nanosheets with dominant (001) facets serving as the electron collector.~~

~~Several deposition techniques have been used in the past to deposit TiO_2 films on silicon substrates, including reactive DC sputtering, RF magnetron sputtering, ion beam induced chemical vapor deposition, metal-organic chemical vapor deposition, chemical vapor deposition, mist CVD and the atomic layer deposition (ALD). The ALD has emerged as a modern chemical reaction based technique to deposit monolayers of inorganic compounds. ALD possesses unique film deposition uniformity and exact composition control with atomic precision and absolute conformality.~~

~~Crystalline TiO_2 films of 500 nm thickness were synthesized using ALD on p-type Si (100) substrates. The crystal structures of the TiO_2 thin films were characterized by the X-ray diffraction (XRD). The film thickness and surface morphology were inspected using field emission scanning electron microscopy (FE-SEM) and AFM. The nanomechanical properties were measured using a nanoindenter equipped with a three-sided Berkovich diamond tip to evaluate the hardness and modulus of the TiO_2 thin films. Due to low temperature ALD deposition, the X-ray diffraction revealed a single phase TiO_2 anatase growth and the FE-SEM images indicate columnar grain structure growth with primarily vertical directions of the polycrystalline TiO_2 films. The measured hardness of the anatase ALD TiO_2 films at 20% film thickness has been measured as 5 Gpa, which is considerably softer compared to the reported benchmark values of the better known rutile phase of ~ 12 Gpa. The elastic modulus of the TiO_2 thin films was estimated as 138 and 145 Gpa.~~

AA4-TuP11 Encapsulation of Magnetic Nanostructures by ALD for Improved Stability and Performance*, **Devika Choudhury**, Y. Zhang, K. Gao, A. Mane, J.W. Elam,* Argonne National Laboratory

Morphology of magnetic nanoparticles is an important aspect responsible for controlling the optical, electrical and magnetic properties. Their interesting shapes and sizes result in novel properties significantly different from their bulk counterparts. For example, 1D magnetic nanostructures often exhibit significantly modified properties and enhanced coercivity as compared to the their bulk magnets thus making them attractive for wide range of applications. These materials are not only extensively used in high-density magnetic data-storage mediums, magnetic sensors and spintronic devices, but also suitable for valuable biomedical applications as well.

Metal alloys such as PtCo, SmCo, FeNi and FeCo are well known for their desirable magnetic properties and use. However, due to their nanosize scale, these materials readily oxidize under ambient conditions. Poor chemical stability results in diminished magnetic properties thus limiting their practical usage.

Atomic Layer Deposition (ALD) has emerged as one of the most widely accepted techniques to provide conformal coating of controlled thickness on high curvature structures and a popular method for encapsulation of various type of microstructures. In this work, we report the coating of magnetic metallic alloys using ALD method to improve stability and performance of the nanostructures. Different chemistries are used for the deposition of a variety of protecting layers. Comparison on the effectiveness of the coatings are drawn from the stability and their magnetic properties such magnetic saturation values obtained from SQUID measurements.

AA4-TuP12 Diffusion Barrier Properties of ALD TiSiN Films*, **Jerry Mack**, J. Heo, S. Chugh, H.Y. Kim, S. Rathi, N. Mukherjee,* Eugenus, Inc.

The decreasing feature sizes and increasing aspect ratios in semiconductor process flows have imposed stringent requirements on the physical and electrical properties of metal-to-semiconductor interfaces. This has resulted in fundamental material challenges for low-resistance contacts and ultra-thin diffusion-barrier films. Physical vapor deposition (PVD) based TiN film is a widely used diffusion barrier layer. However, deposition of ultra-thin TiN exhibits pronounced islanding which leads to rough film with polycrystalline grain structure. Furthermore, inhomogeneities due to grain boundaries offer diffusion pathways and lead to device degradation. In the current study, we present our findings on the diffusion barrier properties of amorphous ternary alloy films composed of Ti, Si and N (TiSiN), an excellent alternative to TiN films. These films were grown using Atomic Layer Deposition (ALD) technique on the Eugenus 300mm QXP commercial mini-

batch reactor. In one set of experiments, TiSiN films were deposited on highly-doped polycrystalline Si:B films followed by diffusion studies of boron. In another set of experiments, fluorine precursor based CVD Wsi_x film was deposited on TiSiN, followed by diffusion studies of fluorine. Secondary Ion Mass Spectrometry (SIMS) and High-resolution electron energy loss spectroscopy (HREELS) were utilized to detect the effectiveness of the barrier film to prevent boron and fluorine diffusion.

ALD Applications
Evergreen Ballroom & Foyer - Session AA5-TuP
Emerging Applications Poster Session

AA5-TuP1 Bottom up Stabilization of Perovskite Quantum Dots LED via Atomic Layer Deposition*, **Rong Chen**, K. Cao, Q. Xiang, B. Zhou,* Huazhong University of Science and Technology, China

Flexible displays are becoming the most promising and attractive techiques in the future. Quantum dots(QDs) have attracted great attentions due to their excellent optical properties, such as tunable wavelength, narrow emission, long carrier diffusion length, and high photoluminescence quantum efficiency. These properties make QDs the most promising optical materials for flexibles displays. However, as the instability of QDs based light emitting diodes limits their practical applications, QDs based LEDs are still under laboratory developments.

In this talk, we will discuss ALD based protection approaches from nanoscale QDs passivation to macroscopic encapsulation to improve the stability and boost its performance of QD-LEDs. First, the low-temperature selective ALD method has been developed for defects elimination. This protection method can preserve QDs monomers without damaging surface ligands and improving the quantum efficiency. For the QD light emitting layers, voids are formed during the stacking which may induce instability from electric, heat transfer. The ALD based filling process has been developed to improve charge transport within the layer. To study the surface interaction mechanisms of ALD precursors with the QDs layer, in-situ characterizations such as quartz crystal microbalance (QCM), infrared spectrometer (IR) are utilized to monitor the ALD process and the interactions with QDs layers. The oxides filling between quantum dots could reduce the carrier transport barrier and enhance carrier injection. Finally, it is imperative to develop efficient and ultrathin encapsulation to improve the stability towards ambient environments and flexibility of displays. Ultrathin multi-stacking films are designed and fabricated based on the combination of spatial ALD, molecule layer deposition and chemical vapor deposition. Such composite films could greatly enhance the water and oxygen resistance, while retain low stress and flexibility of the devices. It has demonstrated that the ALD approaches are versatile and useful for several fabricating steps in flexible QDs displays.

AA5-TuP2 ALD Bilayers for X-ray Windows with Long Lifetime*, **Agnieszka Kurek**, Y. Shu,* Oxford Instruments Plasma Technology*; H. Knoops,* Oxford Instruments Plasma Technology, UK*; A. O'Mahony, O. Thomas, R. Gunn,* Oxford Instruments Plasma Technology*; Y. Alivov, C. McKenzie, B. Grigsby, A. Degtyaryov,* Oxford Instruments X-ray Technology

X-ray-emitting devices require a window transparent to low energy X-rays while keeping the device at vacuum. Polycrystalline Be windows are often used since they have high X-ray transparency due to the low atomic number of Be. However, Be is sensitive to environmental moisture and shows degradation over time via two routes. Firstly, ambient gas can penetrate the Be window through the crystalline grain boundaries deteriorating the vacuum. Secondly, water vapour reacts with Be material causing corrosion and forming an oxide layer which can delaminate and reduce the window thickness over time. The window can become so thin it can no longer hold a vacuum inside the X-ray device – effectively ending the lifetime of the tube. Here, we show how the application of conformal, pinhole-free ALD bilayer coatings can extend the lifetime of X-ray windows more than five times with negligible influence on X-ray transmittance.

We have developed and patented (US20180061608A1) a robust solution using a combination of Al_2O_3 and TiO_2 less than 200 nm in thickness. The ALD coatings were deposited in an Oxford Instruments Plasma Technology FlexAL™ system at 350 °C. Thermal Al_2O_3 (~40 nm) was used as an adhesion layer, followed by in-situ deposition of thermal TiO_2 (~80 nm) as a harder, protective layer, using trimethylaluminum and tetrakis(dimethylamino) titanium, respectively. The relatively low atomic numbers of Al and Ti mean that the maximum allowed film thickness to maintain clarity of the X-ray spectra is 800-1000 nm, which is much higher than the used thickness. This window coating is an effective moisture barrier and attenuates the transmitting X-rays by less than 5 % compared to the attenuation of an uncoated window. Importantly, the ALD coating does not contaminate the output X-ray spectra. No fluorescence contamination of Al and Ti could be detected. The lifetimes of ALD coated windows were compared with that of uncoated window by determining how long they could sustain ultra-high vacuum. For all sixteen coated samples, the windows survived the test at least 5 times longer and, in many cases, >15 times longer.

The ALD coating of the X-ray windows increases lifetime of X-ray emitting equipment by more than five times minimising specialist maintenance. The excellent conformality of ALD is furthermore expected to help close off grain boundaries present in the Be windows which can be up to 100 nm deep and could otherwise be pathways for gas diffusion into the vacuum of the system. Future options include making the coating conductive as a further advantage for X-ray equipment.

AA5-TuP3 ALD for 3D Nano MEMS Applications*, **Dorothee Dietz**,* Fraunhofer Institute for Microelectronic Circuits and Systems IMS, Germany

In the area of MEMS and nano sensor structures, the ALD becomes ever more important. Because of the highly isotropic and highly conformal deposition method, ALD is the best choice for structures with large aspect ratios or structures with complex cross sections. Moreover it is possible to deposit several different materials in the same tool, so that the functionality of the material can be tuned by stacks or doping as good as possible. Because of the low deposition temperature, ALD can be applied in post-CMOS-processes.

ALD techniques enable the fabrication of free standing 3D structures as follows: In a first step, a sacrificial layer is deposited onto a (CMOS-) substrate. Small holes or trenches are etched through it as pillars and an ALD layer is deposited and structured. In the end, the sacrificial layer is removed. This technique can be used e.g. for the processing of different gas sensors or for realizing 3D multi electrode arrays (MEA).

The first type of gas sensor, which is based on conductometric semiconductor gas sensing, operates with metal oxide (MOx) nano wires, 350 nm in width and 150 µm in length. The metal oxide (e.g. ZnO or SnO_2) is used as a functional layer but also for forming the 3D structure. Because the metal oxides need to be heated for gas sensitivity, a heater is realized with the same technology as described above. In this case, Ru, TiN or TiAlCN, is used as heater material, deposited also by ALD.

The second gas sensor is acting as a nano pellistor. The heater has to be a free standing 3D structure, because the sensor has to be thermally decoupled from the substrate underneath. All materials are deposited with ALD to achieve the high aspect ratio and because of the material properties. The heater consists of Ru, the surrounding isolation layer can be Al_2O_3 and the catalytic layer is made of Ru again.

To increase the sensitivity of the sensor, the surface of the catalyst can be increased by using a porous Al_2O_3 layer instead of a solid one. A porous Al_2O_3 layer can be achieved by doping it during the ALD in a first step e.g. with ZnO and by a selective etching of the doping material in a second step.

Another application for using this technology is processing 3D MEA. They can penetrate biological cell membranes for measuring intracellular electrical signals directly. As a conductive and biocompatible material, Ru is used for these electrodes. They are 200 nm in diameter and a few microns in height. With an additional step, the diameter at the tips can be reduced so that they can penetrate membranes easier, without the risk of destroying them.

AA5-TuP4 Tribological Properties of Plasma Enhanced Atomic Layer Deposition TiMoN*, **Mark Sowa**,* Veeco-CNT*; A. Kozen,* U.S. Naval Research Laboratory*; B. Krick, N. Strandwitz,* Lehigh University

In our previous study, we demonstrated a tertiary plasma enhanced atomic layer deposited transition metal nitride (TiVN) with exceptional wear rates and friction coefficients. We have extended that work with an investigation of another tertiary transition metal nitride system, $Ti_xMo_yN_z$. For films deposited at 250°C and 300W on a Veeco CNT G2 Fiji PEALD system, we have demonstrated how the ratio of TiN:MoN cycles (1:0, 3:1, 1:1, 1:3, 0:1) provides linear control of the Ti:Mo in the resulting film. Through application of an 13.56MHz RF substrate bias (0-250V) during the plasma step, ion bombardment energy of the substrate can be varied, providing a means for tweaking the films physical and chemical characteristics which in turn are shown to impact the resulting film's tribological properties. As PEALD metal nitrides have broader interest than wear layers and to gain insights on the interrelationships of the mechanical properties, the

processing details, and other film properties, we also report on the resulting film composition/impurities, density, crystallinity, optical properties, resistivity, and morphology.

AA5-TuP5 Thickness Optimization of Alumina Thin Film for Microchannel Plate Detector*, **Baojun Yan**, S. Liu,* Institute of High Energy Physics, Chinese Academy of Sciences, China

Conventional lead glass microchannel plate (MCP) detector has been used in a variety of applications. The MCP performance can be improved by coating high secondary electron emissive layers, such as alumina (Al_2O_3) and magnesium oxide (MgO), via atomic layer deposition (ALD). In this poster, the alumina thin films with varied thicknesses were deposited by ALD on polished Si substrates and MCPs, respectively. The secondary electron yield (SEY) of the alumina thin films on silicon substrate were measured by pulsing electron beam. The MCPs used in our experiment had a high length to diameter ratio ~80:1 and worked in photon counting mode. The optimal thickness of alumina was obtained through comparative study the MCP performance before and after coating. In addition, the DC gain variation as a function of total charge per unit area Q (C/cm^2) were investigated.

~~**AA5-TuP6 Optical Coatings Deposited on Nonlinear Crystals by Atomic Layer Deposition***, **Ramutis Drazdys**, R. Buzelis, M. Drazdys,* Center for Physical Sciences and Technology, Lithuania~~

~~Growing requirements for optical coatings deposited on temperature and environment sensitive crystals force to look for alternatives to conventional physical vapor deposition technologies. KDP, DKDP, $LiNbO_3$ are nonlinear optical materials that have been difficult to coat due to specifics of surface adhesion and thermal properties. Atomic layer deposition (ALD) is widely used in nanotechnology and semiconductor devices [1] and recently attracted more interest in manufacturing of optical components [2,3]. The main goal of our research was to develop antireflection (AR) coatings on nonlinear crystals with high laser induced damage threshold (LIDT). HfO_2 and Al_2O_3 thin layers deposited using TDMAH and TMA precursors and H_2O as oxidant by Savannah 200 system from Ultratech at low temperature (<100°C) were investigated. Experimental deposition processes of HfO_2 and Al_2O_3 thin film 150 nm thickness single layers were made at temperatures from 40°C to 100°C with different pulse and purge time duration parameters. To prevent the HfO_2 layer crystallinity we used the nanolaminate concept [4] where each HfO_2 layer with thickness of 20 nm incorporate a certain number of Al_2O_3 monolayers. Growth rates, dependency on precursor pulse and chamber purge durations were determined by using quartz crystal monitoring and optical spectra data. Refractive index and absorption dispersions were determined. Setup with the Nd:YAG laser (from EKSPLA co.) generating pulses with repetition rate 15 Hz, pulse duration ~3 ns was used for LIDT measurements. The investigation of the optical transmission and reflection of produced thin layers allowed to determine optical loses in UV region. These results gave us the possibility to choose optimal technological parameters for AR coating formation on nonlinear crystals substrates. The following design of experimental AR coating was selected: substrate / 75nm HfO_2 / 200nm Al_2O_3. In previous investigations determined growth rates per pulse cycle were used for layers thickness control. The same coating design was used to manufacture AR coatings by IBS and e-beam evaporation. The LIDT measurements of AR coatings demonstrated comparable or higher damage levels for ALD coatings.~~

~~[1] M. Ritala, *et al.* Nanotechnology 10 (1999) p.p. 19-24.~~

~~[2] K. Pfeiffer, *et al.* Opt. Express Vol 6 Nr.2 (2016).~~

~~[3] Y. Wei, *et al.* Nanoscale Research Letters 10;44 (2015) p.p.1-7.~~

~~[4] S. Zaitsu, *et al.* Japanese Journal of Applied Physics Vol. 43, No. 3 (2004) p.p. 1034–1035 .~~

AA5-TuP7 Atomic Layer Deposition of Nickel and Nickel Oxide Thin-Films for Astronomical X-ray Optics Applications*, **Hossein Salami**, A. Uy, A. Vadapalli,* University of Maryland*; V. Dwivedi,* NASA Goddard Space Flight Center*; R. Adomaitis,* University of Maryland

Nickel and nickel oxide films have optical, electrical and magnetic properties that when combined with good chemical stability makes them attractive for many applications. Nickel oxide is a p-type semiconductor that can be used as a transparent electrode, or in manufacturing nonvolatile resistance random access memories, or for chemical sensing purposes. In its pure form, nickel film can be used as adhesion layer for copper interconnects [1]. Because of its X-ray reflecting property, another application of pure nickel film is in multi layer coatings for X-ray optics [2,3].

In this talk, we will discuss atomic layer deposition process for Ni and NiO thin-films using two different metal precursors, nickelocene and nickel acetylacetonate, in combination with ozone as the oxygen source. We will present two different routes to depositing metallic Ni: direct metal deposition or metal-oxide deposition with a subsequent reduction step. Our initial results confirm the deposition of NiO film and its reduction using molecular hydrogen predicted by thermodynamic analysis. Advantages of each route and their effect on the properties of the final product will be presented. Furthermore, specifically for astronomical applications, roughness and X-ray reflectivity of the prepared thin-films and the conformal coating of high aspect-ratio X-ray optics will be discussed in detail.

[1] H.L. Lu, G. Scarel, C. Wiemer, M. Perego, S. Spiga, M. Fanciulli, G. Pavia, "Atomic layer deposition of NiO films on Si (100) using cyclopentadienyl-type compounds and ozone as precursors." Journal of the Electrochemical Society, 155(10), (2008).

[2] P. Gorenstein, "Focusing X-ray optics in astronomy", X-ray Optics and Instrumentation, 2010, (2010).

[3] M. Sarr, N. Bahlawane, D. Arl, M. Dossot, E. McRae, D. Lenoble, "Tailoring the properties of atomic layer deposited nickel and nickel carbide thin films via chain-length control of the alcohol reducing agents.", The Journal of Physical Chemistry C, 118(40), (2014).

AA5-TuP8 Atomic Layer Deposition and Chemical Vapor Deposition of Zirconium Boride for Various Applications: New Work Function, Barrier Metal, Hard Mask and Area Selective Deposition*, **Jun-Hee Cho**, J.J. Park, W.-M. Chae, J.-H. Park, S.I. Lee, M.W. Kim,* DNF Co. Ltd, Republic of Korea

Zirconium boride is an attractive material for microelectronic, hard coating, and other applications. Because, it has high melting point (3040 °C), a high mechanical hardness, excellent wear properties, and excellent corrosion resistance toward molten metals [1]. In this work, we talk about new applications of ZrB_x for new work function, barrier metal, hard mask and area selective deposition (ASD). ZrB_x film have been deposited both by sputtering and chemical vapor deposition (CVD) routes. An inherent shortcoming of sputtering is its non-conformal nature. In conventional CVD of ZrB_x films, the $ZrCl_4$ and BCl_3 precursors are reduced with H_2, but the incorporation of residual chlorine atoms has proven to be detrimental to film properties. In addition, thermal atomic layer deposition (ALD) was not studied in detail [2, 3]. In this study, ZrB_x films have been deposited by thermal ALD and CVD process using single precursor $Zr(BH_4)_4$ for new work function, barrier metal, hard mask and ASD. The work function of deposited ZrB_x film by ALD at 250 to 350 □ is 3.93 to 3.96 in the bulk and 3.86 to 3.64 in the surface respectively (Fig. 1). The step coverage was showed 100 % in aspect ratio 19:1 pattern at 250 □(Fig. 2). The resistivity of ZrB_x film was about 450 μΩ ㎝ and showed amorphous structure.

The deposited ZrB_x film on Si(100) by CVD is sufficient to prevent copper diffusion into silicon during a 600 °C anneal for 30 min (Fig. 3, 4). The ZrB_x film on SiO_2 by CVD has a very slow etch rate for CF_x, while a very fast etch rate for BCl_3 (Fig. 5). The wet etch was not showed in 0.5% HF solution (Fig. 5). The ZrB_x film has resistance to oxygen. ASD of $Zr(BH_4)_4$ was showed selectivity of W metal and SiO_2 substrate for ZrB_x film (Fig. 6). The deposited ZrB_x films were showed amorphous phase. The possibility of applying a new work function, barrier metal, hard mask and ASD is expected.

[1]Silvia Reich, Hnrald Suhr, Klhra Hanko,and Laszlro Szepes, Adv. Mater., 4(10), (1992).

[2] Sreenivas Jayaraman, Yu Yang, Do Young Kim, Gregory S. Girolami, and John R. Abelson, J. Vac. Sci. Technol. A., 23(6), (2009).

[3] Dean M. Goedde, Gregory S. Girolami, and John R. Abelson, J. Appl. Phys., 91(6), (2002).

~~**AA5-TuP9 Comparative Study of $Mo_{1-x}W_xS_2$ Alloy Gas Sensor by Atomic Layer Deposition***, **Minjoo Lee**, Y. Kim, J. Park, H. Kim,* Yonsei University, Republic of Korea~~

~~Two-dimensional (2D) Transition metal dichalcogenides (TMDCs) are a layered structure, which stacked via weak van der Waals interaction. 2D TMDCs have attracted great attention because of their remarkable electronic and optoelectronic properties such as indirect-to-direct bandgap transition with reducing layers, superior electrical properties and strong spin-orbit coupling. Furthermore, recently the 2D TMDCs have shown the potential as a gas sensing material due to their very large surface-to-volume ratio, semiconducting property, and low power consumption. Thus,~~

~~the WS_2 or MoS_2 that is the one of the most popular TMDCs has been studied for its gas sensing properties and demonstrated an excellent response to various gas molecules, such as nitrogen dioxide (NO_2), ammonia (NH_3), acetone, etc. However, due to the difficulty of uniform synthesis of 2D TMDCs and the highly sensitive characteristic of these TMDCs gas sensors, there are few researches about direct comparative study of each materials. Although only a theoretically calculated studies were reported, the result is often different according to adapted model.~~

~~In this study, layer controlled 2D MoS_2 and WS_2 synthesized with $Mo(CO)_6$ and $W(CO)_6$ and H_2S gas as precursors and a reactant using ALD in same equipment under similar conditions. Furthermore, we synthesized $Mo_{1-x}W_xS_2$ alloys using ALD super-cycle and confirmed that W composition in alloys can be controlled by changing super cycle configuration. Synthesized 2D TMDCs were fabricated for gas sensors for comparison of gas sensing property and It showed different response and response time according to composition in alloy.~~

AA5-TuP10 Fabrication of High-Aspect-Ratio Nanometric Gold Gratings*, O. Makarova,* Creatv MicroTech Inc*; **Ralu Divan**, L. Stan,* Argonne National Laboratory*; C.-M. Tang,* Creatv MicroTech Inc

High-aspect-ratio gold gratings have broad applications in x-ray optics, and their quality and aspect ratio strongly affect the quality of the generated images. To fabricate the gratings, two key technological challenges must be addressed: (i) creating a high-aspect-ratio trenches with smooth vertical walls, and (ii) filling the trenches uniformly with gold.

We report fabrication of 450 nm half-pitch gold gratings with an aspect ratio of 26 using laser interference lithography (LIL), reactive etching (RIE), atomic layer deposition (ALD), and gold electroplating techniques. In the first step, gratings are patterned on the resist/chromium coated silicon wafer *via* LIL. Then, the chromium, which served as a hard mask for silicon etching is etched using RIE. This step is followed by cryogenic RIE to create deep trenches in silicon. Then, a platinum seed layer is deposited by ALD, and finally the mold is electroplated with gold.

RIE of high-aspect-ratio dense and narrow trench/wall structures of gratings imposes significantly more difficulties than the etching of isolated narrow lines or trenches, since the undercut and the negative taper can damage the thin walls. High-aspect-ratio nanoscale silicon gratings were obtained by carefully tuning all etching parameters (Figure 1a).

A continuous, conductive and conformal seed layer is essential for uniform electroplating. We performed ALD of platinum as a seed layer. To improve platinum adherence, a 10 nm alumina adhesion layer was deposited by ALD as well. The high-exposure platinum ALD was optimized to assure conformal coating of the high-aspect-ratio trenches. The nanometric trenches were filled with gold *via* conformal electroplating, when plating occurred from all surfaces. The method has an advantage of much shorter electroplating time, compare to bottom-up plating technique. However, it is challenging to avoid voids formation due to prematurely trench sealing. and achieve uniform plating over the entire trench depth because of the gold ions depletion inside the narrow and deep trenches (Figure 1b).

Use of the Center for Nanoscale Materials, an Office of Science user facility, was supported by the U. S. Department of Energy, Office of Science, Office of Basic Energy Sciences, under Contract No. DE-AC02-06CH11357.

Area Selective ALD
Evergreen Ballroom & Foyer - Session AS-TuP
Area Selective ALD Poster Session

AS-TuP1 Laterally-Structured Dielectrics by Area-Selective Atomic-Layer-Deposition on 3D Substrates*, **Philip Klement**, D. Anders, F. Michel, J. Schörmann, S. Chatterjee,* Justus Liebig University Giessen, Germany

Industrial semiconductor fabrication combines lithography, etching, and deposition processes to create electronic devices. The quest for miniaturization of those devices has led to complex fabrication processes with multiple patterning and etching steps to achieve area-selective deposition. However, with conventional top-down fabrication reaching its limits in pattering resolution and alignment, a tool for bottom-up processing in advanced technology must deposit different combinations of materials area-selectively. Atomic-layer-deposition (ALD) is a technique for depositing high-quality, ultrathin films of dielectrics with the potential of area-selective deposition. It could reduce the number of manufacturing steps and allow for continued miniaturization, yet no area-selective deposition of lateral heterostructures has been realized.

Here, we show the successful direct patterned deposition of TiO_2 on complex SiO_2 substrates creating smooth surfaces of alternating dielectrics. Our approach demonstrates area-selective deposition on three-dimensional substrates, and we identify factors to consider that are not present in area-selective deposition on conventional two-dimensional substrates. We use a combination of electron beam lithography using a polymer mask, ion beam etching, plasma treatment, and ALD similar to established semiconductor fabrication processes to realize lateral heterostructures of dielectrics. Several process parameters were varied, and their effect on the resulting structure was investigated by atomic force microscopy, scanning electron microscopy, and X-ray photoelectron spectroscopy. We investigated different polymer mask surfaces and precursor diffusion in terms of area-selective deposition, and found that a number of factors must be considered in design, patterning, and deposition to achieve reproducible results. Our work enables the realization of lateral heterostructures of dielectrics as building blocks for advanced technology applications.

AS-TuP2 Light Assisted Area Selective Atomic Layer Deposition on Plasmonic Nanoantennas*, **Chengwu Zhang**, T. Gao, B. Willis,* University of Connecticut

Plasmonic nanoantennas, especially with gaps less than 10 nm, can greatly enhance electric fields through excitations of surface plasmons, which are collective oscillations of electrons excited by light. Arrays of plasmonic nanoantennas can be designed to concentrate and manipulate light at the nanoscale, and have wide applications such as surface enhanced spectroscopy, photo-driven chemical conversion, and optical information processing. Atomic layer deposition (ALD) is a thin-film deposition technique capable of producing conformal thin films with precise control of thickness and composition at the atomic level. Area selective ALD provides a way to precisely tune nanogaps to enhance their optical and electronic properties. The optical properties of plasmonic nanostructures offer the possibility to enhance selective growth through resonant excitations. In this work, we investigate the effect of light in area selective ALD on plasmonic nanoantennas.

We present a case study of Cu area selective ALD on Pd nanoantennas. The sizes of antenna dimers range from 25 nm to 200 nm, with 20 nm gaps. The gaps are measured and compared before and after thermal ALD with and without light irradiation. Results show GPC (growth per cycle) is enhanced at lower temperatures using irradiation, which yields better selectivity. As an example, for nanoantennas with lengths of 75 nm and widths of 25 nm, ALD growth at 150 with light yields almost the same GPC as 230 without light. Compared with thermal ALD, only 1/3 number of cycles are required for the same growth with irradiation. Using various nanoscale antenna designs and array configurations, we analyze the role that plasmonic heating or hot electrons may contribute to the enhanced growth.

AS-TuP3 Area-Specific Atomic Layer Deposition (ALD) of Cobalt As Mediated by Thermally Induced Dehydrocoupled Self-Assembled Monolayers (SAMs)*, **Barry Arkles**, J. Goff, C. Brick,* Gelest, Inc.*; A. Kaloyeros,* SUNY Polytechnic Institute

Organic trihydridosilanes can provide an elegant route for generating self-assembled monolayers (SAM)s by vapor phase transport on a variety of substrates. Under mild conditions, these precursors can be made to interact with a variety of clean metal and hydrogenated metalloid surfaces, including those of interest for nanoscale integrated circuitry (IC) applications, such as titanium, copper, and silicon, to form near-zero-thickness SAMs. As shown in the figure below, the resulting SAMs can be customized with specific functionality (depending on the choice of the R substituent) to activate or deactivate subsequent ALD Co on the underlying substrate of choice, leading to area-specific Co deposition. In this work, negative and positive ALD Co protocols under low substrate temperature conditions will be presented and discussed.

AS-TuP4 Investigation of *In-situ* Surface Cleaning of Cu Films using O_3/O_2 and N_2H_4*, **Su Min Hwang**, A.L.N. Kondusamy, Q. Zhiyang, H.S. Kim, L.F. Peña, K. Tan, J. Veyan,* University of Texas at Dallas*; D. Alvarez, J. Spiegelman,* RASIRC*; J. Kim,* University of Texas at Dallas

Copper is widely used in semiconductors as interconnects due to its low resistivity, high resistance to electromigration, low temperature coefficient of resistance, and good thermal stability.[1] Recent demonstration of atomic layer deposition (ALD) of Cu thin films is expected to overcome the limitations of the PVD process and could be used to deposit a highly conformal film over high-aspect ratio structures with precise thickness control. Several processes on ALD Cu have been reported requiring an additional reduction step to obtain metallic Cu.[2] Therefore, it is imperative

to explore reducing agents capable of reducing the oxide on Cu at low temperatures. Among the various available reducing agents, N_2H_4 (Hydrazine) can be used in the reduction of copper oxide due to its higher reduction capability.[3] Inspired by Hydrazine's unique characteristics, we explore the feasibility of vapor-phase reduction of copper oxide using N_2H_4 to achieve an ideal metallic Cu film in an ALD environment. Additionally, a detailed *in-situ* surface analysis of the reduction with N_2H_4 has not been reported yet.

In this work, Cu samples were oxidized using an O_3/O_2 mixture, followed by N_2H_4 using a rapid thermal ALD system to investigate the reduction effectiveness of N_2H_4. From the XPS analysis, Cu samples treated with O_3/O_2 showed the diffusion of oxygen into the sample and the formation of Cu_2O layer that is approximately 4 nm thick. With N_2H_4 treatment, a significant amount of copper oxide was reduced to metallic copper with approximate thickness of 1 nm, the comparable reduction capability of N_2H_4 agent. In addition, *in-situ* reflection absorption infrared spectroscopy (RAIRS) was employed to elucidate the individual surface chemistry of copper films during the oxidation (O_3/O_2) and reduction (N_2H_4) step. The detailed experimental results will be presented.

This work is partially supported by Rasirc Inc. by providing N_2H_4. We also acknowledge TMEIC (Toshiba Mitsubishi-Electric Industrial Systems Corporation) for providing the O_3 generator.

[1] R.P. Chaukulkar, N.F.W. Thissen, V.R. Rai, and S. Agarwal, J. Vac. Sci. Technol. A **32**, 01A108 (2014).

[2] L.F. Pena, J.F. Veyan, M.A. Todd, A. Derecskei-Kovacs, and Y.J. Chabal, ACS Appl. Mater. Interfaces **10**, 38610 (2018).

[3] D.M. Littrell, D.H. Bowers, and B.J. Tatarchuk, J. Chem. Soc. Faraday Trans. 1 Phys. Chem. Condens. Phases **83**, 3271 (1987).

AS-TuP5 Area-Selective Deposition of SiO_2 based on Spatial ALD with Interleaved Etching Steps to Obtain High Selectivity*, **Alfredo Mameli,*** TNO/Holst Center, Netherlands*; F. Roozeboom,* Eindhoven University of Technology and TNO, Netherlands*; P. Poodt,* TNO/Holst Center, Netherlands

Area-selective atomic layer deposition (AS-ALD) has been envisioned as a potential technological solution for advanced patterning. However, the selectivity that can be obtained is often very limited and the throughput of most AS-ALD methods is low, which hampers its industrial acceptance.[1,2] In this work, we present a process for AS-ALD of SiO_2 using intermittent plasma etching steps to obtain high selectivity.[3] At the same time, the deposition process itself is performed in a spatial ALD mode at atmospheric pressure that allows for achieving high throughput.[4]

AS-ALD of SiO_2 on a pre-patterned substrate with SiO_2 and ZnO was demonstrated using a chemoselective inhibitor that chemisorbs preferentially on the non-growth area (ZnO) while it allows for depositing SiO_2 on the growth area (SiO_2). In order to obtain high selectivity, a blanket fluorocarbon plasma etching step was interleaved after every 110 ALD cycles. This way, up to ~ 30 nm-thick selective SiO_2 deposition was demonstrated, as shown in Figure 1 of the supplemental PDF file. Furthermore, X-ray photoelectron spectroscopy was carried out to verify the selectivity of the process. No Si was detected on the non-growth area, demonstrating the high selectivity of this process.

The process presented in this work combines selective inhibitor chemisorption, plasma-based spatial ALD at high deposition rates and plasma etch-back steps to correct for selectivity loss. Being compatible with roll-to-roll and sheet-to-sheet concepts, this approach can enable high-throughput AS-ALD on large-area and flexible substrates as well.

[1] A. Mameli et al., *ACS Nano*, **2017**, 11, 9303-93

[2] F.S.M. Hashemi et al., *ACS Nano*, **2015**, 9, 8710-8717

[3] R. Vallat et al., *JVSTA*, **2017**, 35, 01B104

[4] P. Poodt et al. *JVSTA*, **2012**, 30, 01802(1-10)

AS-TuP6 Defect Mitigation Solution for Area-Selective Atomic Layer Deposition of Ru on TiN/SiO_2 Nanopatterns*, J. Soethoudt,* KU Leuven – University of Leuven/IMEC, Belgium*; F. Grillo,* ETH Zurich, Switzerland*; E. Marques, R. van Ommen,* Delft University of Technology, Netherlands*; B. Briggs, H. Hody, V. Spampinato, A. Franquet, B.T. Chan,* ***Annelies Delabie,*** IMEC, Belgium

Area-Selective Deposition (ASD) receives increasing attention as a bottom-up approach for nanopatterning. Implementation of ASD is however limited by undesired particle growth on the non-growth surface. This work provides a demonstration of defect mitigation strategies based on insight into the particle growth mechanism on the non-growth surface. Ru is selectively deposited by 1-(ethylbenzyl)-1,4-(ethylcyclohexadienyl) ruthenium (EBECHRu) and oxygen atomic layer deposition on TiN/SiO_2 nanopatterns pretreated with dimethylamino-trimethylsilane. This material system is relevant for a tone inversion patterning application, where a hard material (Ru) is selectively deposited inside holes in a soft material (SiO_{-2}) which is more straightforward than patterning the hard material directly[1]. Ru films are selectively deposited on TiN, while particle growth is observed on dielectrics (Figure 1a). The thickness of the selectively deposited Ru layer on TiN is independent of feature dimensions in the entire investigated size range of 90µm-25nm (Figure 1b). We propose two strategies to mitigate defectivity based on the first stages of EBECHRu/O_2 growth on dielectrics. Initially, the Ru particles are too small to catalytically dissociate oxygen, thereby suppressing direct deposition on the particles[2]. Ru particles at first grow only through surface diffusion and coalescence until they reach a sufficient size for catalytic O_2 dissociation, at which point the particles start to rapidly grow through direct deposition on the particles. A first defect mitigation strategy employs the initial growth regime in which particles are smaller compared to the ASD-grown film. During this regime, the particles can be fully etched with limited thickness reduction of the ASD Ru layer. Self-Focusing Secondary Ion Mass Spectrometry (SF-SIMS) is used as a probe for ASD defectivity due to its low limit of detection and the potential to analyse over 10^4 structures simultaneously[3,4]. A window was identified in which an ASD Ru layer fully covers the growth surface while no defects are observed by SF-SIMS (Figure 2). The second defect mitigation strategy limits the diffusion-mediated growth of particles during the initial regime, thereby extending its length and significantly enhancing selectivity (Figure 3). The size-dependent nanoparticle reactivity in EBECHRu/O_2 ALD suppresses particle growth on the non-growth surface. As such, particles can be completely etched while retaining the integrity of the ASD pattern.

[1]B. Briggs et al., *CSTIC* (2018)

[2]J. Soethoudt et al., *Adv. Mater. Int.* (2018)

[3]A. Franquet et al., *App. Surf. Sci.* (2016)

[4]V. Spampinato et al., *App. Surf. Sci.* (2019)

Nanostructure Synthesis and Fabrication
Evergreen Ballroom & Foyer - Session NS-TuP
Nanostructures Synthesis and Fabrication Poster Session

NS-TuP1 Molybdenum Disulfides and Diselenides by Atomic Layer Deposition*, **Raul Zazpe**, J. Prikryl, M. Krbal, J. Charvot, F. Dvorak, F. Bures, J. Macak,* University of Pardubice, Czech Republic

The discovery and success of graphene paved the way for developing two-dimensional materials with outstanding properties [1]. In particular, monolayers of two-dimensional transition metal dichalcogenides (2D TMDCs) possess a direct band gap [2] that is crucial for optoelectronic applications. Additionally, the direct band gap can be easily tuned by either chemical composition or external stimuli. In parallel to monolayer TMDCs structures, a high surface area layer of TMDCs flakes shows promising properties for hydrogen evolution [3], photodegradation of organic dyes [4] or as electrodes in Li ion batteries [5].

To date, various top-down (e.g. exfoliation) and bottom-up techniques, such as chemical vapor deposition (CVD) and atomic layer deposition (ALD) have been reported for the preparation of 2D-TMDCs [1]. However, ALD is the only technique enabling sub-nanometer thickness control, which is revealed as a crucial factor in the properties of 2D TMCDs materials. In the last years, it has been reported the possibility to employ ALD as a technique to grow MoS_2, which has been extensively studied for many different applications. In these works $(CH_3)_2S_2$ [6] or H_2S [7, 8] were used as the S precursor and $Mo(CO)_6$ [6], $MoCl_5$ [7] or $Mo(thd)_3$ [8] as the Mo precursors. Further, important efforts have also been devoted to attain the ALD fabrication of $MoSe_2$, since it possesses higher electrical conductivity than MoS_2 [9, 10]. Recently, we have shown that ALD deposition of $MoSe_2$ [11] or Mo-O-Se [12] is feasible using $(CH_3)_2S_2$ as the Se precursor and the $MoCl_5$ or $Mo(CO)_6$, respectively, as the Mo precursors.

The presentation will focus on the synthesis of MoS_2 and $MoSe_2$ by ALD, their characterization and applications in various fields. Experimental details and some recent photocatalytic, battery and hydrogen evolution results will be presented and discussed.

[1] A. V. Kolobov, J. Tominaga, Two-Dimensional Transition-Metal, Dichalcogenides. Springer Series in Materials Science, Springer International Publishing AG, Switzerland 2016

[2] B. Radisavljevic et al, Nat. Nanotechnol. 6 (2011) 147

[3] L. Wang et al, Adv. Mater. Interfaces. 2 (2015) 1500041

[4] Y. Wu et al, Nanoscale. 8 (2016) 440

[5] D. Ilic et al, J.Power Sources. 14 (1985) 223

[6] Z. Jin et al, Nanoscale. 6 (2014) 14453.

[7] L. K. Tan et al, Nanoscale. 6 (2014) 10584

[8] M. Mattinen et al., Adv. Mater. Interfaces 2017, 4, 1700123.

[9] D. Kong, H. et al, Nano Lett. 13 (2013) 1341.

[10] A. Eftekhari, Appl. Mater. Today 2017, 8.

[11] M. Krbal et al., Phys. Stat. Sol. RRL. 12 (2018) 1800023

[12] S. Ng et al., Adv. Mater. Interfaces. (2017) 1701146.

NS-TuP2 Wafer-scale MoS_2 Thin Film Deposition via H_2S Plasma Sulfurization of ALD-grown MoO_3 at Low Temperature*, **Jeong-Hun Choi**,* Korea Maritime and Ocean University, Republic of Korea

Molybdenum disulfide has attracted great interest due to its outstanding mechanical, electrical and optical properties. These unique properties make MoS_2 investigated as a promising candidate material for opto-electronic, sensing and catalysis applications. MoS_2 thin films have been achieved by a variety of methods such as sputtering and chemical vapor deposition. Nevertheless, these methods are limited to controlling the number of layer and uniformity over wafer scale. The most crucial problem of these methods is that they demand high growth temperature or additional heat treatment. High temperature process hinders the application of MoS_2 to a wide range such as flexible and transparent devices. In this work, MoS_2 thin films were deposited by H_2S plasma sulfurization of ALD-grown MoO_3 thin films. While ALD-grown MoO_3 provided precise thickness control and uniformity, H_2S plasma process effectively sulfurized MoO_3 into MoS_2 at low temperature. The sulfurization behavior and physical quality of MoS_2 thin films were investigated under various plasma conditions. The film thickness was measured by ellipsometry and Raman analysis. X-ray photoelectron spectroscopy was carried out to analyze the chemical composition of MoO_3 and MoS_2 thin films. The crystallization behavior of the films was characterized by X-ray diffraction. Furthermore, the potential of MoS_2 for electric device component was investigated.

NS-TuP3 ALD-based Synthesis of Few-layer Transition Metal Disulfides with Wafer-scale Uniformity for Device Integration*, **Tao Chen**, Y. Wang, H. Zhu, L. Chen, Q.Q. Sun, D.W. Zhang,* Fudan University, China

Different transition metal disulfides (TMDs) ultra-thin films with wafer-scale uniformity have been successfully synthesized by ALD-based process. Two growth routes have been developed: sulfurizing transition metal oxides deposited by ALD, and annealing amorphous TMD films deposited by ALD. Molybdenum hexacarbonyl and ozone were used as precursors to deposit MoO_3 film by plasma enhanced ALD followed by sulfurization in a tube furnace to form MoS_2 TMD films. Tungsten hexachloride and hexamethyldisilathiane (HMDST) were used as ALD precursors to deposit WS_2 films which were further annealed at high temperature to improve crystallinity. Both approaches can produce high-quality and thickness-controllable TMD films with wafer-scale uniformity, which have been confirmed by AFM, XPS, Raman and TEM characterizations. Field-effect transistor (FET) device arrays have been further fabricated based on both films showing excellent homogeneous and reproducible electrical performance. The FET on/off ratio was about ~10^4 with decent mobility over 10 $cm^2V^{-1}s^{-1}$. These experimental results demonstrated attractive and promising potentials of the novel two-dimensional TMD films in future micro-/nanoelectronics device integrations and applications by using ALD-based techniques.

NS-TuP4 Overcoming Agglomeration and Adhesion in Particle ALD*, **Benjamin Greenberg**, J. Wollmershauser, B. Feigelson,* U.S. Naval Research Laboratory

The fundamental challenge of particle ALD (pALD) is that small particles are sticky. Nanoparticles (NPs) in particular are highly susceptible to van der Waals, dipole-dipole, electrostatic, and chemical forces. When NPs are fluidized or agitated to expose their surfaces to ALD precursors, these forces can cause persistent agglomeration and adhesion to reactor surfaces, preventing conformal coating and reducing core-shell NP yield. To understand and overcome these obstacles, we examine NPs coated in a reactor with two agitation modes, rotation and vibration. We analyze high-speed videos of NP motion while varying agitation parameters (velocity, frequency, timing) as well as NP material and size. After pALD, we weigh the coated powders and study core-shell NP composition and morphology via TEM and N2 adsorption measurements.

NS-TuP5 Density Function Theory for Nucleation of MoF_6 with Oxide Surfaces in Atomic Layer Deposition of MoS_2*, **Matthew Lawson**,* Boise State University

Several two-dimensional (2D) atomic-layered transition metal dichalcogenides (TMDs) are of great interest for electronic and optoelectronic applications due to their wide direct band gaps for few layer materials. Beyond mechanical or liquid exfoliation of bulk materials, high quality 2D TMDs have been grown via chemical vapor deposition (CVD) but growth is typically performed at high temperatures. Several studies have reported atomic layer deposition (ALD) of thin TMD films at lower temperatures, but as-deposited films are typically amorphous our nano-crystalline. Complementary to *in-situ* experimental studies of the growth and nucleation of nanoscale films, we have employed density functional theory (DFT) to understand the nuanced interactions during precursor nucleation. Hydroxyl groups are commonly found on metal oxide surfaces and play an important role during many ALD processes. To develop a deeper understanding of the ALD of MoS_2 from MoF_6 and H_2S, we studied the reactivity of MoF_6 with three substrates: Al_2O_3, MgO, and HfO_2 without hydroxyls and fully saturated with hydroxyls using DFT. We calculated the electronic distribution of the surfaces, how the electronic structures changed with single MoF_6 precursors, and calculated the valence electron transfer. Our calculations support the important role of hydroxyls in the nucleation of MoF6 with oxide surface and provide insight into the formation of precursor bonds at the surface.

ALD Applications
Grand Ballroom H-K - Session AA1-WeM
ALD for Memory Applications II

Moderators: Seung Wook Ryu, SK Hynix, Myung Mo Sung, Hanyang University

8:00am **AA1-WeM1 ALD/ALE Process in Commercially Available Leading-Edge Logic and Memory Devices***, **Rajesh Krishnamurthy**,* TechInsights **INVITED**

In 2018, we saw the introduction of a new generation of logic products, featuring FinFET transistors from Intel with their 10 nm generation microprocessor, followed by 7nm devices from competing foundries, primarily targeting high-end application processors in mobile devices. We also saw memory product manufacturers Samsung, Hynix, Toshiba and Micron introducing 64- or 72- stacked layer 3D-NAND devices, and move into 1x generation DRAM devices.

As a supplier of competitive intelligence to the semiconductor and electronics industries, TechInsights performed structural analyses to examine the features and manufacturing processes of all of these innovative devices.

This presentation will examine some of the different structures we have seen through the evolution of these technologies, in particular 7nm and 10-nm logic, 3D-NAND and DRAM parts, that have been introduced. We will also look at several historical applications of ALD/ALE technology that have been observed through reverse engineering. We will highlight the importance of ALD/ALE process in advanced logic and memory devices. In many cases, the technology could not have advanced without the implementation of ALD technology

8:30am **AA1-WeM3 Atomic Layer Deposited Crystalline Zinc Oxide for Silver-based Ultra-Steep Threshold Switching Selector***, **Harrison Sejoon Kim**, A. Sahota, J. Mohan, H. Hernandez-Arriaga, J. Kim,* The University of Texas at Dallas

Along with the growth of emerging non-volatile memory (NVM), developing an outperforming selector is also required to pave the way for realization of neuromorphic networks. Ideally, when cointegrated with the memory element, the role of a selector is to prevent the sneak-current from neighboring devices in a cross-point array [1]. To thrust the emerging NVM at the technological cutting edge, various kinds of selectors have been developed so far [1]. Also, different deposition techniques have been employed to deposit the selector layer. Atomic layer deposition (ALD) provides excellent atomic thickness controllability, thus amongst them, it is the most favorable technique for fabricating the selectors having their switching threshold dependent on the electric field. Electric field dependent conduction mechanism is significant as threshold voltage (V_{th}, voltage that turns on the selector) can be controlled by changing the physical thickness of switching layer. Controllability of V_{th} makes the selector highly compatible with the memory element. Ag or Cu-based threshold switching (TS) selectors are exemplary for the electric field driven selectors, and moreover, they possess superior characteristics over many kinds of the selectors developed so far [2].

In this work, we demonstrate Ag-based TS selectors fabricated with ALD grown crystalline zinc oxide (ZnO) unlike the most prevalent cases where switching layers have been deposited amorphously. The selector device has simple metal-insulator-metal (MIM) structure. Stacked Ag electrodes are assumed to act as the reservoir for providing Ag metal atoms to form metallic filament within insulating ZnO layer (Fig. 1a). As a result, we have obtained robust TS behavior using ALD ZnO with high selectivity ($>10^7$), ultra-low off-state leakage current (~ pA), high on-state current density (> 0.01 MA/cm^2), and ultra-steep slope (< 10 mV/decade) (Fig. 1b). To suppress cycle-to-cycle variability found in Ag-based TS selectors, we have proposed "Ag delta-doping" concept (Ag-doped ZnO) for minimizing the stochastic issue (Fig. 2). Here, we expect crystalline ZnO would benefit reducing randomness providing better controllability on Ag diffusion (as illustrated in Fig. 2). This will be achieved through a technique so called "super-cycle ALD", followed by further investigation on the reliability of Ag-doped ZnO switching layer.

The authors thank Semiconductor Research Corporation (SRC) for providing financial support in this work.

[1] G. W. Burr *et al.*, *J. Vac. Sci. Technol. B*, vol. 32, no. 4, p. 040802, 2014.

[2] Z. Wang *et al.*, *Adv. Funct. Mater.*, vol. 28, no. 1704862, pp. 1–19, 2018.

8:45am **AA1-WeM4 ALD Ge-Se-Te OTS Selectors with Controlled Composition for PCM Applications***, **Valerio Adinolfi**, L. Cheng, R. Clarke, S. Balatti, K. Littau,* Intermolecular, Inc.

The increasing need for faster high-capacity NV-memories have led researchers to explore chalcogenide materials as a solution to fabricate PCM memories and OTS selectors. Memories and selectors are vertically integrated in X-point arrays to produce storage devices. In order to meet the stringent requirements on integration chalcogenide stacks will have to be integrated in 3D structures (as is currently happening for FLASH NANDs). 3D architectures can be enabled exclusively by ALD depositions – providing the necessary conformality and film quality – of the active layers. A limited number of ALD chalcogenide films have been demonstrated but, despite intense efforts, these processes fail in controlling the film composition – fine control over the composition of chalcogenide systems is indispensable for producing performing OTS and PCM devices.

Here we present, for the first time, ALD of binary and ternary films of Ge – Te – Se with controlled composition evaluated in devices as two terminal threshold switches. A unique process involving $HClGe_3$, btms -Te(Se), and Te ethoxide was developed by alternating semiconducting GeTe(Se) and metallic Te/Se layers. Nucleation and growth mechanisms are thoroughly investigated by means of an in-situ ellipsometer. We demonstrate the ability to cover a large part of the ternary triangle plot (see figure attached) by using RBS, XPS, and calibrated XRF. X-SEM and AFM reveal smooth surfaces and compact films. Conformality is assessed by uniformly filling trench structures with a high aspect ratio (40:1).

Finally we electrically characterized $Ge_xTe_ySe_z$ thin films contacted with tungsten and TiN bottom plugs and top contacts (respectively). Different compositions produce dramatically different devices; germanium rich compositions exhibit resistive or PCM behaviors while Te – Se rich compositions produce OTS selectors (see figure attached). DC current-voltage (IV) measurements, transient IVs, and threshold voltage characterizations are performed over a large number of devices and a statistical analysis is presented.

This work shows for the first time ternary ALD chalcogenide films with controllable composition and their electrical operation as memory devices (PCM and OTS); this novel ALD process poses the foundation for the imminent development of chalcogenide based 3D X-point memory arrays.

References:

1) A. Chen, *Solid State Electronics* **2016**, *125*, 25.

2) L. Perniola et al., *IEEE Electron Device Lett.* **2010**, *31*, 488.

3) A. Velea et al., *Scientific Reports* **2017**, *7*, 8103.

4) V. Pore, T. Hatanpaa, M. Ritala, M. Leskela, *J. Am. Chem. Soc.* **2009**, *131*, 3478.

5) T. Gwon, et al., *Chem. Mater.* **2017**, *29*, 8065.

9:00am **AA1-WeM5 Pulsed CVD of Amorphous GeSe for Application as OTS Selector***, A. Haider,* IMEC, Belgium*; Shaoren Deng,* ASM, Belgium*; E. Schapmans,* IMEC, Belgium*; J.W. Maes,* ASM, Belgium*; J.-M. Girard,* Air Liqude Advanced Materials, France*; G. Khalil,* imec*; G.S. Kar, L. Goux, R. Delhougne,* IMEC*; **M. Caymax**,* IMEC, Belgium

Alongside advances in RRAM structural design to scale down the memory, the problem of sneak currents, which frustrate the accurate reading/writing of data in each cell, remained a critical issue. An attractive approach is to add a selection device operating for example by means of the Ovonic threshold switching (OTS) mechanism to each memory element that suppresses sneak currents through highly nonlinear current-voltage (IV) characteristics. Amorphous germanium selenide (GeSe) is a well-known candidate for OTS selector which so far has only been grown by physical vapor deposition (PVD) for planar RRAM devices. The 3D RRAM approach, which has the advantage of ultra-high storage density with low cost, calls for a uniform and highly conformal deposition technique to deposit this amorphous GeSe selector material on 3D structures.

Here, we report pulsed chemical vapor deposition (CVD) of amorphous GeSe using germanium chloride and alkylsilylselenide precursors. We learned from a study of precursor chemisorption kinetics based on Total Reflection X-ray Fluorescence (TXRF) that both precursors cover the wafer surface only quite slowly. The same measurements also show that Se precursors need Cl sites (from the Ge precursor) for precursor ligand exchange reactions. Further investigation reveals that higher GPC is obtained in pulsed CVD mode (so, no purge steps between the pulses). Based on this basic understanding, we developed a pulsed CVD growth process (GPC=0.3 Å/cycle) of GeSe using $GeCl_2.C_4H_8O_2$ and $(TMS)_2Se$ as Ge

and Se source, respectively. TEM images reveal that ~20 nm grown GeSe layer is amorphous while EDX and RBS measurements revealed stoichiometric GeSe films with traces of Cl impurities. EDX mapping revealed uniform Ge and Se distribution throughout the film. Elastic recoil detection (ERD) measurements show ~5 % carbon inside the grown GeSe film. AFM images show an RMS surface roughness of 1.7-1.9 nm. GeSe grown on 3D test structures showed excellent film conformality.

Currently work is ongoing to apply conformally grown GeSe layers as OTS selector devices in electrical test vehicles. We will report electrical switching and endurance characteristics of conformal, pulsed CVD grown OTS GeSe selector layers and bench mark these with PVD grown GeSe layers.

9:15am **AA1-WeM6 Thin Film Challenges in 3D NAND Scaling**, ***Jessica Kachian**, D. Pavlopoulos, D. Kioussis,* Intel Corporation **INVITED**

In today's datacentric society, 3D NAND has become a storage architecture of focus through increased bit density, relative to 2D architectures. Continuing bit density increase through 3D NAND scaling requires clever manufacturing strategies, centered on discovery and patterning of target materials. Thin film deposition steps face daunting aspect ratios with unforgiving quality specs. The inherent conformality afforded by ALD makes it an attractive process for 3D NAND. However, many relevant ALD processes do not deliver film quality as-deposited. This talk focuses on general material and patterning requirements for key steps in 3D NAND fabrication and considers how ALD may address these challenges, with attention to target properties towards performance.

ALD Applications
Grand Ballroom H-K - Session AA2-WeM
ALD for ULSI Applications I

Moderators: Ravindra Kanjolia, EMD Performance Materials, Jae Hyoung Choi, Samsung Electronics

10:45am **AA2-WeM12 The Journey of ALD High-k Metal Gate from Research to High Volume Manufacturing**, ***Dina Triyoso**, R. Clark, S. Consiglio, K. Tapily, C. Wajda, G. Leusink,* TEL Technology Center, America, LLC **INVITED**

In the early days of the search to find a replacement for SiO_2-based gate oxides the goal was to find a material with a very high k value which could be incorporated into CMOS production for multiple technology nodes. A historical overview of the many promising high k materials considered for SiO_2 replacement leading to the selection of ALD HfO_2 as "the winner" will be presented. ALD HfO_2 has successfully been implemented in CMOS production for over a decade, starting at the 45nm node. There are two general integration approaches for implementing ALD High-k/Metal Gate stacks (HKMG) in production: gate first and gate last. Challenges with each integration approach, leading to the wider adoption of gate last will be discussed. Furthermore, as the dielectric constant of HfO_2 is only ~20 and a thin SiO_2-base interface was still required to maintain mobility and reliability, HfO_2 provided essentially a one-time scaling benefit. Further thinning of HfO_2 resulted in unacceptable leakage and thus to continue transistor scaling fully depleted devices such as FINFET and Ultra Thin Planar SOI (FDSOI) were pursued. High volume manufacturing flows for FINFET (with gate last integration) and FDSOI (with gate first integration) come with their own unique challenges. For example, with FINFET maintaining gate height uniformity is crucial for Vt targeting and control. With FDSOI, maintaining gatestack stability at high temperature is key. To continue future scaling, new device architectures (e.g. GAA, Vertical FETs, etc.) will pose further challenges for gate stack integration. Recent and historical progress in HfO_2 growth, interface control, selective deposition, morphology and etching will be discussed with respect to the possibility for future gate stack engineering.

References:

R.D. Clark, *Materials*, 7(4), 2913-2944, https://doi:10.3390/ma7042913 (2014).

D.H. Triyoso et al., *ECS Transactions*, 69 (5) 103-110 (2015).

R.J. Carter et al., *ECS Transactions*, 85(6) 3-10 (2018).

R.D. Clark et al., *ECSarXiv.* October 3. https://doi:10.1149/osf.io/qtxnd (2018).

R.D. Clark et al., *APL Materials* 6, 058203; https://doi.org/10.1063/1.5026805 (2018).

11:15am **AA2-WeM14 Effects of Er Doping on Structural and Electrical Properties of HfO_2 Grown by Atomic Layer Deposition.**, ***Soo Hwan Min**, B.-E. Park, C.W. Lee,* Yonsei University, Republic of Korea*; W. Noh,* Air Liquide Laboratories Korea, South Korea*; I.-K. Oh,* Yonsei University, Republic of Korea*; W.-H. Kim,* Hanyang University, Republic of Korea*; H. Kim,* Yonsei University, Republic of Korea

Gate dielectric materials with high-*k* are required for further scaling down in future years. As an alternative of conventional high-*k* materials such as HfO_2, the addition of elements to host high-*k* materials has attracted attention. Among various elements, rare-earth elements, such as Y, La, Dy, or Er has been known to transform the crystal structure of HfO_2 from the first-principles study. The theoretical study showed that the doping into HfO_2 can energetically stabilize the cubic or tetragonal phase at lower temperature than thermodynamic conditions of pure HfO_2. Since cubic (k~29) or tetragonal (k~70) HfO_2 has much higher dielectric constant than that of amorphous (k~16-19) and monoclinic (k~20-25) phases, it is noteworthy that the structural modulation by doping of rare-earth elements can enhance the electrical properties of HfO_2.

In this work, Er doping into HfO_2 was experimentally carried out using atomic layer deposition (ALD) super-cycle process with $Er(MeCp)_2$(N-iPr-amd), $HfCl_4$, and H_2O co-reactant. ALD Er-doped HfO_2 with a variety of Er/(Er+Hf) compositions were systematically examined, mainly focusing on structural and electrical properties. X-ray photoelectron spectroscopy (XPS) and X-ray diffraction (XRD) were utilized to investigate the film composition and crystal structure. In addition, MOS capacitors were fabricated with various compositions to evaluate the electrical properties from capacitive-voltage (C-V) and current-voltage (I-V) measurements. In specific ratio, the dielectric constant and the interface trap density of Er-doped HfO_2 were found to have significantly improved compared to undoped HfO_2. Structural and electrical characterization revealed that the addition of Er to HfO_2 induces phase transformations from the monoclinic to the cubic or tetragonal phases, even at low post-annealing temperatures of 600°C. This study identifies optimum conditions to improve the electrical properties of Er-doped HfO_2 films which have potential applications in future nanoscale devices.

11:30am **AA2-WeM15 Improvement of Electrical Performances of Atomic Layer Deposited ZrO_2 MIM Capacitors with Ru Bottom Electrode**, ***Jaehwan Lee**, B.-E. Park,* Yonsei University, Republic of Korea*; W. Noh,* Air Liquide Laboratories Korea, South Korea*; I.-K. Oh,* Yonsei University, Republic of Korea*; W.-H. Kim,* Hanyang University, Republic of Korea*; H. Kim,* Yonsei University, Republic of Korea

With accelerated scaling down and three-dimensional structuring of integrated circuits, it becomes very challenging to fabricate metal-insulator-metal (MIM) capacitors with low leakage current and high capacitance density. Specifically, the introduction of high-k dielectrics in conjunction with TiN electrodes has improved electrical properties in sub-100 nm processes. Various high-k dielectrics layers combined with TiN electrodes in MIM capacitors were studied for further improvement of MIM capacitors. Controlling an interfacial layer formation between dielectric layer and metal electrode is essential for depositing high-k dielectric thin film on a TiN electrode. When high-k dielectric films were placed on the TiN, interfacial layer was formed due to high reactivity of TiN. The interfacial layer acts as charge traps causing degradation of electrical properties. Surface treatment like plasma treatment on the TiN has been known to help suppress formation of an interfacial layer, but it would be hard to apply for mass-production of DRAM process due to difficulty of uniform treatment without damage caused by energetic species such as ions and radicals on the devices formed inside deep trenches with high aspect ratio.

Alternatively, selection of stable metal electrodes with high work function is required to improve electrical properties. Among several metals, Ru electrode can be appropriate option due to its good thermal and chemical stability, low resistivity, high work function. In this paper, we investigated effects of bottom electrodes on the thin film properties of atomic layer deposited (ALD) ZrO_2, concentrating on correlation between interfacial layer formation and electrical properties. Transmission electron microscopy (TEM) showed thinner thickness of the interfacial layer on the Ru electrode than TiN electrode. Chemical composition of the interfacial layer was analyzed by X-ray photoelectron spectroscopy (XPS) analysis, and ZrO_2 on Ru was less intermixed with bottom electrode due to good thermal and chemical stability of Ru electrode. Introducing Ru electrode improved symmetry of the normalized C-V characteristics. Simultaneously, the introduction of Ru electrode affects decrease of leakage current density from ~10^{-5} A/cm^2 to ~10^{-7} A/cm^2 in I-V characteristics. These results are very meaningful capacitor with Ru electrode can be a very promising device for MIM capacitor in DRAM production.

11:45am **AA2-WeM16 Perfecting ALD-Y_2O_3/GaAs(001) Interface with Ultra-High Vacuum Annealing***, Keng-Yung Lin, Y.-H. Lin,* ***W.-S. Chen****, H.-W. Wan, L.B. Young,* National Taiwan University, Republic of China*; C.-P. Cheng,* National Chia-Yi University, Republic of China*; T.-W. Pi,* National Synchrotron Radiation Research Center, Republic of China*; J. Kwo,* National Tsing Hua University, Republic of China*; M. Hong,* National Taiwan University, Republic of China

High-performance metal-oxide-semiconductor field-effect transistors (MOSFETs) require the semiconductor/high-κ interface with high-temperature thermal stability and a low interfacial trap density (D_{it}). Previously, *in-situ* atomic layer deposition (ALD) or molecular beam epitaxy (MBE) Y_2O_3 has effectively passivated GaAs(001) surface.[1,2] The growth was achieved in an integrated ALD/MBE ultra-high vacuum (UHV) system. Despite the difference in deposition, both Y_2O_3/GaAs interfaces withstand 900 ^oC annealing, and the D_{it}'s lie below 5×10^{11} $eV^{-1}cm^{-2}$. MOS capacitors (MOSCAPs) with such interface outperform those with *ex-situ* deposited Al_2O_3.[3] By *in-situ* synchrotron radiation photoemission study on ALD-Y_2O_3/GaAs(001)-4×6, we found that the faulted surface As atoms were removed and lines of Ga-O-Y bonds stabilized the interface.[4] The interfacial Ga_2O (Ga^+)-like state explains the low D_{it}.

In this work, we have improved the electrical characteristics in ALD-Y_2O_3/GaAs by *in-situ* UHV annealing the initial 1-nm Y_2O_3. The idea is motivated by removing the freed As atoms and hydrocarbons remained in the ALD layer. Note that, an amount of hydrocarbons at such critical interface can degrade the device performances. ALD-Y_2O_3 was grown by thermal ALD with sequential $Y(EtCp)_3$ and H_2O pulses, and *in-situ* UHV annealing up to 600 ^oC was conducted in another chamber in our system right after the ALD growth. MBE-Y_2O_3 is relatively pure and employed as a reference.

Fig. 1 shows the capacitance-voltage (CV) and quasi-static CV (QSCV) curves for MOSCAPs. The UHV-annealed ALD-Y_2O_3/GaAs was improved with a reduced frequency dispersion (F.D.) in the accumulation/depletion region, and a lowered trap-induced hump in the inversion region. Fig. 2 presents the D_{it} spectra extracted from QSCVs. The UHV-annealed ALD-Y_2O_3/GaAs shows a reduced D_{it}, also hinted by the sharp transition of QSCVs and the narrow gap between QSCVs and CVs. Fig. 3 shows the O 1s core-level spectra, where O-Y is from the stoichiometric Y_2O_3 and O* is from the interfacial Ga-O-Y and the surface Y-O-H.[4] Note that the ratios of O-Y of our 1-nm Y_2O_3 films are significantly higher than the one reported.[5] Upon UHV annealing, the residue O* may be attributed to the interfacial Ga-O-Y with the surface Y-O-H mostly removed. This UHV annealing approach is significant in perfecting ALD-Y_2O_3/GaAs and is applicable to many other material systems.

References:

[1] Y. H. Lin *et al.*, *Appl. Phys. Express* **9**, 081501 (2016).

[2] H. W. Wan *et al.*, *J. Cryst. Growth* **447**, 179 (2017).

[3] T. Yang *et al., Appl. Phys. Lett.* **91**, 142122 (2007).

[4] C. P. Cheng *et al.*, *ACS Omega* **3**, 2111 (2018).

[5] P. de Rouffignac *et al.*, *Chem. Mater.* **17**, 4808 (2005).

Atomic Layer Etching
Regency Ballroom A-C - Session ALE1-WeM
Integration & Application of ALE

Moderators: Bert Ellingboe, Dublin City University, Wei Tian, Applied Materials

8:00am **ALE1-WeM1 ALD and Etch Synergy to Enable the Next Scaling Innovations***,* ***Angelique Raley****, K.L. Lee, X. Sun, Q. Lou, Y.T. Lu, M. Edley, S. Oyola-Reynoso, P. Ventzek, R. Clark, P. Biolsi, H. Masanobu, A. Ranjan,* TEL Technology Center, America, LLC **INVITED**

As logic nodes continue to scale below 7 nm, the back-end-of-line (BEOL) critical pitch has moved to sub-40 nm and is forecasted to scale down to 14 nm according to the latest International Roadmap for Devices and System (IRDS). In addition to the patterning and integration complexities that arise with scaling, pitch reduction has a direct impact on the plasma-processing window. Conventional continuous wave processes can no longer achieve stringent aspect ratio dependent etching (ARDE), selectivity and profile control requirements and have gradually given way to pulsed plasma processes, decoupled process sequence plasmas or remote plasmas to widen the process space. In this talk, we will discuss implementation of atomic layer deposition (ALD) and decoupled or cyclic plasma etch in the BEOL to overcome challenges of mask loss, ARDE, low k damage and LER/LWR and look to future technology enablement with area and topographically selective processes.

ALD processes are achieved by using sequential, self-limiting reactions. ALD technology is widely used to go beyond lithography resolution limits, to increase selectivity and to enable self-alignment. For dielectric etches with fluorocarbon plasma chemistry a decoupled plasma etch process can achieve the benefits of an ARDE free etch with improved mask selectivity.

Integrations combining ALD and etch can yield further improvements in profile such as chamfer control and via CD control which have a direct impact on device reliability and yield. Finally, cyclic combinations of ALD and etch can drive down line width roughness through smoothing benefits of front growth merging and preferential etching of asperities.

8:30am **ALE1-WeM3 On the Role of Individual Etching Components in Selective Atomic Layer Processing: Etch and Deposit to Obtain High Selectivity***,* ***Alfredo Mameli****,* TNO/Holst Center, Netherlands*; F. Roozeboom,* Eindhoven University of Technology and TNO, Netherlands*; P. Poodt,* TNO/Holst Center, Netherlands **INVITED**

In the domain of Atomic Layer Processing both Atomic Layer Etching (ALE) and area-selective Atomic Layer Deposition (ALD) are becoming increasingly popular because of their potential in advancing nanomanufacturing.[1, 2] Yet, the selectivity in terms of layer thickness and defectivity requirements has major limitations to overcome. Here, the combination of selective deposition and etching can play a key role in tackling these challenges.[3, 4] The complementarity of deposition and etching techniques offers great potential for reaching the targeted requirements for advanced applications.

In this presentation, the combination of spatial area-selective ALD using chemoselective inhibitors and interleaved etching steps to increase the process selectivity will be discussed. The focus will be on two different etching steps: the self-limiting etching of the inhibitor and a blanket etch-back step of the growing material. The former enables cyclic selective deposition when using a plasma-based ALD process while the latter allows for further maximizing the selectivity.

Finally, the concept of area-selective ALD combined with etching techniques in an integrated cyclic etch/dep spatial-tool for high-throughput Atomic Layer Processing will be presented.

[1] S. M. George *et al*, *ACS Nano*, **2016**, 10, 4889-4894

[2] A. Mameli *et al*, *ACS Nano*, **2017**, 11, 9303-9311

[3] K. J. Kanarik *et al*, *J. Phys. Chem. Lett.*, **2018**, 9, 4814-4821

[4] F. Roozeboom *et al*, *ECS J. Solid State Sci. Technol.*, **2015**, 4, N5067-N5076

9:00am **ALE1-WeM5 Area-Selective Deposition of TiO_2 on Various Surfaces by Isothermal Integration of Thermal TiO_2 ALD and ALE***,* ***Seung Keun Song****, G.N. Parsons,* North Carolina State University

As transistor size is shrinking, area selective deposition process is becoming more important than before. Atomic Layer Deposition (ALD) and Atomic Layer Etching (ALE) are promising processes for area selective deposition of metallic and dielectric materials as they can deposit and etch nanoscale thickness of thin film conformally. ALD precursors usually have different affinity to solid surfaces, which enables ALD processes to have surface dependent selectivity. For examples, thermal TiO_2 ALD, employing sequential doses of $TiCl_4$ and H_2O, shows initial growth delay on hydrogen-terminated silicon (Si-H) but rapid growth on oxide silicon surface (SiO_2) at 150-190℃. To extend this surface dependent selectivity, we created isothermal integrated ALD/ALE process, where TiO_2 ALD cycles are combined with a few cycles of thermal TiO_2 ALE, employing sequential doses of WF_6 and BCl_3, under isothermal condition. Using the integrated ALD/ALE sequence, we achieve ~ 7 nm of TiO_2 on SiO_2, before noticeable TiO_2 nucleation on Si-H, as determined by SEM, ellipsometry and TEM analysis. Process and materials analysis using in-situ QCM and ex-situ AFM and XPS further confirm our findings. Beyond TiO_2 selectivity on Si/SiO_2 surfaces, some metal surfaces (Cu, Au, Co) showed some extent of initial growth delay during TiO_2 ALD cycles, as observed by in-situ QCM. Thus, TiO_2 selectivity on various kinds of surfaces was also studied with ex-situ XPS, SEM, and ellipsometry. We expect that this demonstrated ALD/ALE process on various surfaces provides useful information about ALD/ALE precursors reactions on various surfaces, and this information offers opportunities to integrate ALD and ALE process with optimum process controls.

9:15am **ALE1-WeM6 Limited Dose ALE and ALD Processes for Local Film Coatings on 3D Structures***, **Thomas Seidel**,* Seitek50*; M. Current,* Current Scientific

The use of limited dose ALE and ALD are described for producing localized film coatings on 3D, non-planar structures such as trenches and fins. Limited dose ALD (LD-ALD) has been described for improved ALD film deposition rate (thickness/unit time)[1] and for local masking applications of DRAM bottle trenches.[2] In this paper we describe Limited Dose Atomic Layer Etch (LD-ALE) to obtain localized films on trenches and fins using various combinations of standard ALD, LD-ALD and LD-ALE. Three cases for localized film coatings are described:

(I) a film localized at the bottom of a trench or fin, by using standard ALD followed by LD-ALE,

(II) a film localized at the center of a trench or fin, using LD-ALD followed by LD-ALE, and

(III) a film localized at the top and bottom of a trench or fin, using ALD followed by LD-ALE, and this in turn followed by LD-ALD.

In case (I), the LD-ALE step is carried out using a prescribed limited ALE precursor modification[3] dose. The limited dose is prescribed to attain the desired local film etching and removal of a specified depth near the top of the non-local feature. As an application example, the local doping at the bottom of a bulk finFETs, is described using doped ALD films[4] at the bottom of a fin to counter dope the base of the fin. Separately, doping the source – drain region at the top of the fin is described. Examples of mask applications on trenches and fins will be described, as well as film localized thickness adjustments. Limited Dose implementation challenges as well as various equipment opportunities are briefly discussed. If experimental demonstrations are available, they will be presented.

1. G.Y. Kim et al, US 7,981,473, “Transient enhanced atomic layer deposition.”

2. T. Hecht, et al, US 7,344,953 B2, “Process for vertically patterning substrates in semiconductor process technology by means of nonconformal deposition.”

3. Lee, Y. et al., Chem. Mater. 28, 7657 (2016). Selectivity in Thermal Atomic Layer Etching Using Sequential, Self-Limiting Fluorination and Ligand-Exchange Reactions.”

4. A.U. Mane, et.al, "Atomic layer disposition of boron-containing films using B_2F_4", J. Vac. Technol. A34(1) (2016).

9:30am **ALE1-WeM7 Formation of Ohmic Contacts to Si using In-situ Chemical Cleaning of the Substrate***, **Sara Iacopetti**,* Technion - Israel Institute of Technology, Israel*; R. Tarafdar, S. Lai, M. Danek,* Lam Research Corp.*; M. Eizenberg,* Technion - Israel Institute of Technology, Israel

The implementation of novel device geometries in CMOS technology such as FinFETs, allowed a further downscaling of the logic nodes to 45 nm and below, reaching nowadays mass production of devices of 7 nm and studies on sub-5 nm nodes. To such feature sizes and complex geometries, the well-established technology of Source and Drain (SD) contacts by metal silicide formation produces bulky contacts that cause short-channel effects, detrimental to the transistor performances. Shallow ohmic contacts must be implemented in the future.

This work focuses on the feasibility of producing ohmic contacts using in-situ chemical cleaning (CC) of the native SiO_2 layer prior to the deposition of the contact metal (Co) without air break. The two main aspects investigated are the amount of Si consumption as a function of heat treatment, and the resultant contact resistivity.

Si blanket wafers were exposed to different number of cleaning cycles (increasing: No CC, CC-, CC+ and CC++); Co was deposited by PVD to isolate the effect of cleaning on the interface. Compositional and microstructural studies were carried by ToF-SIMS, XRD and HRTEM (STEM-EDS) on Si + 30 nm PVD Co, as-deposited and vacuum annealed. The CC removes completely the native oxide but creates a disordered interlayer of 2 nm thickness at the metal/semiconductor interface. Cobalt silicides formation is accelerated as a consequence of the removal of the native oxide, leading to the formation of a Co and Si intermixed layer from 200°C, and the onset of crystalline CoSi and $CoSi_2$ formation as early as 350°C and 450°C, respectively. As the resulting contacts are very thick (> 60 nm for the low thermal budget annealing), the approach to shallow contact fabrication moved to Si(CC) + PVD Co 10nm/TiN 30 nm/Co 200nm, without air break between depositions. The thin silicide formation with annealing of the contacts was checked by TEM and XRD and it follows the same silicide formation as seen in the Si + PVD Co 30nm case.

The contact resistivity was studied by fabrication of structures for transmission line measurement (TLM) by photolithography on Si/Co/TiN/Co, followed by wet or reactive ion etching of the metals. The contacts are ohmic and specific contact resistivities of 10^{-6} Ωcm^2 were measured, higher for the CC++ samples with respect to the non-cleaned and other cleaned samples, suggesting that the disordered interface plays a role as a thin dielectric barrier across the interface.

The ongoing research is focusing on the quantitative study of the interface composition and its influence on the contact resistivity, crucial for moving to an ALD metallization scheme.

9:45am **ALE1-WeM8 SADP Spacer Profile Engineering by Quasi-Atomic Layer Etching***, **Tsai Wen (Maggie) Sung**, C. Yan, H. Chung, J. Lo, D. Desai, P. Lembesis, R. Pakulski, M. Yang,* Mattson Technology, Inc.

As the size of modern device shrinks, self-aligned double patterning (SADP) and quadruple patterning (SAQP) has gained increasing interest in the fabrication of 14nm technology node and beyond. Plasma reactive ion etching (RIE) with inductively coupled plasma (ICP) is a common technique utilized in the SADP/SAQP process flow because of its etch anisotropy and tunability. Higher bias power is usually employed to achieve sufficient directionality; however, it can lead to sloped, sharp, and asymmetric spacer profiles. These undesired profiles may cause inadequate pattern transfer and the error may be amplified as it moves down the process line, such as pitch-walking and nonuniform fin formation. Furthermore, a high bias power can also severely damage the bottom substrate due to strong ion bombardment, resulting in an uneven etch. Recently, a method for quasi-atomic layer etching (QALE) was developed where it was found that the reactivity of a material increased with exposure to an active species.[1]

In this work, a chemical dry etch (CDE) equipment with an ICP radical source and a capacitively coupled plasma (CCP) plasma source was utilized to perform QALE. A RF bias was applied to the substrate to produce highly selective radicals and to promote vertical implantation of the active species into the top surface of SADP spacers. The implantation “activates” the spacer top surface by increasing its etch rate during a subsequent etch step, while keeping the etch rate of the unexposed sidewalls at a minimum, thereby improving the etch anisotropy. The activation-etch process is self-limiting and the etch depth scales linearly with the activation-etch cycles. By modulating this QALE method, we successfully demonstrated a significant reduction of the spacer shoulder slope and tip angle, thus flattened the spacer profile. Moreover, the QALE technique can be further developed and utilized to engineer the spacer surface profile and applied in other device fabrication processes.

[1]S.D. Sherpa and A. Ranjan, J. Vac. Sci. Technol. A **35**, 01A102 (2017).

Atomic Layer Etching
Regency Ballroom A-C - Session ALE2-WeM

Materials Selective ALE

Moderators: Fred Roozeboom, Eindhoven University of Technology and TNO, Geun Young Yeom, Sungkyunkwan University

10:45am **ALE2-WeM12 Dynamic Temperature Control Enabled Atomic Layer Etching of Titanium Nitride***, **He Zhang**, Y.S. Kim, D. Paeng,* Lam Research Corp.

TiN ALE was achieved with Rapid Thermal Sources using O_2 plasma and Cl_2. TiN surface was oxidized to TiO_2 and the following Cl_2 flow absorbed Cl on the oxidized surface. This modified layer can be thermally removed under intense light source irradiation. Full removal of few nm blank ALD TiN layer is demonstrated. XPS observed surface composition change after each step. Surface smoothen was also observed after etching. The ultra-short thermal pulses enabled fine control of surface reactions in each ALE steps. Thermal ALE of Ge under similar approach will also be discussed.

11:00am **ALE2-WeM13 Rapid Thermal-Cyclic Atomic Layer Etching of Thin Films with Highly Selective, Self-Limiting, and Conformal Characteristics***, **Kazunori Shinoda**,* Hitachi, Japan*; H. Kobayashi,* Hitachi*; N. Miyoshi, M. Izawa,* Hitachi High-Technologies*; K. Ishikawa, M. Hori,* Nagoya University, Japan **INVITED**

Etching processes with atomic level precision are important in order to provide next-generation of semiconductor devices that have densely arrayed high-aspect-ratio structures. There is thus considerable interest in the development of isotropic atomic layer etching (ALE) for a variety of materials used in semiconductor manufacturing. One approach for isotropic ALE is rapid thermal-cyclic ALE, which consists of cyclic repetitions

of plasma exposure at lower temperature and infrared (IR) lamp annealing. The plasma exposure produces self-limiting modified layers on the surface of the target materials, and the IR lamp annealing removes the modified layer by thermal desorption. The authors demonstrated rapid thermal-cyclic ALE of a variety of materials such as Si_3N_4, SiO_2, TiN, and W over the last several years.

Rapid thermal-cyclic ALE processes were originally developed on the basis of an understanding of plasma-surface reactions using in-situ analysis. As for Si_3N_4, in-situ x-ray photoelectron spectroscopy (XPS) analysis revealed that hydrogen and fluorine containing plasmas produce a self-limiting layer of ammonium hexafluorosilicate on the surface of Si_3N_4. Thermal desorption spectroscopy (TDS) analysis showed that lamp annealing decomposes the ammonium hexafluosilicate into SiF_4, HF, and NH_3. The result of TDS is consistent with the result of thermodynamic calculation of the decomposition of ammonium hexafluorosilicate. This technology is also applicable to other nitride films besides Si_3N_4. The authors have demonstrated self-limiting isotropic ALE of TiN using this technology.

A 300-mm ALE apparatus that consists of an inductively coupled plasma (ICP) source for downflow radicals, IR lamps for rapid thermal annealing, and in-situ ellipsometry for thickness monitoring was developed for rapid thermal-cyclic ALE. A self-limiting nature in both the plasma exposure step and the lamp annealing step has previously been demonstrated for Si_3N_4, TiN, and W. Conformal, highly selective etching for patterned samples was confirmed by transmission electron microscopy (TEM). Layer by layer ALE for Si_3N_4 of more than 100 cycles was confirmed by in-situ ellipsometry. Moreover, it was demonstrated that etching selectivity between different materials could be switched from infinitely selective to nonselective by adjusting the lamp annealing time. In this talk, applications of rapid thermal-cyclic ALE for a variety of dielectric and metal films will be presented.

11:30am **ALE2-WeM15 Atomic Layer Etching of HfO_2 with Selectivity to Si by Utilizing Material-Selective Deposition Phenomena***, **Kang-Yi Lin**, C. Li,* University of Maryland*; S. Engelmann, R.L. Bruce, E.A. Joseph,* IBM T.J. Watson Research Center*; D. Metzler,* IBM Research - Albany*; G.S. Oehrlein,* University of Maryland

Atomic layer etching (ALE) applies sequential deposition, reactant purge and etching steps with a short processing step length to establish self-limited material removal and atomic scale precision. The reactants during the ALE deposition steps may exhibit material-selective deposition based on the chemical affinity of precursor gases to the substrate material and nature of interfacial bonding. Integrating the feature of material -selective deposition with an etching step opens a new processing window for selective ALE. In this work, we evaluated the deposition behaviors of different hydrofluorocarbon (HFC) precursors, i.e. mixtures of methane (CH_4) with trifluoromethane (CHF_3) and mixtures of methane with octafluorocyclobutane (C_4F_8), on Si and HfO_2 surfaces, respectively. This is followed by the investigation of substrate-dependent selective deposition using a mixture of HFC precursors to achieve HfO_2 etching and etching selectivity relative to Si. Our results show that during the purge step of ALE sequences using CH_4/CHF_3 selectively deposit a fraction of a nm thick FC layers on Si surface while self-desorption is observed on the HfO_2 surface . In contrast, mixtures of CH_4 with C_4F_8 etchant do not show this self-desorption behavior for HfO_2. By utilizing the selective deposition behavior seen for CH_4/CHF_3-based ALE in conjunction with low energy Ar ion bombardment, we were able to remove the top HfO_2 layer while simultaneously forming a FC passivation layer on the underlying Si surface. In order to confirm the etching performance of CH_4/CHF_3-based ALE of HfO_2, X-ray photoelectron spectroscopy (XPS) was used to study whether any HfO_2 remains on the sample at the end of the processing cycle where the in-situ ellipsometry indicated a depletion of the HfO_2 layer . The XPS results show that after the ALE processing the Hf-O peaks no longer exist in the Hf4f and O1s spectra. Instead, a weak intensity of the fluorinated Hf peaks are observed, suggesting the HfO_2 layer with an initial thickness of 2.9 nm was removed and a few hafnium etching byproducts were left on the substrate. These results support the concept that gas pulsing of complex HFC precursors during ALE sequences provides the opportunity to achieve material-selective deposition and enable ALE selectivity of HfO_2 relative to Si.

11:45am **ALE2-WeM16 Enhancing Etch Selectivity in Plasma-Assisted ALE of Silicon-Based Dielectrics using Surface Functionalization***, **Ryan Gasvoda**,* Colorado School of Mines*; S. Wang, E. Hudson,* Lam Research Corp.*; S. Agarwal,* Colorado School of Mines

Stringent processing windows are required for the fabrication of sub–7–nm semiconductor devices, which in turn places severe constraints on conventional plasma-–assisted etching. Atomic layer etching (ALE) is a promising etching technique that can provide high etch fidelity, directionality, layer–by–layer removal, and selectivity to meet the stringent processing demands. Plasma–assisted ALE of SiO_2 and SiN_x typically consists of two sequential half–cycles: fluorocarbon (CF_x) deposition from a fluorocarbon plasma followed by an Ar plasma activation step. Typically, selectivity is achieved through manipulating the plasma and processing parameters. Recently, we proposed a methodology to further increase etch selectivity by selective prefunctionalization of the SiO_2 or SiN_x surface with hydrocarbons. We show that the abundance of hydrocarbon on the prefunctionalized surface promotes the formation of an etch inhibiting graphitic carbon film after just a few ALE cycles.

In this study, we used *in situ* attenuated total reflection Fourier transform infrared (ATR–FTIR) spectroscopy and *in situ* 4–wavelength ellipsometry during ALE to monitor the surface reactions, film composition, and net film thickness. We show that cyclic azasilanes can be used to selectively functionalize SiO_2 over SiN_x. Figure 1 shows the infrared spectra after 5 ALE cycles of SiO_2 etching with (blue) and without (black) surface prefunctionalization. For the prefunctionalized surface, we observe an increase in absorbance from ~1500 – 1800 cm^{-1}, assigned to a graphitic hydrofluorocarbon film. After just 4 ALE cycles, this graphitic hydrofluorocarbon film reaches a thickness that acts as an etch stop layer. As a result, after 10 cycles, the etched thickness of SiO_2 was ~23% of the case where there was no surface functionalization. This methodology can therefore be used to enhance overall etch selectivity for SiN_x over SiO_2. Further, we will discuss the role of Ar^+ ion energy during the Ar plasma activation step on graphitic hydrofluorocarbon film formation. The length and structure of the hydrocarbon chain on the prefunctionalized surface will also be addressed.

ALD for Manufacturing
Grand Ballroom E-G - Session AM1-WeM
Spatial ALD, Fast ALD, and Large-Area ALD

Moderators: John F. Conley, Jr., Oregon State University, Paul Poodt, TNO/Holst Center

8:00am **AM1-WeM1 Impact of Operating Parameters on Precursor Separation in "Air Hockey" Spatial Atomic Layer Deposition Reactor***, **John Grasso**, B. Willis,* University of Connecticut

A defining characteristic of atomic layer deposition (ALD) is the sequential exposure of a surface to self-limiting, saturating reactions. Temporal ALD operates through intermittent purge cycles, while spatial ALD relies on physical separation accomplished by delivering reactants through a deposition head located in close proximity to the substrate's surface. An inert gas stream placed between precursors acts as a diffusional barrier to prevent mixing. A dysfunctional barrier results in gas phase reaction and non-ALD growth. To understand the impact system parameters have on the efficiency of the gas barrier, this work presents a COMSOL Multiphysics study of the fluid dynamics and concentration diffusion for the system.

We present a case study for ALD of alumina by trimethylaluminum (TMA) and water using a novel spatial ALD system analogous to an air hockey table. In contrast to other spatial ALD reactors that are limited by mechanical constraints, dispersed nitrogen inlets float a substrate overtop an injector region to deposit films within a deposition gap of less than 100 µm. The flotation height, or deposition gap, is a function of the fluid pressure underneath the substrate. An accurate height estimation from the parameters is necessary to evaluate the efficiency of the gas barrier. *In-situ* -height measurements are used to validate the COMSOL model, and the results are in good agreement for different operating conditions.

This work investigates how diffusivity, deposition gap, inert flow rate, and geometric design influence the effectiveness of precursor separation by evaluating the concentration of the precursors at the substrate surface. Small deposition gaps prevent precursor intermixing, however the diffusional barrier is not effective when the inert flow rate is low. Specifically, high diffusivity enables the precursors to readily diffuse beyond their ideal zone, cause gas phase reactions, and lead to CVD

growth. Additionally, the uniform surface exposure of reactant is altered, leading to non-uniform growth at the edges of the deposition area. Successful precursor separation can be achieved at large flotation heights when the inert flow is large; however, the precursor concentration at the surface becomes low. These conditions may lead to insufficient saturation of the surface and non-ideal ALD growth. Stationary deposition experiments are utilized to demonstrate the ability of the model to predict non-ALD behavior. Additionally, the geometric design of the reactor plays a critical role in preventing precursor intermixing.

8:15am **AM1-WeM2 Plasma Enhanced Spatial ALD of Silver Thin Films at Atmospheric Pressure***, **Tim Hasselmann**,* University of Wuppertal, Germany*; N. Boysen,* Ruhr University Bochum, Germany*; D. Theirich,* University of Wuppertal, Germany*; A. Devi,* Ruhr University Bochum, Germany*; T. Riedl,* University of Wuppertal, Germany

A wide range of opto-electronic devices, such as solar cells and light emitting diodes, require electrodes that are highly conductive and at the same time transparent. Ultra thin (thickness < 10 nm) silver (Ag) films can provide these properties.[1,2] Plasma enhanced atomic layer deposition (PE-ALD) would be a suitable coating technique that allows for homogenous film growth on large areas at low temperatures with precise thickness control. Since ALD is originally a vacuum based technique, limitations towards high throughput processing and low-cost manufacturing occur. These drawbacks can be overcome by spatial PE-ALD at atmospheric pressure.[3] In our earlier work, we have shown outstanding (conductive) gas diffusion barriers and more recently, the growth of Ag films from a novel halogen-free precursor, by spatial PE-ALD at atmospheric pressure.[4-6] In this work, we provide detailed growth studies of Ag thin films grown from this novel 1,3-di-tert-butyl-imidazolin-2-ylidene silver(I) 1,1,1- trimethyl-N-(trimethylsilyl) silanaminide [(NHC) Ag(hmds)] precursor by spatial PE-ALD. An atmospheric pressure dielectric barrier discharge with Ar/H_2 as working gas is used. Saturating behavior with growth rates of about $2.4x10^{14}$ atoms/(cm^2 cycle) (corresponding to an equivalent of 0.42 Å/cycle), determined by RBS, at a very low deposition temperature of 100°C is shown, with only small amounts of residual carbon (~1.5 at.%) and Si (~0.8 at.%) in the films. Percolated and conductive Ag films with a low sheet resistance of 0.9 Ω/sq (resistivity: 10^{-5}Ωcm) are demonstrated. Furthermore, the influence of the deposition temperature in a range from 80°C to 120°C on the growth characteristics is discussed. All results are compared to those obtained from the more established precursor [Ag(fod)(Pet_3)] (FOD).[7] The prospects to use these ALD grown Ag layers to create highly conductive electrodes for perovskite solar cells are discussed.

[1] K. Zilberberg et al., J. Mater. Chem. A 4, 14481–14508 (2016)

[2] Y. J. Yun et al., Adv. Funct. Mater. 27, 1701513 (2017)

[3] P. Poodt et al., J. Vac. Sci. & Technol. A 30, 01A142 (2012)

[4] L. Hoffmann et al., ACS Applied Mater. & Interfaces 9, 4171 (2017)

[5] L. Hoffmann et al., J. Vac. Sci. & Technol. A 36, 1, 01A112 (2018)

[6] N. Boysen et al., Angew. Chem. Int. Ed. 57(49) 16224-16227 (2018)

[7] M. Kariniemi et al., Chem. Mater., 23(11), 2901–2907. (2011)

8:30am **AM1-WeM3 Low Temperature Spatial PEALD of Silicon Nitride Films from Aminosilane Precursors and DC Direct Plasma***, **Eric Dickey**,* Lotus Applied Technology **INVITED**

PEALD of silicon nitride using aminosilane precursors in combination with N_2, N_2:H_2, or NH_3 plasma has been widely studied in recent years. Most of this research has been conducted in conventional pulse-purge reactors, employing RF plasma from either indirect Inductively Coupled Plasma (ICP) or direct Capacitively Coupled Plasma (CCP). While the use of RF plasma is a necessity for pulse-purge ALD reactors, Spatial ALD provides an opportunity to use a simple DC direct plasma. This is due to the fact that most interior surfaces of the reaction chamber, including the plasma electrode, are not coated with the dielectric film, as growth occurs only on the surfaces that are exposed to both the plasma and the precursor. In this work, a spatial ALD system incorporating a rotary disc substrate holder and DC diode plasma was used to deposit silicon nitride at temperatures between 300 and 350°C, from bis(diethylamino)silane (BDEAS), bis(tertbutylamino)silane (BTBAS), diisopropylaminosilane, (DIPAS), and "New SAM" supplied by Air Liquide. N_2 and N_2:H_2(4%) were used as the plasma gas, with an operating pressure between 0.5 and 1.2 Torr. Refractive index values as high as 2.14 at 633nm were attained, and wet etch rates in dilute hydrofluoric acid (1%) as low as 1 nm per minute were measured. RBS compositional analysis for stoichiometry and contamination was performed on a subset of samples, and showed significant variation depending on the precursor and plasma gas used.

9:00am **AM1-WeM5 Development and Characterization of an Atmospheric Pressure Plasma Reactor Compatible with Open-Air Spatial ALD***, H. Rabat, F. Zoubian, O. Aubry, N. Dumuis, S. Dozias,* GREMI Université d'Orléans/CNRS, France*; C. Masse de la Huerta, A. Sekkat, V.H. Nguyen,* LMGP Grenoble INP/CNRS, France*; M. Bonvalot, C. Vallée,* LTM-UGA, France*; D. Hong,* GREMI Université d'Orléans/CNRS, France*; **David Muñoz-Rojas**,* LMGP Grenoble INP/CNRS, France

Dielectric Barrier Discharges (DBD) are widely used for atmospheric pressure plasma generation. The possibility of their adaptation in custom-made configurations makes them potential candidate to assist deposition processes. In fact, the increased need of high-quality thin films forces to improve the deposition techniques. New processes should be able to work in less constrained conditions such as atmospheric pressure rather than vacuum and to have faster deposition rates while respecting the same high quality of the deposited films. In this paper we present the development of a surface dielectric barrier discharge plasma reactor to assist an atmospheric spatial atomic layer deposition process. The plasma was generated by a surface dielectric barrier discharge powered by a microsecond pulsed high voltage power supply. The dissipated power was measured for different configurations, and thanks to the micro discharges imaging, it was observed that the thickness and the shape of the dielectric barrier influenced the micro discharges distribution on the dielectric surface. The plasma reactor exhaust gas was chemically analyzed by FTIR spectroscopy and micro gas chromatography. The ozone concentration was determined as function of frequency of the power supply. Initial results of utilization of the new compact atmospheric plasma head to deposit functional materials by open-air high-throughput plasma-activated SALD will be provided.

9:15am **AM1-WeM6 Fast Plasma ALD Employing de Laval Nozzles for High Velocity Precursor Injection***, **Abhishekkumar Thakur**, J. Sundqvist,* Fraunhofer Institute for Ceramic Technologies and Systems IKTS, Germany*; S. Wege,* Plasway Technologies GmbH, Germany

ALD based self-aligned multiple patterning (SAxP) has been the key process to continued chip scaling. SAxP demands PEALD for low temperature and conformal deposition of spacers on photoresist features for the subsequent etch based pitch splitting. ALD is limited by low thru put that can be improved by raising the growth per cycle (GPC), using new ALD precursor, preforming batch ALD or fast Spatial ALD, shrinking the ALD cycle length, or omitting purge steps to attain the shortest possible ALD cycle. Today's latest and highly productive platforms facilitate very fast wafer transport in and out of the ALD chambers. Current 300 mm ALD chambers for high volume manufacturing are mainly top-down or cross-flow single wafer chambers, vertical batch furnaces, or spatial ALD chambers.

In our research developing fast PE ALD processes, we use top down gas flow via showerhead to ignite a 60 MHz plasma (CCP) in a 300 mm chamber. The chamber has been modified to attain ultra-short (≤10 ms) ALD precursor pulses along with good uniformity using a ring injector (WO2017194059A1) with integrated de Laval nozzles enabling high speed, all-round precursor injection across the wafer. We used the well-known TMA-O_2 PEALD process to deposit Al_2O_3 for the hardware development and the productivity benchmarking.

Initially we used a single capillary injector for PEALD of Al_2O_3 at room temperature (30 °C), wherein we shrunk the TMA pulse length from 2000 ms down to 15 ms maintaining the constant 1.7 Å GPC (Fig. 1), which confirmed the self-limiting nature of the TMA half-reaction. With the de Laval ring injector the saturation started at 10 ms of TMA pulse length (Fig. 2), which is the tested switching limit of the electro-pneumatic ALD valve. The process linearity (Fig. 3) and the saturation curve indicated the ALD nature of the process. For 50 ms of TMA pulse, a wide ALD temperature window (30-120 °C) with constant 1.3 Å GPC was extracted (Fig. 4). Even with very short pulses we achieved a very good uniformity from wafer center to the edge. XPS analysis of the deposited Al_2O_3 indicated that the film deposited at 120 °C were more oxidized than the films at 30 °C with the single injector. However, the elemental composition for films deposited with TMA pulse of 10 ms vs. 50 ms was indistinguishable. A surface carbon contamination (Table 1) was observed due to the wafer exposure to the outer atmosphere post processing. However, angular XPS depth profiling revealed no detectable amounts of carbon in the "bulk of the film". The complete ALD process optimization results including plasma pulse optimization, conformality and 300 mm wafer scale uniformity will be presented at the conference.

9:30am **AM1-WeM7 Development of a Meter Scale ALD Optical Coating Tool for Astronomical Mirror (and other) Applications***, D. Fryauf,* University of California Santa Cruz*; A. Phillips,* University of California Observatories*; A. Feldman,* Structured Material Industries, Inc.*; N. Kobayashi,* University of California Santa Cruz*; **Gary Tompa,*** Structured Material Industries, Inc.

Atomic Layer Deposition (ALD) is best known for depositing electronic device films, but it also offers great promise for producing transparent barrier films on optics - such as large concave metal-coated astronomical observatory telescopic mirrors. To date, ALD coatings on mirrors has been limited to relatively small-sized optics and certainly not ones with their mounting hardware attached. We have designed, constructed, and tested a new ALD tool to apply uniform ALD coatings on planar and curved substrates up to 1m in diameter. The new tool has been named the Meter Scale ALD (MS-ALD) tool. The MS-ALD tool employs a unique chamber design that isolates a large substrate surface to be coated by utilizing the substrate itself as an internal wall of the process chamber. This configuration allows the backside of the optic to be isolated from the front side process environment allowing robust transparent uniform protective dielectric coatings to be grown on telescope mirrors with their backside support hardware in place. Conceptual design, modeling, implementation, results, scalability, and future direction of this new tool are discussed for coating large astronomical telescope optics, specifically protective coatings for aluminum and silver surfaced mirrors as well as other future large structures and, ultimately, semiconductor wafers. To demonstrate the potential of this new design, aluminum oxide has been deposited by thermal ALD using trimethylaluminum and water at a reaction temperature of 60°C. Growth rates, dependence on precursor pulse times, and chamber purge times, show that the two half-reactions occur in a saturated regime, matching characteristics of ideal ALD behavior. The aluminum oxide deposition process parameters of the MS- ALD are compared with those of a conventional 100 mm wafer-scale ALD tool. Saturated ALD growth was realized with a simple scaling factor applied to precursor pulse and purge times. Growth was demonstrated using more than fifty 100 mm diameter wafers mounted on a glass substrate to represent a meter scale mirror. The results show promising application of transparent robust dielectric films as uniform barriers across large, and at times complex, optical components at the meter scale are now possible.

9:45am **AM1-WeM8 From Wet-lab to Cleanroom: An Integrated ALD-CVD Process for the Large-area Deposition of Ultrathin Zeolitic Imidazolate Framework Films***, **Ivo Stassen**, A.J. Cruz, R. Ameloot,* KU Leuven, Belgium

Robust and scalable thin film deposition methods are key to realize the potential of the combined nanoporosity and hybrid organic-inorganic chemical modularity of metal-organic frameworks (MOFs) in electronic devices [1]. Here, we report the first fully integrated and highly-controllable vapor deposition process for MOFs (MOF-CVD) [2], as recently implemented in a 200 mm modified commercial ALD reactor. The process consists of two-steps: (1) atomic layer deposition for the metal oxide precursor, and (2) subsequent stop-flow reaction with the sublimated organic linker at elevated pressure and non-isothermal temperature conditions. As our selected test case, the optimized MOF-CVD process for ZIF-8 (zinc-2-methylimidazolate) showcases smooth, pinhole-free and large-area uniform ultrathin films that are highly nanoporous. Our process distinguishes itself from previous works as it permits single-chamber deposition, under mild conditions and without the need for a separate post-deposition crystallization steps; to the best of our knowledge, it is the only MOF thin film deposited *via* an integrated ALD-CVD method on large area substrates to date. Through its implementation in a single-chamber, the MOF-CVD reaction mechanism was studied using a combination of time-resolved *in situ* ellipsometry and QCM monitoring, and *ex situ* thin film characterization techniques. We will present the impact of relevant deposition parameters in the form of a MOF-CVD deposition-rate process chart. Our method shows great promise to ease the manufacturing of devices based on MOF thin films, as will demonstrated by a sneak preview of ongoing application projects.

[1] Stassen, I., Ameloot R., *et al.* An updated roadmap for the integration of metal–organic frameworks with electronic devices and chemical sensors. Chem Soc Rev 46, 3185–3241 (2017).

[2] Stassen, I., Ameloot R., *et al.* Chemical vapour deposition of zeolitic imidazolate framework thin films. Nat. Mater. 15, 304–310 (2016).

Emerging Materials
Grand Ballroom A-C - Session EM1-WeM

Molecular Layer Deposition

Moderators: Stacey F. Bent, Stanford University, Charles L. Dezelah, ASM

8:00am **EM1-WeM1 Molecular Layer Deposition of Titanicone Films using TiCl and Fumaric or Maleic Acid: Growth Mechanism and Ambient Stability***, **Yan-Qiang Cao**, A.-D. Li,* Nanjing University, China

Atomic layer deposition (ALD) has been widely used for synthesizing a myriad of inorganic materials. With the development of ALD, it was also used to deposit a relatively new class of organic-inorganic hybrid films, called as molecular layer deposition (MLD) due to the molecular nature of the deposition process. Although MLD has prepared some types of organic-inorganic hybrid films, it is still in its infancy now. Compared to inorganic precursors, organic precursors for MLD have much more selections in the functional groups, chain backbone, chain length and molecular structure. Moreover, there are a special group of organic molecules called isomers, which possess the same functional groups and backbones with different structures. To date, the research about organic isomer precursors on MLD growth is rather rare.

Therefore, this work systematically investigated the effect of organic precursors of isomer of fumaric acid (FA) and maleic acid (MA) on MLD growth and stability of inorganic-organic hybrid films of titanicones. T itanicones films were fabricated by MLD using $TiCl_4$ and FA or MA at various growth temperatures. It was found that the *cis*-/*trans* configurations of organic precursors can influence the MLD growth behavior, the preference for bonding mode and ambient stability of hybrid films. $TiCl_4$-MA and $TiCl_4$-FA MLD processes exhibit quite different growth mechanism. The composition ratio of C : O : Ti of Ti-MA films from X-ray photoelectron spectroscopy (XPS) analyses has little change with deposition temperature, whereas Ti-FA shows the temperature dependent composition. Moreover, both *ex situ* XPS and *in situ* quartz crystal microbalance (QCM) demonstrate that the as-deposited MLD Ti-MA hybrid films are consisted of inorganic Ti-O-Ti units and organic-inorganic Ti-MA units. In addition, density function theory (DFT) calculation was performed to characterize the possible reaction mechanism of $TiCl_4$-MA MLD process. The DFT results are in accordance well with experiment data. Ti-MA and Ti-FA hybrid films show the preference for bidentate and bridging bonding mode, respectively. Furthermore, the inorganic Ti-O-Ti units in hybrid films can improve ambient stability of Ti-MA hybrid films. As a result, Ti-MA hybrid films are much more stable in open air for one year than Ti-FA ones. These results are very important for understanding the MLD process and choosing proper organic precursors.

8:15am **EM1-WeM2 Temperature Dependent Surface Chemistry in Molecular Layer Deposition of Polyimide on Cu and Si***, **Chao Zhang**, M. Leskelä, M. Ritala,* University of Helsinki, Finland

Polyimides (PIs), a class of high-performance polymers widely used in semiconductor industry, exhibit excellent electrical, mechanical and thermal properties[1]. PIs have been originally prepared by solution-cast method. However, solvent-free processes with capability to deposit high-quality PI films with precisely controlled thickness are needed in thin film device fabrication. So, molecular layer deposition (MLD) of PIs as an alternative approach has been getting more attention lately.

In this work, MLD growth of PI was first compared on Cu and Si substrates by using 1,6-hexanediamine (DAH) and pyromellitic dianhydride (PMDA) as precursors at deposition temperatures of 170-220 ^{o}C (Fig. 1). At 170-180 ^{o}C the PI growth rate on Si is around 5 Å/cycle and close to 4 Å/cycle on Cu. On the other hand, at higher temperatures from 200 to 210 ^{o}C much more PI was deposited on Cu with a growth rate of 7-8 Å/cycle whereas only a tiny amount of PI was grown on Si. The significant contrast of the PI growth rate on Cu and Si at 200 ^{o}C shows potential for area-selective MLD, which also encourages us to explore further the surface chemistry of PI MLD on Cu and Si. Based on our study with ATR-FTIR, XRD, AFM and XPS a surface reaction mechanism is proposed for the PI growth on Cu and Si at 170 and 200 ^{o}C. For the PI MLD on Si (Fig. 2 a), cyclic PI formation can be accomplished via two pathways[2-4]: 1) reversible amidization (step 1) followed by imidization (step 4); 2) the same amidization (step 1) but different imidization with inter-chain polyimide forming as intermediate (step 2, 3). After the rapid amidization there is a competition between the reversed amidization (precursor re-evaporation) and imidization (cyclic PI formation). At 170 ^{o}C imidization dominates while at 200 ^{o}C reversed amidization dominates resulting in minor PI film growth on Si. On Cu (Fig. 2 b), the resulting films consist of not only cyclic PI but also inter-chain PI

since Cu ions can diffuse into the deposited film and further catalyze and/or stabilize the inter-chain polyimide by forming metal-organic complexes with the partially ordered system inside. However, at 170 °C ring-closed imidization seems to dominate, whereas at 200 °C inter-chain PI formation dominates.

References:

[1] G. Maier, Progress in Polymer Science **26,** 3 (2001).

[2] E. Sacher, Journal of Macromolecular Science, Part B **25,** 405 (1986).

[3] J. H. Jou and P. T. J. M. Huang, **24,** 3796 (1991).

[4] E. Spassova, Vacuum **70,** 551 (2003).

8:30am **EM1-WeM3 Integrated MLD Supercycle for the Direct Deposition of Zeolitic Imidazolate Framework Films***, **Alexander John Cruz**, I. Stassen, R. Ameloot,* KU Leuven, Belgium

Intrinsic nanoporosity and synthetic tunability position nanoporous materials, such as metal-organic frameworks (MOFs) at the center-stage of some emerging applications in microelectronics [1]. For example, these materials have shown promising properties for device integration ranging from gas sensing to low-k dielectrics for future logic microprocessors. Essential for capitalizing on the disruptive potential of MOFs on such device-oriented valorization is a solvent-free process for the deposition of ultrathin, defect-free films with unprecedented control over thickness and properties [2]. We herein present an ongoing proof-of-concept study on the direct molecular layer deposition of thermally and chemically stable nanoporous MOF films using a modified commercial ALD/MLD reactor. In our ZIF-8 (zinc-2-methylimidazolate) test case, sequential reactions of diethylzinc, water, and 2-methylimidazole are assembled into a supercycle to yield layer-by-layer deposition of films that are crystalline and nanoporous as-synthesized, in the absence of separate post-deposition treatments. To explore a variety of chemical handles for molecular-level control of the thickness and film characteristics, we introduced modulators such as water, methanol and ethylene glycol during different stages of the supercycle by means of ALD pulses. The present contribution will highlight our most recent works on MLD ZIF-8 and a brief introduction on a catalog of new MOF chemistries *via* integrated ALD-MLD-CVD processes, as well as a demonstration of potential integration routes to applications in microelectronics. Furthermore, we will elaborate the steps on how we took advantage of *in situ* ellipsometry and QCM in combination with complementary *ex situ* techniques for unraveling mechanistic insights into the reaction-crystallization processes. We will clarify and explain optimization guidelines and high-level design rules on how to implement MOF-MLD formulations to other laboratory setups and fabrication facilities.

[1] Stassen, I., Ameloot R., *et al.* An updated roadmap for the integration of metal-organic frameworks with electronic devices and chemical sensors. Chem Soc Rev 46, 3185–3241 (2017).

[2] Stassen, I., Ameloot R., *et al.* Chemical vapor deposition of zeolitic imidazolate framework thin films. Nat. Mater. 15, 304–310 (2016).

8:45am **EM1-WeM4 Understanding Molecular Layer Deposition Nucleation Mechanisms in Polyurea via Time Domain Thermoreflectance***, **Rachel Nye**, M. Fusco,* North Carolina State University*; E. Radue, A. Kelliher, P. Hopkins,* University of Virginia*; G.N. Parsons,* North Carolina State University

Despite the high utility of molecular layer deposition (MLD) polymer films in applications such as sensors and electronics, the underlying chemistry behind these processes remains unclear. While the effects of active site termination, polymer chain orientation, and monomer absorption are areas of current interest to understanding MLD growth mechanisms, the role of diffusion in polymer films has not yet been considered. This is due to lack of an efficient analytical approach to understanding diffusion mechanisms. To address this issue, we introduce a technique new to the field, time domain thermoreflectance (TDTR), to explore the possibility of monomer diffusion as an alternate growth mechanism to previously reported linear or absorption mechanisms.

Polyurea films are deposited from p-phenylene diisocyanate (PDIC) and ethylenediamine (ED) or hexanediamine (HD) to provide different polymer compositions. Traditional MLD analysis techniques including atomic force microscopy (AFM), spectroscopic ellipsometry, and Fourier Transform infrared spectroscopy (FTIR) are used to characterize surface roughness, growth characteristics, and chemical composition, respectively. AFM results indicate the presence of two different growth regimes based on trends in surface roughness versus cycle number. At small cycle numbers, surface roughness increases with film thickness, indicating nonconformal growth on isolated nucleation “islands”. After approximately 50 cycles (20 nm), surface roughness decreases, indicating conformal film growth due to the convergence of islands. Further investigation into these regimes is performed with picosecond acoustics data from TDTR measurements, which has not previously been available for MLD films. Our results demonstrate that the speed of sound increases with increasing film thickness, hence the film’s density decreases. Both the decrease in density and surface roughness can be explained by monomer diffusion from the surface into the bulk polymer film after the film reaches a certain threshold thickness. These findings provide a basis for understanding and characterizing monomer diffusion in organic/hybrid films, which will ultimately clarify the overall growth mechanisms of MLD processes.

9:00am **EM1-WeM5 Molecular Layer Deposition of Indicone Thin film using Indium Precursor and Hydroquinone***, **Seung-Hwan Lee**, G.H. Baek, J.-H. Lee,* Hanyang University, Republic of Korea*; T.T. Ngoc Van, B. Shong,* Hongik University, Republic of Korea*; J.-S. Park,* Hanyang University, Republic of Korea

Flexible electronics are obtaining attention for potential to be used in various applications because of their light, thin, conformable design advantages.[1] However, most inorganic materials have limitations to be used for flexible devices due to high elastic modulus and weakness on external stress or strain, regardless of their superior electrical properties. On the other hand, organic materials are often elastic so that they are resistant to external stress or strain, but with poor electrical performance. Therefore, hybrid materials combining advantages of organic and inorganic materials are are of much research interest. Molecular layer deposition (MLD) is a promising technology for deposition of organic and organic-inorganic hybrid thin films for conformality and excellent thickness controllability.[2] In this work, indicone thin films containing indium and organic diol linkage are deposited by MLD. [1,1,1-trimethyl-N-(trimethylsilyl)-silanaminato]-indium (InCA-1) and hydroquinone (HQ) are used as the indium and the organic precursor, respectively, at deposition temperature between 100-250℃. The MLD properties are demonstrated from growth behavior; Fourier transform infrared (FTIR) spectroscopy and X-ray photoelectron spectroscopy (XPS) are used to analyze the chemical characteristics in the material. Density functional theory (DFT) calculations are utilized to investigate the chemical mechanism of the deposition reaction. Indium-based hybrid films are grown by supercycles of indium oxide atomic layer deposition (ALD) and indicone MLD. Structural, optical and electrical properties with respect to the super-cycle ratio are investigated. As the fraction of indicone incorporated in the hybrid films increases, crystallinity decreases while electrical resistivity increases. The hybrid film, which has 99:1 indium oxide and indicone ratio, shows slightly increased resistivity, but shows enhanced resistance toward mechanical deformation compared to pure ALD indium oxide thin films. The hybrid film has superior mechanical property for future flexible devices.

[1] Y. Sun, J.A. Rogers, Inorganic semiconductors for flexible electronics, Advanced materials (2007), 19(15), 1897-1916.

[2] Steven M. George et al, Growth and properties of hybrid organic-inorganic metalcone films using molecular layer deposition techniques, Advanced Functional Materials, (2013), 23, 532

9:15am **EM1-WeM6 Air Stable Alucone Thin Film Deposited by Molecular Layer Deposition using Hetero Bifunctional Organic Reactant***, **GeonHo Baek**, S.-H. Lee, J.-H. Lee, J.-S. Park,* Hanyang University, Republic of Korea

Molecular layer deposition (MLD) is fundamentally a modified Atomic Layer Deposition (ALD) principle, where conformal thin films are fabricated with self-limiting surface reaction chemistry. The ALD/MLD hybrid process makes it possible to deposit thin film by in-situ process only by changing the precursor and to manufacture excellent organic-inorganic hybrid thin films. Many researcher groups reported “metalcone” films using various metal and organic precursors but there are not many studies on hetero bifunctional group organic precursors. [1] Because of its two different functional groups, it has different thin film properties, and this reinforces the moisture-sensitive problems of most MLD films. Therefore, it will be very useful in the application field of the organic thin film.

In this work, we fabricated alucone thin films using Trimethylaluminum (TMA) and 4-mercaptophenol(4MP) by MLD and the properties of the thin films were analyzed as annealing progressed with increasing temperature. In particular, we observed the alucone film characteristics from 4MP with different functional groups of -OH and -SH group. Growth per cycle tends to decrease due to the difference in reactivity between the -OH and the -SH group but it forms a denser thin film due to the bonding angle close to 90°

when bonded to the -SH group. XPS analysis confirmed that some elements including S were reduced during the annealing and SE analysis indirectly confirmed that the film was dense by increasing the refractive index. Annealed alucone film was occurred thermal polymerization in the high temperature region and carbon ring structure trans the graphene flake by graphitization. Raman and XPS analysis carried out various characterization related to carbon. At the annealing temperature of 750°C, the resistance can be measured while changing from insulator to conductor. Annealed MLD alucone thin film as a hybrid semiconducting material has various potential applications such as electronic, capacitor or thermoelectric devices.

reference

[1] Steven M. George et al, Growth and properties of hybrid organic-inorganic metalcone films using molecular layer deposition techniques, Advanced Functional Materials, (2013), 23, 532

9:30am **EM1-WeM7 Molecular Layer Deposition of "Magnesicone", a Magnesium-based Hybrid Material, as a Matrix Material for Solid Composite Electrolytes***, Jeroen Kint, F. Mattelaer, M. Minjauw,* Ghent University, Belgium*; P. Vereecken,* IMEC, Belgium*; J. Dendooven,* ***C. Detavernier,*** Ghent University, Belgium

Porous thin films are a very versatile class of materials for a wide range of applications due to their high (reactive) surface area. Numerous deposition methods are available, yet when conformality on complex 3D structures and sub-nm uniformity and thickness control and are requirements for the envisioned application, these deposition methods often don't meet these demands. Atomic and molecular layer deposition (ALD/MLD) are generally accepted as the go-to methods when conformality, uniformity and sub-nm thickness control are necessary conditions. When the application requires porous films, organic/inorganic hybrids (metalcones) can be deposited using MLD, and with a post-treatment, they can be made porous. This has already been shown for alucones. A wide variety of these metalcones exist, yet no Mg-based flavours are available. In this work, MLD and a post-deposition anneal were used to obtain porous MgO thin films.

A novel magnesium-based organic-inorganic hybrid process was developed using magnesium bis-(methylcyclopentadienyl) and ethylene glycol or glycerol. The growth characteristics of both processes were characterized using in-situ ellipsometry. For both flavours of the magnesicone, saturated growth could be achieved in a broad temperature window (100-250°C). The hybrid nature of these films was confirmed using FTIR and EDX. Exposure of these "magnesicone" films to ambient atmosphere was investigated using FTIR. Both flavours reacted with ambient air, absorbing water.

As deposited magnesicone films were annealed in oxidizing ambient at different heating/cooling rates, while being monitored using real-time spectroscopic ellipsometry (RTSE). The influence of the heating/cooling rates on pore formation was extracted from the changes in refractive index (linked to the density) and the film thickness. Three regimes could be discerned. Firstly, moderate heating/cooling rates lead to porous films (corresponding to a sudden drop in density and increase in porosity). Secondly, it was observed that pores collapse when a rapid cool-down takes place, as seen from an increase in density and a decrease in thickness. Finally, heating at high ramp rates causes no pore formation. These findings were backed up by subsequent ellipsometric porosimetry measurements. For high ramp rates (≥400°C/h), no pores were formed, whereas at lower ramp rates (≤200°C/h) pore formation was confirmed.

A novel process for the deposition of a magnesium-based hybrid organic-inorganic material, "magnesicone" was developed. It's response to different annealing conditions was investigated using RTSE and EP. By doing so, porous MgO films with porosities up to 45% could be achieved.

9:45am **EM1-WeM8 Molecular Layer Deposition of Polyamide Films on Particles Using a Rotating Cylinder Reactor***, **Tyler Myers**, S.M. George,* University of Colorado - Boulder

Molecular layer deposition (MLD) utilizes sequential, self-limiting surfaces reactions to deposit polymeric thin films. Depending on the precursors, the MLD polymeric film can be all-organic or a mixed organic-inorganic hybrid film. In this study, all-organic polyamide MLD films are deposited on particles using adipoyl chloride and ethylene diamine as precursors. This polyamide MLD film is designated as Nylon 6,2. The MLD is performed in a rotating cylinder reactor to agitate the particles. The rotating cylinder reactor is also located inside an isothermal enclosure to eliminate cold spots that cause difficulties when using low vapor pressure precursors.

The polyamide MLD was performed at low temperatures ranging from 37°C to 80°C. These low temperatures allow the polyamide MLD film to be deposited on thermally sensitive organic particles such as pharmaceutical particles. Using witness wafers in the reactor, the sequential adipoyl chloride and ethylene diamine exposures led to a growth rate of 4 Å/cycle at 67 °C for the Nylon 6,2 MLD film as determined by x-ray reflectivity (XRR) measurements. These growth rates were in good agreement with the film thicknesses measured by transmission electron microscopy (TEM) on inorganic particles (ZrO_2 and TiO_2) and organic particles (cellulose and active pharmaceutical ingredients) (See Supplemental Figure 1). The polyamide MLD growth rates were inversely dependent on temperature as observed earlier for previous polyamide MLD and alucone MLD film growth.

The TEM images revealed that the polyamide MLD films were smooth and conformal on the various particle substrates (See Supplemental Figure 1). Fourier Transform Infrared (FTIR) vibrational analysis of the polyamide MLD films revealed the presence of N-H, C-H, C-N, and C=O stretching vibrations and CO-N-H bending modes. X-ray photoelectron spectroscopy (XPS) analysis on witness wafers yielded peaks corresponding to C, N, O, and a small amount of Cl. Energy Dispersive Spectroscopy (EDS) mapping of the polyamide MLD film grown on cellulose particles observed N and Cl in the polyamide coating. The deposition of all-organic polymer MLD films on particles may have many interesting applications because of their high elasticity and chemical stability.

Emerging Materials
Grand Ballroom A-C - Session EM2-WeM

Organic-Inorganic Hybrid Materials

Moderators: Gregory N. Parsons, North Carolina State University, Jonas Sundqvist, Fraunhofer Institute for Ceramic Technologies and Systems IKTS

10:45am **EM2-WeM12 Vapor Phase Infiltration: A Route for Making Insulating Polymer Fibers Conductive***, **Mato Knez**,* CIC nanoGUNE, Spain*; I. Azpitarte,* CTECHnano, Spain

Future technological devices rely in large parts on flexible functional materials. Polymers play an important role for this approach as the combination of low weight and mechanical flexibility makes them unavoidable within this technological concept. However, for a variety of technological approaches, not only the mechanical properties, but also electronic properties of polymers need to satisfy the technological needs.

A promising strategy to implement conductivity into polymer fibers is based on vapor phase infiltration (VPI), if it was successfully applied for an infiltration of a conductive or semiconducting material. VPI is a modification of Atomic Layer Deposition (ALD) which allows synthesis of hybrid materials by infiltration of inorganic materials into organic substrate. With this technique diffusion of precursors into polymeric materials from the gas phase is enforced and yields new composites with inorganic moieties coordinated or covalently linked with the polymeric matrix.

Fibers of poly(p-benzamides), for example Kevlar®, are known since decades and are of great commercial importance primarily because of their exceptional mechanical strength and flexibility as well as an established industrial fabrication process. The polymer gains its mechanical properties through the high molecular order and the intermolecular hydrogen bonds, which in turn makes it very complex to introduce further functionalities into the material. This seriously limits the application range. For example, Kevlar is an electrical insulator and as such by default not suitable as active component in wearable electronic applications.

The present work shows a VPI-based approach towards functionalization of Kevlar fibers in two aspects. In the first instance, electrical conductivity of the intrinsically insulating fibers was induced. This was performed by infiltration of conductive metal oxides. In the second instance the resulting hybrid polymer-inorganic fibers became photocatalytically active upon irradiation with visible light. The photocatalytic effect relies on the insertion of ZnO into the fiber matrix and the chemical interaction between the inorganic and polymeric phase, which eventually result in back-doping of the ZnO with nitrogen hand in hand with the alteration of the electronic structure of the polymeric chain.

11:00am **EM2-WeM13 Vapor Phase Infiltration of Metal Oxides into Microporous Polymers for Organic Solvent Separation Membranes***, **Emily McGuinness**, F. Zhang, Y. Ma, R. Lively, M. Losego,* Georgia Institute of Technology

Membrane-based organic solvent separations promise a low-energy alternative to traditional thermal separations but require advanced materials that operate reliably in chemically aggressive environments. While inorganic membranes can withstand demanding conditions, they are costly and difficult to scale. Polymeric membranes, such as polymers of intrinsic microporosity, are easily manufactured into form factors consistent with large-scale separations (e.g., hollow fibers), but perform poorly in aggressive solvents. Here, a new post-fabrication membrane modification technique, vapor phase infiltration (VPI) is reported that infuses polymer of intrinsic microporosity 1 (PIM-1) with inorganic constituents to improve stability while generally maintaining the polymer's macroscale form factor and microporous internal structure **(Figure 1)**. The atomic-scale metal oxide networks within these hybrid membranes protect PIM-1 from swelling or dissolving in organic solvents including: tetrahydrofuran, dichloromethane, and chloroform **(Figure 2a)**. This atomic-scale metal oxide network further decreases the molecular weight cutoff (MWCO; the smallest molecular weight the membrane "successfully" rejects) in n-heptane and toluene from a MWCO of about 600 g/mol for pristine PIM-1 thin film composite membranes to 204 g/mol for hybrid AlOx/PIM-1 membranes **(Figure 2b)**. The hybrid membranes further retain this MWCO and high levels of rejection (>95%) in solvents that traditionally swell or even dissolve pristine PIM-1 (such as ethanol and tetrahydrofuran). The decrease in MWCO and increase in stability of AlOx/PIM-1 hybrid membranes allows them to perform separations not only between solutes and solvents, but also separations of more challenging systems such as those comprising multiple solvents. For example, the hybrid AlOx/PIM-1 membranes are capable of enriching the toluene concentration in a mixture of 90 wt% toluene, 5 wt% 1,3,5-triisopropylbenzene, and 5 wt% 1,3-diisopropylbenzene from 90.0 wt% to 97.8 ± 0.3 wt%. In this talk, we will discuss the chemical mechanisms of the infiltration process that we believe create the hybrid structures necessary to support this enhanced stability and separation performance.

11:15am **EM2-WeM14 ZnO-Infiltrated Hybrid Polymer Thin Films with Enhanced Gravimetric Water and Oxygen Vapor Sensing Properties***, E. Muckley, L. Collins, A. Ievlev,* Oak Ridge National Laboratory*; X. Ye, K. Kisslinger,* Brookhaven National Laboratory*; B. Sumpter, N. Lavrik,* Oak Ridge National Laboratory*; **Chang-Yong Nam**,* Brookhaven National Laboratory*; I. Ivanov,* Oak Ridge National Laboratory

Organic-inorganic hybrids generated by infiltration synthesis, a hybridization technique derived from atomic layer deposition (ALD), can feature various unique materials properties and functionalities not observed in conventional materials. In this work, we discover that the ZnO-infiltrated polymer hybrid nanocomposite thin film exhibits remarkably enhanced light-activated gravimetric gas vapor sensing properties. The hybrid nanocomposite thin film prepared by infiltrating molecular ZnO in SU-8, a common negative-tone, epoxy-based polymer resist, features up to 20-fold greater gravimetric responses to oxygen and water vapors compared with control ZnO or SU-8 thin films in a dark environment. Additional 50 – 500% enhanced responses are detected under ultraviolet (UV) irradiation. Experimental interrogation shows that the increased gravimetric response of the hybrid film is attributed not only to the higher analyte accessibility to active ZnO sites in the matrix but also to the reversible, light-induced increase of surface potential and adsorption energy. Density function theory calculations suggest that the UV enhancement is caused by the light-induced, reversible generation of hydrophilic fluoroantimonic acid from the photoacid generator (PAG) residual in the SU-8 film matrix. A gravimetric sensor based on the ZnO-infiltrated SU-8 hybrid finally enables 96% accurate classification of water and oxygen environments with sub-10 mTorr detection limits. The results highlight the utility of infiltration synthesis for advancing sensor technologies.

11:30am **EM2-WeM15 Physically Interpenetrated Organic-Inorganic Sub-Surface Layers Created via Vapor Phase Infiltration for Improved Film Adhesion***, **Mark Losego**, S. Dwarakanath, R. Tummala,* Georgia Institute of Technology

Like atomic layer deposition (ALD), vapor phase infiltration (VPI) uses sequential pulsing of gaseous precursors to chemically modify a substrate. In VPI, these precursors sorb into the subsurface (bulk) of the polymer substrate, eventually becoming entrapped and forming a new organic-inorganic hybrid material. We have been studying the effects of just a few (< 5) VPI exposure cycles on the structure and properties of various polymeric materials and often find that significant inorganic loading can be achieved through a single exposure step (from 2 wt% to up to 20 wt%). Beyond loading, the chemical structure of these materials is still not well understood. While in some cases, chemical bonding between the organic and inorganic components is evident, often we do not observe any chemical changes. For these materials, we believe the metal-organic precursor is forming an adduct to one of the polymer's functional groups, but upon exposure to a co-reactant (e.g., H_2O or O_2), the metal oxide cluster product becomes detached from the polymer. The resulting physically intertwined network of organic and inorganic constituents offers a unique hybrid structure with new property space to explore. This talk will focus on one such system, a redistribution layer (RDL) polymer used for electronic packaging infiltrated with AlO_x. We have found VPI of this RDL polymer can improve adhesion strength to metallic electrode layers by 3x (~200 g/cm for untreated versus ~600 g/cm treated). At failure, these infiltrated interfaces show bulk polymer fracture, indicating the polymer fails before the interface. Extensive spectroscopic investigations show no indication of change to the RDL polymer chemistry, suggesting that the inorganic is physically interpenetrated with the polymer chains creating a "root system" that improves adhesion through physical entanglement. Optimization of the VPI process temperature for adhesion will be discussed. Low process temperatures impede sufficient diffusion depth of the inorganic, while high process temperature preclude sufficient inorganic loading because sorption is thermodynamically limited.

11:45am **EM2-WeM16 Inorganic-Organic Thin Film Layer-Structures and Thermal Conductivity***, **Fabian Krahl**,* Aalto University, Finland*; A. Giri, P. Hopkins,* University of Virginia*; M. Karppinen,* Aalto University, Finland

We utilize a combined atomic/molecular layer deposition approach to engineer layered ZnO-benzene structures that are meant to show precisely tailorable thermal conductivity values. We deposit a wide range of different layer sequences from regular superlattices to linear gradients (a linear increase in the space between benzene layers) and even more complex layering structures (see attached picture).

In superlattice structures with 12 benzene layers the thermal conductivity is effectively suppressed by decreasing the thermal conductivity from around 54 W $m^{-1}K^{-1}$ in pure ZnO down to values of around 4 W m^{-1} K^{-1}[1,2]. The thermal conductivity in the ZnO-benzene system is most probably suppressed by scattering the phonons that are responsible for the heat conduction in ZnO [2,3]. We are investigating deviations from the superlattice structure and reported our first findings last year [4], more samples are currently measured. We want to understand the connection between the films thermal conductivity and their internal structure to design materials with a high electrical but low thermal conductivity which would be of tremendous use for thermoelectric devices.

References

[1] T. Tynell, A. Giri, J. Gaskins, P.E. Hopkins, P. Mele, K. Miyazaki, and M. Karppinen, Journal of Materials Chemistry A **2**, 12150 (2014).

[2] A. Giri, J.-P. Niemelä, T. Tynell, J.T. Gaskins, B.F. Donovan, M. Karppinen, and P.E. Hopkins, **93**, 115310 (2016).

[3] A.J. Karttunen, T. Tynell, and M. Karppinen, **22**, 338 (2016).

[4] F. Krahl, A. Giri, J.A. Tomko, T. Tynell, P.E. Hopkins, and M. Karppinen, Advanced Materials Interfaces **5**, 1701692 (2018).

Emerging Materials
Grand Ballroom E-G - Session EM3-WeM
Epitaxial Growth and III-V Materials

Moderator: John Ekerdt, University of Texas at Austin

10:45am **EM3-WeM12 Atomic Layer Epitaxy of Zinc Oxide on C-plane Sapphire from Diethylzinc and Water using Pulsed-Heating Atomic Layer Deposition***, **Brandon Piercy**, M. Losego,* Georgia Institute of Technology

A challenge to atomic layer epitaxy (ALEp) is the mismatch between low-temperature windows for certain ALD precursors and the higher thermal budgets required for epitaxial growth. A common solution is to use precursors with higher ALD temperature windows, but these do not necessary exist for all desired chemistries. Therefore, ALEp is limited to material combinations having low lattice mismatch and high temperature precursor stability. To circumvent this challenge, we are exploring a new technique called pulsed-heating ALD (PH-ALD) that interleaves individual ALD growth cycles with a fast, high-temperature heat pulse using a high-

power resistive heater. As proof-of-concept, we study epitaxial growth of ZnO on c-plane sapphire using a diethylzinc (DEZ) / water chemistry. DEZ is known to decompose above about 180˚C, and the DEZ-H_2O system cannot be grown epitaxially on c-sapphire with traditional thermal ALD approaches. Here, we explore the use of pulse heating to temperatures of up to 900˚C and for various ALD cycle ratios. X-ray diffraction shows the best epitaxial alignment and ZnO rocking curve, with a FWHM of <0.5˚, at a pulse temperature of 900˚C and a 1:1 ALD:heat pulse ratio. Crystal quality and intensity drop significantly with pulse temperatures less than 800˚C. Reducing the ALD cycles:heat pulse ratio also lowers crystal quality, but epitaxial growth is retained down to 5 ALD cycles per heat pulse. Photoluminescence spectroscopy of the D0x band shows that the 1:1 PH-ALD samples have 1.3x the intensity of post-annealed ZnO ALD and 10x the intensity of as-deposited ZnO ALD. Finally, we study growing a few layers of PH-ALD ZnO followed by standard thermal ALD with no pulsed heating. We find that a template layer of only 20 PH-ALD cycles is sufficient to template ZnO epitaxial films up to 100 nm thick.

11:00am **EM3-WeM13 Growth of AlN Barriers in Al/AlN/Al SIS Josephson Junctions by Low Temperature Atomic Layer Epitaxy***, **Charles Eddy, Jr.,*** U.S. Naval Research Laboratory*; D.J. Pennachio, J. Lee, A. McFadden,* University of California, Santa Barbara*; S.G. Rosenberg,* U.S. Naval Research Laboratory*; Y.H. Chang, C.J. Palmstrom,* University of California, Santa Barbara

Superconductor-Insulator-Superconductor (SIS) structures are of increasing interest for the creation of Josephson junctions that can serve as the basis for quantum qubit transmons, which hold significant promise for quantum computing technologies. Traditionally, these devices have been developed using amorphous AlO_x in Al/AlO_x/Al structures and have enabled fundamental demonstrations of transmon performance. However, improved performance may be expected with an epitaxial insulator. Even in these structures, the nature of the superconductor/substrate interface and the superconductor/ambient interface limits coherence and, consequently, qubit performance.

In an effort to address this challenge, we employ low temperature atomic layer epitaxy (ALEp) to grow crystalline AlN insulators on crystalline aluminum films. Smooth epitaxial aluminum films are grown by evaporation on cryogenically-cooled, buffered GaAs(001) substrates [1]. These epitaxial surfaces are “frozen” using a low temperature nitridation atomic layer process (ALP) before the samples are ramped to 300° C for low temperature ALE of AlN using semiconductor grade trimethylaluminum and UHP argon and nitrogen inductively coupled plasmas (ICPs). In this study, we evaluate the structural effects of variations in the initial nitridation ALP, growth conditions of ALEp AlN barriers, and SIS barrier thickness using transmission electron microscopy. We have found that at one end of the spectrum, a simple 5 cycle nitridation ALP of epitaxial aluminum at ~90° C, where each cycle is a 30 second exposure to 300W UHP argon/nitrogen (200/75 sccm) ICP , consumes a significant fraction of the aluminum to make an amorphous AlN insulator that is roughly 2 nm thick. When this surface is subjected to another low temperature Al evaporation, the top Al films are a mixture of amorphous and polycrystalline. When the same nitridation ALP is employed and followed by 5nm of ALEp AlN growth at 300° C, a similar amount of the aluminum film is consumed and an amorphous ALEp AlN layer results. Finally, when the nitridation ALP is reduced to a single cycle of nitridation, less of the aluminum film is consumed and the 5nm AlN ALEp film shows polycrystallinity with small regions demonstrating sharp, potentially epitaxial interfaces. This result suggests that proper ALP nitridation of the epitaxial aluminum can support epitaxial growth of AlN by ALE. Further studies of the influence of number of cycles, cycle duration, plasma chemistry and plasma power on both the nitridation ALP and AlN ALEp will be presented.

[1] S. Gazibegovic et al., Nature 548, 434 (2017).

11:15am **EM3-WeM14 Investigating Plasma Parameters and Influence of Argon to the Crystallinity of GaN Films Grown by Plasma-Assisted ALD***, **Deepa Shukla**, I. Saidjafarzoda, A. Mohammad, B. Brian Willis, N. Biyikli,* University of Connecticut

Gallium nitride has attracted significant attention in (opto)electronic and RF-chip industry mainly due to its wide bandgap of about 3.4 eV,which revolutionized lighting as well as high-power and high-frequency electronic devices. However, conventional crystal growth methods employ substrate temperatures typically around ~1000 °C, which is incompatible with post-CMOS integration and other temperature-sensitive substrates. To broaden the application spectrum of GaN, lower temperature growth methods are highly needed. Plasma-assisted ALD (PA-ALD) is a strong candidate which also provides unmatched conformality and uniformity performance. In this work, GaN thin films were grown on Si (100) substrates using PA-ALD. Trimethylgallium (TMG) and N2 /H2/Ar plasma were used as metal precursor and co-reactants. GaN deposition experiments were performed with and without Ar plasma at different plasma powers (150W, 175W, 200W) and different temperatures ranging within 120-240°C. An optimal growth per cycle (GPC) of ~0.7 was observed at 150°C using in-situ ellipsometer and was confirmed by ex-situ x-ray reflectivity (XRR) analysis. The hexagonal wurtzite crystal peaks were observed in the grazing-incidence x-ray diffraction (GI-XRD) analysis. Among the films deposited, GaN samples grown at 240°C showed crystalline character with a preferred orientation along the (002) plane signifying GaN crystal formation temperature above 200°C. Moreover, the absence of Ar gar in the plasma showed a notable reduction in the peak intensities of (100) and (101) crystal domains, resulting in a predominantly preferred (002) orientation. Effect of plasma power and plasma duration on the quality of GaN was carried out with N2/H2-plasma during deposition cycles. No considerable change in crystal orientation was observed with change in plasma power, however increase in plasma duration from 10 to 40 sec suppressed the formation of (100) and (101) domains, resulting in a dominant (002) diffraction peak.

11:30am **EM3-WeM15 Ultrathin GaN Epilayer by Low-temperature Atomic Layer Annealing and Epitaxy***, **Wei-Chung Kao**, W.-H. Lee, Y.-T. Yin,* National Taiwan University, Republic of China*; J.-J. Shyue,* Academia Sinica*; H.-C. Lin, M.J. Chen,* National Taiwan University, Republic of China

Conventionally, GaN epilayers have been grown by metal-organic chemical vapor deposition (MOCVD) at very high growth temperatures (>1000°C) in order to achieve high crystal quality. However, the high-temperature growth technique is challenged by thermal stress and cracking due to the large difference in thermal expansion coefficients between GaN and the substrate. In this research, high-quality GaN heteroepitaxy has been achieved by atomic layer annealing and epitaxy (ALAE) at a low growth temperature of 300°C. By introducing a layer-by-layer, *in-situ* He/Ar plasma treatment at a low plasma power in each cycle of atomic layer deposition, the crystal quality of the GaN is significantly enhanced. The significant improvement of the GaN crystal quality is attributed to the effective annealing effect due to ion bombardment from the He/Ar plasma to each as-deposited layer. The nano-beam electron diffraction, high-resolution transmission electron microscopy, and atomic force microscopy reveal a high-quality nanoscale single-crystal GaN epilayer with a very smooth surface. The full width at half-maximum of the X-ray rocking curve of the GaN epilayer is as low as 168 arcsec. This research demonstrates the impact of the low-temperature ALAE technique for growing high-quality nanoscale GaN epilayers for high-performance solid-state lighting, solar cells, and high-power electronics.

~~11:45am **EM3-WeM16 High-Quality ALD Formation of Group-III Nitrides and their Applications in FTO-based Thin Film Solar Cells***, **Xinhe Zheng**, H. Wei, P. Qiu, M. Peng, S. Liu, Y. He, Y. Song, Y. An,* University of Science and Technology Beijing, China~~

~~Group-III nitrides semiconductors (GaN, AlN, InN), grown by high-temperature MOCVD or MBE methods, have been widely utilized in optoelectronic and microelectronic devices. However, due to some benefits like low deposition temperature, precise thickness control and good conformality, ALD has recently attracted much attention in the fabrication of group-III nitrides materials. Here, we report high-quality growth of nitrides using plasma-enhanced ALD (PEALD). By optimizing the ALD window parameters, a single-crystalline nitride thin film can be achieved. Their optical, electrical, structural properties and impurities content are in detail characterized.~~

~~For some thin film solar cells using FTO glass substrates, interface modification and/or carrier transportation have been mainly focused for the improvement of device performance. So far, various metal oxides (TiO_2, Al_2O_3, ZrO_2, SiO_2, etc) deposited by ALD have been used in the CIGS and perovskite solar cells. However, there are still no reports about the application of group-III nitrides in FTO-based thin film solar cells using quantum dots (QDs) and perovskite compounds as solar energy materials. In this study, we successfully fabricate high-quality GaN and AlN onto the FTO glass substrates at a very low temperature by PEALD. It was found that the existence of ultrathin AlN coating can efficiently reduce quantum loss in the interface between TiO_2 and CdSeTe QDs. An enhancement of open-circuit from 0.642 V to 0.679 V, corresponding to an increase of conversion efficiency from 8.51 % to 9.31% under AM 1.5G irradiance, is achieved for an insertion of AlN. The results show that the ultra-thin AlN layer on~~

~~TiO_2/QDs surfaces can create an energy barrier for electron injection from QDs into the electrolyte and the injected electron from TiO_2 into the electrolyte, thus effectively inhibiting photo-generated electron recombination. The ALD GaN thin film on FTO glass here could serve electron transport layer for perovskite solar cells. The results indicate that GaN thin-film thickness has a significate effect on the electron transport and collection of the photovoltaic cells. It is found that the devices based on the 50-cycle GaN thin-film (~4 nm) show the best cell performance with efficiency of 15.2%. The introduction of group-III nitrides has shown promise for improving solar cell performance and could open up a way in designing novel thin film solar cells.~~

~~References~~

~~1, H. Wei, X. Zheng*, et.al, Appl. Surf. Sci., to be issued.~~

~~2, S. Liu, X. Zheng*, et.al, Chin. Phys. B, to be issued.~~

~~3, M. Peng, X. Zheng*, et.al, Nanoscale, to be issued.~~

~~4, S. Liu, X. Zheng*, et.al, Nano. Res. Lett., 12(279), 1-6(2017).~~

ALD Applications
Grand Ballroom A-C - Session AA1-WeA
Emerging Applications II

Moderators: Arrelaine Dameron, Forge Nano, Se-Hun Kwon, Pusan National University

1:30pm **AA1-WeA1 Atomic Layer Deposited Nano-Coatings to Protect $SrAl_2O_4$ Based Long-Life Phosphors from Environmental Degradation***,* ***Erkul Karacaoglu****,* Georgia Institute of Technology*; E. Ozturk,* Karamanoglu Mehmetbey University, Turkey*; M. Uyaner,* Necmettin Erbakan University, Turkey*; M. Losego,* Georgia Institute of Technology

Strontium aluminate ($SrAl_2O_4$) phosphors activated with Eu^{2+} and co-doped with RE^{3+} elements (RE: Nd, Dy, etc) are long-life phosphors (>12 hrs of persistent luminescence) of significant commercial relevance. These phosphors have been widely used as luminescent additives in many commercial products including plastics and textiles. Today, these phosphors are of interest for zero-energy safety lighting both in residential markets and on roadways. However, these phosphors are prone to degradation in moist or humid conditions. This talk will discuss our work to use ALD to protect these phosphors from degradation in aggressive aqueous environments. We specifically study degradation of $SrAl_2O_4$ powders co-doped with Eu_2O_3 and Dy_2O_3 and then coated with Al_2O_3 or TiO_2 by atomic layer deposition (ALD). ALD coatings of about 10 to 250 nm in thickness are investigated. Uncoated phosphor powders dispersed directly in water show rapid hydroxylation as tracked with increasing water basicity from pH 7 to 13. XRD analysis, FT-IR spectroscopy, and optical microscopy all confirm post-mortem that these uncoated powders readily decompose to SrO, $Al(OH)_3$, and Al_2O_3 within 3 hours of water exposure and fully degrade to $Sr_3Al_2O_6$ and $Al_2O_3{\cdot}H_2O$ after 48 hrs of water exposure. This degradation results in a severe loss of phosphorescence. Powders that are ALD coated with even 5 nm of Al_2O_3 or TiO_2 show minimal change in aqueous pH and no change in morphological appearance after 48 hours of direct water exposure. 10 nm coatings are found to protect the phosphor powders for up to 2 weeks in direct water exposure. XRD confirms no emergence of secondary phases and photoluminescence properties are retained. Achieving good conformality over all powder surfaces appears to be an important requirement. Interestingly, the photoluminescence intensity of the raw powders also appears to increase with Al_2O_3 ALD coating thickness. This photoemission increase continues even up to a 250 nm coating thickness which shows a 1.5x increase in phosphorescence. This enhancement of emission intensities for ALD coated samples could be attributed to increased radiation absorption caused by surface defects or surface strain introduced by the coatings. Prior work on other luminescent materials has shown similar effects, and our current understanding of these photophysics phenomena will be discussed.

1:45pm **AA1-WeA2 Enhanced Interfacial Fracture Toughness of Polymer-Epoxy Interfaces using ALD Surface Treatments***,* ***Yuxin Chen****, N. Ginga, W. LePage, E. Kazyak, A. Gayle, J. Wang, M.D. Thouless, N.P. Dasgupta,* University of Michigan

Polymer interfaces play a critical role in a variety of applications, including consumer products, structural components, biomedical devices, and flexible electronics. In many cases, polymers need to be bonded with adhesives to create structural joints or multi-layer structures. For adhesives to efficiently wet and bond to a substrate, the surface free energy of the substrate must be equal to or higher than the surface free energy of the adhesive. However, the surface energy of most polymers is low, which makes adhesion difficult. Thus, there often is a need to increase the surface energy of a polymer without changing the bulk mechanical and chemical properties.

In this work, we demonstrate that atomic layer deposition (ALD) can be applied on poly(methyl methacrylate) (PMMA) and fluorinated ethylene propylene (FEP) to increase their surface energies and, hence, to increase the interfacial fracture toughness when bonded to an epoxy adhesive.

ALD alumina films were deposited on each type of polymer to modify the surfaces towards high energy surfaces of metal oxide. Transmission-electron microscopy (TEM) and atomic-force microscopy (AFM) were used to study the film morphology on the polymers. These indicated that the ALD treatment increased the surface roughness and changed the sub-surface chemistry by vapor-phase infiltration (VPI). The increase in surface energy after ALD was measured by the sessile-drop test with water, ethylene glycol and glycerol.

The interfacial fracture toughness of each polymer-epoxy interface was measured using a customized motor-controlled wedge tester. After ALD film growth, the interfacial fracture toughness of the PMMA-epoxy and FEP-epoxy interfaces increased by factors of up to 7 and 60, respectively. The two ALD samples and two control samples were tested at the same level of humidity. Furthermore, we observed stress-corrosion cracking of the ALD-polymer interfaces. By conducting wedge tests in different levels of humidity, we found that although ALD increased equilibrium interfacial fracture toughness at all humidity, the effect decreased as humidity increased. Scanning-electron microscopy (SEM) of samples after testing provided additional evidence for stress-corrosion cracking of the ALD-polymer interface. These results suggest a new application of ALD for engineering the mechanical properties of chemically inert surfaces.

2:00pm **AA1-WeA3 Atomic Layer Deposition of Pd on ZnO Nanorods for High Performance Photocatalysts***,* ***Jong Seon Park****, B.J. Kim, G.D. Han, K.-H. Park, E.H. Kang, H.-D. Park, J.H. Shim,* Korea Univ., Republic of Korea

The metal oxide-metal heterostructure is reported to be effective for improving the performance of photocatalysts. Zinc oxide (ZnO) is widely used as a photocatalyst due to its proper band gap (3.3 eV) that enables outstanding semiconducting characteristics. Also, ZnO has been fabricated in variety of forms including thin film, particles or nanowires, that are useful for catalysis with high surface area. Palladium (Pd) is considered as a well-matching metal with ZnO to synergistically improve photocatalytic performance with an appropriate Fermi level. Recombination of generated charges are prohibited since Pd catches excited charges from ZnO leading to highly improved photocatalytic efficiency.

In this study, ZnO nanorods coated with Pd nanoparticles is evaluated as photocatalysts. The ZnO nanorods are prepared by hydrothermal growth on silicon wafers. The Pd nanoparticles are fabricated by atomic layer deposition (ALD). ALD Pd is conducted using Pd(II) hexafluoroacetylacetonate ($Pd(hfac)_2$) precursor with formalin in a customized ALD chamber (ICOT Inc.). The growth temperature is 90ºC. To evaluate the photocatalytic performance, the degradation rate of methylene blue is measured under the ultraviolet radiating condition. As a result, it is confirmed that the degradation rates are accelerated with the ZnO-ALD Pd catalysts compared to bare ZnO nanorods. This result will be discussed in more details at the presentation.

2:15pm **AA1-WeA4 Accelerating Light Beam (ALB) Generation through Dielectric Optical Device Fabricated by Low Temperature Atomic Layer Deposition (ALD)***, W. Zhu, C. Zhang, A. Agrawal, H. Lezec,* National Institute of Standards and Technology*;* ***Huazhi Li****,* Arradiance LLC

Accelerating light beam (ALB) or bended light along an arbitrary curvature enables many intriguing applications such as particle manipulation, optical illusion and cloaking[1]. To date, one common method to generate ALBs is based on spatial light modulators (SLMs)[2], which are large and lack spatial resolution due to the large pixel size of the SLMs. Acceleration control of Airy beams (one representative form of ALB) in a photorefractive crystal by applying ultrahigh voltages have been recently reported[3]. However, the scheme usually only operates at a specific wavelength, or imposes a stringent requirement on the ALB generation process. Furthermore, the ALB is generated inside the crystal, not in free-space.

In this presentation we successfully demonstrated a novel scheme to generate ALBs through an ultrathin all- dielectric optical metasurface consisting of nano-posts with cylindrical cross-sections. By properly configuring the lateral dimensions of the nano-post (major axis length and short axis length), as well as its orientation angle, arbitrary phase modulations of an incident beam can be created, thus providing an efficient approach to generate ALBs. The dielectric metasurfaces are fabricated by first creating the reverse patterns in an electron beam (E-beam) resist, followed by low-temperature atomic layer deposition (ALD) of TiO_2, which fills the openings in the exposure E-beam resist in a conformal manner without causing any degradation of the resist (enabled by low temperature ALD).

The proof-of-concept devices demonstrated include: 1) Generation and switch between two arbitrary ALBs that follow different caustic trajectories in free-space (schematically represented in the following figure); 2) simultaneously achieving efficient and broadband generation and dynamic control of ALBs across the visible region. Our study opens up the possibility of creating ultra-compact, fine-spatial-resolution, and flat-profile nanophotonic platforms for efficient generation and dynamical control of structured light beams.

Literature:

1. Cai, W.; Chettiar, U. K.; Kildishev, A. V.; Shalaev, V. M. *Nat. Photonics* 2007, 1, 224−227; Valentine, J.; Li, J.; Zentgraf, T.; Bartal, G.; Zhang, X. *Nat. Mater*. 2009, 8, 568−571.

2. Siviloglou, G. A.; Broky, J.; Dogariu, A.; Christodoulides, D. N. *Phys. Rev. Lett.* 2007, 99, 213901.

3. Ye, Z.; Liu, S.; Lou, C.; Zhang, P.; Hu, Y.; Song, D.; Zhao, J.; Chen, Z. *Opt. Lett.* 2011, 36, 3230−3232.

2:30pm **AA1-WeA5 Tunable Plasmonic Colours Preserved and Modified by Atomic Layer Deposition of Alumina***, J-M. Guay, A. Lesina, G. Killaire,* University of Ottawa, Canada*; **Peter Gordon,*** Carleton University, Canada*; C. Hahn,* University of Ottawa, Canada*; S. Barry,* Carleton University, Canada*; L. Ramunno, P. Berini, A. Weck,* University of Ottawa, Canada

Decorative colouring of pure silver and gold surfaces is an important application for jewelry and coinage, particularly collector's coins. In order to preserve the purity of these substrates, colours created by adding materials like inks or patinas should be avoided. A novel colouring method that uses careful laser treatment to create a surface with nanoscale, plasmonic features has been developed but the bare surface features undergo dynamic coalescence that dulls and shifts the available colour palette. This work demonstrates that colours generated by nanostructured plasmonic silver surfaces can be preserved and tuned by overcoating with alumina films by ALD. These colours were observed to shift with increasing alumina film thickness.

Two types of laser treatment were used to create surface features on silver that gave rise to colours in the visible spectrum: burst and nonburst. For burst surfaces, the colours first degrade with increasing alumina film thickness but recover at larger thicknesses with an expanded colour range. For nonburst surfaces the colours degraded with increasing thickness without any recovery. Underlying periodic structures specific to the burst method are responsible for this behavior. FDTD modeling of representative surfaces, including the conformal alumina layer, helps explain these colour changes. For alumina thicknesses smaller than the nanoparticle gaps, the changes in the perceived colours are due to the perturbation of plasmonic resonances. For alumina thicknesses larger than the nanoparticle gap, the change in colours originates primarily from the complex reflectance response of the alumina coated structures and modification of the refractive index of the resulting complex surface.

The coloured surfaces were evaluated for applications in colourimetric and radiometric sensing showing large sensitivities of up to 3.06/nm and 3.19 nm/nm, respectively. The colourimetric and radiometric sensitivities are observed to be colour dependent.

2:45pm **AA1-WeA6 TFE of OLED Displays by Time-Space-Divided (TSD) PE-ALD and PE-CVD Hybrid System***, **Bongsik Kim,*** JUSUNG Engineering, Republic of Korea

In this paper we introduce a time space divided (TSD) plasma assisted deposition equipment available to in-situ atomic layer deposition (ALD) and chemical vapor deposition (CVD) process and a thin film encapsulation (TFE) of organic light emitting diodes (OLEDs) deposited by the above mentioned equipment, TSD hybrid system. Figure 1 represents a structure of the TSD hybrid system. The 1st electrode, included protruding rod-like metal bars, is composed of two types of gas injection systems and the protruded parts are inserted into holes of the 2nd electrode. Each electrode is rigorously designed considering the hollow cathode effect (HCE), the plasma sheaths and the surface area for optimizing RF power efficiency. The remote plasma source cleaning (RPSC) system enables an in-situ cleaning to etch away the film residue in the chamber.

Figure 2 show cross-sectional views of two kinds of TFEs in particle environments. Figure 2-1 represents seam defect of general SiO film, deposited by using the hexamethyldisiloxane (HMDSO), and figure 2-2 represents the cross-sectional view of the coated particle by flowable SiO, named pp-HMDSO. Because deposited films generally growth to the direction from which the gas is flowing, almost films which are deposited by the general CVD process cannot avoid to growth of the defect from the blind spot. So, we, by controlling process conditions, fabricated the TFE which includes flowable SiO film in order to fill the blind spot and hardened the film to reinforce the adhesion to neighbored layers.

Figure 3 show measured characteristics of the TFE structure of the figure 2-2, deposited by the TSD hybrid system at low substrate temperature (<100□). In order to suppress film defects, induced by particles, first, we coated particles with the pp-HMDSO and then, the ALD SiO layer is deposited as a second barrier and a buffer layer between the SiO and the SiN. Even if the film coats conformally without any defect, the permeation of water and oxygen through the film bulk direction would be occurred. So, finally, we coated with the CVD SiN layer for an ultra-low water vapor transmission rate (WVTR). As shown in figure 3, the WVTR of $<5x10^{-5}$g/m^{2}day at 40 □ /100%RH conditions is measured by MOCON Aquatran2 and also we get the optical transmittance (>95%) and the low film stress (<100MPa) data.

The TSD hybrid system can make various kinds of thin films, such as CVD SiN, SiON, SiO, ALD SiO, SiN, etc, by in-situ ALD or CVD process and also can control characteristics of thin films widely by changing the process conditions. By TSD hybrid system, manufactured by JUSUNG engineering, we expecting to contribute the OLED industry development.

3:00pm **AA1-WeA7 Tailoring the Ferroelectricity of ZrO_2 Thin Films using Ultrathin Interfacial Layers Prepared by Plasma-Enhanced Atomic Layer Deposition***, **Sheng-Han Yi,** B.-T. Lin, T.-Y. Hsu, J. Shieh, M.J. Chen,* National Taiwan University, Republic of China

In recent years, HfO_2/ZrO_2-based ferroelectric thin films have been recognized as promising candidates for memory devices and negative-capacitance field-effect-transistors to achieve a further improvement of device performance. The ferroelectric(FE) and antiferroelectric(AFE) properties of these CMOS-compatible oxides have been confirmed to originate from the polar orthorhombic phase and non-polar tetragonal phase, respectively. In this work, we report the significant impact of ALD-deposited interfacial layers on the microstructures and FE/AFE properties of ZrO_2 thin films. Sub-nanometer interfacial layers deposited by plasma-enhanced atomic layer deposition are intentionally introduced between the ZrO_2 thin film and the electrodes of metal-insulator-metal structures to tailor the crystalline phase and ferroelectricity of the ZrO_2. The interfacial layers boost the formation of orthorhombic ZrO_2, leading to significant enhancement of the ferroelectricity with a significant increment of the remanent polarization. On the other hand, another interfacial layers contribute to the formation of tetragonal ZrO_2, giving rise to the dramatic transformation of ZrO_2 from ferroelectricity to antiferroelectricity. The findings indicate that interface engineering by ALD is an effective and advantageous approach to tailor the FE/AFE characteristics of materials.

3:15pm **AA1-WeA8 Spin-Hall-Active Platinum Thin Films Grown Via Atomic Layer Deposition***, **Michaela Lammel,*** IFW Dresden, Germany*; R. Schlitz,* Technische Universität Dresden, Germany*; A.A. Amusan,* IFW Dresden, Germany*; S. Schlicht,* FAU Erlangen, Germany*; T. Tynell,* IFW Dresden, Germany*; J. Bachmann,* FAU Erlangen, Germany*; G. Woltersdorf,* Martin-Luther-Universität Halle-Wittenberg, Germany*; K. Nielsch,* IFW Dresden, Germany*; S.T.B. Goennenwein,* Technische Universität Dresden, Germany*; A. Thomas,* IFW Dresden, Germany

Due to its strong spin orbit coupling platinum (Pt) is often used as a spin injector/detector in spintronics. We used atomic layer deposition (ALD) to fabricate platinum thin films on a substrate consisting of liquid phase epitaxy grown yttrium iron garnet ($Y_3Fe_5O_{12}$, YIG) on gadolinium gallium garnet ($Gd_3Ga_5O_{12}$). Magnetotransport experiments were performed on the YIG/Pt heterostructures in three mutually orthogonal rotation planes, revealing the fingerprint of spin Hall magnetoresistance. Samples with different platinum thicknesses were used to estimate the spin transport parameters of the Pt thin films. Comparing the values for the spin Hall angle as well as the spin diffusion length with literature we found the spin diffusion length in the ALD Pt thin films agrees well with results reported for high-quality sputtered platinum. The spin Hall magnetoresistance however is smaller by approximatley a factor of 20. Clearly, further experiments will be required to optimize the interface quality in such ALD-based heterostructures. Nevertheless, our results show that spin Hall active Pt thin films can be fabricated by ALD featuring an appropriate quality for spin transport. The reported results build the framework for establishing conformal coatings for non-planar surface geometries with spin Hall active metals via ALD which in the future can provide the basis for developing 3D spintronic devices [1].

[1] Schlitz et al., Appl. Phys. Lett. **112**, 242403 (2018)

ALD Applications
Grand Ballroom H-K - Session AA2-WeA

ALD for ULSI Applications II

Moderators: Haripin Chandra, Versum Materials, Inc., Robert Clark, TEL Technology Center, America, LLC

1:30pm **AA2-WeA1 Silicon-Based Low k Dielectric Materials with Remote Plasma ALD***, **Hyeongtag Jeon**,* Hanyang University, Republic of Korea **INVITED**

As the devices continue to shrink in size, resistive-capacitive (RC) time delay due to parasitic capacitance of devices is becoming a major problem. Low dielectric films with having high thermal stability and excellent step coverage is needed for applications such as barriers and gate sidewall spacers. Silicon oxycarbide (SiOC), silicon oxycarbonitride (SiOCN), silicon carbon nitride (SiCN) are possible candidates for these requirements because the carbon content and bonding state in the low dielectric materials can control the dielectric constant.

Atomic layer deposition (ALD) can be an ideal method for the high conformality with its self-limited reaction. The introduction of the plasma is necessary to decompose the ligands in the precursor for the ALD reaction by the plasma power. We used remote plasma ALD (RPALD) to prevent films from substrate damages caused ion bombardment.

In this work, we will discuss the trend of low k dielectric ALD studies and report the results of SiOC, SiOCN, and SiCN ALD. We used remote plasma ALD system. Octamethylcyclotetrasiloxane (OMCTS) and O_2, Ar, H_2, N_2 and CH_4+Ar plasmas were respectively used as a precursor and reactants for SiOC and SiOCN thin film deposition. Bis[(diethylaminohigh) dimethylsilyl](trimethylsilyl)-amine (DTDN-2) and N_2 plasma were used as a precursor and reactant for SiCN thin film deposition. X-ray photoelectron spectroscopy (XPS), Auger electron spectroscopy (AES), transmission electron microscopy (TEM), I-V measurement, C-V measurement, and wet etch rate (WER) test were performed for investigating the characteristics of low k dielectric films.

2:00pm **AA2-WeA3 SiOC Films by PEALD with Excellent Conformality and Wet Etch Resistance***, **Young Chol Byun**, E. Shero,* ASM

As memory devices shrink, electrical and integration constraints have become tighter. As an example, digit line spacer stacks need to demonstrate a low dielectric constant (k<4.5), excellent wet etch rate resistance (an order of magnitude lower than thermal SiO2) and excellent conformality and growth over composite structures comprising a metal, hardmask and poly-Si. Conventional furnace-deposited ALD nitrides (SiN) tend to demonstrate good wet etch rate resistance but suffer high k (>7.0). PEALD oxides (SiO2) have a low-k but poor wet etch resistance and sub-optimal conformality on the composite stack due to the directional nature of the capactively-coupled plasma. But CCP plasma reactors typically offer higher throughput. This motivates the search for SiOC class of films to leverage Si-O bonding for low-k and Si-C bonding for step coverage, preferably deposited by PEALD.

Here, we demonstrate SiOC films with a low-k value (<4.5) with excellent step coverage and wet etch rate resistance due to Si-C backbonding (80X lower than furnace nitride and 500X lower than thermal oxide in hydrofluoric acid). The films also show good step coverage of 100% in upto 10:1 aspect ratio structures. In summary, these PEALD films show a pathway to aggressively scale k and wet etch resistance for front end memory applications.

2:15pm **AA2-WeA4 ALD TiN for Superconducting Through-Silicon Vias***, **Kestutis Grigoras**, S. Simbierowicz, L. Grönberg, J. Govenius, V. Vesterinen, M. Prunnila, J. Hassel,* VTT Technical Research Centre of Finland Ltd, Finland

Through-silicon vias (TSVs) are a widely used interconnect technique, allowing the creation of non-planar integrated circuits. Recently, the use of TSVs in multichip packages was proposed as a way of improving the addressability and integration of superconducting qubits – the core elements of superconducting quantum processors [1, 2]. In this approach, the primary quantum-coherent elements of a quantum integrated circuit can be separated from the readout and control elements by fabricating them on separate chips, which are then combined with flip-chip bonding. Here, routing signals through TSVs enables the addressability of a large number of qubits. The main requirements for TSV films are superconductivity, small dimensions, and conformality. To satisfy these challenging requirements, we use atomic layer deposition (ALD).

In this work, we investigate the performance of TiN TSV interconnects. We etch arrays of 60 µm diameter TSVs in 495 µm thick 6-inch silicon wafers by deep reactive ion etching using the Bosch process (Omega i2L, Aviza Technology). We use 2 µm thick oxide layers both as a mask (top side) as well as an etch stop layer (back side). We coat the TSVs with a TiN layer by ALD (SUNALE R-150B, Picosun), performing 2,500 cycles at 450°C, using $TiCl_4$ and ammonia as precursors and nitrogen as a carrier gas. The superconducting behaviour of thin TiN layers has been previously investigated for layers deposited by plasma-ALD [3], but this technique is not applicable for coating high-aspect-ratio trenches (the aspect ratio of our TSVs is about 8:1). Therefore, we use thermal ALD in this work.

Initially, the deposited layers did not become superconducting even at 0.1 K. Optimization of the ALD process by tuning precursor pulse/purge times finally led to superconducting TiN layers with a T_c of approximately 0.85 K. The room temperature sheet resistance for a 47 nm thick layer is approximately 60 Ω/sq, as measured on the flat area of the samples. We confirm the conformality of the TiN inside vias using scanning electron microscopy. Future plans include increasing the T_c as well as integrating TSVs on chips with other structures (resonators, qubits).

[1] Rosenberg et al., npj Quantum Information 42 (2017) 1-5.

[2] Vahidpour et al., arXiv:1708.02226 [https://arxiv.org/abs/1708.02226] [physics.app-ph].

[3] Shearrow et al., arXiv:1808.06009v1 [cond-mat.mtrl-sci]

2:30pm **AA2-WeA5 Physical and Electronic Properties of Annealed ALD-deposited Ru from Ru(DMBD)(CO)$_3$ and Oxygen***, **Michael H. Hayes**,* Oregon State University*; C.L. Dezelah, J.H. Woodruff,* EMD Performance Materials*; J.F. Conley, Jr.,* Oregon State University

Ru metal is promising for MOS gate electrode and interconnect applications due to its relatively low bulk resistivity, high work-function, conductive oxide (RuO_2), and ease of etching. Because it is insoluble in and adheres well to Cu, Ru also has potential as a liner for metal interconnects. The earliest precursors used for ALD of Ru were often characterized by long nucleation delays (~200 cycles) and island-like growth, both unfavorable for producing uniform thin (< 10 nm) films. Recently, Austin et. al.[1] demonstrated a thermal ALD process using dimethylbutadiene Ru tricarbonyl [Ru(DMBD)(CO)$_3$] and O_2 that results in zero nucleation delay, low resistivity (14 µΩ-cm), and low RMS roughness (0.6 nm). While the resistivity is among the lowest reported, it is still higher than bulk crystalline Ru. In this work, we examine the impact of inert and forming gas anneals on the resistivity (ρ_{Ru}), effective workfunction ($\Phi_{Ru\text{-}eff}$) on ALD Al_2O_3 and HfO_2, crystal structure, and composition of ALD Ru films deposited using Ru(DMBD)(CO)$_3$ and O_2.

ALD Ru films of at least 30 nm in thickness are annealed at 400, 450, and 500 °C in either N_2 or 3% H_2/N_2 ambient in 20 minute increments up to a total of 60 min (Fig. 1). Whereas annealing in pure N_2 reduces ρ_{Ru} from an average of 16 µΩ-cm to 13 µΩ-cm, H_2/N_2 annealing results in a greater reduction in resistivity with the lowest ρ_{Ru} of 9.1 µΩ-cm obtained after 60 min at 500 °C, approaching the bulk value of 7.1 µΩ-cm. ρ_{Ru} vs. Ru film thickness will be discussed at the meeting.

X-ray diffraction (Fig. 2) of the as-deposited films indicates hexagonal Ru with slight (001) preferred orientation and average crystallite size of 6.3 nm. After H_2/N_2 annealing, the relative intensity of the (001) peak is reduced and the crystallite size increased to 12.4 nm. Atomic force microscopy confirmed a slightly rougher film post anneal (2.1 nm RMS). XPS shows low impurity content.

Capacitance-voltage measurements are used to determine the flat-band voltage (V_{FB}) of a series of Ru/Al_2O_3/p-Si and Ru/HfO_2/p-Si MOS capacitors with various thickness ALD dielectrics for both as-deposited and 500 °C 60 min H_2/N_2 annealed samples. The extrapolated zero-oxide-thickness V_{FB} was then used to determine $\Phi_{Ru\text{-}eff}$ for each dielectric (Fig. 3). Annealing increases $\Phi_{Ru\text{-}eff}$ to 4.9 eV and 5.3 eV for the Ru/Al_2O_3/p-Si and Ru/HfO_2/p-Si devices, respectively. Fast nucleation, low ρ_{Ru} comparable to bulk, and large $\Phi_{Ru\text{-}eff}$ comparable to sputtered films indicate ALD Ru using Ru(DMBD) and O_2 may offer advantages compared to previous reports.

[1] D. Z. Austin *et al.*, "ALD of Ru and RuO_2 Using a Zero-Oxidation State Precursor," *Chem. Mater.* 29(3), 1107 (2017).

2:45pm **AA2-WeA6 Fluorine Free Boron-Containing Composite Layers for Shallow Dopant Source Applications***, **Anil Mane**, D. Choudhury, K. Pupek, R. Langeslay, M. Delferro, J.W. Elam,* Argonne National Laboratory

Conformal and uniform coatings of boron-containing thin films via atomic layer deposition (ALD) could be used as a shallow dopant source for

advanced 3D-transistor structures in VLSI manufacturing. Targeting this application, we evaluated three non-halogenated boron compounds for their suitability as ALD precursors: boric acid ($B(OH)_3$), trimethyl borate ($B(OCH_3)_3$), and hafnium borohydride $Hf(BH_4)_4$. The $B(OH)_3$ and $B(OCH_3)_3$ were used in combination with trimethyl aluminum to deposit $B_xAl_{2-x}O_3$ ALD films, and the $Hf(BH_4)_4$ was used with H_2O to deposit HfB_xO_y films. We evaluated the ALD surface chemistries for these processes using in-situ quartz crystal microbalance (QCM) and Fourier transform infrared spectroscopy (FTIR) studies. The QCM measurements also confirmed self-limiting behavior and helped to optimize the ALD timing. The resultant boron containing nanocomposite films were analyzed using X-ray photoelectron spectroscopy (XPS), secondary ion mass spectrometry (SIMS), ellipsometry, and electrical capacitance measurements. The boron content in the $B_xAl_{2-x}O_3$ and HfB_xO_y composite films was controllable by tuning the ALD cycle ratio and the precursor sequence. We performed rapid thermal annealing of composite films as a function of time and temperature and determined the B-diffusion in silicon as well as changes in the optical properties of the $B_xAl_{2-x}O_3$ and HfB_xO_y layers. Here we will present a detailed investigation of ALD methods for creating B-containing layer for shallow dopant application.

3:00pm **AA2-WeA7 Impact of Medium Energy Ions on the Microstructure and Physical Properties of TiN Thin Layers Grown by Plasma Enhanced Atomic Layer Deposition (PE-ALD).***, S. Belahcen, C. Vallée, A. Bsiesy,* ***Marceline Bonvalot****,* LTM-UGA, France

Titanium nitride TiN has been extensively used in common microelectronic devices as an electrode material, where it serves as an interfacial connecting material between a device and the metallic contacts used to drive it, while simultaneously preventing any diffusion of the metal into silicon. TiN is also involved in biological Micro-Electro-Mechanical Systems (bioMEMS) as an electrode material, for instance in cardiac pacemakers or neural stimulation applications, thanks to its unequalled conducting properties at reduced dimensions, as compared to traditional noble metals, and also thanks to its high corrosion resistance to human body fluids. For such applications, a deep knowledge of the microstructural properties of TiN are of utmost importance.

In this work, the impact of processing parameters on the physical properties of TiN has been investigated in details. TiN thin layers (20 nm) have been prepared on SiO_2 (100 nm)/Si substrates by Plasma Enhanced ALD (PE-ALD), using TDMAT as a precursor and N_2 as a plasma gaz. The PE-ALD setup used for this purpose has been equipped with an original Atomic Layer Etching (ALE) kit positionned at the back-face of the substrate holder, which allows medium energy ions to be extracted from the plasma during the ALD growth. Several bias values ranging from 0 W to 90 W have thus been tested during the plasma step to investigate the impact of ions with varying kinetic energies on the morphological properties of TiN.

The rugosity of as deposited TiN layers has been obtained from AFM measurements. XRD and XRR analyses have been systematically carried out in order to evaluate the texturation, cristallinity and mechanical stress in the layer. The impact of medium energy ions during TiN growth has been correlated to the rugosity, density and residual stress. These results will be discussed in view of potential applications of TiN as an electrode material in microelectronic devices.

3:15pm **AA2-WeA8 ALD Process Monitoring for 3D Device Structures***,* ***Jiangtao Hu****,* Lam Research Corp.

Semiconductor device structures have become increasingly complex, requiring new measurement techniques to support manufacturing. Measurement of high aspect ratio (HAR) structures requires a response signal to depth and profile, and the bottom may be invisible to top-down optical signals. Likewise, certain thick films are opaque to optical thickness measurement. Lateral processing steps occur too deeply in a structure to be visible, and thin conformal deposition films need to be characterized inside the feature.

For ALD applications, a critical requirement is to have complete and uniform coverage from the top to the bottom of a 3D device. A thinner or incomplete deposition at the bottom of a device can often lead to high leakage and high failure rates. Conventional optical thickness measurements of ALD films can identify thickness variations at the top of a high aspect ratio (HAR) device but may not identify process deviations at the bottom of this type of device.

Monitoring ALD using mass metrology is a potential solution to this issue. The direct measurement of mass change due to process enables detection of process excursions. Measurement of the wafer mass before and after a process is a simple and direct means of monitoring and control. This is particularly true for ultra- opaque films and complex stacks, film density monitoring, and conformal and ALD/sidewall deposition, where traditional optical metrology techniques may not be effective.

Conformal deposition typically involves an area much greater than a blanket deposition layer, and even more so on severe/strong/high device topologies. Mass sensitivity to film on a patterned wafer can be as much as 10 times greater than on a blanket wafer (Fig 1).

More importantly, mass metrology directly monitors the amount of material change in a device across the entire HAR structure while conventional optical film metrology typically measures these changes on a test pad or blanket test wafer. Mass metrology instrumentation can detect low coverage of ALD films at the bottom of a HAR device which otherwise would be missed using optical measurement. For example, we can compare mass change induced by flow rate reduction on blanket or patterned wafers (Fig 2). Significant mass change occurs on patterned wafers after a 3% of flow rate reduction, while on patterned wafers this deviation is pronounced after a 1% reduction.

In this discussion, we will discuss how Mass Metrology can be used to monitor ALD process variations in 3D semiconductor devices, along with the applications and benefits of this technology in ALD.

Emerging Materials
Regency Ballroom A-C - Session EM1-WeA

Ternary and Quaternary Oxide Materials

Moderator: Bart Macco, Eindhoven University of Technology

1:30pm **EM1-WeA1 Rhenium(III)-based Ternary Oxides: Novel Materials from Straightforward Synthesis *via* ALD Comprising Uncommon Reaction Pathways***,* ***Max Gebhard****, S. Letourneau, D. Mandia, D. Choudhury, A. Yanguas-Gil, A. Mane, A. Sattelberger, J.W. Elam,* Argonne National Lab

Oxides of rhenium, such as ReO_2 and ReO_3, exhibit high conductivity in the order $\sigma = 10^3 - 10^4\ (\Omega cm)^{-1}$, close to that of metals. This property is of high importance regarding applications with high demands on tailored electrical properties. An example of such an application are microchannel plates (MCPs), which are used as signal amplifiers in advanced detector units for UV-light (space aviation) and photoelectrons (XPS). Also, MCPs play a crucial role in the development of large area photodetectors.[1] MCPs are comprised of a glass capillary array. By applying a material with high secondary electron emission (SEE) yield, an incident electron/photon can create an electron avalanche that eventually increases the signal-to-noise ratio and thereby allows the detection of event starters. Below the SEE layer, a resistive coating must be applied, exhibiting the right range of resistivity to avoid electrons from being drained and to act as electron supplier. This material must be operable at elevated temperatures, *i.e.* it must have a low temperature-coefficient of resistance (TCR) to avoid decreased device performance at higher temperatures. Metal nanoparticles embedded in an Al_2O_3-matrix have been shown to provide the right resistivity for MCP application.[2] However, their TCR values demand for the development of materials with improved properties.

In this context, the development of ternary oxides, comprising ReO_x units with electrical conductivity and other components with dielectric character, provide a good opportunity to overcome the limitations of existing coatings.

Herein, we present two new materials, namely $ReAl_yO_x$ and $ReSi_yO_x$. These materials, where $ReSi_yO_x$ is reported for the first time, have been deposited using ALD and detailed mechanistic studies revealed that during the growth, reductive elimination reactions cause the formation of uncommon but stable Re(III) oxide species. Furthermore, fascinating mechanisms allowing the formation of unsaturated hydrocarbons and hydrogen, were identified during the growth. The processes were explored in great detail employing *in-situ* tools such as QCM, QMS and FTIR. Furthermore, the materials were fully characterized in terms of composition, structure, and electrical properties using XPS, RBS/HFS, XRD, XRR and XAS.

[1] J. Wang, K. Byrum, M. Demarteau, J. Elam, A. Mane, E. May, R. Wagner, D. Walters, L. Xia, J. Xie, and H. Zhao, *Nucl. Instruments Methods Phys. Res. Sect. A Accel. Spectrometers, Detect. Assoc. Equip*. **2015**, 804, 84

[2] J. W. Elam, A. U. Mane, J. A. Libera, J. N. Hryn, O. H. W. Siegmund, J. McPhate, M. J. Wetstein, A. Elagin, M. J. Minot, *et al*., *ECS Trans*. **2013**, 58 (10), 249

1:45pm **EM1-WeA2 Growth Behavior and Electronic Characterization of $PbZrO_3$ and $PbZr_xTi_{1-x}O_3$ Grown by Atomic Layer Deposition with Several Zr Precursors***, **Nicholas Strnad**,* University of Maryland*; D. Potrepka,* U.S. Army Research Laboratory*; A. Leff,* General Technical Services, LLC*; J. Pulskamp,* U.S. Army Research Laboratory*; R. Phaneuf,* University of Maryland*; R. Polcawich,* U.S. Army Research Laboratory

Process, structural, chemical, and electrical characterization is presented for $PbZr_xTi_{1-x}O_3$ (PZT) deposited by ALD using different combinations of precursors with thicknesses suitable for piezoelectric microelectromechanical systems (piezo-MEMS). PZT grown by ALD is desired for integration into 3-D MEMS [1] whereby actuators are grown on high aspect-ratio sidewalls, which greatly increases the areal work-density. To determine the viability of ALD PZT for MEMS, the films were integrated into micromachined, released cantilever structures. ALD $PbTiO_3$ (PTO) has been previously grown using lead bis(3-N,N-dimethyl-2-methyl-2-propanoxide) [$Pb(DMAMP)_2$] and tetrakis dimethylamino titanium [TDMAT] as the lead and titanium cation precursors, respectively [2]. Incorporation of tetrakis dimethylamino zirconium [TDMAZ] yielded PZT, but the growth rate of $PbZrO_3$ (PZO) and PZO-rich PZT was suppressed compared to PTO-rich PZT, resulting in a Zr/Ti composition less than the desired morphotropic phase boundary (MPB) composition of 52/48. The PTO-rich ALD PZT (Zr/Ti = 22/78) films were annealed at 700 °C in O_2 to crystallize into the perovskite phase. Micromachined trench structures 45 µm deep were coated with conformal ALD $PbZr_{22}Ti_{78}O_3$ to demonstrate that the process conditions fell within the ALD-window. Transmission electron microscopy images revealed that the ALD PZT films crystallized with grains tens of nanometers in diameter. Rutherford backscattering was used to characterize the chemical composition of the films. In-situ ellispometry indicated that the as-grown PZT thickness was a linear function of the number of supercycles. For 200 nm-thick ALD $PbZr_{22}Ti_{78}O_3$ films, planar metal-insulator-metal capacitors were created to evaluate the ferroelectric and dielectric properties. The films exhibited an average remnant polarization of 20 µm/cm^2, a dielectric constant at zero volts of 475, a tuning range of 212-548 from 0 to 450 kV/cm, and a corresponding Tan delta of 0.025 (see supplemental). The ferroelectric properties of the ALD PZT presented here rivals PZT grown at similar compositions and thicknesses by other well-accepted processing methods. Several other zirconium precursors were investigated for inclusion into ALD PZT including zirconium tert-butoxide [$Zr(OtBu)_4$] and tetrakis ethylmethylamino zirconium [TEMAZ]. The incorporation of $Zr(OtBu)_4$ led to improved tunability of the zirconium concentration but also resulted in a lower overall growth rate of PZT.

References

[1] Three dimensional piezoelectric MEMS, US8966993 B2, J.S. Pulskamp and R. G. Polcawich (19 Dec 2012)

[2] N. A. Strnad et al. *J. Vac. Sci. Technol. A* 37(2) Mar/Apr 2019

2:00pm **EM1-WeA3 Understanding Growth Characteristics of ALD $NiAl_yO_x$: The Role of Ozone***, **Jonathan Baker**, J. Schneider, S.F. Bent,* Stanford University

ALD of ternary films has grown in interest as applications requiring the advantages of ALD (including sub-nanometer thickness control, uniformity, compositional control and conformality) have demanded more complex materials. However, depositing ternary materials by ALD is typically more complicated than the binary ALD systems from which the ternary materials are derived. As a result, the growth of a ternary material by ALD often deviates from ideal growth behavior described by the "rule of mixtures." In this work, ALD of $NiAl_yO_x$ was studied using the nickelocene ($NiCp_2$)/O_3 and trimethyl aluminum (TMA)/H_2O precursor systems for nickel oxide and aluminum oxide respectively. Depositions of $NiAl_yO_x$ were performed using the supercycle method, allowing a wide range of compositions to be achieved by altering the cycle ratio of nickel oxide to aluminum oxide ALD cycles. However, composition as a function of cycle ratio was found to be nickel deficient compared to the ideal rule of mixtures. The cause of the observed non-ideality was explored to help elucidate the ALD reaction mechanisms. Characterization of the films revealed that the growth rate of aluminum oxide was significantly enhanced following a $NiCp_2$/O_3 cycle. Modification of the rule of mixtures to account for the enhanced growth rate of Al_2O_3 resulted in a model which fits observed properties well, accounting for both the observed compositions and growth rates. In addition, $NiAl_yO_x$ has shown to be an interesting case study for understanding the deposition of ternary materials of first-row transition metal oxides grown with O_3. Similar to ALD of Fe_2O_3 and MnO_x, which utilize metallocene-derivatives and O_3, NiO ALD requires long precursor and O_3 exposures to achieve fully self-limiting growth. The root cause for this behavior is hypothesized to stem from the use of the strong oxidizer O_3, which may oxidize the metal centers to higher oxidation states or otherwise introduce extra oxygen into the film. For the deposition of $NiAl_yO_x$, low O_3 exposures were used to develop the initial $NiAl_yO_x$ system. To understand the effects of O_3 exposure on the deposition of the ternary ALD film and binary NiO system, growth of $NiAl_yO_x$ as a function of O_3 exposure was explored with an aim to understand the ALD reaction mechanisms at play when using O_3 as an oxidizer. The effect of high O_3 exposures will be discussed.

~~2:15pm **EM1-WeA4 Atomic Layer Deposition of $B_xMg_{1-x}O$ Films: Progress Towards Shallow Boron Doping***, **David Mandia**, D. Choudhury, M. Gebhard,* Argonne National Laboratory*; J. Liu,* Northwestern University*; A. Yanguas-Gil, A.U. Mane, A. Nassiri, J.W. Elam,* Argonne National Lab~~

~~Preparation of $B_xMg_{1-x}O$ films through an ABC-type ALD program employing bis(cyclopentadienyl) magnesium (II), trimethyl borate ($B(OCH_3)_3$), and water as precursors is presented herein. The thin film properties are extensively characterized by X-ray photoelectron (XPS), diffraction (XRD), and reflectivity (XRR). Moreover, optical properties of the as-grown and post-deposition annealed films are assessed through spectroscopic ellipsometry measurements with a particular focus on the effective optical properties of the B_2O_3 film component, which is an attractive shallow-boron dopant source material. Instead of using the highly toxic diborane (B_2H_6) as a boron doping source, the present work employs ALD to generate MgO stablized B_2O_3. Interestingly, as observed from *in situ* quartz crystal microbalance (QCM) and Fourier transform infrared (FTIR) analysis, stabilization of B_2O_3 occurs by dosing $Mg(Cp)_2$ after the $B(OCH_3)_3$ pulse which forms Mg-B-O* surface species that undergoes further reaction to B_2O_3 in the succeeding water pulse. Without the $Mg(Cp)_2$ pulse (or MgO "AB" sub-cycle) preferential formation of boric acid ($B(OH)_3$) occurs instead of B_2O_3. Post-deposition annealing treatments along with follow-up spectroscopic ellipsometry and high-resolution XPS/depth profiling measurements were performed to characterize the composite films' optical and electronic structural properties, respectively. The thermal ALD synthesis of $B_xMg_{1-x}O$ composite films on silicon in concert with post-deposition annealing is a potentially viable approach towards shallow-boron dopant layer or junction formation through the stable B_2O_3 component and could find use in solid-state electronics applications.~~

2:30pm **EM1-WeA5 Enhanced Doping Control of Metal Oxide Thin Films Using a Modified ALD Process***, E. Levrau,* IBM TJ Watson Research Center*; **Yohei Ogawa**,* ULVAC, Japan*; M. Frank, M. Hopstaken, E. Cartier,* IBM T.J. Watson Research Center*; K. Schmidt,* IBM Research - Almaden*; M. Hatanaka,* ULVAC, Japan*; J. Rozen,* IBM T.J. Watson Research Center

The introduction of controlled amounts of dopants into logic and memory devices has been extensively used in nanoelectronics in order to alter the properties of a material and make it suitable for a specific application. Doping thin films can be complicated because of the difficulty to control thickness and dopant gradient distribution.

Atomic Layer Deposition allows for excellent thickness control and doping is usually achieved by varying the cycle ratio of two metal oxides during deposition, M1O and M2O, in what are called super-cycles. We refer to this method as the standard nanolaminate process [1]. Here, we propose a modified ALD process that allows for finetuning the dopant concentration down to a few atomic % in the metal oxide (MO) thin film. This doping control can happen at thicknesses much thinner than standard nanolaminates thus allowing for a better trade-off between stack functionality and leakage. Doping levels of less than 10cation% are desired, specifically for higher k phases of HfO_2 for ferroelectric devices [2].

In figure 1, a comparison of the minimum deposition thickness required for each method, is given for varying dopant concentrations. This illustrates that the modified ALD process allows for films to be ~6x thinner than the standard nanolaminate process from the studied precursors for Zr-doped HfO_2, while exhibiting less than 5% 1-sigma thickness variation across a 200mm wafer. The process does not involve BEOL thermal budget or partial reactions associated with plasma oxidation and can therefore be very conformal. This makes it compatible with FEOL integration for 3D thin film depositions.

It has been demonstrated that doping can be beneficial for non-volatile memories as it can enhance the endurance and the switching stability of the devices [3]. Here, HfZrO thin films with varying dopant levels of Zr are deposited through the modified ALD method on 200mm substrates. Dopant concentrations are determined by RBS analysis. Film properties are

analyzed with spectroscopic ellipsometry and XPS. Thin-film HfO_2-based ferroelectric devices with different dopants will be evaluated.

[2] Fischer D., Kersch A., J. of Appl. Phys., 104(8), 084104 (2008).

[3] Ryu S. W., Cho S., Park J., Kwac J., Kim H., Nishi Y., Appl. Phys. Lett., 105, 072102 (2014).

2:45pm **EM1-WeA6 As Deposited Epitaxial $LaNiO_3$ and $La(Ni,Cu)O_3$ with Controllable Electric Properties***, **Henrik Hovde Sønsteby,*** University of Oslo / Argonne Natl. Labs, Norway*; O. Nilsen, H. Fjellvåg,* University of Oslo, Norway

Depositing complex oxides by ALD is a rapidly emerging field, with new materials with excellent properties published every month. $LaNiO_3$ is a perovskite type oxide with metallic behaviour, thought to play a major role in functional multilayer stacks and integrated electronics. Although routes for depositing $LaNiO_3$ has been reported in literature, an annealing step has always been necessary to obtain eptaxial films. In many applications this hinders monolithic device integration, and can cause unwanted strain effects and cracking.

In this presentation we show a facile route for direct epitaxial growth of $LaNiO_3$ by thermal ALD at temperatures as low as 250 °C. The films show excellent conductive properties as deposited, with specific resistivity as low as 10^{-4} Ohm cm. The functional properties of the films are slightly improved upon annealing, reaching specific resitivites in the 10^{-5} Ohm cm order of magnitude. Furthermore, we show that the order of precursor pulses plays a fundamental role in obtaining high quality as deposited epitaxial films.

$LaNiO_3$ is a remarkable member of the $RENiO_3$ series of materials (RE = La, Pr, Nd, Sm, Eu, Gd, Dy, Ho, Er, Y, Lu),as it is the only member that remains metallic to 0 K. All other members observe a metal-insulator-transition (MIT) at temperature varying from ~100 K (Pr) to ~600 K (Lu). Controllably tuning the MIT is highly awaited by the community.

In this presentation we also show how substution by Cu on the Ni-site alters the electric properties and MIT temperature of $LaNiO_3$. We show that a full range of compositions is attainable, from $LaCuO_x$ to $LaNiO_3$, and that the electronic properties vary smoothly over this composition range. ALD can be used to obtain a remarkable cation composition control. Furthermore, we hypothesize on the reason behind the varying properties of this material system, and try to explain it by showing how oxygen vacancies are introduced by copper substitution. This may help shed light on the surprising properties of $LaNiO_3$ itself, but more importantly the films can be directly used in applications where a tunable MIT is necessary.

This presentations highlights the use of complex oxide ALD as a real alternative to MBE, with several key advantages such as conformality and low temperature deposition.

3:00pm **EM1-WeA7 Time Dependence of Pyroelectric Response in Ferroelectric $Hf_{0.58}Zr_{0.42}O_2$ Films***, **Sean Smith**, M.D. Henry, M. Rodriguez,* Sandia National Laboratories*; J. Ihlefeld,* University of Virginia

HfO_2 based ferroelectrics are a promising family of ferroelectrics stable as thin films. The ferroelectric response in HfO_2 thin films is associated with a metastable orthorhombic phase, typically seen in films < 30 nm thick, stabilized by doping, electrode material, deposition conditions and annealing. Thin HfO_2 based ferroelectrics are attractive for use in memory, energy harvesting, and sensing applications, however the polarization response of the thinnest of these films, <~5 nm, has been reported to be unstable over time. In this work we show that the pyroelectric response of 5 nm $Hf_{0.58}Zr_{0.42}O_2$ with TaN electrodes decreases logarithmically after biasing, decreasing from an initial value of -58 $\mu Cm^{-2}K^{-1}$ to ~-40 $\mu Cm^{-2}K^{-1}$ in the first 24 hours. While films 10 nm and thicker have a pyroelectric response that is constant on the same timescale.

Sandia National Laboratories is a multimission laboratory managed and operated by National Technology & Engineering Solutions of Sandia, LLC, a wholly owned subsidiary of Honeywell International Inc., for the U.S. Department of Energy's National Nuclear Security Administration under contract DE-NA0003525.

3:15pm **EM1-WeA8 Tailoring Nickel Oxide Conductivity by Introducing Transition Metals: From First-principles to Experimental Demonstration***, **Md. Anower Hossain**, T. Zhang, D. Lambert,* University of New South Wales, Australia*; Y. Zakaria,* Hamad Bin Khalifa University, Qatar*; P. Burr,* University of New South Wales, Australia*; S. Rashkeev, A. Abdallah,* Hamad Bin Khalifa University, Qatar*; B. Hoex,* University of New South Wales, Australia

Transition metal oxides, such as MoO_3, WO_3, V_2O_5, and NiO have shown potential for application as hole-selective passivating contact for silicon (Si) solar cells. Among them, NiO is a p-type semiconductor which possesses notoriously poor hole-conducting properties. Doping of metal oxides with multivalent metal cations is one of the most effective ways to improve electronic band structure properties of resulting ternary metal oxides because dopants create favorable defect states crucial for charge carrier transport. Therefore, we used first-principles density functional theory (DFT) computations as a predictive tool to identify suitable dopants. The density of states, defect formation energies, and thermodynamic transition levels of various charge states within the band gap of doped NiO were calculated and promising dopants were identified. We synthesized Al-doped NiO ($Al_xNi_{1-x}O$) and Zn-doped NiO ($Zn_xNi_{1-x}O$) films onto 2.0 Ω.cm *p-Si* wafers using atomic layer deposition (ALD). We used a supercycle approach alternating *N* (10, 25, 50) NiO cycles and 1 Al_2O_3 cycle. Cross-sectional transmission electron microscopy and energy dispersive x-ray spectroscopy mapping showed conformal films with the elemental distribution of Ni, O, and Al. X-ray photoelectron spectroscopy (XPS) measurements revealed the presence of Ni^{2+}, Ni^{3+} and Al^{3+} oxidation state in the films. The Al content was found to scale with the number of AlO_x ALD cycles. The density of the Ni^{3+} and Al^{3+} oxidation state increased with the increasing number of AlO_x ALD cycles, confirming the Al incorporation into the host lattice of NiO. However, a significantly higher Al concentration was found in the $Al_xNi_{1-x}O$ film as was expected from the supercycle ratio. This was resulting from a significantly higher growth per cycle of AlO_x compared to NiO. While undoped NiO was found to be resistive, the Al_xNi_{1-x} films showed the contact resistivity of 41.6 - 113 $m\Omega\cdot cm^2$ after annealing in a rapid thermal processing furnace at 200-300 °C under N_2 for 10 minutes. In addition, the $Zn_xNi_{1-x}O$ films deposited by supercycle of NiO and ZnO cycle also showed the Ohmic contact with *p-Si*. The $Zn_xNi_{1-x}O$ films were also thermally stable up to 500 °C with the best contact resistivity of approximately 21.5 $m\Omega\cdot cm^2$. This indicates a significant improvement of contact performance as compared to the undoped NiO counterparts. This work demonstrates that a ternary $Al_xNi_{1-x}O$ and $Zn_xNi_{1-x}O$ films are suitable hole-selective passivation contact for the *p-Si* solar cells.

Nanostructure Synthesis and Fabrication
Grand Ballroom E-G - Session NS-WeA

2D Nanomaterials by ALD (including Transition Metal Dichalcogenides)

Moderators: Annelies Delabie, IMEC, Harm Knoops, Oxford Instruments Plasma Technology

1:30pm **NS-WeA1 Modified ALD Process to Achieve Crystalline MoS_2Thin Films***, **Li Zeng**, C. MacIsaac, J. Shi, N. Ricky, I.-K. Oh, S.F. Bent,* Stanford University

Stimulated by the discovery of two-dimensional (2D) graphene, 2D transition metal chalcogenides (TMDs) are attracting much attention owing to their similar layered structure and graphene-analogous properties. Numerous research efforts are under way to explore their wide ranging potential applications, including but not limited to optoelectronics, electrochemical cells, and energy harvesting devices. However, challenges still remain regarding the development of controllable growth methods for TMDs with large-scale conformality at moderate synthesis temperature. For the past half-decade, there has been an increasing trend toward resolving these issues by employing atomic layer deposition (ALD) due to its inherent growth characteristics. Over a dozen metal sulfide/selenide materials have been explored by ALD and yielded promising results, such as wafer-scale uniformity and compatibility with electrical devices and photochemical cells.

Despite the promise brought by the ALD approach, further effort is needed because the TMD films that are deposited at lower, more desirable temperatures often show non-ideal stoichiometry and require high-temperature post-annealing to improve the film quality. Using the notable molybdenum disulfide (MoS_2) as an example, one of the known processes uses $Mo(CO)_6$ as the Mo ALD precursor and H_2S as the co-reactant with an ALD window of 150 ~ 175 °C. Results from both literature and our laboratory show that the S to Mo ratio is close to 1.5:1—relatively far from the ideal value of 2:1—with the presence of undesired MoO_x species. We performed an investigation into fundamental mechanisms of this ALD process. Based on that understanding, a new methodology was developed that produces higher-quality MoS_2 films from these same precursors. These results were achieved by elevating the growth temperature and shifting the typical ALD process into a pulsed chemical vapor deposition regime. A series of MoS_2 films were synthesized on Si substrates by this modified

process, resulting in controllable linear growth behavior, a S-to-Mo ratio of 2-to-1, and strong characteristic MoS_2 Raman peaks. Additional characterization tools, including grazing incident X-ray diffraction (GIXRD), X-ray reflectivity (XRR) and atomic force microscopy (AFM), were also used to examine the film crystallinity, density and surface morphology. By characterizing the material as a function of process conditions, we are able to elucidate fundamental mechanisms and key kinetic factors behind the MoS_2 growth process using $Mo(CO)_6$ and H_2S. This study may help shed some light on future design of ALD processes for 2D TMDs.

1:45pm **NS-WeA2 Nucleation and Growth of ALD MoS_2 Films on Dielectric Surfaces***, S. Letourneau,* ***Anil Mane****, J.W. Elam,* Argonne National Lab

Molybdenum disulfide (MoS_2) is a promising two-dimensional (2D) semiconductor. Similar to graphite, MoS_2 has a layered structure comprising weak van der Waals bonding between layers, and strong covalent bonding within layers. The weak secondary bonding allows for isolation of these 2D materials to a single layer, like graphene. While bulk MoS_2 is an indirect band gap semiconductor with a band gap of ~1.3 eV, monolayer MoS_2 exhibits a direct band gap of ~1.8 eV, making it an attractive candidate for replacing Si in electronic devices. Atomic layer deposition (ALD) has been used previously to grow MoS_2 films using a variety of molybdenum and sulfur precursors. However, many of these precursors are solids at room temperature, require high temperature vapor transport, and have the potential to result in carbon incorporation. Recently, MoS_2 ALD using molybdenum hexafluoride (MoF_6), a high vapor pressure liquid at room temperature, and hydrogen sulfide (H_2S) has been demonstrated. For device applications, the ALD MoS_2 must be integrated with dielectrics. While the nucleation of MoS_2 during chemical vapor deposition (CVD) is understood, the nucleation of MoS_2 ALD using MoF_6 and H_2S on dielectric surfaces has yet to be explored. Unlike films grown by high temperature CVD, ALD MoS_2 is amorphous and must be annealed to crystallize the film. In this study, we utilized *in situ* quartz crystal microbalance (QCM) and Fourier transform infrared (FTIR) spectroscopy measurements to investigate the first few cycles of MoS_2 ALD on Al_2O_3 and HfO_2 surfaces prepared *in situ* by ALD. Self-limiting growth of MoS_2 was observed on a wide range of dielectric surfaces including alumina, and hafnia. The MoS_2 nucleation was found to depend strongly on the substrate. These studies provide insight into the low-temperature ALD of MoS_2 and provide guidance for the integration of MoS_2 and other ALD TMDC films.

2:00pm **NS-WeA3 Plasma-Enhanced Atomic Layer Deposition of Transition Metal Dichalcogenides: From 2D Monolayers to 3D Vertical Nanofins***,* ***Ageeth Bol,*** Eindhoven University of Technology, Netherlands **INVITED**

2D materials have been the focus of intense research in the last decade due to their unique physical and chemical properties. The synthesis of crystalline transition metal dichalcogenide nanolayers (TMDs) using atomic layer deposition (ALD) has attracted a lot of interest lately as ALD offers monolayer thickness control, scalability and low temperature growth (T ≤450°C). However, ALD grown films have been reported in literature to exhibit a high density of out-of-plane 3D structures in addition to 2D horizontal layers[1, 2]. The presence of such 3D structures are a benefit for catalysis, as it increases the density of active edge sites. However, these structures can hinder charge transport and consequently raise film resistivity, which hampers both electrocatalysis and nanoelectronic applications. Hence it is essential to understand and control 3D structure formation during atomic layer deposition of TMDs.

In this presentation I will first focus on the formation mechanism of 3D structures. Extensive high resolution transmission electron microscopy studies in our lab have shown that grain boundaries and the grain orientation of adjacent 2D crystals play an important role in 3D structure formation.

Then I will demonstrate that we can control both the shape and density of the 3D structures during plasma-enhanced ALD. The shape of the 3D structures can be varied by modulating the plasma gas composition (H_2/H_2S ratio) in the co-reactant step. This has a direct influence on the number a catalytic edge sites in WS_2 films. The density of 3D structures can be suppressed by introducing a novel three step (ABC) ALD process, which involves the addition of an extra Ar and/or H_2 plasma step (step C) to the conventional AB-type ALD process. This reduces the 3D structure density and consequently reduces the resistivity of the TMD film by an order of magnitude.

Our work showcases the versatility of plasma-enhanced ALD for the controlled synthesis of transition metal dichalcogenide nanolayers, which can enable applications in both the nanoelectronics and catalysis field.

[1] A. Sharma *et al*, *Nanoscale***10,** 8615–8627 (2018).

[2] T.A. Ho *et al*, *Chem. Mater.* **29**, 7604-7614 (2017).

2:30pm **NS-WeA5 Atomic Layer Deposition of Emerging 2D Semiconductors HfS_2 and ZrS_2***,* ***Miika Mattinen****, G. Popov, M. Vehkamäki, P. King, K. Mizohata, P. Jalkanen, J. Räisänen, M. Leskelä, M. Ritala,* University of Helsinki, Finland

Two-dimensional (2D) materials are being studied intensively due to their unique electronic, optical, and catalytic properties and the wide range of potential applications arising from their layered crystal structures. However, the majority of studies focus on only a few of the large group 2D materials, such as the semimetallic graphene, insulating h-BN, and semiconducting MoS_2. Semiconducting 2D materials, in particular, are promising for electronics applications including field-effect transistors (FETs), photodetectors, and sensors. HfS_2 and ZrS_2, members of the transition metal dichalcogenide (TMDC) group, are indirect band gap semiconductors that have recently emerged as potential alternatives to MoS_2 and other 2D semiconductors.[1] They have an indirect band gap suitable for many semiconductor applications, 1.7–1.8 (ZrS_2) or 1.8–2.1 eV (HfS_2) in bulk.[2] A notable benefit of HfS_2 and ZrS_2 is that their native oxides, HfO_2 and ZrO_2, are well-known high-k oxides, a situation analogous to Si and SiO_2.[3]

We present the first ALD processes for HfS_2 and ZrS_2 using simple, thermally stable and industrially applied halide precursors $HfCl_4$ and $ZrCl_4$ with H_2S. Crystalline, continuous, high-quality 2D HfS_2 and ZrS_2 films with thicknesses from a few to tens of monolayers (monolayer = 0.58 nm) are deposited at 400 °C once care is taken to minimize the presence of impurities such as water in the ALD reactor. Good ALD characteristics, including rapid saturation and linear growth rate at approximately 0.1 Å/cycle are achieved. The HfS_2 and ZrS_2 films can be grown on a variety of substrates, including oxides, metals, and sulfides. Single-crystalline substrates, such as sapphire and muscovite mica, enable tailoring the morphology and texture of films and even epitaxial growth. Due to the sensitivity of HfS_2 and ZrS_2 towards oxidation, we demonstrate encapsulation of the sulfide films "in situ" with an ALD-grown oxide layer using an oxidant-free process. We are currently studying the use of HfS_2 and ZrS_2 films as photodetectors to highlight the potential of the films for electronic applications.

[1] Yan et al., *Adv. Funct. Mater.*, **2018**, 28, 1803305

[2] Abdulsalam and Joubert, *Phys. Status Solidi B*, **2016**, 253, 705–711

[3] Mleczko et al., *Sci. Adv.*, **2017**, 3, e1700481

2:45pm **NS-WeA6 Low Temperature ALD for Phase-controlled Synthesis of 2D Transition Metal (M=Ti, Nb) *di-* (MX_2) and *Tri-* (MX_3) Sulfides***,* ***Saravana Balaji Basuvalingam****, M. Verheijen, W.M.M. Kessels, A. Bol,* Eindhoven University of Technology, Netherlands

The synthesis of two-dimensional transition metal dichalcogenides (TMDCs, MX_2) by atomic layer deposition (ALD) has gained a lot of attention lately due to the need for precise thickness control over a large area at low temperatures for future applications in opto-electronics[1]. There is also another class of two-dimensional materials involving similar elements as in TMDCs, which are known as transition metal trichalcogenides (TMTCs, MX_3). Contrary to TMDCs, TMTCs have quasi-1D properties which give added freedom for applications as they have strong anisotropy in both electrical and optical properties[2]. The present study is the first exploration of the synthesis and characterization of TMTCs using ALD.

The most commonly used technique for synthesizing TMTCs is chemical vapour transport (CVT), which is a non-scalable, high temperature and time consuming technique that grows crystals having dimensions of the order of a few cm. Therefore there is a need for synthesising TMTCs on a large scale at low temperature with a good control over the phase and thickness.

In this work, we report the first results on the controlled synthesis of TMTCs (TiS_3 and NbS_3) by ALD using metalorganic precursors and H_2S at low temperatures (100°C – 300°C). We demonstrate that by controlling deposition conditions one can tailor the phase (di- or trichalcogenide) of the material. In order to gain control over the phase of the materials we studied the effect of the deposition temperature, co-reactant (thermal ALD versus plasma-enhanced ALD) as well as co-reactant gas composition on the materials phase (Figure 1). The phase of the materials as a function of deposition parameters was studied by X-ray photoemission spectroscopy

(XPS) and Raman spectroscopy (Figure 2). The quality and the composition of the films were studied using Rutherford back scattering (RBS). It was observed that TMTCs (TiS_3 and NbS_3) can be synthesized using plasma-enhanced ALD using H_2S plasma as co-reactant at low temperatures, while TMDCs (TiS_2 and NbS_2) were synthesized by both plasma-enhanced ALD (at high temperatures) and thermal ALD. The morphology and crystallinity of the synthesized films were investigated using scanning electron microscopy (SEM) and transmission electron microscopy (TEM), which revealed the two-dimensional and nano/poly-crystalline nature of the films. Our experiments show that ALD enables the controlled synthesis of both TMDCs and TMTCs at low temperatures over large scales, which opens up new avenues to include both TMDCs and TMTCs in nano- or optoelectronic applications.

[1] W. Hao et. al, 2D Mater. **6**, 012001 (2018).

[2] J.O. Island et. al, 2D Mater. **4**, 022003 (2017).

3:00pm **NS-WeA7 ALD Boron Nitride Coated and Infiltrated Carbon Materials for Environmental Applications***, W. Hao, C. Journet, A. Brioude,* Université Lyon, France*; H. Okuno,* Université Grenoble-Alpes, France*;* ***Catherine Marichy****,* Université Lyon, France

Atomic Layer Deposition (ALD) has proven to be an effective approach for surface modification and fabrication of carbon based heterostructures [1]. Nevertheless, ALD BN coating of carbon material has been poorly studied up to date. Our group recently reported a two-step ammonia-free ALD approach for BN allowing the coating of various substrates such as inorganic and polymeric nanostructures [2,3]. While successful deposition of BN layers on carbon nanomaterial has been realized, it has been observed that some BN precursor diffuses into some polymers [4].

Herein various carbon nanostructures (nanoparticles, nanotubes, nanofibers) coated with ALD are discussed. The inertness of highly graphitic carbon inhibiting the initiation of ALD growth, the influence of the crystalline nature of the substrate on the BN coating is investigated in term of growth and structure, using different graphitized/amorphous carbon supports. Nucleation delay and impact on the crystalline quality (amorphous, turbostratic, hexagonal phase) of BN films are observed as a function of the degree of graphitization. Furthermore, obtained from vapor infiltration of polymers, BN-carbon hybrid structures are briefly introduced. The obtained materials are characterized by advanced electron microscopy and related techniques. Finally, the potential of such a coating to improve the oxidation resistance of carbonaceous material is demonstrated.

[1] C. Marichy, N. Pinna, Coordination Chemistry Reviews, (2013), 257, 3232.

[2] W. Hao, Marichy C., Brioude A., ChemNanoMat., 3, (2017), 656.

[3] Hao W. Marichy C., Journet C., Brioude A., Enviro. Science Nano., 4, (2017), 2311.

[4] Hao W. PhD thesis, (2017)

Author Index

Bold page numbers indicate presenter

— A —
Aarik, J.: AF5-MoP2, 81
Aav, J.: AF5-MoP2, 81
Abdallah, A.: EM1-WeA8, 148
Abdulagatov, A.: ALE1-TuM3, **97**
Abelson, J.: AS1-TuA4, 111
Abrams, L.: AA1-TuM5, 88
Acharya, J.: AA2-TuP15, **121**
Adams, D.: ALE-SuP4, 50
Adinolfi, V.: AA1-WeM4, **131**; AF3-MoA16, 62
Adomaitis, R.: AA1-MoA5, 55; AA1-MoA8, 55; AA5-TuP7, 127
Agarwal, S.: ALE2-WeM16, 135; AS1-TuA3, 111; AS2-TuA111, 112
Agbenyeke, R.E.: AA2-MoA13, 56
~~Ageev, O.~~: ~~ALE-SuP3~~, 50
Aghazadehchors, S.: AA4-TuP9, 125
Agrawal, A.: AA1-WeA4, 143
Aguinsky, L.F.: ALE2-TuA12, **109**
Ah-Leung, V.: ALE2-TuM14, 98
Ahmmad Arima, B.: AA4-TuP5, 124
Ahmmad, B.: AA4-TuP3, 124; AF4-MoP1, 78
Ahn, J.: EM-MoP5, 85
Ahn, J.-H.: AA1-TuP2, 115
Ahvenniemi, E.: AF5-MoP2, 81
Akbashev, A.R.: AF5-MoP2, 81
Akimoto, K.: **ALE2-MoA16**, 67
Albert, M.: AF1-TuM2, 91
Ali, S.: AF5-MoP2, 81
Alivov, Y.: AA5-TuP2, 126
Allemang, C.: AS1-TuA7, 112
Alphonse, A.: AF5-MoP7, 82
Altamirano Sanchez, E.: AS1-TuM16, 100
~~Alvarado, J.~~: ~~AA2-TuP11~~, **120**
Alvarez, D.: AF2-MoP7, **73**; AF4-MoA17, 64; AM-MoP8, 84; AS-TuP4, 128
~~Ambrozic, G.~~: ~~AF4-MoA13~~, 63
~~Ameloot, R.~~: AM1-WeM8, 137; ~~AS2-TuA113~~, 113; EM1-WeM3, 138
Amusan, A.A.: AA1-WeA8, 144
An, J.-S.: AF1-MoP6, 70; AF2-MoP14, **75**
~~An, Y.~~: ~~EM3-WeM16~~, 141
Andachi, K.: AF2-MoP7, 73
Anders, D.: AS-TuP1, 128
Anderson, V.: AF-TuA6, 107
~~Antony, A.~~: ~~AA1-TuP1~~, 115
Antoun, G.: ALE1-MoA8, **66**; ALE-SuP11, 52
Appiah, E.: AF5-MoP1, 80
Arachchilage, H.J.: AF1-MoP2, **69**
Arellano, N.: AS1-TuA6, 111
Arepalii, V.: AA1-TuP17, 117
Arkles, B.: AS-TuP3, **128**
Armini, S.: AS1-TuM12, **99**; ~~AS2-TuA113~~, 113
Arts, K.: **AF3-MoA12**, 61; AF-TuA2, **105**
Asakawa, K.: EM-MoP6, 86
Asundi, A.: AA1-TuM6, 89
Aubry, O.: AM1-WeM5, 136
Avila, J.: AF2-MoP11, **74**; AF-TuA6, 107; AF-TuA7, 107
Awakowicz, P.: AF1-MoP12, 71
Azpitarte, I.: EM2-WeM12, 139
— B —
Babcock, S.E.: EM-MoP11, 87
Bača, D.: AF2-MoP17, 76
Bachmann, J.: AA1-WeA8, 144
Bacic, G.: AF2-TuM6, **94**
Bačić, G.: AF2-MoA4, 59; AF2-TuM4, 94
Bacquie, V.: ALE2-TuM14, **98**
Baek, G.H.: EM1-WeM5, 138; EM1-WeM6, **138**
Baets, R.: AF-TuA4, 106
Bahat Treidel, E.: AA2-TuP16, 121
Baik, S.J.: EM-MoP14, 87
Bailey, M.: EM-MoP2, 85
Baker, J.: EM1-WeA3, **147**
Balatti, S.: AA1-WeM4, 131
Balder, E.: AA2-TuA13, 103
Balme, S.: AA1-MoA3, 54
Barger, P.: AA1-TuM5, 88
Barlage, D.: AA2-TuP10, 120; AF1-MoA2, 57; EM-MoP12, 87
Barnola, S.: ALE2-MoA14, 67
Barry, S.: **AA1-TuA5**, 101; AA1-WeA5, 144; AF1-MoP4, 69; AF2-MoA3, **59**; AF2-MoA4, 59; AF2-TuM3, 93; AF2-TuM4, 94; AF2-TuM6, 94; AF-TuA4, 106
Bartha, J.W.: AF1-TuM2, 91
Bartlett, B.: AA1-TuM7, 89
Barton, K.: AS1-TuA7, 112
Basaldua, I.: AA1-TuA7, 102
Basuvalingam, S.B.: NS-WeA6, **149**
Baum, T.: AF1-MoP9, 70; AF3-MoP2, 76; AS1-TuA8, 112
~~Baumgart, H.~~: ~~AA2-TuP9~~, 120; ~~AA4-TuP10~~, 125; ~~AM-MoP3~~, 83
Bechelany, M.: AA1-MoA3, 54; AA4-TuP1, 123; AF5-MoP2, 81
Beer, S.M.J.: AF1-MoP13, **71**; AF1-MoP8, 70
Beladiya, V.: AM-MoP2, 83
Belahcen, S.: AA2-WeA7, 146; AS2-TuA112, 112
Bellet, D.: AA4-TuP9, 125
Bellido-Gonzalez, V.: AF-TuA3, 106
Bent, S.F.: AA1-TuM6, 89; AS1-TuA1, 110; AS1-TuA2, 110; EM1-WeA3, 147; NS-WeA1, 148
Benz, D.: **AA1-TuA5**, 101; AA1-TuM8, **89**; EM-MoP2, 85
Berdova, M.: AF5-MoP2, 81
Berini, P.: AA1-WeA5, 144
Berry, J.J.: AA2-MoA11, 56
Bertuch, A.: AA1-TuA6, 102; AA2-TuP8, **119**
Bhatia, R.: AA1-TuA6, **102**
Bickel, N.: AA2-TuP16, **121**
Bielinski, A.: AA1-TuM7, **89**; AA2-TuM12, 89
Bin Afif, A.: AF3-TuM12, 95
Biolsi, P.: ALE1-WeM1, 133
Biyikli, N.: AF3-MoP7, **77**; AF3-TuM13, 95; AF3-TuM16, 96; AF4-MoP3, 79; EM3-WeM14, 141
Blomberg, T.: AA1-MoA4, **54**; ALE1-TuM6, 97
Bochevarov, A.: AF1-MoA5, 58
Bock, C.: AF1-TuM3, 91
Bodalyov, I.: AF5-MoP2, 81
Bol, A.: NS-WeA3, **149**; NS-WeA6, 149
Bonvalot, M.: AA2-WeA7, **146**; AM1-WeM5, 136; AS2-TuA112, 112
Boris, D.: AF-TuA6, **107**; AF-TuA7, 107; ALE-SuP7, 51
Bosnick, K.: AA1-TuP6, **115**
Bosund, M.: AF3-TuM14, **96**
Boyadjiev, S.: AF5-MoP2, 81
Boysen, N.: AF1-MoP8, 70; AF2-MoA5, **59**; AM1-WeM2, 136
Brancho, J.: AA1-TuM7, 89
Breitung, E.: AA1-TuA6, 102
Brian Willis, B.: EM3-WeM14, 141
Brick, C.: AS-TuP3, 128
Briel, O.: AM-MoP1, 82
Briggs, B.: AS-TuP6, 129
Brindley, J.: AF-TuA3, **106**
Brinkmann, K.: ALE2-TuM16, 99
Brioude, A.: NS-WeA7, 150
Bruce, R.L.: ALE2-WeM15, 135
Brüner, P.: AF3-MoA15, **62**
Bsiesy, A.: AA2-WeA7, 146; AS2-TuA112, 112
~~Buhmann, H.~~: ~~AA2-TuP18~~, 121
Bull, S.: AA2-MoA14, **56**
Bures, F.: NS-TuP1, 129
Burgmann, S.: AF3-TuM12, **95**
Burkins, P.: AA1-TuA7, 102
Burr, P.: EM1-WeA8, 148
Burtin, P.: ALE2-MoA14, 67
Buttera, S.: AF2-TuM3, **93**
Büttner, T.M.: AA3-TuA13, 104
~~Buzelis, R.~~: ~~AA5-TuP6~~, 127
Byun, J.Y.: AF4-MoP11, 80
Byun, Y.C.: AA2-WeA3, **145**
— C —
Cabrini, S.: ALE1-MoA4, 65
Cadien, K.: AA1-TuP6, 115; AA2-TuP10, 120; AF1-MoA2, 57; EM-MoP12, 87
Caha, O.: AF2-MoP17, 76
Cai, J.: AF2-MoP12, 74
Cameron, D.: AF2-MoP17, 76; AF5-MoP2, 81
Cano, A.: ALE1-TuM5, **97**; ALE2-TuA14, 109
Cao, K.: AA5-TuP1, 126
Cao, Y.-Q.: AA3-TuP7, **123**; EM1-WeM1, **137**
Carbajal, D.: AS1-TuM16, 100
Cartier, E.: EM1-WeA5, 147
~~Castán, H.~~: ~~EM-MoP7~~, 86
Cavanagh, A.: AS1-TuM14, 99
Caymax, M.: AA1-WeM5, 131
Cecchini, R.: AA1-TuA3, 101
Cha, M.H.: ALE-SuP10, 51
Cha, T.: ALE-SuP9, 51
Chae, H.: AA1-TuP3, 115; ALE-SuP9, 51
Chae, W.-M.: AA5-TuP8, 127; AF1-MoP11, 71
Chaker, A.: AS2-TuA112, 112
Chan, B.T.: AS1-TuM16, 100; AS-TuP6, 129
Chandra, H.: AF2-MoP8, 73
Chang, H.S.: AA1-TuP10, 116; AA1-TuP12, 116; AA1-TuP9, 116
Chang, Y.H.: AF1-TuM4, 92; EM3-WeM13, 141
Charvot, J.: NS-TuP1, 129
Chatterjee, S.: AS-TuP1, 128
~~Chávez, M.~~: ~~AA2-TuP11~~, 120
Chekurov, N.: AF5-MoP2, 81
~~Chen, C. W.~~: ~~AF2-MoP5~~, **73**
Chen, H.-H.: AF-TuA1, **105**
Chen, K.-H.: AA2-TuM12, 89; AA2-TuM13, 90; AA2-TuM15, **90**
Chen, L.: NS-TuP3, 130
Chen, M.J.: AA1-WeA7, 144; AA3-TuA14, 104; EM3-WeM15, 141
Chen, R.: AA5-TuP1, **126**
Chen, T.: NS-TuP3, **130**
Chen, W.-S.: **AA2-WeM16**, 133
Chen, Y.: AA1-WeA2, **143**; EM-MoP11, 87
Cheng, C.-P.: **AA2-WeM16**, 133
Cheng, E.: ALE2-TuA11, 109
Cheng, L.: AA1-WeM4, 131; AF3-MoA16, 62
Cheng, P.-H.: AA3-TuA14, 104
Cheng, R.: AF5-MoP2, 81
Chesser, J.: EM-MoP9, 86
Chevolleau, T.: **ALE2-MoA16**, 67
Chin, G.: AF3-MoP6, **77**
Chin, T.-K.: AA1-TuM4, **88**
Cho, C.-H.: ALE1-MoA6, 65
Cho, J.-H.: AA5-TuP8, **127**; AF1-MoP11, 71
Cho, J.-Y.: AA1-TuP6, 115
Cho, M.H.: AA1-TuP7, **115**
Cho, S.: AA2-TuP6, 119
Cho, S.-J.: ALE2-MoA11, 66
Cho, T.: AS1-TuA7, **112**
Cho, Y.: ALE-SuP9, 51
Cho, Y.J.: AA1-TuP9, **116**
Choi, B.-H.: AA4-TuP4, 124
Choi, H.J.: AA2-MoA17, 57
Choi, J.H.: AA3-TuA16, **105**

Author Index

Choi, J.-H.: NS-TuP2, **130**
Choi, J.S.: ALE-SuP10, 51
Choi, Y.: AF2-MoP3, 72
Chopra, S.: AS2-TuA111, 112
Choudhury, D.: AA2-TuA11, **102**; AA2-WeA6, 145; AA4-TuP11, **125**; EM1-WeA1, 146; ~~EM1-WeA4~~, 147
Chowdhury, V,: AF5-MoP1, **80**
Christensen, S.: AA2-MoA11, 56; AA2-MoA15, 56; AA2-MoA16, 57; AF2-MoP4, 73
Chubarov, M.: AF5-MoP2, 81
Chugh, S.: AA2-TuP17, 121; AA4-TuP12, 125
Chung, C.W.: ALE-SuP10, 51
Chung, H.: ALE1-WeM8, 134
Chung, T.-M.: AA2-MoA13, 56
Chung, Y.-D.: AA1-TuP17, 117
Ciftyurek, E.: AF1-TuM3, 91
Ciftyürek, E.: AF2-MoA7, 60
Clancey, J.: ALE1-TuM5, 97; ALE2-TuA14, 109
Clark, R.: AA2-WeM12, 132; AF2-MoP16, 75; ALE1-WeM1, 133
Clarke, R.: AA1-WeM4, 131
Clendenning, S.B.: ALE1-TuA5, 108; ALE-SuP2, 50
Clerix, J.-W.: AS1-TuM16, 100
Coati, A.: AF1-TuM7, 92
Collins, L.: EM2-WeM14, 140
Concepcion, J.: AA1-TuP14, 117
Conley, Jr., J.F.: AA2-WeA5, 145; AF2-TuM5, 94; AF5-MoP6, 82
Consiglio, S.: AA2-WeM12, 132; AF2-MoP16, **75**
Cooke, M.: ALE1-MoA4, 65
Creange, S.: AA1-TuA6, 102
Creatore, M.: AA1-TuM3, **88**
Cremer, T.: AA1-TuP13, 117
Cremers, V.: AF5-MoP2, 81
Cruz, A.J.: AM1-WeM8, 137; EM1-WeM3, **138**
Cunnane, D.: AA1-MoA6, 55
Current, M.: ALE1-WeM6, 134
Cuthill, K.: AF2-MoP8, 73
— D —
Dadlani, A.: AF3-TuM12, 95
Dallorto, S.: ALE1-MoA4, **65**
Dameron, A.: AA1-TuM5, 88
Danek, M.: ALE1-WeM7, 134
Daniel, B.: AF-TuA3, 106
Darling, S.: AS2-TuA215, 113
Dasgupta, N.P.: AA1-TuM7, 89; AA1-WeA2, 143; AA2-TuM12, **89**; AA2-TuM13, 90; AA2-TuM15, 90; AS1-TuA7, 112
Daubert, J.: AA4-TuP2, **123**
Davis, A.: AA2-TuM12, 89; AA2-TuM13, **90**; AA2-TuM15, 90
~~De Gendt, S.~~: ~~AS2-TuA113~~, 113
Degtyaryov, A.: AA5-TuP2, 126
del Hoyo, J.: ALE-SuP7, 51
Delabie, A.: AS1-TuM16, **100**; AS-TuP6, **129**
Delferro, M.: AA2-WeA6, 145
Delhougne, R.: AA1-WeM5, 131
Dendooven, J.: AF1-TuM6, 92; AF1-TuM7, **92**; AF3-MoA15, 62; AF-TuA4, 106; **EM1-WeM7**, 139
Deng, S.: AA1-WeM5, **131**
Denkova, A.: AA1-MoA2, 54
Desai, D.: ALE1-WeM8, 134
Detavernier, C.: AF1-TuM6, 92; AF1-TuM7, 92; AF3-MoA15, 62; AF-TuA4, 106; **EM1-WeM7**, 139
Devi, A.: AF1-MoP12, 71; AF1-MoP13, 71; AF1-MoP8, **70**; AF1-TuM3, 91; AF2-MoA5, 59; AF2-MoA6, 60; AF2-MoA7, 60; AF2-TuM6, 94; AF5-MoP2, 81; AM1-WeM2, 136
Dezelah, C.L.: AA2-WeA5, 145; AF2-TuM5, 94
Dhakal, T.: AA1-TuP5, **115**
Dhuey, S.: ALE1-MoA4, 65
Di Palma, V.: AA1-TuM3, 88
Dickey, E.: AM1-WeM3, **136**
Dietz, D.: AA5-TuP3, **126**
Divan, R.: AA5-TuP10, **128**
Djenizian, T.: AA2-TuA16, 104
~~Dolak, J.~~: ~~AF4-MoP8~~, 80
Dopita, M.: AA3-TuA11, 104
Downey, B.: AF-TuA7, 107
Doyle, S.: AA2-TuP3, **118**
Dozias, S.: AM1-WeM5, 136
Draeger, N.: AS1-TuA2, 110
~~Drazdys, M.~~: ~~AA5-TuP6~~, 127
~~Drazdys, R.~~: ~~AA5-TuP6~~, **127**
Driess, M.: AF3-MoA11, 61
Drozd, V.E.: AF5-MoP2, 81
~~Dueñas, S.~~: ~~EM-MoP7~~, 86
~~DuMont, J.~~: ~~EM-MoP8~~, **86**
Dumuis, N.: AM1-WeM5, 136
Durand, C.: **ALE2-MoA16**, 67
Dussarat, C.: **ALE2-MoA16**, 67
Dussart, R.: ALE1-MoA8, 66; ALE-SuP11, 52
Dvorak, F.: NS-TuP1, 129
Dwarakanath, S.: EM2-WeM15, 140
Dwivedi, V.: AA1-MoA5, **55**; AA1-MoA8, 55; AA5-TuP7, 127
— E —
Eddy Jr., C.R.: AF-TuA7, 107
Eddy, C.R.: AS2-TuA214, 113
Eddy, Jr., C.R.: AF1-TuM4, 92; AF-TuA6, 107; EM3-WeM13, **141**
Eden, J.G.: AF-TuA5, 106
Edley, M.: ALE1-WeM1, 133
Eizenberg, M.: AF3-TuM15, 96; ALE1-WeM7, 134
Ekerdt, J.: AF4-MoA11, **63**; AS2-TuA111, 112
Elam, J.W.: AA1-TuP11, 116; AA1-TuP13, 117; AA2-TuA11, 102; AA2-TuA12, 103; AA2-WeA6, 145; AA4-TuP11, 125; AF1-MoA1, 57; EM1-WeA1, 146; ~~EM1-WeA4~~, 147; NS-WeA2, 149; PS1-MoM5, **53**
Elhadj, S.: EM-MoP9, 86
Eller, B.: AF4-MoP4, 79
Ellingboe, A.R.: AF4-MoP11, 80
Elliot, S.: AF1-MoA5, 58; ALE1-TuM5, 97
Elliott, S.D.: ALE2-TuA14, **109**
~~Elmustafa, A.~~: ~~AA4-TuP10~~, 125
Elnikova, L.: AF5-MoP2, 81
Endo, K.: ALE2-TuM12, 98
Engelmann, S.: ALE2-WeM15, 135
Engeln, R.: AF1-TuM5, 92
~~Eom, S.~~: ~~AA2-TuP20~~, **122**
Eom, T.: AA2-MoA13, 56
Eperon, G.: AA2-MoA11, 56
Ermert, D.: AF1-MoP9, **70**
Esarey, S.: AA1-TuM7, 89
~~Etinger-Geller, Y.~~: ~~AF5-MoP10~~, **82**
Evans, P.G.: EM-MoP11, 87
— F —
Faguet, J.: ALE1-MoA8, 66; ALE-SuP11, 52
Fanciulli, M.: AA1-TuA3, 101
Farjam, N.: AS1-TuA7, 112
Feigelson, B.: NS-TuP4, 130
Feldman, A.: AM1-WeM7, 137
Feng, J.-Y.: AF1-TuM7, 92
Ferguson, I.: AA1-TuP16, **117**
~~Ferretti, A.M.~~: ~~EM-MoP1~~, 85
Fjellvåg, H.: EM1-WeA6, 148
Floros, K.: AA2-TuP6, 119; ALE2-MoA11, 66
Folestad, S.: AA1-MoA1, 54; EM-MoP2, 85
Foody, M.: AF1-MoP14, 71; AF4-MoA14, **63**
Foss, A.E.: AF4-MoP10, 80
Fourkas, J.: ALE1-MoA5, 65
Frank, M.: EM1-WeA5, 147
Frankel, I.: AF2-TuM6, 94
Franquet, A.: AS-TuP6, 129
Frey, A.: AM-MoP1, 82
Friz, A.: AS1-TuA6, 111
Fryauf, D.: AM1-WeM7, 137
Fu, H.: ALE2-MoA15, 67
Fu, K.: ALE2-MoA15, 67
Fu, Y.-C.: ALE2-MoA11, 66
Fujii, T.: ALE2-TuM12, 98
Fujisaki, S.: ALE1-TuM8, **98**
Fusco, M.: EM1-WeM4, 138
— G —
~~Gallardo, S.~~: ~~AA2-TuP11~~, 120
Gao, F.: **AF3-MoA12**, 61; AF3-MoA16, 62
Gao, K.: AA4-TuP11, 125
Gao, T.: AS-TuP2, 128
Garcia-Mendez, R.: AA2-TuM13, 90
Gargouri, H.: AA2-TuP16, 121; AM-MoP2, **83**
Gaskell, A.: AA3-TuA11, 104
Gassilloud, R.: AS2-TuA112, 112
Gasvoda, R.: ALE2-WeM16, **135**
Gaulding, A.: AA2-MoA16, 57
Gavartin, J.: AF1-MoA5, 58
Gayle, A.: AA1-TuM7, 89; AA1-WeA2, 143
Gebhard, M.: AA1-TuP11, **116**; AA1-TuP13, 117; EM1-WeA1, **146**; ~~EM1-WeA4~~, 147
Gennett, T.: AA2-MoA15, 56; AA2-MoA16, 57
George, S.M.: AF4-MoA15, 63; ALE1-TuM3, 97; ALE1-TuM5, 97; ALE1-TuM7, 97; ALE2-MoA13, **66**; ALE2-TuA14, 109; AS1-TuM14, 99; EM1-WeM8, 139
~~Geyer, S.~~: ~~AA3-TuP3~~, 122
Gheeraert, E.: **ALE2-MoA16**, 67
Ghods, A.: AA1-TuP16, 117
Gill, Y.J.: ALE-SuP14, 52
Gillespie, C.: EM-MoP9, 86
Ginga, N.: AA1-WeA2, 143
Girard, J.-M.: AA1-WeM5, 131
Giri, A.: EM2-WeM16, 140
Girolami, G.: AS1-TuA4, 111
Givens, M.: AA3-TuA13, 104; AF2-TuM7, 95
Go, D.: AM-MoP5, **84**
Goeke, R.: ALE-SuP4, 50
Goennenwein, S.T.B.: AA1-WeA8, 144
Goff, J.: AS-TuP3, 128
Gokhale, V.: AF-TuA7, 107
Golka, S.: AM-MoP2, 83
Goncharova, L.: AA2-TuM14, 90
Gonon, P.: AS2-TuA112, 112
Goodyear, A.: ALE1-MoA4, 65
Goorsky, M.: AF-TuA7, 107
Gordon, P.: AA1-WeA5, **144**
Gottardi, G.: AF5-MoP2, 81
Gottscho, R.: ALE1-MoA1, 64
Gougousi, T.: AA1-TuA7, **102**
Goul, R.: AA2-TuP15, 121
Goux, L.: AA1-WeM5, 131
Govenius, J.: AA2-WeA4, 145
Graniel, O.: AA1-MoA3, 54
Grasso, J.: AM1-WeM1, **135**
Greeley, J.P.: AA2-TuA12, 103
Greenaway, A.: AF2-MoP4, **73**
Greenberg, B.: NS-TuP4, **130**
Greer, F.: AA1-MoA6, **55**
Gregory, S.: AA1-TuA8, **102**
Greth, K.D.: ALE-SuP4, 50
Griffiths, M.: **AA1-TuA5**, 101; AF2-MoA3, 59; AF2-MoA4, **59**; AF-TuA4, 106
Grigoras, K.: AA2-WeA4, **145**
Grigsby, B.: AA5-TuP2, 126
Grillo, F.: **AA1-TuA5**, 101; AF1-MoA3, **58**; AS-TuP6, 129
Grob, C.: AA1-MoA8, 55
Grönberg, L.: AA2-WeA4, 145

Author Index

Gross, K.: AA2-MoA15, 56
Grzeskowiak, J.: AF1-TuM4, 92
~~Gu, C.~~: ~~AA2-TuP2~~, **118**
Gu, J.: AF2-MoP14, 75
Guay, J-M.: AA1-WeA5, 144
Guinney, I.: AA2-TuP6, 119
Guisinger, N.: AA1-TuP19, 118
Gunn, R.: AA5-TuP2, 126
Guo, X.: ALE1-MoA7, **66**; ALE1-TuM4, 97
Gutierrez Razo, S.: ALE1-MoA5, 65
— H —
Haeger, T.: ALE2-TuM16, 99
Hahn, C.: AA1-WeA5, 144
Haider, A.: AA1-WeM5, 131
Halls, M.: AF1-MoA5, 58
~~Hamaguchi, S.~~: AF4-MoP6, 79; ALE1-TuM1, 96; ~~ALE2-TuA15~~, **110**; ~~ALE-SuP8~~, 51
Hampel, N.A.: AF1-TuM2, 91
Han, G.D.: AA1-WeA3, 143; AA4-TuP7, **124**
Han, Y.: EM-MoP15, 87
Hao, M.: ALE2-MoA15, 67
Hao, W.: NS-WeA7, 150
~~Haridas, A.~~: ~~AA1-TuP1~~, **115**
Harris, K.: AA1-TuP6, 115
Hartig, J.: AF1-MoA6, **58**
~~Hartinger, S.~~: ~~AA2-TuP18~~, 121
~~Hartmann, G.~~: ~~AF3-MoP5~~, 77
Hasegawa, M.: AA1-MoA5, 55; ALE2-MoA17, **67**
Hashemi, F.S.M.: **AA1-TuA5**, **101**
Hassel, J.: AA2-WeA4, 145
Hasselmann, T.: AF2-MoA5, 59; AM1-WeM2, **136**
Hatanaka, M.: EM1-WeA5, 147
Hatanpää, T.: AF2-TuM2, 93
Hatase, M.: AF1-MoP10, 70
Hatch, K.: ALE2-MoA15, **67**
Haufe, N.: AF3-MoA13, 61
Haukka, S.: ALE1-TuM6, 97
Haung, Z.: AF4-MoP4, 79
Hausmann, D.: AS1-TuA2, 110; AS1-TuA3, 111; AS1-TuA5, 111
Haverkate, L.: AA2-TuA13, 103
Hayes, M.H.: AA2-WeA5, **145**; AF5-MoP6, 82
He, C.: ALE1-TuM4, 97
~~He, Y.~~: ~~EM3-WeM16~~, 141
Heikkilä, M.J.: AF2-TuM2, 93
Heinonen, O.: AS2-TuA215, 113
Heiska, J.: AA2-TuA14, **103**
Hemakumara, D.: AA2-TuP6, **119**; ALE2-MoA11, 66
Hendrix, B.: AS1-TuA8, 112
Hennessy, J.: AA1-MoA7, **55**
Henry, M.D.: EM1-WeA7, 148
Heo, J.: AA2-TuP17, 121; AA4-TuP12, 125
Hermida-Merino, D.: AF1-TuM7, 92
Hernandez-Arriaga, H.: AA1-WeM3, 131; AA3-TuA15, 104
Hess, A.: AS1-TuA6, 111
Hidayat, R.: AF1-MoP11, **71**; ~~AF2-MoP15~~, 75; AF2-MoP3, 72
Higashi, S.: AF2-MoA8, 60
Hikichi, K.: AF3-MoP1, 76
Hilt, O.: AA2-TuP16, 121
Hintzen, H.: AA1-TuM8, 89
Hirose, F.: AA4-TuP3, 124; AA4-TuP5, 124; AF4-MoP1, 78
Hirose, M.: AA2-TuP19, **122**; AF4-MoA16, 64
Hock, A.: AF1-MoP14, **71**
Hody, H.: AS-TuP6, 129
Hoex, B.: AA1-TuP18, 118; EM1-WeA8, 148
Holden, K.: AF2-TuM5, **94**; AF5-MoP6, 82
Hong, D.: AM1-WeM5, 136
Hong, K.P.: AF5-MoP7, 82
Hong, M.: AA2-TuP12, 120; **AA2-WeM16**, 133
Hong, W.P.: AA3-TuP1, 122; AA3-TuP5, 122
Hopkins, P.: EM1-WeM4, 138; EM2-WeM16, 140
Hopstaken, M.: EM1-WeA5, 147
Hori, M.: ALE1-MoA3, 65; ALE1-TuA3, 107; ALE2-MoA17, 67; ALE2-WeM13, 134
Hossain, M.A.: AA1-TuP18, 118; EM1-WeA8, **148**
Hössinger, A.: ALE2-TuA12, 109
Hsu, T.-Y.: AA1-WeA7, 144
Hu, J.: AA2-WeA8, **146**
~~Huang, G.~~: ~~AA3-TuP6~~, 123
Huang, J.: AF5-MoP1, 80
Huang, J.-H.: AA2-TuP12, 120
Huber, C.: AS1-TuA7, 112
Hudson, E.: ALE2-WeM16, 135
Hughes, T.: AF1-MoA5, 58
Humlíček, J.: AF2-MoP17, 76
Humphreys, C.: AA2-TuP6, 119
~~Huong, C.~~: ~~EM-MoP3~~, **85**; EM-MoP4, 85
Hurst, K.: AA2-MoA16, **57**
~~Hussain, M.N.~~: ~~ALE-SuP5~~, **51**
Hwang, B.K.: AF4-MoP10, 80; AF4-MoP5, 79
~~Hwang, G.~~: ~~AF3-MoP5~~, **77**; ALE2-TuA11, **109**
Hwang, K.: AA3-TuA16, 105
Hwang, S.M.: AF4-MoA17, 64; AF4-MoP10, 80; AF4-MoP5, **79**; AS-TuP4, **128**
Hwangbo, H.: AA1-TuP3, 115
Hyttinen, P.: **AF3-MoA12**, 61
— I —
Iacopetti, S.: ALE1-WeM7, **134**
Ievlev, A.: EM2-WeM14, 140
Ihlefeld, J.: EM1-WeA7, 148
Ikeda, N.: AA2-TuP19, 122; AF4-MoA16, 64
Ilhom, S.: AF3-MoP7, 77; AF3-TuM13, 95; AF3-TuM16, **96**; AF4-MoP3, **79**
~~Ilyn, M.~~: ~~AF4-MoA13~~, 63
Inbar, H.S.: AF1-TuM4, 92
Inoue, K.: AF3-MoP1, 76
Inoue, M.: AF2-MoA8, 60; AF4-MoA16, 64
Iordanov, I.: AM-MoP6, 84
Irokawa, Y.: AA2-TuP19, 122
~~Ishibashi, K.~~: ~~AF3-MoP5~~, 77
Ishikawa, K.: ALE2-MoA17, 67; ALE2-WeM13, 134
~~Isobe, M.~~: ~~ALE2-TuA15~~, 110
Ito, K.: AF4-MoA16, 64
~~Ito, T.~~: AF4-MoP6, 79; ALE1-TuM1, **96**; ~~ALE2-TuA15~~, 110; ~~ALE-SuP8~~, 51
Ivanov, I.: EM2-WeM14, 140
Ivanov, S.: AF1-MoP1, 69; AF2-MoP2, 72
Ivanova, T.: AA3-TuA13, **104**; AF2-TuM7, 95
~~Iwao, T.~~: ~~AF3-MoP5~~, 77
Izawa, M.: ALE2-WeM13, 134
— J —
Jacobson, L.: AF1-MoA5, 58
Jacopin, G.: **ALE2-MoA16**, 67
Jalkanen, P.: NS-WeA5, 149
Jang, J.H.: AA1-TuP3, 115
Jang, S.J.: AA4-TuP8, 125
Jayakodiarachchi, N.: EM-MoP11, **87**
~~Jelovica Badovinac, I.~~: ~~AF4-MoA13~~, 63
Jenkins, M.: AF5-MoP6, **82**
Jeon, H.: AA2-WeA1, **145**
Jeon, N.: AS2-TuA215, 113
Jeon, N.J.: AA2-MoA13, 56
Jeong, B.H.: ALE-SuP14, 52
Jeong, J.: AA1-MoA4, 54; ALE-SuP12, 52
Jeong, J.Y.: EM-MoP15, **87**
Ji, H.: AF2-MoP18, 76
Ji, Y.J.: AF4-MoP11, 80
Jiang, Y.-S.: AA3-TuA14, 104
Jimenez, C.: AA4-TuP9, 125
~~Jõgiaas, T.~~: ~~EM-MoP7~~, 86
Johnson, A.: AA1-TuA7, 102
Johnson, N.: ALE2-MoA13, 66
Johnson, S.D.: AS2-TuA214, 113
Johs, B.: AF3-TuM13, 95
Jongen, R.: AS1-TuA5, 111
Joseph, E.A.: ALE2-WeM15, 135; PS2-MoM11, **53**
Journet, C.: NS-WeA7, 150
Jung, S.H.: AA2-TuP17, 121
Jung, Y.C.: EM-MoP5, 85
Junghans, T.: AA4-TuP6, 124
— K —
Kääriä, M.: AF5-MoP4, 81; AM-MoP9, 84
Kachian, J.: AA1-WeM6, **132**
Kagaya, M.: AF4-MoP6, 79
Kalaitzidou, K.: AA1-TuA4, 101
~~Kalam, K.~~: ~~EM-MoP7~~, **86**
Kalliomäki, J.: AF5-MoP4, 81; AM-MoP9, 84
Kaloyeros, A.: AS-TuP3, 128
Kanarik, K.J.: ALE1-MoA1, 64
Kang, D.: AA2-TuA12, **103**
Kang, E.H.: AA1-WeA3, 143
Kang, H.-K.: AA3-TuA16, 105
Kang, M.: AA2-TuP8, 119
Kanomata, K.: AA4-TuP3, 124; AA4-TuP5, 124; AF4-MoP1, 78
Kao, W.-C.: EM3-WeM15, **141**
Kar, G.S.: AA1-WeM5, 131
Karacaoglu, E.: AA1-WeA1, **143**
~~Karahashi, K.~~: AF4-MoP6, 79; ALE1-TuM1, 96; ~~ALE2-TuA15~~, 110; ~~ALE-SuP8~~, **51**
Karppinen, M.: AA2-TuA14, 103; EM2-WeM16, 140
~~Kasikov, A.~~: ~~EM-MoP7~~, 86
~~Katsman, A.~~: ~~AF5-MoP10~~, 82
Kazyak, E.: AA1-TuM7, 89; AA1-WeA2, 143; AA2-TuM12, 89; AA2-TuM13, 90; AA2-TuM15, 90; AS1-TuA7, 112
~~Kei, C. C.~~: ~~AF2-MoP6~~, 73
Kelliher, A.: EM1-WeM4, 138
Kelliher, J.: AA4-TuP2, 123
Kemell, M.: AF2-TuM4, 94
Kenny, T.W.: AF5-MoP8, 82
Kessels, W.M.M.: AA1-TuM3, 88; AF1-TuM5, 92; **AF3-MoA12**, 61; AF-TuA2, 105; AS1-TuA5, 111; AS2-TuA111, 112; NS-WeA6, 149; PS1-MoM2, **53**
Khalil, G.: AA1-WeM5, 131
Khan, A.: AA3-TuA11, 104
Khan, S.: ALE1-TuA1, **107**
Khosravi, A.: AA3-TuA15, 104
Kia, A.M.: AF3-MoA13, 61
Killaire, G.: AA1-WeA5, 144
Killge, S.: AF1-TuM2, 91
Kim, B.: AA1-WeA6, **144**
Kim, B.J.: AA1-WeA3, 143
Kim, C.G.: AA2-MoA13, 56
~~Kim, C.-M.~~: ~~AA2-TuP7~~, 119
Kim, D.: AF1-MoP3, **69**; AF2-MoP1, 72
Kim, D.H.: AA2-MoA17, **57**; AF1-MoP7, **70**
Kim, D.S.: ALE-SuP14, **52**
Kim, G.J.: AA2-MoA13, 56
Kim, G.W.: AF4-MoP12, 80
Kim, H.: AA2-WeM14, 132; AA2-WeM15, 132; ~~AA5-TuP9~~, 127; AF2-MoP10, 74; AF2-MoP13, 75; AF2-MoP9, 74
Kim, H.J.: AF5-MoP8, 82; AM-MoP5, 84
Kim, H.-L.: AF1-MoP11, 71; AF2-MoP3, 72
Kim, H.S.: AA1-WeM3, **131**; AA3-TuA15, 104; AF4-MoP5, 79; AS-TuP4, 128
Kim, H.Y.: AA2-TuP17, **121**; AA4-TuP12, 125
~~Kim, I.S.~~: ~~AA1-TuM1~~, 88
Kim, J.: AA1-TuP17, **117**; AA1-TuP3, **115**; AA1-WeM3, 131; AA3-TuA15, 104; AF2-

Author Index

MoP3, **72**; AF3-MoP10, **78**; AF4-MoA17, 64; AF4-MoP5, 79; AF-TuA5, **106**; AS-TuP4, 128
Kim, J.E.: ALE-SuP14, 52
~~Kim, J.H.~~: ~~AF4-MoP8~~, **80**
Kim, J.-H.: AA2-TuP1, 118
Kim, J.Y.: AF4-MoP10, 80
Kim, K.H.: AF4-MoP11, **80**
Kim, K.Kim.: AA1-TuP10, **116**
Kim, K.S.: AF4-MoP11, 80
Kim, M.-S.: AF1-MoP1, 69; AF2-MoP2, **72**; AF4-MoP2, 78
Kim, M.W.: AA4-TuP8, 125; AA5-TuP8, 127
Kim, S.: AF2-MoP14, 75; ~~AF2-MoP15~~, 75; AF2-MoP3, 72
Kim, S.G.: AA4-TuP8, 125
Kim, S.-H.: AA1-TuP7, 115; AF1-MoP7, 70; AF2-MoP10, 74; ~~AF2-MoP15~~, 75
Kim, S.J.: AA1-TuP3, 115
Kim, S.-J.: ALE1-MoA6, 65
Kim, S.Y.: EM-MoP5, 85
~~Kim, T.H.~~: ~~AF2-MoP15~~, **75**
Kim, W.-H.: AA2-WeM14, 132; AA2-WeM15, 132
Kim, Y.: AA3-TuA16, 105; ~~AA5-TuP9~~, 127; AF2-MoP14, 75; ALE-SuP9, **51**; EM-MoP14, **87**
Kim, Y.S.: ALE2-WeM12, 134; ALE-SuP13, 52
Kimes, W.: AF2-TuM1, 93
Kimmerle, B.: AM-MoP4, 83
Kimmerle, K.: AF2-TuM1, 93; AM-MoP4, 83
Kimmerle, W.: AF2-TuM1, 93
King, P.: NS-WeA5, 149
Kint, J.: **EM1-WeM7**, **139**
Kioussis, D.: AA1-WeM6, 132
Kishimoto, A.: AA2-TuA15, 103
Kisslinger, K.: EM2-WeM14, 140
Kivioja, J.: AF5-MoP4, **81**
Kiyono, H.: AA2-TuP19, 122; AF4-MoA16, 64
~~Kleinlein, J.~~: ~~AA2-TuP18~~, 121
Klement, P.: AS-TuP1, **128**
~~Klimin, V.~~: ~~ALE-SuP3~~, **50**
Knaut, M.: AF1-TuM2, 91
Knemeyer, K.: AF3-MoA11, **61**
~~Knez, M.~~: ~~AF4-MoA13~~, 63; EM2-WeM12, **139**; ~~EM-MoP8~~, 86
Knoops, H.: AA2-TuP6, 119; AA5-TuP2, 126; AF-TuA2, 105
Ko, D.-H.: ALE-SuP12, 52
Kobayashi, A.: ALE1-MoA3, 65
Kobayashi, H.: ALE2-WeM13, 134
Kobayashi, N.: ALE1-MoA3, 65; ALE1-TuA3, 107; AM1-WeM7, 137
Koeck, F.: AF4-MoP4, 79
Koh, W.: EM-MoP14, 87
Koide, Y.: AA2-TuP19, 122
~~Kolympadi Markovic, M.~~: ~~AF4-MoA13~~, 63
Komachi, J.: ALE1-TuA7, 108
Kondati Natarajan, S.: ALE1-TuA5, 108; ALE-SuP2, 50; ALE-SuP6, 51
Kondo, H.: ALE2-MoA17, 67
Kondusamy, A.L.N.: AF4-MoA17, **64**; AF4-MoP10, 80; AF4-MoP5, 79; AS-TuP4, 128
~~Kong, M.~~: ~~AA2-TuP20~~, 122
Konh, M.: ALE1-TuM4, 97; ALE-SuP1, **50**
Koo, J.: AA2-MoA17, 57; AA4-TuP7, 124
Korchnoy, V.: AA2-TuP5, **119**; AF3-TuM15, **96**
Kostamo, J.: AM-MoP9, **84**
Kozen, A.: AA5-TuP4, 126; ALE-SuP7, 51
Krahl, F.: EM2-WeM16, **140**
Krbal, M.: NS-TuP1, 129
Kreutzer, M.: AA1-TuM8, 89
Krick, B.: AA5-TuP4, 126
Kriegner, D.: AA3-TuA11, 104
Krishnamurthy, R.: AA1-WeM1, **131**
~~Krishtab, M.~~: ~~AS2-TuA113~~, **113**
Kropp, J.A.: AA1-TuA7, 102
Krüger, O.: AA2-TuP16, 121
Krumpolec, R.: AF2-MoP17, **76**
Krylov, I.: AF3-TuM15, 96
Kuboi, N.: ALE1-TuA7, **108**
Kubota, S.: AA4-TuP3, 124; AA4-TuP5, 124
Kubota, T.: AF-TuA1, 105
Kuech, T.F.T.: EM-MoP11, 87
Kuis, R.: AA1-TuA7, 102
~~Kukli, K.~~: ~~EM-MoP7~~, 86
Kulkarni, S.: ALE2-TuA13, **109**
Kumano, M.: AF3-MoP1, **76**
Kurek, A.: AA5-TuP2, **126**
Kurihara, H.: ALE2-TuM12, 98
Kuyel, B.: AF5-MoP7, **82**
Kwak, S.: AF1-MoA5, 58
Kwo, J.: AA2-TuP12, 120; **AA2-WeM16**, 133
Kwon, J.-D.: AA1-TuP2, **115**
~~Kwon, S. H.~~: ~~AA2-TuP7~~, 119; AA3-TuP1, 122; AA3-TuP5, 122
— L —
La Zara, D.: AA1-MoA1, **54**; EM-MoP2, **85**
Lai, S.: ALE1-WeM7, 134
Laiwalla, F.: AA1-MoA4, 54
Lam, D.V.: AA2-TuP1, 118
Lambert, D.: EM1-WeA8, 148
Lammel, M.: AA1-WeA8, **144**
Lancaster, A.: AF1-MoA1, 57
Land, M.: AF1-MoP4, **69**
Lange, A.: EM-MoP9, 86
Langeslay, R.: AA2-WeA6, 145
Larrabee, T.J.: AF3-MoP8, **78**
Lasso, J.: AA2-TuM12, 89
Lavrik, N.: EM2-WeM14, 140
Lawson, M.: NS-TuP5, **130**
Layne, B.: AA1-TuP14, 117
Lazzarini, L.: AA1-TuA3, 101
Le Roux, F.: ALE2-MoA14, **67**
Lee, B.: AA2-TuP8, 119
Lee, C.: AF1-MoP1, **69**; AF4-MoP10, 80; AF4-MoP2, 78
Lee, C.W.: AA2-WeM14, 132
Lee, H.B.R.: AF2-MoP9, 74
Lee, H.I.: AA3-TuA16, 105
Lee, J.: AA2-WeM15, **132**; AF1-MoP3, 69; AF2-MoP1, **72**; EM3-WeM13, 141; EM-MoP14, 87
Lee, J.-H.: EM1-WeM5, 138; EM1-WeM6, 138
Lee, J.-J.: ALE1-MoA6, 65
Lee, K.L.: ALE1-WeM1, 133
~~Lee, M.~~: ~~AA5-TuP9~~, **127**
Lee, M.Y.: AF2-MoP10, 74; ~~AF2-MoP15~~, 75
Lee, S.: AA1-TuM7, 89; AF2-MoP10, 74
Lee, S.D.: AA4-TuP8, 125
Lee, S.-H.: ALE1-MoA6, 65; EM1-WeM5, **138**; EM1-WeM6, 138
Lee, S.I.: AA4-TuP8, 125; AA5-TuP8, 127; AF1-MoP11, 71
Lee, S.-M.: AA2-TuP1, **118**
Lee, S.-W.: ~~AA2-TuP7~~, **119**; AF1-MoP1, 69; AF2-MoP2, 72; AF4-MoP2, **78**
Lee, T.: EM-MoP5, 85
Lee, W.-H.: EM3-WeM15, 141
Lee, W.-J.: AA1-TuP17, 117; AA3-TuP1, 122; AA3-TuP5, 122; AF1-MoP11, 71; AF2-MoP14, 75; ~~AF2-MoP15~~, 75; AF2-MoP3, 72; EM-MoP14, 87
Lee, W.O.: ALE-SuP14, 52
Lee, Y.: ALE2-MoA13, 66
~~Lee, Y.B.~~: ~~AF4-MoP8~~, 80
Lee, Y.-J.: ALE2-TuM12, 98
Lee, Y.K.: AA2-MoA13, 56
Lee, Y.-S.: ALE1-MoA6, **65**
Lefaucheux, P.: ALE1-MoA8, 66; ALE-SuP11, 52
Leff, A.: EM1-WeA2, 147
Lehto, T.: AF5-MoP4, 81; AM-MoP9, 84
Lei, X.: AF2-MoP8, 73; AF4-MoP2, 78
Leick, N.: AA2-MoA15, **56**; AA2-MoA16, 57
Leijtens, T.: AA2-MoA11, 56
Lemaire, P.C.: AS1-TuA3, 111
Lembesis, P.: ALE1-WeM8, 134
LePage, W.: AA1-WeA2, 143
Lesina, A.: AA1-WeA5, 144
Leskelä, M.: AF2-MoA7, 60; AF2-TuM2, 93; AF2-TuM4, 94; EM1-WeM2, 137; NS-WeA5, 149
Letourneau, S.: AF1-MoA1, 57; EM1-WeA1, 146; NS-WeA2, 149
Leusink, G.: AA2-WeM12, 132; AF2-MoP16, 75
Levrau, E.: EM1-WeA5, 147
Lezec, H.: AA1-WeA4, 143
Li, A.-D.: AA3-TuP7, 123; EM1-WeM1, 137
Li, C.: ALE2-WeM15, 135
Li, F.: AF3-MoP3, 77
Li, H.: AA1-WeA4, **143**; ~~AA3-TuP3~~, **122**; AF4-MoP6, **79**
Li, R.: AA2-TuM14, 90
Li, T.: AA1-TuM5, 88; AA2-TuP13, 121
Li, X.: AA2-TuP6, 119; ALE2-MoA11, **66**
Li, Y.: AA1-TuA4, 101; ALE2-TuM12, 98
Lim, E.T.: ALE-SuP10, **51**
Lim, H.-D.: AA4-TuP8, 125; AF1-MoP11, 71
Lim, H.-J.: AA3-TuA16, 105
Lim, T.: AA1-TuP12, **116**
Lin, B.-T.: AA1-WeA7, 144
~~Lin, C.-L.~~: ~~AF2-MoP6~~, 73
Lin, H.-C.: EM3-WeM15, 141
Lin, K.-Y.: AA2-TuP12, 120; **AA2-WeM16**, **133**
Lin, K-Y.: ALE1-MoA5, 65; ALE2-WeM15, **135**
~~Lin, P.~~: ~~AA2-TuP9~~, 120; ~~AA4-TuP10~~, 125; ~~AM-MoP3~~, **83**
Lin, X.: ALE1-TuM4, 97
~~Lin, Y. C.~~: ~~AF2-MoP6~~, **73**
Lin, Y.-H.: AA2-TuP12, 120; **AA2-WeM16**, 133
Linford, M.: EM-MoP13, 87
~~Link, J.~~: AF2-TuM2, 93; ~~EM-MoP7~~, 86
Lisiansky, M.: AA2-TuP5, 119
Littau, K.: AA1-WeM4, 131; AF3-MoA16, 62
Liu, B.: AA2-TuP15, 121
~~Liu, B. H.~~: ~~AF2-MoP6~~, 73
~~Liu, J.~~: ~~AA2-TuM16~~, 90; AA2-TuP12, 120; ~~EM1-WeA4~~, 147
Liu, M.: AA1-TuP14, 117
~~Liu, S.~~: AA5-TuP5, 127; ~~AF4-MoP9~~, **80**; AS1-TuA4, 111; ~~EM3-WeM16~~, 141
Liu, T.-L.: AS1-TuA1, 110; AS1-TuA2, **110**
Lively, R.: EM2-WeM13, 140
Lo, J.: ALE1-WeM8, 134
Long, N.V.: AA1-TuP15, 117; EM-MoP4, 85
Longo, E.: AA1-TuA3, **101**
Longo, M.: AA1-TuA3, 101
Losego, M.: AA1-TuA4, 101; AA1-TuA8, 102; AA1-WeA1, 143; EM2-WeM13, 140; EM2-WeM15, **140**; EM3-WeM12, 140
Lou, Q.: ALE1-WeM1, 133
Lu, Y.T.: ALE1-WeM1, 133
Lucero, A.T.: AF4-MoA17, 64; AF4-MoP10, 80
Ludwig, K.F.: AS2-TuA214, 113
Lushington, A.: AA2-TuM14, **90**
— M —
Ma, A.: AA2-TuP10, **120**
~~Ma, F.~~: ~~AA3-TuP6~~, 123
Ma, X.: AA2-TuP13, 121

Author Index

Ma, Y.: EM2-WeM13, 140
Macak, J.: AA2-TuA16, **104**; NS-TuP1, 129
Mack, J.: AA2-TuP17, 121; AA3-TuA11, 104; AA4-TuP12, **125**
Mackus, A.J.M.: AS1-TuA5, 111; AS2-TuA111, 112
Maclsaac, C.: NS-WeA1, 148
Maeda, E.: AA2-TuP19, 122; AF4-MoA16, **64**
Maekawa, K.: ALE1-MoA8, 66; ALE-SuP11, 52
Maes, J.W.: AA1-WeM5, 131
Mahuli, N.: AF4-MoA15, **63**
Mai, L.: AF1-MoP12, **71**; AF1-MoP8, 70
Makarova, O.: AA5-TuP10, 128
Mallick, B.: AF2-TuM6, 94
Mallikarjunan, A.: AF2-MoP8, 73
Mameli, A.: ALE1-WeM3, **133**; AS1-TuA5, 111; AS-TuP5, **129**
Mandia, D.: AA1-TuP19, **118**; AS2-TuA215, 113; EM1-WeA1, 146; ~~EM1-WeA4~~, **147**
Mane, A.: AA1-TuP11, 116; AA1-TuP13, **117**; AA2-TuA11, 102; AA2-TuA12, 103; AA2-WeA6, **145**; AA4-TuP11, 125; EM1-WeA1, 146; NS-WeA2, **149**
~~Mane, A.U.~~: ~~EM1-WeA4~~, 147
Mannequin, C.: **ALE2-MoA16**, **67**
Manstetten, P.: ALE2-TuA12, 109
Mantovan, R.: AA1-TuA3, 101
Mäntymäki, M.: AM-MoP9, 84
Marichy, C.: NS-WeA7, **150**
Mariette, H.: **ALE2-MoA16**, 67
Marques, E.: AS-TuP6, 129
Marshall, C.: AA1-TuM5, 88
Marshall, J.: AF5-MoP7, 82
Martinez, M.: AA2-MoA16, 57
~~Martinson, A.~~: ~~AA1-TuM1~~, **88**; AA1-TuP19, 118; AS2-TuA215, 113
Masanobu, H.: ALE1-WeM1, 133
Maslar, J.: AF2-TuM1, **93**; AM-MoP4, 83
Masse de la Huerta, C.: AM1-WeM5, 136
Masuda, J.: AF2-TuM6, 94
Matsukuma, M.: AF4-MoP6, 79
Mattelaer, F.: AF1-TuM6, 92; **EM1-WeM7**, 139
Mattinen, M.: AF2-MoA7, 60; AF2-TuM2, 93; AF2-TuM4, 94; NS-WeA5, **149**
McBriarty, M.E.: AF3-MoA16, 62
McCarthy, M.: AA2-MoA12, 56
McFadden, A.: EM3-WeM13, 141
McGehee, M.: AA2-MoA11, 56
McGettigan, C.: AA1-TuA8, 102
McGuinness, E.: AA1-TuA8, 102; EM2-WeM13, **140**
McKee, T.: AA1-MoA4, 54
McKenzie, C.: AA5-TuP2, 126
~~Mei, Y.F.~~: ~~AA3-TuP6~~, **123**
Meng, X.: AF2-MoP12, **74**; AF4-MoA17, 64
Merkx, M.: AS1-TuA5, **111**
Messina, D.: AF4-MoP4, **79**; ALE2-MoA15, 67
Metzler, D.: ALE2-WeM15, 135
Mey-Ami, L.: AF3-MoP3, 77
Meyer, D.: AF-TuA7, 107
Meyler, B.: AA2-TuP5, 119
Meynaerts, B.: AS1-TuM16, 100
Michel, F.: AS-TuP1, 128
Miele, P.: AA1-MoA3, 54
~~Mikkor, M.~~: ~~EM-MoP7~~, 86
Miller, J.: EM-MoP9, **86**
Millward, A.R.: AF4-MoP10, 80
Min, S.H.: AA2-WeM14, **132**
Minjauw, M.: AF1-TuM7, 92; AF-TuA4, 106; **EM1-WeM7**, 139
Minot, M.: AA1-TuP13, 117
Mione, M.A.: AF1-TuM5, **92**
Mironov, A.: AF-TuA5, 106
Misra, V.: AA2-TuP8, 119
Mitschker, F.: AF1-MoP12, 71
Miura, M.: AA4-TuP3, 124; AA4-TuP5, 124; AF4-MoP1, 78
Miyoshi, N.: ALE2-WeM13, 134
Mizohata, K.: AF2-TuM2, 93; AF2-TuM4, 94; NS-WeA5, 149
Mizubayashi, W.: ALE2-TuM12, 98
Mizutani, F.: AF2-MoA8, **60**
Modreanu, M.: AA2-MoA12, 56; AA2-TuA15, 103
Mohammad, A.: AF3-MoP7, 77; AF3-TuM13, **95**; AF3-TuM16, 96; AF4-MoP3, 79; EM3-WeM14, 141
~~Mohammed, Y.~~: ~~AA4-TuP10~~, **125**
Mohan, J.: AA1-WeM3, 131; AA3-TuA15, **104**
Mokhtarzadeh, C.: ALE1-TuA5, 108; ALE-SuP2, 50
~~Molenkamp, L.~~: ~~AA2-TuP18~~, 121
Monaghan, S.: AA2-MoA12, 56
Moore, D.: AA2-MoA11, 56
Moran, D.: AA2-TuP6, 119; ALE2-MoA11, 66
Moret, J.: AA1-MoA2, 54
Mori, Y.: AA4-TuP5, **124**
Morisato, T.: AF1-MoA5, 58
Moriya, T.: AF4-MoP6, 79
~~Morrison, W.~~: ~~AF5-MoP3~~, 81
Motamedi, P.: AA1-TuP6, 115
Muckley, E.: EM2-WeM14, 140
Mudrick, J.: ALE-SuP4, **50**
~~Muenstermann, D.~~: ~~AA2-TuP11~~, 120
Mukherjee, N.: AA2-TuP17, 121; AA3-TuA11, **104**; AA4-TuP12, 125
Mullins, R.: ALE2-TuA14, 109; ALE-SuP6, **51**
Muneshwar, T.: AA2-TuP10, 120; AF1-MoA2, 57; EM-MoP12, **87**
Muñoz-Rojas, D.: AA4-TuP9, **125**; AM1-WeM5, **136**
Murdzek, J.A.: ALE1-TuM7, **97**
Mustard, T.: AF1-MoA5, **58**
Myers, T.: EM1-WeM8, **139**
— N —
Nabatame, T.: AA2-TuP19, 122; AF2-MoA8, 60; AF4-MoA16, 64
Naghibolashrafi, N.: AA2-TuP17, 121
Nakane, K.: ALE1-TuA3, 107
Nam, C.-Y.: AA1-TuP14, **117**; EM2-WeM14, **140**
Nam, S.W.: AA3-TuA16, 105
Nam, T.: AF2-MoP13, **75**; AF2-MoP9, 74
Nanayakkara, S.: AA2-MoA11, 56
Nandi, D.K.: AA1-TuP7, 115; AF1-MoP7, 70; ~~AF2-MoP15~~, 75
Narasimhan, V.K.: AF3-MoA16, **62**
Nardi, K.: AS1-TuA2, 110
~~Nassiri, A.~~: ~~EM1-WeA4~~, 147
Natarajan, S.K.: ALE1-TuM5, 97; ALE2-TuA14, 109
Nathan, S.: AA1-TuM6, **89**
Naumann d'Alnoncourt, R.: AF3-MoA11, 61
Naumann, F.: AA2-TuP16, 121; AM-MoP2, 83
Nelson, A.: EM-MoP9, 86
Nemanich, R.: AF4-MoP4, 79; ALE2-MoA15, 67
Nepal, N.: AF2-MoP11, 74; AF-TuA6, 107; AF-TuA7, 107; AS2-TuA214, 113
Ngoc Van, T.T.: EM1-WeM5, 138
Nguyen, C.T.: AF3-MoA14, **62**
Nguyen, N.D.: AA4-TuP9, 125
Nguyen, V.H.: AA4-TuP9, 125; AM1-WeM5, 136
Nicholas, C.: AA1-TuM5, 88
Nie, B.: AA2-TuP17, 121
Nielsch, K.: AA1-WeA8, 144
Niiranen, K.: AF3-TuM14, 96
Nilsen, O.: EM1-WeA6, 148
Nim, M.-H.: AF1-MoP6, 70; AF2-MoP14, 75
~~Nishida, A.~~: ~~AS1-TuM15~~, **100**
Noda, S.: ALE2-TuM12, 98
Noh, H.: EM-MoP15, 87
Noh, W.: AA2-WeM14, 132; AA2-WeM15, 132; AF1-MoP3, 69; AF2-MoP1, 72
Nolan, M.: ALE1-TuA5, 108; ALE2-TuA14, 109; ALE-SuP2, 50; ALE-SuP6, 51
~~Nowak, D.~~: ~~AF5-MoP3~~, 81
Nozawa, T.: AF-TuA1, 105
Nugteren, H.: AA1-TuM8, 89
Nurmikko, A.: AA1-MoA4, 54
Nyakiti, L.: AF-TuA7, 107
Nye, R.: EM1-WeM4, **138**
— O —
O'Brien, S.: AA2-MoA12, 56; AA2-TuA15, 103
Oehrlein, G.S.: ALE1-MoA5, 65; ALE2-WeM15, 135
Ogawa, Y.: EM1-WeA5, **147**
Oh, I.-K.: AA2-WeM14, 132; AA2-WeM15, 132; AS1-TuA1, **110**; NS-WeA1, 148
Oh, J.D.: AF1-MoP6, **70**
Oh, S.-J.: AA3-TuP1, 122; AA3-TuP5, **122**
Ohi, A.: AA2-TuP19, 122; AF4-MoA16, 64
Ohori, D.: AF-TuA1, 105; ALE2-TuM12, **98**
Okada, N.: AF1-MoP10, 70; ~~AS1-TuM15~~, 100
~~Okada, Y.~~: ~~ALE2-TuA15~~, 110
Okuno, H.: NS-WeA7, 150
Okuyama, Y.: AA2-TuP17, 121
Okyay, A.K.: AF3-TuM13, 95
O'Mahony, A.: AA2-TuP6, 119; AA5-TuP2, 126
Opila, R.: ALE1-TuM4, 97
Ostermay, I.: AA2-TuP16, 121
O'Tani, J.: EM-MoP13, 87
Overbeek, M.D.: AA1-TuA3, 101; EM-MoP10, **86**
Oyola-Reynoso, S.: ALE1-WeM1, 133
Ozaki, T.: AF-TuA1, 105; ALE2-TuM12, 98
Ozturk, E.: AA1-WeA1, 143
— P —
Paeng, D.: ALE2-WeM12, 134; ALE-SuP13, 52
Pakulski, R.: ALE1-WeM8, 134
Pallem, V.: ALE1-MoA7, 66; ALE1-TuM4, 97
Palmstrom, A.F.: AA2-MoA11, **56**
Palmstrom, C.J.: EM3-WeM13, 141
Palmstrøm, C.J.: AF1-TuM4, 92
~~Pan, D.~~: ~~AF3-MoP4~~, **77**
Pan, Y.: ALE1-MoA1, 64
Pandiyan, S.: AF1-MoA5, 58
Pannier, C.: AS1-TuA7, 112
~~Pantò, F.~~: ~~EM-MoP1~~, 85
Papanastasiou, D.: AA4-TuP9, 125
Parala, H.: AF1-MoP8, 70
Parise, R.: AM-MoP6, **84**
Park, B.-E.: AA2-WeM14, 132; AA2-WeM15, 132; AF2-MoP10, 74
Park, G.J.: AA4-TuP8, 125
Park, H.: ALE-SuP12, 52; EM-MoP15, 87
Park, H.-D.: AA1-WeA3, 143
Park, H.H.: AA2-MoA13, **56**
~~Park, H.S.~~: ~~AF4-MoP8~~, 80
Park, I.-S.: AF2-MoP18, 76; EM-MoP5, **85**
Park, J.: AA1-TuP15, **117**; ~~AA5-TuP9~~, 127; EM-MoP4, 85
Park, J.H.: AA2-MoA17, 57
Park, J.-H.: AA5-TuP8, 127
Park, J.J.: AA4-TuP8, **125**; AA5-TuP8, 127; AF1-MoP11, 71
Park, J.-R.: AF2-MoP14, 75
Park, J.S.: AA1-WeA3, **143**; AA4-TuP7, 124
Park, J.-S.: AA1-TuA1, **101**
Park, J.-S.: EM1-WeM5, 138
Park, J.-S.: EM1-WeM6, 138
Park, J.-W.: AF1-MoP6, 70; AF2-MoP14, 75

Author Index

Park, J.Y.: AA3-TuP1, **122**; AA3-TuP5, 122
Park, K.-H.: AA1-WeA3, 143
Park, S.: AF2-MoP18, **76**; ~~AF5-MoP3~~, **81**
Park, S.-J.: AF-TuA5, 106
Park, S.M.: AF2-MoP10, **74**
Parsons, G.N.: ALE1-WeM5, 133; EM1-WeM4, 138
~~Patanè, S.~~: ~~EM-MoP1~~, 85
Patel, D.: EM-MoP13, 87
Pattison, T.: AS1-TuA6, 111
Pavlopoulos, D.: AA1-WeM6, 132
Pedersen, H.: AF1-MoA7, **58**; AF2-TuM3, 93
Peek, B.: AF1-MoP15, **72**; AF-TuA3, 106
Pelissier, B.: AS2-TuA112, 112
~~Pellin, M.~~: ~~AA1-TuM1~~, 88
Pemble, M.: AA2-MoA12, 56
Peña, L.F.: AS-TuP4, 128
~~Peng, M.~~: ~~EM3-WeM16~~, 141
Pennachio, D.J.: AF1-TuM4, 92; EM3-WeM13, 141
Perng, T.-P.: AA1-TuM4, 88
Pesce, V.: AS2-TuA112, 112
~~Peter, R.~~: ~~AF4-MoA13~~, 63
Peterson, R.: AS1-TuA7, 112
Petersson, G.: AA1-MoA1, 54; EM-MoP2, 85
Pfeiffer, K.: AM-MoP2, 83
Phaneuf, R.: EM1-WeA2, 147
Phillips, A.: AM1-WeM7, 137
Pi, T.-W.: **AA2-WeM16**, 133
Pidko, E.: AA1-MoA2, 54
Piercy, B.: EM3-WeM12, **140**
Piernavieja Hermida, M.: AF3-MoA11, 61
Pilvi, T.: AA1-MoA4, 54
~~Pinna, N.~~: AF2-TuM8, **95**; ~~EM-MoP1~~, 85
Poduval, G.K.: AA1-TuP18, **118**
~~Pokroy, B.~~: ~~AF5-MoP10~~, 82
Polakowski, P.: AA3-TuA13, 104
Polcawich, R.: EM1-WeA2, 147
Pollet, O.: ALE2-TuM14, 98
~~Ponti, A.~~: ~~EM-MoP1~~, 85
Poodt, P.: AA2-TuA13, **103**; ALE1-WeM3, 133; AS-TuP5, 129
Popecki, M.: AA1-TuP13, 117
Popov, G.: AF2-TuM4, **94**; NS-WeA5, 149
Popov, I.: AA2-TuP5, 119
~~Poruba, A.~~: ~~AF4-MoP8~~, 80
Posseme, N.: ALE2-MoA14, 67; ALE2-TuM14, 98
Possémé, N.: AS2-TuA112, 112
Potrepka, D.: EM1-WeA2, 147
Potter, R.: AF-TuA3, 106
Povey, I.: AA2-MoA12, 56; AA2-TuA15, **103**
~~Pradhan, A.~~: ~~AA2-TuP9~~, 120
Pranda, A.: ALE1-MoA5, **65**
Prasanna, R.: AA2-MoA11, 56
Pribil, G.: AA1-TuA6, 102
Prikryl, J.: NS-TuP1, 129
Prinz, F.: AF5-MoP8, 82
Provine, J.: AF3-TuM12, 95; AF5-MoP8, 82
Prunnila, M.: AA2-WeA4, 145
Pudas, M.: AA1-MoA4, 54
Pulskamp, J.: EM1-WeA2, 147
Pupek, K.: AA2-WeA6, 145
Puurunen, R.: **AF3-MoA12**, 61; AF3-MoA13, 61; AF3-MoA16, 62; AF5-MoP2, 81; AF-TuA2, 105
— Q —
Qadri, S.: AF-TuA7, 107
Qin, Y.: AF3-MoA17, 62
Qin, Z.: AF4-MoA17, 64
~~Qiu, P.~~: ~~EM3-WeM16~~, 141
Quayle, M.J.: AA1-MoA1, 54; EM-MoP2, 85
Quijada, M.: ALE-SuP7, 51
Quinn, B.: AM-MoP6, 84
— R —
Rabat, H.: AM1-WeM5, 136
Radue, E.: EM1-WeM4, 138
~~Rähn, M.~~: ~~EM-MoP7~~, 86
Rahul, R.: AA1-TuP7, 115
Räisänen, J.: AF2-TuM2, 93; AF2-TuM4, 94; NS-WeA5, 149
Rajbhandari, P.: AA1-TuP5, 115
Raley, A.: ALE1-WeM1, **133**
Ramachandran, R.: AF1-TuM7, 92
Ramos, C.: AM-MoP8, 84
Ramunno, L.: AA1-WeA5, 144
Rangelow, I.: ALE1-MoA4, 65
Ranjan, A.: ALE1-WeM1, 133; ALE2-TuA11, 109
Rao, M.: AF2-MoP8, 73
Rao, M.B.: AF2-MoA1, **59**
Rashkeev, S.: EM1-WeA8, 148
Rathi, S.: AA2-TuP17, 121; AA3-TuA11, 104; AA4-TuP12, 125
Ravikumar, V.: **AA1-TuA5**, 101
Raza, A.: AF-TuA4, 106
~~Raza, H.~~: ~~EM-MoP1~~, 85
Reeves, R.: EM-MoP9, 86
Reif, J.: AF1-TuM2, **91**
Resende, J.: AA4-TuP9, 125
~~Rezvan, A.~~: ~~ALE-SuP3~~, 50
Ricky, N.: NS-WeA1, 148
Riedl, T.: AF2-MoA5, 59; ALE2-TuM16, 99; AM1-WeM2, 136
Ritala, M.: AF2-MoA7, 60; AF2-TuM2, **93**; AF2-TuM4, 94; EM1-WeM2, 137; NS-WeA5, 149
Ritasalo, R.: AA1-MoA4, 54
~~Ritslaid, P.~~: ~~EM-MoP7~~, 86
Ritter, D.: AF3-TuM15, 96
Robertson, K.: AF1-MoP4, 69
Robinson, Z.R.: AF1-TuM4, 92; AS2-TuA214, 113
Rodin, D.: AA1-TuA8, 102
Rodriguez, M.: EM1-WeA7, 148
~~Rogero, C.~~: ~~AF4-MoA13~~, 63
Roozeboom, F.: AF1-TuM5, 92; ALE1-WeM3, 133; AS-TuP5, 129
Rosenberg, S.G.: AF1-TuM4, **92**; AF-TuA6, 107; AS2-TuA214, 113; EM3-WeM13, 141
Rosowski, F.: AF3-MoA11, 61
Rozen, J.: EM1-WeA5, 147
Ruppalt, L.B.: AF3-MoP8, 78
Ryan, L.: AA2-MoA12, **56**
Ryu, J.S.: ALE-SuP10, 51
— S —
Sahota, A.: AA1-WeM3, 131; AA3-TuA15, 104
Saidjafarzoda, I.: EM3-WeM14, 141
Saito, K.: AA4-TuP3, 124; AF4-MoP1, **78**
Sakamoto, J.: AA2-TuM13, 90
Sakurai, A.: AF1-MoP10, **70**
Salami, H.: AA1-MoA5, 55; AA1-MoA8, 55; AA5-TuP7, **127**
Salmi, E.: AF3-TuM14, 96
Samukawa, S.: AF-TuA1, 105; ALE2-TuM12, 98
Sanchez, A.: AA2-TuM12, 89; AA2-TuM15, 90
Sandoval, T.: AS1-TuA1, 110
~~Santangelo, S.~~: ~~EM-MoP1~~, **85**
Saravade, V.: AA1-TuP16, 117
~~Saric, I.~~: ~~AF4-MoA13~~, **63**
Sarnet, T.: AF5-MoP4, 81; AM-MoP9, 84
Sasaki, M.: **ALE2-MoA16**, 67
Sasao, N.: EM-MoP6, **86**
Sato, D.: ALE2-TuM12, 98
Sattelberger, A.: EM1-WeA1, 146
Sawant, S.Y.: AA1-TuP7, 115
Scanlan, D.: ALE1-TuA4, **108**
Schapmans, E.: AA1-WeM5, 131
Scheppe, A.: EM-MoP9, 86
Schierbaum, K.D.: AF1-TuM3, 91; AF2-MoA7, 60
~~Schlereth, R.~~: ~~AA2-TuP18~~, 121
Schlicht, S.: AA1-WeA8, 144
Schlitz, R.: AA1-WeA8, 144
Schlögl, R.: AF3-MoA11, 61
Schmidt, K.: EM1-WeA5, 147
Schnabel, H.-S.: AA4-TuP6, **124**
Schneider, J.: EM1-WeA3, 147
Schneidewind, J.: ALE2-TuM16, 99
Schörmann, J.: AS-TuP1, 128
Scowen, P.: AF4-MoP4, 79
~~Seemen, H.~~: ~~EM-MoP7~~, 86
Seidel, K.: AA3-TuA13, 104
Seidel, T.: AA1-TuP8, **116**; ALE1-WeM6, **134**
Sekine, M.: ALE2-MoA17, 67
Sekkat, A.: AM1-WeM5, 136
Selberherr, S.: ALE2-TuA12, 109
Seo, J.: AA2-MoA13, 56
~~Seo, K.~~: ~~AA2-TuP20~~, 122
Seo, S.: AF2-MoP9, **74**
Seok, J.-H.: AF1-MoP6, 70; AF2-MoP14, 75
Seong, I.-H.: ALE1-MoA6, 65
Seong, S.: EM-MoP5, 85
Shaffer, D.: AA1-TuP14, 117
Shah, D.: EM-MoP13, **87**
~~Shamim, S.~~: ~~AA2-TuP18~~, 121
Shamsi, Z.: AM-MoP8, 84
Sharma, K.: AS1-TuA3, 111
Sharma, V.: ALE1-TuM6, **97**
Shekhar, A.: **AA1-TuA5**, 101
~~Shekhar, P.~~: ~~AA2-TuP18~~, **121**
~~Sheng, Y.~~: ~~AA2-TuP11~~, 120
Shero, E.: AA2-WeA3, 145
Shi, J.: NS-WeA1, 148
Shi, Y.: ALE1-TuA6, 108
Shieh, J.: AA1-WeA7, 144; AA3-TuA14, 104
~~Shigeno, S.~~: ~~ALE2-TuA15~~, 110
Shigeru, K.: AF4-MoP1, 78
Shim, J.H.: AA1-WeA3, 143; AA2-MoA17, 57; AA4-TuP7, 124
Shimizu, M.: AF3-MoP1, 76
Shin, D.: ALE-SuP12, **52**
~~Shin, H.~~: ~~AS2-TuA216~~, **114**
Shin, J.W.: AM-MoP5, 84
Shin, S.S.: AA2-MoA13, 56
Shin, Y.: AF4-MoP12, 80
Shinoda, K.: ALE2-WeM13, **134**
Shkura, E.: ALE2-TuM16, **99**
Shong, B.: AF2-MoP9, 74; EM1-WeM5, 138
Shoute, G.: AF1-MoA2, **57**
Shu, Y.: AA5-TuP2, 126
Shukla, D.: AF3-MoP7, 77; AF3-TuM13, 95; AF3-TuM16, 96; AF4-MoP3, 79; EM3-WeM14, **141**
Shukla, S.: AM-MoP9, 84
Shul, R.: ALE-SuP4, 50
Shyue, J.-J.: EM3-WeM15, 141
Siebert, M.: ALE2-TuM16, 99
Siegel, D.: AA2-TuM12, 89
Sigurdsson, S.: AA1-MoA4, 54
Simbierowicz, S.: AA2-WeA4, 145
Singh, J.: AA1-TuM6, 89
Sippola, P.: AA3-TuA13, 104; AF2-TuM7, **95**
Smith, S.: EM1-WeA7, **148**
Sobell, Z.: AS1-TuM14, **99**
Soethoudt, J.: AS1-TuM16, 100; AS-TuP6, 129
Sohn, H.: EM-MoP15, 87
Solano, E.: AF1-TuM7, 92; AF3-MoA15, 62
Son, J.-P.: ALE1-MoA6, 65
Son, J.-W.: AA2-MoA17, 57
Song, C.: AF4-MoP12, **80**

Author Index

Song, E.-J.: AA1-TuP2, 115
Song, H.: ALE-SuP12, 52
Song, S.H.: AA4-TuP4, **124**
Song, S.K.: ALE1-WeM5, **133**
~~Song, Y.~~: ~~EM3-WeM16~~, 141
Sønsteby, H.H.: EM1-WeA6, **148**
Sopha, H.: AA2-TuA16, 104
Sowa, M.: AA5-TuP4, **126**
Spampinato, V.: AS-TuP6, 129
Sperling, B.: AF2-TuM1, 93
Spiegelman, J.: AF2-MoP7, 73; AF4-MoA17, 64; AM-MoP8, **84**; AS-TuP4, 128
Sprey, H.: AA3-TuA13, 104
~~Sreenivasan, M.G.~~: ~~AA1-TuP1~~, 115
Sridhar, S.: ALE2-TuA11, 109
Stafford, N.: ALE1-MoA7, 66
Stan, L.: AA5-TuP10, 128
Stassen, I.: AM1-WeM8, **137**; EM1-WeM3, 138
Stephenson, D.: ALE1-TuA4, 108
~~Stern, R.~~: AF2-TuM2, 93; ~~EM-MoP7~~, 86
Stover, A.: ALE1-TuA4, 108
Strandwitz, N.: AA5-TuP4, 126
Strnad, N.: EM1-WeA2, **147**
Sugimura, S.: EM-MoP6, 86
Sumpter, B.: EM2-WeM14, 140
Sun, K.: AA1-TuM7, 89
Sun, P.: AF5-MoP1, 80; AM-MoP6, 84
Sun, Q.: AA2-TuM14, 90
Sun, Q.Q.: NS-TuP3, 130
Sun, X.: AA2-TuM14, 90; ALE1-WeM1, 133
Sunderland, T.L.: AF4-MoP10, 80
Sundqvist, J.: ALE1-TuA1, 107; AM1-WeM6, 136
Sung, T.: ALE1-WeM8, **134**
Suyatin, D.: ALE1-TuA1, 107
Suzuki, K.: AF2-MoP7, 73
Sweet, W.: AA4-TuP2, 123
Szeghalmi, A.: AM-MoP2, 83
Szornel, J.: ALE1-MoA4, 65
— T —
Tadjer, M.: AF-TuA7, 107
~~Tak, Y.D.~~: ~~AF4-MoP8~~, 80
Takahashi, M.: AF4-MoA16, 64
Tamboli, A.: AF2-MoP4, 73
~~Tamm, A.~~: ~~EM-MoP7~~, 86
Tan, .: ALE1-MoA1, **64**
Tan, K.: AS-TuP4, 128
Tanaka, S.: AF3-MoP1, 76
Tang, C.-M.: AA5-TuP10, 128
Tanide, A.: ALE2-MoA17, 67
Tanimoto, Y.: ALE2-TuM12, 98
Tapily, K.: AA2-WeM12, 132
Tarafdar, R.: ALE1-WeM7, 134
Tasneem, N.: AA3-TuA11, 104
Tatsumi, T.: ALE1-TuA7, 108
Teeter, G.: AA2-TuM13, 90
Teplyakov, A.: ALE1-TuM4, **97**; ALE-SuP1, 50
Teramoto, T.: **ALE2-MoA16**, 67
Teranishi, T.: AA2-TuA15, 103
Tesfaye, A.: AA2-TuA16, 104
Teslich, N.: EM-MoP9, 86
Thakur, A.: AM1-WeM6, **136**
Thayne, I.: AA2-TuP6, 119; ALE2-MoA11, 66
Theirich, D.: AF2-MoA5, 59; ALE2-TuM16, 99; AM1-WeM2, 136
Theofanis, P.: ALE1-TuA5, **108**; ALE-SuP2, **50**
Thomas, A.: AA1-WeA8, 144
Thomas, O.: AA5-TuP2, 126
Thompson, T.: AA2-TuM12, 89
Thouless, M.D.: AA1-WeA2, 143
Thu, H.: AA1-TuP15, 117
Tillocher, T.: ALE1-MoA8, 66; ALE-SuP11, **52**
~~Tinacba, E.J.~~: ~~ALE2-TuA15~~, 110
Tompa, G.: AM1-WeM7, **137**
Tonner, R.: AS1-TuA1, 110
Torgesen, J.: AF3-TuM12, 95
Torres, A.: ALE2-MoA14, 67
Toyoda, N.: ALE2-TuM15, **99**
Tracy, R.: AA1-TuM5, 88
Tran Vo, H.C.: AA1-TuP3, 115
Tränkle, G.: AA2-TuP16, 121
Trejo, O.: AS1-TuA7, 112
~~Triolo, C.~~: ~~EM-MoP1~~, 85
Triyoso, D.: AA2-WeM12, **132**
Trunschke, A.: AF3-MoA11, 61
Tsai, Y.: ALE1-TuA6, 108
Tsampas, M.: AA1-TuM3, 88
Tsuchibuchi, G.: AF2-MoP7, 73
Tsutsumi, T.: ALE1-MoA3, **65**; ALE1-TuA3, 107; ALE2-MoA17, 67
Tulodziecki, M.: AA2-TuA13, 103
Tummala, R.: EM2-WeM15, 140
Tuominen, M.: ALE1-TuM6, 97
Tynell, T.: AA1-WeA8, 144
— U —
Uematsu, K.: ALE2-TuM15, 99
Unnikrishnan, S.: AA2-TuA13, 103
Utriainen, M.: **AF3-MoA12**, 61; AF3-MoA13, 61; AF3-MoA16, 62; AF-TuA2, 105
Utsuno, M.: AF-TuA1, 105
Uvarov, V.: AA2-TuP5, 119
Uy, A.: AA1-MoA5, 55; AA1-MoA8, **55**; AA5-TuP7, 127
Uyaner, M.: AA1-WeA1, 143
— V —
Vadapalli, A.: AA1-MoA8, 55; AA5-TuP7, 127
Vallée, C.: AA2-WeA7, 146; **ALE2-MoA16**, 67; AM1-WeM5, 136; AS2-TuA112, **112**
Van Daele, M.: AF1-TuM7, 92; AF-TuA4, **106**
van de Sanden, R.: AA1-TuM3, 88
van den Bruele, F.: AA2-TuA13, 103
Van Elshocht, S.: AS1-TuM16, 100
van Helvoort, A.T.J.: AF3-TuM12, 95
van Ommen, J.R.: AA1-MoA1, 54; **AA1-TuA5**, 101; AF5-MoP2, **81**; EM-MoP2, 85
van Ommen, R.: AA1-MoA2, **54**; AA1-TuM8, 89; AS-TuP6, 129
Varga, A.: AF2-MoA4, 59
Väyrynen, K.: AF2-TuM2, 93
Vehkamäki, M.: AF2-TuM4, 94; NS-WeA5, 149
Ventrice, Jr., C.A.: AF1-TuM4, 92
~~Ventzek, P.~~: ~~AF3-MoP5~~, 77; ALE1-WeM1, 133; ALE2-TuA11, 109
Vereecken, P.: **EM1-WeM7**, 139
Verheijen, M.: AS2-TuA111, 112; NS-WeA6, 149
Verni, G.: AF2-TuM7, 95
Vervuurt, R.: ALE1-TuA3, **107**
Vesterinen, V.: AA2-WeA4, 145
Veyan, J.: AS-TuP4, 128
Volk, A.: AF3-MoP10, 78
Vos, M.: AS2-TuA111, **112**
— W —
Waduge, W.L.I.: EM-MoP11, 87
Wajda, C.: AA2-WeM12, 132; AF2-MoP16, 75
Waldman, R.: AS2-TuA215, **113**
Wallace, R.: AA3-TuA15, 104
Wallas, J.: AF4-MoA15, 63
Walton, S.: AF-TuA6, 107; AF-TuA7, 107; ALE-SuP7, **51**
Wan, H.-W.: AA2-TuP12, 120; **AA2-WeM16**, 133
Wang, H.: AS1-TuA8, **112**
Wang, J.: AA1-WeA2, 143; AF3-MoP3, **77**
Wang, L.: AA1-TuP14, 117
Wang, M.: AF2-MoP8, **73**; ALE1-TuA6, 108
Wang, S.: ALE2-WeM16, 135
Wang, W.: AA2-TuP13, 121
Wang, X.: AA2-TuP13, 121; AF1-TuM1, **91**; AF2-MoP12, 74; ALE2-MoA15, 67
Wang, Y.: NS-TuP3, 130
Wang, Z.: AA3-TuA11, 104; ALE1-TuM4, 97
Warburton, R.F.: AA2-TuA12, 103
Weber, M.: AA1-MoA3, **54**; AA4-TuP1, **123**
Weck, A.: AA1-WeA5, 144
Wege, S.: AM1-WeM6, 136
~~Wei, H.~~: ~~EM3-WeM16~~, 141
Weimer, A.: AA2-MoA14, 56; AF1-MoA6, 58
Weinbub, J.: ALE2-TuA12, 109
Weinfeld, K.: AF3-TuM15, 96
Weinreich, W.: AF3-MoA13, **61**
Werbrouck, A.: AF1-TuM6, **92**
Wheeler, V.: AF2-MoP11, 74; AF-TuA6, 107; AF-TuA7, **107**
Wiemer, C.: AA1-TuA3, 101
Wilk, A.: AM-MoP1, **82**
Wilken, M.: AF1-MoP8, 70
Willis, B.: AF3-MoP7, 77; AF3-TuM13, 95; AF3-TuM16, 96; AF4-MoP3, 79; AM1-WeM1, 135; AS-TuP2, 128
Wilt, J.: AA2-TuP15, 121
Winter, C.H.: AA1-TuA3, 101; AF1-MoP2, 69; EM-MoP10, 86; EM-MoP11, 87
Winterkorn, M.M.: AF5-MoP8, **82**
~~Woehl, J.~~: ~~ALE-SuP5~~, 51
Woelk, E.: AF2-TuM1, 93; AM-MoP4, **83**
Wojtecki, R.: AS1-TuA6, **111**
Wollmershauser, J.: NS-TuP4, 130
Wolterbeek, B.: AA1-MoA2, 54
Woltersdorf, G.: AA1-WeA8, 144
Wood, K.: AA2-TuM13, 90
Wooding, J.: AA1-TuA4, **101**
Woodruff, J.H.: AA2-WeA5, 145
Woodward, J.M.: AF1-TuM4, 92; AF-TuA6, 107; AS2-TuA214, **113**
Wree, J.-L.: AF1-MoP8, 70; AF2-MoA7, **60**
Wright Jr., R.: AF1-MoP9, 70
Wright, R.: AF3-MoP2, **76**
Wu, J.: AA2-TuP15, 121
Würfl, J.: AA2-TuP16, 121
— X —
Xiang, J.: AA2-TuP13, **121**
Xiang, Q.: AA5-TuP1, 126
Xiao, M.: AF2-MoP8, 73
Xie, Q.: AF2-TuM7, 95
Xu, W.: AS1-TuA3, **111**
Xu, X.: AF3-TuM15, 96
— Y —
Yamakawa, S.: ALE1-TuA7, 108
Yamashita, A.: AF1-MoP10, 70; ~~AS1-TuM15~~, 100
Yamazaki, K.: ALE1-MoA8, 66; ALE-SuP11, 52
Yan, B.: AA5-TuP5, **127**
Yan, C.: ALE1-WeM8, 134
Yan, D.: AA1-TuP14, 117
Yang, B.C.: AM-MoP5, 84
Yang, B.-I.: AF1-MoP11, 71
Yang, H.: AF2-MoP18, 76
Yang, M.: ALE1-WeM8, 134
Yang, T.-Y.: AA2-MoA13, 56
Yang, W.: ALE1-MoA1, 64
Yanguas-Gil, A.: AF1-MoA1, **57**; EM1-WeA1, 146; ~~EM1-WeA4~~, 147
Yatsuda, K.: ALE1-MoA8, 66; ALE-SuP11, 52
Ye, X.: AA1-TuP14, 117; EM2-WeM14, 140
Yee, S.: AA1-TuA8, 102
Yeo, S.M.: AA2-MoA13, 56
Yeom, G.Y.: AF4-MoP11, 80; AF4-MoP12, 80; ALE-SuP14, 52
Yeom, W.K.: AF4-MoP12, 80
Yi, S.: AF4-MoP2, 78
Yi, S.-H.: AA1-WeA7, **144**

Author Index

Yin, Y.-T.: AA3-TuA14, **104**; EM3-WeM15, 141
Ylivaara, O.: **AF3-MoA12**, **61**
Yoneda, M.: AA2-TuA15, 103
Yoo, S.-W.: ALE1-MoA6, 65
Yoon, H.: AF2-MoP10, 74
Yoon, H.R.: EM-MoP4, **85**
Yoon, S.: AF2-MoP18, 76
Yoshida, K.: AA4-TuP3, **124**; AA4-TuP5, 124
Yoshikawa, Y.: AA2-TuA15, 103
~~Yoshino, T.~~: ~~AS1-TuM15~~, 100
Yosida, K.: AF4-MoP1, 78
You, C.: **ALE2-MoA16**, 67
You, S-J.: ALE1-MoA6, 65
Young, E.C.: AF1-TuM4, 92
Young, L.B.: AA2-TuP12, **120**; **AA2-WeM16**, 133
Yu, S.: AA2-TuM12, 89
~~Yu, Y. S.~~: ~~AF2-MoP6~~, 73
Yuan, B.: ALE1-TuM4, 97
— Z —
Zafeiropoulos, G.: AA1-TuM3, 88
Zakaria, Y.: EM1-WeA8, 148
Zanders, D.: AF1-MoP8, 70; AF1-TuM3, **91**; AF2-TuM6, 94
Zazpe, R.: AA2-TuA16, 104; NS-TuP1, **129**
Zeng, D.: AM-MoP1, 82
Zeng, L.: NS-WeA1, **148**
Zeng, T.: AF2-TuM6, 94
Zhang, B.: AF3-MoA17, **62**
Zhang, C.: AA1-WeA4, 143; AS-TuP2, **128**; EM1-WeM2, **137**
Zhang, D.: AA1-MoA1, 54; ALE1-TuA6, **108**
Zhang, D.W.: NS-TuP3, 130
Zhang, F.: EM2-WeM13, 140
Zhang, H.: ALE2-WeM12, **134**; ALE-SuP13, **52**
~~Zhang, K.~~: ~~AA2-TuP9~~, **120**; ~~AA4-TuP10~~, 125; ~~AM-MoP3~~, 83
Zhang, T.: EM1-WeA8, 148
Zhang, Y.: AA4-TuP11, 125
Zhang, Z.: AS1-TuA4, **111**
Zhao, Y.: AA2-TuM14, 90; AF1-MoP14, 71; ALE2-MoA15, 67
~~Zhao, Y.T.~~: ~~AA3-TuP6~~, 123
Zheng, L.: AA1-TuM5, **88**
~~Zheng, X.~~: ~~AF4-MoP9~~, 80; ~~EM3-WeM16~~, **141**
Zhiyang, Q.: AF4-MoP5, 79; AS-TuP4, 128
Zhou, B.: AA5-TuP1, 126
Zhou, C.: AA1-TuP16, 117
Zhou, L.: AA2-TuP13, 121
Zhou, X.: AF4-MoP10, **80**; AF4-MoP5, 79
~~Zhu, H.~~: ~~AA2-TuM16~~, **90**; NS-TuP3, 130
Zhu, K.: AA2-MoA11, 56
Zhu, W.: AA1-WeA4, 143
Zoubian, F.: AM1-WeM5, 136
Zuo, P.: EM-MoP11, 87
Zywitzki, D.: AF1-MoP8, 70; AF2-MoA6, **60**

Innovative Chemistries for Advanced Thin Films

Leading Advanced Materials supplier for Semiconductor industry, We offer a unique range of gaseous, liquid and solid precursors for leading edge CVD and ALD films and applications:

-Advanced Epitaxy of Germanium & Silicon materials
-PE-ALD and T-ALD for high-k and advanced patterning
-LPCVD and FCVD materials for gap fill oxide
-BEOL dielectrics & metallization materials

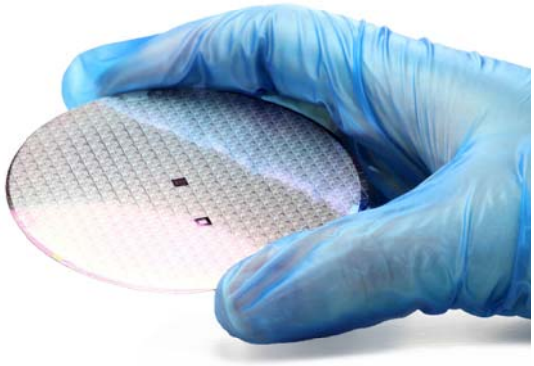

Beyond Semiconductor, our Innovative Chemistries are helping our customer to tune thin film properties and functionalization:

Electrical	Optical	Mechanical
Barrier	Hydrophobic	Passivation
Protective	Encapsulation ...	

Air Liquide Advanced Materials researchers and product specialists are dedicated to the **screening of new molecules**, the development and scaling of efficient manufacturing processes, and the design of smart and safe packaging solutions development. Air Liquide Advanced Materials also provides our customers and development partners with the product stewardship and guidance to **safely introduce new substances into high volume manufacturing**.

From gram-scale to Multi-tons ALD/CVD precursors

5 B Boron 10.811	21 Sc Scandium 44.956	22 Ti Titanium 47.88	25 Mn Manganese 54.938	27 Co Cobalt 58.933	28 Ni Nickel 58.693	29 Cu Copper 63.546	39 Y Yttrium 88.906	40 Zr Zirconium 91.224
14 Si Silicon 28.086	32 Ge Germanium 72.61	41 Nb Niobium 92.906	42 Mo Molybdenum 95.94	44 Ru Ruthenium 101.07	72 Hf Hafnium 178.49	73 Ta Tantalum 180.948	74 W Tungsten 183.85	78 Pt Platinum 195.08
57 La Lanthanum 138.906	58 Ce Cerium 140.115	59 Pr Praseodymium 140.908	63 Eu Europium 151.966	64 Gd Gadolinium 157.25	66 Dy Dysprosium 162.50	68 Er Erbium 167.26	70 Yb Ytterbium 173.04	71 Lu Lutetium 174.967

aloha@airliquide.com

Shaping the Future

Applied Materials is the leader in materials engineering solutions used to produce virtually every new chip and advanced display in the world. Our expertise in modifying materials at atomic levels and on an industrial scale enables customers to transform possibilities into reality. At Applied Materials, our innovations make possible™ the technology shaping the future.

Learn more: **www.appliedmaterials.com**

APPLIED MATERIALS®
make possible

ARRADIANCE

World leader in high performance Benchtop ALD Systems™

...Yes, we do custom

Molecular Innovation ™

www.arradiance.com

ARRADIANCE®

ALD LEADERSHIP

We were one of the first companies to have the vision to realize the potential of ALD technology for the semiconductor industry. In 1999, we acquired Microchemistry in Finland, forming ASM Microchemistry. We dedicated a further eight years of R&D to turning it into a process that could be used reliably and efficiently by advanced semiconductor chip manufacturers. ASM is now a leader in ALD equipment and process solutions for a wide range of semiconductor production applications.

FOR FURTHER INFORMATION, PLEASE CONTACT INFO@ASM.COM

ASM.COM

EMD Performance Materials

Accelerating

the next generation of deposition materials.

From Lab to Fab...

Molecule Design & Synthesis

Molecule Characterization

Deposition Screening &
Film Characterization

Precursor Flux Measurement

High Volume Manufacturing

We have you covered

EMD is a business of Merck KGaA, Darmstadt, Germany

Leverage our Ereztech 25 grams™ approach for synthesizing new ALD precursors and high volume production scale-up.

25 grams™

Ereztech 25 grams™

Learn More, Scale Faster

- **Low risk:** we'll synthesize your new molecule for a minimum as small as 25g
- **Low cost:** we provide this service at our cost
- **Big results:** test your new ALD precursor faster via with our BridgeForward® scale-up methodology

Visit us at booth #200 & 201 and find out how we can help you speed up your chemical innovation!

EREZTECH

BRIDGING CHEMICAL GAPS

ereztech.com

GET THE EUGENUS EDGE

FOR YOUR ALD APPLICATIONS

Introducing a new breed of semiconductor equipment manufacturing

Built on the success of Genus—the original ALD thin films innovator—we're creating a bold future for our customers, with breakthrough ALD performance, results, and efficiency.

We offer a unique blend of rapid, Silicon Valley R&D with world-class Korean manufacturing. The result? The Eugenus edge.

For more information, visit **www.eugenustech.com**.

EUGENUS

ALD 150 LX

Patented Precursor Focusing Technology™

Designed for POWER & *Performance*

- Designed for Advanced R&D
- Remote Plasma
- Real-time Ellipsometry
- Cluster Tool Integration
- Precursor Focusing Technology™ for Optimal Performance
- Extended Intervals Between Maintenance Cycles
- eKLipse™ Control Software

Kurt J. Lesker® Company

www.lesker.com

Enabling Technology for a Better World

18-054

Metryx® Mass Metrology for 3D Device Process Monitoring & Control

Memory Array

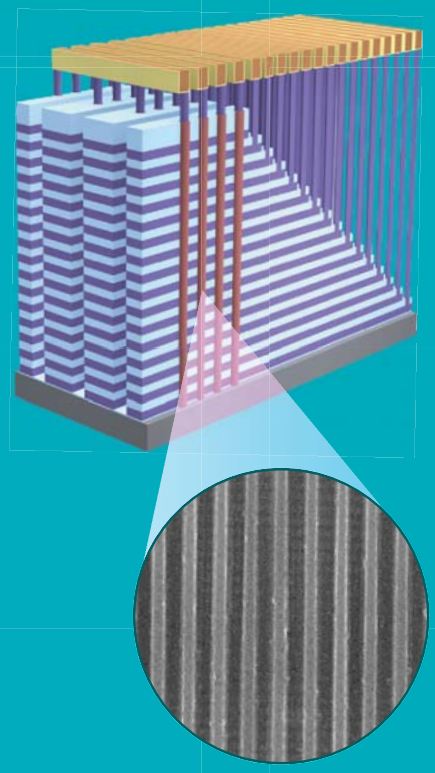

Conformal Deposition over High Aspect Ratio Features

Lam® RESEARCH

Connect with us

www.lamresearch.com

Leadmicro 微导

www.leadmicro.com

JIANGSU LEADMICRO NANO-EQUIPMENT TECHNOLOGY LTD.

Semiconductor

Integrated Circuit

LED&MEMS

Photovoltaics

Flexible Electronics

Emerging Technologies

Industry Solutions

Phone: +86-(0)510-81164688

General enquiry: info@leadmicro.com

Product and technology enquiry: sales@leadmicro.com

Driving innovation at the atomic scale

OXFORD INSTRUMENTS

Atomic Layer Etch

- **Ultra low** damage
- **High selectivity**
- **Ultra accurate** depth control
- **Process solutions** for GaN, AlGaN, Si, SiO_2 & 2D materials

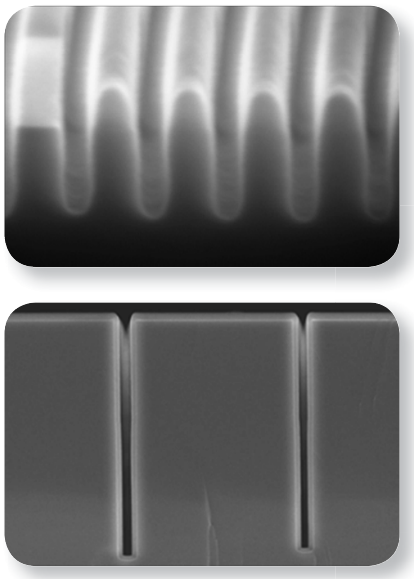

Atomic Layer Deposition

- **Conformal coating**
- **Low damage** plasma
- **Solutions** for a wide variety of materials:
  - High-*k* dielectrics
    e.g Al_2O_3 & HfO_2
  - Dielectrics
    e.g SiN_x & SiO_2
  - Conductive materials
    e.g. TiN, NbN, Pt

Plasma.oxinst.com

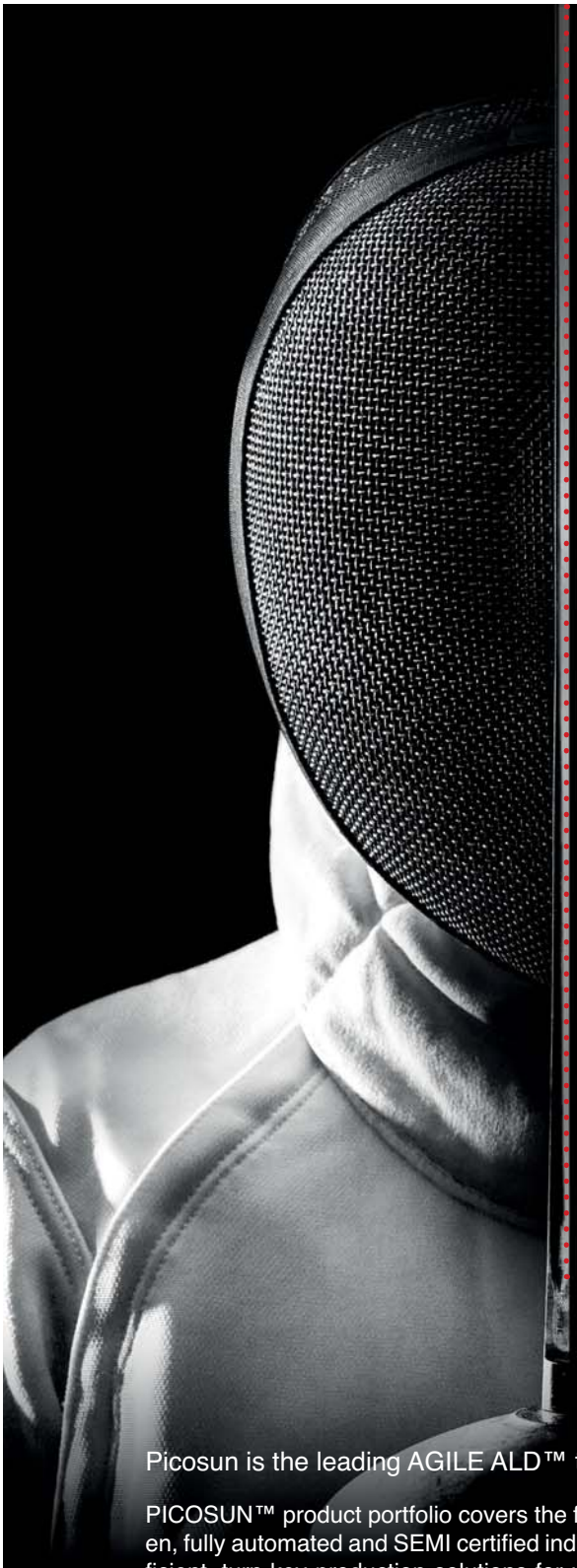

picosun
AGILE ALD

for companies driven by
innovation

Picosun is the leading AGILE ALD™ technology provider for microelectronics and other industries.

PICOSUN™ product portfolio covers the full range of ALD, from market-leading research tools to production-proven, fully automated and SEMI certified industrial ALD systems for up to 300 mm wafers. Our specialties are cost-efficient, turn-key production solutions for up to 200 mm wafer markets, and coating of 3D items such as medical devices and implants, coins, watches, and machinery parts.

COME HEAR THE LATEST NEWS FROM THE HQ OF AGILE ALD™ AT BOOTH 511-513!

www.picosun.com

info@picosun.com

TEL™

TECHNOLOGY ENABLING LIFE™

TOKYO ELECTRON

tel.com

VERSUM MATERIALS:
ACCELERATING THE FUTURE

We are an innovation-driven electronic materials company with more than 2,300 global employees who bring a deeper understanding of materials, a long history of collaboration and an extensive track record of success to the electronics industry. So whether you need help developing game-changing technology, improving an existing product, or making a manufacturing process more productive, we'll get you to the next place you want to be.

What can we help you advance?

VERSUM MATERIALS

VERSUMMATERIALS.COM

ARRADIANCE®

Enabling Technologies for Our World and Beyond

Molecular Innovation ™

www.arradiance.com

AVS 66TH INTERNATIONAL SYMPOSIUM & EXHIBITION

SYMPOSIUM: OCT. 20-25, 2019 | EXHIBIT: OCT. 22-24, 2019

Greater Columbus Convention Center, Columbus, Ohio

"Shaping Our Future: Materials, Technologies & Processes for Energy Transition"

Exciting Sessions are being planned in the following topical areas:

- 2D Materials
- Actinides & Rare Earths
- Advanced Ion Microscopy
- Advanced Surface Engineering
- Applied Surface Science
- Atomic Scale Processing
- Biomaterial Interfaces & Plenary
- Chemical Analysis & Imaging at Interfaces
- Complex Oxides: Fundamental Properties & Applications
- Electronic Materials & Photonics
- Energy Transition
- Frontiers of New Light Sources Applied to Materials, Interfaces, & Processing
- Fundamental Aspects of Material Degradation
- Fundamental Discoveries in Heterogeneous Catalysis
- Magnetic Interfaces & Nanostructures
- Manufacturing Science & Technology
- Materials & Processes for Quantum Information, Computing, & Science
- MEMS & NEMS
- Nanometer-scale Science & Technology
- New Challenges to Reproducible Data & Analysis
- Plasma Science & Technology
- Spectroscopic Ellipsometry
- Surface Science
- Thin Film
- Vacuum Technology

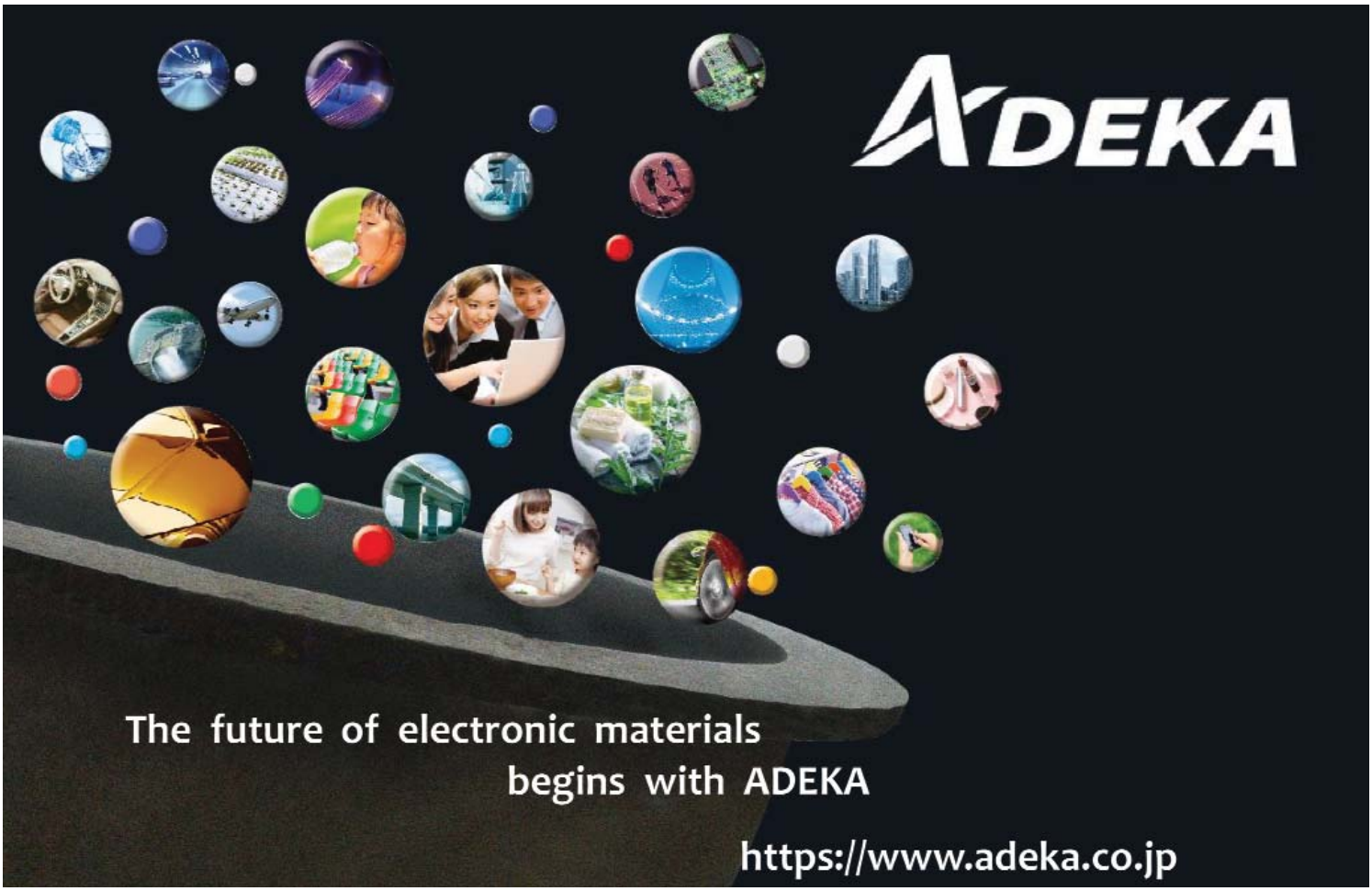
ADEKA
The future of electronic materials
begins with ADEKA
https://www.adeka.co.jp

Hansol
Chemical
Global specialty chemical Company
delivering innovation value
Advanced precursor technology
Our innovative precursor solutions lead to develop next generation semiconductor.
Customer-oriented business
With our own quality system and efficient BCP, we ensure to meet customer's needs.
www.hansolchemical.com

Pegasus Chemicals

Precursors for ALD and CVD

Supporting Innovation with Chemistry...

Pegasus

QUALIFICATION
Process fixed

PRECURSOR FIXED DESIGN
Fixed manufacture/fixed supply

PRECURSOR SCALE UP
Proven increased manufacture platform

MATERIAL SELECTION
Electrical properties
Optical properties

PRECURSOR ANALYSIS

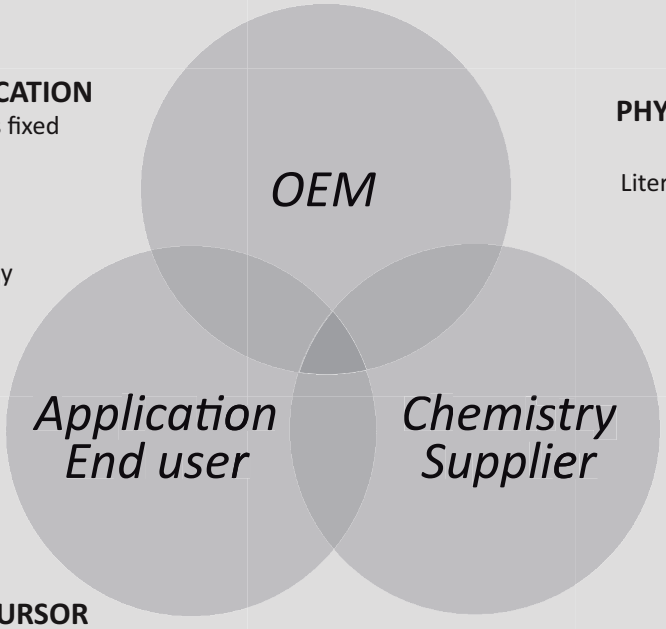

PHYSICAL PROPERTY STUDY
Literature/patent search

DEVELOPMENT
Precursor molecular design

DEPOSITION AND CHARACTERISATION
Growth rate
Layer composition

Pegasus

www.pegasuschemicals.com

BRUTE® Chemicals

King of the Gas Jungle

BRUTE Chemicals attack the challenges of low temperature ALD.

There is no hiding from **BRUTE Chemistry**, while plasma needs line-of-sight to act.

Super dry **BRUTE Hydrazine** reduces the chance of oxygen contamination in nitride films grown below 400°C.

BRUTE Peroxide actively hydroxylates surfaces, without ozone or plasma.

Contact **RASIRC** for your guide to the Gas Jungle.

RASIRC®

www.rasirc.com

New! OG-60H *Launched*

- N2 non-doping **O3** ⇒ Better Quality Film
- 350g@1slm ⇒ *Just Right* **for R&D**

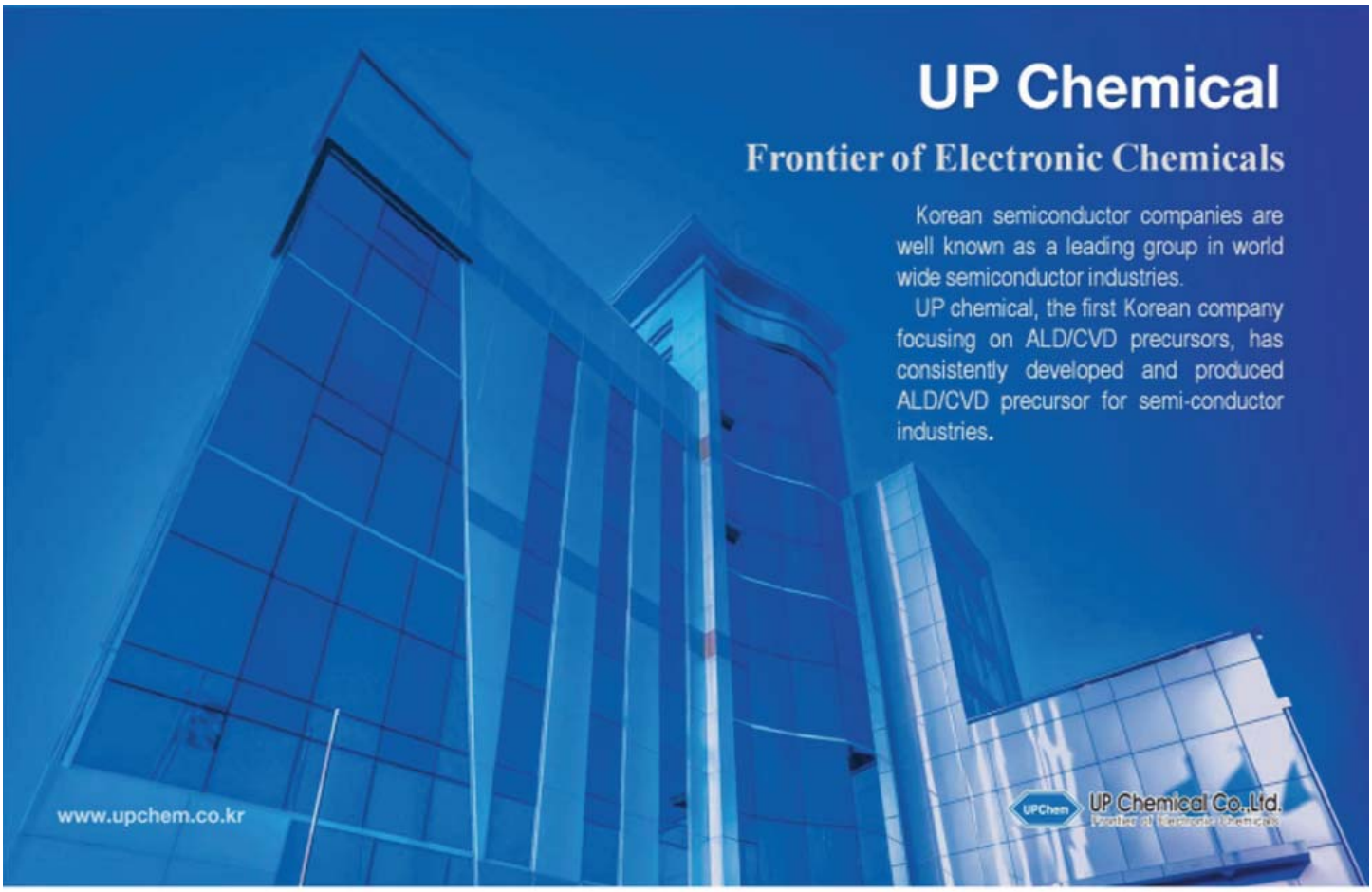

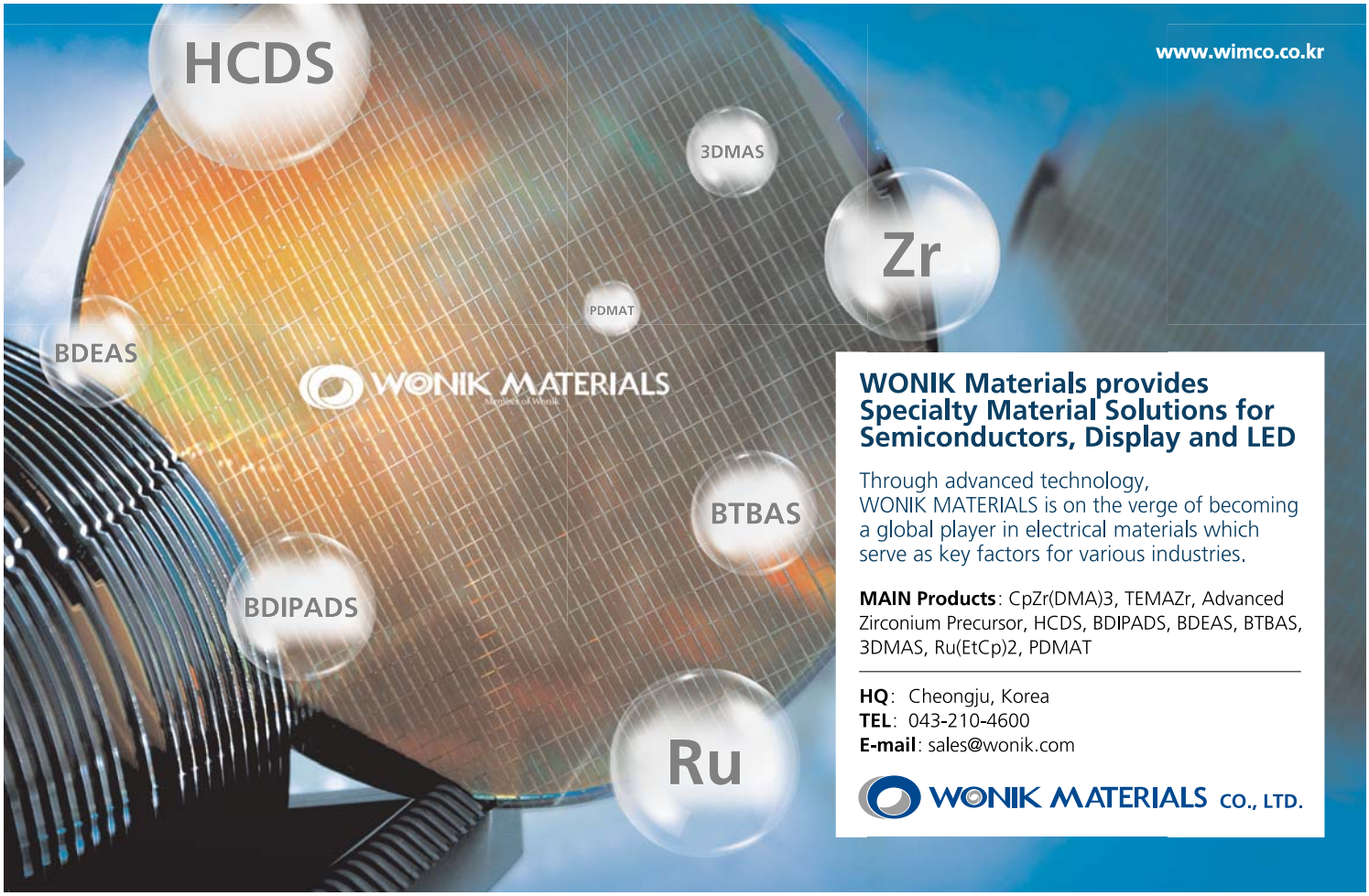

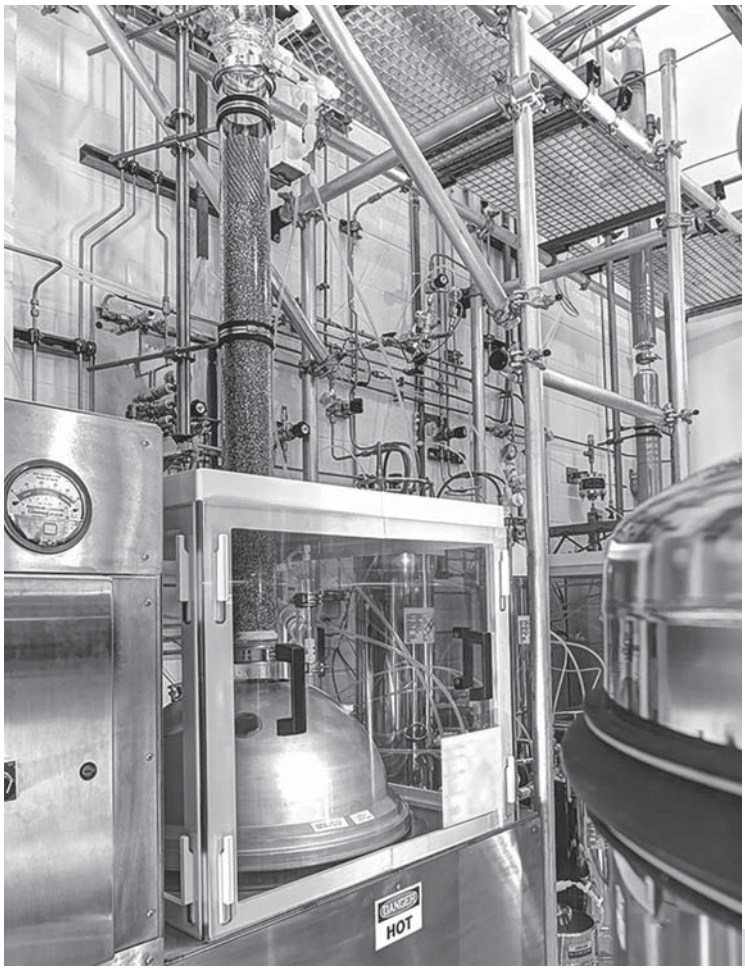

Materials that Matter

As a global provider of customized precursors and delivery systems, we specialize in bringing new materials to the semiconductor industry through high-volume purification, packaging systems, advanced material characterization, and process controls. Vaporizers designed to allow for higher transport of solid precursors at lower temperature, and delivery test stands with flow monitoring exemplify our focus to help customers solve ALD and CVD process and integration challenges.

Visit entegris.com to learn more.

Entegris®, the Entegris Rings Design®, and other product names are trademarks of Entegris, Inc. as listed on entegris.com/trademarks.

©2019 Entegris, Inc. | All rights reserved.

Entegris

NSI IS A TOTAL SOLUTIONS PROVIDER FOR AMPOULES/ BUBBLERS, AND LIQUID LEVEL SENSORS USED IN ALD PRECURSORS AS WELL AS EQUIPMENT NEEDED FOR GAS AND CHEMICAL MANAGEMENT. WE HELP RESEARCHERS AND CHEMICAL MANUFACTURERS BY GETTING THEM THE PARTS, THEY NEED FAST. OUR DEDICATED TEAM OF ENGINEERS AND TECHNICIANS WILL BRING YOUR VISION TO REALITY. WE BUNDLE DEVELOPMENT MECHANICAL DESIGN, ELECTRICAL DESIGN, CONTROL, SOFTWARE DEVELOPMENT, INTEGRATION, AND TESTING FOR COMPLEX ULTRA-HIGH PURITY GAS & CHEMICAL DELIVERY SYSTEMS.

JVSTA
Journal of Vacuum Science & Technology A

Call for Research Articles

Special Topic Collection: Atomic Layer Deposition and Atomic Layer Etching

Journal of Vacuum Science & Technology A is soliciting research articles for publication in a 2020 Special Topic Collection on Atomic Layer Deposition and Atomic Layer Etching.

This special topic collection is planned in collaboration with ALD 2019 and the ALE 2019 Workshop to be held in Bellevue, WA from July 21—July 24, 2019. The Special Topic Collection will feature sections dedicated to the science and technology of atomic layer controlled deposition and to the science and technology of controlled etching of thin films. While a significant number of articles will be based on material presented at ALD 2019 and the ALE 2019 Workshop, research articles on ALD and ALE but not presented at this conference are also welcome. The special topic collection will be open to all articles on the science and technology of ALD and ALE.

Submit your manuscripts to JVST online at http://jvsta.peerx-press.org. Helpful instructions for contributors, which may be found at http://avs.scitation.org/jva/authors/manuscript. Authors are encouraged to use the JVST template. Online, you will have an opportunity to tell us that your paper is a part of the Special Topic Collection by choosing either the "ALD Special Topic Collection" or the "ALE Special Topic Collection."

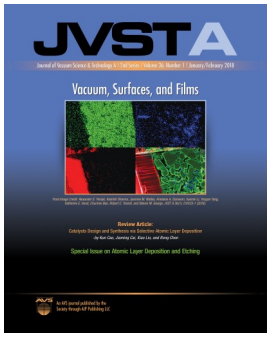

Manuscript Deadline:
November 1, 2019

Manuscript Details & Submission:
www.jvsta.org

Image Credit:
Giovanni Marin et al.
avs.scitation.org/doi/full/10.1116/1.5079614

Conference Office: 110 Yellowstone Dr., Suite 120, Chico CA 95973
Ph: 530-896-0477 • Fx: 530-896-0487 • E-mail: della@avs.org • Web: www.ald-avs.org